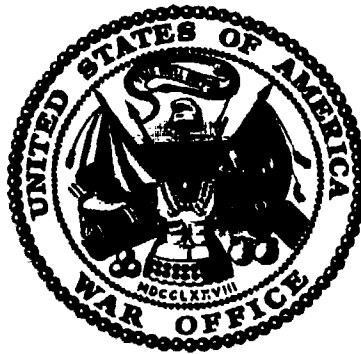


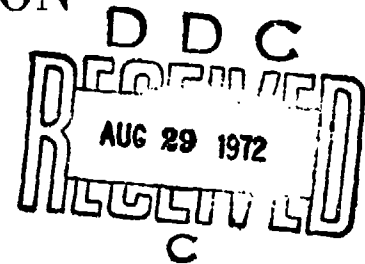
AD 747336

AD



BOUNDARY LUBRICATION

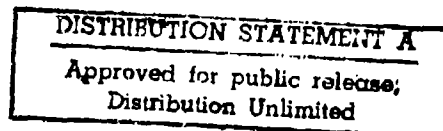
- 1972 -



SCIENTIFIC AND TECHNICAL APPLICATIONS FORECAST

Reprinted by
NATIONAL TECHNICAL
INFORMATION SERVICE
U.S. Department of Commerce
Springfield, VA 22151

OFFICE OF THE CHIEF OF RESEARCH AND DEVELOPMENT
DEPARTMENT OF THE ARMY
WASHINGTON, D.C. 20310



353

ACCESSION for		White Section	<input checked="" type="checkbox"/>
RTIS		Def Section	<input type="checkbox"/>
DDC		UNANNOUNCED	<input type="checkbox"/>
JUSTIFICATION			
BY	DISTRIBUTION/AVAILABILITY CODES		
DISC	AVAIL. 22/27 27 27 27		
A			

NOTICES

Distribution

This document has been approved for public release and sale; its distribution is unlimited.

Availability

Qualified requestors may obtain copies of this document from the Defense Documentation Center, Cameron Station, Alexandria, Virginia. Others may purchase copies from the Clearinghouse for Federal Scientific and Technical Information, U.S. Department of Commerce, Springfield, Virginia 22151.

Disposition

Destroy this report when no longer needed. Do not return it to the originator.

Disclaimer

The findings in this report are not to be construed as an official Department of the Army position unless so designated by other authorized documents.

Rights

Reproduction in whole or in part is allowed for purposes of the U.S. Government.

Unclassified
Security Classification

DOCUMENT CONTROL DATA - R & D

(Security classification of title, body of abstract and indexing annotation must be entered when the overall report is classified)

1. ORIGINATING ACTIVITY (Corporate author) Esso Research and Engineering Company P.O. Box 8 - Government Research Laboratory Linden, New Jersey 07036		2a. REPORT SECURITY CLASSIFICATION Unclassified	
		2b. GROUP N/A	
3. REPORT TITLE Boundary Lubrication			
4. DESCRIPTIVE NOTES (Type of report and inclusive dates) Scientific and Technical Applications Forecast (1972) Final Report (June 1969 - June 1972)			
5. AUTHOR(S) (First name, middle initial, last name) Alan Beerbower			
6. REPORT DATE June 1972		7a. TOTAL NO. OF PAGES 351	7b. NO. OF REFS
8a. CONTRACT OR GRANT NO. DAHC-19-69-C-0033		8b. ORIGINATOR'S REPORT NUMBER(S) GRU.1GBEN.72	
9. PROJECT NO.		9b. OTHER REPORT NO(S) (Any other numbers that may be assigned this report)	
10. DISTRIBUTION STATEMENT Approved for public release; distribution unlimited.			
11. SUPPLEMENTARY NOTES		12. SPONSORING MILITARY ACTIVITY Office of the Chief of Research & Dev. Department of the Army Washington, D.C. 20310	
13. ABSTRACT This report reviews the state-of-the-art of Boundary Lubrication and presents the prospects of such improvements in the lubrication of highly-loaded bearings as virtually to eliminate bearing failures and the need to relubricate machinery in the field. It includes a survey of instances of anomalously successful boundary lubrication and of mathematical models which might explain the low wear observed. These models are shown to be inadequate and some steps are taken to complete them. It is shown that 27 out of the 28 anomalies are explained by the expanded models. A plan for applying this knowledge to design practices is outlined.			

DD FORM 1473

REPLACES DD FORM 1473, 1 JAN 64, WHICH IS OBSOLETE FOR ARMY USE.

Security Classification

BOUNDARY LUBRICATION

An
Army Research Office
Scientific and Technical Applications
Forecast

By
Alan Beerbower
Esso Research and Engineering Company
Linden, N. J.

Contract No. DAHC19-69-C-0033

JUNE 1972

10

FOREWORD

The documents known as Scientific and Technical Applications Forecasts (STAF) form a series designed to supplement the U. S. Army Long Range Technological Forecast. A STAF is intended to provide an insight into one specific field, and is for use by persons inside and outside of the Department of the Army who have need for such background information. A STAF is primarily an encyclopedic summary of the current knowledge and a projection of the expected technological environment during the next 20 years. It is also a research plan designed to achieve the forecast. It includes an extensive bibliography, and its purpose is to enable scientifically, technically and operationally oriented individuals to communicate across disciplinary lines in order to achieve programmed Army goals.

U.S. Army RDT&E agencies are encouraged to publish STAF's on specific scientific and technical subjects falling within their area of assigned responsibilities. Additionally, recommendations concerning desired

Headquarters, Department of the Army
Office of the Chief of Research and Development
Attn: Science and Technology Division
Washington, DC 20310

This particular STAF on boundary lubrication is more than a summary in that it has developed new insights beyond those in the literature, and its technological forecast includes the prospect of Army vehicles and machinery whose moving parts will require no field re-lubrication and will experience negligible wear during the expected useful life of the machine. It contains a suggested research plan to aid in achieving that goal.

The conclusions in this report are subject to evolution in the light of new developments and information. Accordingly, readers are urged to submit comments to fill in gaps in current knowledge, report new findings or applications, and suggest new programs.

HAROLD F. DAVIDSON
Physical Scientist
Office of the Chief of Research
and Development



ESSO RESEARCH AND ENGINEERING COMPANY

GOVERNMENT RESEARCH LABORATORY

P. O. BOX 8, LINDEN, N. J. 07036

R. F. NEBLETT
DIRECTOR

PREFACE

This Scientific and Technical Applications Forecast (STAF) on Boundary Lubrication constitutes the final report in accordance with Contract No. DAHCl9-69-C-0033, dated 1 June, 1969. Mr. Harold F. Davidson of the Army Research Directorate, Science and Technology Division originated the project and monitored its progress.

The author wishes to express the deepest appreciation to those who aided in various ways during the project. In particular, Dr. Henry Gisser, Pitman-Dunn Laboratories, Frankford Arsenal, was consulted many times and served as one of the final reviewers. The other reviewers were:

Prof. Ernest Rabinowicz, Massachusetts Institute of Technology,
Dr. L. S. Akin, Marine Turbine and Gear Dept, General Electric,
Mr. R. L. Johnson, NASA, Lewis Research Center,
Mr. Henry Mahncke, SKF Industries,
Mr. Harold Ravner, U. S. Naval Research Laboratory, and
Mr. Harry Ammlung Aberdeen Proving Ground.

Several co-workers also provided vital assistance; Dr. I. L. Goldblatt in the organic chemistry, Mr. A. R. Garabrant in mathematical programming and correlations, and Dr. J. A. Brown in organization of the material. Mr. L. Berkowitz supervised the project.

Correspondence about any aspect of this STAF would be welcomed by the author, especially where extropulations or interpretations of theory are involved.

ESSO RESEARCH AND ENGINEERING COMPANY

A. Beerbower

TABLE OF CONTENTS

	<u>Page</u>
1. SUMMARY	1
2. THE REGIMES OF LUBRICATION	5
3. THE PROSPECTS FOR ENHANCED LUBRICANT PERFORMANCE	8
3.1 The Limitations of Current Engineering Practice	8
3.2 Instances of Extraordinary Performance	9
3.3 Prospects for an Advanced Design Manual	10
4. ANOMALIES IN LUBRICATED SLIDING	12
4.1 The Anomalous Base Case - Ordinary Lubrication	12
4.2 Anomalies Involving Lead	13
4.3 Anomalies Involving Calcium	14
4.4 Anomalies Involving Other Elements	15
4.4.1 Zinc and Cadmium	15
4.4.2 The Chalcogenes	16
4.4.3 The Halogens	16
4.4.4 Tungsten	18
4.5 Optima in Blended Lubricants	18
4.6 Competition of Additives for Surfaces	20
4.7 Ambiguous Roles of Humidity and Oxygen	21
4.8 The Sharp Transition to Scuffing Wear	24
4.9 Effect of Anti-Wear Additives on Fatigue	26
4.10 Benefits of a Break-In Period	26
4.11 Miscellaneous Anomalies	27
4.11.1 Anomalously Low Friction	27
4.11.2 Anomalous Wetting Energy	27
4.11.3 Metals of Group B in the Periodic Chart	27
4.11.4 Multilayers of Stearic Acid	28
4.11.5 Freshly Purified Cetane	28
4.11.6 Complex Organic Phosphates	28
4.11.7 Diesel Engine Scuffing	28
4.11.8 Wear Due to Suspended Abrasive Particles	28
4.11.9 Delay of Scuffing Transition	28
4.11.10 Gold Appears to Oxidize	30
4.11.11 Water Plus Phenothiazine Shows Low Wear	30
4.11.12 Two Consistent Sets of Friction Data	30
4.11.13 High Friction on Titanium	30
4.11.14 Austenite Versus Martensite	30
4.12 Summary of Anomalies	30
5. ADVANCED MODELS OF BOUNDARY LUBRICATION	31
5.1 Introduction: Current Design Practices	31
5.1.1 Design of Rubbing Bearings	31
5.1.2 Design of Gears	32

TABLE OF CONTENTS (Continued)

	<u>Page</u>
5.2 New Concepts	41
5.3 The Empirical Model for Zero and Finite Wear (Model I)	43
5.3.1 Analysis for Zero Wear (Model IA)	47
5.3.2 Testing Model IA	51
5.3.3 Analysis of Finite Wear (Model IB)	52
5.3.4 Testing Model IB	59
5.4 Adhesive Wear (Model II)	59
5.4.1 Adhesive Wear With Simple Lubricants (Model IIA)	70
5.4.2 Testing Model IIA	74
5.4.3 Adhesive Wear With Gas and Vapor Lubricants (Model IIB)	77
5.4.4 Adhesive Wear With a Compounded Lubricant (Model IIC)	78
5.4.5 Severe Wear (Model IID)	81
5.5 The Irreversible Chemistry Models - Reaction With the Atmosphere and/or the Lubricant (Model III)	81
5.5.1 Corrosive Wear by the Atmosphere (Model IIIA)	83
5.5.2 Testing Model IIIA	89
5.5.3 Corrosion by Additives (Model IIIB)	93
5.5.4 Formation of Surface Resin (Model IIIC)	94
5.5.5 The Charge-Transfer Mechanism (Model IIID)	107
5.5.6 Testing Model IIID	110
5.5.7 Formation of Soap Films (Model IIIE)	114
5.6 Metallurgical Compatibility (Model IV)	114
5.6.1 The Bulk Energy Model (IVA)	115
5.6.2 The Surface Free Energy Model (IVB)	116
5.6.3 Testing Model IVA (Metallurgical Compatibility)	119
5.7 Mixed Film Lubrication (Model V)	125
5.7.1 Empirical Load-Sharing (Model VA)	125
5.7.2 A Two-Dimensional Model (VB)	127
5.7.3 The One-Dimensional Model (VC)	132
5.7.4 Gear Surface Damage (Model VD)	138
5.7.5 A Tentative Break-In Mechanism (Model VE)	140
5.7.6 Testing Model V (Mixed Film Lubrication)	140
5.8 Rolling Contact Fatigue (Model VI)	142
5.8.1 The Interfacial Free Energy (γ_{12}) Theory (Model VIA)	142
5.8.2 Testing the Interfacial Free Energy Model VIA	143
5.8.3 The Hydrogen Embrittlement Theory (Model VIB)	143
5.9 Abrasive Wear (Model VII)	148
5.9.1 Two-Body Abrasion (Model VIIA)	149
5.9.2 Automotive Abrasion (Model VIIB)	152
5.9.3 Three-Body Abrasion (Model VIIC)	153
5.10 Fretting Corrosion (Model VIII)	158

TABLE OF CONTENTS (Continued)

	<u>Page</u>
5.11 Auxiliary Models on Surface Free Energy	159
5.11.1 Surface Free Energy of Liquids	159
5.11.2 Surface Free Energy of Solids	160
5.11.3 Surface Free Energy of Mixtures	161
5.11.4 Interfacial Free Energy	161
5.11.5 Interfacial Entropy	168
5.12 Predicting the Coefficient of Friction (F)	168
6. COMPARISON AND COMBINATION OF THE MODELS WITH EACH OTHER	172
6.1 Reduction to Standard Format	172
6.2 Checking Models Against Each Other	176
6.3 Comparison with Literature Data	178
6.4 Perspective on the Modes of Wear	184
6.4.1 Increasing Load	184
6.4.2 Decreasing Viscosity	184
6.4.3 Decreasing Velocity	186
6.4.4 Decreasing Work of Adhesion	186
6.4.5 Break-In	186
6.4.6 Abrasion	186
6.4.7 Fatigue	186
6.4.8 EP Lubrication	186
6.5 Combining the Models for Design Purposes	186
7. REVIEW AND EXPLANATION OF THE ANOMALIES	189
7.1 The Base Case	189
7.2 Anomalies Involving Lead	190
7.3 Anomalies Involving Calcium	191
7.4 Other Elements	191
7.5 Optima in Blended Lubricants	192
7.5.1 The DuPont Patents	192
7.5.2 The Silicone Anomaly	195
7.5.3 Aromatic-Aliphatic Blends	195
7.6 Competition of Additives for Surfaces	198
7.7 Roles of Humidity and Oxygen	198
7.8 The Sharp Transition to Scuffing Wear	200
7.9 Effect of Anti-Wear Additives on Fatigue	201
7.10 Break-In Anomalies	203
7.11 Miscellaneous Anomalies	
7.11.1 Anomalously Low Friction in Transmissions	205
7.11.2 Anomalous Wetting Energy	205
7.11.3 Group B Metals	207
7.11.4 Multilayers of Stearic Acid	207
7.11.5 Freshly Purified Cetane	209
7.11.6 Complex Organic Phosphates	209

TABLE OF CONTENTS (Continued)

	<u>Page</u>
7.11.7 Diesel Engine Scuffing	209
7.11.8 Suspension of Particles	210
7.11.9 Delay of Transition	210
7.11.10 Formation of Gold-Oxygen Layer	210
7.11.11 Water Solutions as Lubricants	213
7.11.12 "Bifurcated" Wear Data	213
7.11.13 High Friction on Titanium	213
7.11.14 Austenite Versus Martensite	215
7.12 Recapitulation of Anomaly Explanations	215
7.13 Immediate Applications of Anomalies	218
7.13.1 Lead	218
7.13.2 Calcium	218
7.13.3 Diesel Scuffing	218
7.13.4 Particle Suspension	218
 8. RECOMMENDED RESEARCH PLAN	 219
8.1 The Incentives for Further Work	219
8.2 Forecast of Possible Achievements	221
8.3 The Plan of Attack	222
 APPENDIX I - Nomenclature	 224
APPENDIX II - Bibliography	227
APPENDIX III - Surface Free Energy: A New Relationship to Bulk Energies (reprint)	253
APPENDIX IV - The Surface Free Energy of Solids	260
APPENDIX V - Interfacial Energies of Pure Liquids on Solids	270
APPENDIX VI - Surface and Interfacial Free Energies of Mixtures	295
APPENDIX VII - Surface and Interfacial Entropies	303
APPENDIX VIII - Solubility Parameters (reprint)	310
APPENDIX IX - List of Experts Interviewed	332
APPENDIX X - Publications Resulting from This Contract	335
Distribution List	336

List of Tables

<u>Number</u>	<u>Page</u>	<u>Title</u>
2-I	7	Regimes and Modes of Lubrication and Wear
4-1	22	Effect of Tricresyl Phosphate (TCP) in Various Lubricants and Atmospheres
4-II	29	Anti-Wear Additives Increase Diesel Scuffing
5.1-1	36-37	Material Classes for IMB Charts 5.1-2 and 5.1-3
5.1-II	39	Critical Scoring Index Numbers
5.3-1	46	Lubricants Used to Develop Model 1
5.3-II	48	Distribution of Fatigue and Adhesive Modes in Model 1
5.3-III	53	Predicted Zero-Wear Travel (Inches) for Copper Ball on Steel Disk
5.3-IV	54	Noble Metal Alloy Tests of Zero-Wear Model
5.3-V	55	Critical Relative Humidities of Alloys
5.3-VI	56	Zero-Wear Predictions on Pure Hydrocarbons
5.3-VII	60	Predicted Wear Rates for Model 1B
5.4-1	67	Specific Wear Rates for Various Metal Combinations
5.4-II	73	Input Data for Model IIA
5.4-III	75	Heats of Adsorption of Pure Hydrocarbons on Steel Calculated from Wear Rates
5.4-IV	76	Heats of Adsorption of Commercial Liquids on Steel Calculated from Wear Rates
5.4-V	80	Time Scale for Film Renewal
5.5-1	90	Comparison of Activation Energies for the Oxidation of Iron
5.5-II	108	The Charge Transfer Mechanism

List of Tables (Continued)

<u>Number</u>	<u>Page</u>	<u>Title</u>
5.5-III	112	Absolute Rate for Capture of a Water-Solvated Electron
5.5-IV	113	Heteroatom Molecules Show Prowear or Increased Friction in Mixed (50/50) Isoparaffin-Aromatic Base Stock
5.6-I	117	Value of Compatibility Parameter C_2
5.6-II	120	Publications on Laboratory Tests of Adhesion, Friction and Wear of Various Metallic Pairs
5.6-III	121	Predictions of Scoring Resistance on Iron
5.6-IV	122	Prediction of Scoring Resistance - Nonferrous Couples
5.6-V	124	Success of Compatibility Predictions
5.7-I	130	Gear Surface Distress as a Function of Specific Film Thickness
5.7-II	139	Roughness Conversion Factors for Various Gear Manufacturing Methods
5.8-I	145-6	Fatigue of Steel Balls in Various Lubricants
6.1-I	177	Wear Modes Expressed as Exponents in $(V/d) = Kd^mV^nU^p$
6.3-I	179	Variation of Wear Rate with Load in Various Atmospheres
7-I	194	Friction and Wear of Laves Phase Alloy With Various Liquid Lubes
7-II	196	Mass Spectral Analysis of 1000 Coastal Distillate Oil
7-III	197	Wear Data for Components of 1000 Coastal Distillate Oil
7-IV	199	Various Roles of Water in Lubrication Models
7-V	202	Estimated Properties of Blok's Oils at Standard Temperatures
7-VI	212	"Zero-Wear" Periods at High Loads on the 4-Ball Machine with Cetane as Lubricant
7-VII	216	Summary of Explanations for the Anomalies in Section 7

List of Tables (Continued)

<u>Number</u>	<u>Page</u>	<u>Title</u>
V-I	279	Results of Panzer Plots
V-II	282	Typical Works of Adhesion on Chromium by Washburn-Anderson Balance
V-III	286	Temperatures of Melting (T_m) and Transition (T_t) for Various Compounds ($^{\circ}\text{C}$) ^m
V-IV	288	Partial Solubility Parameters of Metal Surfaces
V-V	292	Methods for Heat of Immersion in Pure Liquids
VI-I	299	Heats of Displacement from White Oil by Frewing (1943) Dynamic Method
VI-II	302	Methods for Heat of Displacement
VIII-1	313-6	Solubility Parameters of Various Liquids at 25°C
VIII-2	317	Group Contributions to Partial Solubility Parameters
VIII-3	327	"Liquid" Volumes and Solubility Parameters for Gaseous Solutes at 25°C
VIII-4	328	Rates of Change for Two Liquids

List of Figures

<u>Number</u>	<u>Page</u>	<u>Title</u>
2-1	5	Regimes of Lubrication
4-1	17	Effect of Iodine on Friction
4-2	19	Optima Obtained in Blending an Isoparaffin (Bayol 35) with a Polynuclear Aromatic (1-methylnaphthalene)
4-3	23	Behavior of 1-Methylnaphthalene as Affected by Moisture and Oxygen
5.1-1	33	ASLE Design Chart for Various Bearing Materials
5.1-2	34	IME Pressure-Velocity Curves for Journal Bearings Using Machineable Materials
5.1-3	35	IME Pressure-Velocity Curves for Journal Bearings Using Unmachineable Materials
5.1-4	40	Scoring Probability of Gears with Different Lubricants
5.3-1	44	Successful Boundary Lubrication
5.3-2	45	Failure of an Asperity by Elastic Deformation
5.3-3	61	Comparison of Measured and Predicted Wear Rates - Copper Sphere on Steel Disk
5.4-1	63	Asperities before Collision
5.4-2	64	Start of Adhesive Wear
5.4-3	65	Continuation of Adhesive Wear
5.4-4	66	Completion of Adhesive Wear
5.4-5	69	The Interlocked Dislocation Model
5.4-6	72	Heat of Adsorption of Vapor versus Fraction Not Covered
5.5-1	82	The Hydrated Iron Oxide Layer
5.5-2	84	The Post-Wear Process
5.5-3	87	Alternative Methods of Correlating Wear Versus Time
5.5-4	91	Rate Constant for Static Oxidation of Iron versus Temperature
5.5-5	92	Correlation of Wear Rate with Hydrocarbon Density
5.5-6	95	Corrosion of Steel Wire by Phosphorus Lube Additives as a Function of Reaction Time

List of Figures (Continued)

<u>Number</u>	<u>Page</u>	<u>Title</u>
5.5-7	98	Correlation of Activation Energies of Metals for Ethane - Deuterium Exchange
5.5-8	99	Polymer Formed from Vapor in Air
5.5-9	100	Dislocations at Surfaces
5.5-10	104	Data Analysis on Hermance and Egan Friction Polymer
5.5-11	105	Solubility Parameter of Resin Formed from Naphthenic Base Stock
5.5-12	106	Solubility Parameter of Resin Formed from Aromatic + Isoparaffin Lubricant
5.5-13	109	Chemical Model for Lubrication in the Presence of Polynuclear Aromatics
5.6-1	118	Compatibilities of Metal Pairs
5.7-1	126	Effect of White Oil Viscosity on Wear
5.7-2	128	Two Dimensional Physical Model
5.7-3	131	Integrated Values of $G_H(h_o)$ and $G_C(h_o)$
5.7-4	133	Two-Dimensional Solution for a Journal Bearing
5.7-5	135	One and Two Dimensional Physical Models
5.7-6	136	Stribeck-Type Diagram from the One-Dimensional Model
5.7-7	137	Film Collapse due to Thermal Instability - Theoretical Prediction
5.7-8	137	Film Collapse Due to Thermal Instability - Experimental Verification
5.7-9	141	Experimental Dependence of Wear Rate on Apparent Bearing Pressure
5.8-1	144	The Interfacial Free Energy Theory of Fatigue Cracking
5.8-2	147	Fatigue Results with One Crystallized Glass and Three Steel Balls
5.9-1	150	Two-Body Abrasive Wear

List of Figures (Continued)

<u>Number</u>	<u>Page</u>	<u>Title</u>
5.9-2	150	Abrasive Wear as a Function of Hardness
5.9-3	151	Effect of Heat-Hardening on Abrasive Wear
5.9-4	151	Effect of Work-Hardening on Abrasive Wear
5.9-5	154	Automotive Bearing Wear Correlation
5.9-6	156	Wear Rate as a Function of Particle Size and Concentration
5.11-1	162	Hansen Plot of Friction on Polyethylene (Untreated)
5.11-2	163	Hansen Plot of Friction on Polyethylene Treated with $H_2S_2O_7$ for Two Minutes
5.11-3	164	Hansen Plot of Friction on Polyethylene Treated with $H_2S_2O_7$ for Five Minutes
5.11-4	166	Determination of Interaction Parameters for Freshly Cut Aluminum
5.11-5	167	Correlation of Cutting Ratio with Interaction Parameters
5.12-5	170	Correlation of Coefficient of Friction with Wear and Velocity
6.1-1	174	Transformation of Exponential into a Power Function
6.1-2	175	Torque Balance for Removal of an Oxide Cap (Corrosive Wear)
6.3-1	180	Variation of Wear Rate with Travel in Various Atmospheres
6.4-1	185	Regime and Modes of Wear (Excluding Abrasion) on Broken-In Machine Parts
6.5-1	187	Illustrative Design Scheme for Military Power Gearing
7-1	204	Correlation of Surface Free Energy with Hardness
7-2	206	Zisman-Gans Plot of Wetting Power of Organic Liquids on Metals
7-3	211	Seizure Delay Travel as a Power Function of Load
7-4	214	Probable Mechanism for High Friction on Titanium

List of Figures (Continued)

<u>Number</u>	<u>Page</u>	<u>Title</u>
III-1	255	Comparison of Calculated and Observed Surface Free Energies
III-2	257	Surface Free Energies of the Liquid Metals at Their Melting Points
III-3	258	Surface Free Energy of the Fused Metal Halides
IV-1	269	Change in Surface Free Energy on Fusion of Solids
V-1	275	Homomorph Chart for Non-Cyclic Compounds
V-2	277	Prediction of London Parameter from Refractive Index
V-3	281	Works of Adhesion of Liquids on Mercury
V-4	282	Changes in Oil Lens/Metal Plate/Water Layer System in Measuring Spreading Pressure of Oil on a Metal Surface
V-5	289	The Rehbinder Effect
V-6	290	The Joffé Effect
VI-1	300	Scuffing Tests with Hexadecane plus Additives
VIII-1	319	Solubility Plot for Poly (methyl methacrylate)
VIII-2	320	Solubility Parameter Plot for Common Solvents
VIII-3	321	Bimodal 25% Swell Contour of Polysulfide Rubber
VIII-4	322	Correlation of Swell of Natural Rubber with Radius of Spheroid
VIII-5	327	Fugacity of Hypothetical Liquid at 1 atmosphere

1. SUMMARY

This STAF reviews the state of the art of Boundary Lubrication and presents the prospects of such improvements in the lubrication of highly-loaded bearings as virtually to eliminate bearing failures and the need to re-lubricate machinery in the field.

The field of lubrication is one which has grown up empirically and in which the practical art has far outstripped the basic understanding. There has been steady improvement in machine life and performance, but this has been due in the main to incremental improvements, empirically proved; and it is still not possible for a scientist to design a new lubricant for a new application and say with confidence, "This will work." There is, of course, a general body of experience and some limited Handbooks which guide lubrication engineers; but exceptions and anomalies are so common as to preclude any great feeling of confidence on their part, and it is still necessary to demonstrate new lubricants and new lubrication designs by iterative field trials, often lasting for a year or more.

However, a number of examples are known of really spectacular performances by lubricants - far beyond anything the state of the art would predict - and there is a growing body of understanding of the basic physics and chemistry of surfaces. These recent advances, taken together, promise important improvements in machine and lubricant design; because if it is once really understood why spectacular lubricant performance is sometimes obtained, it should be possible to capitalize on the understanding and make it to order in all cases, not just in happy accidents.

This happy situation has not yet been realized, but this STAF points the way by an in-depth study of the contributory art, including:

- A survey of observed cases of extraordinary lubrication.
- An analysis of the common factors and practical applications.
- An outline of advanced mathematical models of wear in the boundary regime to account for the extraordinary performance.
- A research plan to derive a unified, quantitative wear model and a design manual for the actual engineering of bearing-lubricant systems which will run without attention until obsolete.

The advances reported are such as to make realistic the hope of virtual elimination of the re-lubrication of Army machinery in the expected lifetime of the equipment, and the consequent virtual elimination of lubricant storage at operating bases. The elimination of field re-lubrication should actually result in longer equipment life; because it has been found that field servicing is frequently harmful (by such things as the introduction of abrasive contamination into a precision bearing) and that most breakdowns occur shortly after servicing.

This survey uncovered 28 anomalies - phenomena inexplicable in the state of the art as available to designers at that time - in the performance of lubricants, including the surprising fact that two very ancient liquids - petroleum and fats - are good lubricants while most liquids are rather poor lubricants. Among the most striking of the anomalies are:

- Leaded metals and lubricants carry extreme loads without scuffing.
- Calcium additives prevent scuffing and wear.
- Other elements such as zinc, cadmium, sulfur, iodine and tungsten give unexpectedly lower wear or friction - by as much as 99% over the base lubricant.
- Blending dissimilar liquids can produce superior lubricants.
- With the right lubricants, oxygen and humidity can improve performance.
- The transition from mild wear to severe scuffing can be delayed.
- Anti-wear additives can increase or decrease fatigue life.

While not all of these techniques offer equal rewards, an explanation of any of them IN TERMS WHICH THE DESIGNER CAN USE would offer some promise for pay-off. Plausible explanations have been obtained in 25 cases of the 28 anomalies, two others still require special "ad hoc" theories, and one is still unexplained.

The working approach of this study was to attempt to understand the fundamental phenomena of lubrication in quantitative terms, using the achievements of "ordinary good practice" as the starting point and the much better achievements of the "anomalous cases" as tests of the new models and theories. Lubrication is so complex a phenomenon that no one, all-encompassing model was found; but seven overlapping models of wear point the way toward a complete understanding:

- EMPIRICAL - A quantitative but empirical set of design criteria for very lightly loaded bearings, such as in office machines.
- ADSORPTIVE CHEMISTRY - Which takes into account adsorption of gases, additives and base stocks onto bearing surfaces.
- REACTIVE CHEMISTRY - Which provides for metal oxidation and the reaction of (some) additives with metal surfaces to form both harmful structures such as flakes and also the protective surface resin.

- METALLURGY - Which clarifies the shifts in the scuffing transition.
- MIXED FILM - A concept still under development, which connects boundary lubrication with the better-understood hydrodynamic lubrication.
- FATIGUE - Which considers the harmful or beneficial effects of additives on this failure mode.
- ABRASION - Which covers the effect and the fate of particulates generated in the above wear modes.

In addition to this critical review, it was expedient to create four auxiliary models which help in various ways to implement the seven main ones. These are:

- A new approach to surface and interfacial free energies, useful in the adsorptive and fatigue models.
- Correlations of the coefficient of friction with the wear rate for two clearly identifiable wear modes.
- Means for "fingerprinting" wear modes, which led to a master-model concept for dealing with the mixed modes found to predominate under non-idealized conditions.
- A combination of the models for reactive chemistry and mixed film, which explains a great deal about both ordinary and anomalous lubrication.

The last of these came, in the end, to dominate the picture on successful boundary lubrication. It proceeds by three steps. First, a bearing or gear breaks in by chopping off the oxide layer, and often some metal, from the highest asperities. Second, the raw metal interacts with the lubricant to form surface resin, which partly fills the micro-valleys to produce a "glazed" surface of lessened roughness. Third, this smoothing increases the hydrodynamic lift and reduces the rate of wear to where resin no longer forms. The system is now in homeostatic balance; loss of resin causes wear, which produces resin until wear is again reduced. Failure would be the result of sudden heating (due to overload, etc.) which dissolves the resin, throwing much of the load onto the asperities and causing whole patches to rip off as "scuffing."

These models, now semi-quantitative, sketch out a greatly improved understanding of lubrication and wear. Confirmed and quantified, they would provide the basis for a design manual for the engineering of lubricant/bearing systems with sealed-at-the-factory lubrication and wear rates low enough to give a zero maintenance life expectancy equal to the obsolescence time of the machine. This assumes that such designs would use only the best quality lubricants, to prevent the failures due to oxidation which presently limit system life. Present or easily foreseeable industrial, automotive and aircraft lubricants can be confidently expected to provide severe service (300°F) for 5 to 10 years by the time such design changes could reach the field. Realization of this goal requires further R&D effort in three interwoven phases, involving original study as opposed to the compilations in this STAF:

- Complete and quantify the models where gaps and inadequacies exist.
- Test the models by comparison with published data and with new experiments to verify crucial points.
- Translate the quantified and verified models into a practical design manual, useful and intelligible to industrial factory engineers and to military planners.

The design manual would be based on the principle of system analysis, rather than the present practice of assembling pre-designed components into a machine. Given the basic environmental parameters of load, speed, temperature and any special atmospheric condition, the designer would undertake simultaneous optimization of

- Metallurgy of both contacting surfaces
- Geometry of contacting surfaces
- Physical and chemical properties of lubricant
- Chemical properties of additives
- Chemistry and geometry of seals
- Filtration - need, fineness, service life

Preliminary estimates suggest that the program would require approximately a three-man effort over a period of approximately three years.

Several of the anomalies uncovered and explained in this STAF appear to be ready for immediate application to field problems without waiting for further research. These are:

- Increased use of leaded alloys, platings and lubricants,
- Application of high calcium content lubricants in new areas,
- Reduce diesel scuffing with glaze-forming additives, and
- Use anti-abrasion additives to decrease the need for filtration.

2. THE REGIMES OF LUBRICATION

Lubrication is a complex and technical subject, and it is essential to establish a common language at the outset. DO NOT SKIP THIS SECTION, no matter how expert you are.

This STAF follows the usage of the new glossary just released by the International Research Group on Wear of Engineering Materials (Rowe, 1969) except where they did not provide a word for a specific situation. In the discussions of lubrication and wear, "regime" is used to describe the outward symptoms (e.g., "hydrodynamic" or "boundary" lubrication) and "mode" is used to name the underlying mechanisms (e.g., "mixed film" lubrication or "scuffing" wear - as defined on the next page). Distinctions are sometimes difficult; Table 2-I, on page 7, summarizes the intent.

The following figure diagrams the relationship between bearing wear and bearing load as it is currently known in "normal good practice." The anomalies discussed in this STAF would by definition fall either below or above the wear rate curve at the appropriate relative load, but not on it.

Figure 2-1
REGIMES OF LUBRICATION

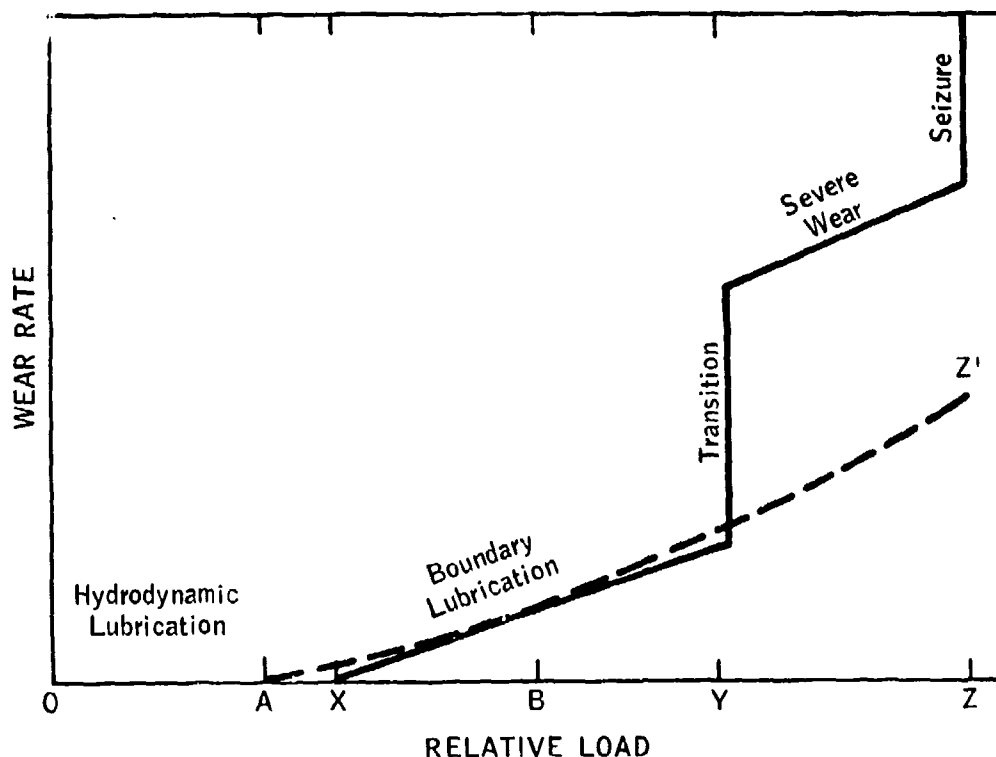


Figure 2-1 is highly idealized (see Fig. 6.4-1), but helps set some definitions:

Region O-A is the regime of hydrodynamic lubrication in which the entire load is borne by the liquid film and there is no metal-to-metal contact. There is little or no wear, and the friction is due solely to the viscous shear of the lubricant. As the load rises to enough to distort the curvature of the surfaces, the term becomes elastohydrodynamic lubrication.

Region A-X is the regime of quasi-hydrodynamic or mixed-film lubrication, which depends upon the roughness of the surfaces for its onset. The main part of the load is carried by the hydrodynamic film in the micro-grooves or "anti-asperities", while most of the friction and all the wear result from asperity contacts. It is often transitory, as the running-in process smooths down the higher asperities; and Point A moves toward Point X.

Region X-Y is the regime of boundary lubrication proper, the territory of this STAF. There is some metal-to-metal contact on the asperity tips, and the degree of metal-to-metal contact increases as the load increases. Most of the load, however, is still carried by the liquid film. Wear is mild and tends to be due to corrosion to the left of Point B. Point B represents a change in wear mode, from corrosive and abrasive to adhesive wear in which material is transferred from one surface to the other by cold welding. The location of Point B is variable; under non-corrosive conditions, metallic wear particles occur as far left as Point X, while with corrosive additives, they are not found until Z' is reached, far outside the boundary region.

Region B-Y is characterized by "hemispherical" wear particles, which are much too short and thick to be simply the planed-off tops of asperities. Some believe they are compressed or even rolled up during formation, but others believe they are plucked out of the surface. In many cases, a particle is transferred back and forth several times before release. The wear rate tends to be greater than in X-B, but is still called "mild."

Region Y-Z is one of prohibitively severe wear, and bearings cannot operate there except very briefly. Bearing surfaces to the left of Point Y are apt to be as smooth as the original one, even though quite worn; but those on the right are scored or scuffed. The transition Point Y is not always as clear-cut as shown in the Figure, and can fail to appear at all with some systems. The use of "extreme pressure" additives, for example, can extend the wear curve up along line B-Z'. However, the scuffing transition is so often found as to represent the "normal" situation. For the purpose of this STAF, it represents a limit beyond which designers must not go, and the objective is to locate it without experiencing it. The line B-Z' is outside the scope of boundary lubrication, and so will not be discussed in any detail.

The subject of fatigue needs mention. It cannot be located in any particular regime because it is characterized by a variable wear rate. It is important, partly because it can set a limit to the life of a bearing which shows negligible wear up until failure and partly because it can be aggravated by some improved boundary lubricants. It can become a limiting factor in rolling contact bearings which share a lubricant with some boundary-regime mechanism such as gears.

The remainder of this STAF concerns the region from X to Y, with excursions into the hydrodynamic or scuffing regimes only when it is necessary to illuminate some point pertinent to the boundary regime. Lifetime design is no problem in the hydrodynamic regime; such bearings (in steam turbines) run for years without erasing pencil marks made on the surface by the machinist. No one tries to operate machines in the scuffing regime Y-Z, and the extreme pressure (EP) regime Y-Z' is a special case which is not widely applicable.

TABLE 2-I

REGIMES AND MODES OF LUBRICATION AND WEAR

<u>Regime</u>	<u>Modes</u>
Hydrodynamic	No Wear
Elastohydrodynamic	"Zero-Wear" Molecular Wear
Quasi-Hydrodynamic	Break-in Mixed Film Sliding (Contact) Fatigue
Mild Wear	Sliding Fatigue Adhesive Wear Corrosive Wear Mixed Corrosive-Adhesive Mixed Corrosion Fatigue
Severe Wear	Scuffing Scoring Severe Abrasion ("Wire-Wool", "Plowing") Violent Corrosion
Seizure	Welding

3. THE PROSPECTS FOR ENHANCED LUBRICANT PERFORMANCE

The scope of this STAF has been focused on liquid lubrication in the boundary regime under "reasonable" conditions. Solid and gaseous lubricants are excluded from discussion, as are the effects of unusually corrosive atmospheres and extreme temperatures. The hydrodynamic and extreme pressure regimes are also not treated in any detail.

In the discussions of lifetime lubrication and zero maintenance design which follow, it is assumed that the liquid maintains its integrity; that is, that seals are adequate to prevent abrasive contamination from outside and that the lubricant is effectively stabilized with anti-oxidants. This assumption may appear optimistic in view of the fact that oxidation is responsible for most current lubrication failures, but current progress in industrial, automotive and aircraft lubricants indicates that oxidation problems will be well under control by the time the design practices outlined herein can reach the field. By 1977, premium quality lubricants can be expected to give 5 to 10 years service at 300°F before oxidizing. The zero-maintenance design concept carries with it the requirement to use only premium quality lubricants and to consider them part of the capital investment in the machine itself.

3.1 The Limitations of Current Engineering Practice

Designers tend to size their bearings on the well-established hydrodynamic models. The 1968 ASLE-sponsored Handbook of Lubrication Engineering (O'Connor 1968) devotes only five pages (99-104 in Chapter 5) to designing "Thin-Film, Mixed-Film and Dry Bearings". This forces the designer to use the dry-sliding models, since boundary models are not in acceptable form, and so results in very over-conservative designs.

Despite the efforts of many of the best minds from the universities as well as the bearing, lubricant and machine industries, the Handbook fails to provide the designer with a plan for simultaneously optimizing metallurgy, shape factors and lubricant. This probably reflects the true situation on commercial designs, in which the bearing (or gear, etc.) manufacturer decides the metallurgy, the machine designer then selects a shape from the bearing catalog, the maintenance engineer selects a lubricant of the viscosity specified in machine instruction booklet, and the lubricant formulator modifies one of his regular products to fit if complaints start to build up. Occasionally, there are conferences, on a spot basis, if the machine designer foresees an unusual problem, and there may be an attempt to review some possibilities before the design is "frozen". However, this is all too rare.

Military designing differs from the above discussion mainly in that everyone involved knows that the lubricant must, barring exceptional circumstances, meet one or another of the existing MIL specifications. There may also be some intervention by a technical expert from the procuring agency, if something out of the ordinary is being designed. However, the tendency is to let the contractor use his best judgment.

The tendency in both commercial and military design offices is to overemphasize the viscosity of the lubricant, as if most bearings were going to operate with a hydrodynamic film at all times. This is definitely not true, as stop-and-start operation is always in the boundary regime. This is pointed out in the ASLE Handbook, but the treatment is scanty and admittedly oversimplified due to the lack of more sophisticated mathematical models than the two primitive ones cited there. Neither of these includes any factor for lubricant quality; one is based on an allowable temperature rise and the other on an allowable wear rate. The result of this dependence on full-film and dry-sliding models often is over-design, except in the aircraft and aerospace industries where weight is of prime importance. If such optimization is required, an iterative shop program is usually employed in which a prototype is built, tested to failure, rebuilt and so on until an acceptable compromise is achieved.

In the United Kingdom, a serious effort has been made in the last few years to improve lubrication practices. This stems from a report (Jost 1966)* in which potential annual savings of \$1,000,000,000 were estimated for that country. Among the many steps taken has been encouragement by the government of courses in advanced design. The charts issued by The Institution of Mechanical Engineers certainly appear to be simpler, and easier to use than the ASLE Handbook, but still suffer from the lack of suitable equations for wear in the boundary regime.

3.2 Instances of Extraordinary Performance

As part of this program, a number of examples of what improved lubricant-metal systems can do were collected. Some of the anomalies which are not predicted by current understanding are:

- Lead metals and lubricants carry extreme loads without scuffing.
- Calcium additives prevent scuffing and wear.
- Other elements such as zinc, cadmium, sulfur, iodine and tungsten give unexpectedly lower wear or friction - up to 99%.
- Blending dissimilar liquids can produce superior lubricants.
- With the right lubricants, oxygen and humidity can improve performance, even though they usually degrade it.

* All such references are given in Appendix II, by author and year. In case an author published more than one report that year, they are flagged (1966A), (1966B), etc.

- Additives can interfere with each other's activities, but can be chosen to avoid interference.
- The transition from mild wear to severe scuffing can be shifted to higher loads by changes in lubricant-plus-metal chemistry and physics.
- Anti-wear additives often reduce fatigue life, but not always.
- Break-in practices can be shortened and otherwise improved.

While not all of these anomalies offer equal rewards, and few are totally understood, it can be shown that most of them can be generalized sufficiently to permit wider use. A number of partial explanations are given in ASME's "Boundary Lubrication - An Appraisal of World Literature" (Ling 1969) but usually in the language of chemists and often with several untested alternatives. In this STAF, the anomalies are used to test the various mathematical "models" of lubrication and wear which are presented - a model being defined as an equation or a set of equations which can be adapted to the needs of a designer.

3.3 Prospects for an Advanced Design Manual

In view of the examples of extraordinary success shown above, it might seem that it is only necessary to replace all ordinary lubricants with these anomalous ones, and the problem is solved. However, most of these successes are for special situations and cannot be widely applied until understanding of the fundamental principles involved is available.

It must be recognized that "understanding" exists on a number of levels in any process involving growing sophistication about complex phenomena. In the first stage, technologists create a body of empirical knowledge which is usually mysterious and contradictory but which works well enough to attract users. Design engineers then pick this body over for a few threads of general applicability and start using them. In due course, scientists are drawn in and produce a body of verified experimental data, with theories of a phenomenological nature (e.g., chemical mechanisms).

Next, a group of mathematical theorists forms and distills the generalizations into model equations, far different from the empirical expressions of the first designers, containing some of the same parameters originally used but with new ones replacing some originally considered essential. Usually these equations are quite clear to the theorists, but only vaguely useful to the designers. A translation process is needed to convert the scientific equations into design equations, and the resulting forms often shock the theorists. However, the design equations produce results quite commensurate with the scientific principles.

In this STAF, "model" is used to describe a hypothetical wear process and the equations showing its response to changes in load, speed, chemistry, etc. "Design equations" describe a set of computations to be applied to a preliminary machine design to determine how and when it will fail. Such equations tend to be oriented to computer programming, and include failures due to lack of mechanical strength as well as lubrication.

Boundary lubrication is now in the latter part of the generalization phase, and almost ready to start the last step. In fact, one wear model has already been converted into a design model, even though it is definitely limited to conditions of low loads, speeds and humidities and so is not in wide use. Another model has achieved similar status and is being advocated for gear use, although it also lacks some forms of input which are very likely to be needed soon.

This STAF presents a battery of seven models of lubrication and wear which have been distilled from the literature and in some cases extended in the course of this effort. They are mostly in the generalization, or model equation, phase; but they explain most of the instances of extraordinary lubricant performance. They contain gaps, and they need firming up by some crucial experiments. If this were done and the models validated, it would only remain to reduce them to suitable form for use by designers - a design manual for achieving extraordinary performance routinely.

4. ANOMALIES IN LUBRICATED SLIDING

The initial step of this project was to "survey all accessible examples of extraordinary lubrication", in which performance was spectacularly beyond current understanding. This has also been referred to as "anomalous lubrication", with the emphasis on those anomalies which were better than predictable by conventional theory, but in addition taking into account a few cases in which performance was limited by unknown factors to a level far below what might reasonably be expected.

It must be recognized that "anomalous" is a transitory state, without permanent meaning, since as soon as an explanation is validated the phenomenon becomes part of the accepted pattern. Thus, we must define the word on a time scale; for engineering purposes it indicates anything not predictable from the current design manuals sponsored by the American Society of Lubrication Engineers (O'Connor 1968), the Institution of Mechanical Engineers (Neale 1968) and the American Gear Manufacturers Association (Dudley 1965). However, this is so all-inclusive as to be misleading, and in this STAF indicates approximately "unpredictable by the formalized engineering models of 1965".

In this section, the ten outstanding cases which were selected for further study are reviewed. In a few cases, these are individual anomalies; but others consist of groups which appear to have something in common. It must be emphasized that not all of these cases are new; on the contrary, some are so old that they are taken for granted even though they are still as mysterious as when they were first observed.

The study of anomalies serves two purposes. First, these more or less isolated successes forecast what could be done if we really understood their causes. Second, they serve as tests for advanced theories; any theory which merely explains routine success predicting the anomalies can scarcely be considered an advance.

4.1 The Anomalous Base Case - Ordinary Lubrication

Before reviewing the other cases, it would be best to consider briefly what may be the greatest anomaly of all, that two of the cheapest metals and two of the cheapest lubricants known work so well together that it is necessary to search rather deeply to find anomalies that are really extraordinarily better than fatty oil and petroleum films on bronze and steel.

Historically, fatty oils were recognized as lubricants about 6,000 years ago. This is not their natural function; biological joints are lubricated with synovial fluid, a complex visco-elastic aqueous solution of polymers, and the fats are fuel to the organisms that make them. Stone age technologists soon recognized that fat's viscosity and adhesion to surfaces solved many problems on moving parts. This knowledge increased in value with the bronze age, and again during the iron age. Petroleum joined this team only about a hundred years ago. While it may well have been originally derived from fat (an unsettled controversy which need not concern us here), fitting this complex hydrocarbon mixture into the already developed technology required a good deal of effort.

It is noteworthy that of all the other viscous liquids discovered in the meantime, only "synthetic" esters have yet found a high volume market as lubricants. Of the seventy or so metals now available, only lead has been added to the list of widely used bearing materials. (Babbitt may be regarded as a special case of the bronze in which the copper/tin ratio is approximately reversed, from the usual 82 Cu/16 Sn/2 Zn to 89 Sn/7 Sb/4 Cu. Rabinowicz (personal communication) notes that aluminum-tin is becoming common, but it has not gone nearly as far).

4.2 Anomalies Involving Lead

As mentioned in 4.1, lead was added within historic times to the basic list of copper, tin and steel. This began many years ago, but has grown greatly in importance during the past few years. The use of lead-base "white metal" as a cheap substitute for babbitt is old, but these are both solid-solution alloys of fairly predictable behavior. They contain a second phase of SbSn and Cu₆Sn₅, which is harder than the solid solution; this was once believed to be important. This view is not supported by the success of the two-phase alloys which were later introduced (Morris 1967).

The most important of these is the 70 Cu/30 Pb alloy which has been used in automotive bearings since about 1920, in which the lead is dispersed as a separate soft phase. The results were sufficiently good to justify a great deal of work in preventing the corrosion which resulted when the unsophisticated motor oils of those days became oxidized. More recently, leaded bronzes have attracted favorable attention from NASA (Demorest 1969), and TNO in Holland (de Gee 1969). Both leaded bronze and lead-plated steels were tested for aerospace use, in air and vacuum (Harris 1966); he found good results were not always obtained but the overall picture was favorable. Some results seemed to depend on the presence of tungsten in the steel (see 4.4.4).

Leaded steels were studied in depth by the U.S. Army Tank Automotive Command (Warke 1969). Their excellent machinability (low friction during cutting, turning, etc.) was duly noted, but the main purpose of the study was to determine the extent to which these steels suffered from high temperature embrittlement. It was concluded that the fatigue life, compared to an unleaded steel, was unchanged at up to 300°F but suffered a 90% loss at 600°F. Very good results have been obtained with an iron alloy "Bishiralloy" loaded with 15 to 30% lead (Anonymous 1970) as slider-bar material on the electrical power pantographs of Japanese National Railways. Slider life went from less than 2.3 hours to over 10,000 hours.

It appears that the mechanism is that the small drops of lead which are emulsified in the matrix just before pouring extrude during use, and provide a surface coating similar to lead plating but self-renewing (Bowden 1950). The physical properties of lead - insolubility in most other metals, plasticity and low surface free energy - cause it to spread rapidly, so the cases cited so far are scarcely anomalous. However, these low free energy surfaces seem to be exceptionally easy to lubricate. Demorest (1969) found that ordinary automotive pressure gun grease was adequate, though it contains no additives (except the lithium stearate thickener, which contributes little to lubrication). His earlier work (1966) had shown that very sophisticated additives

were not adequate to support the very heavy loads in his simulated rocket hauling vehicle. The anomaly lies in the fact that such a low surface free energy metal should not, according to theories current in 1965, bond any better to lubricants than a harder metal; quite the opposite would be predicted.

The anomaly is even more pointed when we consider the effect of lead compounds as additives. There is a long history on this (Klemgard 1937, Boner 1954) and the list continues to grow. Industrial gear oils of the 1920's frequently contained lead soaps, thus combining the lead anomaly with fatty oils and acids. The advent of the automotive hypoid gear depended very largely on this background, though the next step was replacement of the fatty oil with the relatively non-lubricating petroleum naphthenic acids to improve solubility of the soap. The fact that such a change could be made without sacrificing lubricating quality emphasizes that lead was the key component.

Lead alkyls give powerful lubrication enhancement (Antler 1959, 1963; Feng 1963) and their removal from gasoline has run into difficulties in the form of increased exhaust valve wear. Triphenyl thiomethyl lead, developed by the Ethyl Corporation (Beatty 1967) for the International Lead and Zinc Research Organization (Carr 1967) shows phenomenally low wear rates at low concentrations. In the solid phase, both white lead ($\text{Pb}_3(\text{CO}_3)_2(\text{OH})_2$) and red lead (Pb_3O_4) are well known pipe thread lubricants, and the former is still standard for lubricating dead centers on lathes.

While none of these additives has been shown to deposit a film of lead metal on the surface, this has been postulated and would combine the alloy and additive phenomena tidily. The electromotive series favors this reaction on iron, and the analogous reaction with gold compounds was recently reported (Dickert 1971). Both Blok and the writer observed this with silver salts, but neither published it.

4.3 Anomalies Involving Calcium

Calcium has never made much impact as an alloying agent, due partly to its high susceptibility to corrosion (Morris 1967). However, its action as an additive is quite adequate to justify its inclusion as anomalous. It is interesting to note that calcium is second only to lead in its insolubility in other metals (Rabinowicz 1971B).

The oldest case of calcium as a lubricant additive comes from analysis of the "grease" in an ancient Egyptian chariot's wheels. Probably the gelling powers of the calcium soap motivated the addition of lime to the fatty oils, but there is no doubt that the increase in load-bearing capacity helped to perpetuate the use of lime-based greases to the present and future. The literature is replete with examples (Klemgard 1937). All effect of the gelling power can be ruled out by comparison with sodium and lithium base greases, which show no more load-bearing capacity than can be accounted for by the thickened base oil. Strontium and especially barium greases have been prepared, but no noteworthy effects on load bearing capacity were reported.

A new generation of calcium base greases and oils appeared about 1955. These were based on calcium acetate with just enough calcium laurate, etc. to make it compatible with the oil. The high calcium content led to film strengths that would previously have required corrosive sulfur or chlorine additives (Kolfenbach 1959). Simultaneously, the use of calcium alkylbenzene sulfonates containing excess lime in motor oils and in oils for diesel engines operated at high sulfur fuels became common. Much of the benefits in the latter case can be attributed to the ability of the excess calcium to neutralize sulfuric acid formed in the combustion chamber, but some anti-wear effects appear to be present even with low sulfur fuel. A striking fact is that replacement of the calcium with magnesium, equally potent in neutralizing acid, did not give good anti-wear action (unpublished data, Esso Research and Engineering Co.).

Another instance of the anomalous effect of calcium is the use of lime as an additive to wire-drawing lubricants (Wistreich 1957). The action seems fairly specific to iron and steel wire, but may be used on some stainless steels. Copper, brass and aluminum do not benefit, but this may be because the stresses do not require much film strength with these soft metals. The film strength is not due to chemical action as with sulfur or chlorine extreme pressure (EP) lubricants (see 4.4.2 and 4.4.3) and the technique remains an art even after 120 years of use. Lime is either coated on the wire from a water slurry, or applied as a dispersion in cup grease, and the wire comes out smooth and bright. Attempts to substitute any other hydroxide or carbonate result in a dull, rough surface with increased friction in the die as an extra penalty.

4.4 Anomalies Involving Other Elements

Several other elements have shown unexpected effects on lubrication - mostly favorable. In most cases, plausible (though not necessarily accurate) explanations exist. These may be considered in a few groups.

4.4.1 Zinc and Cadmium

These elements have a good deal in common with calcium, and may end up being grouped with it as a single anomaly. However, the present main use of zinc is very different from that of calcium, in that it is usually applied as the dialkyl dithiophosphate. This complicates things greatly as both sulfur and phosphorus have strongly beneficial effects. Attempts to replace the zinc with other elements have led to cadmium as the only usable substitute, but toxicity has prevented its use.

Zinc oxide has enjoyed a wide reputation as a solid additive in greases, under the general brand name of "Lubriplate" (trademark of Fiske Bros.). However, their basic patent ran out a few years ago, and the expected rush to copy the products has not developed. Perhaps the only "anomaly" was the white color and hiding power of this additive.

4.4.2 The Chalcogenes

Sulfur, and to a limited extent selenium and tellurium, have been long used to increase load bearing capacity. The latter two are usually ruled out by toxicity, cost or both. The mechanism by which sulfur acts was long thought to be simply corroding the surface to an FeS film, but there are new data to indicate that more goes on than had been supposed (Allum 1968). Perhaps it is best to reserve judgment on the anomalous status of this important class of additives.

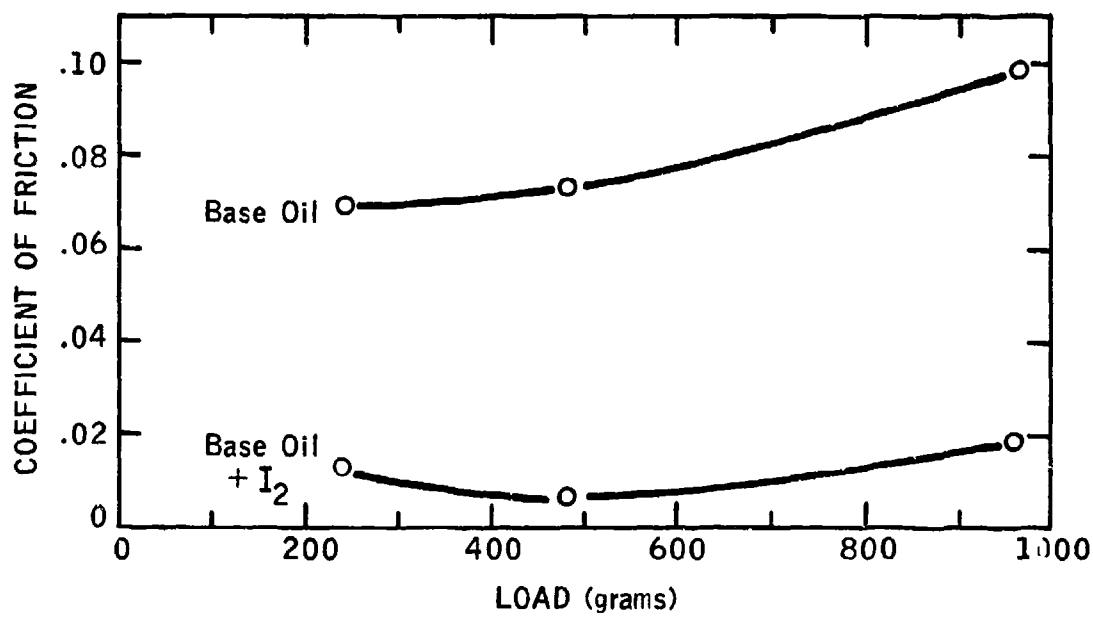
4.4.3 The Halogens

Fluorine, the lightest member of the family, tends to behave quite predictably. Its C-F bond strength keeps it from any exchange reactions, and the fluorocarbons are the least reactive of all liquids. This is not true of chlorine. It is generally well understood that chlorine will leave an aliphatic molecule readily (an aromatic less readily) for hot metal, and form an FeCl₂ film. There may be more complicated hypotheses, but this fits all the facts. Bromine behaves about the same way; a little more activity per mole, about the same by weight. These cannot be regarded as anomalous, though chlorine is extremely useful in gear lubricants and cutting oils.

Iodine, on the other hand, has been shown by two different groups (Furey 1966, Brown 1968) to exhibit additive qualities that are not predictable from its greater atomic weight and the lower strength of the carbon-halogen bond. In addition to the anti-scuff qualities shown by chlorine, it has a demonstrated capability to reduce friction to as little as 1% of dry or 10% of base oil value in a steel-to-steel system (Fig. 4-1). This is quite an enormous effect. For both cases - with and without iodine - lubrication was in the ordinary wear regime; the reduction in friction is not simply a case of going from a scuffing situation to one of mild wear. Moreover, in many well-known cases where wear is reduced by about 50% from that of the base oil (e.g., with conventional fatty acids, other halogens, organic phosphates), friction is generally reduced by no more than 20-30%. Reductions in friction of 50% are considered unusual. Thus, the 90% reduction due to iodine in the present example is rare indeed.

It does not matter whether the iodine is present as solvated molecules (brown solutions) or as diatomic molecules (violet solutions). As little as 0.0075% I₂ in either form does the job; the "charge-transfer complex" form (Roberts 1963A) is not required. Moreover, iodine is much more effective than chlorine or bromine, other members of the halogen family that are usually more reactive than I₂. And it is quite interesting that iodine by itself as a solid lubricant is ineffective (Peterson 1955).

Figure 4-1
EFFECT OF IODINE ON FRICTION



4.4.4 Tungsten

In a number of instances, it has been observed that the addition of a moderate amount of tungsten to steel has a strong effect in reducing the wear rate. This might appear to be merely an example of the old rule that hard metals wear less than softer ones, but in pump vanes the two alloys were heat-treated to exactly the same hardness of 60-62 Rockwell C. Running them in the author's laboratory showed a consistent difference of about five-fold. A very desirable effect was also noted (see 4.2) in lead-plated ball bearings, where alloys without tungsten (i.e., 440 C stainless steel) failed to show much benefit from the plating. The mystery is deepened by the fact that high surface energy elements are less abundant at the surface, in accord with the Gibbs-Duhem principle discussed further below. Tungsten is also quite vulnerable to oxidation (Kubaschewski 1962) which would lead to its rapid removal from the surface.

Some vital information may be found in 7 recent patents to duPont (1971), covering a system for producing lubricants "in situ" by the polymerization of thin liquids which are passing through the equipment. The vital step is a reaction at the rubbing surfaces of two alloys, one of which must contain 6 to 12 atom percent of tungsten or molybdenum. Most of the data covers molybdenum, with tungsten only being tested once out of ten examples (and coming off second-best that time), but they are given equal weight in the claims. Also cited, as third-rate choices, are chromium and manganese. This anomaly will be further discussed in Section 5.5 under the subject of "surface resin", and in Section 7.5.1.

4.5 Optima in Blended Lubricants

There have been observations for some time that blending together two different types of liquid lubricants would sometimes result in a product which was far more satisfactory than either. One of the first reported examples was blending low molecular weight dimethyl silicone oil with diesters. Testing on the Ryder Gear Machine, the silicone alone carries very little load before scuffing. The diester, typical of base stocks for jet engine lubricants, scuffs at 1800 lb/in. Blending 4% by weight of 4 centistokes at 25°C dimethyl silicone into this ester raised the scuff load to over 3000 lb/in. Unfortunately, these blends foam excessively, since silicone in solution acts similarly to soap in water. (Silicone acts as an anti-foam agent only when not in solution.) Hence, this work received only scanty attention and some rather fanciful explanations (Matuszak 1959). Recently, one of the silicone manufacturers has come up with what might be called an "internal blend", in which tetradecyl replaces one of the methyls (Brown 1966, 1970). The resulting liquid is reported to have quite exceptionally good properties, even protecting aluminum-on-aluminum in reciprocating motion.

In passing, it may be noted that the poor performance of dimethyl silicone constitutes a negative anomaly. These fluids appear to have ideal properties, but fail rapidly due to wear at light loads and scuffing at moderate loads. This is caused by the polymerization of the silicone to a hard, sandy resin which acts as an abrasive (Currie 1950, Tabor 1965, 1969).

A much more important example of an anomaly in blending arose during an investigation of high pump wear in aircraft fuel systems (Appeldoorn 1966, 1967A, 1968B). In Figure 4-2, the results obtained in air and in argon atmospheres with blends of isoparaffinic and polynuclear aromatic components are shown. The conclusion was that over-refining the fuel (i.e., removing nearly all the aromatics) caused the high wear. While this is a perfectly valid conclusion, it is evident from the Figure that atmosphere affects the optimum blending ratio. This will be discussed in Section 4.7.

Some anomalies in re-blending components extracted from lubricating oil by silica gel proved to be more complicated (Groszek 1967-8, Beerbower 1971D). This work is discussed in detail in Section 7.5.3.

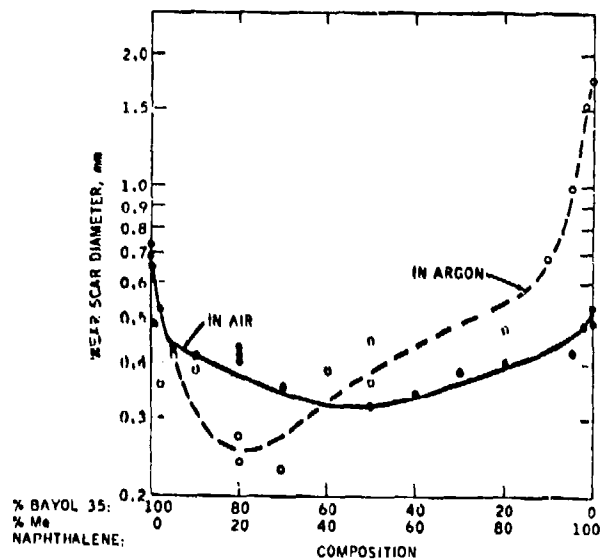


Figure 4-2

Optima Obtained by Blending an Isoparaffin
(Bayol 35) with a Polynuclear
Aromatic (1-methylnaphthalene)

4.6 Competition of Additives for Surfaces

A phenomenon which has been under investigation since the 1920's is the ability of additives to seek out the surface and, in effect, act as the real lubricant while the base oil merely serves as a solvent or carrier (plus its functions as a viscous-film former in the mixed-film regime, as a heat transfer medium and a flushing agent to remove wear particles from the action zone). No doubt this work was sparked by observed differences between the fatty oils and mineral oils, since it took the form of putting small doses of the former into the latter. The results must have seemed miraculous, as they proved that less than 1% of fatty acid converted the hydrocarbon lubricant into the equivalent of a fatty oil.

This "Germ Process", as it was first called, was mysterious only because the principles laid down by Willard Gibbs had not yet been reduced to usable form. We now know that such behavior is simply the universal tendency of a system to equilibrate at the configuration which has the lowest free energy, and that is when the metal surface is nearly 100% covered with oleic acid.

However, in the 1930's and 1940's, many other types of additives were introduced, sometimes with very embarrassing results. A highly complex lubricant of the 1950's might well include:

- "Oiliness" agent, such as oleic acid,
- Antioxidant,
- Sludge dispersant, typically calcium sulfonate
- Pour depressant, usually alkylated naphthalene
- VI improver, either polybutene or polyacrylate
- Antifoam, a dimethyl silicone
- Rust inhibitor, often a complex acid or amine.

The results were difficult to predict, and led to a set of rules on "antagonisms" and "synergisms". Loosely translated, these mean that the experimenter did not know what happened, but disliked or liked the result.

At the "base-line" date of 1965, many of these interactions were routinely explained on generally accepted grounds, but anomalies still exist. At one time, it was believed that sulfur additives (see 4.4.2) functioned simply by reacting with the metal surface to form metal sulfide (and presumably an olefin), but new data indicate that physical adsorption plays a major role. Vere (1969) has shown that thiophene derivatives in jet fuel play a role in lubricating pumps; Forbes (1970) has shown that aliphatic sulfur compounds wet the surface in a complicated but predictable fashion, and Grew (1969) has shown that the action of even a very active compound, dibenzyl disulfide, can be blocked by the non-lubricating hexadecyl amine. Chlorine additives have also been regarded as working by simple irreversible chemistry

resulting in metal chloride (see 4.4.3), but Studt (1968) has shown that they can be blocked by lauric acid. While such effects can vaguely be foreseen from the Gibbs principle, detailed predictions are not possible.

An even more unpredictable effect is shown in Table 4-I (Appeldoorn 1967A, 1968B, 1969). Gibbs' principle cannot explain how an active anti-wear agent such as tricresyl phosphate can be forced off a surface by such bland materials as hydrocarbons, nor especially by a mixture of two kinds. The first group of data show what may be regarded as the normal effect of TCP; in paraffinic lubricants it acts by coating the surface and so reduces wear. Even the failure to perform this function in dry argon is predictable, since the tri-ester must be split to become truly a surfactant.

The mystery starts when we consider the failure to improve the poor performance of aromatics, regardless of atmosphere. Aromatics do wet a little more energetically than paraffins, but scarcely can compare with TCP and its hydrolysis product dicresyl hydrogen phosphate. The real anomaly develops when we try to improve the already good performance of the paraffin-aromatic blend; not only does the attempt fail, but wear becomes even greater than it was with the aromatic alone in some atmospheres. Discussion of the last line of Table 4-I will be reserved for the next section.

So far, it appears that all the effects of competition are bad, in that effective additives are driven off by inferior materials. This is, of course, what tends to be published in the journals. Cases of synergism tend to appear in the form of patents, usually so obscured with irrelevant speculations as to be very hard to isolate. The fact that this STAF failed to turn up many useful cases should not be taken as an indication that the phenomenon cannot be turned to advantage. For instance, Studt (1968) went on to demonstrate that tetrachloro-lauric acid would displace the simple acid, and have the virtues of both fatty oil and chlorinated aliphatic. Once quantitative explanations of the interaction are available, such models will serve to make Studt's success routine.

4.7 Ambiguous Roles of Humidity and Oxygen

Until the atomic energy program forced the matter on our attention, it was not generally realized that the atmosphere surrounding a bearing/lubricant system had anything to do with its performance. The space program added to this recognition, and it is now coming to be realized that essentially all lubrication data obtained before 1960 (and a good deal since) is worse than useless. Not only did experimenters fail to control the humidity in their laboratories; they seldom even bothered to record it. The observed effects are sketched in Table 4-I, most of which was discussed in the previous section from a different standpoint, as well as in Figure 4-2. Additional information is provided in Figure 4-3 (Goldman 1970), showing the special nature of the interaction of aromatics with the atmosphere. The region below the line was originally called "scuffing", but Goldman (1969) later re-examined the test pieces and found it to be a special sort of corrosive wear. (These dates are correct; the later work happened to be published earlier.)

TABLE 4-1

EFFECT OF TRICRESYL PHOSPHATE (TCP)
IN VARIOUS LUBRICANTS AND ATMOSPHERES

(Wear Rate, Steel on Steel)

<u>Lubricant</u>	<u>Dry Argon</u>	<u>Wet Argon</u>	<u>Dry Air</u>	<u>Wet Air</u>
Isoparaffin (P)	Low	Medium	Medium	Very high
P + TCP	Low	Low	Low	Low
Polynuclear Aromatic (A)	High	Medium	Medium	Medium
A + TCP	High	Medium	Medium	Medium
Blend (P + A)	Low	Medium	Low	Low
P + A + TCP	High	High	High	High

Based on Appeldoorn (1969).

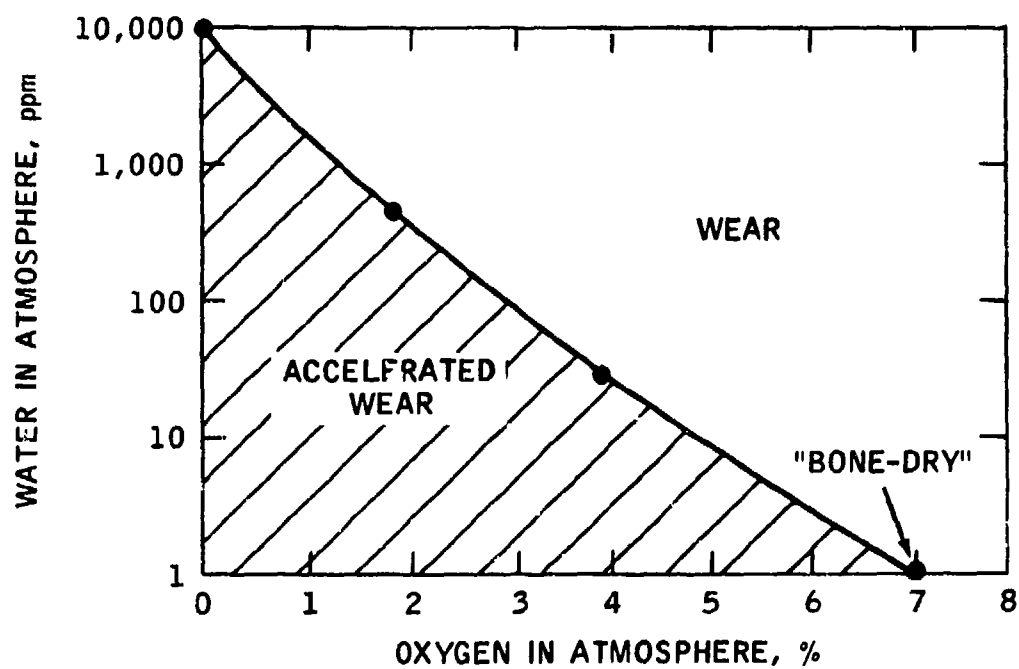


FIGURE 4-3

BEHAVIOR OF 1-METHYLNAPHTHALENE AS AFFECTED BY MOISTURE AND OXYGEN.

The situation is obviously very complicated; it appears that both water vapor and oxygen can act to reduce or increase wear, depending on the lubricant. They can replace one another, as shown in Figure 4-3, but wet argon is not quite equivalent to dry air, as shown by the P + A blend in Table 4-I.

The addition of TCP to the P + A blend in Table 4-I apparently shows that this additive is simulating the worst effects of water and oxygen, while its addition to the P oil has exactly the opposite effect.

There are certainly relations between the additive competition discussed in 4.6 and these atmospheric anomalies - at least where TCP is involved. Oxygen can be regarded as an "additive", at a concentration of about 200 ppm in paraffinic and 50 ppm in aromatic oils. Water is also soluble at about 50 ppm in paraffinic and 500 ppm in aromatic oils. These are not too low to permit competition, especially since the effects are apt to be irreversible. On the other hand, both oxides and hydroxides are quite capable of accepting some classes of additive, so that competition with the atmosphere may result in a different outcome of the conflict between two additives.

4.8 The Sharp Transition to Scuffing Wear

One of the most startling phenomena in boundary lubrication is the sudden change from moderate to severe wear and friction, on application of a small increment in severity, as shown at point Y in Figure 2-1. As long as this transition was associated merely with a load increment, it could be written off as being parallel to the familiar yielding from elastic to plastic deformation in testing the strength of materials. However, it has been clearly demonstrated that the same transition can be triggered off by a minor increase in ambient temperature; in fact, as will be discussed in Section 5, there is every reason to believe that the load increment causes transition primarily because it leads to an increase in contact temperature. Furthermore, this cannot be equated with the known (but rarely demonstrated) phenomenon of yielding under constant load at a certain point while increasing the temperature, because the friction/wear transition is at least as dependent on the lubricant as on the metallurgy. While this argument is weakened later on, by considerable evidence that the yield point of solids is indeed affected by the nature of the surrounding liquid or gas, (see Section 5.8 and Appendix V) the currently accepted view that the scuffing transition is uniquely related to lubrication will be pursued here.

The vertical line at Y in Figure 2-1 is schematic, and may very well represent a very steep S-shaped curve (Model II-C) or even a backward-bent one (Model V-C). The physical events are not subject to very precise examination due to their violent nature, and the scatter of data is sufficient to fit equally well on a number of models (Section 5). Usually, a small load step is followed by a brief period of mild wear, and stopping the test during this period shows a typically smooth surface. Pike (1970) describes this period as "seizure delay" and cites some interesting 4-ball data. Very suddenly, the friction rises and characteristic noises come from the machine: squealing, groaning, chattering or grinding, depending on the speed and geometry of the

test machine. (This description applies to machines with test parts of simple geometry. When actual gears are used, the change is much less dramatic since it takes place at the tooth tips and only propagates under further load increments.) Stopping for examination now shows a rough surface, sometimes with scuff marks forming a vague pattern reminiscent of overlapping circles. In other cases, linear marks known as "scoring" appear; the relation of these to scuffing proper is still the subject of debate, but in this report no distinction will be made.

Often, scuffing wear generates large particles. Unlike those seen in moderate wear, which are near the limit of optical microscope resolution (3 to 5 μm), scuffing particles may be visible to the naked eye.

If the load remains constant a wear rate several times as high as that recorded at the last pre-scuffed load step is maintained. Increasing the load causes a regular increase in the wear rate as shown in Figure 2-1, eventually followed by sudden welding. Decreasing the load will reduce this rate along a line parallel to the normal wear rate/load relation. Sometimes, at considerably reduced load, healing will take place and a new break-in period leads to the normal wear rate again. The surface is apt to show wave or ripple marks, and other evidence of the rough contour period.

Another evidence of scuffing is the generation of a "swarf", or feather edge of the wear scar. On the Timken machine, which has a cylinder rubbing on a flat block and producing a narrow wear scar 0.50 in. long, it is common to find that one or two small areas have scuffed at the end of the standard 10-minute test period under loads near transition. The writer believes this to be a transient situation, and that continued running at the same load would cause the scuffing to spread all the way along the scar. This experiment has not been carried out, partly because the standard procedure allows the temperature to rise due to frictional heat. Hence, the anticipated effect could be attributed (if found) to either time or temperature. Fitting the machine with a cooling system would provide an interesting opportunity to study the "seizure delay" previously reported only on the 4-ball machine and mentioned above (Pike 1970).

Unlike those previously considered, the transition anomaly is entirely to the disadvantage of the machine designer. However, as shown in Table 4-I, it is possible to find cases in which the competition of additives, the atmospheric effects, and their interaction with one another can aid in shifting the transition point Y (Figure 2-1) to a higher load. In fact, it is this phenomenon that makes possible operation of gears under modern conditions. Automotive hypoid gears, in particular, could not be operated at all due to their high proportion of sliding to rolling motion until suitable additives were developed in the late 1930's. This is done by a deliberate sacrifice; as shown by the line ending at Z' in Figure 2-1, operation at loads above Y not only involves higher than normal wear there, but also at loads below Y when the same lubricant is used. This is undoubtedly due to the corrosive or chemically reactive nature of the additives. Despite this insight, we may still call operation in this "extreme pressure" (EP) region anomalous, since recent work has shown that the mechanisms long accepted for the prevention of scuffing by controlled corrosion are not valid (see 4.4.2 and 4.4.3 above).

4.9 Effect of Anti-Wear Additives on Fatigue

As the lubricant industry has responded to demands for lubricants with better anti-wear and anti-scuff properties, it has been noticed that trouble seemed to be arising in an unexpected crop of fatigue failures, often after prolonged service but sometimes earlier than anticipated. This has been particularly the concern of the rolling element bearing users (Rounds, 1962, 1967), who have reported some data. It is difficult at this point to discuss the matter because of contradictions in the data (partly due to lack of humidity control), but it certainly seems likely that some very good anti-wear additives are responsible. A far less clear-cut case concerned the gear people a few years ago, but has been set aside for the present as being of less pressing importance.

Complicating the situation is the fact that there are several phenomena grouped together as "fatigue." One of these is rapidly coming under control; it is known as "subsurface fatigue" and arises from slag, etc., inclusions in the metal. This had nothing to do with the lubricant, as the fatigue crack arose at the impurity and only reached the surface at the time of failure; it is currently being brought under control by vacuum melting.

What may be called "rolling fatigue" arises from micro-cracks in the metal surface that propagate downward and then turn parallel to the surface. Eventually, a piece snaps out and bearing failure results at a catastrophic rate. This phenomenon seems to be definitely related to the lubricant.

"Corrosion fatigue" merges into the rolling sort, and may sometimes result from high humidity causing the formation of hydrogen by the reaction $\text{Fe} + \text{H}_2\text{O} = \text{FeO} + \text{H}_2$. If so, it must result in more rapid failure as hydrogen has a very bad effect on hard steels (Berry 1967). The possible roles of lubricants and additives in this mode of wear will be discussed later.

"Sliding fatigue" may be defined as that coming from sliding motion. It is rather more controversial than the first three, but may well be lubricant-related. It must certainly include a "sliding corrosion fatigue" as a fifth sub-species. The effect is to cause the asperities on the surface to fail by repeated elastic stressing, and spring loose as much smaller particles than those found in rolling fatigue.

So far, this anomaly appears to be largely harmful. However, some data can be interpreted so as to provide hope for positive results from properly selected additives - at least in preventing the accelerating effects of corrosion on rolling fatigue.

4.10 Benefits of a Break-In Period

It has been long and widely recognized that gear and bearing surfaces show less wear in service if they have been subjected to a moderate period of operation under partial load. One factor that was obvious from the beginning of this practice was that the break-in served as a final lapping step during which poorly finished surfaces lost their high spots, which turned up as

visible metal particles in the oil. Various additives were tried; some proved so powerful that they prevented lapping, and when the special break-in oil was replaced with ordinary lubricant, rapid wear resulted (Crook 1958/59). In other cases, there proved to be a chemical factor involved (especially in units designed for EP service) and clear-cut films of reaction products could be identified (Grew 1969).

In many cases, however, the process was mysterious - and remains so. With modern finishing and fitting methods available, it should not be necessary for the new owner to serve as an amateur machinist by lapping the surfaces to perfection. Nevertheless, the best finishes from the machine shop still showed excessive wear until broken in, unless given a pre-treat in a chemical bath which formed the equivalent of an EP film. It was evident in some cases that smoothing was taking place; cast iron cylinders in particular show a "glaze" that has never been analyzed completely. Speculation led to the concept of a "Bielby layer" of highly cold-worked metal which was both smoother and harder than the original surface, but it could not be detected in some cases and shop processes designed to produce it led to disappointing results.

We now believe that the formation of surface resin is a factor; this will be discussed in detail in 5.5.4 and 5.5 below.

4.11 Miscellaneous Anomalies

In the course of this investigation, a large number of workers were asked to report on any peculiar phenomena that might be added to the list of anomalies. These are listed below simply in chronological order of acquisition. Some are discussed further in Section 7, but others remain to be investigated.

4.11.1 Anomalously Low Friction was reported by Finkin (1968A) in transmissions, where moderate friction is required for operation. This was a copper-based sintered material sliding on steel. There was a long low-friction period, followed by a metal transfer mode. Friction appeared to be a step-function of temperature. This is discussed further in 7.11.1.

4.11.2 Anomalous Wetting Energy was published by Bennett (1968), and Zisman was unable to explain (1969) this effect. They had measured the contact angle (θ) of various liquids on metals polished with abrasive in water. All the metals had the same "critical surface tension" of 44 ± 2 ergs./cm² at $\cos \theta = 1$, but the slopes ($\Delta \cos \theta / \Delta \gamma_2$) varied widely. The latter fact may be considered anomalous, since it is not widely believed that metallic forces can reach out through the layers of oxide, hydroxide and bound water to affect the behavior of liquids - especially the non-polar ones used as probes. (Further discussion in 5.5, 7.11.2 and Appendix V).

4.11.3 Metals of Group B in the Periodic Chart were found (Roach 1956) to have special properties in preventing the scuffing transition. Other people have found similar behavior but have connected it with other metal properties, such as hexagonal crystal structure (Buckley 1966). As this goes far beyond the calcium, etc., effects, it is treated below as Model IV in Section 5.6.

4.11.4 Multilayers of Stearic Acid have been investigated by several groups (Allen 1969A). This may or may not have special meaning in regard to lubrication. Others have found that stearic acid forms only 40% of a monolayer (Anderson 1969). Askwith (1966) found optimum lubrication when oil and additive molar volumes matched; this leads to 50% coverage (Beerbower 1971C). (Further discussion in 7.11.4.)

4.11.5 Freshly Purified Cetane is a far poorer lubricant than material which has stood a little while. Tests run on material kept in the dark show higher friction than on that exposed to light (Johnson 1950). (Further discussion in 7.11.5.)

4.11.6 Complex Organic Phosphates have quite extraordinarily low friction (Blok 1970). Castor oil reacted with P_2O_5 carried over 1000 kg on the 4-ball machine at 1500 rpm, with F values as low as 0.006. Despite the low friction, the heat and pressure extruded part of the top ball into a rod projecting among the other three. A suspension of bone meal (largely calcium phosphate) in oleic acid or linseed oil was so slippery the top ball could scarcely be held in its chuck, and the F readings were exceptionally low (limited discussion in 7.11.6).

4.11.7 Diesel Engine Scuffing shows very peculiar effects; the usual anti-wear additives turn out to be prowear (Pike 1970, Davies 1969) as shown in Table 4-II. The scuffing could be related to conversion of grey cast iron to cementite (Fe_3C) (Rogers 1970). "Scuffing" in this case may be something quite different from the sort of transition discussed above (4.8) and related more to sliding fatigue (4.9) but the complexity of the metallurgy, motion, corrosive atmosphere and anti-corrosion (calcium base) additive interactions render analysis difficult. An attempt is made to relate it to additive-induced fatigue via Model II in Section 7.11.7.

4.11.8 Wear Due to Suspended Abrasive Particles is dramatically reduced by the addition of minor amounts of additives. Tao (1970) found that small amounts of oleic acid essentially reduced the wear of an iron or iron oxide particle suspension to that of the clean oil, while stearyl amine did the same for silica. He was able to explain this only in generalities, not very useful in predicting how to control abrasive wear. This is discussed in 5.9.3 and 7.11.8.

4.11.9 Delay of Scuffing Transition appears to be more unpredictable (Pike 1970) than transition temperature, which could serve as a check on the numerous transition theories (further discussion in 7.11.9).

TABLE 4-II

ANTI-WEAR ADDITIVES INCREASE DIESEL SCUFFING

<u>Additive</u>	<u>Relative Wear Rate</u>	
	<u>On Steel Balls</u>	<u>In Diesel Engines</u>
None	100	100
Oleic Acid	80	100
Dibenzyl Disulfide	50	145
Isopropyl Oleate	60	195
Zinc Dialkyl Dithiophosphate	40	245

4.11.10 Gold Appears to Oxidize, though this is in conflict with all ordinary chemical thermodynamics. The evidence is that melted gold will not spread on ceramics in bone-dry argon, but spreads freely in air (Pask 1970). While this is not a lubrication anomaly, it may be related to some of the effects of atmosphere on friction and wear. This matter is given some further attention in 7.11.10.

4.11.11 Water plus Phenothiazine Shows Low Wear, enough so to be used as hydraulic fluid, even though emulsions of 5% of oil in water show high wear. Break-in is very important; if high wear ever starts it tends to continue to destruction (limited discussion in 7.11.11).

4.11.12 Two Consistent Sets of Friction Data can result from repeated tests on a single system (Ling 1962). Apparently some chance event starts one or the other of two mutually exclusive processes going, and the result is a pair of wear or friction curves known as "bifurcation". Johnson (1970B) and various others have observed similar effects. These frequently are "explained" as instances of borderline scuffing transition (Y on Figure 2-1), but may have deeper significance as explained in 7.11.12).

4.11.13 High Friction on Titanium is notorious; this is usually accompanied by scuffing. The problem is so severe that special care must be taken at the rolling mills in stacking finished sheets, as they will scuff one another seriously enough to be rejected merely by this mild contact. The only lubricants that have shown any real promise are those based on iodine (Brown 1968) (Section 4.4.3 and Figure 4-1), and these have been used despite serious corrosive tendencies in the earlier versions. Rabinowicz (personal communication) questions this conclusion, as discussed further in 7.11.13.

4.11.14 Austenite Versus Martensite. These two structures of steel have long been recognized to have different mechanical properties. Recently it was realized that their response to lubricants was also very different (Grew 1969). The discoverers put forth the following explanation: Martensite is the main constituent of ordinary, highly reactive steels. Most of the properties of stainless steels are connected with their austenitic structure. Thus, it is reasoned that austenite is relatively non-reactive. The fine needles of martensite certainly would be easier to attack than the coarse grains of austenite. No literature is cited on reaction rates under static conditions, but a number of cases of high wear attributable to austenite, both preformed and generated by rubbing, were quoted (no further discussion - see 7.11.14).

4.12 Summary of Anomalies. This list shows that, in about ten areas, friction or wear is markedly less than would be predicted by 1965 models. In another ten, lack of understanding is leading to incorrect predictions, that may be either too optimistic or too pessimistic. In three cases, machine operation is considerably more difficult than was anticipated. It seems reasonable to expect that improved understanding would permit more general use of the ten favorable anomalies, and also avoiding the dangers of working with the ten which are imperfectly predictable. Understanding the three cases where unexpected difficulties arise might point the way to new solutions of these vexing problems.

5. ADVANCED MODELS OF BOUNDARY LUBRICATION

This chapter presents a detailed discussion of seven advanced models of boundary lubrication which have emerged from this study. Each is applicable to a limited range of conditions, and each is to some extent incomplete; but together they provide at least qualitative explanations for nearly all the anomalies and they open the way to a quantitative understanding deep enough to make what is now anomalously good performance into routine.

A "model" is defined, for the purposes of this STAF, as an equation or set of equations predicting the wear rate (or a transition to another mode of wear) for some specific mechanism of particle generation. Minor exceptions to this definition are made in a number of cases where multiple mechanisms were found to be at work, but the overall process is described by essentially the same equations. At the end of this section, two auxiliary "models" are introduced which lead only to values required for use in the true wear models.

5.1 Introduction: Current Design Practices

Aside from the specialized model proposed by the American Gear Manufacturers Association (Dudley 1965) and discussed below, only the "PV" (pressure times velocity) or "rubbing-factor" model has received the backing of any professional society. It is recommended in the Handbook sponsored by ASLE (O'Connor 1968), and IME (Neale 1968) in the UK for unlubricated bearings. Both societies recognize the boundary lubrication will give less wear than predicted by "PV", but in the absence of suitable equations they recommend it as the "worst possible case." The following discussion attempts to combine the best features of both publications. ASLE uses equations and one chart, while IME gives charts which are far more detailed, but no equations. The latter publication is far easier to use. Both depend on the designer meeting two criteria: a simple heat balance, and the "PV" system mentioned above.

5.1.1 Design of Rubbing Bearings

The first of these is a simple balance of work lost = heat dissipated:

$$\text{"PV"} = WU/A_p = Jk_1 \Delta T/F \quad (5.1-1)$$

where:

W = load, U = velocity, A_p = projected area, J = mechanical equivalent of heat, k_1 = thermal conductivity, ΔT is the allowable temperature rise, F the coefficient of friction and "PV" has a more or less constant maximum allowable value for any given material. This formulation is from ASLE; IME merely discusses the matter in general terms, and gives typical values, for 16 classes, of allowable temperature, coefficient of friction and thermal conductivity. Equation (5.1-1) is not even dimensionally balanced; it would also require the length of the heat leakage path to complete a valid calculation.

In general, nomenclature (Appendix I) is based on the ASLE standard as far as is possible. However, "PV" is so widely used that it is used on this and the next few pages.

ASLE shows a correlation of published "PV" values for various materials with $k \Delta T/F$ (Figure 5.1-1), which could be expressed as

$$\log "PV" = \log (WU/A_p) = 0.35 \log (k_1 \Delta T/F) + 2.35 \quad (5.1-2)$$

though ASLE does not take that step.

The second criterion is somewhat more sophisticated. According to ASLE,

$$"PV" = W U/A_p = h P_m/k_w t \quad (5.1-3)$$

where h/t = allowable wear rate, P_m = hardness of material, and k_w is a wear constant. This is the equation of a hyperbola, in P and V coordinates, but the IME charts (Figures 5.1-2 and 5.1-3) show it as being more or less flattened in the middle. Originally the flat portion was used as a measure of load bearing capacity but, as IME points out, this "is an oversimplification and can be misleading." The materials coded in Figures 5.1-2 and 5.1-3 are listed in Table 5.1-1.

This model is related to the well-accepted Archard wear equation

$$V/d = K W/P_m \quad (5.1-4)$$

where V = wear volume and d = distance traveled = Ut , but since V is not exactly equivalent to hA_p , k_w cannot be quite the Archard constant K . The exact relation of V to h would require precise knowledge of the shape of the wear groove in the bushing, or else assurance that all wear is on the shaft. The latter is very rare, and wear groove shapes depend on many factors, so that $k_w \approx K$ is a good example of an "unscientific" (because the wear area is not really A_p) approximation that solves a very vexing engineering problem.

Equation (5.1-4) is of the utmost importance in wear theory and will be constantly referred to in this STAF. The constant K will sometimes be called the "specific wear rate."

ASLE states that "PV" based on allowable wear rate will usually have a smaller value than "PV" based on allowable temperature rise, while IME advises calculating both and accepting the more conservative result.

5.1.2 Design of Gears

By far the most sophisticated model officially recognized for design purposes in the boundary regime is the AGMA "Gear Scoring Design Guide for Aerospace Spur and Helical Power Gears" (Dudley 1965). The title is quite descriptive of its scope and limitations, to the reader who is well grounded already in such matters. It is concerned only with scoring (location of point Y in Figure 2-1 and offers no guidance on friction or wear. It contains specific parameters for two oils commonly used in military aircraft, MIL-L-7808 and

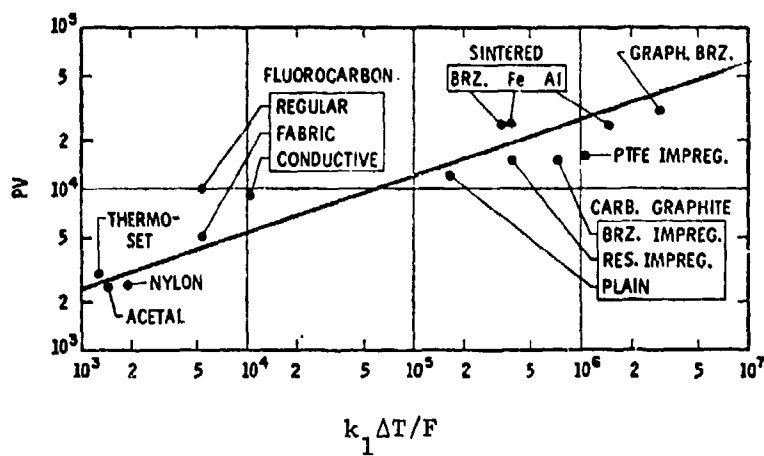


Fig. 5.1-1 ASLE Design Chart for Various Bearing Materials

Figure 5.1-2
IME PRESSURE-VELOCITY CURVES FOR JOURNAL BEARINGS
USING MACHINEABLE MATERIALS

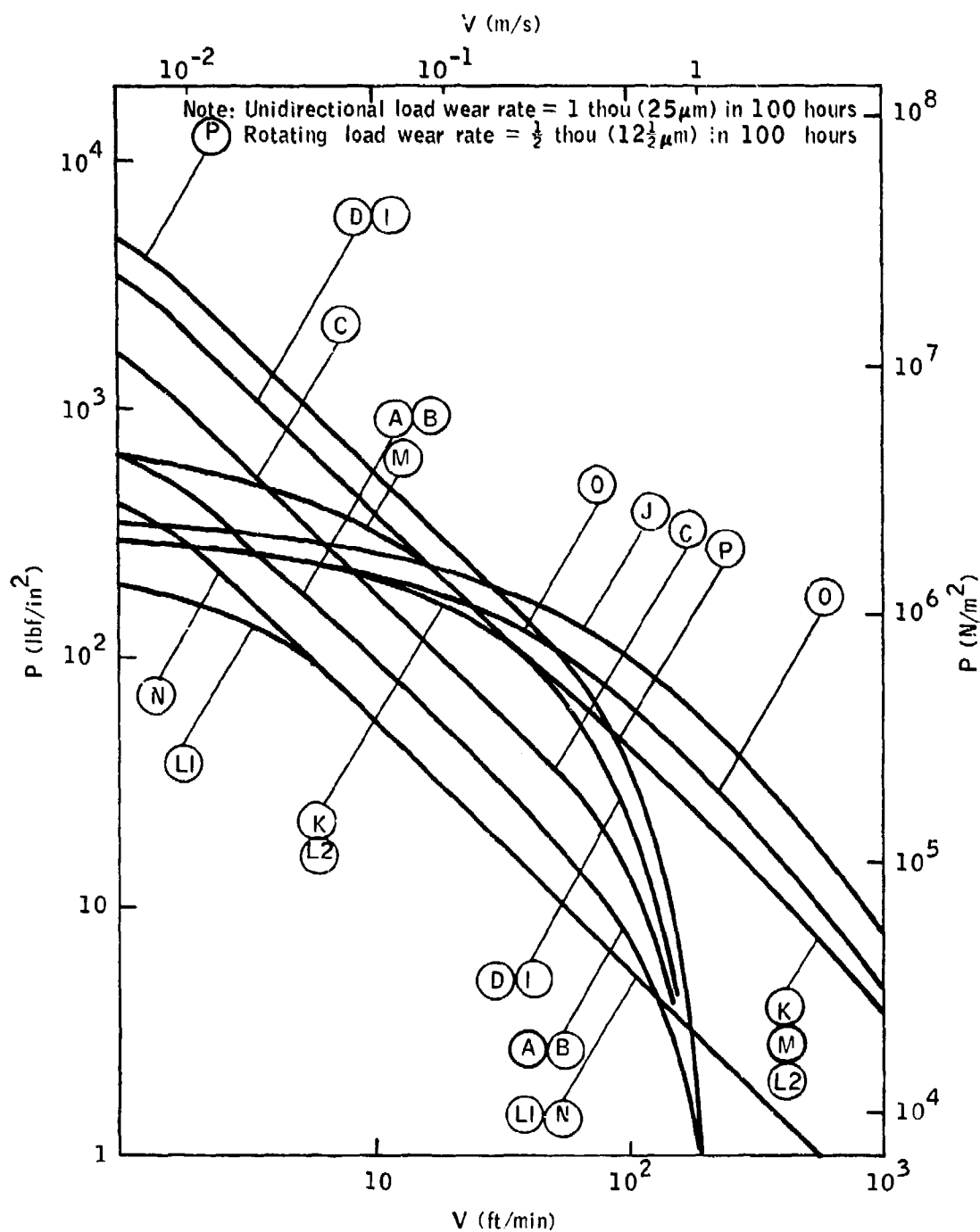


Figure 5.1-3
IME PRESSURE-VELOCITY CURVES FOR JOURNAL BEARINGS
USING UNMACHINEABLE MATERIALS

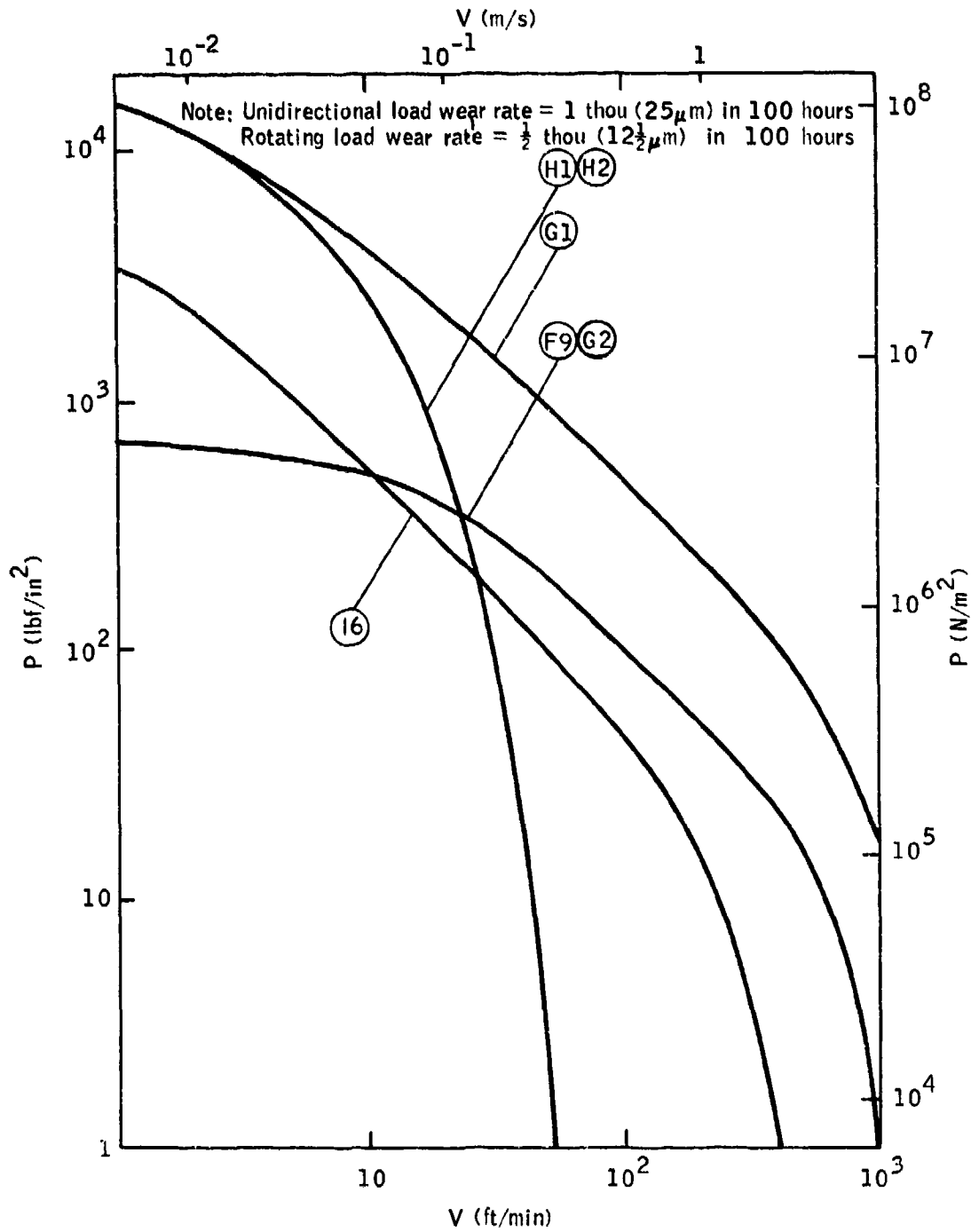


TABLE 5.1-1 MATERIALS FOR IME CHARTS
5.1-2 AND 5.1-3

Group	Description	No	Material	Description	Form Available (see Key opposite)	Manufacturer
A	Thermoplastic	1	Delrin ⁽¹⁾	Polyacetal	P R	Polypenco Ltd
		2	Glacetal ⁽²⁾	Polyacetal	S.S.I.W.	The Glacier Metal Co. Ltd
		3	Monocast Nylon	Polyamide (Nylon)	R.T.	Polypenco Ltd
		4	Nyliner ⁽³⁾	Polyamide (Nylon)	SI	Kellett Engineering Co. Ltd
		5	Nylon 66 ⁽²⁾	Polyamide (Nylon)	P.R.S.T.	Polypenco Ltd
B	Thermoplastic - Metal Backed	1	Nyliner ⁽³⁾	Polyamide (Nylon)	CU.	Kellett Engineering Co. Ltd
C	Thermoplastic with Filler	1	Nylasint 20	Graphite filled nylon	TO.	Polypenco Ltd
		2	Nylasint 60	Graphite filled nylon	TO.	Polypenco Ltd
		3	Nylasint M4	Molybdenum disulphide (MoS ₂) filled nylon	TO.	Polypenco Ltd
		4	Nylasint MS	MoS ₂ filled nylon	TO.	Polypenco Ltd
		5	Nylatron GS ⁽²⁾	MoS ₂ filled nylon + rust inhibitors	B.P.Pr.R.S.T.	Polypenco Ltd
		6	Nylatron GSM	MoS ₂ filled nylon	R.P.R.	Polypenco Ltd
D	Thermoplastic with Filler - Metal Backed	1	Glacier DX ⁽⁵⁾	Polyacetal + patented additive-impregnated porous bronze on steel	B.H.C.W.S.	The Glacier Metal Co. Ltd
E	PTFE	1	PTFE ⁽²⁾	Polytetrafluoroethylene	P.R.S.T.	Polypenco Ltd
F	PTFE with Filler	1	CP2	Glass filled PTFE	R.	Crane Packing Ltd
		2	Fluoroint ⁽²⁾	Mica filled PTFE	R.S.T.	Polypenco Ltd
		3	Glacier DQ1	Bronze-graphite filled PTFE	R.T.	The Glacier Metal Co. Ltd
		4	Glacier DQ2	Graphite filled PTFE	R.T.	The Glacier Metal Co. Ltd
		5	Glacier DQ3	Bronze-lead oxide filled PTFE	R.T.	The Glacier Metal Co. Ltd
		6	M7	Graphite filled PTFE	TO.	Nohrac Carbon Ltd
		7	Permaflon	Glass filled PTFE	B	Permall Ltd
		8	Rulon ⁽⁴⁾ LD	Ceramic type filled PTFE	P.R.Sh.T.W.	Henry Crossley (Packings) Ltd
		9	Rulon ⁽⁴⁾ T-Liner Tape	Ceramic type filled PTFE	S.S.I.W.	Henry Crossley (Packings) Ltd
G	PTFE with Filler - Metal Backed	1	Glacier DU ⁽⁵⁾	PTFE lead impregnated porous bronze on steel	B.H.C.W.Rd.S.Sp. ⁽⁸⁾⁽⁹⁾	The Glacier Metal Co. Ltd
		2	Rulon T-Liner Bearing ⁽⁴⁾⁽⁶⁾	Ceramic type filled PTFE	CU.	Henry Crossley (Packings) Ltd
H	PTFE-Novon	1	Fiberglide ⁽¹¹⁾	PTFE cotton weave reinforced with a thermoset reinforced cotton backing + graphite	⁽⁸⁾⁽⁹⁾ R.Rd.Sp.W.	Aspep Industrial Products Ltd
		2	Fiberglide ⁽⁷⁾⁽¹¹⁾	PTFE glass weave reinforced with a thermoset reinforced glass backing	⁽⁸⁾⁽⁹⁾ R.Rd.Sp.W.	Aspep Industrial Products Ltd
I	Thermoset Reinforced with Filler	1	Adder Brand	Asbestos cloth-thermoset laminate with graphite	R.Sh.T.	Tufnol Ltd
				Asbestos cloth-thermoset laminate with MoS ₂	R.Sh.T.	Tufnol Ltd
		2	AL2	Asbestos cloth-thermoset laminate with graphite	R.Sh.T.	Railko Ltd
		3	AL12	Asbestos cloth-thermoset laminate with graphite	R.Sh.T.	Railko Ltd
		4	Bear Brand	Cotton-thermoset laminate with graphite	R.Sh.T.	Tufnol Ltd
		5	Ferobestos	Asbestos cloth-thermoset laminate with MoS ₂	R.Sh.T.	Tufnol Ltd
I	Thermoset Reinforced with Filler	6	PX	Asbestos cloth-thermoset laminate with graphite	R.Sh.T.	J.W.Roberts Ltd
				Textile-thermoset laminate with PTFE based surface layer	B.Sh.	Railko Ltd

(Continued)

TABLE 5.1-I (Continued)

Group	Description	No	Material	Description	Form Available (see Key below)	Manufacturer
I	Thermoset - Reinforced with Filler (Continued)	7	Orkot RL	Textile-thermoset laminate with graphite	TO.	United Coke and Chemicals Co. Ltd
				Textile-thermoset laminate with MoS ₂	TO.	United Coke and Chemicals Co. Ltd
				Textile-thermoset laminate with graphite	TO.	United Coke and Chemicals Co. Ltd
		8	Orkot RH	Textile-thermoset laminate with MoS ₂	TO.	United Coke and Chemicals Co. Ltd
				Textile-thermoset laminate with graphite	TO.	United Coke and Chemicals Co. Ltd
		9	Orkot TL	Textile-thermoset laminate with MoS ₂	TO.	United Coke and Chemicals Co. Ltd
J	Thermoset - Carbon Graphite with Filler	1	ERB14J	Thermoset bonded carbon/ graphite + PTFE + MoS ₂	TO.	Nobrac Carbon Ltd
		2	MB	Thermoset bonded carbon/ graphite + PTFE + MoS ₂	TO.	Nobrac Carbon Ltd
K	Carbon/Graphite - High Carbon	1	CY2	Carbon/graphite	R.	Morganite Carbon Ltd
L	Carbon/Graphite - Low Carbon	1	EY9106	Electro-graphite ⁽¹²⁾	R.	Morganite Carbon Ltd
		2	CY9 ⁽⁶⁾	Carbon/graphite	R.	Morganite Carbon Ltd
M	Carbon/Graphite with Copper and Lead	1	MY3A	Carbon/graphite + copper	R.	Morganite Carbon Ltd
		2	MY3D	Carbon/graphite + copper + lead	R.	Morganite Carbon Ltd
N	Carbon/Graphite with Whitewall	1	MY104	Carbon/graphite + babbitt	R.	Morganite Carbon Ltd
		2	MY106	Carbon/graphite + antimony	R.	Morganite Carbon Ltd
O	Carbon/Graphite impregnated with a Thermoset	1	CY9C	Carbon/graphite impregnated with a thermoset	R.	Morganite Carbon Ltd
		2	M12	Carbon/graphite impregnated with a thermoset	TO.	Nobrac Carbon Ltd
P	Graphite impregnated Metal	1	Devn Metal (Irons)	Graphite filled metal ⁽¹⁰⁾ + MoS ₂	B. C. U. P. S. Sp. W.	The Universal Metallic Packing Co. Ltd
		2	Devn Metal (Bronzes)	Graphite filled metal ⁽¹⁰⁾ + MoS ₂	B. C. U. P. S. Sp. W.	The Universal Metallic Packing Co. Ltd

KEY

B	Bush
CU	Composite Unit - sleeve in a metal housing
HC	Hemispherical Cup
P	Plate
Pr	Profile - various standards or produced to order
R	Rod
Rd	Rod End Bearing
S	Strip
Sh	Sheet
Sl	Sleeve
Sp	Spherical Bearing
T	Tube
TD	No Standard Range Stocked - to order only
W	Washer

NOTES

- (1) Trade name of du Pont (U.K.) Ltd.
- (2) Can be used as a sleeve which is mounted by the user in a housing.
- (3) Trade name of Thomson Industries, Inc.
- (4) Trade name of The Dixon Corporation.
- (5) Plastic layer bonded to a metal back.
- (6) Not available or suitable as a thrust washer.
- (7) Various known as Fabroid and Fabrilube.
- (8) Spherical Bearing (9)



A Rod End Bearing



A Spherical Bearing

- (10) Metals used are bronze, lead bronze, tin bronze, iron and nickel.
- (11) Fiberglide and Fiberslip can be bonded to various materials e.g. steel.
- (12) Carbon content negligible.

and MIL-O-6081, Grade 1005, on which 48 and 24 gear sets were run, respectively. MIL-O-6081, Grade 1010, was run on only 6 gear sets (all of which failed) so no explicit parameters are given for that oil. Additional tests were run on MIL-O-6086 (4 sets), MIL-L-25336 (3 sets), MIL-L-6082 (3 sets), MIL-L-15016 (1 set) and MIL-L-2104 (1 set). Analysis of this data is left to the reader.

The model is one of those used for calculating "flash temperature". This term is perhaps unfortunate as it has been used by chemists in another sense, but it seems so well accepted in boundary lubrication that OECD (Rowe 1969) lists it with no alternative. However, they do show it with a double meaning. Note (1) of their definition #195 says "at areas of real contact", which is in line with AGMA usage. Note (3) says "may also mean the average temperature over a restricted contact area", which is appropriate to Equation (1) and the ASLE model. Thus, the two models have a common principle, but AGMA has implemented it in a far less naive way than did ASLE. Their model equation is:

$$T_f = T_b + \left[\frac{W_t}{F_e} \right]^{1/4} \left[\frac{50}{50 - Z_s} \right] \left[\frac{Z_t (n_p)^{1/4}}{(P_d)^{1/4}} \right] \quad (5.1-5)$$

Where:

T_f = flash temperature index, degrees F

T_b = initial temperature, degrees F (may be oil inlet)

W_t = effective tangential load, pounds

F_e = effective face width, inches

Z_s = surface finish, rms (after running in), μ inches

Z_t = scoring geometry factor

n_p = pinion rpm

P_d = diametral pitch, transverse operating

Z_t is a complicated function involving several angles, the tooth count on both gears, and the distance between gear centers. W_t is also somewhat complicated. It is the tooth loading tangential to the pitch circle, corrected for the sharing of load by more than one pair of teeth, and for three combinations of roll angles

By comparison with the goals set forth in detail below, the model lacks almost everything that a chemical engineer would desire. In addition to requiring laborious testing for each oil, it lacks any means for predicting the effect of changing metallurgy. In fact, the document does not even mention the alloy, heat treatment, hardness or thermal conductivity of the gears used,

though this information is accessible through AGMA. An annoying limitation is that the surface finish D_s must be measured or estimated after running-in; it has no clear-cut relation to the original surface finish D , and the user is advised to pick a number between 10 and 30, and then warned that his choice "will throw irregularity into the results." Since D_s is subtracted from 50, choosing 30 would give twice the temperature rise of that incurred by choosing 10. This corresponds to an allowable loading ratio of $2^{1.33}$ or 2.5 times as much load capacity with $D_s = 10$ as with $D_s = 30$. This is an acceptable engineering safety factor, but the logical extrapolation that gears of 50 micro-inch RMS finish will score under the most trivial loading is not.

The "flash temperature index" alone does not contain any lubricant parameter; that must be supplied from experimental data. For MIL-O-7808, the scoring risk is considered "low" up to $T_f = 276$, medium from 276 to 339, and high above that. The final conclusion, however, is based on a very sophisticated statistical analysis of the available data. The risks for both oils are shown in Figure 5.1-4, from which the designer can read them at once; "low" proves to be 5.5% probability, and "high" 30% probability. It is rather obliquely suggested that 10% probability could be used as a maximum design limit, but the actual choice is left open.

A simpler and older model is also described but not recommended; it is the "Scoring Index." It does not take into account nonstandard tooth proportions, nor does it have any parameter for lubricant quality:

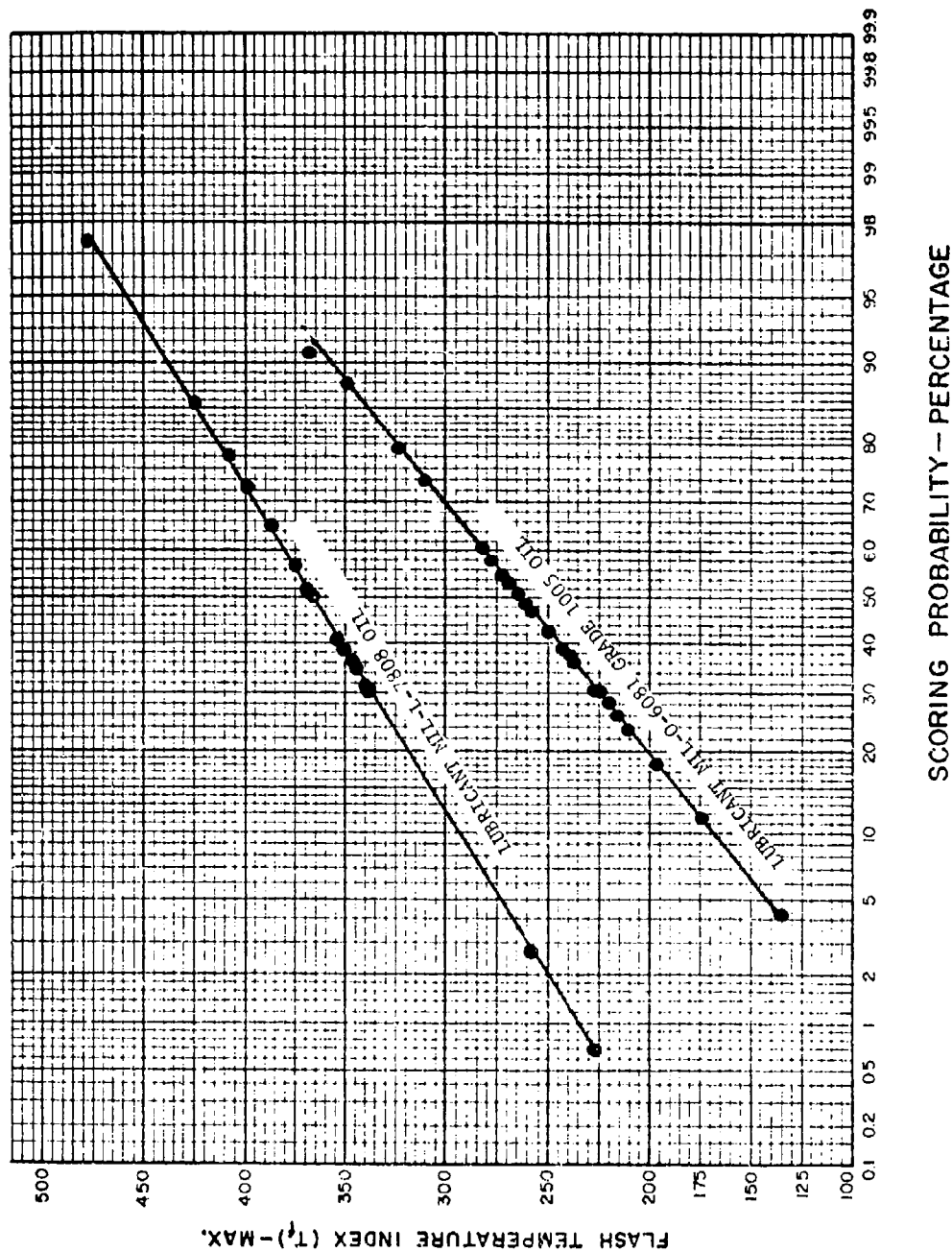
$$SI = \frac{(W_e/F_e)^{3/4} (n_p)}{(P_d)^{1/4}} \quad (5.1-6)$$

with symbols as in Equation (5.1-5). This equation is still recommended by ASLE, with the critical scoring index numbers shown in Table 5.1-II. Presumably Equation (5.1-5) would have been included by ASLE if it had been ready at the time their Handbook (O'Connor 1968) was written, several years before the date of publication.

TABLE 5.1-II Critical Scoring Index Numbers

Gear blank temp, F	100	150	200	250	300
Kind of oil	Critical scoring index numbers				
AGMA 1	9,000	6,000	3,000		
AGMA 3	11,000	8,000	5,000	5,000	2,000
AGMA 5	13,000	10,000	7,000	4,000	
AGMA 7	15,000	12,000	9,000	6,000	
AGMA 8A	17,000	14,000	11,000	8,000	
Grade 1065, MIL-O-6082B	15,000	12,000	9,000	6,000	
Grade 1010, MIL-O-6082B	12,000	9,000	6,000	2,000	
Synthetic (Turbo 35)	17,000	14,000	11,000	8,000	5,000
Synthetic MIL-L-7808D	15,000	12,000	9,000	6,000	5,000

FIGURE 5.1-4
SCORING PROBABILITY OF GEARS WITH DIFFERENT LUBRICANTS



5.2 New Concepts

Although the designers are not yet exploiting them, there are a number of published mathematical models for boundary lubrication which show promise of design value. They are summarized here for orientation and discussed in detail in the following sections.

EMPIRICAL MODEL - Model I was developed for design of office equipment. It offers two possible modes: IA predicts the load that can be supported without incurring appreciable wear for a pre-selected amount of travel (speed times time). Model IB predicts the wear rate under loads somewhat greater than IA, but still light by military standards. Both have completely developed geometrical concepts, but are very deficient in lubricant chemistry - including limitations on atmospheric humidity. Each includes two modes of wear: low transfer, probably due to sliding fatigue, and high transfer due to some form of metal/metal "adhesion" (MacGregor 1964).

REVERSIBLE CHEMISTRY MODEL - Model II is based on reversible chemistry and provides a means for varying the lubricant and metal properties over a wide range. It is used for moderate loads and can be shown to join Model I without any gap despite the very different forms of the equations. Its weakness is in failure to take into account irreversible chemistry such as oxidation of metals. Model IIA covers base stock only, IIB adsorbed gases only, and IIC additives dissolved in base stocks (Rowe 1966, 1967, 1970).

IRREVERSIBLE CHEMISTRY - Model IIIA provides for metal oxidation, but not for any sort of adsorption of lubricants and additives onto the metal or oxide. It has not been evaluated on metals other than steel, but it appears adaptable to all other easily oxidizable metals. It also contains a secondary potential for metals of low oxidation rate (Quinn 1967; Tao 1968A).

Model IIIB covers corrosion of the metal by additives of the extreme pressure (EP) class. Since this follows essentially the equations of Model IIIA, and is borderline to the scope of this STAF, it is given a fairly short treatment (Sakurai 1965, 1966, 1967, 1970).

Model IIIC represents catalytic decomposition of the base stock by freshly deformed metal. This results in polymerized base stock (usually hydrocarbon), hydrogen and metal carbides. Free radicals are intermediate products and may discharge their energy by several alternate pathways (Eischens 1969, Beerbower 1971A).

Model IIID requires the presence of a charge-transfer agent such as a polynuclear aromatic. Again, free radicals are produced, and one of their pathways is the formation of a surface resin containing oxygen and even nitrogen from the atmosphere. This is the newest, and perhaps most important, of the models (Goldblatt 1971).

Model IIIE covers the irreversible interaction of additives with metal, and particularly hydrated metal oxide surfaces. This reaction is probably limited to organic acids, but these may include acids formed by oxidation of the products of Models IIIC and IIID (Kreuz 1969).

METALLURGY - Model IV covers metallurgical compatibility and serves mainly to clarify conditions in which the metal pair is responsible for shifting the scuffing transition to higher loads. (Hildebrand 1950, Rabinowicz 1965B, 1971A).

MIXED FILM - Model V is a concept, still under quantitative development, in which the load is largely supported by the partial liquid film remaining in the valleys (anti-asperities) of the metal surface. Work has progressed far enough to state that moderately rough surfaces can be 99% supported by this hydrodynamic film and still be wearing at a significant rate. (Thompson 1972, Christensen 1971).

FATIGUE - Model VI involves fatigue due to rolling, as opposed to sliding fatigue in Model I, and the effect of additives on this failure mode. (Rounds 1962, 1967).

ABRASION - Model VII covers the effect and fate of wear particles generated by the above modes. (Khrushchov 1956-1965).

Several concepts which are extremely promising will require further work before they can be seriously considered for actual design use:

- Neither Model II nor III contains any means for adaptation to realistic geometries, but this can readily be transferred from Model I.
- Models IIIC and IIID are based on metal-organic interactions that have not been quantified to engineering mathematics. Both research and mathematical formalization will be required.
- Model V is being actively formalized by several groups, but has two gaps which need to be filled. First, it requires entering the roughness of the surfaces into the equations, and this depends on the history of the surfaces - the "as-received" roughness is largely wiped out during use, and no model seems available for computing the resulting roughness. Second, the interaction with Model III is of utmost importance as the surface resin reduces the roughness and thus decreases wear by lightening the load on the asperities. If this happens promptly enough, it will also decrease the amount of change in the metal topography; so an iterative solution is likely.
- Model VI is borderline to the project, being aimed only at predicting the effect of additives on anti-friction bearing fatigue. However, there is evidence that the optimum additives for gears may shorten the life of the bearings lubricated by a common source - but the extent of the problem is not yet clearly defined.

In the following sections, the models will be presented essentially as the authors prepared them, reduced to the common nomenclature of Appendix I. Where applicable, each sub-model will then be criticized on theoretical grounds. Next, such tests as have been feasible through the use of published data on ordinary lubrication will be presented and discussed. In Section 6, the models will be compared with one another, and preliminary steps taken towards combining them into a "mixed-mode" model. Applicability to explaining the anomalies will be tested in Section 7.

5.3 The Empirical Model for Zero and Finite Wear (Model I)

This model has a rather instructive history. It arose at the IBM Laboratories as the result of their accumulating a large amount of data to be used in the design of office equipment. Due to this end use, the experimenters studied wear and friction under lighter loads than commonly used, and came to the conclusion that operation on a wear-free basis for a selected lifetime could be achieved by proper selection of materials, with due attention to geometry. In order to handle this increasingly bulky set of data (eventually over 1500 data points) a scheme was devised to reduce the observations to a table of two parameters for each combination of slider metal, fixed plate material and lubricant (MacGregor 1964), plus the mechanical properties of the two solids.

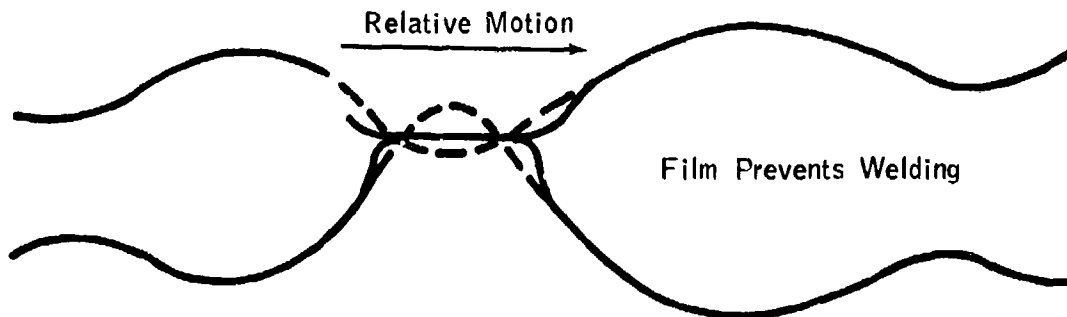
The tabulated parameters were the coefficient of friction, and a much less obvious one describing the mode of failure at the end of the zero-wear period. Two modes were designated as "high transfer" and "low transfer", and only recently have been assigned the more conventional names of "adhesive wear" and "fatigue wear" (Bayer 1962, 1968A). A third mode is described as "quasi-hydrodynamic", but it was not considered necessary to list any parameters for this condition in the tables.

The existence of a fatigue mode of wear between sliding surfaces was new and has been quite controversial, but it appears now to be both real and prevalent. It is distinct from the more generally accepted fatigue of rolling element bearings and is more closely related to the original observations of fatigue in flexed rods. In this case, continued elastic deformation of an asperity (Figure 5.3-1) leads to its eventual spalling off after a microcrack at its leading edge has propagated to a point where the friction force equals the tensile strength of the remaining metal. The writer's concept of this process is shown in Figure 5.3-2. While the originators of Model I disclaim anything other than an empirical approach, followed by recognition that their equation was consistent with the Palmgren function (Lundberg 1949), they must intuitively have used concepts compatible with Figure 5.3-2. Unfortunately, a peculiar jargon of terms, unfamiliar to lubrication engineers in general, accompanied this evolution.

More controversy has arisen from the fact that the model was presented without adequate warnings of its limits of applicability. One of these is implicit. When the equations are solved, it is found that allowable loads are quite small. Others appear in the tables which accompanied the principal publication (MacGregor 1964); only three metals were used as the ball in the Bowden-Leben type machines used for the test work, and no clear-cut means is provided for estimating the effect of using other metals for this vital part. The other materials were all used in the platen. In addition, only four grades of oil, and in many cases only three, plus dry sliding, are listed. No means was provided for estimating the effect of other lubricants. All changes from the ball and lubricant materials are to be handled by a worst-case assumption that they will result in adhesive wear.

Figure 5.3-1
SUCCESSFUL BOUNDARY LUBRICATION
WITH ELASTIC DEFORMATION ONLY - THE
"ZERO-WEAR" PERIOD

Vertical Scale Exaggerated
about 6X:

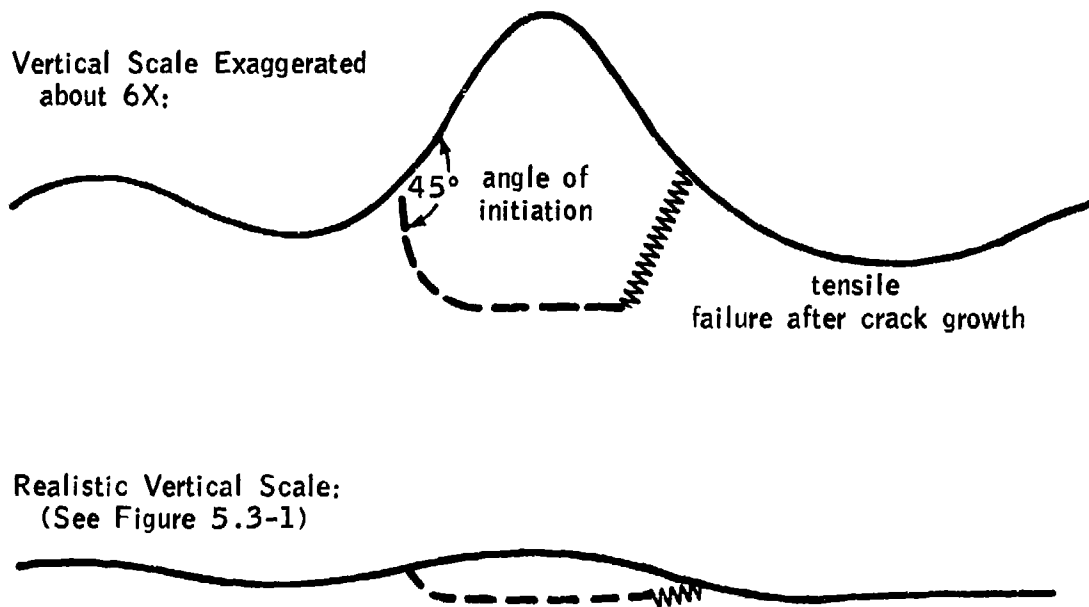


Realistic Vertical Scale:



Note: In this and similar drawings, the roughness is assumed to have a Gaussian distribution of asperity heights, corresponding to 4μ in rms and an average slope of 8° . Hence, the contact spot has a diameter of about 200μ in (5μ m), as discussed by Williamson (1968).

Figure 5.3-2
FAILURE OF AN ASPERITY BY ELASTIC
DEFORMATION (FATIGUE WEAR)



It is possible to adjust the model for different heat treatments of the same alloy, as the hardness is a third parameter. However, that requires assuming the coefficient of friction to be independent of the hardness. As discussed below in Section 5.12, this assumption is very hard to justify. The restricted choice of oils is very irksome to lubricant chemists (Table 5.3-I).

TABLE 5.3-I

LUBRICANTS USED IN DEVELOPING
MODEL I

OIL A: (Socony-Mobil Gargoyle PE 797)

Paraffinic base stock, 32 cst @ 100°F, with antioxidant and anti-rust.

Flash = 405, Pour = +20, Gravity = 33.0 API, VI = 105, Neut. No. = 0.05

OIL B: (Esso Standard Millicot K-50)

Naphthenic base stock, 85 cst @ 100°F, 1% tricresyl phosphate and about 0.04% of 200,000 M.W. (Staudinger) Polybutene.

OIL C: (Texaco MIL-0-5606)

Naphthenic base stock, 15 cst @ 100°F, 0.5% tricresyl phosphate, a zinc dialkyl dithiocarbamate and a benzothiazole, plus 5-10% of polymethacrylate (Private communication from R. S. Fein, May 17, 1971).

Flash = 200, Pour = -75, Gravity = 1.15/1.18 sp. gr., VI = 188.

OIL D:

OIL A + 0.1 wt. % Stearic acid.

Another limitation that is clearly expressed is that sliding velocities must not be high enough to generate a temperature rise that would affect the parameters. Although it has not been published, the IBM workers have determined that suitable parameters can be obtained by heating the test machine to the anticipated temperature rise (Bayer 1970). Metal properties do not change much, but those of plastics do. Coefficients of friction tend to be lower under the "high speed" conditions.

The most serious restriction of all is that the published data were all obtained at 10% relative humidity (Bayer 1962). They are not generally applicable at humidities greater than 35%, but this was not recognized until about 1969 and has just been published (Vaessen 1971). It will be discussed in Section 5.3.3.

As a result of these limitations and the way they were expressed, in unfamiliar terms and by casual mention in the articles, lubrication engineers have tended to be very critical of Model IA. Actually, the criticism seems to be based on attempts to use it completely outside its limitations, both expressed and unexpressed. It is the feeling of the writer that such an attitude is quite unsound; instead, it is much more to the point to find out what is good about Model I that permits it to correlate all the observations on 520 systems, and then to try various means towards generalizing it. The authors (Bayer 1970) do not plan to extend the model as it already serves its purpose at IBM. However, they suggest that anyone interested in doing so could prepare tables for other temperatures and humidities. Plastics in particular need such special handling.

5.3.1 Analysis for Zero-Wear (Model IA)

All of Model I is tied to a concept of unit travel called a "pass" and defined as the distance of sliding equal to the Hertz contact area dimension in the direction of motion. Model IA uses the criterion for zero wear that the maximum shear stress in the contact area τ_{\max} must be smaller than a certain fraction, G , of the yield stress in shear of the material, τ_y . Hence, the following inequality defines "zero wear conditions":

$$\tau_{\max} \leq G \tau_y \quad (5.3-1)$$

When the number of passes (N) is 2000, G has the reference value G_R . G_R can have one of three possible values, depending on the materials and lubricant. For full hydrodynamic lubrication $G_R = 1.00$. For boundary lubrication $G_R = 0.54$ designates systems with low susceptibility to transfer and $G_R = 0.20$ for those with high susceptibility. No systems showing G_R values intermediate between 0.20 and 0.54 have ever been detected, indicating that these represent different sub-regimes. Values of G_R are tabulated for over 500 systems, and for unlisted systems $G_R = 0.20$ is usually assumed. For $N \geq 2000$ passes

$$G = G_R \left(\frac{2000}{N} \right)^{1/9} \quad (5.3-2)$$

It must be realized that these two values of G_R can lead to very much wider differences in design than just their ratio of 2.7, which applies only to the Hertzian stress. In terms of allowable load, the ratio is $(2.7)^3 = 19.5$, or in zero-wear life at a given load it is $(2.7)^9 = 131,136$. Thus, a false assumption of $G_R = 0.20$ leads to a very conservative design, and a more certain means for selection is highly desirable. Scanning MacGregor's Table III-3, we find that the lubricant tends to dominate the situation, as shown in Table 5.3-II. Essentially all unlubricated systems fail by adhesive wear, and all stearic acid solution lubricated systems by fatigue. Beyond that, the pattern is less clear.

TABLE 5.3-II
Effect of Materials on Mode of Wear
(Ratio of Fatigue Mode to Total Tests)

Alloys in Platen								
<u>Ball</u>	<u>Lubricant</u>	<u>Stainless</u>	<u>Steel</u>	<u>Nickel</u>	<u>Copper</u>	<u>Aluminum</u>	<u>Total</u>	<u>% Total</u>
52100	None	0/7	1/20	0/3	0/3	0/6	1/39	2.5
	A	2/7	9/20	0/3	2/3	6/6	19/39	48.5
	B	3/7	10/20	2/3	2/3	4/6	21/39	54.0
	C	0/7	4/20	0/3	2/3	3/6	10/39	25.5
	D	4/4	13/13	0/0	3/3	6/6	26/26	100.0
302SS	None	0/7	1/19	0/3	0/3	0/6	1/38	2.5
	A	6/7	12/19	0/3	2/3	5/6	25/38	66.0
	B	5/7	13/18	0/3	1/3	6/6	25/37	67.5
	C	3/7	7/18	0/3	2/3	5/6	17/37	46.0
	D	4/7	13/13	0/0	2/2	6/6	24/24	100.0
BRASS	None	0/7	0/19	0/3	0/3	0/6	0/38	0.0
	A	0/7	0/19	1/3	1/3	2/6	4/38	10.5
	B	4/7	10/19	3/3	2/3	1/6	20/38	52.5
	C	0/7	0/19	0/3	2/3	0/6	2/38	5.5
	D	1/1	9/9	0/0	0/0	0/0	10/10	100.0

It is evident that the mode of failure is highly dependent on both ball and platen metallurgy. The three oils might be expected to line up according to their tricresyl phosphate content B C A, but actually come closer to their viscosity ranking B A C. It appears that the numbers from which Table 5.3-II was compiled still contain some hydrodynamic lifting, despite the authors' efforts to screen this out into the $G_R = 1.00$ mode. Recent advances in this area are discussed below, in Section 5.7.

Use of the model is by stepwise calculation. First, the contact stress τ_{\max} is calculated from the Hertz formula appropriate to the geometry, the load, the radii of curvature, the Young's modulus and Poisson's ratio of the materials, and the coefficient of friction of the system, F. A stress concentration factor may be used to correct the Hertz formula for sharp corners, and non-Hertz cases can also be handled. A very ingenious system is provided for handling plated, case-hardened and other nonhomogeneous materials. Values of F must be looked up from the same table as G_R , obtained experimentally or estimated by analogy from listed systems. As will be discussed below, this estimate must be made with care, as an error at this point can have unexpectedly large consequences.

The number of passes for zero wear (N_0) may be estimated by combining Inequality (5.3-1) with Equation (5.3-2):

$$N_0 = 2000 \left(\frac{\tau_y G_R}{\tau_{\max}} \right)^9 \quad (5.3-3)$$

However, the lifetime of each member must be considered separately. For the "fixed spot" member, on which the contact spot does not move, the zero-wear travel d_0 in inches of relative travel is given by

$$d_0 = SL_0 = HN_0 \quad (5.3-4)$$

where H is the length of the Hertz contact spot in the direction of travel, S the distance traveled per revolution or stroke and L_0 the lifetime in revolutions or strokes.

For the "moving spot" member, on which the contact spot keeps moving,

$$d_0 = SL_0 = SN_0 \quad (5.3-5)$$

The lower of these d_0 values is taken as the lifetime of the system.

The equation for the sphere is

$$\tau_{\max} = q_0 \sqrt{(1 - 2\nu_0)^2 \frac{16}{3} + F^2} \quad (5.3-6)$$

where q_0 is the maximum stress in the τ_{\max} Hertz contact area and ν_1 is Poisson's ratio for the metal of the sphere. For this geometry

$$q_0 = \left[\frac{6W}{\pi \left[\frac{1-\nu_1^2}{E_1} + \frac{1-\nu_2^2}{E_2} \right] r^2} \right]^{1/3} \quad (5.3-7)$$

where W is the load, E_1 , and E_2 are Young's modulus for sphere and plane, and r is the radius of the sphere. By definition

$$q_0 = 6 W/H^2 \quad (5.3-8)$$

where H is the Hertz dimension in the direction of travel.

Combining all these equations,

$$d_o = \frac{2000(\tau_y G_R)^{0.9} 1.06}{(\sqrt{(1-2\nu_1)^2/16 + F^2})^9 (6W)^{2.67} (E')^{6.34}} \quad (5.3-9)$$

where

$$1/E' \equiv (1-\nu_1^2)/E_1 + (1-\nu_2^2)/E_2$$

As Poisson's ratio is usually about 1/3, the first term in the denominator of Equation (5.3-9) can be approximated by

$$(0.007 + F^2)^{4.5}$$

This simplification helps to illustrate the serious consequences of mis-estimating F . Taking the example of a copper ball on 52100 steel used by Beerbower (1971A) and discussed briefly in 5.3.2, an error of 0.01 in F leads to an 18-fold change in d_o . Mathematical methods for estimating F are discussed in some detail in 5.12.

Equation (5.3-9) also demonstrates the approximate equivalence of Model IA to the Palmgren (Lundberg 1949) function $d_o W^3 = \text{constant}$ since F is assumed to be a constant for any given combination of materials, regardless of load and geometry. Thus, Model IA has the correct dimensional relationship for a fatigue failure; its application to adhesive failure must, at this point, be regarded as empirical.

The fact that "zero-wear" periods are rarely reported in the adhesive mode probably reflects the relatively low d_o values which could easily be missed. The IBM workers observed this to happen in 313 cases (out of 520), which should be proof enough of the reality of the phenomenon.

This model is given a brief numerical evaluation in Section 5.3.2. For the present, it can be concluded that Model IA is useful in locating point A in Figure 2-1 but needs generalization for higher speeds and humidities. It also needs more reliable methods for estimating G_R and F (see Section 5.12).

5.3.2 Testing Model IA

Tests were built around using the data obtained by Rowe (1966) in developing Model II. This involved similar geometry and many other factors in common. It was not realized at first, but the low humidity was also important. Two differences did cause some concern; Rowe loaded his machine more heavily than Bayer would have, and he conducted his test in a nitrogen atmosphere. The latter proved to be of little significance as Bayer reported his wear to be largely metallic, so his dry air had little corrosive effect in the Model III sense.

The results have already been published (Beerbower 1971A), and it would not be valuable to go through them in great detail. A computer was programmed to print out the zero-wear distance for various loads and coefficients of friction; the results are shown in Table 5.3-III. It was rather disappointing to find that these distances were so short Rowe would scarcely have observed them. Fortunately, another set of data turned up at the last moment. Vaessen and de Gee (1971) had mentioned these tests to the writer during a visit to their laboratory. Their data are shown in Table 5.3-IV. While they do not coincide 100% with Model IA, it is evident that they achieved satisfactory predictions only if the humidity at their test machine was kept as low as that in the IBM laboratory. Their data are too fragmentary to serve this purpose, but it is evident that they have established the need for a substantial increase in the scope of Model I. It will be necessary to provide some sort of tabulation of the "critical relative humidity" for various metals, above which they are coated with a film of water which is presumably bound by the corrosion products. Table 5.3-V shows the observations of Vaessen and de Gee, in comparison with those of Hudson (1929). It also appears that fatigue failure may well show a proportionate response to relative humidity, through hydrogen embrittlement, on hard steels but not on most other metals (Berry 1967). The water is not "anomalous" but is simply bound to the oxides (Dal 1965) as confirmed by interviewing J. P. Roberts.

Comparison of Model IA with Appeldoorn's (1967A) data on 13 pure hydrocarbons in air at $50 \pm 15\%$ RH proved very conclusively that the model is not applicable to steel at that humidity. Out of 72 points, 28 were predicted for zero wear, and none were observed. Oil selection was not a problem, as actual F values were used. The details are shown in Table 5.3-VI.

The writer published the results of the latter tests as comments on the Vaessen and de Gee paper (Beerbower 1971F). The authors responded with essentially a fresh development of Model IA, "in a classical manner". Changed to the symbols of this STAF, they proceed from the premise that surface fatigue is the main process, and any other modes mentioned are merely tendencies during the zero-wear period. Hence, all contacts are elastic (cf. Figure 5.3-1), which implies polymeric or very lightly loaded metal surfaces.

TABLE 5.3-III

PREDICTED ZERO-WEAR TRAVEL (inches)
FOR COPPER BALL ON STEEL DISK

Coefficient of Friction (F):	Load (W) Pounds						
	.08	.16	.24	.32	.40	.48	.56
.001	286.	4.63	0.205	1.88×10^{-2}	2.78×10^{-3}	5.68×10^{-9}	1.46×10^{-4}
.004	7.10	0.115	2.08×10^{-3}	4.66×10^{-4}	6.89×10^{-5}	1.41×10^{-5}	3.63×10^{-6}
.015	0.209	3.38×10^{-3}	1.50×10^{-4}	1.37×10^{-5}	2.03×10^{-6}	4.15×10^{-7}	1.16×10^{-6}
.065	4.19×10^{-3}	6.78×10^{-5}	3.09×10^{-6}	2.75×10^{-7}	4.06×10^{-8}	8.31×10^{-9}	2.14×10^{-5}
.250	1.15×10^{-4}	1.86×10^{-6}	8.24×10^{-8}	7.57×10^{-9}	1.12×10^{-9}	2.29×10^{-10}	5.90×10^{-11}
							1.81×10^{-11}

NOTE: All values below the line are unreliable (Bayer 1970) since the zero-wear travel (d_0) is less than the Hertz spot diameter (H).

TABLE 5.3-IV

NOBLE METAL ALLOY TESTS OF ZERO-WEAR MODEL

Pin = 70% Ag, 20% Au, 10% Cu; Disc = 55% Cu, 18% Ni, 27% Zn

Test duration = 72 hrs

<u>LOAD</u> <u>(gms)</u>	<u>WEAR RATE OF</u> <u>PIN ($\mu\text{m/hr}$)</u>	<u>ZERO-WEAR PERIOD</u> <u>(hrs)</u>	<u>COEFFICIENT</u> <u>OF FRICTION (F)</u>	<u>PREDICTED</u> <u>ZERO-WEAR (hrs)</u>
Relative Humidity = 0%				
7	<0.01	>72	-	1820
8	<0.01	>72	-	530
10	0.7	3	0.8 \pm 0.6	72
15	1.8	1	0.8 \pm 0.6	2
40	2.4	<0.02	0.6	3.10 ⁻⁴
60	4.1	<0.02	0.6	8.10 ⁻⁶
Relative Humidity = 60%				
20	<0.01	>72	0.6	57000
30	<0.01	>72	0.6	1520
40	<0.01	>72	0.6	110
50	42	9	0.6 \pm 0.5	15
60	50	0.5	0.5	3
70	62	0.5	0.5	0.75

TABLE 5.3-V

CRITICAL RELATIVE HUMIDITIES OF ALLOYS

<u>Alloy Composition</u>	<u>Critical RH</u>	<u>2% Weight Gain</u>	<u>Method and Reference</u>
55 Cu, 18 Ni, 27 Zn	55%	-	Wear Test (Vaessen 1971)
90 Cu, 9.5 Sn, 0.5P	45	-	"
85 Cu, 15 Zn	35	-	"
70 Ag, 20 Au, 10 Cu	55	-	"
99.9 Cu	30	-	"
70 Cu, 30 Zn	60	70	Weight gain (Hudson 1929)
60 Cu, 40 Zn	~60	75	"
70 Ni, 30 Cu	~60	75	"
Zn	~75	80	"
Cu	~75	80	"
Al	~80	95+	"
Ni*	42	60	"
Ni	65	70	"
80 Ni, 20 Cr	65	70	"
80 Cu, 20 Ni	70	75-80	"
Fe	~80	~100	"

TABLE 5.3-VI

ZERO-WEAR PREDICTIONS ON PURE
HYDROCARBONS

<u>Code</u>	<u>Hydrocarbon</u>	<u>Load (grams)</u>						
		<u>30</u>	<u>60</u>	<u>120</u>	<u>240</u>	<u>480</u>	<u>1000</u>	<u>2000</u>
1	n-Octane	-	-	-	-	-		
2	n-Nonane	- *	+	-	-			
3	n-Butylbenzene	-	-	-	-	-	-	
4	Diethyl cyclohexane	-	-	-	-	-		
5	n-Dodecane	+	+	+	-	-		
6	Tetralin	+	+	+	-	-		
7	Decalin	+	+	-	-	-	-	
8	1-Methyl naphthalene	+	+	+	-	-		
9	1-Hexadecene	+	+	+	-	-	-	-
10	n-Hexadecane	+	+	+	+	-	-	
11	Heptamethyl nonane	+	+	+	-	-	-	
12	i-Propyl bihexyl	+	+	+	-	-		
13	Dimethano decalin	+	+	+	-	-		

Code: + predicted zero-wear, not observed
- predicted finite wear, observed.

Materials: 52100 steel ball on 52100 steel cylinder

Conditions: 50±15% relative humidity air, 240 rpm, 32 minutes.

*Reversal due to an abnormally high F value at 30 gm.

Most materials show surface fatigue in 10^3 to 10^4 cycles if $\tau_{\max} = \alpha\tau_y$ for $0.95 < \alpha < 1.00$. However, we must consider that on a microscale the true asperity stress ($\bar{\tau}_{\max}$) is greater than the mean τ_{\max} used by Bayer by a stress concentration factor (ψ) so that

$$\bar{\tau}_{\max} = \psi \tau_{\max} \quad (5.3-10)$$

If, for a certain material, N is the endurance for $\bar{\tau}_{\max} = \alpha\tau_y$, then

$$\bar{\tau}_{\max} = \alpha\tau_y / \psi \quad (5.3-11)$$

Applying the Lundberg-Palmgren (1949) relation

$$N_o = N \left(\frac{\alpha\tau_y}{\psi\tau_{\max}} \right)^9 \quad (5.3-12)$$

where the exponent 9 is a rough value. This is identical to (5.3-3) if $G_R = \alpha/\psi$ and $N = 2000$. Because of the 9th power, the value of N is not very critical, and use of (say) 16000, about the upper limit of cycles to failure, τ_{\max} increases not more than 26%. Thus, 2000 is a plausible value, and Model IA is no longer empirical.

The reason for G_R values clustering around 0.2 and 0.5 must lie in the adhesive bonding tendency of the materials. The authors feel that every dry system starts running with G_R around 0.5 (or $\psi \approx 2$). If adhesion is high, transfer takes place in the first few passes. Even if continued transfer is prevented (as by oxidation) the result will be a drastic increase in ψ . It seems reasonable that ψ would level off at about 5; hence, $G_R \approx 0.20$ is the result. If this does not happen, adhesive wear takes over and fatigue never "gets a chance" to become the principal mode of wear.

They end "A consequence of this reasoning is that, in each system with $G_R \approx 0.2$, it must be possible to find evidence of weld formation and transfer after a small number of passes. Further, although it is reasonable to assume that the usual machining processes all result in roughly the same "start" value of $\psi \approx 2$, it should be possible to produce surfaces with higher ψ values by machining alone. We recommend that future research aimed at clarification of the model, should be performed along these lines."

5.3.3 Analysis of Finite Wear (Model IB)

The end of the zero-wear period represents an abrupt transition into another regime. The criteria already discussed are used to classify this into one or the other of the two modes - fatigue with $G_R = 0.54$ or adhesive with $G_R = 0.20$. However, it is quite possible for the mode to change almost immediately after finite wear starts on a ball, since the contact geometry soon becomes flat-on-flat.

Under fairly light loads, this can cause a shift from adhesive to fatigue wear, so that an experiment may be necessary to avoid a very serious error in prediction. A shift from fatigue to adhesion is highly improbable.

It must be recognized at the start that only one of the surfaces is expected to show finite wear, while the other one is expected to remain in the zero-wear condition described in Equation (5.3-1). The wear on the first surface is predicted by a differential equation which is basically a statement that wear is a function of the energy dissipated per pass:

$$d[A_t/\tau_{\max} W^{0.2}] = C' dN \quad (5.3-13)$$

This equation can be integrated only for specific situations, of which only the Bowden-Leben type machine used at IBM will be illustrated. Converting A_t , the cross-sectional area of the wear track, to the more useful wear track width (in this case, equal to ball scar diameter) is done by an approximation based on a triangular area formula

$$A_t \approx \frac{w^3}{16r} \quad (5.3-14)$$

Wear on the ball results in a flat-to-flat geometry, so that

$$\tau_{\max} H = \frac{4W(0.25 + F^2)^{0.5}}{\pi w} \quad (5.3-15)$$

Making these substitutions and integrating for ball wear,

$$w = C(LrS)^{0.118} W^{0.530} (0.25 + F^2)^{0.265} \quad (5.3-16)$$

where C includes the original C' times several numerical constants. Neither C' nor C can be developed directly from material properties.

By establishing a formalization of the definition of zero wear, it is possible to establish a useful relationship between Models IA and IB. This is done by defining the depth of the "zero" wear scar as half the surface roughness, D. From this and the triangle approximation, the zero wear scar width

$$w_0 = (8rD)^{1/2} \quad (5.3-17)$$

Assuming that all the other factors in Equation (5.3-16) remain constant,

$$w = w_0 (L/L_0)^{0.118} \quad (5.3-18)$$

For platen wear the exponent becomes 0.133; for adhesive wear of the ball, 0.250 and of the platen 0.333.

These exponents may be converted to a volume/distance wear rate for comparison with Equation (5.1-4) and other models, by using an approximate formula for ball wear:

$$V \approx \pi w^4 / 64r \quad (5.3-19)$$

where r is the ball radius. Combining this with Equations (5.3-4, 6, 8 and 18) results in the working equation for fatigue wear on the ball:

$$(V/d) = 4.80 \times 10^{-3} \frac{D_W^{1.26} (E')^3 [(1 - 2\nu_1)/16 + F^2]^{2.12}}{d^{0.528} r^2 (\tau_y G_r)^{4.25}} \quad (5.3-20)$$

Similar equations may be built up for ball adhesive wear, and platen wear in both modes. All resemble (5.3-20) except for the exponents. Both adhesive situations have d to the 0 power, as in Equation (5.1-4), but they do not have W to the first power due to involvement of F . This is discussed further in 6.1.

Bayer demonstrated that L_0 is independent of surface finish (1962). It is proper to substitute the L_0 value obtained from Equation (5.3-1) into Equation (5.3-14) as this point represents the intersection of the zero wear line with the finite wear curve. This is a discontinuity, where the ball ceases to have a spherical contact on the plane. Another discontinuity comes when the second member starts to wear, and Equation (5.3-14) is not applicable above this point.

It is evident that Equation (5.3-20) shows a much greater dependence of wear on surface finish than most investigators find in the boundary regimes (de Gee 1969). Bayer's tying D to the coarser surface (1968A) has been reconsidered and the writer believes it best to use the roughness of the surface expected to first show wear. This is necessary by the definition (5.3-14) and is compatible with the general nature of adhesive wear. It is important to use peak-to-valley (PTV) values for D . If only root-mean-square (RMS) values are available, they must be multiplied by $2\sqrt{2}$ (Beerbower 1971A), if the surface is assumed to be sinusoidal as was done in all calculations in this STAF. Akin (1971) uses an empirical factor of 4.5 for less idealized surfaces, and also a factor of 5.4 for center line average (CLA) values (personal communication, March 14, 1972).

There is a case in which the roughness of the nonwearing surface is significant, but it is so special as to be outside the scope of this study. It is usually the result of very poor design in which the harder member acts as a file on the softer one. This is known as "two-body abrasive wear", and is set aside. However, the similar case in which hard foreign matter embeds in one surface to create the "file" is covered in 5.9.

At this point it is necessary to look again at the definitions of "anomalous". Figure 2-1 is predicated on the idea, expressed in Equation (5.1-4), of a wear rate that does not vary with time. Fatigue wear as described above varies as the -0.528 or -0.60 power of the distance (or time at any constant velocity) counted from the start of finite wear. Prior to that, it is "zero" as defined in Equation (5.3-17). Rather than to attempt to broaden the concept of Figure 2-1 to accommodate this special case, it seems preferable to live with the fact that in fatigue mode "wear rate" must imply "relative to the standard lubricant, in fatigue mode, after the same distance of travel."

5.3.4 Testing Model IB

The finite wear Model IB was screened against the same three sets of data. Table 5.3-VII has already been published (Beerbower 1971B) and need not be further discussed, but the comparison with Rowe's (1966) data in Figure 5.3-3 is new. This plot required a little thought, as Rowe did not report details such as individual run length. Hence, the lines for Model IB represent about the upper and lower limits of his experiments (39,000 and 390,000 inches in Table 5.3-VII). The upper limit of Bayer's criterion $d \leq H$ falls below Rowe's lowest load, but his correlation line was transferred (along with most of his points) to Figure 5.3-3. The worst problem was that when the fatigue constants ($G_R = 0.54$ and exponent = 0.118) were used, predictions were far too low; when the high transfer constants ($G_R = 0.20$ and exponent = 0.250) were used, predictions were too high. Bayer was consulted by phone; he had encountered cases where the zero wear period was high-transfer and the change to finite wear also produced a change to fatigue mode. The reverse (fatigue to transfer) was most unlikely. The combination $G_R = 0.20$ and exponent = 0.118 proved an excellent fit to the data, as shown in Figure 5.3-3. While this is plausible, it does represent one more caution on Model I that had never been published.

The Vaessen and de Gee (1971) data are too limited for a numerical comparison, but again the low RH predictions seem to be about right.

The Appeldoorn (1967A) data, as might be expected from Model IA, were completely different from the predictions. At low loads, wear rates were several thousand times those predicted. The gap narrowed until at about 1000 grams load (incipient scuffing) the predicted and actual lines crossed. Thus, not only was the model inapplicable, but apparently a mixed mode existed. This is discussed further below. (see 6.3 and 7.12).

At present, we can only conclude, as before, that Model I is adequate for 10-30% RH, and capable of expansion.

5.4 Adhesive Wear (Model II)

It is evident from Section 5.3.1 that a value of G_R (the allowable fraction of yield stress for a zero-wear life of 2000 passes) = 0.2 means adhesive wear, but in symbols more appropriate to the fatigue mode. It might even be considered to be a way of expressing the negative anomalies from that mode, just as $0.54 < G_R < 1.00$ expresses the positive anomalies, due to quasi-hydrodynamic lubrication.

The main line of development of the adhesive mode goes back to Bowden and Tabor (1950), though its primary source is lost in antiquity. Their laboratory work led Archard (1956) to formulate Equation (5.1-4). The development of this is instructive enough to justify pausing for a brief review. The original assumption was that the asperities are plastically deformed by the load. However, this was quite illogical and an alternative derivation based on elastic deformation of a surface covered with asperities of random height was shown to yield results which are at least dimensionally consistent.

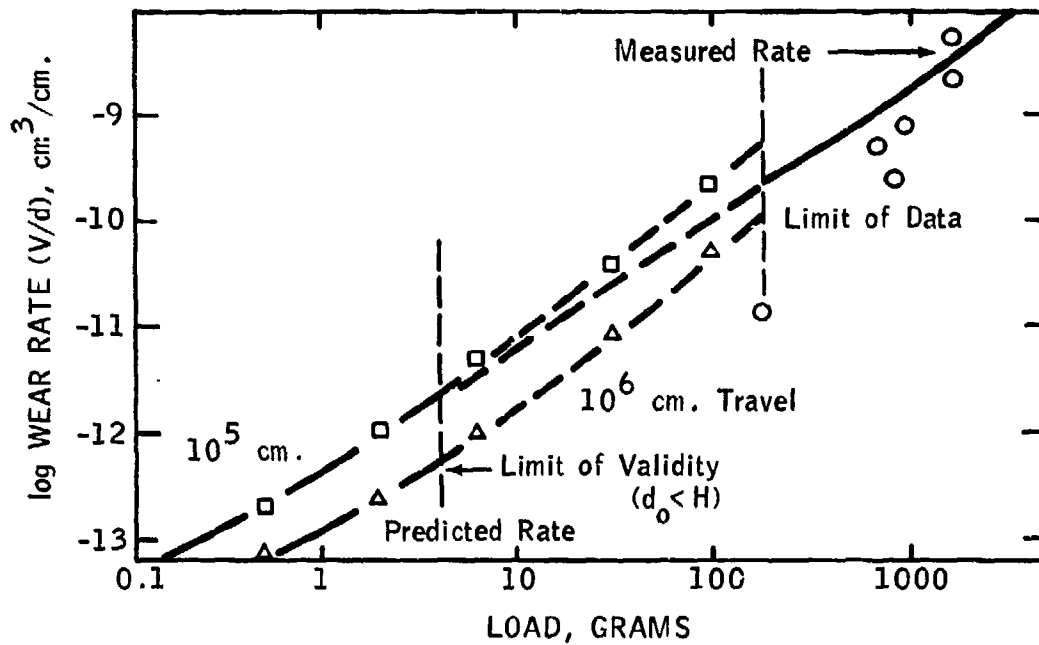
TABLE 5.3-VII

PREDICTED WEAR RATES
FOR MODEL IB (cm³/cm)

Load (gms)	Sliding Distance (cm)	Coefficient of Friction (F)							
		.08	.16	.24	.32	.40	.48	.56	.64
0.45	10 ⁴	1.8 x 10 ⁻¹⁴	1.2 x 10 ⁻¹³	7.1 x 10 ⁻¹³	2.2 x 10 ⁻¹²	4.6 x 10 ⁻¹²	9.4 x 10 ⁻¹²	1.7 x 10 ⁻¹¹	2.9 x 10 ⁻¹¹
1.8	10 ⁴	1.0 x 10 ⁻¹³	7.2 x 10 ⁻¹³	3.7 x 10 ⁻¹²	1.0 x 10 ⁻¹¹	2.4 x 10 ⁻¹¹	5.0 x 10 ⁻¹¹	9.5 x 10 ⁻¹¹	1.6 x 10 ⁻¹⁰
6.8	10 ⁴	7.4 x 10 ⁻¹³	4.3 x 10 ⁻¹²	1.7 x 10 ⁻¹¹	5.1 x 10 ⁻¹¹	1.2 x 10 ⁻¹⁰	2.6 x 10 ⁻¹⁰	5.0 x 10 ⁻¹⁰	8.7 x 10 ⁻¹⁰
29.5	10 ⁴	4.3 x 10 ⁻¹²	2.4 x 10 ⁻¹¹	1.0 x 10 ⁻¹⁰	3.2 x 10 ⁻¹⁰	7.8 x 10 ⁻¹⁰	1.7 x 10 ⁻⁹	3.2 x 10 ⁻⁹	5.5 x 10 ⁻⁹
113.5	10 ⁴	1.8 x 10 ⁻¹¹	1.3 x 10 ⁻¹⁰	5.6 x 10 ⁻¹⁰	1.7 x 10 ⁻⁹	4.3 x 10 ⁻⁹	9.2 x 10 ⁻⁹	1.8 x 10 ⁻⁸	3.1 x 10 ⁻⁸
0.45	10 ⁵	4.6 x 10 ⁻¹⁴	5.1 x 10 ⁻¹⁴	2.1 x 10 ⁻¹³	5.2 x 10 ⁻¹³	1.3 x 10 ⁻¹²	2.6 x 10 ⁻¹²	4.8 x 10 ⁻¹²	8.6 x 10 ⁻¹²
1.8	10 ⁵	1.0 x 10 ⁻¹³	2.5 x 10 ⁻¹³	9.8 x 10 ⁻¹³	2.9 x 10 ⁻¹²	7.0 x 10 ⁻¹²	1.5 x 10 ⁻¹¹	2.8 x 10 ⁻¹¹	4.9 x 10 ⁻¹¹
6.8	10 ⁵	1.7 x 10 ⁻¹³	1.1 x 10 ⁻¹²	4.8 x 10 ⁻¹²	1.5 x 10 ⁻¹¹	3.7 x 10 ⁻¹¹	7.8 x 10 ⁻¹¹	1.5 x 10 ⁻¹⁰	2.6 x 10 ⁻¹⁰
29.5	10 ⁵	1.1 x 10 ⁻¹²	7.0 x 10 ⁻¹²	3.0 x 10 ⁻¹¹	9.4 x 10 ⁻¹¹	2.3 x 10 ⁻¹⁰	5.0 x 10 ⁻¹⁰	9.5 x 10 ⁻¹⁰	1.7 x 10 ⁻⁹
113.5	10 ⁵	5.5 x 10 ⁻¹²	3.8 x 10 ⁻¹¹	1.7 x 10 ⁻¹⁰	5.2 x 10 ⁻¹⁰	1.3 x 10 ⁻⁹	2.8 x 10 ⁻⁹	5.3 x 10 ⁻⁹	9.4 x 10 ⁻⁹
0.45	10 ⁶	6.5 x 10 ⁻¹⁵	1.4 x 10 ⁻¹⁴	5.2 x 10 ⁻¹⁴	1.6 x 10 ⁻¹³	3.6 x 10 ⁻¹³	7.6 x 10 ⁻¹³	1.5 x 10 ⁻¹²	2.5 x 10 ⁻¹²
1.8	10 ⁶	1.7 x 10 ⁻¹⁴	6.9 x 10 ⁻¹⁴	2.7 x 10 ⁻¹³	8.3 x 10 ⁻¹³	2.1 x 10 ⁻¹²	4.4 x 10 ⁻¹²	8.3 x 10 ⁻¹²	1.4 x 10 ⁻¹¹
6.8	10 ⁶	5.0 x 10 ⁻¹⁴	3.3 x 10 ⁻¹³	1.4 x 10 ⁻¹²	4.4 x 10 ⁻¹²	1.1 x 10 ⁻¹¹	2.3 x 10 ⁻¹¹	4.4 x 10 ⁻¹¹	7.7 x 10 ⁻¹¹
29.5	10 ⁶	3.0 x 10 ⁻¹³	2.1 x 10 ⁻¹²	9.1 x 10 ⁻¹²	2.8 x 10 ⁻¹¹	7.0 x 10 ⁻¹¹	1.5 x 10 ⁻¹⁰	2.8 x 10 ⁻¹⁰	5.0 x 10 ⁻¹⁰
113.5	10 ⁶	1.6 x 10 ⁻¹²	1.1 x 10 ⁻¹¹	5.0 x 10 ⁻¹¹	1.6 x 10 ⁻¹⁰	3.9 x 10 ⁻¹⁰	8.4 x 10 ⁻¹⁰	1.6 x 10 ⁻⁹	3.0 x 10 ⁻⁹

Note: All values below the line are unreliable (Bayer 1970) since the zero-wear travel (d_0) is less than the Hertz spot diameter (H).

Figure 5.3-3
COMPARISON OF MEASURED AND PREDICTED WEAR RATES -
COPPER SPHERE ON STEEL DISK, $F = 0.25 \pm 0.01$



- Legend
-
- Predicted by Model IB for 10⁵ cm. travel
 - △ Predicted by Model IB for 10⁶ cm. travel
 - Actual wear rate measured by Rowe (1966)

The plastic model gives as the true area of contact W/P_m , where P_m is the hardness (i.e., the yield stress in compression under penetration hardness geometry). The adhered junctions formed by the deformation are assumed to have a consistent shear strength per unit area (τ_y) which creates the force due to friction, the coefficient of friction

$$F = \tau_y / P_m \quad (5.4-1)$$

which is consistent with Amontons' law since F is independent of load and apparent contact area, and dependent only on material properties.

From the same concept comes the wear model, by assuming that these junctions are sometimes stronger than the bulk material. This is justified on the basis that the surface is work-hardened while there are stress cracks beneath this "Bielby layer". Then, if each encounter produces a wear particle, as shown in Figures 5.4-1 through 5.4-4, the wear volume (V) will be proportional to the distance traveled (d) and the true area of contact (W/P_m). This is the source of Equation (5.1-4), $(V/d) = KW/P_m$. The constant K has come to be known as the "specific wear rate". If the wear particle is assumed to be hemispherical, $K = 1/3$. This is sometimes included in the equation, so any "wear constant" quoted must be identified.

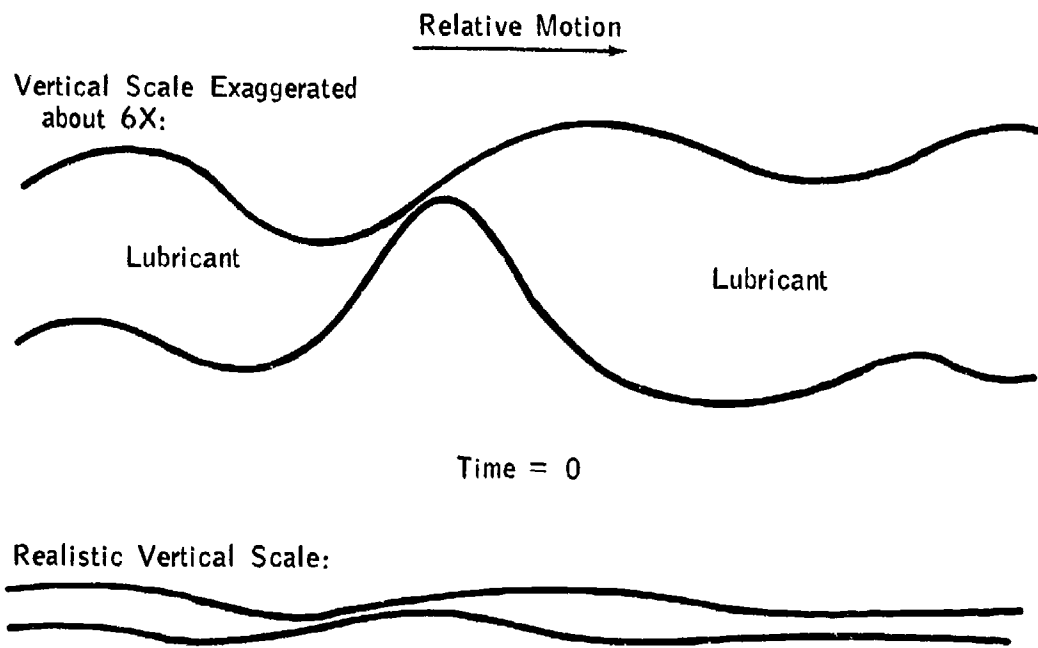
Experience shows that it is extremely rare for each encounter to yield a particle, so that K values usually are far below $1/3$. Rabinowicz' (1968) K values are shown in Table 5.4-I; these were originally published as " $3K$ " but were adjusted to fit Equation (5.1-4).

Equation (5.1-4) is so simple, and fits so much of the accumulated data, that there is a tendency to raise it to the status of a "law" of nature. Not everyone is in agreement; this includes Prof. Archard who realizes the limitations of his model far better than many of his followers. Bickerman (1970) has been particularly critical of the whole adhesion theory of friction and wear. Unfortunately, his criticism is usually stated so broadly, and so much oriented to his main career as an adhesives technologist, that lubrication engineers tend to turn away without considering any of the points he is trying to make. His principal one is that Amontons' law can be derived from non-adhesion concepts. However, his model equation

$$F = \tan \theta_1 \quad (5.4-2)$$

where θ_1 is the asperity slope, requires a slope of 45° , far beyond those found on surfaces, to explain the very ordinary value of $F = 1.0$. This tends to lend support to over-emphasis of the adhesion theory; as will be shown below, several other wear modes are required to explain even ordinary lubrication, and adhesion is not necessarily even the most important.

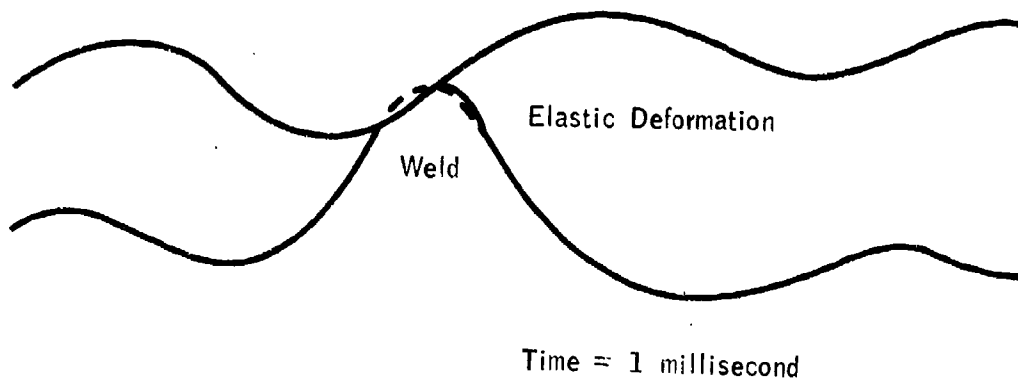
Figure 5.4-1
ASPERITIES BEFORE COLLISION



See Note on Figure 5.3-1

Figure 5.4-2
START OF ADHESIVE WEAR

Vertical Scale Exaggerated about 6X:



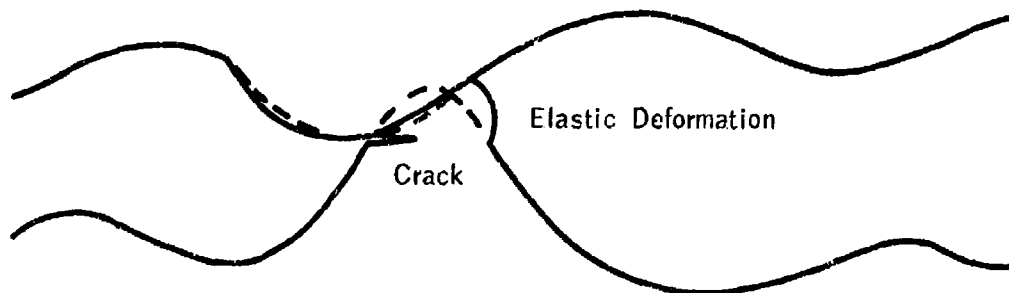
Realistic Vertical Scale:



See Note on Figure 5.3-1

Figure 5.4-3
CONTINUATION OF ADHESIVE WEAR

Vertical Scale Exaggerated about 6X:



Time = 3

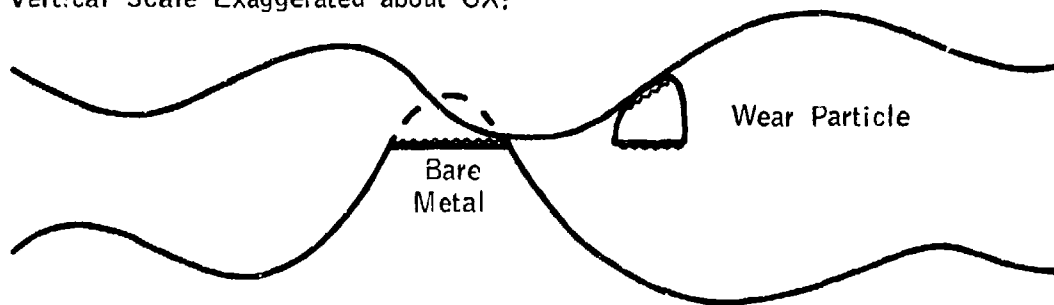
Realistic Vertical Scale:



See Note on Figure 5.3-1

Figure 5.4-4
COMPLETION OF ADHESIVE WEAR

Vertical Scale Exaggerated about 6X:



Time = 13

Realistic Vertical Scale:



See Note on Figure 5.3-1

TABLE 5.4-I

Specific Wear Rates for Various
Metal Combinations *

<u>Combination</u>	<u>Rate x 10⁻⁵</u>	<u>Combination</u>	<u>Rate x 10⁻⁵</u>
Cu-Pb	0.3	Zn-Zn	39.
Ni-Pb	0.7	Mg-Al	52.
Fe-Ag	2.3	Zn-Cu	62.
Ni-Ag	2.3	Fe-Cu	64.
Fe-Pb	2.3	Ag-Cu	66.
Al-Pb	4.7	Pb-Pb	79.
Ag-Pb	8.3	Ni-Mg	95.
Mg-Pb	8.7	Zn-Mg	97.
Zn-Pb	8.7	Al-Al	99.
Ag-Ag	11.3	Cu-Mg	101.
Al-Zn	13.0	Ag-Mg	108.
Al-Ni	15.7	Mg-Mg	122.
Al-Cu	16.0	Fe-Mg	128.
Al-Ag	17.7	Fe-Ni	198.
Al-Fe	20.0	Fe-Fe	258.
Fe-Zn	28.0	Cu-Ni	270.
Ag-Zn	28.0	Cu-Cu	420.
Ni-Zn	36.7	Ni-Ni	952.

* Data by H. H. Hultgren, B. S. Thesis, MIT 1966, cited by Rabinowicz (1971B). See also comments on Merchant (1968) and unsigned article in Product Engineering (August 15, 1966, p11). Conditions were unlubricated sliding in air, according to Rabinowicz (personal communication, March 3, 1972), between two contacting annular specimens, OD = 1", ID = 0.75", pressed together with a force of 400 gm, and rotated together at a relative angular speed of 120 rpm.

A more constructive criticism was made by Feng (1952, 54A, 55, 57B, 58), who stressed the difficulty of losing the wear particle from the opposing surface (Figure 5.4-4) if it is truly welded in place. His alternative is the highly plausible one that the wear particle locks to the opposing asperity by means of step-dislocations, which form a saw-tooth-like profile and its replica (Figure 5.4-5). Since this lock holds only as long as the force causing rupture lasts, the particle may drop off at once, or perhaps be retained as transfer. Another of Feng's points was used above in explaining the Archard model, that work hardening and subsurface cracking help to explain the separation of a more or less uniformly sized crop of particles. Since the energy consumed is the same as in the Archard model, Amontons' law is valid for the Feng model. The friction-reducing ability of contamination and lubrication is explained both by reduced dislocation amplitude and also by increased film thickness. This model was not carried on to a complete wear equation, but appears to be leading towards Equation (5.1-4). It has the very important property that V is the difference between a maximum transfer V_0 , depending on load, speed, work-hardening, etc., but not on environment, and V_L which depends on environment only. There is no explicit way to introduce any parameters for lubricant quality, but V_L includes lubricant. With due respect for the fact that Figures 5.4-1 to 5 are exaggerated in the vertical scale by about 6-fold, it appears that the mechanism shown in Figure 5.4-3 would permit a relatively small weld to peel off a piece of metal by compressing it horizontally while progressive tension failure extends the crack across the asperity. Since a shear stress parallel to the surface can be viewed as a compressive stress in the leading zone combined with a tensile stress in the trailing zone, this mechanism results in Equation (5.4-1) though the meaning of τ_y may not be exactly what Archard had in mind. Thus, the Archard and Feng models are by no means mathematically incompatible.

The Archard model was directly concerned with dry sliding, and the introduction of lubricant terms was due to Rowe, who presented his modifications in three papers of increasing degrees of sophistication (1966, 1967, 1970). The basic equation is a modification of Equation (5.1-4)

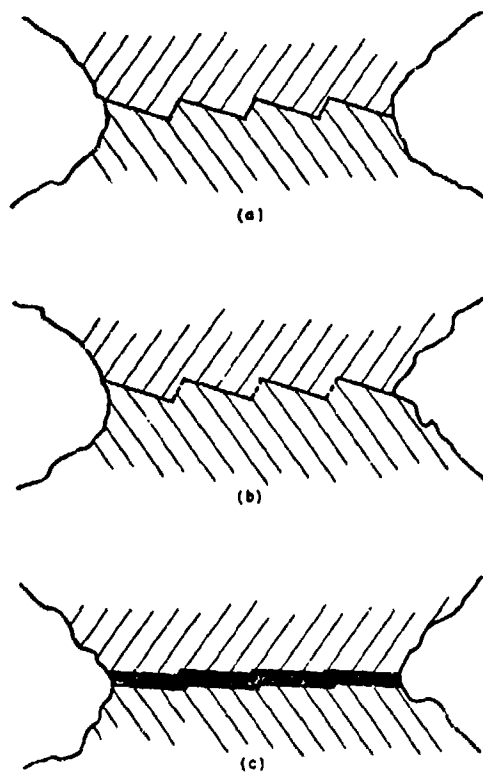
$$\frac{V}{d} = \frac{k_m \gamma \alpha W'}{P_m} \quad (5.4-3)$$

where k_m is what is left of K and presumably now equal to $1/3$. γ is the von Mises function for plastic flow which also appears in Equation (5.3-15).

$$\gamma = (1 + 3F^2)^{0.5} \quad (5.4-4)$$

There is room for debate on the use of 3, 4 or even 12 in Equation (5.4-4). Spurr (1964) has thrown some light on this matter, which helps to justify 3 in the most relevant cases. There may also be some justification for making it a function of Poisson's ratio (ν), as in Equation (5.3-6).

FIGURE 5.4-5
THE INTERLOCKED DISLOCATION MODEL



Sketch showing roughened interface of pair of actually contacting high spots with contaminated surfaces. (a) For case that surface film is tenacious, and thin as compared to average roughening of interface. (b) Same as (a) except that surface film is brittle. Establishment of metal-to-metal contact on regions shown by dotted lines is possible. (c) For case that thickness of surface film is close to or greater than average depth of roughening of interface.

VERTICAL SCALE EXAGGERATED ABOUT 50X.

5.4.1 Adhesive Wear With Simple Lubricants (Model IIA)

The key concept in Equation (5.4-3) is the fractional film defect (α) as defined by Kingsbury (1960)

$$\alpha = 1 - \exp \left[\frac{-X \exp(-E/RT_s)}{U t_o} \right] \quad (5.4-5)$$

where X is the diameter of the spot associated with an adsorbed molecule, E the heat of adsorption, R the gas constant and U the sliding velocity.

The surface temperature is

$$T_s = T_b + 1.040 \times 10^{-5} \frac{FU(WP_m)^{0.5}}{(k_1 + k_2)} \quad (5.4-6)$$

where T_b is the bulk lubricant temperature and k_1 and k_2 the thermal conductivities of both surfaces. This is the "surface temperature rise" equation used by Rowe. Many other versions are available, the most sophisticated being that of Francis (1971).

The fundamental time of vibration of an adsorbed molecule is

$$t_o = 4.75 \times 10^{-13} \left(\frac{MV_m^{2/3}}{T_m} \right)^{0.5} \quad (5.4-7)$$

where M is the molecular weight of the lubricant, V_m its molecular volume and T_m its melting point.

All of these input values can be estimated or are known quite precisely. Rowe tested this equation by back-calculating from wear experiments, but the present plan is to use it for design purposes and then judge the results against both general and anomalous experience. For this purpose one may regard W , U , M , V_m and t_o as preselected parameters. P_m is obtainable from the Diamond Pyramid Hardness, Vickers Hardness Number, etc. or from MacGregor's Table III-4. k_m has a theoretical value for hemispherical wear particles of 0.33, shown by Rowe to be of the right order of magnitude.

The values of X are not so generally available, and it is proposed to use a simpler parameter, $(6V_m/\pi N_a)^{1/3}$ which has proved to be of great value in predicting surface free energies. This is the diameter of the sphere associated with the surface molecule. Hence,

$$\alpha = 1 - \exp \left(\frac{- \exp(-E/RT_s)}{3.23 \times 10^{-5} U(M/T_m)^{0.5}} \right) \quad (5.4-8)$$

As Rowe pointed out, values of α do not often exceed 0.01, so the exponent in Equation (5.4-8) is also quite small and a very close approximation may be made by simplifying to

$$\alpha \approx \frac{-\exp(-E/RT_s)}{3.23 \times 10^{-5} U(M/T_m)^{0.5}} \quad (5.4-9)$$

Values of T_m are readily available for pure compounds, but for mixtures such as lubricating oils they simply do not exist. (The pour point only indicates that enough wax has coagulated to gel the liquid, or that the oil has reached a viscosity of about 300,000 centistokes.) Hence, in such cases a generalized melting point based on the liquid/vapor critical point will be used.

$$T_m = 0.40 T_c \quad (5.4-10)$$

It must be mentioned that de Boer (1968) has recently taken considerable exception to the practice of regarding t_o as the vibration time. A way of using his new ideas and also eliminating Equation (5.4-10) is discussed in 5.4.2.

As in Model I, the lack of a reliable method for predicting F is an embarrassment, and possible methods are discussed in 5.12. As a start, the tabulated values for Model I cover many likely combinations of materials and lubricants.

A serious question raised by the writer (Beerbower 1971A) still remains unanswered. This concerns the nature of α when viewed as the fractional defect in two films. Rowe, and Kingsbury before him, used α as if it concerned only one member and the other were bare. Since that is most unlikely,

$$\alpha = \frac{\alpha_r \alpha_s}{r s} \quad (5.4-11)$$

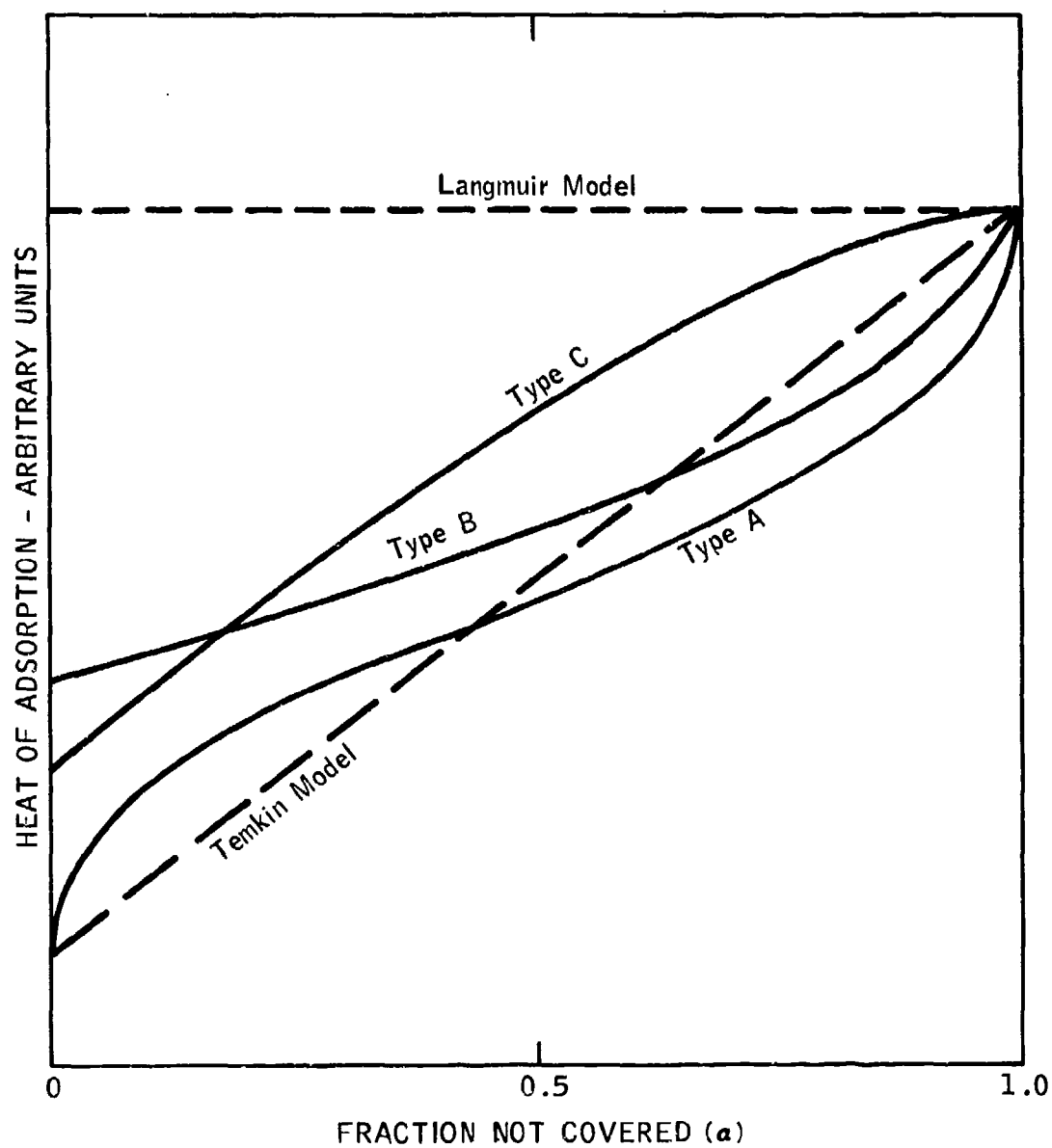
where α_r and α_s are the defects for the two surfaces, would be the logical solution based on the probability of matching two bare spots. However, this has the effect of cutting in half Rowe's eminently satisfactory value of $E = 11700$ cal/mole. To preserve this, we will arbitrarily define

$$\alpha = \sqrt{\alpha_s \alpha_r} \alpha \exp [-(E_s + E_r)/2RT] \quad (5.4-12)$$

and attempt to justify this geometric mean submodel.

Evaluation of E is quite difficult; fortunately, at the low α values involved, high precision is not required. Very few values are available in the literature, and Rowe was forced to compare his experimental energies (or heats, synonymous in this case) with works of adhesion from the literature. The work represents only about 60% of this energy (Philippoff 1960) but that seems trivial compared to other uncertainties. One vexing problem is what to do about the variation of E with α , as shown in Figure 5.4-6, drawn from data quoted by Bond (1962). It is evident that the metal surface varies, with a few "active sites" having up to 3 times the heat of adsorption of the average surface. Which is the correct value of E for use in Equation (5.4-9)? Obviously, not the maximum value at $\alpha = 1.00$, since these are the sites least likely to be uncovered by the process described in Equation (5.4-8), nor the

Figure 5.4-6
HEAT OF ADSORPTION OF VAPOR
VERSUS FRACTION NOT COVERED



mean value from Figure 5.4-6 which includes them. On the other hand, is it likely that the energy at $\alpha = 0.01$ on Figure 5.4-6 corresponds to that on a bearing surface, when the data was obtained from a vacuum evaporated film and the real surface was formed by the violent process shown in Figure 5.4-5?

Some effort is made to answer these questions in 5.4.2 and Appendix V, but the best answer seems to be that only E values obtained from friction and wear data should be used for design purposes. It is to be hoped, but not promised, that E will depend only on materials and lubricant with a minor adjustment for T_s .

Viewed for design purposes, Model IIA would require considerable input data. These are listed in Table 5.4-II.

TABLE 5.4-II

INPUT DATA FOR MODEL IIA

Engineering Data: $W, U, T_b, F^*, r_1,$

Lubricant Data: $M, V_m, \Delta H_v, \gamma_1^*, T_c, \epsilon^*$

Metals Data: $P_m, E_{1m}, \gamma_1^*, B, \Delta H_s^*, V_m^*$
(Two sets
Required)

* Redundant for alternate paths.

For Model IIC, the same data must be provided on additives as indicated above for "lubricant".

5.4.2 Testing Model IIA

Once again, the Appeldoorn (1967A) data was used for comparison with Model IIA. The computation plan was to set $k_m = 1/3$ and use actual values of $F, V/d$ and W to calculate first T_s , then α , then E . Thus, the working equation assembled within the computer was

$$(V/d) = \frac{(1 + 3F^2)^{0.5} W}{3P_m} \left(1 - \exp \left(\frac{-\exp [E/R(T_b + 1.040 \times 10^{-5} F U W^{0.5} P_m^{0.5} / (k_1 + k_2))] }{3.23 \times 10^{-5} U (M/T_m)^{0.5}} \right) \right) \quad (5.4-13)$$

Since actual T_m values were available, Equation (5.4-10) was not used. The results are shown in Table 5.4-III. It is evident that the values of E obtained are by no means constant for a given hydrocarbon and are more or less independent of hydrocarbon type. This is a very serious blow to the entire concept, and it was seriously questioned whether the data might be at fault, due to loose control on humidity. Another set of data from the same report, in which atmosphere control was excellent but commercial fuels without additives were tested, was then analysed by the same procedure (using ASTM D 2386 freezing point for T_m). The results, shown in Table 5.4-IV, are equally discouraging. Finally, a small amount of data using one of the fuels and varying the metallurgy was put through the same routine. This time a slight trend could be found, harder metal giving higher E for a given load.

Empirically, it was observed that the ratio E/T_s was essentially a constant for each hydrocarbon. This was startling, since it also makes $\exp(-E/RT_s)$ a constant, thus throwing all the variation in α into t_o (since U is constant). This violates Rowe's equation (5.4-7) if V_m is considered constant; even when corrected for expansion to T_s , the change in $V_m^{2/3}$ is not enough to account for the variation in α . Another explanation is considered in Appendix V.

DeBoer (1968) has seriously questioned the use of such equations as (5.4-7) for t_o . He does not offer any simple substitute, but only a series of increasingly complex expressions for various cases:

5.4.2.1 For a freely translating and rotating molecule of such low frequency (ν_z) that $h\nu_z \ll kT_s$, where h is Plank's and k is Boltzman's constant,

$$t_o = 1/\nu_z \quad (5.4-14)$$

which corresponds to Equation (5.4-7).

5.4.2.2 If the perpendicular vibration is practically in its lowest state,

$$t_o = h/kT_s \quad (5.4-15)$$

which corresponds to gas adsorbed near 25°C.

5.4.2.3 If either translation or rotation is seriously hindered,

$$t_o < h/kT_s \quad (5.4-16)$$

This is comparable to benzene on charcoal, and seems most appropriate to Model IIA.

5.4.2.4 If all translation mobility is lost, Inequality (5.4-16) is still obeyed, but t_o is smaller than before. This case seems appropriate to Model IIC. The molecule cannot slide, but it can hop from site to site; deBoer cites an example of $E = 10000$ cal/mole, and assumes ΔQ for hopping to be 5000 cal/mole. The time of adsorption (t) may be about 3×10^{-6} sec.,

TABLE 5.4-III

HEATS OF ADSORPTION OF PURE HYDROCARBONS
ON STEEL CALCULATED FROM WEAR RATES

Load (gms): Code	Lubricant	Heat of Adsorption (kcal/mole)						Ratio (E/T _a) (cal/mole deg K)							
		30	60	120	240	480	1000	2000	30	60	120	240	480	1000	2000
1	n-Octane	12.7	12.8	13.5	14.3	15.6	--	--	38.5	40.6	39.8	40.6	43.0	--	--
2	n-Nonane	12.4	12.1	12.0	12.7	--	--	--	38.4	38.5	35.3	35.1	--	--	--
3	n-Butylbenzene	12.5	11.9	12.0	13.0	15.7	15.9	--	38.0	36.4	35.4	36.5	39.2	38.0	--
4	Diethyl cyclohexane	13.3	13.1	13.2	14.0	15.1	--	--	39.5	39.5	38.8	39.6	39.8	--	--
5	n-Dodecane	12.2	12.6	13.3	14.0	15.7	--	--	39.0	40.0	40.9	40.9	42.1	--	--
6	Tetralin	12.7	12.9	13.4	13.9	14.7	18.1	24.5	40.6	40.3	41.1	41.0	40.2	41.1	41.7
7	Decalin	13.0	13.0	13.8	14.3	14.5	15.8	--	41.2	40.9	38.5	41.0	40.2	39.9	--
8	1-Methyl naphthalene	13.1	13.6	14.1	14.8	15.7	--	--	41.7	43.2	43.6	44.3	44.5	--	--
9	1-Hexadecene	12.7	13.2	13.5	14.1	15.0	16.3	18.2	40.6	42.0	41.7	42.5	43.3	43.8	43.4
10	n-Hexadecane	12.6	13.1	13.5	14.1	15.0	16.3	--	41.0	41.9	42.5	43.3	42.0	42.3	--
11	Heptamethyl nonane	12.4	12.7	13.4	14.0	15.0	16.4	--	40.0	40.3	41.3	41.7	41.0	41.5	--
12	i-Propyl bihexyl	12.7	13.3	13.8	14.3	15.1	--	--	41.6	42.7	42.8	42.8	43.5	--	--
13	Dimethano decalin	13.1	13.6	--	14.7	15.5	--	--	42.9	43.2	--	43.5	43.8	--	--
Mean		40.2 40.5 40.2 41.0 41.5 41.1 42.4													
Grand Mean		----- 40.7 -----													

TABLE 5.4-IV

HEATS OF ADSORPTION OF COMMERCIAL LIQUIDS
ON STEEL CALCULATED FROM WEAR RATES

Load (gms): Liquid	Atmosphere	Heat of Adsorption (kcal/mole)			Ratio (E/T _s)		
		240	480	1000	240	480	1000
Synth. Isopar.	Dry Argon	16.4	17.9	20.0	43.1	44.5	45.7
	Wet Argon	16.1	17.5	20.4	43.5	44.8	45.8
	Dry Air	16.2	16.9	17.6	42.5	40.5	41.7
	Wet Air	15.3	15.2	18.5	40.4	36.8	38.1
JP-5	Dry Argon	17.1	17.7	20.0	44.8	44.3	44.5
	Wet Argon	17.2	17.8	18.6	44.5	44.2	42.3
	Dry Air	19.2	18.1	28.4	44.7	42.0	42.2
	Wet Air	15.5	16.5	25.2	38.6	40.0	40.0
RAF-176-64	Dry Argon	16.6	17.2	18.5	46.0	44.0	45.0
	Wet Argon	16.7	17.6	18.4	44.3	45.0	43.7
	Dry Air	17.4	16.9	--	43.7	41.9	--
	Wet Air	15.6	16.7	17.6	41.3	41.0	40.7
PW-523	Dry Argon	17.9	17.2	19.2	45.2	42.9	46.2
	Wet Argon	17.4	18.0	19.3	44.1	44.3	45.2
	Dry Air	14.8	15.5	22.0	39.4	40.1	39.7
	Wet Air	15.7	15.7	19.5	38.7	38.8	38.2
JP-4	Dry Argon	17.0	18.1	22.2	45.0	46.3	46.2
	Wet Argon	17.3	18.5	19.8	45.1	45.9	44.5
	Dry Air	16.7	18.2	--	44.7	45.6	--
	Wet Air	16.2	15.8	--	42.8	38.4	--
Conditions: 52100 Steel, 240 rpm, 32 minutes.							
Grand Mean for Argon					-----44.5-----		
Grand Mean for Air					-----40.9-----		

in which case the temporary "halting time"

$$t' = t_0 \exp (\Delta Q/RT_s) \quad (5.4-17)$$

comes to 5×10^{-10} sec and the molecule makes about 6000 hops before being desorbed.

Inequalities are not very promising, but it must be remembered that all this means is setting k_m free again to become an "adjustable parameter", which can now be defined as

$$k'_m \equiv h/3t_0kT_s \quad (5.4-18)$$

which helps to explain why Rowe never was able to get $k_m = 1/3$. This means either returning to his approach of evaluating both k_m and E from data, or arriving at E by the surface free energy methods discussed above and in Appendix V. Since we have the additional complication of an iterative solution for F , it would seem unwise to simultaneously attempt his graphical method for E . Hence, it is proposed to revise Model IIA into:

$$(V/d) = \frac{k_m W}{P_m} \gamma \alpha = \frac{k_m W}{P_m} \gamma \frac{X}{U t_0} \exp(-E/RT_s) = \frac{k_m W}{P_m} \gamma \frac{3kT_s X}{hU} \exp(-E/RT_s) \quad (5.4-19)$$

Unfortunately, time has not permitted any testing of Equation (5.4-18), even to the extent of determining whether the presence of T_s outside the exponential will permit E to remain constant. However, its derivation seems to justify its being high on the agenda for future study.

5.4.3 Adhesive Wear with Gas and Vapor Lubricants (Model IIB)

In his second article, Rowe (1967) carried the model to include the reversible adsorption of vapor lubricants. To do this, he established a slightly different definition of X , the diameter of the circular spot associated with an adsorbed molecule

$$X = 2/(\pi n)^{0.5} \quad (5.4-20)$$

where n is the number of molecules per unit area. While this is compatible with his X in Model IIA, it is not related to $V^{1/3}$ in the way proposed for Equation (5.4-19) until adsorption approaches a compact monolayer. This permitted him to relate X to Henry's law and the Langmuir isotherm principle.

While Model IIB is a notable scientific achievement, its engineering application is too limited for consideration in this study. Like all Rowe's models, it involves reversible processes, which exclude the interactions of oxygen and humidity with most engineering materials. Those concerned with graphite, or unlubricated wear in inert atmospheres, may wish to test it further.

5.4.4 Adhesive Wear With a Compounded Lubricant (Model IIC)

Model IIA was designed only for pure liquids, and IIB for pure gases. These limitations were removed by development of the idea of temporary residence of both additive and base fluid on the metal surface in a dynamic equilibrium. If α and β represent the fractional film defects of the area occupied at rest by the two species, respectively

$$\frac{V}{d} = \frac{k_m[\beta + (\alpha - \beta)\phi] \gamma H'}{P_m} \quad (5.4-21)$$

where ϕ is the area fraction occupied at rest by additive. Since each of these develops a film defect related to its heat of adsorption as in Equation (5.4-9), this becomes

$$\frac{V}{d} = \frac{k_m \gamma}{P_m} \left[1 + \left(\frac{V}{V_0} e^{\frac{\Delta E}{RT}} - 1 \right) \right] \frac{H' X}{t_0} e^{-\frac{\Delta E}{RT}} \quad (5.4-22)$$

where ΔE is the difference in heats of adsorption, x the ratio of molecular areas, t_0' the ratio of vibration times, X the molecular area of the base fluid, and t_0 its vibration time.

It is now necessary to evaluate ϕ , and Rowe chose one of the several possible ways. He set up an equilibrium constant for the adsorption-desorption processes of both species which will eventually result in ϕ satisfying the Gibbs-Duhem requirement of minimum free energy in the system. This results in a special expression for $x = 1$, relating the wear rate to friction function ratio $(V/\gamma d)$ for a lubricant with concentration c of an additive, to the same ratio $(V/\gamma d)_b$ for the base fluid;

$$\left(\frac{V}{\gamma d} \right)_c = \frac{e^{\frac{\Delta S}{R}}}{e^{\frac{\Delta E}{RT_c}}} \left[\left(\frac{V}{\gamma d} \right)_b - \left(\frac{V}{\gamma d} \right)_c \right] + \left(\frac{V}{\gamma d} \right)_b \frac{e^{\frac{\Delta E}{RT_c}}}{t_0} \quad (5.4-23)$$

where ΔS is the entropy change of the entire system.

For the case where x values are not similar, Rowe ran into more difficulty in eliminating ϕ . This arose largely because his goals included evaluating x from wear data. If the approach shown under Model IIA is taken, this problem is minimized since x simply equals the cube root of the ratio the molar volumes for additive and base fluid. In addition, t_0 becomes the ratio of the critical temperatures of the two species. When, as often happens, T_c for the additive is not known, it can usually be estimated by the Lydersen method as discussed in Reid and Sherwood (1966), if the boiling point (T_b) is known.

It is also quite possible to avoid these difficulties by precalculating the composition of the adsorbed layer at equilibrium. Everett (1965) provides means for doing this from activity coefficients, which can be derived from solubility parameters as described by Prausnitz (1969). Another approach is to apply the necessary x corrections to Equation (5.4-15) and evaluate the entropy change as discussed in Appendix VII. Groszek (1971) gives a procedure for the direct determination of ΔE in a flow microcalorimeter.

In any case, the tools are available to perform the necessary manipulation on binary or multicomponent systems. The choice of going into Model IIC with corrections for $x \neq 1$ or into Model IIA with a weighted average value of E would be largely one of convenience.

One factor completely ignored in Model II is the fact that pure metals are rarely, if ever, encountered in lubrication engineering. This is not particularly hard to deal with in the case of solid-solution alloys. Buckley (1969) has shown that even 1 atomic percent or less of aluminum alloyed in copper or iron will diffuse to the surface to produce a highly enriched layer. This is not any specific reaction of aluminum but merely the same principle that causes soap to coat the surface of water. It is commonly believed that Gibbs postulated attraction of low energy components to the surface, but this is not the case. This principle merely states that when they are brought to the surface by any process, they will tend to remain there because their departure would cause an increase in free energy, a Second Law violation. The Gibbs-Duhem equation merely predicts equilibrium, and the rate of attaining it is controlled by relatively sluggish solid diffusion.

This raises the question of the time scale of Model IIC. When two asperities impact as shown in Figures 5.4-1 through 5.4-5, the result may be a surviving film or a bare spot. Assuming that even the survival case requires renewal of the film due to partial rupture, we may calculate certain times on any reasonable set of parameters. Table 5.4-V shows a typical case. The "wearing" members were calculated on the basis of time to wear a depth of $D/2$ peak-to-peak ($\text{RMS} \sqrt{2}$), and the "non-wearing" members on Model IA. It is evident that the time for diffusion of additive from solution is very limited for the "fixed spot" (ball) member, and quite generous for the "moving spot" (plane) member, regardless of where the wear is taking place. Whether the time is sufficient for metallic diffusion on the "moving spot" member remains to be investigated. If it is, such alloys can be handled simply by the Hildebrand (1950) method for mixtures (see Equation 5.5-14). The low surface free energy component may be a metal, or sometimes a carbide, etc.

Table 5.4-V represents an example of the sort of new information that arises from this type of analysis. Neither Model I nor II alone would lead to the valuable conclusion that additives must be tailored to fit the "moving spot" member if they are to be effective. As far as the writer knows, this principle has never been recognized before, but there is every reason to accept it as valid based both on its derivation and on practical experience. On this basis, E must be calculated for the "moving spot" member, but E_b for the harder member, for use in Equation (5.4-21). A more rigorous solution, in terms of α and α_s , may be justifiable in the future.

Model II may also be useful in predicting the transition point at Y in Fig. 2-1, by reason of the rapid rise of the double exponential in Equation (5.4-5), as pointed out by Kingsbury (1960) whose early work led to Model IIA. He went so far as to set up an equation for this "characteristic temperature", T_t :

$$T_t = \frac{E}{2R} \left(1 - \frac{V}{V_0} e^{-E/RT} \right) \quad (5.4-24)$$

TABLE 5.4-V

TIME SCALE FOR FILM RENEWAL

Conditions:	Wear Rate	$V/d = 10^{-8} \text{ cm}^3/\text{cm}$
	Surface Finish	$D = 3 \times 10^{-6} \text{ cm peak-to-peak}$
	Wear Scar	$w = 0.02 \text{ cm diameter or width}$
	Hertz Diameter	$H = 0.02 \text{ cm}$
	Speed	$U = 10 \text{ cm/sec}$
	Path on Plate	$S = 20 \text{ cm}$

Ball Not Wearing

$$t_b = \frac{H}{U} = 0.0020 \text{ sec}$$

Ball Wearing

$$t_b = \frac{\pi H^2 D / 2}{UV/d} = 0.0024 \text{ sec}$$

Plate Wearing

$$t_p = \frac{wSD/2}{UV/d} = 3.0 \text{ sec}$$

Plate Not Wearing

$$t_p = \frac{S}{U} = 2.0 \text{ sec}$$

which defines the conditions for a maximum $d\alpha/dT$. While this model does not produce a vertical line transition as shown in Figure 2-1, the latter must be regarded as schematic. Data in the Y region scatter enough to fit a very steep sigmoid curve equally well.

In view of the difficulties encountered with IIA, no tests were run on model IIC. Probably the application of Equation (5.4-18) will open up the way to do this. In spite of the difficulties encountered in the tests, it appears that the Bayer, Feng, Archard and Rowe approaches are converging to a common solution to the problems of reversible surface energetics. With the geometry of Model I put in, this would produce a design program which, with additional inputs shown in Table 5.4-II, appears fairly complete. Actually, there is a great deal missing from it, as will be shown below under Model III.

5.4.5 Severe Wear (Model IID)

Brockley (1965) proposed a model for wear so severe that it must be classified as "scuffing" and so outside the scope of this STAF. For the sake of completeness, it results in the equation

$$K = (\pi/4) \sec^2 \theta_1 = \pi/4 \cos^2 \theta_1 \quad (5.4-25)$$

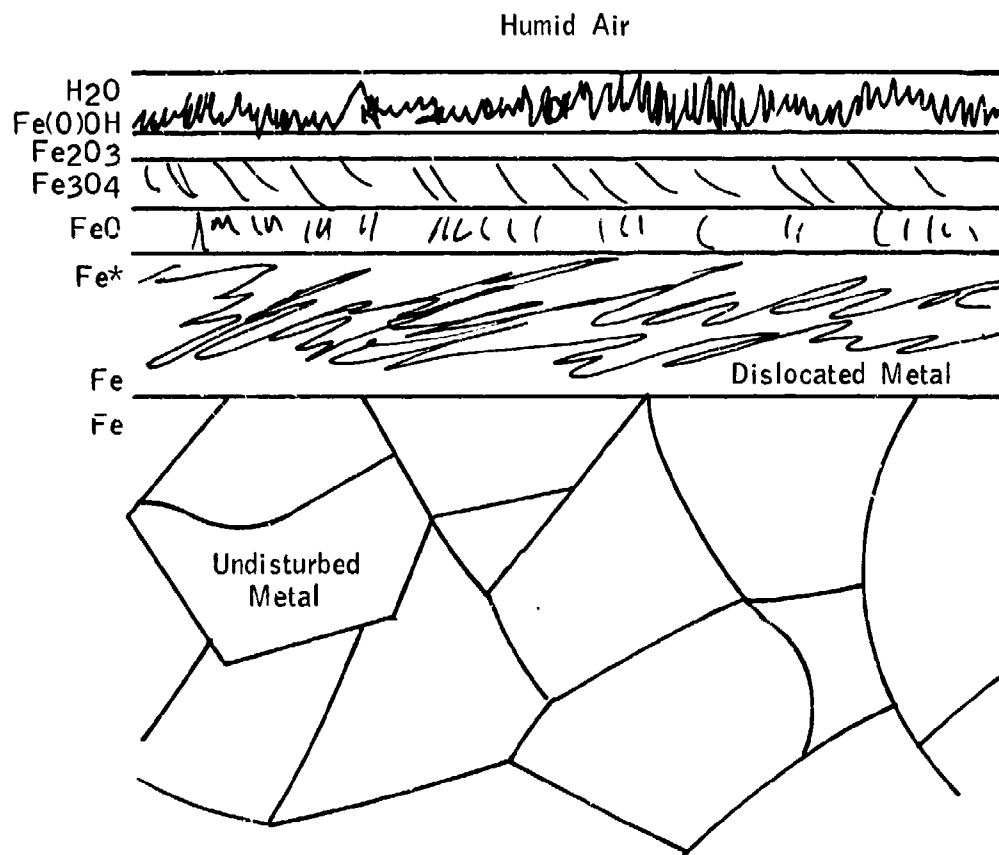
where θ_1 is the angle of the asperity slope at the impact point. Since this model generates spheroidal particles, the maximum value of K is 1.0 rather than 1/3. This corresponds to an angle of 27.6° , high enough not to interfere with the use of Model IID on any surface likely to be encountered.

Brockley provides one test for this model, which seems adequate for the purpose of this STAF and not worth discussing here.

5.5 The Irreversible Chemistry Models - Reaction With the Atmosphere and/or the Lubricant (Model III)

Model II was based on what might be termed reversible interactions; the adhesion of a metal to another, to a lubricant or to an additive by means of forces ranging from purely physical ones to temporary chemical bonds. As a borderline case between these and reactions, we may use the fatty acids which have provided so much information to the scientists and practical help to the lubrication engineers. Opinions vary a great deal as to how these substances bond to surfaces. It appears that, as is typical in boundary lubrication, every one is partly right and partly wrong. There is every reason to believe that acids first are attached to the surface by hydrogen bonds through a complex layer as shown in Figure 5.5-1. In due course, through the combined effects of temperature, pressure and time, it is probable that elimination of water leads to covalently bonded soaps. These will be dealt with in Section 5.5.7; the point to be made now was how this is the dividing line between Models II and III, and also how important it is.

Figure 5.5-1
THE HYDRATED OXIDE LAYER ON IRON



Note: Interfaces are drawn as planes since actual contours are not known.

The irreversible reactions may be put into four groups: corrosion of the metals by the atmosphere, corrosion of the metals by the additives, polymerization of the lubricant by catalytic action of the metals, and reaction of the additives with metals - or more often corrosion products - to form solid film lubricants. The last is partly redundant with the second, but must be viewed both ways to appreciate the sacrifice sometimes made in wear rate for the sake of a high scuff load. The general nature of these competitive reactions is illustrated in Figure 5.5-2. Truly, as Prof. Archard described it, "lubrication is a very intense process in a very small reactor."

5.5.1 Corrosive Wear by the Atmosphere (Model IIIA)

All metallic surfaces (except for the noble metals) come into use completely covered with corrosion products, so that the first increment removed from moving, load-carrying surfaces is certain to be "corrosive wear". Subsequent events may continue the same sequence of corroding and removing layers, or may proceed along one of the alternate paths of adhesion, plowing and fatigue. Some confusion arises because these alternates may produce metal particles which then corrode almost instantly, but that is outside the scope of Model IIIA. On the other hand, there is some reason to classify some wear as fatigue of the layer of corrosion products, which is definitely within the scope. As a result, there is some uncertainty as to how much wear is due to corrosion phenomena, but an increasing number of cases are being identified as corrosive wear. Detailed attempts to render this mechanism predictable have isolated four specific cases, all of which have been fitted with mathematical models of potential value in engineering design.

5.5.1.1 Oxidative Wear of Unlubricated Steel Surfaces (Model IIIA-1) has been studied by Quinn (1967, 1968-9, 1971A & B). He has evolved three models and made some progress in fitting them to his experimental data on steel in air at 150°C to 450°C. Starting from the "parabolic oxidation" equation, in which the depth of the oxide layer varies with the square root of the time, he first developed a rate equation which contained four adjustable parameters. These included the distance along which a wearing contact is made, and the critical thickness of the layer before breaking, as well as the two constants needed for an Arrhenius rate equation. His model was improved by Rowe (1968), who showed that the distance could be eliminated, and the fit to the data improved, by using a more rigorous definition of the probability of a contact producing a wear particle. This "Quinn-Rowe" equation, in the present symbols, is:

$$(V/d) = KWA \exp(-Q/RT_s) / \rho_c^2 h_c U P_m \quad (5.5-1)$$

where V/d = wear volume of metal per unit travel (cm^3/cm)

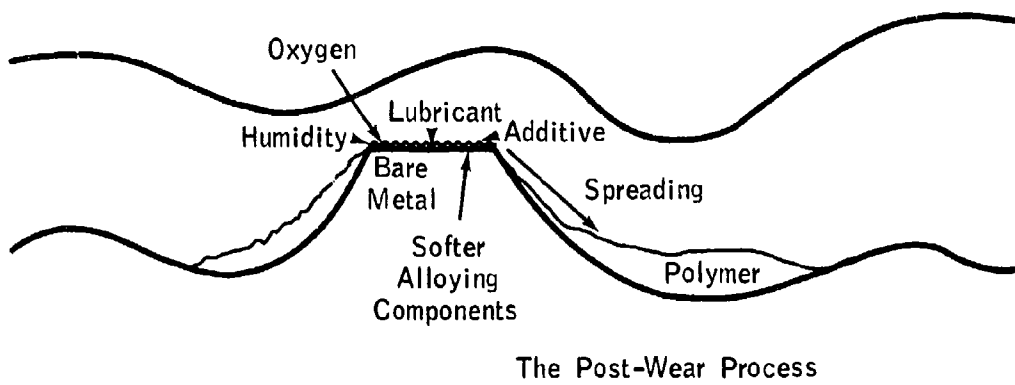
K = a wear constant

W = load (gm force)

A = Arrhenius constant for "parabolic" oxidation

Figure 5.5-2

Vertical Scale Exaggerated about 6X:



- Q = activation energy for "parabolic" oxidation (cal/mole)
- R = gas constant (cal/mole, °C)
- T_s = contact temperature (°K)
- Ø = molar volume of oxide/molar volume of metal
- h_c = critical oxide thickness = wear particle thickness (cm)
- U = relative velocity (cm/sec)
- P_m = hardness of asperities (gm force/cm²)

K is related to the probability, P, that a contact will produce a wear particle by $K/h_c = P/2r$, where r is the radius of a wearing contact junction. Rowe suggested a different means for converting oxide volume to metal volume, but Ø is simpler. Very recently, Tenwick and Earles (1971) made a similar analysis and also arrived at Equation (5.5-1). In addition, they corrected P for temperature variation with two empirical auxiliary equations, which add little to the analysis.

Both Quinn (1971B) and Tenwick and Earles (1971) also derived essentially identical equations based on the "linear" oxidation model, a simplification of a logarithmic equation. The result is simpler as it does not contain h_c, which is difficult to measure, but is limited to temperatures below 200°C:

$$(V/d) = (K_1 W A_1 / P_m U \emptyset) \exp(-Q_1 / RT_s) \quad (5.5-2)$$

where

$$K_1 = 1/3 \text{ (according to Tenwick and Earles)}$$

A₁ and Q₁ are constants for the linear Arrhenius equation

Quinn's third model (1971A) was aimed at eliminating h_c while retaining the parabolic oxidation model. It took the form:

$$(V/d) = (W A^{0.5} / P_m t^{0.5} \emptyset) \exp(-Q/2RT_s) \quad (5.5-3)$$

Quinn's assumption for Equation (5.5-3) is "that at all times during the period t of an established wear rate, the real contact area is subject to oxidation at the contact temperature (T_s)," in our symbols (including using W/P for the real contact areas). He then proceeds to calculate total volume of oxide (=V Ø) by the parabolic equation, just as if all of the oxide were still in place. This is a fallacy, as the oxide is flaking off. The parabolic equation is based on the decrease in diffusion due to the build-up of oxide, so t should start at zero after each wear event. As shown by Rao (1969), this leads back to the linear law.

Presumably because he detected this fallacy, Quinn withdrew Equation (5.5-3) before publication (1971B). However, it fits his data remarkably well. In Figure 5.5-3, his Figure 3 (1968-9) is replotted and interpreted both ways; less data need be discarded to fit (5.5-3) than (5.5-1). Hence, (5.5-3) will be retained, on an empirical basis, and discussed in Section 5.5.2.

5.5.1.2 Corrosive wear of lubricated steel surfaces (Model IIA-2) by the atmosphere has been studied by Tao (1968A, 1969). The first paper made a detailed study, based on the diffusion rate of oxygen through hydrocarbons. He started with the basic differential equations for two-dimensional steady-state diffusion, and some simplifying assumptions about the ball-on-cylinder apparatus. These included smooth surfaces, a uniform clearance (ξ), fresh oil saturated with oxygen and humidity brought in by viscous drag, instantaneous reaction of the surface followed by immediate removal of the FeO(OH) , and wear only at the upper (ball) surface. From these he arrived at the following equation:

$$\xi = \frac{1}{1.61 C_0 U_a \rho} \int_0^T \frac{T^2 dt}{1 - 1.08 \exp(-3.718 \lambda T^2 \xi^2 U)} \quad (5.5-4)$$

where T is the time, C_0 the initial oxygen concentration, U_a the mean oil flow velocity, ρ the oil density, H the Hertz contact diameter, w the scar width on the ball (measured parallel to the cylinder axis), λ the mass diffusivity and U the sliding velocity.

Tao was able to use this equation to compute clearances, and obtained quite plausible values based on wear rates in air by neglecting the exponential term and substituting a value of W from a run of known duration. This was based on the fact that the exponential becomes negligibly small as the concentration of oxygen in the oil leaving the action zone approaches zero. With this simplification,

$$w^3 - H^3 = 0.082 \rho \xi C_0 U \quad (5.5-5)$$

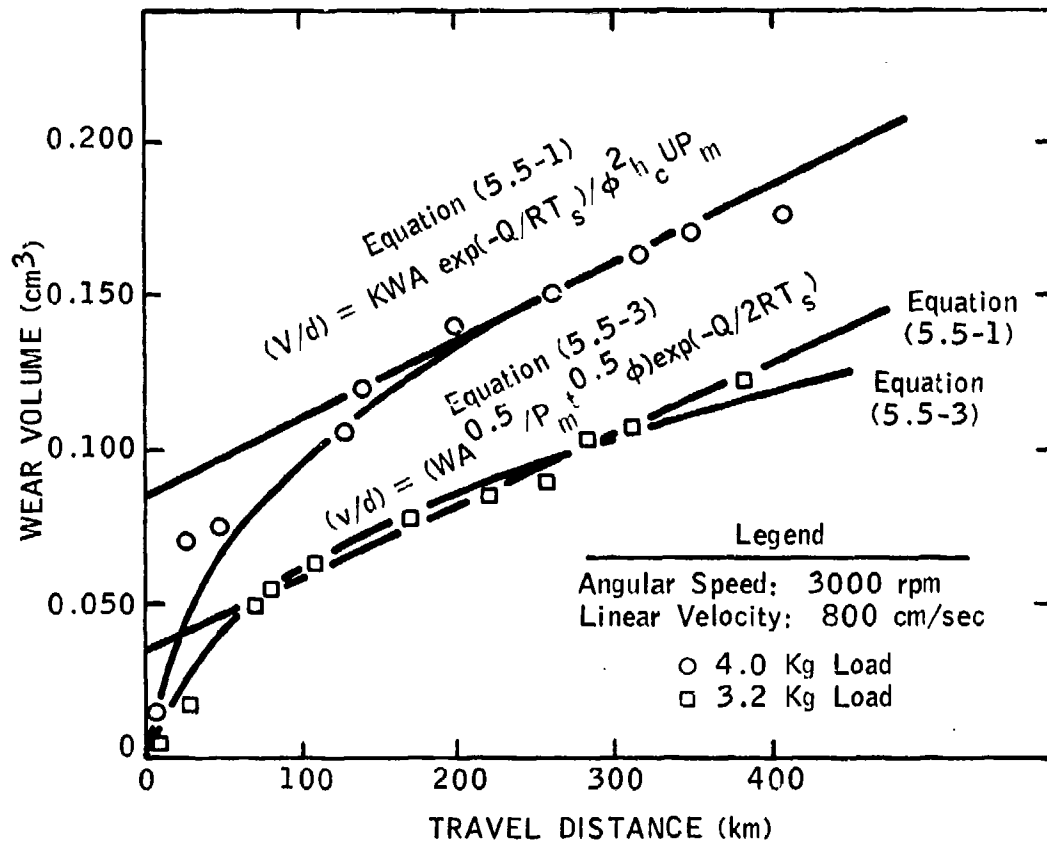
The value of C_0 was shown to be a function of the oxygen partial pressure (p), the density of the lubricant at 60°F (ρ_0) and other factors as defined above, by the writer (ASTM 1970, Method D 2779).

$$C_0 = \frac{3.00 p \rho(0.980 - \rho_a)}{T_b^2 \exp\left(\left[\frac{1.041(T_b - 700)}{T_b}\right] + 5.347\right)} \quad (5.5-6)$$

No equations were set up to handle humidity as it appeared that air of > 50% RH would provide an adequate supply of H_2O to keep the reaction supplied. Tao demonstrated, in fact, that Equation (5.5-5) was only in error by about 10% regardless of the humidity.

A tentative dependence of w on the "compliance", a complex term involving W and D , was demonstrated but the relationship to Model IB cannot be established without a good deal more work.

Figure 5.5-3
ALTERNATIVE METHODS OF CORRELATING
WEAR VERSUS TIME
(Data from Quinn (1967) Figure 3)



Obviously, this is only a partial model, as Equation (5.5-5) would indicate that no wear takes place at $C_0 = 0$. This is not true, as shown in subsequent work by the same group with Argon. However, no attempt was made then to incorporate this observation into Model IIIA.

After conversion to a form consistent with Equations (5.1-4) and (5.4-3), and neglecting Tao's correction for Hertz spot diameter, Equation (5.5-5) becomes

$$(V/d) = (4.92 \rho_o \xi C_0)^{1.33} (Ut)^{0.33} \quad (5.5-7)$$

Later he analyzed the relative importance of metal oxidation and oxide removal in controlling the wear rate by two more models (1969). The first was based on the parabolic oxidation equation followed by an abrupt removal of the oxide layer. Assuming that the oxidation takes place at the Blok-Archard flash temperature, which depends on the square root of the load, it was possible to establish a load-wear relationship by way of the activation energy of oxidation:

$$(V/d) = (kt/Uh_c^2) \exp(-2Q/RT) \quad (5.5-8)$$

The fit to the time data was not as good as for Equation (5.5-5), and fitting the load data left something to be desired.

The second new model assumed instant oxidation, followed by removal of the oxide in accordance with the Archard equation (5.1-4). This fit the data even more poorly than Equation (5.5-8).

Tao did not discuss the role of geometry in either paper, but a personal interview led to further insight into the reasons why the peculiar exponents are required in Equation (5.5-7). The "starvation" for oxygen in the exit oil, which is an essential part of the simplification of Equation (5.5-4), also leads to a special dependence on the geometry. With a spherical member, the wear rate increases with wear since the oil intake area is ξw , and the oxygen flow $\xi w U C_0$. If we altered the geometry to a cylindrical pin, the result would be a special form of Equation (5.1-4):

$$(V/d) = K_s \rho_o \xi C_0 / P_m \quad (5.5-9)$$

where K_s is a special wear coefficient for this "starved" case, and ξ is a function of sW . This will be further discussed in Section 5.5.2.

5.5.2 Testing Model IIIA

Since the unlubricated case is outside the scope of this STAF, Equations (5.5-1) through (5.5-3) were not subjected to any real test. The authors' values of Q are shown in Table 5.5-1 along with some literature values. Obviously, the experimental values are considerably lower. One problem is that the literature values show a discontinuity, as shown in Figure 5.5-4. Another is that the dislocations, etc., discussed above are likely to affect the pre-exponential factor A , and may well have an effect on Q . It all depends on what is limiting the reaction rate. If Sakurai (1967) (see 5.5.3) is correct, and the whole process is limited by the diffusion rate of iron ion vacancy, the dislocations will not affect A or Q , but will have an effect on h_c by weakening the Fe/FeO bond strength.

The Tao Model IIIA-2 for starved corrosion has been checked against two sets of data. However, the procedure used for one depends on simplifications developed in Section 6.1, so the discussion will be given under that heading. The only point to be made at present is that Tao's values of Q in Table 5-XV are as plausible as those of Quinn and Tenwick.

The other point is that Tao's Equation (5.5-5) calls for a linear dependence of wear rate on oxygen content. As shown in Equation (5.5-6), this is in turn a quadratic function of oil density, for hydrocarbons. A test plot was made of the Appeldoorn data on 13 pure hydrocarbons and five jet fuels. The results are not very gratifying, as shown in Figure 5.5-5. (The point numbers refer to the hydrocarbons in Table 5.4-III. Points for the fuels are identified on the Figure). The ASTM constant of 0.980 for zero solubility was replaced by 1.163 derived from Appeldoorn's limited data, as the former would give negative solubility (and wear rate) for 1-Methyl naphthalene and Dimethano decalin. Use of the ASTM constant had not given any better correlation.

Points 2, 3, 15 and 18 were already under suspicion, and may be considered bad data. However, it is obvious that it would be necessary to throw out about half the remaining data to obtain a reasonable correlation coefficient. Apparently some other cause is contributing to high wear on a great many hydrocarbons. On the other hand, it appears that Tao's estimate that all the oxygen would be depleted before leaving the action zone is justified as there is only one point seriously below the line. Thus, we may accept Equation (5.5-7) as being reasonably well verified.

After a good deal of work had been done with it, two weaknesses were found in the Appeldoorn data. The first has been touched on briefly, that wear at some of the higher loads could be called "incipient scuffing". These do not include the 240 gram load used here. The second lies in the fact that the data entered in the notebooks had been processed to the extent of averaging the two diameters of the wear spot by $(a + b)/2$, rather than the more precise \sqrt{ab} . This might be expected to produce a bias rather than increased scatter, if there were no wear whatever on the cylinder, but in fact the ratio a/b does vary, at any given load. Some of this has recently been traced to variations in cylinder finish, but it is impossible to do this for the older data. Thus, it must be recognized that such tests as Figure 5.5-5 are bound to cast more doubt than is proper on the model. Any follow-on program must record the a and b values, as well as more details on cylinder reproducibility.

Table 5.5-I

Comparison of Activation Energies for the Oxidation of Iron

<u>Author</u>	<u>Equation</u>	<u>Q (KCal/mole)</u>
Quinn (1967)	(5.5-1)	7.2 to 18
Tenwick & Earles (1971)	(5.5-1)	5.32
" "	(4.4-1) Corrected for Temperature	2.46
Quinn (1971B)	(5.5-2)	4.4 to 12.2
Quinn (1971B)	Static	49
Tao (1969)	(5.5-5)	3.36
Tao (1969)	Static	9.60

Figure 5.5-4
RATE CONSTANT FOR STATIC OXIDATION
OF IRON VERSUS TEMPERATURE

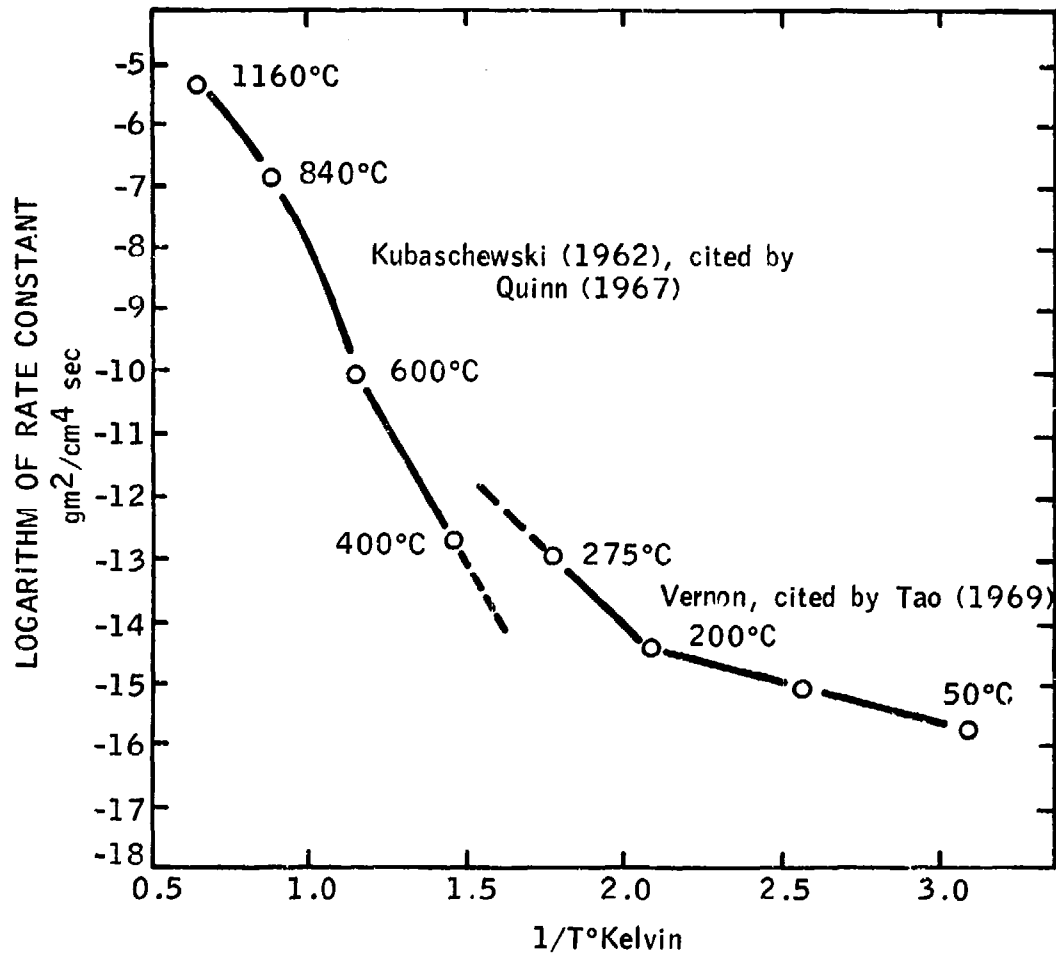
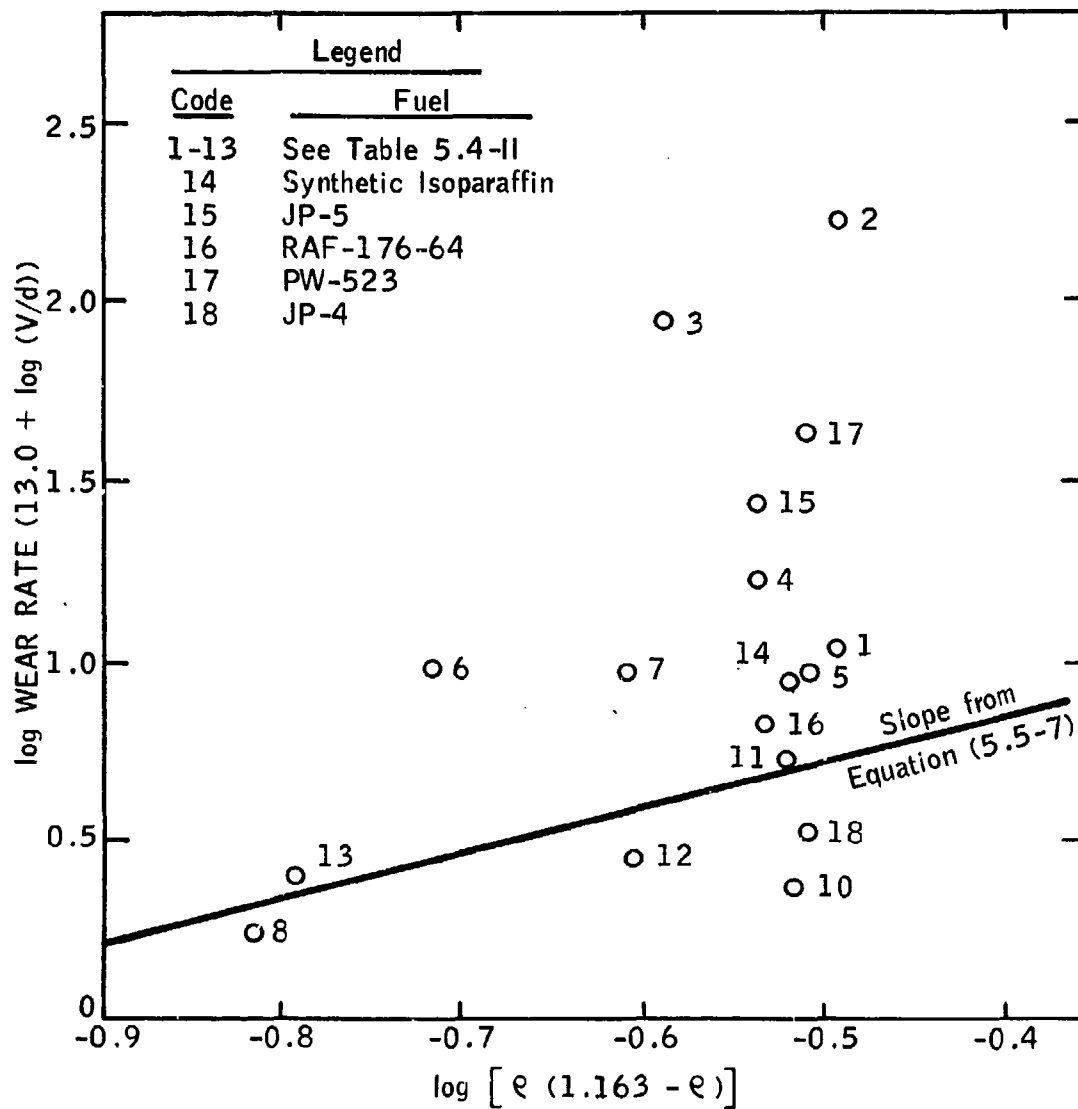


Figure 5.5-5
CORRELATION OF WEAR RATE
WITH HYDROCARBON DENSITY



This criticism was not mentioned under Models I and II, as there is no doubt as to their failure to predict even the order of magnitude of the wear rate.

One subject not yet mentioned here is the formation of alloys, though Quinn touches on it (1968-9). Fowle (1968) has studied the ratios of oxides formed on alloys and found that the fraction coated with each oxide was more closely related to the free energy of formation of the oxide than to the composition of the alloy. This may not be helpful, as rates of oxide formation are not readily predictable from these free energies according to Kubaschewski (1962). In all his examples, the oxide ratios are about as would be predicted by surface free energy considerations (see Equation (5.5-14) and Appendix VI). Thus, the preliminary work for extending Model IIIA to alloys is already laid.

5.5.3 Corrosion by Additives (Model IIIB)

Sakurai has published a series of papers (1965, 1966, 1967, 1970) which concentrate on the kinetics of the reactions at the interface of steel with oil containing "corrosive" additives. The first of these (1965) established three very important points. The most general concerns additives which follow the parabolic corrosion "law" used in developing Equation (5.5-1). These were found to exclude only dibenzyl disulfide, benzyl chloride and zinc dialkyl-dithio-phosphates which follow irregular patterns, and two chlorine compounds which follow a new "cubic law". These latter are hexachlorethane and chlorinated paraffin, both of which appear to form a polymeric film in addition to the layer of corrosion products which leads to the "parabolic law". It appears that this relation to Quinn's work is no coincidence as the second point is that oxides are more prevalent in the layer than sulfides - contrary to past beliefs. (With chlorine, the products tend to be $\text{FeCl}_2 \cdot 4\text{H}_2\text{O}$ and $\text{FeO}(\text{OH})$ after the "parabolic" reactions; whatever causes the "cubic" law was not identified). The third point was that reaction rate was essentially independent of additive concentration, showing that diffusion through the corrosion products layer is limiting. While the authors correlated the reaction rates with Mean Hertz scuff load, no wear model was formulated.

The next paper (1966) used an NACA-type test machine rather than the hot-wire static method, with the added sophistication of radioactively traced additives. However, no direct measurement of wear rates was made, and the only wear equation given is a relationship between wear and the rate constants calculated from Geiger counts. As Rowe commented (Sakurai 1966), this assumes that all the wear involved is corrosive, and that all the sulfide becomes wear debris which is hard to justify on the data as shown. The author agreed with these comments. Otherwise, the paper confirms the previous results (1965).

The third paper (1967) covered the reactions of two phosphates, two phosphites and one trithiophosphite with steel, using the hot wire test, the Timken machine and the 4-ball machine. The film was found to be mainly basic iron phosphate, with traces of phosphides, except with the thiophosphate where FeS predominated and some Fe_2O_3 and phosphate were suspected.

The important finding was that the film resistance to the flow of iron ion vacancy rose very rapidly with time on both acid and neutral phosphites and phosphates. The exponent of film thickness, calculated by the present authors, was from 4.5 to 5.2. Thiophosphate gave the usual sulfur exponent of 2.0. Only sketchy attempts were made to analyze the data, which included four readings:

- (a) Timken OK load (i.e., last step before scuffing).
- (b) Timken wear from 10 lb to OK load.
- (c) Change in surface finish on Timken block.
- (d) 4-Ball wear, load and time not specifically stated.

It should be recognized that the high exponents given above were obtained from the data obtained after an initial period of 1 to 5 minutes of nearly "linear law" corrosion, as shown by the 45° initial slopes in Figure 5.5-6. The same problem arises as on Quinn's data (Figure 5.5-3); where should the "break-in" period be considered to end? However, in this case it is even more crucial, since the possible exponents cover a five-fold rather than a two-fold range. There is not sufficient data to reach a firm conclusion on the exponents before the knee, but the present coauthor feels that future work should be concentrated in that region, since the lifetime of an asperity is probably far less than one minute.

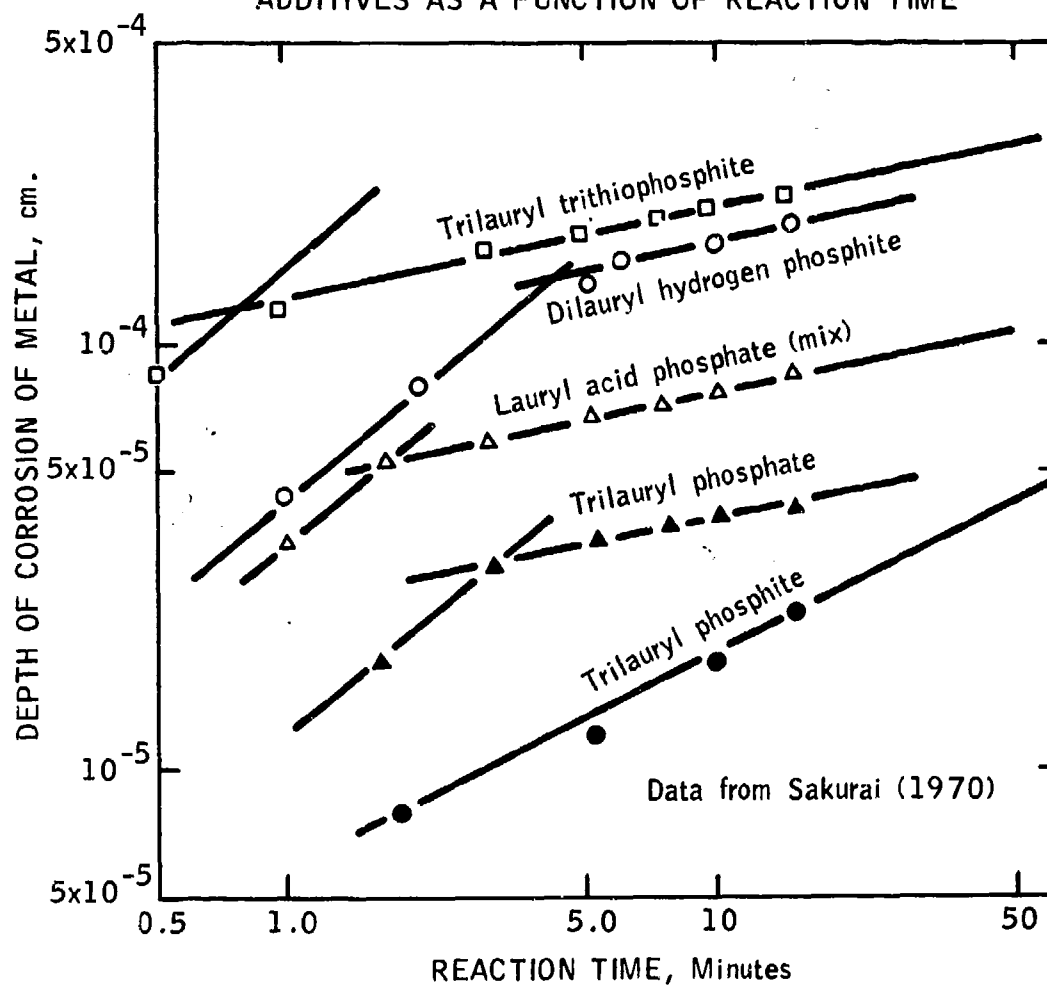
5.5.4 Formation of Surface Resin (Model IIIC)

The growth of an organic material on and around wear spots has probably been casually observed for quite a long time. Unfortunately, products of the air oxidation of lubricant are very similar in appearance and composition and even tend to form preferentially at the air-metal-oil zone of interaction. Such deposits are known as "lacquer," which shades into a thicker version known as "varnish". Eventually varnish may go on to form a black crust known as "coke," even though it is partly soluble in ketones and phenols.

The material we are calling "surface resin" was first reported (1958) as a separate entity by Hermance and Egan. They found it forming on noble metal switch contacts exposed to organic vapors, and named it "friction polymer"--a natural enough choice of words but somewhat misleading as the process is not primarily dependent on friction and the material is not a polymer by accepted terminology. These statements may seem didactic but will be explained in detail below.

Dietrich (1959) in Germany promptly followed up with another study, confirming and supplementing the original paper. Campbell (1962) tried to test their findings, but his equipment and conditions were so different that comparison is difficult. Fein (1965B) followed up Campbell's work and concluded the material was significantly involved in a good boundary lubrication. Chaikin (1967) pursued the original line, and further confirmed it.

Figure 5.5-6
CORROSION OF STEEL WIRE BY PHOSPHORUS LUBE
ADDITIVES AS A FUNCTION OF REACTION TIME



A third line was started by Furey (1965) who set out to deliberately increase the yield by adding a di-acid glycol half-ester to the lubricant. The idea was to set up a reaction at the wear zone to form long chains of ester polymer. The writer found this to be true, but also found much tendency to polymerize outside the contact area, resulting in heavy sludge and varnish. Somewhat earlier Furey (1959) had patented tetra-alkyl titanates which proved useful as anti-scuff additives, and Matuzak covered silicones for the same purpose. Neither patent gives a realistic mechanism; both are now believed to be due to surface resin. The titanates polymerize when heated alone or used in paint; and Tabor (1969) has shown that the silicones polymerize on polished copper.

None of the above work resulted in any sort of mathematical model. The writer consulted with Dr. G. C. Bond, an authority on catalysis by metals and learned that there were fairly substantial grounds for such a development. It was evident from Bond's work in correlating data from many sources that the reactions yielding free radicals at the metal surface followed Arrhenius-type equations, and that there was a relation between the activation energy and the physical (atomic) properties of the metal. In light of other studies, directed at the time to predicting E for Model II, it seemed that the surface free energy (γ_1) would be more appropriate than any parameter Bond had tried, though his included the closely related ΔH_s . Values of γ_1 were calculated (as discussed in Appendix IV) by

$$\gamma_1 = 0.0715 (\Delta H_s - RT)/V^{2/3} \quad (5.5-10)$$

where ΔH_s is the heat of sublimation at 25°C.

Some trial plots were made with data cited by Bond in his book (1962) (in his Table IV, p.195) on the exchange of deuterium with the hydrogen in ethane. The data were reported in terms of $\log r$ (reaction rate), $\log A$, and E . Plotting E versus γ_1 gave a very rough correlation; it was evident that there was an uncontrolled variable. Since $\log A$ was probably related to dehydrogenation, and the given values were fairly constant, the mean value of 23.0 was used to recalculate E' . The resulting plot was much smoother, as shown in Figure 5.5-7, and was fitted by

$$E' = 24300 - 5.36 \gamma_1 \quad (5.5-11)$$

This equation is not dimensionally consistent, as γ_1 is in ergs/cm² and E' in cal/mol. This could have been avoided by using $\Delta E_s (= \Delta H_s - RT)$, but γ_1 has more adaptability as shown later. We may consider that Equation (5.5-11) justifies tentative adoption of two hypotheses:

1. E has linear dependence on γ_1 (or ΔE_s), and
2. A is independent of the metal.

These were tested by plotting the data from Hermance (1958) and Dietrich (1959), after adjusting the latter to a comparable number of wipes and for the partial pressure of naphthalene used. The result was a surprisingly good fit to a modified Arrhenius equation (see Figure 5.5-8):

$$\log r = 30.4 \gamma_1 R'T - 0.25 \quad (5.5-12)$$

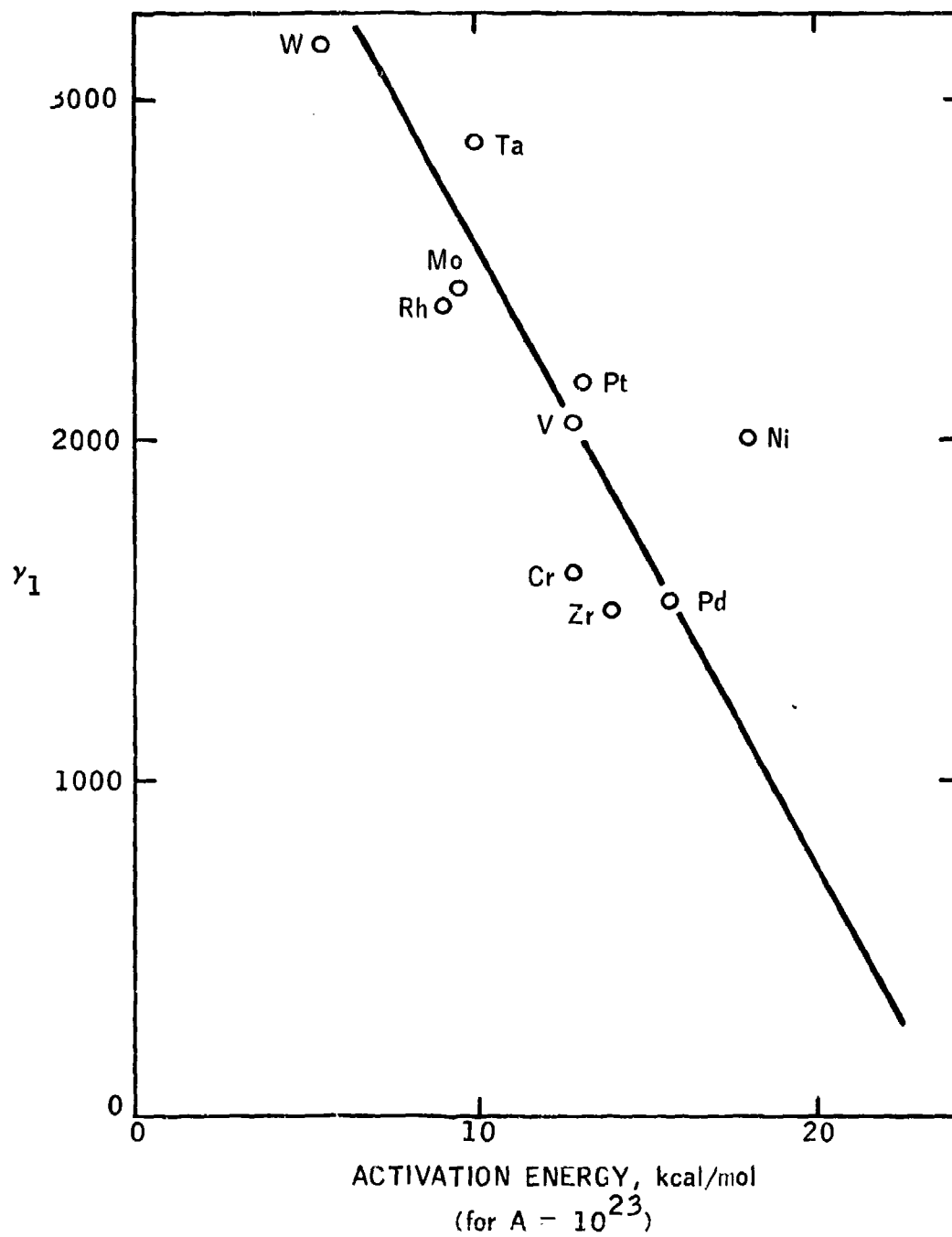
where R' is the gas constant in ergs/mol $^\circ$ K. It is somewhat presumptuous to include T , as all the data were obtained at 25 $^\circ$ C, but it seems logically justifiable. This equation might be said to conceal a third adjustable parameter, as the -0.25 no doubt includes both $\log A$ and a constant related to the 24,300 in Equation (5.5-11). It may be necessary to keep these separate, as discussed in the next section, when other hydrocarbons are involved.

There are two kinds of deviations to be accounted for in Figure 5.5-8. A number of metals completely failed to produce resin. In every case, data either from Hermance and Egan's paper (1958) or Kubaschewski (1962) showed that the metal will oxidize rapidly in air at room temperature. The other exceptions were the excessive activity of platinum for benzene and rhodium for naphthalene, and palladium for both.

In order to explain these results, it is necessary to digress briefly. The fact that metals react more rapidly when they have been distorted is common knowledge, but there has been relatively little quantitative data published. Hoar (1962, 1964) carried out a long series of experiments on the corrosion rates of various stainless alloys which had been subjected to stresses beyond the yield point. The rate ran about 10 times as high as that of annealed metal in the first paper cited (1962). Later work led to dissolution rates of 150 to 1000 times the base case, and the 1964 paper showed a ratio of over 10,000 times. Similar work was independently carried out by France (1970) on mild steel; he found the corrosion rate was increased by a factor of up to 400. A recent survey of German literature (Naeser 1970) revealed 13 cases of metals and 25 of non-metals which showed effects of "mechanical activation". Hoar's coworker Scully (1963) explained this phenomenon on the basis of dislocations which had emerged from the surface, resulting in local high-energy spots. A similar explanation was advanced by Bond (1966) to explain why the heats of adsorption on fresh, vacuum-deposited metal surfaces were far above average. As sketched in Figure 5.5-9, the step edge (B) of a screw dislocation has twice the orbital energy available of a flat surface (A). In the later stages of distortion, one might expect a ridge (C) to show three times the energy of a flat, and finally the tip of pyramid to show about five times the basic value. These local "hot spot" energies must be added to the surface free energy, following the definitions in Appendix IV, and averaged to get the surface stress.

It is the writer's belief that the reason for the platinum and rhodium discrepancies in Figure 5.5-8 is that the experimenters dislocated these specimens during preparation. If they had annealed them, they would have restored the surface free energy, as shown in a recent interchange between Merchant and Bikerman (1968). Thus, it is probable that the surface stress (σ) should be used to replace γ in Equation (5.5-12) but we do not have any sure method for measuring it.

Figure 5.5-7
CORRELATION OF ACTIVATION ENERGIES OF METALS
FOR ETHANE-DEUTERIUM EXCHANGE



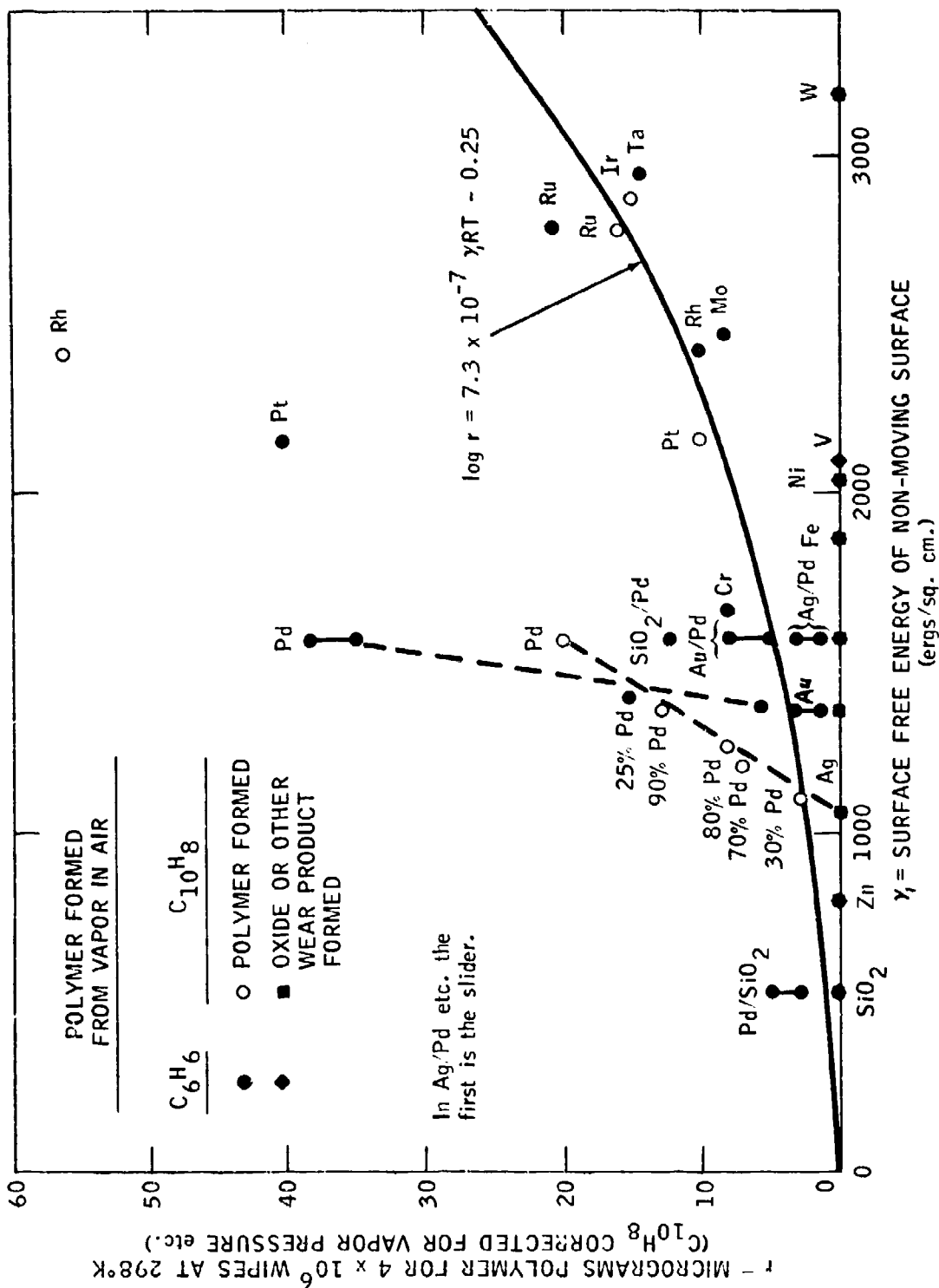
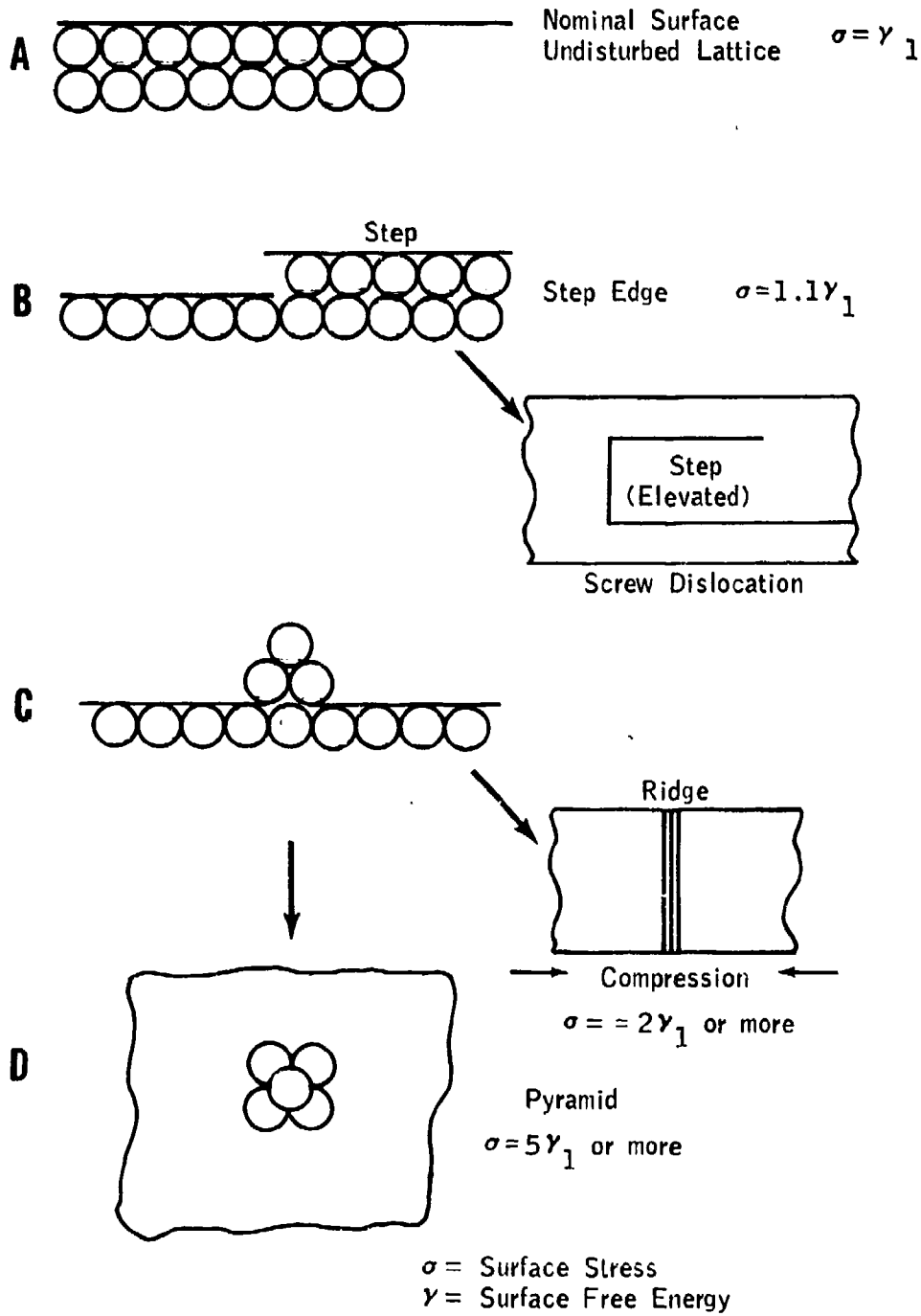
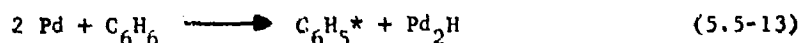


Figure 5.5-9
DISLOCATIONS AT SURFACES



The palladium situation could be explained on the same basis. However, as both Hermance and Dietrich found abnormal activity, even in alloys containing Pd, it would appear that this element has some property which makes it hyperactive. One obvious property is its exceptional capacity for absorbing hydrogen as the hydride. This would tend to drive the reaction



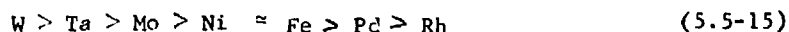
rather more forcibly than the corresponding one for platinum, etc., where H_2 must diffuse away. (The stoichiometric nature of Pd_2H is not firmly established).

One further detail on Figure 5.5-9 is of interest. The surface free energies of the alloys were calculated by an extremely simple model of Hildebrand's (1950, p.408, Equation (26)) in which a "perfect solution" is assumed. For this, we must take $V_m^{2/3}$ as constant; since for palladium, silver and gold, $V_m = 8.9, 10.3$ and 10.3 respectively, for all alloys we may use $V_m^{2/3} = 4.54 \text{ cm}^2$. The equation, in which X_3 represents the mole fraction of the higher surface free energy material, is

$$\gamma_m = \gamma_1 - \frac{RT}{V_m^{2/3}} \left(\ln(1 - X_3) + X_3 \exp \left[\frac{(\gamma_1 - \gamma_3) V_m^{2/3}}{RT} \right] \right) \quad (5.5-14)$$

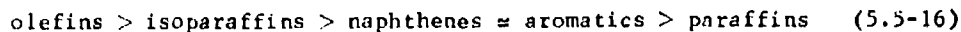
As may be seen in Figure 5.5-8, the alloys respond with very gratifying linearity of r versus γ_m . This matter is discussed further in Appendix VI.

It is also gratifying to see the way the metals line up for some other interactions. The heat of adsorption of hydrogen ranks the following metals appropriately



except that rhodium should come before nickel. Similar data for ethylene are less satisfying, as two sets of data (Bond 1962) neither agree with each other or with the γ ranking. Trapnell (1956) also reports data on ethane adsorption; unlike Figure 5.5-7, his values for molecules adsorbed per 10^{-16} mg of metal form two curves, with Ti, Cr, and Mo about ten times as active as the seven metals which fall into approximate order. It is evident that there is a considerable amount of art in producing the films used in this work, since the reproducibility between laboratories is rather poor. Variations in surface stress and contamination would account for most of the scatter.

Turning next to the reactivity of hydrocarbons in surface resin formation, Dr. Bond (1970) predicted the following ranking:



This is about the same ranking as for many other reactions, including oxidation. Olefins are rare in mineral oils, it being a matter of some note that only oils from Pennsylvania crude show a double bond, and that this has been used as a basis for prosecution of those falsely claiming their oil to be of such origin. It may or may not be coincidence that these oils have always been considered to have peculiarly good lubricating properties. Loomis (1971) has shown that resins from Pennsylvania crude have anti-wear properties.

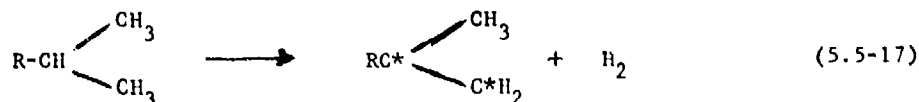
Another source of double bonds in lubricants is the fairly common practice of adding a small amount (up to 10%) of animal fatty oils, largely glyceryl trioleate, to aid in boundary lubrication. The benefits have been attributed to Model II type adsorption on the metal, but the ester does not adsorb very well until it becomes hydrolyzed in service.

A third source of olefin is the use of polymers as viscosity index improvers. These are always made from some olefinic monomer and (unless specially hydrogenated after polymerization) retain a double bond at one end of each chain. Furthermore, these chains tend to break in service, exposing more olefins. The amount is not very large; perhaps 0.1% of the olefinic nature of the monomer is present in fresh additive and no more than 0.3 to 0.5% in used oil. However, Okrent (1961A, 1961B, 1964) found that these additives provide for lower friction and wear in automotive engines than plain oils of the same viscosity. By the time of the third paper cited, he had arrived at an explanation of this fact, based on the theory of elastic relaxation of the polymer under the varying load and shear in an engine, but not everyone is fully satisfied with it.

Thus, we have three cases in which the users are prepared to pay a substantial premium for a lubricant because, for reasons which they do not clearly understand, it does a better job. The decline in sales of Pennsylvania oil was not precipitated by development of solvent refining, which yields products better in physical properties than this "standard of excellence." There was a considerable lag before solvent refined oils were fully accepted (about 20 years) and their acceptance coincided both with the exhaustion of the Pennsylvania fields and the wide-spread use of polymeric additives.

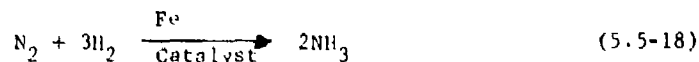
The writer does not mean to imply that these observations prove these three cases all arise from surface resin, but merely that the coincidence that the only olefinic lubricants in common use all are considered to be of premium quality demands a little investigation. In addition, data by Fein (1965B) and Appeldoorn (1967A) indicate that olefins tend to lubricate at least slightly better than saturates of the same viscosity. Buckley (1970) also showed that two unsaturated hydrocarbons, ethylene and acetylene, adsorb more strongly on clean iron surfaces than do methane and ethane, and cause more decrease in the adhesion between two surfaces for equivalent surface coverage. Hansen (1970B) studied the decomposition of these two gases on tungsten, and Morecroft (1971) extended the work to octadecane and decanoic acid. Both reacted to give hydrogen and methane, showing that his evaporated iron film was vigorously reactive.

The attack on isoparaffins is essentially a dehydrogenation, as visualized by Eischens (1969):



The hydrogen is free to diffuse away into the metal or oil. Carbide formation may be very important, as discussed in Section 5.9, due to multiple radicalization. The reaction which takes place with other pure hydrocarbons is essentially similar. The free radicals produced are very prone to form resin with any oxygen present, but even in de-oxygenated helium they can polymerize (Kingsbury 1968). In the latter case, the reaction is fairly slow, and probably proceeds through oil-soluble dimer etc. until an insoluble state is reached.

The course of events in air is considerably more rapid and complicated, due to immediate interaction of the free radicals with oxygen, to form hydroperoxide radical and various other species. Surprisingly, the nitrogen of the air also gets involved; the ability of a bearing to fix nitrogen tells a good deal about the energies involved. The reaction may well be that of the Haber process



which is usually carried out at 200 atmospheres and 500°C.

The product has definitely been shown to contain C=O groups (Fein 1965B), which appear to be in the form of esters, soaps, ketones and amides. This was confirmed by Goldblatt (unpublished). Another evidence of the energies involved is that pure aromatics yield aliphatic surface resin, as observed by Hermance (1958), Fein (1965B) and Goldblatt (unpublished).

Hermance (1958) also published a great deal of data on the solvent resistance of the resin made from benzene vapor. The writer analyzed his data by the Hansen (1967) method, discussed in Appendix V. The results are shown in Figure 5.5-10. Briefly, the three quadrants represent the faces of a three dimensional plot, so that placing the two δ_D axes together would produce a corner of a space in which two spheres hang suspended. Each solvent is represented by a point on each surface, and the spheres by a circle on each surface. The coordinates are δ_D , the contribution of London forces to the Hildebrand (1950) solubility parameter; δ_P , the contribution of the Keesom (permanent dipole) forces; and δ_H , the contribution of the electron-acceptor ("hydrogen bond") and related forces. Non-solvent points fall outside the spheres, and hence outside the circles on two or more quadrants, while solvent points must fall inside the circles on all three quadrants to be properly correlated as discussed in Appendix VIII. It will be noted that all solvents except nitrobenzene ($\text{C}_6\text{H}_5\text{NO}_2$) fall in the proper areas.

The plot required two spheres to contain all the solvents except $\text{C}_6\text{H}_5\text{NO}_2$, and exclude the non-solvents. This pattern is typical of mixtures and copolymers (Beer-bower 1969). In this case, the smaller sphere appears to center around ester-type resins, while the larger sphere is characteristic of acids and amides.

Similar plots of data by Goldblatt (unpublished) are shown in Figure 5.5-11 for resin from naphthenic base-stock. The resemblance to that from benzene is very striking. On the other hand, resin from a mixed aromatic-isoparaffinic lubricant showed a very different pattern, as shown in Figure 5.5-12.

Figure 5.5-10
DATA ANALYSIS ON
HERMANCE AND EGAN FRICTION POLYMER

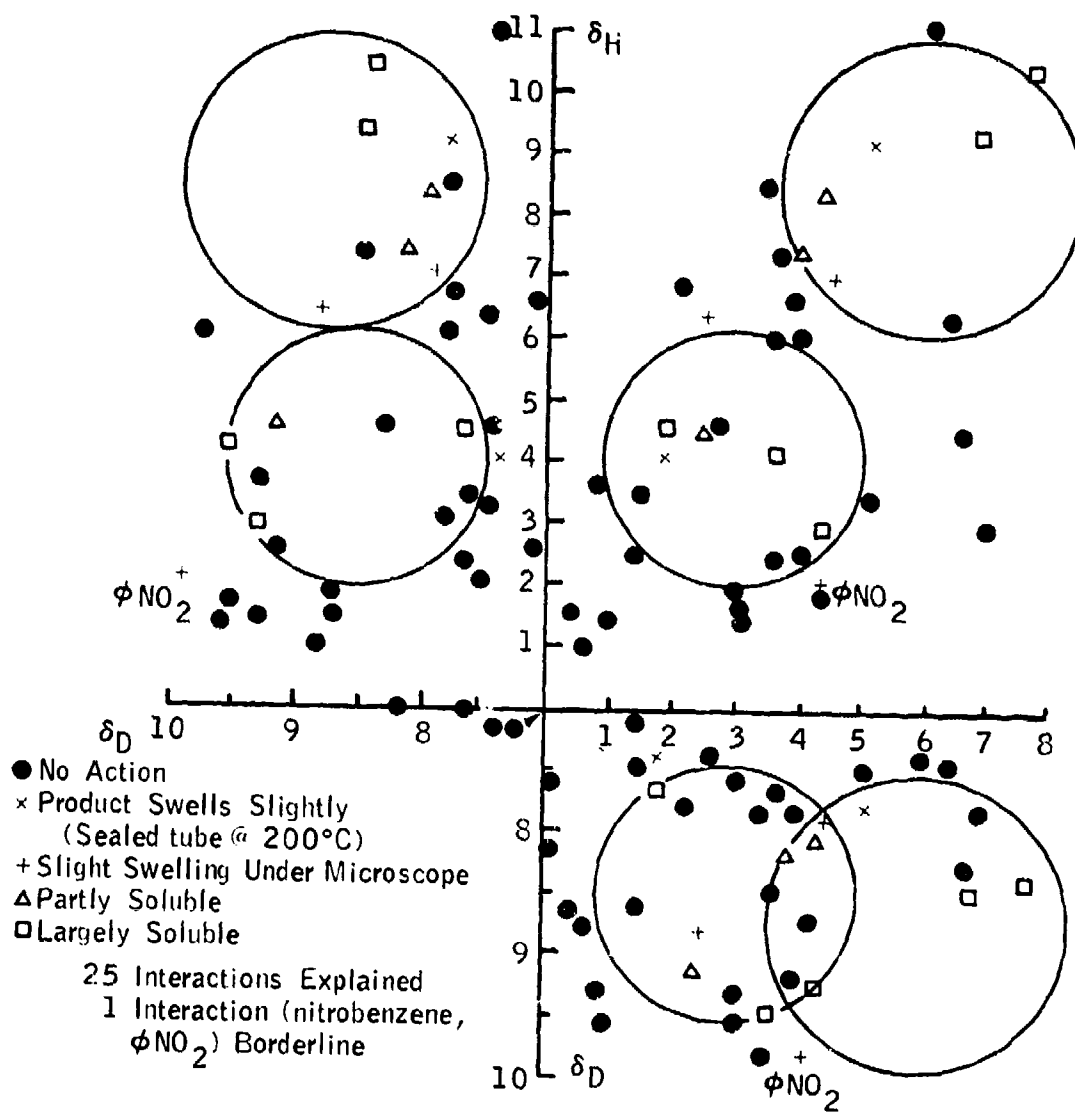


Figure 5.5-11
SOLUBILITY PARAMETER OF RESIN
FORMED FROM NAPHTHENIC BASE STOCK

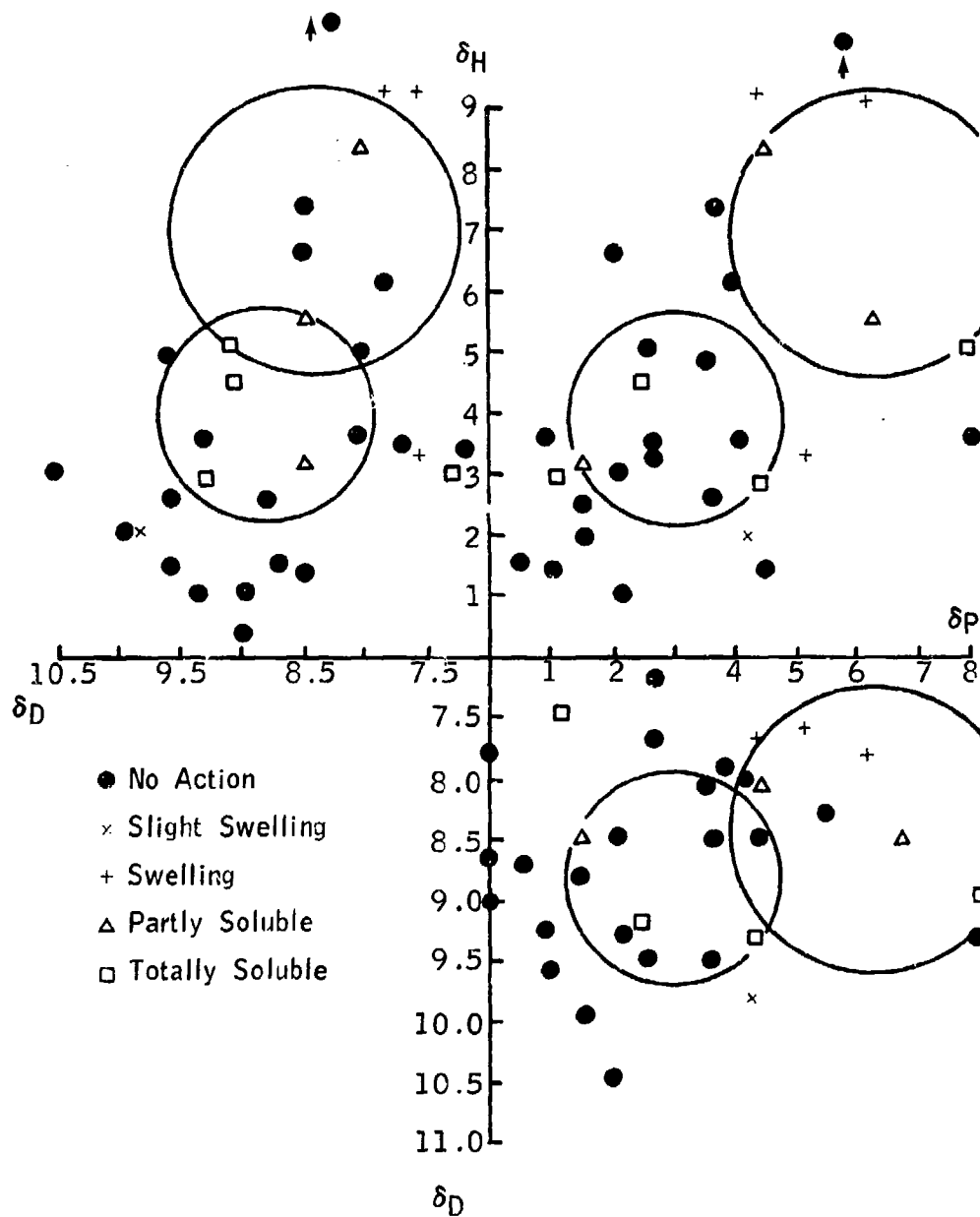
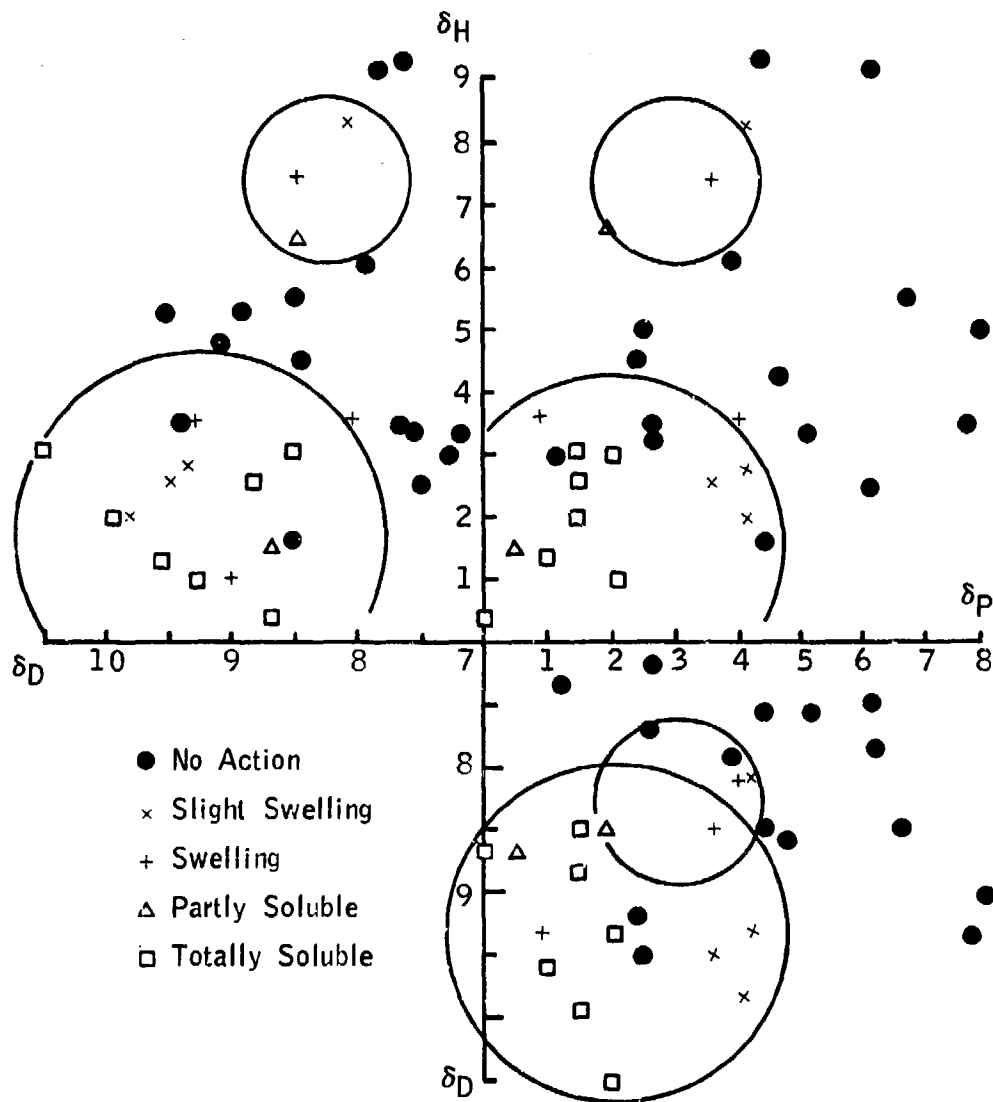


Figure 5.5-12
SOLUBILITY PARAMETER OF RESIN
FORMED FROM AROMATIC +
ISOPARAFFIN LUBRICANT



This is one of the many pieces of evidence which led Goldblatt (1971) to develop a further model to account for the blending anomaly, which is discussed in the next two sections.

5.5.5 The Charge-Transfer Mechanism (Model IIID)

As discussed in the previous section, dehydrogenation followed by polymerization is a fairly straight-forward process. The fact that oxidation frequently accompanies the "polymerization" merely increases the rate of resin formation and does not change the basic mechanism of Equation 5.5-17. Goldblatt's model goes far beyond this, as it depends on another mechanism to supplement the rather sluggish reactions so far discussed. The whole scheme is shown in Table 5.5-II, in slightly different symbols and language from those in the original. Another version, perhaps more easily understood, is shown in Figure 5.5-13.

The first process was discussed in Section 5.5.4, in considerable detail. However, it must be added that the deformation process also releases a considerable flow of electrons from the metal. These "exoelectrons," which are often called after Kramer (who discovered them), are emitted at a rate which falls off exponentially with time as if it were radioactive decay with a few hours half life. This leads naturally to the third process the acceptance of an electron by a polynuclear aromatic which has already been adsorbed in process #2. The presence of the resulting radical anion ($Ar\cdot$) was demonstrated by Goldblatt in several ingenious experiments.

$Ar\cdot$ when set free by process #3a, is a very active chemical, and can participate in the various other processes, #4, 6, 7, and 8. Process #4 is one of those Goldblatt demonstrated; he used $\alpha-Fe_2O_3$ to destroy 1-methyl naphthalenide. Both #3b and #4 can generate wear debris. If $M:Ar\cdot$ dissolves before desorption, very fine metal will result (i.e., the lamp-black like material often associated with mild wear). In process #4, $Ar\cdot$ attacks aged surface and in doing so, detaches oxide which becomes an abrasive to perpetuate step (1) in a chain reaction via process #5.

If $Ar\cdot$ last long enough, it can reach other compounds than those at the surface. In ordinary air, both H_2O and O_2 are at hand to quench $Ar\cdot$ and Goldblatt feels this accounts for air alleviating the high wear observed with dry inert atmospheres. Process #6 results in dihydroaromatic, which is really an olefin and hence prone to oxidize to a resin such as process #7 generates directly.

Process #8 is a major source of resin, and is considered to be the main explanation of the blending effect (Anomaly 3.5). Process #9 is merely a variant in which #7 and #8 take place simultaneously.

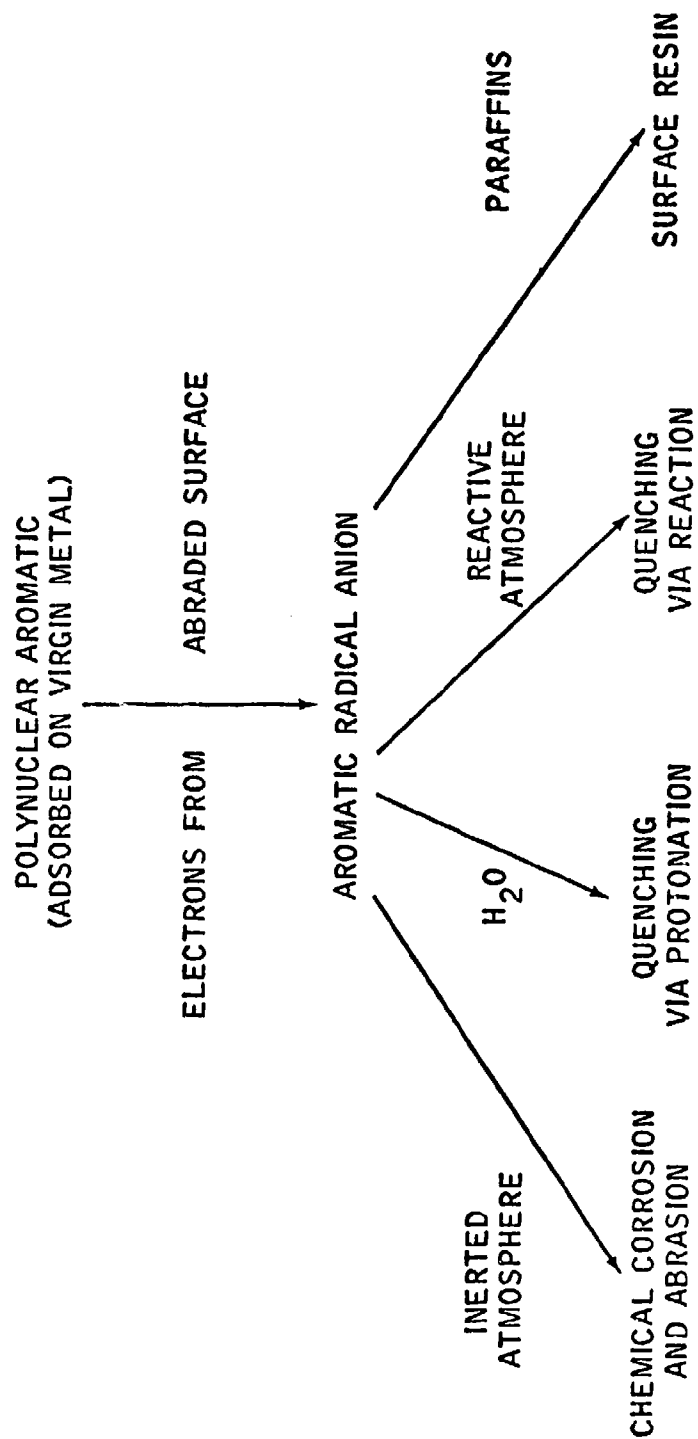
This is too large a set of reactions to include in Equation (5.5-12), which was actually only set up to cover metal + aromatic + O_2 processes corresponding to #1, #2, #3, and #7. Of course, as #6 tends to end in the same way as #7, it can be counted in, but #4, #8, and #9 are new business. Of course, with two empirical parameters Equation (5.5-12) can be adjusted to cover almost any situation, especially as one of them is the difference of two terms. The danger is that it can be adjusted too easily, and so does not serve as a very good screening tool.

TABLE 5.5-II

The Charge Transfer Mechanism

Aged Metal Surface $\xrightarrow{\text{deformation}}$ Active Metal (M)	#1
M + Polynuclear Aromatic (Ar) $\xrightarrow{\text{adsorption}}$ M:Ar	#2
M:Ar $\xrightarrow{\text{ionization}}$ $M^+ : Ar^-$	#3a
$M^+ : Ar^-$ $\xrightarrow{\text{desorption}}$ $M^+ + Ar^-$	#3b
$Ar^- + MO_x \xrightarrow{\text{reduction}}$ MO_{x-1} (abrasive)	#4
Aged Metal + Abrasive $\xrightarrow{\text{deformation}}$ M	#5
$Ar^- + H_2O \longrightarrow Ar-H \cdot + OH^- \longrightarrow ArH_2$	#6
$Ar^- + O_2 \longrightarrow Ar + O_2^- \longrightarrow \text{Peroxide} \longrightarrow \text{Acid or Resin}$	#7
$Ar^- + \text{Aliphatic (Ap)} \longrightarrow Ar:Ap \text{ Adduct} \longrightarrow \text{Resin}$	#8
$Ar^- + Ap + O_2 \xrightarrow{\text{peroxidation}}$ $ApO_2 \longrightarrow \text{Acid or Resin}$	#9

FIGURE 5.5-13
CHEMICAL MODEL FOR LUBRICATION IN THE PRESENCE OF
POLYNUCLEAR AROMATICS



More data are needed to determine whether it is applicable to other aromatics. Actually, benzene is unique, and being able to lump it with naphthalene may have been an accident. If not, (5.5-12) should apply to all non-alkylated aromatics. Alkylated ones must be sharply divided into those having a benzylic hydrogen, and others. The "others" must be tested against (5.5-12), but the "benzylic" class have a special weakness to oxidation that would upset the whole model.

If (5.5-12) is to be extended to more general use, it will be necessary to correct the dimensional imbalance by putting cm^2/mol into the right-hand side, or by going back to ΔE_s . The second would cost us the flexibility of γ_1 in dealing with surface stresses (Appendix IV) and alloys (Appendix VI). However, this might not be too serious as σ is almost impossible to measure directly and the electrical data from Hoar (1964) and Francis (1970) could as easily be applied to augment ΔE_s . Equation (5.5-12) could very easily be converted to a "surface energy of sublimation" ($\gamma V_m^{2/3}$). The effect on Figure 5.5-8 would be trivial as $V \approx 10 \text{ cm}^3$ for most of the active metals.

Assimilating processes #6 and #7 into mathematical form requires knowledge of the solubility of H_2O and O_2 , which is available, and perhaps of their rates of diffusion and reaction. However, on the basis of Tao's Model IIIA work and success with Equation (5.5-5), it appears that these reactions might also be handled on a concentration-only basis. Certainly processes #6 and #7 are as rapid as would be the direct oxidation of metal, but in this case the supply of radical anions is also limiting as was not the case with the metal. Thus, it will be necessary to regard Equation (5.5-12) as the starting point of a rather complex set of equations. These must necessarily involve the concentration of $\text{Ar}\dot{\text{O}}$ as a function of the distance from its points of origin.

One factor not previously considered is the effect of pressure on polymerization. Weale (1967) gives an equation which is adaptable as follows:

$$\ln(k/k_0) = \frac{q_0 \Delta V_m}{V_m RT_0} \quad (5.5-19)$$

where k and k_0 are the rate constants at q_0 pressure and at one atmosphere respectively, and $\Delta V_m/V_m$ is the fractional change in volume on polymerization. This predicts for a typical reaction in which $\Delta V_m/V_m = 0.20$, an acceleration of approximately 10,000 fold under $q_0 = 20,000$ atmospheres. When interviewed, he pointed out that this reasoning does not hold if the lubricant solidifies, and cited a summary by Babb (1963) of data on freezing under pressure.

5.5.6 Testing Model IIID

It is difficult to subject these models to wear rate analysis in view of their incomplete status. First, it will be necessary to formulate equations that express the lubricant composition in terms leading to another equation to join with (5.5-12). The following excerpt from a recent paper by Goldblatt and the writer (Beerbower 1971F) gives some ideas as to how this might be done in terms of measurable parameters of aromatic and heteroatom molecules. The questions to be answered were "Why do heteroatom molecules increase wear in petroleum lubricants?" and "Which types of heteroatom molecules are particularly bad?"

"In this model, the aromatic adsorbs onto the freshly uncovered metal surface, and accepts an electron from it to form a radical anion. This anion may then undergo one or more of three competing reactions:

- [1] React with another hydrocarbon to form "surface resin",
- [2] Be quenched by water, oxygen or another electron acceptor, or
- [3] Form a metal-organic compound, a kind of corrosive wear.

Reaction [1] is the way in which aromatics improve the wear rates of paraffins. The surface resin serves as a solid film lubricant, and also enhances hydrodynamic lubrication by partly filling the anti-asperities (Beerbower 1971A).

"Reaction [2] is the one involved in the questions. The most general answer is that the most efficient electron capturing species will interfere most completely with the enhancement. A special answer is that in the absence of oxygen, this same species would enhance Reaction [3], and so increase wear above that found with paraffin alone."

"One measure of the quenching ability of a species is its capture rate of solvated electrons. Table 5.5-III lists observed rates of capture as determined by Hart (1964). Pyridine and nitrobenzene show high rates, the latter being 100 times as fast as naphthalene. From this one would predict that both would interfere with lubrication by paraffin-aromatic blends. No data was available on ring-sulfur compounds, but the aromaticity of thiophene is slightly greater than that of pyridine (Kanekar 1967), so the rate should also be slightly greater. It has also been found that in competitive metalation of benzothiophene and N-methylindole, the former is preferentially metalated (Shirley 1964). Carbon disulfide is also very efficient at electron capture, the rate being about the same as for nitrobenzene.

"Another criterion for predicting the effects of heteroatom species is the type of reactions the intermediates might undergo. Nitrogen heterocyclic molecules form intermediates that are probably innocuous. On the other hand, sulfur compound intermediates are highly reactive, as shown by their thermal instability (Gerdil 1963), and thus are prowear agents. Since aromatic ring sulfurs are more reactive than aromatic ring nitrogens, one would expect the sulfurs to be the more detrimental.

"A brief screening of some naturally occurring heteroatom species is shown in Table 5.5-IV. It is clear that pyridine and indole do not promote wear, though there is some effect on friction. On the other hand, benzothiophene is extremely prowear. So is nitrobenzene, a nonring nitrogen molecule which was predicted to be quite reactive. Similar data were reported by Rudston (1971) who showed that several sulfur compounds promoted wear in white oil, while nitrogen compounds such as pyridine and indole reduced wear as predicted.

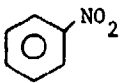
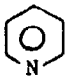
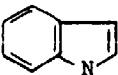
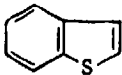
TABLE 5.5-III

ABSOLUTE RATE FOR
CAPTURE OF A WATER-SOLVATED
ELECTRON

<u>Acceptor</u>	<u>pH</u>	<u>Rate ($M^{-1}sec^{-1}$)</u>
Benzene	7	7×10^6
Aniline	11.9	2×10^7
Naphthalene	7	3.1×10^8
Nitrobenzene	7	3×10^{10}
Pyridine	7.3	1×10^9
Carbon Disulfide	7.7	3.1×10^{10}

TABLE 5,5-IV

HETEROATOM MOLECULES SHOW PROWEAR OR INCREASED FRICTION
IN MIXED (50/50) ISOPARAFFIN-AROMATIC BASE STOCK(1)

<u>Additive</u>		<u>Wear Scar Diameter (mm)</u>	<u>Coefficient of Friction</u>	<u>Percent Heteroatom Species in Oil</u>
None		0.38	0.08	0
2% Nitrobenzene		0.55	0.13	0.74
2% Pyridine		0.34	0.12	0.36
2% Indole		0.38	0.09	0.24
2% Benzothiophene		0.53	0.10	0.47

(1) 4-Ball test, 15 mins., 77°F, wet air atmosphere, 1200 rpm,
20 kg load, 52100 steel.

"Based on these studies, it may be concluded that, among the various heteroatom molecules occurring in petroleum, the sulfur compounds are among the most detrimental to wear in mixed paraffin-polynuclear aromatic blends."

Since the comments quoted above were written, we have come to believe that the electron transfer energy (χ_{H}^2) can well be substituted for the values in Table 5.5-III, but further study of this matter is needed.

5.5.7 Formation of Soap Films (Model IIIE)

The concept of additives forming covalent compounds with the metal surface is at least as old as that of reversible adsorption (Bowden 1950). However, no mathematical model has been suggested up to now. The nearest approach has been that of Kreuz (1969) who demonstrated that such films can be removed by the solvent action of the base fluid. This had always been a strong argument for reversible adsorption, as it was hard to explain how a covalent film could ever fail. However, Kreuz did not carry his work to its logical conclusion by applying the Hildebrand (1950) theory of regular solutions. This may have been because Kreuz found quite sharp "solubilization" temperatures for his soap films, which were essentially independent of concentration; in fact, they could be related to the transition point at Y in Figure 2-1. Such behavior is not predicted by the Hildebrand theory because it relates only to London forces and the soaps include major polar and hydrogen bonding. Prediction of the behavior of such systems requires the Hansen (1967) modification, which predicts a rather sharp miscibility when the molar volume of the solid is very large with respect to that of the base fluid, V_m :

$$(\delta_{D1} - \delta_{D2})^2 + 0.25 (\delta_{P1} - \delta_{P2})^2 + 0.25 (\delta_{H1} - \delta_{H2})^2 < RT_c / 2V_m \quad (5.5-20)$$

where δ_{D1} etc. are the partial parameters of the soap, and those with subscript 2 are those for the lubricant.

This method will require more work, especially since δ_P and δ_H for soaps are not so easily calculated as for polymers, but it does offer design possibilities. It also has the complication that it leads back to Model II-C, since dissolved soaps are still "additives" and must be treated according to their E values on the metals.

No published data except that of Kreuz (1969) is available, and that is too scanty for a real test of Equation (5.5-20). However, unpublished data by Goldblatt, Harting and Panzer each, in various ways, support this model. Of the three only Goldblatt has actually carried it through the wear rates; in his opinion, the combination with Model V will be of real significance but only in a limited number of cases.

5.6 Metallurgical Compatibility (Model IV)

The models discussed so far have attempted to provide general coverage of the whole span from 0 to Y in Figure 2-1. The remaining ones are more specialized, and tend to be directed only to locating a limit in the same sense that Model IA serves to locate point O. Model IV serves only to define what happens at point Y, and perhaps beyond it to point Z.

Investigation of the scuffing transition phenomenon has already been mentioned under Models II and III, with some plausible explanations available. However, there is reason to believe that when all lubricating films have failed (including the metal oxide), the nature of the metals in contact may spell the difference between moderate wear and scoring or even welding. Such "self-lubricating" pairs are well known; the steel "worm" driving a bronze gear is a classic example. Naturally, such pairs show high transfer when unlubricated; as Johnson (1970B) pointed out, everything sticks to everything because the London forces present in all matter are totally non-discriminating.

A number of investigators have sought other couples with even more favorable properties than steel + bronze. Rabinowicz, one of the most diligent investigators of Model IV, was able to cite eleven studies (1971A), though he had to discard one of these as it was based on an unfortunate choice of metals. The remaining ten, along with several he failed to cite and the MacGregor data for Model I, are discussed in Section 5.6.3. The consensus of these workers appears to be that transition involves some degree of interpenetration of one metal into the other, to form a solid solution.

This leads to two models, one based on the bulk energies of the metals and the other on the surface energies. As discussed under Model IIIc, these are closely related, but they will be handled separately at present.

5.6.1 The Bulk Energy Model (IVA)

Hildebrand (1950) established a simple rule for the miscibility temperature of two metals which form a regular solution. This usually takes place at around 50/50% by volume. If we adopt this as a model for transition temperature,

$$T_t = \frac{V_1 + V_2}{4R} (\delta_1 - \delta_2)^2 \quad (5.6-1)$$

where V_1 and V_2 are the molar volumes of the metals while δ_1 and δ_2 are their solubility parameters. If T_t is less than the surface temperature T_s , scoring will take place.

A computer run on this model was published (Beerbower 1971A). It showed that unrealistic T_t values (up to 39000°K) resulted, so a less simplified version of the Hildebrand equation which permits insertion of other concentrations was used:

$$T_t = \frac{\phi_1^2 V_1 (\delta_1 - \delta_2)^2}{R [\phi_1 (1 - V_1/V_2) + \ln(1 - \phi_1)]} \quad (5.6-2)$$

Runs were made with ϕ_1 (defined as the volume fraction of the high δ metal) set at 95%, but the predictions were still far higher than ever observed at transition (up to 13,400 °K). However, $\phi_1 = 0.05$ gave quite reasonable-looking values of T_t , with a maximum of 906°K (633°C) for Zn-Zr. There also appears to be an appropriate relation between $T_t = 300^\circ\text{K}$ and behavior at about room temperature, as discussed in Section 5.6.3.

5.6.2 The Surface Free Energy Model (IVB)

Rabinowicz (1965B) cited surface free energy, and especially the ratio of it to hardness (γ/P_m), as a key parameter in friction and wear. In a recent article (1971A), he undertook to link this with the static coefficient of friction

$$F_s \approx 0.2 + C_1 A_{12}/P_{m1} \quad (5.6-3)$$

where C_1 is a constant for constant surface geometry, A_{12} is the work of adhesion ($= \gamma_1 + \gamma_2 - \gamma_{12}$, where γ_{12} is the interfacial free energy), and P_{m1} is the penetration hardness of the softer metal.

Since neither A_{12} nor γ_{12} can be readily measured nor rigorously calculated, he proceeds to make the rather drastic assumption that $A_{12} = C_2 (\gamma_1 + \gamma_2)$, so that

$$F_s \approx 0.3 + C_1 C_2 (\gamma_1 + \gamma_2)/P_{m1} \quad (5.6-4)$$

Values of C_2 were determined empirically, for five situations, from the largest collection (210 pairs) of static friction data ever published. The procedure was to sort the data into sets, based on binary phase diagrams from the literature. The sets were the four categories shown in Figure 5.6-1 plus "identical" for metals sliding on themselves. All five sets were then plotted separately, F_s versus $\log [(\gamma_1 + \gamma_2)/P_{m1}]$, using the log function simply to "spread the points out more effectively". Since the "compatible" group of 97 pairs was largest, it was used as the standard for slope of the resulting best straight line. This line was then transferred to the other plots, and a "best fit" line drawn parallel to it. By arbitrarily setting $C_2 = 0.5$ for the first plot, he eliminated C_1 and arrived at C_2 values for the other four sets. These are shown in Table 5.6-1 as "measured". The measured values were "adjusted" to those in the last column (C_2') "to spread the values out more evenly". It is not made clear how the adjustment process was handled, but it was obviously guided by his awareness that C_2' cannot exceed 1.00. Down to the last line, the adjusted values fit

$$C_2' = 2/3 C_2 + 1/6 \quad (5.6-5)$$

fairly well, but he apparently abandoned linearity to force agreement with his paper (Rabinowicz 1966) even though this was at odds with his book (1965B).

Several steps in this model are far from mathematically rigorous. When the paper was presented, Steijn commented that basing a linear coefficient such as C_2 on a semilog plot was unsound. Rabinowicz admitted this, but indicated that he felt it gave correct results. Setting the "compatible" group at $C_2 = 0.50$ is also a dubious procedure; setting "identical" at 1.00 would be much more defensible. Further discussion will be given in Section 5.6.3.

In his latest article (1971B), Rabinowicz dropped out the surface energy model and merely compared Figure 5.6-1 with ten sets of friction data. These included 70 of his 210 pairs for static friction in air, covering a restricted hardness range since apparently hardness has an independent influence on F_s . Two other sets of static friction in vacuum are also included. Two small sets of adhesion in vacuum data were combined. Six sets of kinetic data, including one previously unpublished, were used.

TABLE 5.6-I

VALUE OF COMPATIBILITY PARAMETER C_2

<u>Condition</u>	<u>Symbol</u>	<u>Measured Value of C_2</u>	<u>Adjusted Value of C_2'</u>
Identical		1.25	1.00
Compatible	○	.50	.50
Limited Compatibility	◐	.25	.32
Limited Compatible	◑	.16	.20
Incompatible	●	.15	.125

The "model" was simply the standard method for correlation coefficient by ranking. The coefficient was determined for each set of data, and for subsets in several cases where atmosphere or temperature was varied. Wear data was also correlated, when available. Both static and kinetic data showed average friction coefficients of 0.28, but the kinetic data showed less scatter. Wear correlated with a coefficient of 0.56, and less scatter than kinetic friction.

These coefficients are cited as evidence that compatibility is a factor in friction and wear. By ordinary standards, coefficients less than 0.85 are considered unconvincing, so that the effect of this paper is to indicate that other factors dominate the process. This "model" does not require further discussion, since IVA appears to provide more satisfactory correlations.

Figure 5.6-1
COMPATIBILITIES OF METAL PAIRS

	W	Mo	Cr	Co	Ni	Fe	Nb	Pt	Zr	Ti	Cu	Au	Ag	Al	Zn	Mg	Cd	Sn	Pb
In				◐	◐				◐	◐	◐	◐	◐	◐	◐	◐	◐	◐	◐
Pb	◐	◐	◐	◐	◐	◐	◐	◐	◐	◐	◐	◐	◐	◐	◐	◐	◐	◐	◐
Sn			◐	◐	◐	◐	◐	◐	◐	◐	◐	◐	◐	◐	◐	◐	◐	◐	◐
Cd			◐	◐	◐	◐		◐	◐	◐	◐	◐	◐	◐	◐	◐	◐	◐	◐
Mg		◐		◐	◐	◐	◐		◐	◐	◐	◐	◐	◐	◐	◐	◐	◐	◐
Zn		◐	◐	◐	◐	◐	◐	◐	◐	◐	◐	◐	◐	◐	◐	◐	◐	◐	◐
Al	◐	◐	◐	◐	◐	◐	◐	◐	◐	◐	◐	◐	◐	◐	◐	◐	◐	◐	◐
Ag	◐	◐	◐	◐	◐	◐	◐	◐	◐	◐	◐	◐	◐	◐	◐	◐	◐	◐	◐
Au	◐	◐	◐	◐	◐	◐	◐	◐	◐	◐	◐	◐	◐	◐	◐	◐	◐	◐	◐
Cu	◐	◐	◐	◐	◐	◐	◐	◐	◐	◐	◐	◐	◐	◐	◐	◐	◐	◐	◐
Ti	◐	◐	◐	◐	◐	◐	◐	◐	◐	◐	◐	◐	◐	◐	◐	◐	◐	◐	◐
Zr	◐	◐	◐	◐	◐	◐	◐	◐	◐	◐	◐	◐	◐	◐	◐	◐	◐	◐	◐
Pt	◐	◐	◐	◐	◐	◐	◐	◐	◐	◐	◐	◐	◐	◐	◐	◐	◐	◐	◐
Nb	◐	◐	◐	◐	◐	◐	◐	◐	◐	◐	◐	◐	◐	◐	◐	◐	◐	◐	◐
Fe	◐	◐	◐	◐	◐	◐	◐	◐	◐	◐	◐	◐	◐	◐	◐	◐	◐	◐	◐
Ni	◐	◐	◐	◐	◐	◐	◐	◐	◐	◐	◐	◐	◐	◐	◐	◐	◐	◐	◐
Co	◐	◐	◐	◐	◐	◐	◐	◐	◐	◐	◐	◐	◐	◐	◐	◐	◐	◐	◐
Cr	◐	◐	◐	◐	◐	◐	◐	◐	◐	◐	◐	◐	◐	◐	◐	◐	◐	◐	◐
Mo	◐	◐	◐	◐	◐	◐	◐	◐	◐	◐	◐	◐	◐	◐	◐	◐	◐	◐	◐

The assumed compatibility relationships, based on the binary phase diagrams. Like metal pairs, not shown, are assumed metallurgically compatible by definition.

- -Two liquid phases, solid solution less than 0.1%.
- ◐ -Two liquid phases, solid solution greater than 0.1%, or one liquid phase, solid solution less than 0.1%.
- ◑ -One liquid phase, solid solution between 0.1% and 1%.
- -One liquid phase, solid solution over 1%.

Blank boxes indicate insufficient information.

5.6.3 Testing Model IVA (Metallurgical Compatibility)

Despite its obvious limitations, Model IV has a fascination about it that has led to an amazing amount of work being done and reported. It has also led to more analysis than it may seem proper to include in a study of lubrication.

The laboratory work cited by Rabinowicz (1971B) in his analysis, and a good deal which he did not cite, is listed in Table 5.6-II. The former includes his own static tests (1971A), some by Tomlinson (1929) on which he casts serious doubt, and two sets of static tests in vacuum. None of these seem useful for testing Model IVA, nor do the two sets of adhesion tests in high vacuum. One of these was already cited by the writer, as was the kinetic work of Roach (1955), Coffin (1956), and Machlin (1954). The work by Grau (1966) had not been previously published, but will be useful here.

Rabinowicz cited only one paper on alloys (Moeller 1967), and handled that quite crudely by assuming that they would perform as if 100% composed of the main constituent. This is by no means in all cases; Equation (4.4-15) shows how binary blends can be handled, while Shain and Prausnitz (1964) carry this idea further. Work on alloys not cited includes Cornelius and Roberts (1961), and five other related papers. Most important, in terms of quantity as well as tie-in with Model I, is the work of MacGregor (1964), which was also neglected.

A partial analysis of four of the sets of data was made, in accordance with Equation (5.6-1) and published (Beerbower 1971A) in the form of predicted temperatures at the 50% miscibility point. The success ratings had to allow for the results from the laboratories containing contradictions, part of which may have been caused by the lack of a clear definition of "scoring". The writer attempted to bring the data to a common basis, in which "rough", "abraded", etc., were converted to "poor" scoring resistance, "smooth" or low wear rates to "good", and intermediate descriptions to "fair". Where data in helium was available, it was given preference over that in air or in air-saturated kerosene. All hexagonal (HCP) metals were excluded from the ratings; as shown by Buckley (1966), these follow different rules than the common cubic metals. The criteria of success were based on an arbitrary choice of Poor = 0-2000°K, Fair = 2000-4000°K, Good = 4000+°K. These unrealistic temperatures result from their being based on complete miscibility at about 50/50% by volume.

As mentioned in Section 5.6.1, new computer runs were made on Equation (5.6-2). The results at $\phi_1 = 0.05$ as shown in Table 5.6-III for various metals on iron, and in 5.6-IV for various nonferrous combinations. This time the success of predictions was rated on an "absolute" basis, with the poor/fair split at 300°K (27°C). The Fair/Good split was made arbitrarily at 400°K, and Very Poor below 75°K. Since the data of Grau and Itoh were obtained by a method comparable to those of Coffin and Machlin, they were included, and this improved three of the HCP ratings. The categories were: Poor ($F = 0.66$ to 1.07), Fair ($F = 0.51$ to 0.65) and Good ($F = 0.36$ to 0.50). The pairs improved were Cu-Zn, Al-Cd, and Ag-Zn, now counted "correct" on the basis of Footnote c in Table 5.6-IV.

TABLE 5.6-II
PUBLICATIONS ON LABORATORY TESTS OF ADHESION, FRICTION,
AND WEAR OF VARIOUS METALLIC PAIRS

SENIOR AUTHOR	YEAR	TEST METHODS	METALLIC PAIRS	ATMOSPHERES	SPECIAL CONDITIONS AND NOTES
Johnson	1967	Adhesion	1 like 2 unlike	High Vacuum	Changed previous conclusion (Keller 1963)
Hordon	1967	Adhesion	8 unlike	High Vacuum	
Sikorski	1963	Adhesion	30 like 5 unlike	Air Air	Humidity not discussed These data contradict other authors
Rabinowicz	1971A	Static	20 like 190 unlike	Air	Humidity controlled to 50% RH max
Shaw	1930	Static	5 like 10 unlike	10^{-2} torr	
Ernst	1940	Static	9 like 15 unlike	10^{-1} torr	See Tables 5-XII and 5-XIII
Tomlinson	1929	Static	9 like 36 unlike	Air	Not correlated by Rabinowicz (1971B).
Spurr	1962 1964 1967 1971	Static Static Static Wear	6 unlike 15 unlike 11 unlike 6 unlike	Air Air Air Air	Solders against glass Against silver, steel and glass Against steel and glass Against steel
Machlin	1954	Static	24 unlike	Air, He, Ar	See Tables 5-XII and 5-XIII
Coffin	1956	Kinetic	23 unlike	Air and He	
Roach	1956	Kinetic	38 unlike	Air	Kerosene lubricant; see Table 5-XII
Grau	1966	Kinetic	35 unlike	Air	See Tables 5-XII and 5-XIII
Hultgren	1956	Wear	8 like 28 unlike 45 unlike	Air Air Air	See Table 4-V Alloys
Moeller	1967	Static, Wear and Kinetic	115 unlike	Air	See Table 4-IV
MacGregor	1964	Kinetic	2 like	Vacuum, He,	Alloys; varied temperature and humidity
Cornelius	1961	Kinetic and Wear	8 unlike	CO ₂ , Air	
Buckley	1966	Kinetic and Wear	9 like 12 unlike	10^{-9} torr	Hexagonal metals. See also numerous NASA Technical Notes since 1965

TABLE 5.6-111

PREDICTIONS OF SCORING RESISTANCE ON IRON

At. No	Metal	Crystal	Rating from Literature					5% Miscibility Temperature Equation (5.6-2)	
			(A)	(B)	(C)	(D)	(E)	deg K	Success
4	Be	HCP	Very Poor	--	--	--	--	13 VP	+c
12	Mg	HCP	Poor	--	Good ^a	Good/Fair	--	528 G	+c
13	Al	FCC	Poor	Poor	--	Fair	--	131 P	+b
14	Si	DIA	Very Poor	--	--	--	--	106 P	+d
20	Ca	FCC	Very Poor	--	--	--	--	604 G	-
22	Ti	HCP	Very Poor	--	--	Fair	--	69 VP	+c
24	Cr	BCC	Very Poor	--	Good	--	--	14 VP	+b
26	Fe	BCC	Very Poor	--	--	--	--	0 VP	+
27	Co	HCP	Very Poor	Poor	--	--	--	12 VP	+
28	Ni	FCC	Very Poor	--	Poor	--	Poor	7 VP	+d
29	Cu	FCC	Fair/Poor	Poor	--	Poor	Fair	17 VP	+
30	Zn	HCP	Poor	Poor	Fair	Fair	Fair	496 G	-
32	Ge	DIA	Good	--	--	--	--	199 P	-
40	Zr	HCP	Very Poor	--	Poor	Fair	--	62 VP	+c
41	Cb(Nb)	BCC	Very Poor	--	--	--	--	54 VP	+
42	Mo	BCC	Very Poor	--	--	--	--	41 VP	+
45	Rh	FCC	Very Poor	--	--	--	--	35 VP	+
46	Pd	FCC	Very Poor	--	--	--	--	33 VP	+
47	Ag	FCC	Good	--	Fair	Good	--	164 P	-
48	Cd	HCP	Good/Fair	Good	Good ^a	Fair	Fair	626 G	+c
49	In	FCC	Good	--	--	--	--	369 G	+
50	Sn	DIA	Good	--	--	--	Good	304 G	+
51	Sb	LAM	Good	--	--	--	--	367 G	+
56	Ba	BCC	Poor	--	--	--	--	687 G	-
58	Ce	HCP	Very Poor	--	--	--	--	285 P	+d
73	Ta	BCC	Very Poor	--	Fair	--	--	194 P	+b
74	W	BCC	Poor	--	Fair	--	--	281 P	+b
77	Ir	FCC	Very Poor	--	--	--	--	129 P	+d
78	Pt	FCC	Very Poor	--	--	--	--	476 G	-
79	Au	FCC	Very Poor	--	--	--	--	77 P	+d
81	Tl	HCP	Good	--	--	--	--	511 G	+c
82	Pb	FCC	Good	--	Good ^a	Good/Fair	Good	476 G	+b
83	Bi	LAM	Good	--	Fair	--	--	502 G	+b
90	Th	FCC	Very Poor	--	--	--	--	130 P	+d
92	U	BCC	Very Poor	--	--	--	--	35 VP	+

BCC = Body Centered Cubic
FCC = Face Centered Cubic
HCP = Hexagonal Close Packed

DIA = Diamond Structure
LAM = Lamellar or Sheet Structure

- (A) Scoring against 1045 steel at 4640 fpm, kerosene lubricant (Roach 1956).
(B) Static coefficient of friction in vacuum (Ernst 1940).
(C) Scar appearance in air and helium (Coffin 1956).
(D) Static friction in air and nitrogen or argon (Machlin 1954).
(E) Kinetic friction in air (Grau 1966).

- = Incorrect
+ = Correct
+ = Conflicting Data

a = In helium only
b = Counted correct on most favorable data
c = HCP, counted correct on favorable data
d = counting Very Poor equal to Poor

TABLE 5.6-IV
PREDICTION OF SCORING RESISTANCE
Nonferrous Couples

Metal Pair	Crystal	Rating From Literature				5% Miscibility Temperature Equation (5.6-2)	
		(B)	(C)	(D)	(E)	deg K	Success
Al-Zn	FCC-HCP	Poor	--	Fair	Poor	210 P	±c
Co-Cu	HCP-FCC	Poor	--	--	--	54 VP	+d
Al-Co	FCC-HCP	Poor	--	--	--	195 P	+
Cu-Cd	FCC-HCP	Poor	--	Poor	Fair	473 G	-
Cu-Zn	FCC-HCP	Poor	--	Poor/Fair	Fair	350 F	±c
Sb-Zn	LAM-HCP	Poor	--	--	--	10 VP	+d
Al-Cd	FCC-HCP	Good	--	--	Fair	337 F	±c
Bi-Cd	LAM-HCP	Good	--	--	--	45 VP	-
Cd-Zn	HCP-HCP	Good	--	--	Fair	30 P	-
Zn-Bi	HCP-LAM	Good	--	--	--	15 VP	-
Cu-Ni	FCC-FCC	--	Poor	--	Poor	43 VP	+d
Cr-Mo	BCC-BCC	--	Poor	--	--	128 P	+
Ti-Zn	HCP-HCP	--	Poor	--	--	404 G	-
Ag-Cu	FCC-FCC	--	Poor	Fair	Poor	85 P	±b
Cr-Ni	BCC-FCC	--	Poor	--	--	38 P	+
Al-W	FCC-BCC	--	Poor	--	--	789 G	-
Cu-Sn	FCC-DIA	--	Good ^a	--	--	202 P	-
Ni-Sn	FCC-DIA	--	Fair	--	Fair	357 F	+
Al-Zn	FCC-HCP	--	Poor	Fair	--	210 P	±c
Ag-Ta	FCC-HCP	--	Good	--	--	811 G	+
Cu-Mo	FCC-BCC	--	Very Good	--	--	145 P	-
Ag-Cr	FCC-BCC	--	Fair/Good	--	--	94 P	-
Cu-Ta	FCC-BCC	--	Good	--	--	435 G	+
Al-Pb	FCC-FCC	--	Good ^a	Fair	Fair	208 P	-
Cu-W	FCC-BCC	--	Good	--	--	504 G	+
Cu-Pb	FCC-FCC	--	--	Poor	Good	348 F	±b
Cu-Ti	FCC-HCP	--	--	Poor/Fair	--	23 P	±c
Al-Cu	FCC-FCC	--	--	Poor	Poor	61 P	+
Cu-Mg	FCC-HCP	--	--	Poor	--	389 F	-
Pb-Ti	FCC-HCP	--	--	Fair	--	345 F	+
Zn-Zr	HCP-HCP	--	--	Poor	--	906 G	-
Ti-Zn	HCP-HCP	--	--	Fair	--	404 G	-
Ag-Zn	FCC-HCP	--	--	Fair	Poor	165 P	±c
Ag-Al	FCC-FCC	--	--	Poor	--	4 P	+
Al-Mg	FCC-HCP	--	--	Poor	--	249 P	+
Al-Ti	FCC-HCP	--	--	Fair/Poor	--	18 P	±c
Al-Ni	FCC-FCC	--	--	Fair	Poor	176 P	±b
Ag-Cu	FCC-FCC	--	--	Poor	--	85 P	+
Ag-Ti	FCC-HCP	--	--	Fair	--	39 P	-
Ag-Zr	FCC-HCP	--	--	Good	--	76 P	-
Cd-Mg	HCP-HCP	--	--	Poor	--	9 P	+
Cd-Ti	HCP-HCP	--	--	Poor	--	538 G	-
Cd-Zr	HCP-HCP	--	--	Good	--	891 VG	+
Mg-Ti	HCP-HCP	--	--	Poor	--	413 G	-
Ag-Mg	FCC-HCP	--	--	Fair	--	206 P	--

See Table 5.6-III for symbols and notes

Both the $\phi_1 = 0.50$ and the $\phi_1 = 0.05$ predictions gave the same total scores on success, which are shown in Table 5.6-V. This is surprising, since 16 pairs are rated differently at $\phi_1 = 0.05$ than at 50/50. The changes, which were mostly from "Fair" to "Poor" or "Good", exactly balanced out. It is evident that Model IV works best on cubic/cubic systems; that diamond and lamellar can be added to this with little loss of precision (75% versus 76% for cubic alone); and that hexagonal metals are not as well predicted with either cubic (68%) or other hexagonal (38%) types.

As pointed out by Hildebrand (1950), perfect success with this model is unlikely due to intermetallic compound formation and also to crystalline transitions of many metals at elevated temperatures. However, as a tool for making a quick estimate on an unknown pair, Model IVA at least offers a 75% chance of success if HCP metals are excluded. At best, it offers some assurance that the Hildebrand blending equation (5.5-14) may also be usable on alloys.

Rabinowicz' Model IVB study of his static friction data has already been discussed. However, the relevance of dry static friction to the present study is slight. It is of more interest to apply his general ideas to the large block of kinetic data from MacGregor (1964). Since most of the metals are alloys, it is not possible to apply Figure 5.6-1. Rather than taking the time to compute γ_m from Equation (5.5-14) for all these alloys, it was most expedient to revert to the original concepts in Rabinowicz' book (1965), that γ_1 is a function of P_m . As pointed out by the writer (Beerbower 1971A), this function is

$$\gamma_1 \approx 300 P_m^{1/3} \quad (5.6-6)$$

As a first pass, the values of F and P_m were plotted directly without taking the cube root. A number of plots had to be made, as three kinds of balls were used. Some of the correlations were strikingly good, and others quite sketchy. Rather than reproduce these charts in detail, only the highlights are given:

1. Six aluminum alloys gave fair to good linear correlations, each ball causing a distinctive slope (F/P_m); brass = -0.0046, 52100 steel = -0.010, 302 stainless = -0.013.
2. Seven stainless steels plot well, except on brass where the scatter is bad. Slopes are 302 stainless = -0.008, 52100 steel = -0.009.
3. Phosphorus bronze seems to be in a class by itself, which is as predicted (deGee 1971).
4. Two other copper and three nickel alloys plot together, with considerable scatter. They lie near the line for the stainless steels.

TABLE 5.6-V

Success of Compatibility Predictions

	<u>Cubic</u> <u>(FCC or BCC)</u>	<u>Hexagonal</u> <u>(HCP)</u>	<u>Irregular</u> <u>(DIA and LAM)</u>
Cubic:	28/37	17/25	5/7
Hexagonal:	(17/25)	3/8	1/3
Cubic plus Irregular:	33/44	18/28	(5/7)

Overall Success = $50/72 = 69.2\%$

5. The carbon and alloy steels are a rather mixed collection, twenty in number (but with a different member not tested on each ball).

The writer is half convinced that the carbon and alloy steel plots can be represented by inverted "v"s, with all the peaks at $P_m = 320 \text{ kg/mm}^2$. The peak heights would then be: brass, $F \approx 0.80$; 302 stainless, $F \approx 1.05$; 52100 steel, $F \approx 0.85$. Scatter is too severe to attempt to read slopes, but they tend to be lower than those reported above for aluminum alloys.

There is hope that a more refined study might produce some usable rules for F , just as Table 5.3-II offers some hope for rules of G_R , but neither promises to be easy. Worst of all will be analysis of the data on oils A, B, and C; there is no evident connection between those F values and those for the dry case discussed below in 5.12.

5.7 Mixed Film Lubrication (Model V)

There may have been a thought, when the term "boundary lubrication" was coined, that it represented a fairly broad band of mixed conditions. However, over the years a mental wall has been built up between the hydrodynamic and the boundary regimes. It seems to have become a literal wall lately; at the joint ASLE/ASME annual conference, the two groups customarily meet simultaneously in separate rooms. Fortunately, several of the experts on both sides are making attempts to explore the interesting possibilities of mixed films, in which the load is shared between the asperity tops and the anti-asperity valleys.

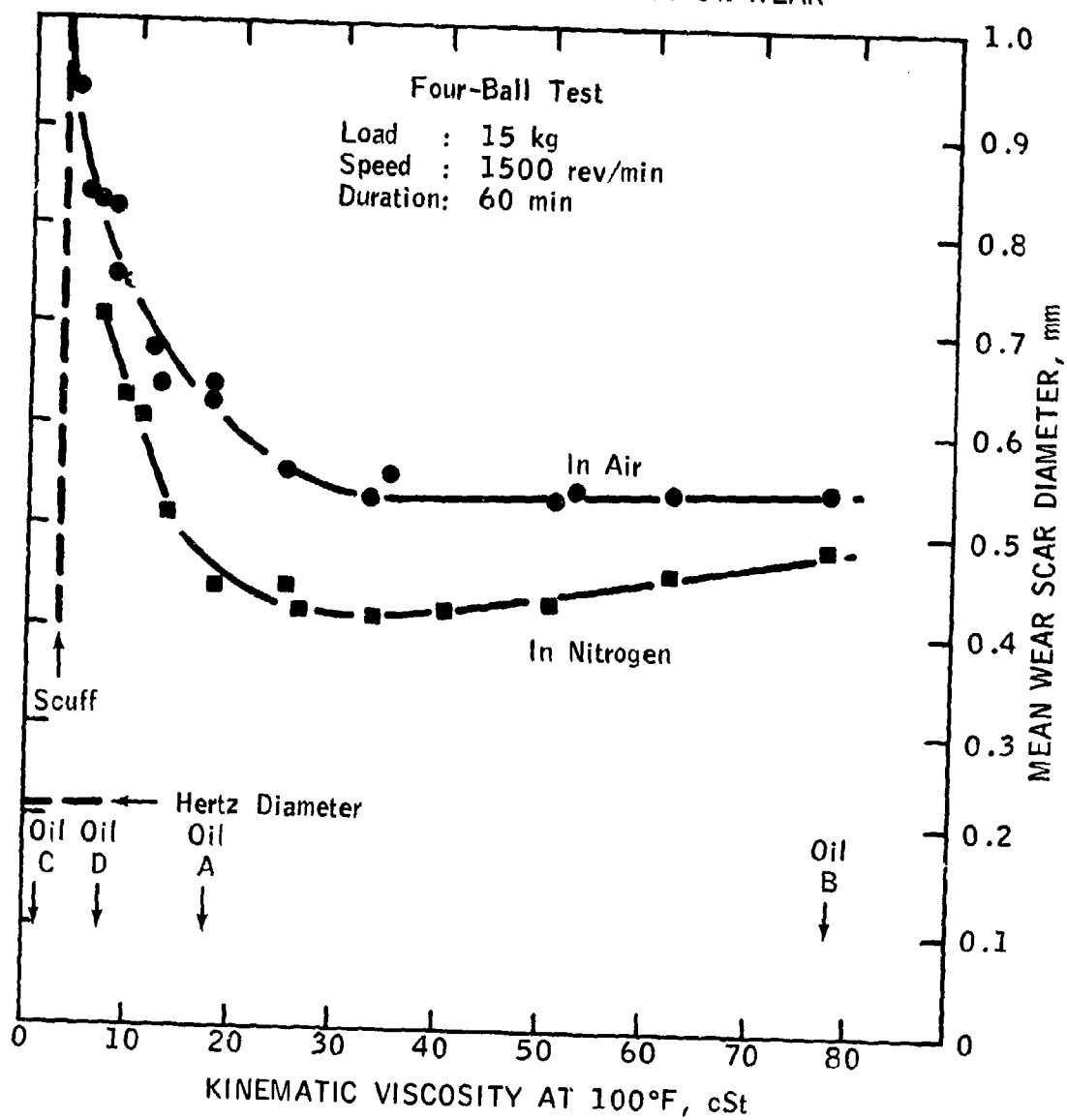
Many of the test machines in common use were designed to provide "pure" boundary conditions. Of these, the 4-ball machine has usually been considered the purest, but even it shows an effect that can be attributed to viscosity, as shown in Figure 5.7-1 by Rudston (1971). Of course, there is reason to believe that higher molecular weight hydrocarbons have a higher heat of adsorption than lower ones, which tends to raise a question on this and similar data as to whether we are not simply seeing a Model II effect. After reviewing the models, none of which are as complete as could be desired, a more serious analysis will be made in Section 5.7.6.

5.7.1 Empirical Load-Sharing (Model VA)

Sakurai (1971) probably has used less theory in his model than any other author cited in this report. Being oriented to boundary lubrication, he ignored all the EHD work cited below and set his own specialty in first place, with the EHD effects appearing as the residual. His final equation is

$$\frac{dV}{dd} = k_2 [P_a - P_{h\infty} + P_{h\infty} \exp(-k_4 U)] \exp(-k_3 U) \quad (5.7-1)$$

Figure 5.7-1
EFFECT OF WHITE OIL VISCOSITY ON WEAR



where k_2 , k_3 and k_4 are empirical constants

P_a = apparent contact pressure

$P_{h\infty}$ = critical pressure of EHD, extrapolated to $U = \infty$

U = velocity

This is developed by the following steps:

1. His tests were made at constant apparent pressure, by repeatedly stopping for an area measurement on his ball-ended pin, and restarting with an increased load to maintain constant P_a .
2. He observed that the wear rates for several runs at different P_a values were each constant, and extrapolated to a positive intercept (P_h) for zero wear rate.

Hence,

$$(V/D) = k_1 (P_a - P_h) \quad (5.7-2)$$

where P_h is the "critical pressure of hydrodynamic lubrication."

3. Both k_1 and P_h proved to vary with velocity.

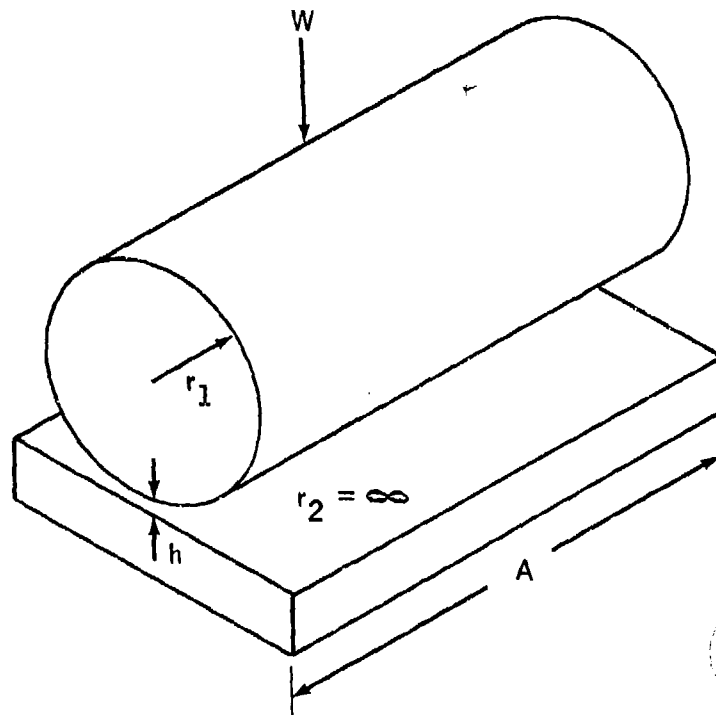
Sakurai, perhaps because of his success with exponentials in Model III B, elected to use them here, though EHD theory would have guided him to power functions (see 5.7.2). Despite this illogical choice, he was able to fit his data quite well. The concept of an infinite velocity is far-fetched, but is good enough for explaining his work with a single white oil containing little or no additive. However, it fails at sulfur concentrations above 0.005 wt %.

The main purpose in citing this unsatisfactory model is to demonstrate that load-sharing is not an artifact of the higher mathematics used in Sections 5.7.2 and 5.7.3, but can be expressed with even the limited tools used here. Sakurai's data deserves further analysis.

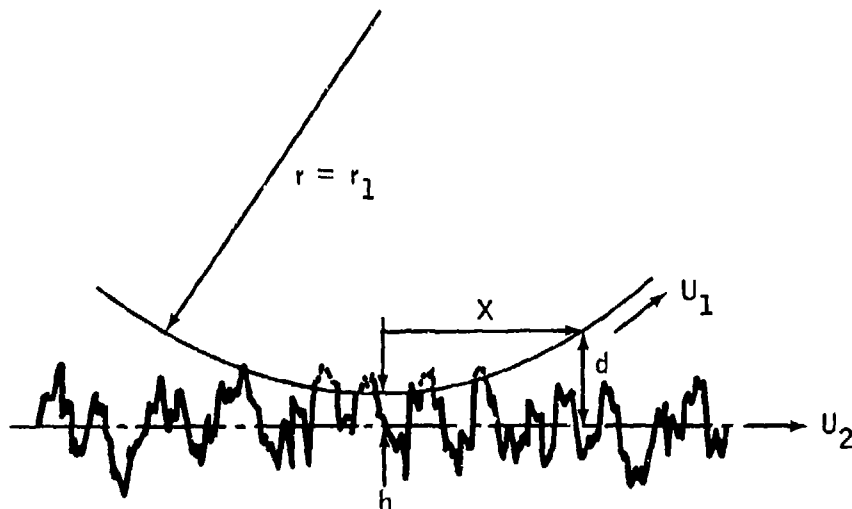
5.7.2 A Two-Dimensional Model (VB)

Thompson and Bocchi (1972) have arrived at a simplified, but apparently workable, means for estimating the distribution of load between asperities and anti-asperities. Working primarily from the hydrodynamic viewpoint, they first established a physical model (Figure 5.7-2) for converting a contact which has roughness on both sides to a dimensionless separation (h_o):

Figure 5.7-2
TWO-DIMENSIONAL PHYSICAL MODEL



a. Model Geometry for Contact of Cylindrical Machine Components



b. A Model for the Micro-Geometry of the Contact Illustrated in a

$$h_o = \xi / \sqrt{D_1^2 + D_2^2} \quad (5.7-3)$$

where D_1 and D_2 are the two surface roughnesses, and h the minimum separation between the centerlines of the two roughness profiles. In this case, D_1 and D_2 are expressed as RMS, as opposed to the peak-to-peak value in Equation (5.3-14). Thompson assumes that ξ also represents the minimum lubricating film thickness. The h_o concept is essentially the same as that used by Tallian (1964) in rolling contacts, and Bodensieck (1965) for gears. The latter calls it "specific film thickness". All agree that it is a highly important concept. Bodensieck goes so far as to tabulate the effects of decreasing h_o on surface distress, as shown in Table 5.7-I.

Thompson arrives at the load carried by EHD (W_2) by the well-known (1966) Dowson-Higginson equation:

$$W_2 = A [1.633 (\Delta\eta/\eta_o \Delta P)^{0.6} (\eta_o U)^{0.7} (E')^{0.03} r^{0.43} (Dh_o)^{-1}]^{7.7} \quad (5.7-4)$$

where 1.633 = factor for English units
 η_o = viscosity at entrance temperature
 $(\Delta\eta/\eta_o \Delta P)$ = viscosity-pressure coefficient
 U = $(U_1 + U_2)/2$, the mean surface velocity (Figure 5.7-2b)
 $1/r$ = $1/r_1 + 1/r_2$ and
 $1/E'$ = $(1 - \nu_1^2)/E_1 + (1 - \nu_2^2)/E_2$

The asperity load (W_1) is based on an equation by Greenwood (1967) for surfaces with Gaussian distribution of roughness. For nonconforming geometry

$$W_1 = 2.26 \chi E' \beta^{0.5} D^2 r^{0.5} G_H(h_o) A \quad (5.7-5)$$

and for conforming geometry

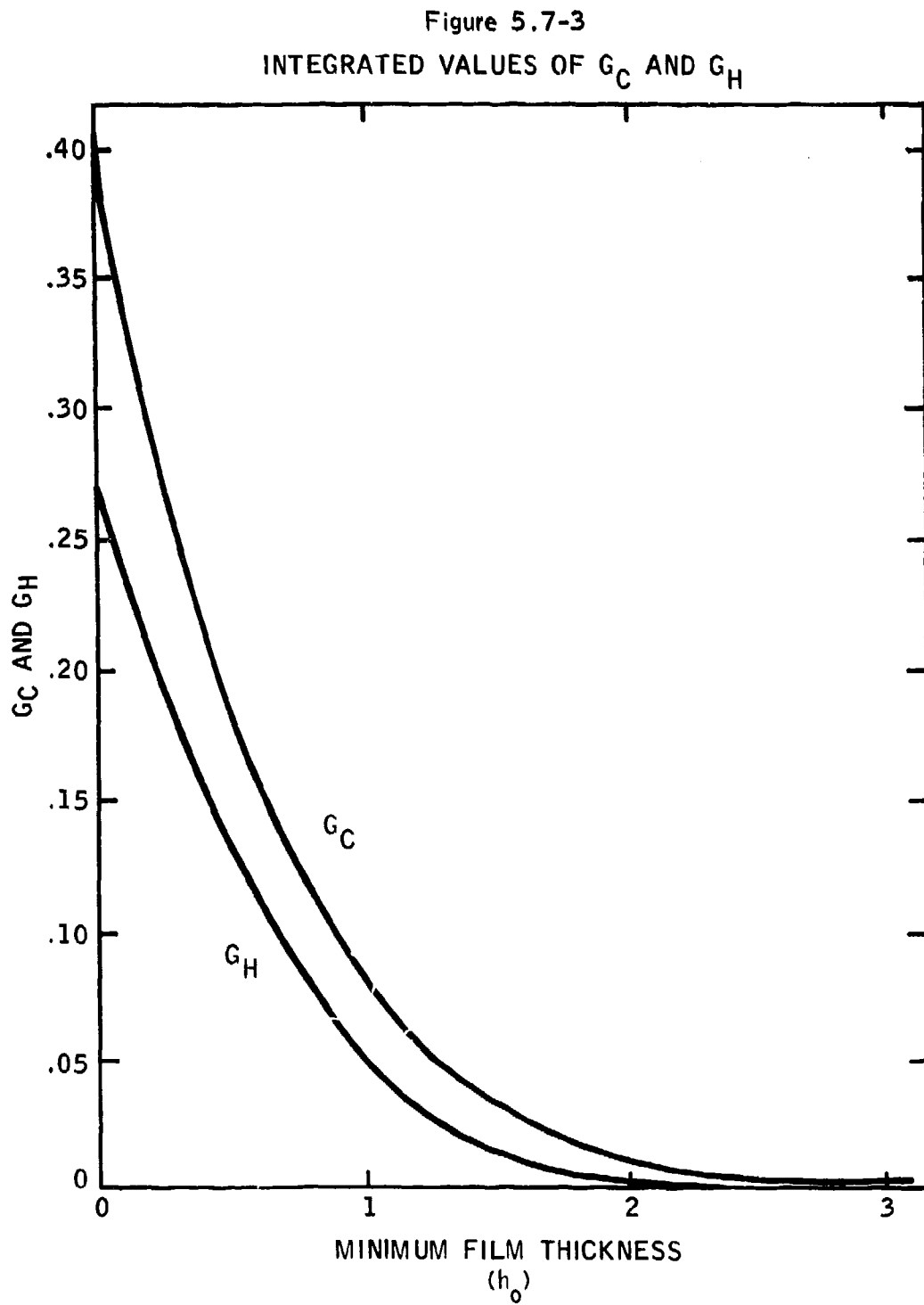
$$W_1 = 0.8 \chi LE' \beta^{0.5} D^{1.5} r^{0.5} G_C(h_o) A \quad (5.7-6)$$

where χ is the asperity density/in², and β = average radius of asperity tips. $G_H(h_o)$ and $G_C(h_o)$ are functions obtained by stochastic integration of the Greenwood equation. ("Stochastic" is the jargon for a process involving the probability formulas.) The values of both may be looked up in Figure 5.7-3. For the present purpose, it is possible to represent $G_H(h_o)$ crudely but effectively by

$$G_H(h_o) \approx 0.055/h_o^{0.75} \quad (5.7-7)$$

TABLE 5.7-I
GEAR SURFACE DISTRESS AS A FUNCTION OF SPECIFIC
FILM THICKNESS

<u>Specific Film Thickness (h_0)</u>	<u>Type of Surface Deterioration</u>
Over 1.5	None (Full hydrodynamic lubrication)
1.3 to 1.5	Slight marking
1.2 to 1.3	Improvement with straight oil
1.1 to 1.3	Improvement with E.P Additives
Below 1.1 (or 1.2)	Scoring, Spalling, Galling, Seizing, Scuffing, etc.
Below 1.0	Pitting (More closely related to surface compressive stress)
Below 0.8	Abrasive wear
Below 0.5	Rippling and Ridging



from $0.20 < h_o < 0.70$, and

$$G_H(h_o) \approx 4.55/h_o^2 \quad (5.7-8)$$

from $0.70 < h_o < 1.50$. As these are the regions of greatest interest, we may obtain a better view of Thompson's result by setting, for the above limits,

$$W_{h_o}^{7.7} - 0.055 J_H h_o^{6.95} - J_L = 0 \quad (5.7-9)$$

$$\text{and } W_{h_o}^{7.7} - 4.55 J_H h_o^{5.7} - J_L = 0 \quad (5.7-10)$$

where J_H = the known portion of (4.5-6), and

J_L = the known portion of (4.5-5).

Since W , the total load, is also known, these equations are readily solvable by machine or graphical methods, though not exactly. A typical solution, for a journal bearing problem described in detail in Thompson's report (1972), is shown in Figure 5.7-4. The results seem plausible, though not much data was cited in support of it.

There has been criticism of this model based on using the $\sqrt{D_1^2 + D_2^2}$ rule for averaging two surface roughnesses, since it was derived for static contacts, and on some other simplifications. None of these appear fatal, but the model can certainly use some more work. A minor effort to test Model VA is made in Section 5.7.6.

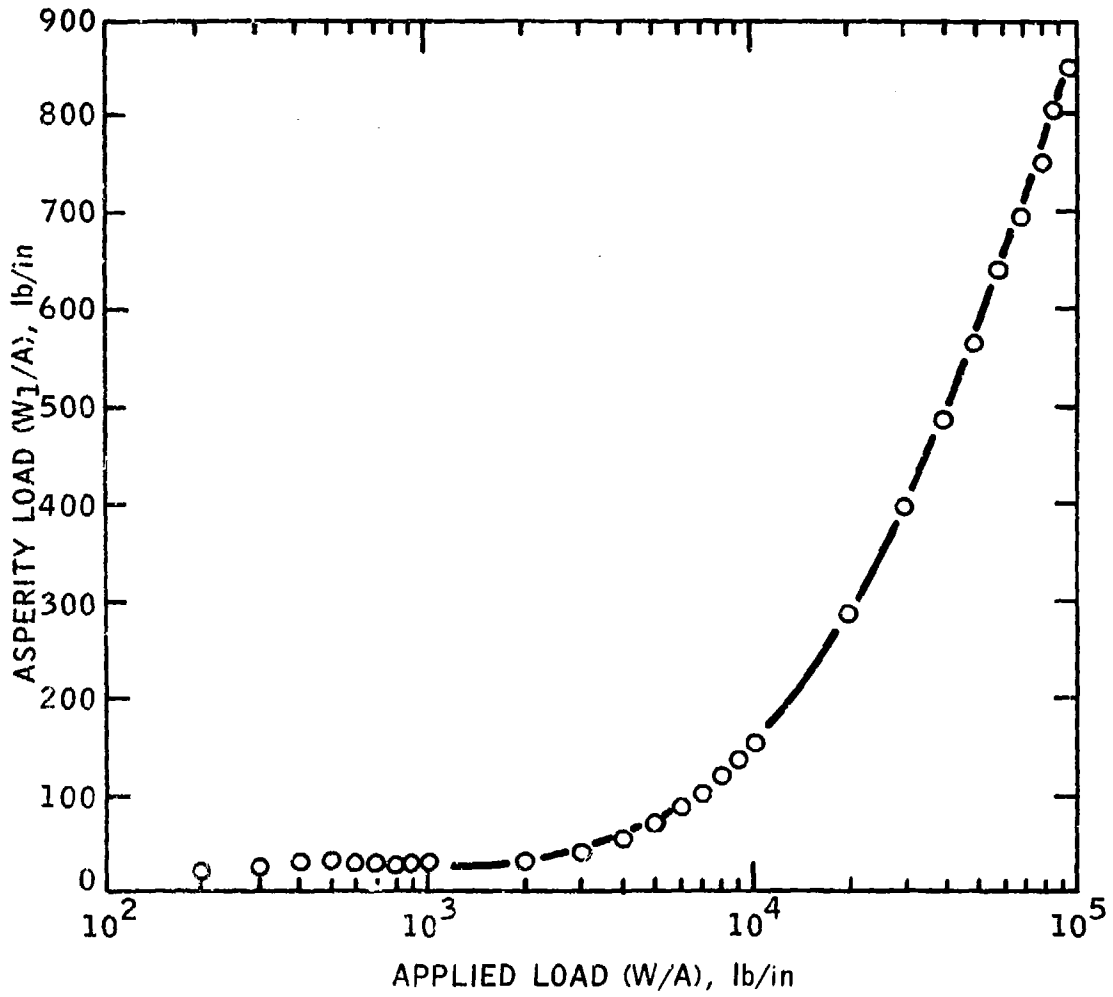
5.7.3 The One-Dimensional Model VC

Christensen (1971), in the latest of a long series of papers, has produced a set of solutions to the load-sharing problem which are more rigorous than Thompson's, but less easily followed. He recognizes three cases:

- a. One-dimensional, longitudinal structure
- b. One-dimensional, transverse structure
- c. Uniform, isotropic structure.

The last of these is relatively difficult to deal with, and Christensen points out that it also is not necessarily the most important. Light wear and running in tend to produce the longitudinal case (a), so that it has special interest. Machining across the direction of sliding would generate case (b), at least until wear converts it to case (c) or eventually (a).

Figure 5.7-4
TWO-DIMENSIONAL SOLUTION FOR A JOURNAL BEARING



These three cases are shown in Figure 5.7-5, in which certain parameters are also defined. To use these, it is necessary to give a measure of the roughness variation. Though this is known to be typically Gaussian, convenience dictates representing it by a probability density polynomial such as

$$f(h_s) = \frac{35}{32} \left[\frac{16}{35} + \left(\frac{h_s}{c} \right) - \left(\frac{h_s}{c} \right)^3 + \frac{3}{5} \left(\frac{h_s}{c} \right)^5 - \frac{1}{7} \left(\frac{h_s}{c} \right)^7 \right] \quad (5.7-11)$$

where h_s takes account of roughness measured from the nominal level, and $2c$ is the maximum peak-to-valley roughness (D in Section 5.3).

He defines an "expectancy operator" $E(\chi)$ by

$$E(\chi) = \int_{-\infty}^{\infty} \chi f(\chi) d\chi \quad (5.7-12)$$

where $f(\chi)$ is the probability density function of the random variable χ .

He then sets up a Reynolds-type equation for the longitudinal structure

$$\frac{\partial}{\partial x} \left[\frac{d\bar{p}}{dx} E(H^3) \right] + \frac{\partial}{\partial y} \left[\frac{\partial \bar{p}}{\partial y} \frac{1}{E(1/H^3)} \right] = 6\eta U \frac{\partial}{\partial x} E(H) \quad (5.7-13)$$

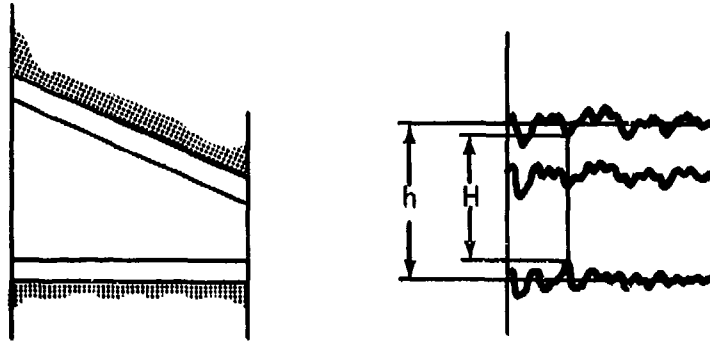
where $\bar{p} = \bar{p}(x, y)$ is the (predetermined) mean hydrodynamic pressure. Similar equations can be set up for cases (b) and (c).

These can be integrated for any specific geometry, and he chose a plane slider of length $l = 1$ and constant inclination m , as shown in Figure 5.7-5. The resulting plots of his film thickness parameter versus load and friction appear to be quite satisfactory. With additional assumptions, he then generalizes into the mixed regime. Figure 5.7-6 shows a Stribeck type diagram for three hypothetical cases, calculated on the above principles. He was much impressed by the fact that, even under conditions of severe roughness, less than 1% of the total bearing area is in boundary lubrication.

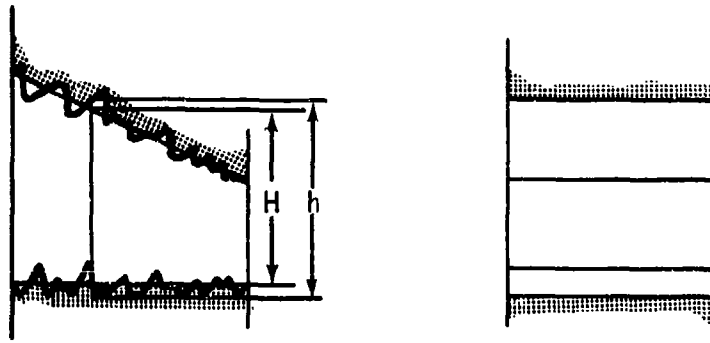
Thus, the friction is dominated by the boundary shear stress, while the load-carrying ability is mainly hydrodynamic in nature. The fact that the curves separate to the left of the dividing line helps to explain why the Stribeck function $\eta U/W$ has never been very helpful in mixed lubrication. Cases A and B differ in material properties, but not in boundary coefficient of friction; evidently all these factors enter into the position of the line. Cases B and C give an even more striking illustration. With all material properties constant, simply shifting the variable from W to ηU changes F by a large factor.

Another example of the end-products to be had from Model VC is shown in Figure 5.7-7 where film collapse due to thermal instability is predicted. Load is slowly increased up to point A. Collapse takes place due to the reverse

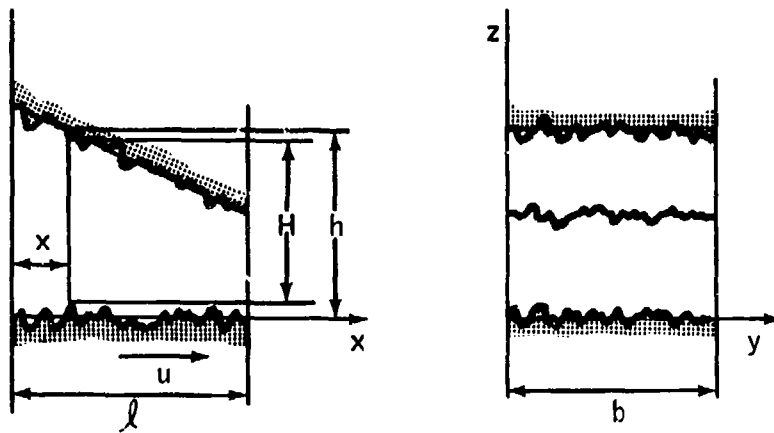
Figure 5.7-5
ONE AND TWO DIMENSIONAL PHYSICAL MODELS



a) Longitudinal roughness

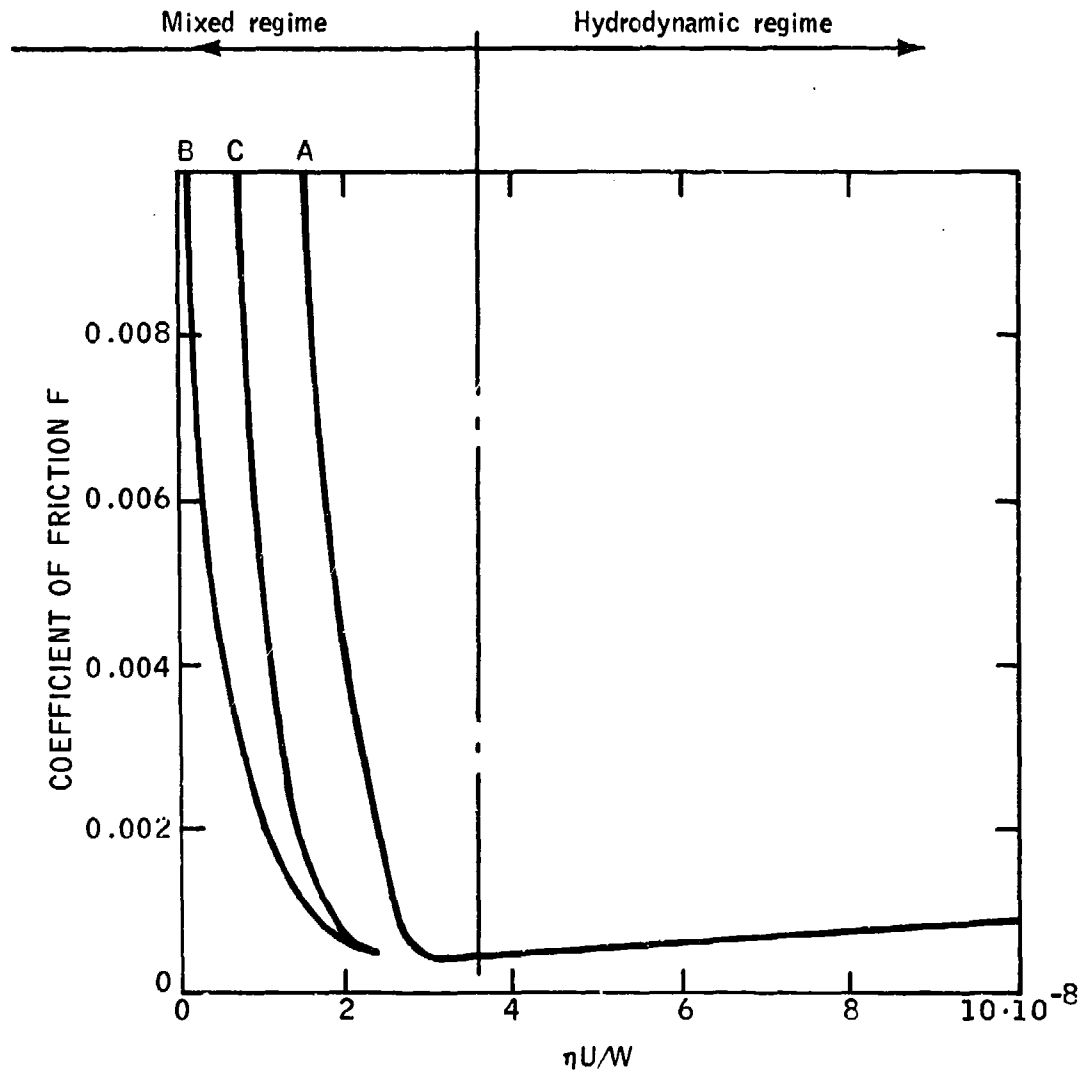


b) Transverse roughness



c) Uniform roughness

Figure 5.7-6
STRIEBECK-TYPE DIAGRAM FROM THE ONE-DIMENSIONAL MODEL



- | | | |
|---------|-------------------------------|----------------------------------|
| Case A: | Material hardness = high | } constant ηU load varying |
| | Boundary shear stress = high | |
| | Boundary frict. coeff. = 0.05 | |
| Case B: | Material hardness = low | } constant load ηU varying |
| | Boundary shear stress = low | |
| | Boundary frict. coeff. = 0.05 | |
| Case C: | Material data as for case B | |

Figure 5.7-7

FILM COLLAPSE DUE TO THERMAL INSTABILITY
THEORETICAL PREDICTION

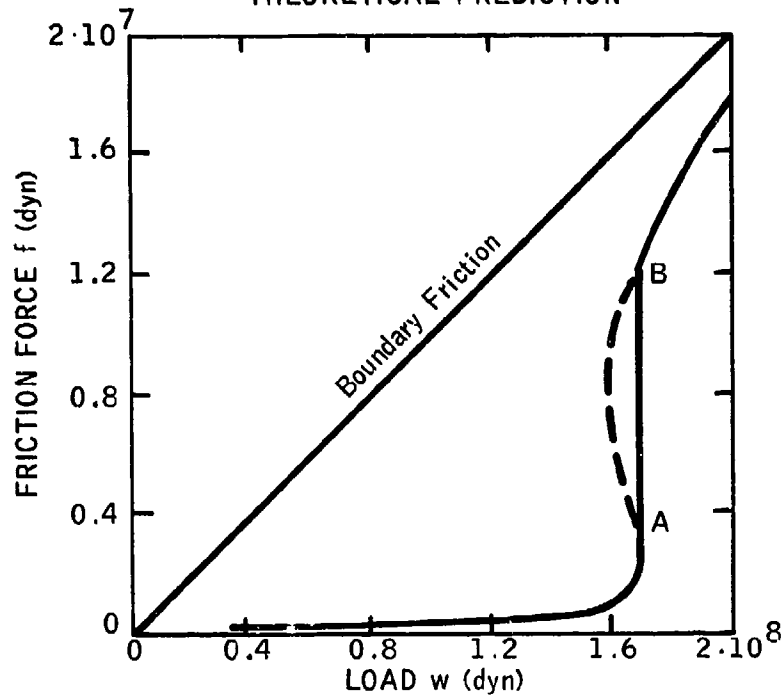
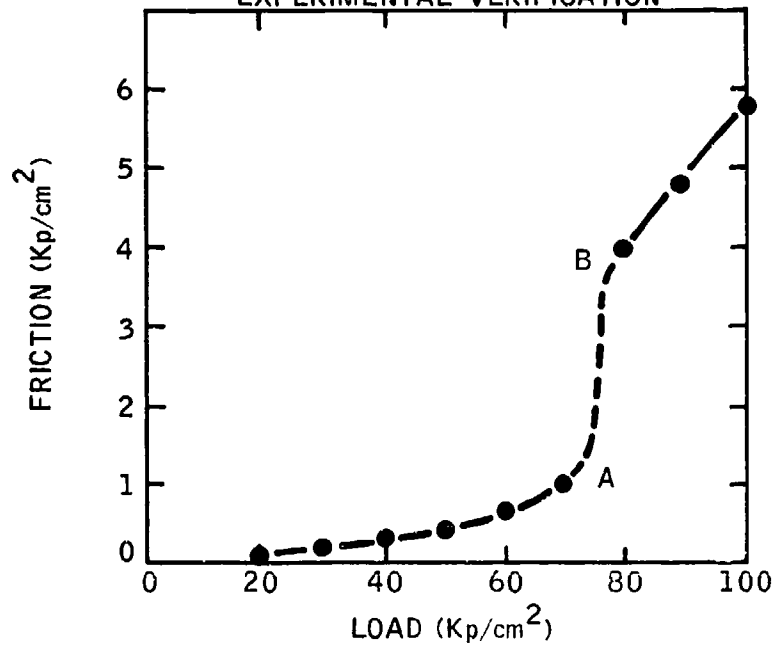


Figure 5.7-8

FILM COLLAPSE DUE TO THERMAL INSTABILITY
EXPERIMENTAL VERIFICATION



curvature of the line, and friction jumps to point B. This is a purely theoretical diagram, but experimental verification is shown in Figure 5.7-8. It is indeed a triumph that the two figures are nearly identical in shape.

The above description of how Figures 5.7-5 through 5.7-7 were calculated is quite incomplete. Although Christensen gave more details than are quoted, he omitted some of his assumptions and methodology for getting from Equation (5.7-13) to the Stribeck diagram and the thermal collapse plot. Publication of these vital details is promised in the near future.

5.7.4 Gear Surface Damage (Model VD)

Bodensieck (1965) has worked out a model, apparently quite independently, which has much in common with Christensen's and also Tallian's (1964). It starts with the definition of specific film thickness

$$h_o \equiv \xi/D = 0.274\eta_s U_R/D \quad (5.7-14)$$

where η_s is the viscosity at surface temperature (T_s) and U_R the rolling velocity. The constant 0.274 applies to English units. He obtains T_s from the equivalent of Equation (5.4-6).

The next step was an empirical observation that the coefficient of friction could be related to h_o by

$$F = (0.0212/h_o) + 0.0125 \quad (5.7-15)$$

which fits a great deal of data from various sources quite well. He felt that the constants might vary with the type of lubricant, but did not find any data to indicate such variation.

The problem of putting D into peak-to-valley terms was solved in a different way than in Section 5.3.3. Table 5.7-II shows the multipliers recommended for various manufacturing methods. He felt that only the value for "ground" was fully verified.

The results obtained on an experimental program designed to test Model VD were shown in Table 5.7-I. The h_o values were calculated from Equation (5.7-14), and the second columns are the test data.

Model VD does not really go the whole way to a load distribution between asperities and EHD, and perhaps should not be included in Section 5.7. However, it does show what might logically be the next step forward by AGMA.

The reader is cautioned that Bodensieck defined h_o from the average roughness of the surfaces rather than the sum as did Thompson, Christensen, and others. His system is self-consistent but must not be mingled with the others indiscriminately.

TABLE 5.7-II

ROUGHNESS CONVERSION FACTORS FOR VARIOUS
GEAR MANUFACTURING METHODS

<u>METHOD OF FINISHING</u>	<u>RATIO: $\frac{\text{PEAK-TO-VALLEY}}{\text{ROOT MEAN SQUARE}}$</u>
Shaping	2.0
Hobbing	1.8
Shaving	1.5
Grinding	1.4*
Lapping or Honing	1.3

*Only grinding has been thoroughly verified on this scale.

5.7.5 A Tentative Break-in Mechanism (Model VE)

At this point, it will not be necessary to develop the detailed mathematics to show that Model III can be combined with Model V in several ways to produce a picture of break-in or running in which has little to do with the conventional ideas. After the initial scraping off of extra-high asperities, the bare spots serve as sites for generating resin. This partly fills the anti-asperities, which increases the EHD share and so relieves the remaining asperities. After this, the system tends to be self-regulating, since depletion of the surface resin produces a negative feed-back in the form of increased asperity contact, which in turn gives the needed relief by generating more resin. Thus, a properly broken in bearing neither scuffs nor generates the excessive amount of resin known as "lacquer" or "varnish", but merely maintains its "glaze".

5.7.6 Testing Model V (Mixed Film Lubrication)

The situation on Model V is still too fragmentary to permit numerical analysis. However, it should be possible to assess the importance of this model in terms of both need and applicability.

5.7.6.1 Need for Model V

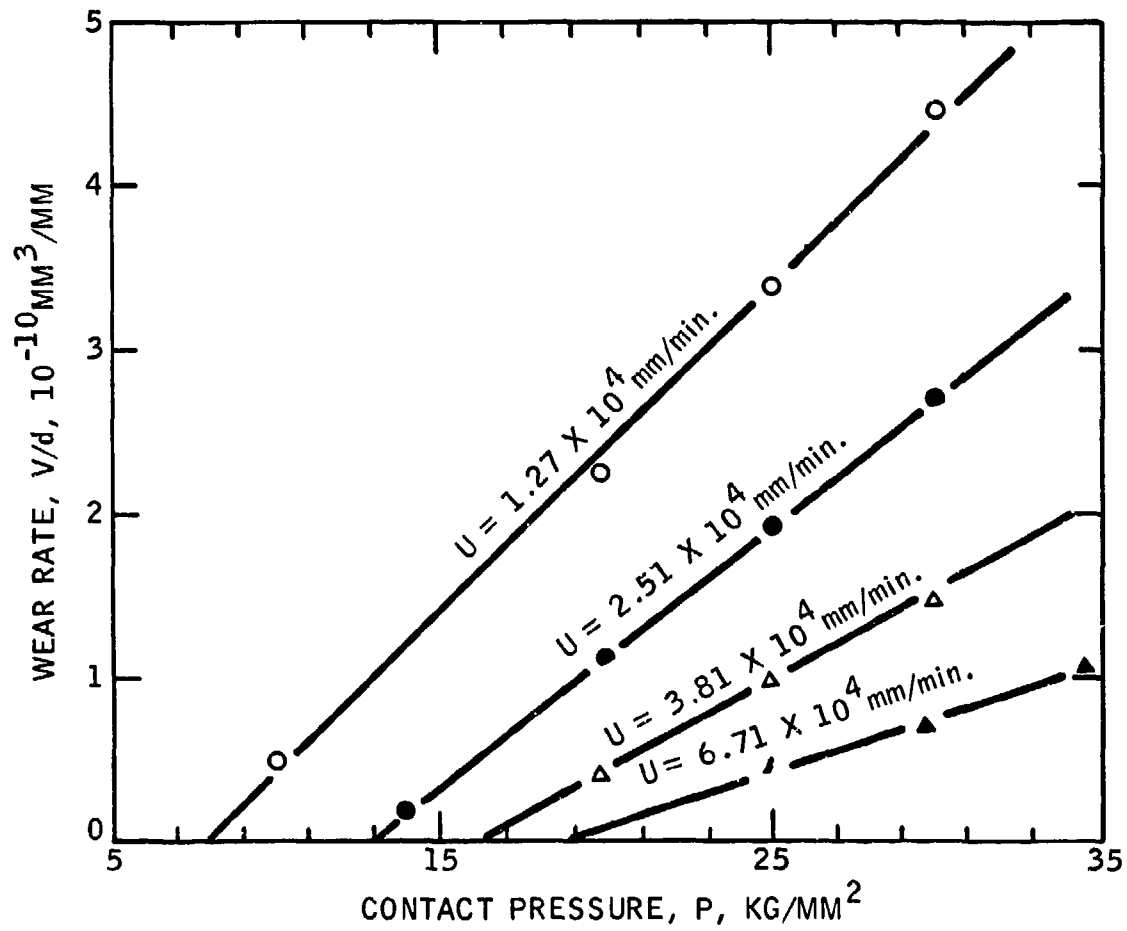
As shown in Figure 5.7-1, not even the 4-ball machine is free from viscosity effects (though, as mentioned in Section 5.7, viscosity is not the only variable in that figure). Sakurai's data also support the concept that even test machines which are designed to rule out EHD effects, as shown in Figure 5.7-9, still respond to velocity.

The internal evidence in Thompson's (1972) paper, as exhibited in Figure 5.7-4, indicates that a fairly constant 1% of the load is carried by the asperities. This is in very reassuring agreement with Christensen's findings of less than 1% in boundary lubrication for Model VC. Thus, the experimentalists and theoreticians agree that the EHD correction is sizable.

5.7.6.2 Applicability of Model V

It appears that Thompson's work shows considerably less load dependence than Sakurai's. The fact that the latter chose to express his load as "apparent pressure" should not create any problem. The trouble becomes evident when an attempt is made to use Model VB with flat-on-flat geometry. For this case, $r_1 = r_2 = \infty$, so that W_1 and $W_2 = \infty$ and the equations become unsolvable. In Model VC, the same situation arises in a different way; when $m = 0$, though not shown in Figure 5.7-6, the solution becomes indeterminate. Model VD does not have any capability for handling pure sliding, as Equation (5.7-14) requires the rolling velocity.

Figure 5.7-9
EXPERIMENTAL DEPENDENCE OF WEAR RATE ON APPARENT
BEARING PRESSURE



Thus, none of the models is capable of being used on Sakurai's data. Rudston's data, on the other hand, could be viewed as spherical geometry and "solved" by Model VB, if we ignore the fact that as soon as wear starts, the geometry becomes essentially flat-on-flat as in Model IB.

Another problem not faced by the model makers is the extremely high probability of a change in D due to break-in. This is the same problem noted in Section 5.1.2; as mentioned there, it will always be a problem. Perhaps Table 5.7-1 represents a good empirical way of handling it. As noted in Section 5.3.3, a survey of lubrication engineers on a world-wide basis showed much less concern with initial D values than is shown by the theoreticians (Beglinger 1969). Østvik (1968-9) shows data on ΔD , but no general model.

Recent work by Tallian (1971), not yet published, will help in throwing some light on these matters.

5.8 Rolling Contact Fatigue (Model VI)

Another of the limiting conditions that may be encountered is a decrease in the lifetime of rolling element bearings in lubricants that have been optimized for boundary lubrication. This is not a point that can be located on Figure 2-1, as noted in Section 2, since it involves fatigue. In many cases, separate lubrication of the ball or roller bearing sounds ideal. However, such a policy applied rigidly would certainly increase the cost of gear boxes and could not be practical at all until sealing of rotating shafts becomes more perfect than can be foreseen at present.

5.8.1 The Interfacial Free Energy (γ_{12}) Theory

Up until recently, it has been taken for granted that strong wetting is an unmitigated blessing, though Bowers (1956) raised the question as to whether this was true. Campbell (1957) investigated and concluded it was not, while Clayfield (1957B) reached the opposite conclusion. Rounds (1962, 1967) has shown that some additives which enhance boundary lubrication can have adverse effects on ball bearing fatigue. Unfortunately, his tests were conducted without controlling the humidity. High humidity promotes fatigue, (see 5.8.3), but there is independent reason to believe his conclusion may be correct. The standard Griffith equation for the minimum force (W_0) to propagate a crack of length (2) in a solid is

$$W_0^2 \propto E_1 \gamma_1 / \ell \quad (5.8-1)$$

where E_1 is the Young's modulus and γ_1 the surface free energy of the solid. For submerged solids, γ_{12} ($= \gamma_1 + \gamma_2 - A_{12}$) must replace γ_1 , tending to lower W_0 . Data on crystalline materials certainly bears this out (Imanaka 1968)

data on glass usually takes the opposite trend. This is somewhat unexpected, since Equation (5.8-1) was basically derived for glassy solids. The reduction in strength of materials on wetting is generally known as the Rebinder effect (Likhtman 1958), while the increase in strength is known as the Joffé effect (Westbrook 1968). Examples of both are shown in Appendix V.

5.8.2 Testing the Interfacial Free Energy Model VIA

Many workers have tested Model VIA. Westwood has been particularly active (1968, 1970A, B), and cites many examples to which Equation (5.8-1) is not applicable. Stoloff (1968) has demonstrated this for many cases of metals wetted by liquid metals. Westwood (1970A) offers specific explanations, some of which are illustrated in Figure 5.8-1. An intruding metal atom (or organic molecule) B in a crack ending at A-A will probably affect the cleavage plane strength (σ) but not the slip plane strength (τ). While simple wetting at A-A₀ tends to decrease σ , chemical reaction at that point may increase it. Since most tension failures include a large ductile component depending on τ , the effect of wetting may be trivial. In many non-metals, the liquid may exert electron-binding effects which completely over-ride surface free energy and result in specific responses to hydrogen bonding. These are not violations of the Gibbs principle nor the second law of thermodynamics, but merely have less obvious explanations than the one shown in Equation (5.8-1).

Some workers object to Equation (5.8-1) on the grounds that it is all too often applied to systems having some degree of ductility without adequate recognition of the need for a large (and non-rigorous) positive correction term. A negative correction term is also needed; as pointed out by Fox (1970), there is a substantial temperature rise in the zone A-A₀ of Figure 5.8-1. This is further developed in Appendix IV.

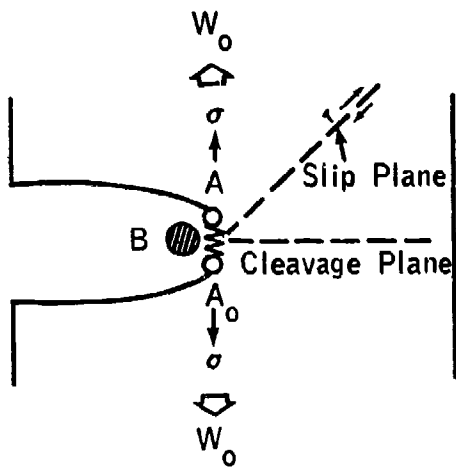
Data by Rounds (1962) on fatigue of steel balls in various lubricants are shown in Table 5.8-I. These have not yet been plotted into a Hansen diagram, as discussed in 5.11.4 below and in Appendix V, but good results will probably not be achieved since the circle would have to enclose paraffinic oils, acids (including the mono- and dialkyl-phosphates) and halogenated fluids, but exclude all other fluids. Thus, wetting does not explain the data. Work by Appeldoorn (1965) using one ceramic ball tends to confirm that point, as shown in Figure 5.8-2. On the other hand, if sliding fatigue data are admissible evidence, Table 5.3-11 makes a strong case for a correlation to high wetting energy as Oil D contains 0.2% stearic acid. Clearly, the choice of both base stocks and additives may be fatigue limited, though in sliding, fatigue is the lesser of two evils.

5.8.3 The Hydrogen Embrittlement Theory (Model VIb)

An important alternative to 5.8.1 is that reduction in fatigue life can come from hydrogen embrittlement. This arose from work by Grunberg (1960), who found strong absorption of hydrogen from wet oil. Schatzberg (1968, 1970A-B) continued this work. Frank (1957) showed that abrasion increased the permeation rate. The fact that high carbon steel is especially prone to such damage is noted by Berry (1967), and Vitovek (1964) traced this to the formation of sub-surface bubbles of methane, which cannot diffuse out again as does hydrogen. This is further discussed in 7.9. As shown by Bradley (1970) paraffins are prone to electron damage; this may generate hydrogen, as may acids, so Rounds' data are partly explainable by H₂, plus the carbon pick-up of Model IIIC.

It is to be hoped that some way around the conflict of interests between rolling and sliding elements can be found. For the moment, it appears that decreasing γ_{12} to protect gears entails some risk of decreasing w_0 on ball bearings in the same housing.

Figure 5.8-1
THE INTERFACIAL FREE ENERGY THEORY
OF FATIGUE CRACKING



Schematic illustration of a crack in a solid, subjected to an increasing force W_0 . The bond A-A₀ constitutes the crack tip, and B is a surface-active liquid metal atom.

TABLE 5.8-I

FATIGUE OF STEEL BALLS IN VARIOUS LUBRICANTS

Chemical composition	Viscosity at, cs			Relative values			
	100 F	210 F	VI	R_{10} life	Wear rate	Running torque	Weibull slope
Mineral oils							
Naphthenic mineral oil	13.8	2.85	36	1.33	31.7	1.52	3.40
Naphthenic mineral oil	33.4	4.49	3	1.24	34.9	1.49	2.35
Naphthenic mineral oil	110	8.17	8	2.13	18.6	1.38	2.33
Naphthenic mineral oil	262	12.3	—26	2.58*	3.6*	1.36*	2.18*
Naphthenic mineral oil	1120	29.0	—5	2.68	3.2	1.27	2.24
Paraffinic mineral oil	5.21	1.74	91	0.64*	873	1.94*	1.63*
Paraffinic mineral oil	10.2	2.55	82	0.61*	683	1.96*	1.50*
Paraffinic mineral oil	59.0	7.45	95	0.95*	92.2*	1.49*	1.57*
Paraffinic mineral oil	262	20.6	100	1.03*	8.8*	1.33*	0.94*
Paraffinic mineral oil	463	30.3	101	0.97*	1.63	1.20*	1.18*
Esters							
Isodecyl pelargonate	4.74	1.69	118	0.5	1.06	1.18	1.72
Dipropylene glycol dipelargonate	9.36	2.64	132	2.98	6.82	1.14	3.63
Di-2-ethylhexyl sebacate	12.8	3.34	154	1.76*	1.94*	1.19*	0.59*
Di-2-ethylhexyl phthalate	20.8	4.23	125	2.61	19.6	1.29	0.59
Trimethylolpropane ester	23.7	4.82	140	1.55	3.40	1.13	0.86
Pentaerythritol ester	25.4	5.01	130	2.95	3.29	1.15	1.66
Tridecyl azelate	36	6.38	134	1.90	5.16	1.44	1.64
Di-alkyl dimerate	81.2	12.0	133	2.91	2.39	1.16	2.02
Diester	188.2	20.4	122	1.03	2.08	1.09	1.34
Diester	273.7	28.9	125	0.60	2.85	1.02	1.26
Fatty acids and alcohols							
Pelargonic acid	5.7	1.92	167	0.49	27.5	0.96	1.39
Oleic acid	20.9	4.94	171	0.23*	29.6*	0.85*	0.90*
Saturated fatty acid	27.3	5.25	136	0.46	2.86	0.91	0.74
Branched C_{18} acid	36.0	6.24	99	0.56	37.0	0.93	0.48
n-Decyl alcohol	9.0	1.93	—209	0.51	76.5	1.36	3.85
Cyclohexanol	26.6	2.39	—639	1.53	38.2	1.61	1.13
Oleyl alcohol	18.9	3.32	13	1.01	2.45	0.85	0.49
Ethylene glycol	9.44	2.01	—57	1.04	17.3	0.73	0.80
Dipropylene glycol	33.8	3.18	—385	1.40	86.5	1.47	1.16
Triethylene glycol	18.7	3.35	23	1.78	72.3	1.14	0.85
Glycerin	224.4	11.56	—15	2.30	16.5	0.68	0.93
Polyglycols							
Polyglycols (propylene oxide, ethylene oxide polymers)	13.10	2.95	78	2.31	545	1.60	2.66
	36.5	6.80	144	1.28*	31.9*	1.23*	0.60*
	65.0	11.0	142	0.88	7.50	1.25	0.93
	141	21.9	140	0.81	45.5	1.28	1.22
Phosphate esters							
Tri(2-ethylhexyl) phosphate	8.03	2.29	107	1.01	2.57	1.06	1.56
2-Ethylhexyl dicresyl phosphate	16.63	3.14	27	0.92	2.30	1.10	2.06
Tricresyl phosphate	30.8	4.12	—35	1.20	4.34	1.81	1.50
Triaryl phosphate	63.4	6.16	10	3.01	29.2	1.82	2.11
Triaryl phosphate	246.4	9.49	—148	2.75	12.3	1.73	4.35
Mono and dialkyl phosphate (C_{12} average)	113.2	15.05	129	0.12	707	0.86	1.41
Di-dodecyl phosphite	13.2	3.55	183	0.54	26.9	0.84	1.20

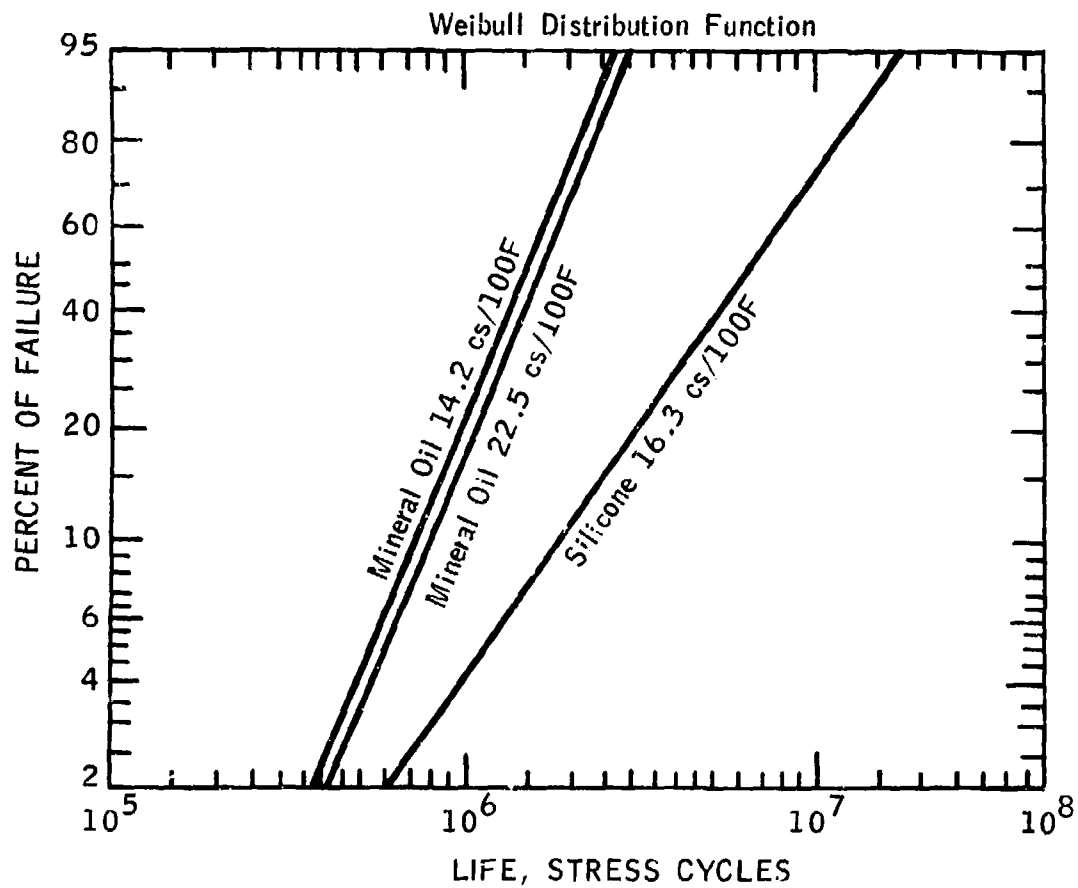
TABLE 5.8-1
(continued)

FATIGUE OF STEEL BALLS IN VARIOUS LUBRICANTS

Chemical composition	Viscosity at, cs			Relative values			
	100 F	210 F	VI	B ₁₀ life	Wear rate	Running torque	Weibull slope
Silicones and silicates							
Methylphenyl silicone	10.59	3.13	176	1.18	4105	2.83	1.83
Hexa(2-ethylbutoxy) disiloxane	10.8	3.81	232	1.10	6.7	1.21	1.67
Methylphenyl silicone	16.1	6.50	213	1.50	100.8	2.29	2.09
Chlorinated methylphenyl silicone	40	16	173	2.22 ^a	37.1 ^a	1.97 ^a	2.07 ^a
Methylphenyl silicone with polyglycol chains	74	16	154	0.44	12.2	1.32	0.84
Methylphenyl silicone	74.5	29.3	156	1.54	625	2.49	3.11
Methylphenyl silicone ^b	77.8	29.8	155	—	1235	3.07	—
Dimethyl silicone	82.9	33.5	153	1.94	332	2.16	1.86
Tetra(2-ethylhexyl) orthosilicate	6.3	2.3	160	2.67	4.77	1.27	4.17
Halogenated fluids							
Trifluorochloroethylene	25	3	—222	0.71	6.97	1.53	0.99
polymers	220	10	—77	0.36	6.42	1.43	0.78
Chlorinated biphenyl	41.6	3.16	—590	0.35 ^a	45.7 ^a	1.23 ^a	1.56 ^a
Polyphenyl ethers							
<i>m</i> -Chlorophenyl- <i>m</i> -phenoxy phenyl ether	16.43	3.06	13	2.95	44.0	1.72	1.64
<i>m</i> -Bis(<i>m</i> -ethylphenoxy) benzene	15.41	3.32	91	1.90	16.0	1.72	7.53
Bis(phenoxyphenyl) ether mixed isomers ^b	69.5	6.26	—7	—	186.5	2.10	—
Bis- <i>m</i> (<i>m</i> -Phenoxyphenoxy) benzene	335.5	12.58	—77	2.95	131.9	2.58	5.11
Bis(phenoxyphenoxy) benzene mixed isomers ^b	389.1	13.58	—81	—	239	2.21	—
Others							
Diamyl naphthalene	30.7	3.67	—140	3.00	3.75	1.35	1.21
Polybutene	23.8	4.37	100	2.40	10.5	1.38	1.33
Polybutene	111.4	12.0	105	2.50 ^a	32.8 ^a	1.65 ^a	5.52 ^a

^a Average of two or more tests.^b Fluid decomposed to form solid material before fatigue failure occurred.

Figure 5.8-2
FATIGUE RESULTS WITH ONE
CRYSTALLIZED GLASS AND THREE STEEL BALLS



On the more optimistic side, in a recent interview Mahncke (1971) of SKF Industries indicated that fatigue cracking of bearing balls was a relatively minor problem compared to those caused by oil oxidation, etc. It appears that until these problems are solved, Model VI will not limit progress.

5.9 Abrasive Wear (Model VII)

As assumed in Section 2, there will be no abrasive wear until the system becomes contaminated with wear products from one of the primary processes. This limits the nature of the abrasive particles to the following classes:

- (a) Bits of the hydrated oxide coating found on all new parts.
- (b) Metallic debris from break-in. This can be minimized by careful fitting, or even by breaking in, flushing and refilling at the factory.
- (c) Metallic particles from fatigue wear (Figure 5.3-2).
- (d) Metallic particles from wear by adhesion or interlocked dislocation and transfer (Figures 5.4-4 and 5).
- (e) Products from corrosive wear.
- (f) Carbide particles from Model IIIC.
- (g) Colloidal particles from Process #3b (Table 5.5-II).
- (h) Oxide particles from Process #4 (Table 5.5-II).

This assortment of material can be described a little more simply if we look at the damage potential rather than the process in question. The ranking might well then be, in increasing severity:

- (g) Colloidal particles are probably harmless.
- (e) Halides, sulfide and phosphate particles are not very harmful.
- (b), (c), (d) Metal particles can vary from mildly to severely abrasive, but tend to the severe side.
- (f) Carbides tend to be severely abrasive.

Once abrasion due to oxide or carbide begins, it can result in another class of particles:

- (i) Metal chips cut off the harder parts. These are in a class with oxides.

The abrasive wear processes are of two kinds; embedded particles (two-body abrasion) and free-moving particles (three-body abrasion).

5.9.1 Two-Body Abrasion (Model VIIA)

Most of the work has been done in this area. Finkin (1968B) made a comprehensive study of abrasive wear in general and was able to cite 42 references, most of them from the UK and USSR. The sole commentator cited 7 more, as evidence of US interest. However, only Rabinowicz (1965A, B) has really done much in the US towards a model.

The mechanism of two-body abrasion is brutally simple, as shown in Figure 5.9-1A, from which

$$(V/d) = r^2 \tan \theta = W \tan \theta / P_m \quad (5.9-1)$$

where r and θ are given special definitions. As shown in the figure, r is the radius (or half-width) of the cut, and θ the angle of contact. This is a special form of Equation (5.1-4), with $K = \tan \theta$.

Krushchov (1956A, B) found Equation (5.1-4) to be valid for 12 commercially pure cubic and hexagonal metals (some in two different grades) and two carbon steels, as shown in Figure 5.9-2. He also performed experiments to test an equation he derived for nonhomogeneous bodies (1958). For such materials, the effective hardness is

$$P_m = \sum (P_i \theta_i) \quad (5.9-2)$$

where P_i is the hardness of phase i , and θ_i its volume fraction. If the body is porous, $(1 - \sum \theta_i)$ is the volume fraction of voids.

Heat hardened steels and work hardened metals showed branched lines in which the annealed metal falls on the line of Figure 5.9-2, but hardening pulls it off as shown in Figures 5.9-3 and 5.9-4. All these can be expressed by

$$(V/d) = K W / [P_o + C_m (P_m - P_o)] \quad (5.9-3)$$

where P_o is the annealed hardness

P_m is the hardness after treatment

C_m is a constant for the metal.

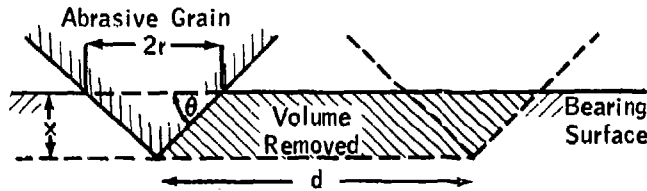
The value of C_m is unpredictable. For steels, it is positive and varies positively with P_o ; for nonferrous metals (including 18% Cr/ 9% Ni stainless steel) it can be zero or even slightly negative.

Spurr and Newcomb (1957) found a relation to Young's modulus (E_1) similar to Equation (5.1-4). Krushchov and Babichev (1960) followed up on this, and changed it to

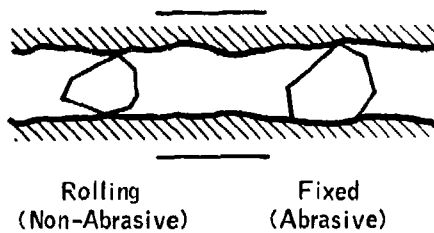
$$(V/d) \propto W/E_1^{1.3} \quad (5.9-4)$$

Figure 5.9-1

TWO-BODY ABRASIVE WEAR



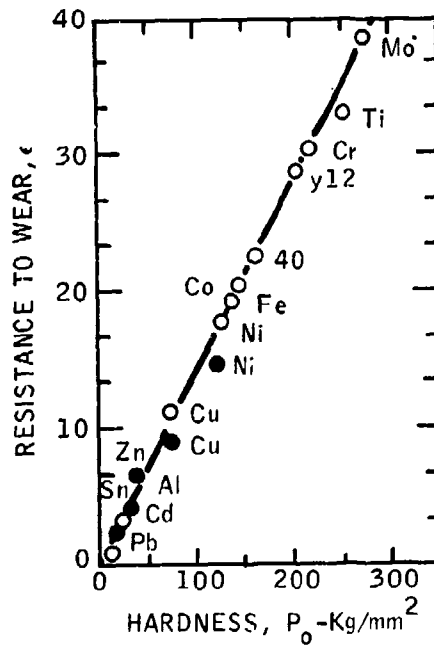
A - Abrasive Wear Model in Which a Cone Removes Material from a Surface



B - Sketch of Abrasive Particles Between Rubbing Surfaces

Figure 5.9-2

ABRASIVE WEAR AS A FUNCTION OF HARDNESS



Wear resistance, ϵ , versus hardness, P_0 . y_{12} is 1.2 percent carbon steel, and 40 is 0.41 percent carbon steel.

Figure 5.9-3
EFFECT OF HEAT-
HARDENING ON ABRASIVE
WEAR

Wear resistance, ϵ , versus hardness, P_m , for four heat treated steels and three pure metals (see Figure 5.9-2 for steel codes)

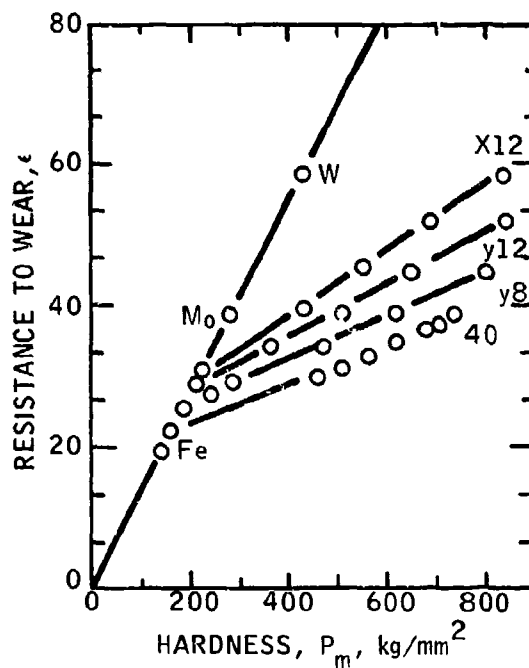
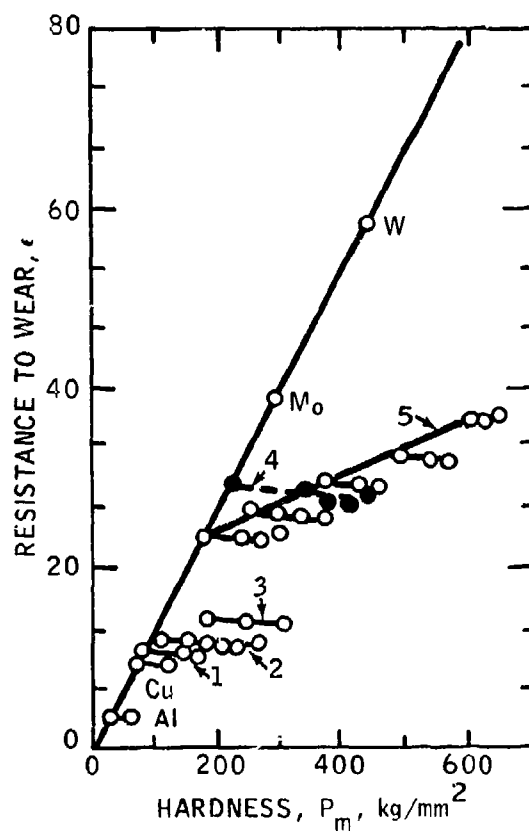


Figure 5.9-4
EFFECT OF WORK-
HARDENING ON ABRASIVE
WEAR

Wear resistance, ϵ , versus hardness, P_m , for work hardened metals: 1-low brass, 2-aluminum bronze, 3-beryllium copper, 4-18Cr-9Ni steel, and 5-0.45 percent carbon steel



but this again showed branching for heat-hardened steels so was no improvement on Equation (5.9-3).

Giltrow (1970) correlated wear coefficient (K) with the square root of cohesive energy, for material from polyethylene to tungsten, but did not include other variables. This is provocative but not immediately useful.

Equation (5.9-3), or a combination of (5.1-4) and (5.9-2), include nothing at all about the abrasive except that it is much harder than the metal. Nathan and Jones (1967) showed that when the ratio of metal to abrasive hardness (P_m/P_a) is less than 30,

$$(V/d) \propto W \log (P_m/P_a) \quad (5.9-5)$$

their previous work had showed that, up to $r = 35 \mu m$,

$$(V/d) = K'r (U + b) W \quad (5.9-6)$$

where $(U + b)$ = velocity plus a constant. Combining these:

$$(V/d) = K'r (U + b) W \log (P_m/P_a) \quad (5.9-7)$$

which has little resemblance to the other work. However, it is probably closer to the situation of self-generated wear particles than Equation (5.9-3), if we limit the particles to those softer than the harder metal of the pair. This situation was considered quite unsatisfactory by Finkin (1968B), and the writer agrees. More research is needed.

5.9.2 Automotive Abrasion (Model VIIB)

Turning from the laboratory use of simulative machines and pure components, at the other extreme are the field tests of Duckworth and Forrester (1957). They dealt with this complicated situation by dimensional analysis. The real heart of the problem was that iron particles from the oil embedded into the soft metal of the bearings so that the principal wear observed was on the hard steel crankshaft. Thus, their model is primarily concerned with the ability of the bearings to "swallow" the abrasive particle to where it ceased to be harmful.

With a large block of data, covering 10 bearing materials in a number of vehicles, they arrived at the conclusion that their results were best correlated by plotting

$$(V/d)_R / \sqrt{T_m C_P} \quad \text{versus} \quad \frac{P_m V_m}{G} \quad (5.9-8)$$

where $(V/d)_R$ = wear rate relative to white metal

T_m = melting point of lowest constituent,

C_p = specific heat (cal/mole °C)

P_m = hardness (kg/m^2)

V_m = molar volume of principal constituent (cm^3)

G = free energy of oxidation of principal constituent (cal/mole)

where all properties are based on bearing metal.

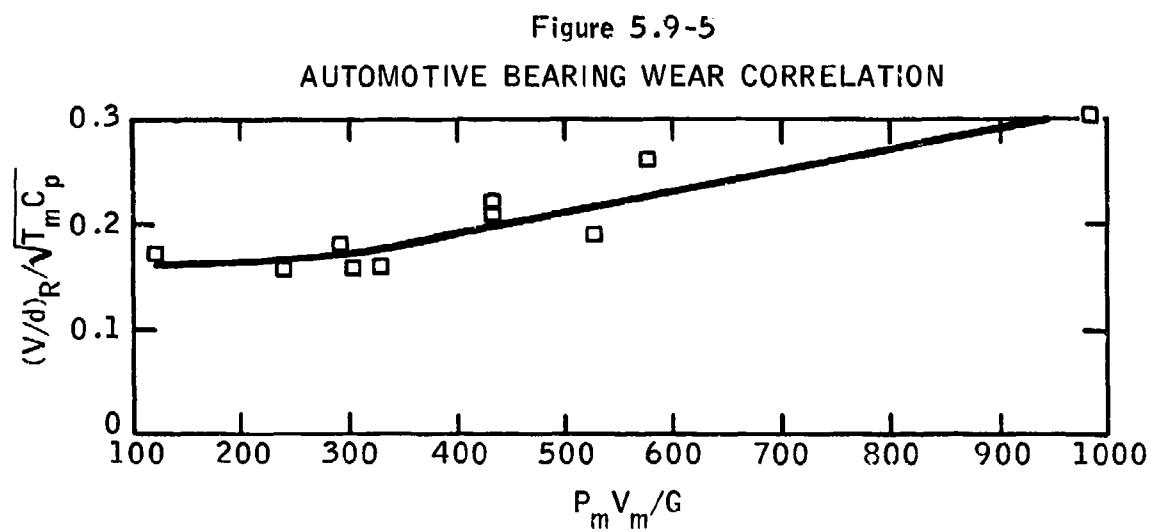
Their plot is shown in Figure 5.9-5. They claim a correlation coefficient of 0.91 and explanation of 84% of the variance. While one may criticize some of their parameters, the results are impressive.

Unfortunately, there is no way to relate this to other situations, as speed and load were subject to continuous variation. This model might be considered for further development, as it appears to be the only one offering help on the embedding mechanism of abrasion control. However, a great deal remains to be clarified on it.

5.9.3 Three-Body Abrasion (Model VIIC)

The situation with a freely moving abrasive particle is shown on the left in Figure 5.9-1, from Rabinowicz (1965B). While this is labeled "Non-Abrasive" in contrast to a similar particle on the right which has become embedded in the surface, it is not fully established that 3-body (left) is not responsible for at least part of the wear. Finkin (1968B) estimates that 90% of the wear in a "3-body" system is actually 2-body. He goes on to assume that: "The relative wear rates of materials experienced in the two situations are identical, however, so one may use a test method employing either principle". Most of the work seems to be done with dry abrasive powders, and even those tests are less common than those with fixed (two-body) abrasive. Rarest of all are the tests of most interest in this report, in which a low concentration of the abrasive is suspended in a viscous lubricant. (High concentration slurries of abrasives, such as lapping compounds, are not relevant). The model must contain, as Babichev (1962) has shown for unlubricated wear, the relation of wear to supply rate of abrasive particles. This consists of an extremely steep initial slope followed by a zero-slope plateau. Lomakin (1956) showed that for pumping a drilling mud containing various concentrations of sharp quartz particles, the 0.15% by weight naturally present gave a wear rate of 5.3 mg/hr. At 1% by weight, wear was 5.9 mg/hr and linear to 20% by weight. If we assume, as he did, that at 0% wear would have been 0 mg/hr, then the "curve" is two straight lines with a ratio in slopes of 133/1, a remarkably abrupt transition.

This phenomenon seems to be substantiated by Rabinowicz (1965A), and by Finkin's observation that doing a moderate job of filtration on industrial equipment frequently does no good at all.



In this case, the minimum concentration is present even when the (typically) inadequate filter is operative, so that clogging it so that the bypass opens really does little additional harm.

Another interesting point about Lomakin's data (1956) is that he observed a time-dependence of wear rate. Like most experimentalists, he was so infatuated with Equation (5.1-4) that he discarded all such data as being some sort of break-in process. Of course, break-in has not been at all characteristic of abrasive wear studies. His unscreened data may be expressed by

$$(V/d) = K_p d^{-0.33} W \quad (5.9-9)$$

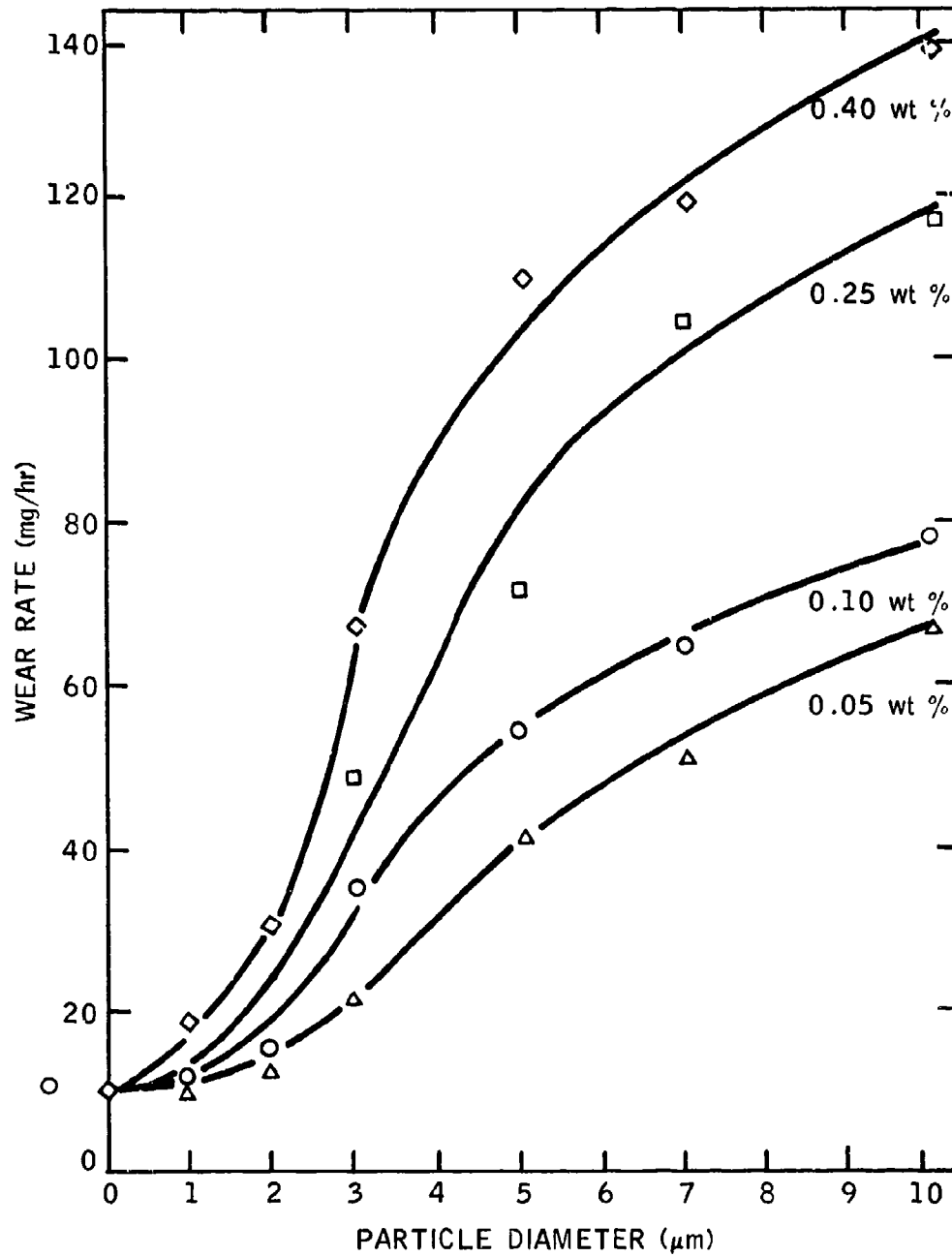
Another member of the Krushchov group published (Maev 1965) an extensive study on abrasion by ingested dust in a simulated Diesel engine cylinder. Sized particles of quartz and corundum were used, with three natural dusts for comparison. The results were fitted to a model which was primarily oriented to air-cleaner efficiency, and so not well suited for the present purpose. Briefly, these observations were made:

- 5.9.3.1 Any injection of abrasive into the system began to lose its effect one to five hours later, presumably due to size reduction. Up to then wear was linear with time.
- 5.9.3.2 Particles of 1 μm diameter had only a minor effect over the concentration range studied, 0.0% to 0.40%. The latter showed about double the rate of clean oil. The clean oil wear rate was established after 40-50 hours run-in.
- 5.9.3.3 The wear rate shows a peculiar variation with particle diameter, with a rapid rise from 1 to 3 μm and a decreasing rate of rise above 3 μm . (Figure 5.9-6) While it does not level off at the maximum tested size of 10 μm , it might do so at a larger diameter.
- 5.9.3.4 The wear rate is characterized by Maev as a linear function of the concentration, for any particle size, from 0.0% to 0.40%. However, the lines do not pass through the zero concentration point (except for 1 μm , which is too low to be very precise), and the lines for 7 and 10 μm show distinct curvature.
- 5.9.3.5 If logically justified, the data could be forced to fit a model

$$(V/d) = kDC_a^{0.5} \quad (5.9-10)$$

where D is the particle diameter and C_a the concentration. This would assume Maev's precision to be considerably less than he states it to be, and involves best-fit straight lines in Figure 5.9-6 in place of his curves, as well as curving his straight lines in 5.9.3.4. These are considerable liberties to take with an experimenter's data, and will be kept in abeyance unless further justification develops.

Figure 5.9-6
WEAR RATE AS A FUNCTION OF PARTICLE
SIZE AND CONCENTRATION



Despite the millions of dollars spent on particulate contamination control in the aerospace industry, very few reports have appeared that give quantitative justification for the "super-cleaning" program. In almost every case where studies have been reported, the benefits cited were freedom from plugging jets, jamming servo valves, etc. In a recent symposium (ASTM 1971A) the same pattern was continued, but Fitch (pp 39-49) gave some data on pump failure which may be attributed largely to abrasive wear. The results were quite surprising in that they indicated thresholds for both particle diameter and concentration below which no damage took place within 30 minutes. In a later paper (Fitch 1971B) he gives further details on a simpler test procedure to obtain the diameter threshold and express it as a sensitivity index. However, he is careful to avoid saying that all the loss in volumetric efficiency is due to wear, so that his model is not quite what we need.

Tao (1970) also added small doses of dusts of controlled diameters to a vane pump test loop, and observed a threshold effect. He did not run enough points to locate it exactly, and his use of a vane pump created an ambiguity which he did not recognize at that time. This type of pump has two modes of failure, both of which were apparently taking place during Tao's experiments. The first is wear, primarily on the ring and vanes, due to the discharge pressure forcing the vanes into intimate contact with the ring. Ordinarily, this continues (after break-in) on a linear basis with time until the vanes are so short that they drop out of the slots. There is little or no loss of volumetric efficiency during this process.

The second mode of failure is by jamming the vanes in the slots, so that the pressure behind the vanes is not transmitted to the vane/ring sealing contact. If this mode is 100% of the failure, essentially no wear takes place. Tao's data indicate that he was operating in a mixture of these two modes most of the time.

A mathematical model arises when we try to predict whether the particle will become fixed. Tao showed that both wear and loss of volumetric efficiency could be brought back to essentially those of the liquid without abrasive, by adding a surfactant with a strong affinity for the particles (oleic acid for Fe or Fe_2O_3 , or C_{18} amine for SiO_2).

It appears to be writer that these effects could all be predicted by the work of Hamaker (who was not concerned with wear or lubrication). He published two papers (1937, 1938) on the mutual attraction of spherical particles, both dry and immersed in a liquid, due to London forces. In addition, his formulation extended to the case of a particle being attracted to an "infinite" solid body. For these cases, he defines A as an attractive energy constant for a given set of materials, D_1 and D_2 as the diameters of the particles, d their separation (surface to surface), and F_y as the force between them. If $D_1 = \infty$ (i.e., a solid body),

$$F_y = AD_2/12d^2 \quad (5.9-10)$$

Hamaker calculated that A must lie between 0.7×10^{-14} and 3×10^{-12} ergs as extremes with most substances around 7×10^{-13} ergs. Immersion in a liquid reduces A , but not very much.

In his second paper, he specifically calculated that a dry sphere of 30 μm diameter will adhere to a surface against the force of gravity, and under water 12 μm was small enough to "adhere completely". It would appear that we have the basis for some selectivity that would lead to the observation of Rabinowicz (1965B) that only 10% adhere (cf Finkin (1968B), above) in that particles are rarely all the same size. In addition, Hamaker shows that shape variations would cause further selectivity.

Gregory (1969) has reviewed the various methods of calculating A, and concluded that, even though they do not produce entirely consistent results, the accuracy is adequate for most purposes. Spielman (1970) illustrates the use of such numbers in predicting the capture of particles from flowing liquids. On the other hand, Donald (1971) warns that electrostatic forces may easily outweigh the London forces. His data were taken in air, but obviously have a direct analogy to liquid systems where both the forces of attraction and washing away are greater.

Vold (1961) made another step forward by calculating the effects of surfactant layers around the particles. The result was a very great weakening of F_y , due mainly to the increase in d. Thus, the effect of acid and amine is explained.

This is a long way from making up a model wear equation, but combining the ideas that wear due to fine, soft particles follows Equation (4.8-7), and that three-body wear is really two-body wear times an "efficiency factor" based on the Hamaker-Vold theory, should be a good start in that direction.

Another matter that needs to be taken care of by such a model is the peculiar effect of humidity on abrasion resistance. Rabinowicz (1967) noted that water vapor increases the wear rate by about 15% in summer over that in winter, on unlubricated tests. He attributes this to a film condensed on the abrasive, comparable to that postulated by Vaessen for the "zero-wear" model (1971).

5.10 Fretting Corrosion (Model VIII)

Fretting corrosion is usually considered as a separate subject from corrosive wear, but the model is so related to III as to warrant brief mention. It also is instructive, being one of the most sophisticated so far developed. Uhlig, Feng, Tierney and McClellan (1953) started with a logarithmic law of oxidation (which was used by Tenwick (1971) but immediately simplified to linear form). Their equation, in consistent symbols, etc., is:

$$(V/d) = (k_0 W^{0.5} / f j \rho_m) - [2k_0 W / f j \rho_m (\pi P_m)^{0.5}] + (k_2 W / \rho_m) \quad (5.10-1)$$

where k_0 and k_2 are empirical constants

j = slip (amplitude),

f = frequency

ρ_m = metal density

The first two terms represent corrosion and the third concerns "mechanical" wear. The authors show appropriate data to establish the dependence of wear or load and frequency. The effect of humidity is also demonstrated, but is not large enough to warrant inclusion in Equation (5.10-1), while the effect of temperature is not regular enough to include. Both of these factors are included in k_o , which must be determined experimentally for any given metals under appropriate environmental conditions.

This model is remarkably sophisticated, especially considering that it is older than any of the work cited above. The authors appear to have anticipated most of the problems encountered by other modelers, and taken care of them for their special case. Especially interesting is their handling of the exponent of W in the first and third terms, so that it varies from 0.5 for pure corrosive wear to 1.0 for noncorrosive wear. (The middle term in the equation represents a more refined treatment of converting the logarithmic oxidation equation to linear form than was used by Tenwick (1971), and is negligible at loads high in comparison with P_m).

This model has held up so well that a recent review (Hurricks 1970) was not able to recommend any change in the mathematics (see also Feng 1953, 1954B, 1956A).

5.11 Auxiliary Models on Surface Free Energy

In order to analyze the models more completely, it will be helpful to establish a few methods for obtaining the surface constants needed for various materials. Several approximations have already been cited (5.4.2, 5.8.1), but several others need to be covered at this point.

5.11.1 Surface Free Energy of Liquids

Very early in this study it appeared that the surface free energies of a number of materials would be required. The work on liquids was carried forward as far as seemed necessary, and was released for publication (Beerbower 1971B). The complete reprint appears as Appendix III.

Briefly, it proved possible to calculate the surface free energy of most liquids from the energy of vaporization. Some exceptional cases (acids, alcohols, metal halides and certain "irregular" metals) required special handling, but most organic and metallic liquids follow the equation

$$\gamma_2 = 0.0715 V_m^{1/3} [\delta_D^2 + 0.632 (\delta_P^2 + \delta_H^2)] \quad (5.11-1)$$

where V_m = molar volume

δ_D^2 = London cohesive energy density

δ_P^2 = Keesom cohesive energy density

δ_H^2 = H-bond cohesive energy density

For regular metals, δ_P and δ_H are zero.

5.11.2 Surface Free Energy of Solids

The surface energies of solids are much more complicated than those of liquids. The whole situation is reviewed in Appendix IV, which is an edited version of the Appendix to Progress Report No. 1 on this project.

In brief, the surface stress (see 5.5.4) cannot be calculated. In most crystals, it is quite feasible to calculate a surface free energy at the melting point by

$$\gamma_{1m} \approx 1.14 \gamma_{2m} \quad (5.11-2)$$

and then to reduce it to working temperature by

$$\gamma_1 = \gamma_o (1 - T_R)^{1.2} \quad (5.11-3)$$

where γ_o is the surface free energy at 0°K, and T_R the ratio of actual to critical temperature, from which

$$\gamma_1 = 1.14 \gamma_{2m} \left[(1 - T_R) / (1 - T_{Rm}) \right]^{1.2} \quad (5.11-4)$$

where T_{Rm} is the reduced temperature at the melting point.

Alternatively,

$$\gamma_1 = 0.0715 v_m^{1/3} (\Delta H_s - RT) \quad (5.11-5)$$

will give about the same result. The problem is that all three kinds of faces have slightly different γ_1 values, and the equations yield only one γ_s value. Which face does it represent - or does it represent an average? In any case, what is the relevance to a typical multicrystalline solid?

A little thought will show that γ_s from liquid or vapor data must represent the smoothest surface, typically the 100 face. This is simply because both are as smooth as it is possible for matter to be. In terms of Fermi surfaces, all interfaces are quite lumpy, and to a nuclear physicist they consist of an array of tiny sharp points.

The multicrystal requires a different approach, based on the Gibbs principle. No doubt most solids violate the principle by exhibiting greater than the minimum free energy, but this is only because they are not in equilibrium. Just as the high surface free energy component in an alloy will be swallowed beneath the surface on annealing as in Equation (4.4-15), so will be more active faces be swallowed. Thus, Equations (5.11-3, 4 and 5) give the surface free energy of the annealed multicrystalline solid. To this must be added corrections for any incomplete crystal reorientation, stress, dislocations and high-energy impurities, when and if such corrections are known.

5.11.3 Surface Free Energy of Mixtures

This has already been partly covered in 5.5.4. However, Clever and his students, Myers (1969) and Schmidt (1967) have gone a step beyond Hildebrand. An article putting their work in more available form is awaiting publication. The problem is further discussed in Appendix VI.

5.11.4 Interfacial Free Energy

As indicated in 5.4.1 and 5.6.2, there is really no good model for interfacial free energy of organic/metal or metal/metal interfaces. Good (1970), who had done the most comprehensive job on interfacial energies, shies away from the metals. The Russians are doing an excellent job of data-gathering, and also have a good record on modeling, so can be expected to solve this problem eventually. Their best effort so far has been by Zadumkin and Karashaev, who set up an electrostatic equation

$$A_{12} = B(\epsilon - 1)/(\epsilon + 1) \quad (5.11-6)$$

where B is a constant for any metal, which is proportional to its contact potential against a hydrocarbon. The supporting evidence on mercury Zadumkin (1965) and gallium (Karashaev 1968) is favorable. The writer has shown (1971A) that B must vary with temperature, and also used Equation (5.11-6) to explain the multi-layers of stearic acid in Anomaly 4.11.4 (see 7.11.4). However, he has some reservations about using only the dielectric constant (ϵ) to characterize a lubricant's boundary action.

The most exciting development in the U.S. is the new approach taken by Hansen (1970A), who simply plotted contours of constant wetting angle on his δ_D , δ_P , δ_H coordinates. At the center of interaction lies the point for the three energies of the solid surface. From these it should be possible to calculate A_{12} for any liquid of known parameters by

$$A_{12} = \frac{0.286 \ V_1 V_2 (\delta_{D1} \delta_{D2} + a \delta_{P1} \delta_{P2} + b \delta_{H1} \delta_{H2})}{(V_1^{1/3} + V_2^{1/3})^2} \quad (5.11-7)$$

but the proof of this equation is none too firm (see below).

As a tool for classifying lubricants, Hansen plots have been made directly from the coefficients of friction, with considerable success. Data by Senior and West (1971) on polyethylene at various levels of surface sulfonation were plotted (Beerbower 1971E) in Figures 5.11-1, 2 and 3. Only the δ_P - δ_H quadrant is shown, as most of the situation in the other two quadrants may be inferred from the distribution of points there. Two facts should be kept in mind -

- (a) All highly interacting liquids (low F) must fall within the circle in all three quadrants, but weakly interacting ones need only fall outside in one to be properly correlated.

Figure 5.11-1
HANSEN PLOT OF FRICTION ON POLYETHYLENE
(UNTREATED)

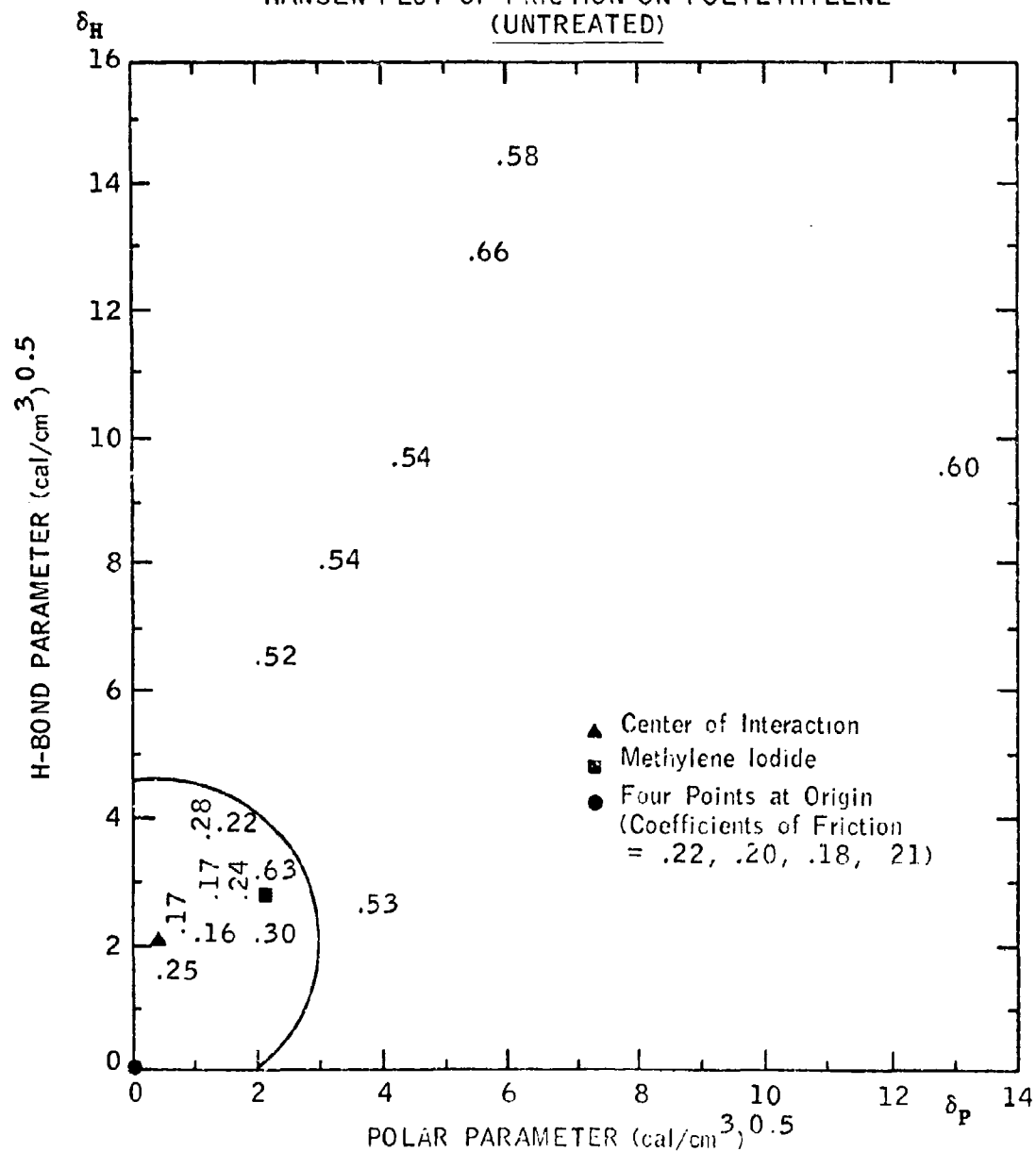


Figure 5.11-2
HANSEN PLOT OF FRICTION ON POLYETHYLENE
TREATED WITH $H_2S_2O_7$ for
TWO MINUTES

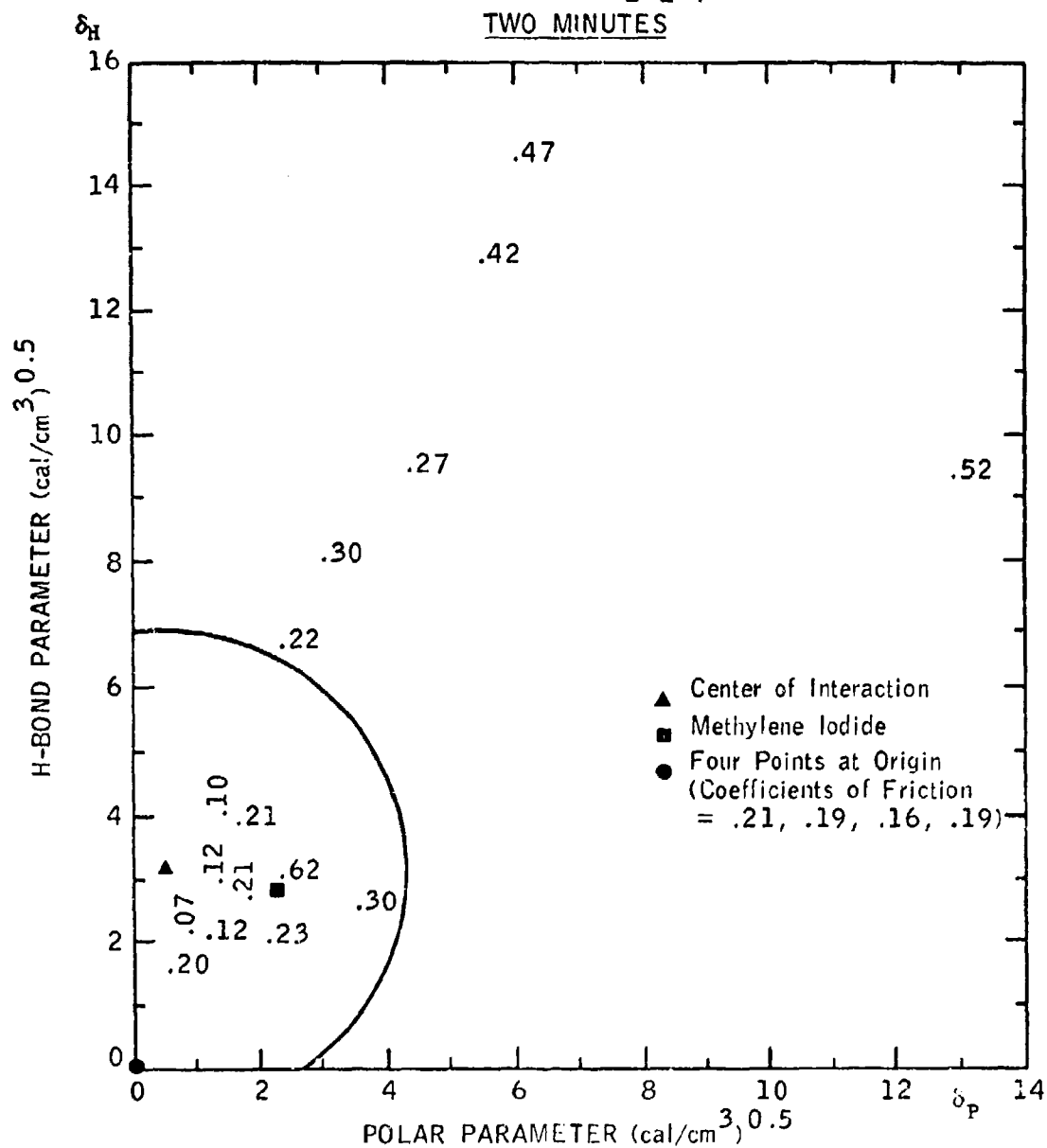
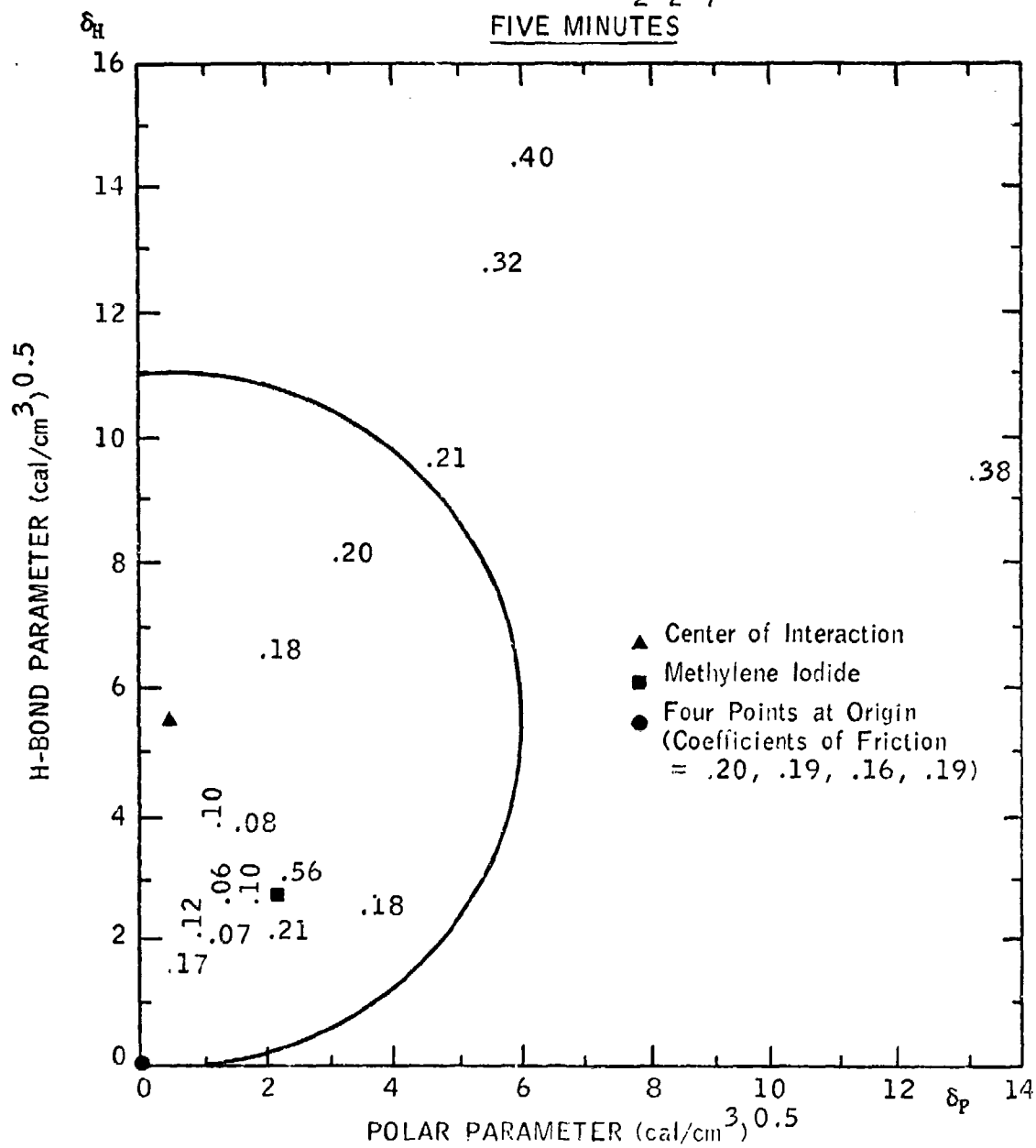


Figure 5.11-3
HANSEN PLOT OF FRICTION ON POLYETHYLENE
TREATED WITH $\text{H}_2\text{S}_2\text{O}_7$ for
FIVE MINUTES



- (b) Methylene iodide, unless repurified just before the test, usually shows up as noncorrelated because of spontaneous decomposition.

It will be noted that, except as cited in (b), all points are correlated satisfactorily. In addition, it is clear that sulfonation of polyethylene not only raises the H bond parameter (as would be expected) but also increases the tolerance on δ_D and δ_P (indicated by increased radius of the circle) and decreases the value of F at the center. Thus, it appears that A_{12} was indeed increased. The authors, in their closure, noted that the center for $\cos \theta = 0$ does not coincide with that for $F = 0.25$. The writer feels this difference is to be expected, due to the distorted surface exposed in the friction tests.

Comparable data on metals is extremely hard to obtain, due to the extraordinary reactivity of freshly cut surfaces. Indeed, one may seriously question whether wetting is a factor in lubricating such surfaces except as a prelude to reaction. One source of data on fresh metal surfaces is metal cutting experiments. One of the most comprehensive was that of Ernst and Merchant (1941), whose data on turning aluminum with a battery of pure liquids have remained unexplained for about 30 years. A complete 3-quadrant plot of the data is shown in Figure 5.11-4, which shows that only CCl_4 , CH_3OH , $C_6H_5NH_2$, and $HCOOC_2H_5$ do not conform. The first is notorious for decomposing under such conditions, so the success score is 37/40 or 92.5%. Turpentine, olive oil, glycerol and water were also successfully predicted but are not counted as the parameters are not very precisely known. The variable used for the contours is the cutting ratio (R_c), which is related to F by

$$F = \cot (2 \sin^{-1} R_c - \Psi) \quad (5.11-7)$$

where Ψ is the rake angle of the cutting tool.

The other way of plotting such data is shown in Figure 5.11-5. In this method, a computer is used to evaluate the two constants shown as 0.25 in Equation (5.5-20). The resulting "heat of mixing" (or wetting) is then plotted against the measured variable; this was elastomer swelling in the original article (Beerbower 1969) but here is a function of R_c devised to linearize the data. The fit is again quite good - but $C_6H_5NH_2$ and $HCOOC_2H_5$, which fitted poorly on Figure 5.11-4, are seen to be fairly well correlated, while C_6H_5Cl , CCl_4 , and CH_3OH proved intractable. $CH_3COOC_2H_5$ and CH_3CHO were further out than expected, but even with them in, the correlation coefficient was 0.85.

There is some reason to believe that what is being correlated in Figures 5.11-4 - 5 is not A_{12} at all, but an energy of chemical reaction. The key compounds are all alcohols, which are known to react with aluminum

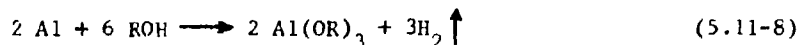


Figure 5.11-4
DETERMINATION OF INTERACTION PARAMETERS FOR FRESHLY CUT ALUMINUM

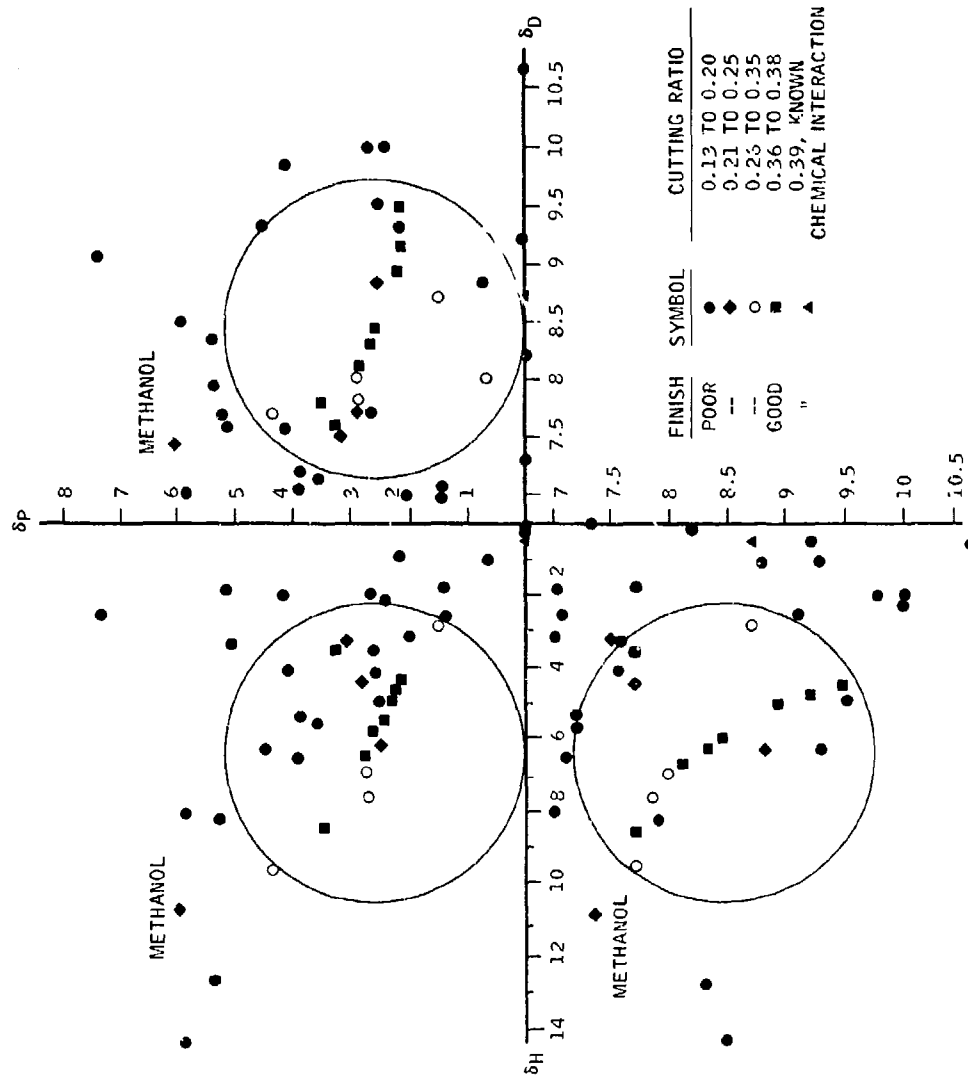
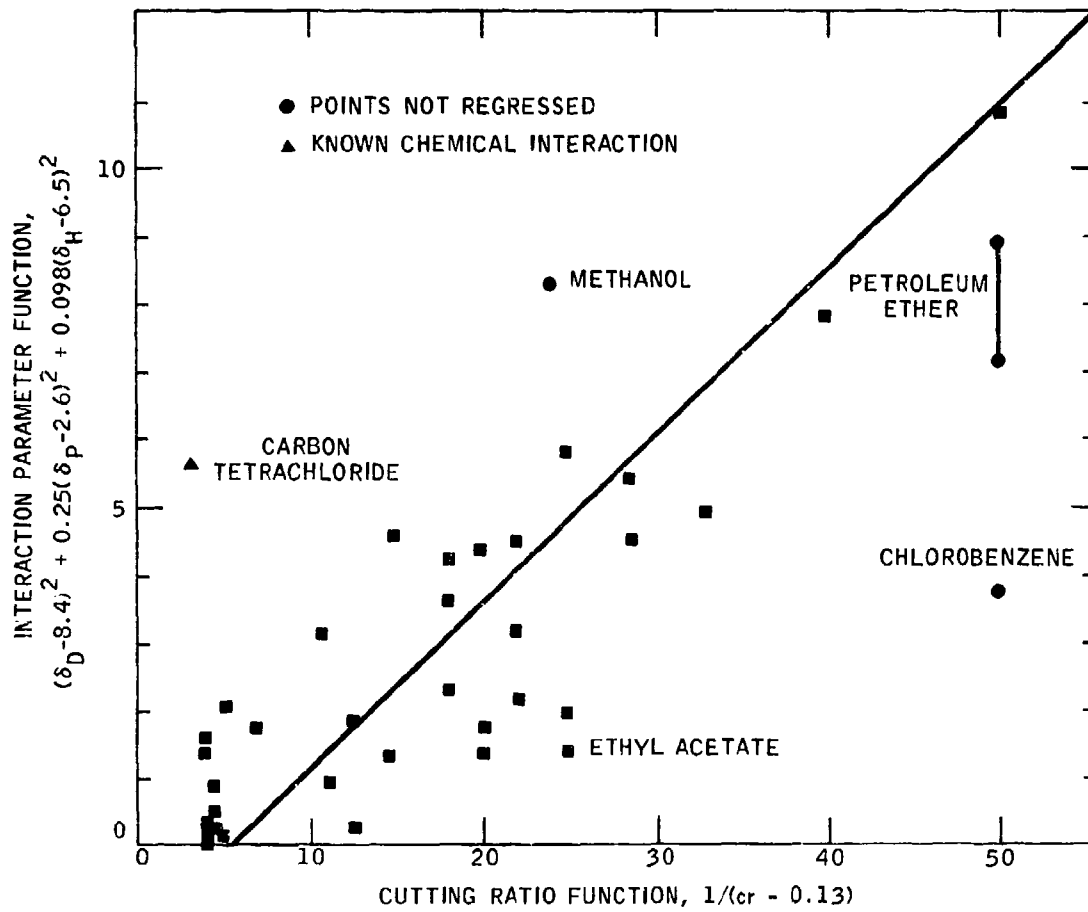


Figure 5.11-5
CORRELATION OF CUTTING RATIO WITH INTERACTION PARAMETERS
CUTTING COMMERCIAL "PURE" Al,
DEPTH OF CUT = 0.005"
CUTTING SPEED = 5.5"/min.



The question is, in the few microseconds available at the edge of the cutting tool, can Reaction (5.11-8) prevail over Equation (5.11-7)? A good deal depends on the answer - or on similar data from a better planned experiment with liquids of modern purity. If Equation (5.11-7) dominates, then it is possible to H-bond to metals and the entire structure built by Fowkes (1967) on the opposite assumption is invalidated. The only other study of metal-wetting of comparable scope is Harkins (1920) on mercury, often analyzed but seldom repeated. The data are about 50 years old, and questions of purity inevitably arise - though Harkins took much more pains on this detail than Ernst and Merchant. Analysis of their data shows about the same level of δ_H (Appendix V), and so does an unpublished study by Panzer on aluminum powder.

5.11.5 Interfacial Entropy

To fit Model II, the total energy of adhesion, often called the heat of adsorption, is required. This is

$$E = W_{12} + T\Delta S_{12} \quad (5.11-9)$$

While some approaches to the entropy of wetting ($T\Delta S_{12}$) are discussed in Appendix VII, this must be classed as a problem for which no validated solution is available.

5.12 Predicting the Coefficient of Friction (F)

As indicated in Section 5.3 it is essential to free the designer from the need for an F value for each combination of two metals, one lubricant and one atmosphere that he might encounter. Adding temperature (T_o) as a parameter, and a modest collection of five metals (taken two at a time) and five each of the other factors, requires tabulation of 55 or 3125 values of F for this very low level of flexibility.

There has always been an intuitive connection between wear rate and F, but those who have sought to express it have been discouraged (by themselves or their co-workers) because of the glaring exceptions to any rule. A recent article on brake design (Eudier 1969) cites "Friction Without Wear" as a realistic goal. Thus, any rule for (V/d) versus (F) must be limited to carefully defined regimes on Figure 2-1.

Abrasive wear has been modeled already by Goddard (1962) as

$$(V/d) = K''W (F - F_o) \quad (5.12-1)$$

where F_o is the coefficient of friction without abrasive. This equation has not been very widely accepted or validated, and certainly must not be used for non-abrasive wear.

Model IB contains within it the assumption of a relation of these variables

$$(V/d) \propto [(1 - 2v_1)^{2/16} + F^2]^{4.50} \quad (5.12-2)$$

which, for Poisson's ratio (ν) = 0.33, approaches the usual fatigue mode ninth power function. This is also applied, with less justification, to high transfer, or "adhesive wear", mode.

To produce an empirical model, the pure hydrocarbon data were taken from Appeldoorn (1967A) and regressed on a $\log (V/d) = m \log F + b$ basis. Of the original 72 points, 21 were discarded because of excessive scatter. Most of those discarded were either at the lowest load where readings were uncertain, or at the highest where incipient scuffing was suspected. The result was $m = 7.45$, with a correlation coefficient of 0.823.

To improve this coefficient, it was decided to follow the precedent of others (Rabinowicz 1965B) and regress the specific wear rate $K (= P_m V/Wd)$. It was also postulated that use of the von Mises function for plastic deformation, used in Equations (5.3-13) and (5.4-4), would be more useful. As mentioned in Section 5.4, several values have been suggested for "n" in $(1 + nF^2)$, such as 3 (Rowe 1967), 4 (Bayer 1962) or 12 (Spurr 1964), so a multiple regression was run with "n" left free. The result was

$$K = (P_m V/Wd) = 4.96 \times 10^{-14} (1 + 10.42F^2)^{4.84} \quad (5.12-3)$$

with a correlation coefficient of 0.87.

Some data is available in Cornelius and Roberts (1961) which may be useful, even though lubricated only by gas (and some inherent lubricating properties of the alloys used). Unfortunately, their data was available only as a semi-log plot, one decade per inch, so that values scaled from it were not precise enough to regress. Replotting their curves on log-log paper (from their Figure 16) gave exponents that were, in some case, quite close to that in Equation (5.12-3). They were an odd assortment of metals and conditions:

Line 2 = 50% Co, 33% Cr, 13% W, 2.5% C shaft in nitrided steel sleeve, CO_2 ,

Line 6b = 53% Co, 31% Cr, 14% W, 1.0% C shaft in 50% Co, 33% Cr, 13% W, 2.5% C sleeve, CO_2 , at 200°C or above,

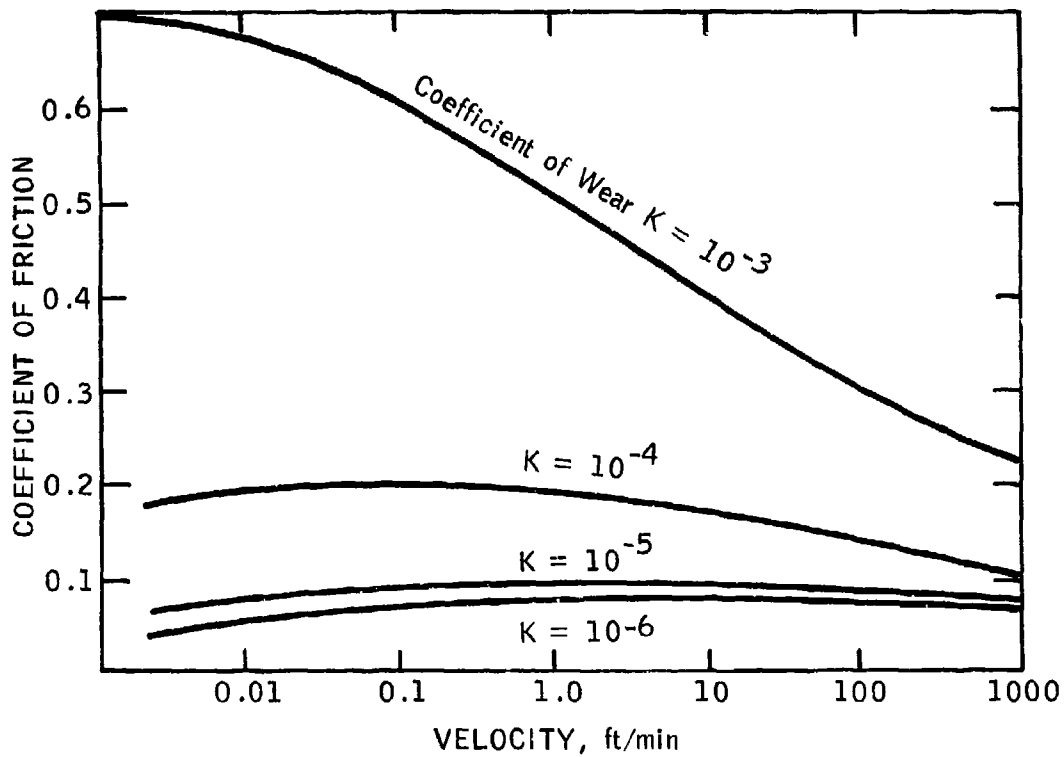
Line 6c = 50% Co, 33% Cr, 13% W, 2.5 C shaft in same alloy sleeve, CO_2 , at 375°C or above,

Line 8 = Nitrided steel shaft in nitrided steel sleeve, He atmosphere.

Several other combinations, not systematically different, gave exponents of 1.93, or $F^{3.85}$. (Lines 1 and 4.)

Cornelius (1961) also quoted some data from Rabinowicz (1958), which had been published without much explanation. The writer took the opportunity to ask Rabinowicz about this at the May, 1971 ASLE Meeting, and learned that the two upper lines on his chart (Figure 5.12-1) represent a different mode from the lower ones.

Figure 5.12-1
CORRELATION OF COEFFICIENT OF FRICTION WITH
WEAR AND VELOCITY



NOTE: According to Prof. Rabinowicz (personal interview, May, 1971) the two upper lines represent a different wear mode from the two lower lines. This information was omitted from the publication (1958) through an editorial error.

This was very gratifying, as the lower ones apparently conform well with Equation (5.12-3), while the others conform well with Cornelius' lines 1 and 4. Apparently the latter mode may relate to incipient scuffing.

It is now possible to return to Model II, and eliminate F as an input parameter. If we assume that

$$\gamma = (1 + 10.24F^2)^{0.5} \quad (5.12-4)$$

in place of Rowe's very similar Equation (5.4-4), solving (5.12-3) for this quantity results in

$$\gamma = (P_m V / 5 \times 10^{-14} W_d)^{0.103} \quad (5.12-5)$$

Substituting this into Equation (5.4-18), which is Rowe's Model IIA with the newer de Boer concept included, we obtain as a working equation

$$(V/d)^{0.897} = 2.19 \times 10^4 k'_m (W/P_m)^{0.897} (V_m)^{0.333} (T_s/U) \exp(-E/RT_s) \quad (5.12-6)$$

As mentioned in 5.4, this requires an iterative solution. The reason lies in the surface temperature (T_s) which must be obtained from Equation (5.4-6) by substituting a value of F computed from Equation (5.12-3). While no exact solution is possible, programming such problems on a modern computer is elementary. Even the substitution of a sophisticated equation for T_s , such as that derived by Francis (1971), would not cause any serious difficulty. The end results could well be given to the designers in the form of charts, such as Figures 5.1-1 through 5.1-4, or Figure 5.7-3 and 5.7-6.

6. COMPARISON AND COMBINATION OF THE MODELS WITH EACH OTHER

In Section 5, each model was considered more or less in its own area of proved performance. The results were not entirely re-assuring, as even the limited testing possible revealed failures to provide correct "predictions" of existing data. It appeared that it would be informative to investigate how the models compared with one another. From this study arose the possibility of combining them to represent mixed modes of wear.

6.1 Reduction to Standard Format

The models as set forth above are a rather heterogeneous collection of equations, which do not lend themselves to easy comparison. It would be very advantageous to put them all into a common form, related to Equation (5.1-4):

$$(V/d) = K d^m W^n U^p \quad (6.1-1)$$

This format also lends itself to analysis of data which does not fit exactly with any of the models. As seen in Section 5, this is all too common.

Starting with Model IA, by definition $(V/d) \approx 0$, and U is of no significance so that $p = 0$. Either m or n , or both, may be $-\infty$.

Model IB is already nearly in proper form. For fatigue,

$$(V/d) = K_f d^{m'} (W \gamma)^{n'} U^0 \quad (6.1-2)$$

For ball wear, $m' = -0.528$ and $n' = 2.12$. If we accept Equation (5.12-4) as the definition of γ , rather than (5.3-15) or (5.4-4), then

$$\gamma^{2.12} = (2 \times 10^{13} P_m V/Wd)^{2.12/9.68} = (2 \times 10^{13} P_m V/Wd)^{0.236} \quad (6.1-3)$$

and

$$(V/d) = K_f d^{m'} W^n U^p \quad (6.1-4)$$

where $K_f = [K_f' (2 \times 10^{13} P_m)^{0.236}]^{1/0.764}$, $m = (m' - 0.236)/0.764 = -1.000$ and $n =$

$(n' - 0.24)/0.764 = 2.64$. For platen wear, $m' = -0.60$ and $n' = 1.65$. Hence, $m = (m' - 0.171)/0.829 = -0.921$ and $n = (n' - 0.171)/0.829 = 1.79$.

In the high transfer mode, for all wear $m' = 0$ and $n' = 2.12$, and for platen wear $m' = 0$ and $n' = 1.65$. Hence, for ball wear $m = (0 - 0.236)/0.764 = -0.31$ and $n = 2.64$. For platen wear $m = (0 - 0.171)/0.829 = -0.206$ and $n = 1.79$.

Models IIA and IIIA require quite a different approach, as the exponential term must be converted to a power function. Expanding it into a series as Uhlig (1953) did for the logarithmic oxidation law yields a cumbersome polynomial as $\exp(-x)$ is slower to converge than $\ln(x)$.

It was simpler to compute the values of the real variable $W\exp(-E/RT)$ and correlate them with W^n . The results are shown in Figure 6.1-1. While the curve is continuous, it can easily be split into two nearly straight portions with the "knee" always at 331 gm load for the standard velocity. The loads were from 30 to 2000 gm, the latter being near the scuff load on the ball-on-cylinder machine, and the E steps from 3 to 15 kcal/mol. The constants for the 52100 steel used were $F = 0.21$, $P_m = 7.46 \times 10^7$ gm/cm², and thermal conductivity = 0.144 cal/°C sec cm, with a velocity of 55.8 cm/sec. Equation (5.4-6) was used for T_s .

The same technique was followed for the evaluation of p. The velocity steps covered were from 4 to 1920 cm/sec, the loads were 120 and 1000 gm, and the values 3 to 15 kcal/mol. The slopes were equal to $E/1400$ above the knees. The latter were located at 24 cm/sec for 120 gm and 46 cm/sec for 1000 gm loads, and are the criteria for the "high U" and "low U" columns in Table 6.1-1. This table presents m, n and p values for all the equations. The loads were put on a "% Scuff Load" basis by dividing by 2000, though that is a very crude approximation. The n and p ranges shown for corrosive wear correspond to minimum and maximum Q values; for adhesive wear, Rowe's value of 11.7 kcal/mol was used.

Model IIIA requires further attention due to the presence of h_c in Equation (5.5-1). This is the critical thickness of the cap of corrosion products on an asperity before it breaks off. As Tenwick (1971) pointed out, many factors may affect h_c , but for the present purposes all of these are to be held constant except load^c and T_s . The potential wear particle may be treated as a rigid body, since it is probably mostly Fe_3O_4 , held to the metal by a bond which is weak due to the volume disparity ϕ and the fact that only the London forces act across the interface. Hence, it will tend to pull off in bending moment - that is, by rotation about the trailing edge as a hinge - when the torque exerted by friction equals that of the bond tensile strength times its lever arm:

$$FWh_c = \pi r^3 \tau_y N \quad (6.1-5)$$

where τ_y is the tensile strength per unit area, which should depend only on the materials involved (and very slightly on T_s). This concept is illustrated in Figure 6.1-2, and the symbols are defined there. At this point, we have substituted two unknown quantities, r and N, for h_c , which appears to be a net loss. However, any one of them can be eliminated by the equation used by Archard in developing Equation (5.1-4). It is

$$\pi r^2 N = W/P_m \quad (6.1-6)$$

Figure 6.1-1
TRANSFORMATION OF EXPONENTIAL
INTO A POWER FUNCTION

$Q = 3000 \text{ cal/mol}$

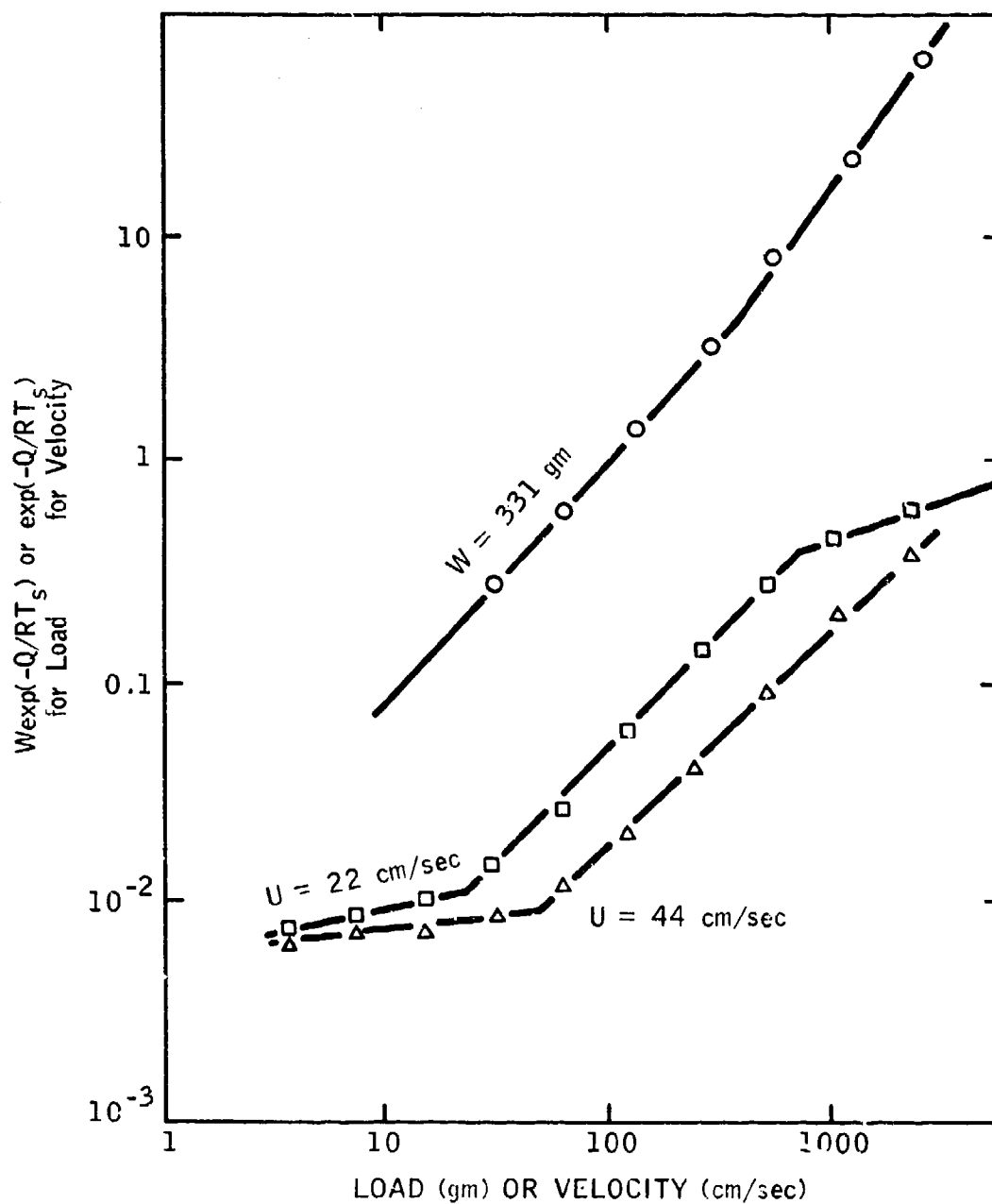
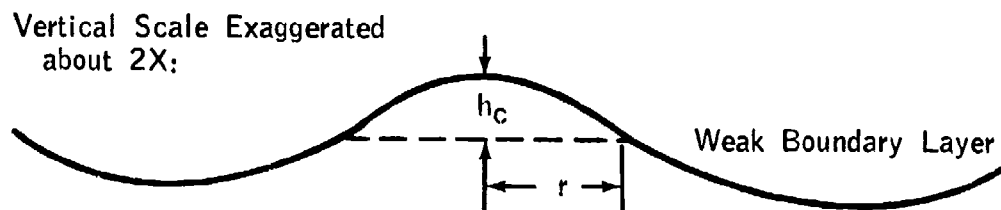


Figure 6.1-2
TORQUE BALANCE FOR REMOVAL OF
AN OXIDE CAP (CORROSIVE WEAR)



h_c = Critical height for Fe_3O_4 cap

r = Radius of cap

F = Coefficient of friction

W = Load τ_y = Tensile yield stress of boundary

For an average asperity

$$h_c F W = \pi r^3 \tau_y N$$

N = Number of asperities involved

The question is, which of the three is least apt to vary with load? All the evidence favors r , since wear particles tend to be fairly uniform in diameter. Hence, we can eliminate N , which certainly varies with W , leaving

$$h_c = \tau_y r / P_m F \quad (6.1-7)$$

Simplifying Equation (5.12-2),

$$F \propto (V/d)^{1/9} \quad (6.1-8)$$

so that

$$h_c \propto (V/d)^{-0.111} \quad (6.1-9)$$

and

$$(V/d)^{1.111} = KWA \exp(-Q/RT_s) / \phi^2 U P_m \quad (6.1-10)$$

Exponents calculated in this way are shown in Table 6.1-I as "Equation (5.5-1)".

Since Equation (5.5-7) expresses load only in terms of ξ , empirical exponents were used in Table 6.1-I for this one case.

The abrasive wear equations present no problems, being already in standard format.

6.2 Checking Models Against Each Other

Table 6.1-I provides an opportunity to review the general nature of what has been accomplished so far. It is clear that fatigue mode stands out quite clearly with high negative "m" exponents. Rather surprisingly, if the empirical Equation (5.5-3) is accepted as fitting Quinn's data (Figure 5.5-3) the possibility arises that his tests were dominated by fatigue rather than corrosion.

Of the three corrosive wear equations, it appears that (5.5-2) is the most rigorous, and also the most appropriate for lubricated systems where the temperature rise is more moderate than in the dry systems for which it was developed.

The two choices for adhesive wear turn out to be less different than appeared from their different formats, provided Equation (5.3-16) is not used outside Bayer's stated conditions. As will be seen, m values from the

TABLE 6.1-1

WEAR MODES EXPRESSED AS
EXONENTS IN $(V/d) = Kd^m W^n U^p$

Mode	Equation	Special Conditions	m for Wear on	n for Wear as under M	p for Wear at low U	p for Wear at high U
Corrosive	(5.5-1)	Surplus of corrodant and 1.5 to 16% of scuff load or 17 to 95% of scuff load	Either 0	1.54 to 2.39	-0.8/-0.45	0.1/3.92
			Either 0	1.80 to 3.60	-0.7/0.0	0.1/3.92
	(5.5-2)	Same as above but T_s below 200°C (low loads)	Either 0	1.23 to 2.16	-0.9/-0.5	0.1/4.35
	(5.5-3)	Empirical, T_s over 200°C Low loads High Loads	Either -0.50	1.73 to 2.66	-0.9/-0.5	0.1/4.35
			Either -0.50	2.00 to 4.00	-0.8/0.0	0.1/4.35
	(5.5-7)	Starved for corrodant	Ball 0.33 Flat 0.92	0.39 to 0.59*	0	0
Fatigue	(5.3-13)	Limited to low loads and velocities	Ball -1.00 Flat -0.60	2.64 1.79	0	-
					0	-
Adhesive	(5.3-13)	Limited to low loads and velocities	Ball -0.31 Flat -0.21	2.64 1.79	0	-
					0	-
Abrasive	(5.4-13)	1.5 to 16% of scuff load 17 to 95% of scuff load	Either 0	1.93	-0.60	3.20
			Either 0	3.49	0	3.20
	(5.9-3)	Suspended in lubricant or imbedded in softer part Soft, fine particles	Either -0.33 to 0 Either 0	1.00 1.00	0 1.00	0 1.00

*Reported as high as 0.88 - See Figure 6.3-1.

laboratories are not so precise as to distinguish between 0 and -0.26 ± 0.05 very often, and $n = 1.93$ for Equation (5.4-3) neatly splits the difference between ball and disc wear which Rowe did not include in Model IIA. Thus, either may be used with roughly similar results, but (5.4-3) is so much less hemmed in with restrictions on load, velocity and humidity that it seems more attractive. The principal difference between the Russian Equation (5.9-3) and Equation (5.9-7) is that the latter recognizes a velocity effect not present with coarse abrasives.

These exponents should not only be useful in data analysis, but also can serve in the wear laboratory as a quick check by the experimenter as to how his test is progressing. Merely plotting three log-log charts would tell him at a glance which mode his machine is running in - or perhaps that he is in a mixed mode as exemplified by Equation (5.10-1) for fretting corrosion.

6.3 Comparison with Literature Data

An interesting set of data by Schatzberg (1970A) was the first indication that this exponent method of analysis might be useful. It was shown to be compatible with the Appeldoorn (1967A) data by the author, but had the virtue of including conditions not covered by the latter. As the writer pointed out (1971A), much of Schatzberg's data appears to be a form of surface fatigue, as its onset appears to be related to the Palmgren function $W^3 d_0 = \text{constant}$. Exponents, similar enough to be explained by the difference in geometry, appeared in Schatzberg's 4-ball data. However, it was the most corrosive condition (wet oxygen) which gave wear rates fitted by $m = 0$, while the least corrosive (dry argon) was fitted by $m = -0.67$. The latter also fitted dry oxygen in 3 out of 4 cases, while wet argon was fitted in 3 out of 4 cases by $m = -0.36$. Bayer had very rarely found cases between $m = 0$ and $m = -0.5$ in both dry and lubricated tests running in air at 10% relative humidity, so the wet argon data seemed to represent a third mode not previously recognized, as shown in Table 6.3-I.

In the present context, we find Archard's equation for adhesive wear, Bayer's for high-transfer, Equations (5.1-1) and (5.5-2) for dry rubbing and Schatzberg's wet oxygen data all in excellent agreement. Can all these be classed as "corrosive wear"? It appears that this would be difficult, and that two different phenomena coincidentally result in $m = 0$. It is interesting to note that Quinn (1968-9) also reported substantial transfer in the first few minutes of his externally heated experiments, so that we might eventually decide that all of the dry-rubbing experiments proceeded by the alternative "wear first, oxidize later" mechanism.

The rest of the situation is even less clear, as shown in Figure 6.3-1. According to Quinn's third interpretation (1971A) of his data, $m = -0.558$, with deviations as low as -0.323 and as high as -0.934 . If, in fact, his specimens were experiencing Bayer's "low-transfer" wear, as implied by the fact that both average $m = -0.50 \pm 0.05$, he should have found a "zero-wear" period at the start of the run, as did Schatzberg for most of his cases. Zero-wear is defined by Bayer as "wear less than half the peak-to-peak surface finish

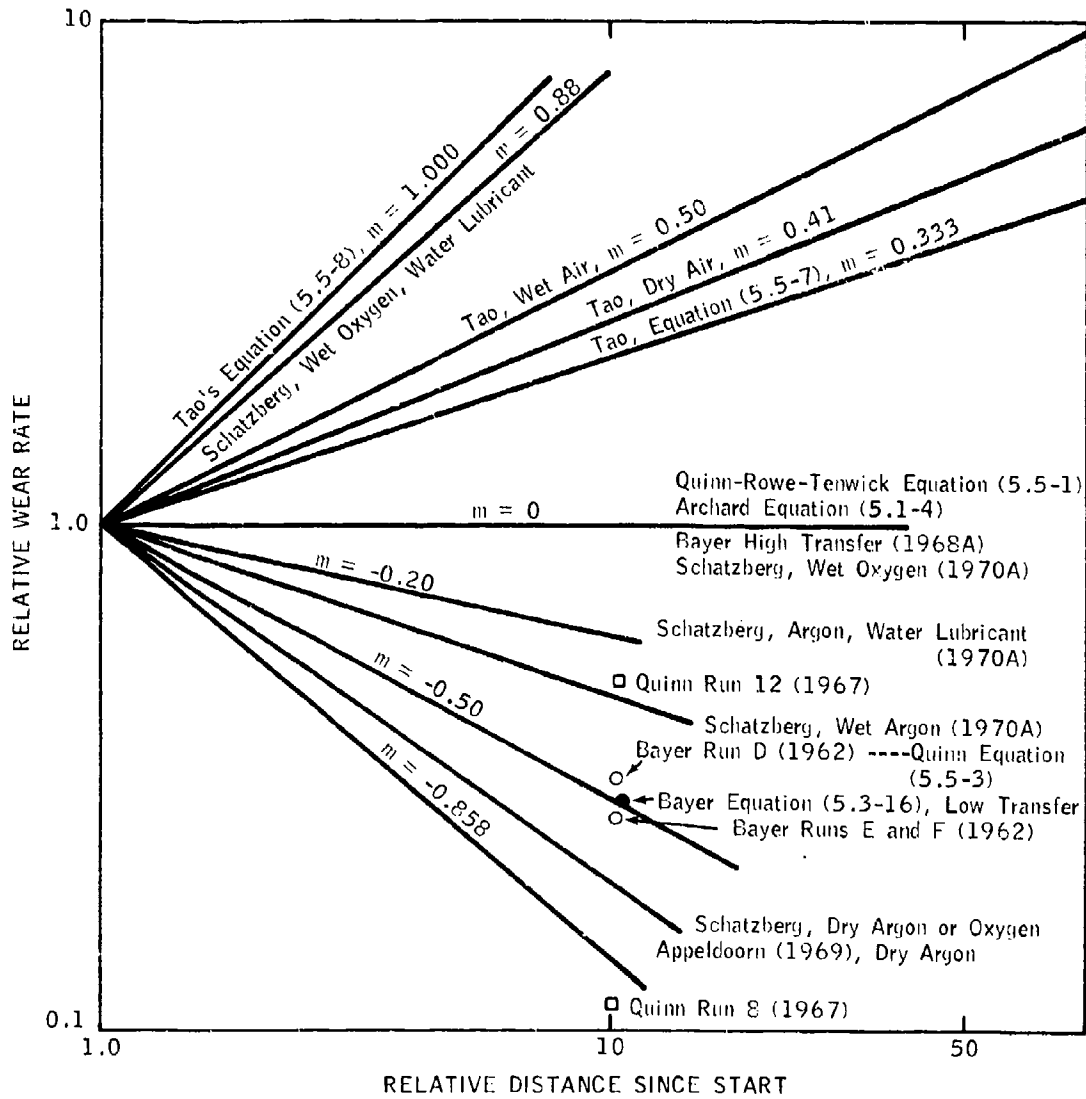
TABLE 6.3-I
VARIATION OF WEAR RATE WITH LOAD
IN VARIOUS ATMOSPHERES

Lubricant	Ratio ($\Delta \log(V/d)/\Delta \log W$) = n				
	Level	Oxidizing		Argon	
		Wet	Dry	Wet	Dry
MIL-H-6083C	O ₂	1.98	--(a)	1.2(b)	1.01
MIL-H-5606B	O ₂	1.45	2.1(a)	0.8(b)	1.24
MIL-L-17672B	O ₂	0.5(b)	2.1(a)	1.16	1.0(b)
Emulsifiable Hydraulic Fluid	O ₂	1.33	1.2(b)	1.6(b)	1.20
Synthetic Isoparaffin White Oil	Air	2.4(b)	1.58	0.12	0.15
JP-5	Air	1.4(b)	2.07	1.77	1.12
RAF-176-64	Air	1.24	2.0(a)	--(b)	--(b)
PW-523	Air	0.9(a)	1.06	0.60	--(b)
JP-4	Air	--(a)	--(a)	--(b)	--(b)

(a) Not enough data for reliable value.

(b) Erratic data.

Figure 6.3-1
VARIATION OF WEAR RATE WITH TRAVEL IN
VARIOUS ATMOSPHERES



of the coarser member." Quinn probably could not have detected a zero-wear period because his measurements were only taken in steps of 10^6 cm travel.

The lowest value of m reported is -0.858 , by Appeldoorn, Goldman and Tao (1969), for dry argon. No zero-wear period was reported; it would be predicted to be less than the 1 minute at which the first measurement was taken, for the 1000 gm load they used (at least for the dry air case discussed further below. Bayer's zero-wear predictions may not be applicable in argon despite the good finite wear results in nitrogen shown in Figure 5.3-3.)

Tao's work is quite unusual in predicting and detecting a case of $m > 0$. This may well be due to the combination of oxygen starvation, in which the wear particles absorb all the oxygen dissolved in the oil between entry and exit, with spherical geometry. The starvation would not appear for Schatzberg with his pure oxygen nor Bayer with his relatively light loading. The spherical geometry causes a rapid increase in total oxygen intake with wear, as this is proportional to wear scar diameter (i.e., to $V^{0.25}$). This leads to his relationship of scar diameter cubed to time, and thus to $m = 0.33$. Quinn used a wedge-shaped pin, and no lubricant, so that Equation (4.4-7) does not apply to his work. Adjusting it to his geometry would lead to $m = 0$ and a version of Equation (5.5-2) containing C_0 as a variable, which might be more generally useful than Equation (5.5-7).

Another case of $m > 1$ was reported by Appeldoorn, Goldman and Tao (1969) and Schatzberg (1970A). This was obtained with water as the lubricant and oxygen as the atmosphere. Again the spherical geometry and oxygen starvation serve to explain the result of $m = 0.88$ (Figure 6.3-1). Although this case might appear to approach the ultimate in corrosiveness, it is oxygen starved because gases are much less soluble in water than in oils.

Neither Quinn's later work (1971B) nor Tenwick and Earle's (1971) were reported in sufficient detail for analysis by this method.

Time dependence of wear has been reported by a number of people on the 4-ball machine. A particularly large study by Appeldoorn, Campion and Tao (1966) resulted in many cases of $m = 0$, using cetane in room air (45-65% RH). All showed an appreciable period of $(V/d) = 0$, but this can hardly be equated with Bayer's zero-wear period since it tends to increase with load and is much longer than his equations would predict for loads of 10 to 50 kg. The only condition deviating from $m = 0$ was 50 kg at 1200 rpm; here $m = -0.32$. It is not legitimate to make a direct comparison as both oil and machine geometry were different, and there is reason to believe that all loads above about 10 kg involved some degree of scuffing wear. (See 7.11.9, Delay of Transition.)

Thus, study of the values of m does not lead to an unambiguous mathematical criterion for distinguishing corrosive wear from the other modes. It seems probable that a better case could be made for using Bayer's zero-wear period (d_0) if there were more data on this model under corrosive conditions. Schatzberg shows that d_0 falls off from its usual level for dry argon or oxygen by a factor of about 3 with wet argon, and as much as ten-fold with wet oxygen. Vaessen and deGee (1971) showed a similar effect of humidity on the

zero-wear life of noble metal contacts. Our study of some data by Appeldoorn (1967A) on the wear of 52100 steel with 13 pure hydrocarbons in air at 35 to 65% relative humidity shows that, while Bayer's model for 100% RH predicted zero-wear for 28 out of 72 tests, actually none were observed (Table 5.3-VI). Thus, d_0 has interesting possibilities.

The study of "n" gives some further insight as to the meaning of the various data. In Equation (5.5-7), n depends on the elastohydrodynamic solution of the relation of h_0 to W. Tao (1969) shows a good relationship of wear to the EHD "compliance"; for humid air, $n = 0.39$ and for dry air $n = 0.59$. Study of the data on 13 pure hydrocarbons (Appeldoorn 1967A) mentioned above yielded n values from 0.44 to 1.18. This excludes n-nonane and n-butyl benzene, which both showed abnormally high wear rates and $n = 2.05$. The variation in n of the 11 best values showed a vague tendency to correlate with density, which is known to have a large effect on oxygen solubility, but obtaining a reasonable correlation coefficient would have meant discarding all but 6 or 7 of the original 13 values.

An analysis was also made of wear data on five commercial liquids: JP-4, JP-5, a UK jet fuel, a U.S. jet fuel, and a synthetic isoparaffinic white oil (Appeldoorn 1967A). None of these liquids contained any surface-active additive. The n-values were quite erratic and did not correlate with the atmospheres, which varied in corrosive tendency from dry argon to wet air. In six cases, the scatter was too bad to arrive at an n value, and in four others n is of dubious value because of scanty or erratic data. These results are shown in Table 5.3-I, along with the breakdown of Schatzberg's (1970A) data for four oils in four atmospheres. Again, some points had to be rated "dubious", four for scanty data and five for erratic data, leaving only 7/16. In one case, there is evidence of the "bifurcated" behavior described by Ling (1962), in which replicate results fall into two distinct groups of high and low wear. This case, Emulsifiable Hydraulic Fluid in dry argon, was counted as valid in Table 6.3-I because there was enough low-wear data to use for an n value. Again, the results show no clear-cut trend with corrosive tendency, though it is notable that in every case worth reporting, wet air or oxygen gives a higher n value than dry argon. The dry air and wet argon data are difficult to explain.

An analysis of variance was made on the wear rates of the five commercial liquids, using only the 240 and 480 gm loads as the 1000 gm load caused scuffing in some cases. The most important of the primary variables were humidity and oxygen content, both of which were significant at the 99% confidence level or greater. Load was significant at the 95% level. The interaction of oxygen with humidity was also significant at the 99% level, and that of load with oxygen at the 95% level. (The significance of liquid tended to be suppressed by the narrow range tested.)

The effects of the primary variables, plus the two interactions shown to be significant, accounted for 64% of the variance. The remaining 36% can be attributed to the sum of minor interactions, experimental errors, unsuspected variables and perhaps to the existence of a bimodal situation.

The above analysis demonstrates the value of the m-n-p "finger-print" system as a diagnostic tool. It also demonstrates rather clearly that many exponents are outside any theoretically predicted range (Table 6.3-I). It is evident that wear in the "pure" modes discussed above is the exception, and that further explanations must be sought. To do so by creating more models appears unwise, since the five already considered work well under the extreme conditions for which only one mode is possible. It would be far preferable to "blend" them on a nonlinear basis. This involves setting up a compound equation of the type

$$(V/d) = (V_f + V_a + V_c + V_{fa} + V_{fc} + V_{ac} + V_{fac})/d + (V_d/d) \quad (6.3-1)$$

where the subscripts f, a, c and d refer to fatigue, adhesion, corrosion and abrasion, respectively. This not only recognizes the prevalence of mixed modes, but permits compensation for their interactions.

In the above equation, abrasion has a unique role. Since all of the mathematical models for primary wear (V_f , V_a , V_c) assume clean parts and lubricant, there will be no abrasion until wear particles have accumulated. Thus, V_d becomes a function of V , of uncertain form but probably a step-function. In order to account for the low n exponents in some of the actual tests, it appears that V_d must become so large as to overshadow all the other terms in these cases.

When V_d does not dominate the equation, it is possible to make some predictions about the interaction terms. For instance, it is known that corrosion greatly accelerates fatigue (for example, by hydrogen embrittlement of iron) so that V_{fc} will tend to be large and positive. On the other hand, Bayer has shown that adhesion and fatigue rarely, if ever, coexist - presumably because adhesive wear destroys the microcracks from which fatigue propagates. Hence, V_{fa} (the wear due to the interaction of fatigue with adhesion) will always be 0. Since adhesion and corrosion are dimensionally similar, it may be hoped that V_{ac} and V_{fac} will prove to be negligible. If so, only V_{fc} needs to be evaluated.

Two other models which are needed to complete the picture are under development. One is a correction for the portion of W carried by the partial hydrodynamic film in the antiasperities (see 5.7). This must be further corrected for any build-up of surface resin, soaps and other organic solids in the antiasperities (see 5.5.4 to 5.5.7).

It appears that adequate models are available for the primary causes of wear. Work should now be concentrated on the secondary or correction models of abrasion, hydrodynamic load-sharing and surface resin with considerable confidence that these six models will contain all the necessary building blocks for a complete system of wear prediction and antiwear design. In fact, it is not too soon to start systematic collection of some of the necessary values for use by design engineers. The key values will include the fatigue parameters already collected, but at several levels of humidity and temperature. They

will also include the activation energies and energies of adsorption as collected by the corrosion and adhesion workers. There is every reason to believe that such values taken under static conditions are useless, due to lack of the dislocations, deformations and electron emission of real bearing surfaces. Hence, compilation of the energy tables should be based on dynamic test results only.

6.4 Perspective on the Modes of Wear

At this point, it is possible to take a broader view of the modes and regimes of wear than was possible in Figure 2-1 or in any individual model. Such perspective is attempted in Figure 6.4-1, in which dimensionless variables are plotted rather than the simple ones used before. The ordinate, specific wear rate, is merely the K from Equation (5.1-4). This contains the hardness, normally constant for a given system, and also the load. A plot of Figure 2-1 on K - W coordinates would be no different from the V/d - W plot, but a chart of K vs $(W - X)$ would consist of two horizontal lines with vertical lines at Y and Z . The major difference in Figure 6.4-1 is in the use of h_0 . Since this is proportional to $W^{-0.13}$, the abscissa scale is inverted from that in Figure 2-1.

The specific film thickness ties Figure 6.4-1 completely to Model V, which seems clearly established as the necessary starting point for all serious study. It consists of the hydrodynamic film thickness as derived by Dowson and Higginson (1966) divided by the effective roughness of the two surfaces (Tallian 1964, Valori 1965). Thus, it includes load, viscosity, velocity and roughness as parameters as shown in Equation (5.7-4) but with $W_2 = W$.

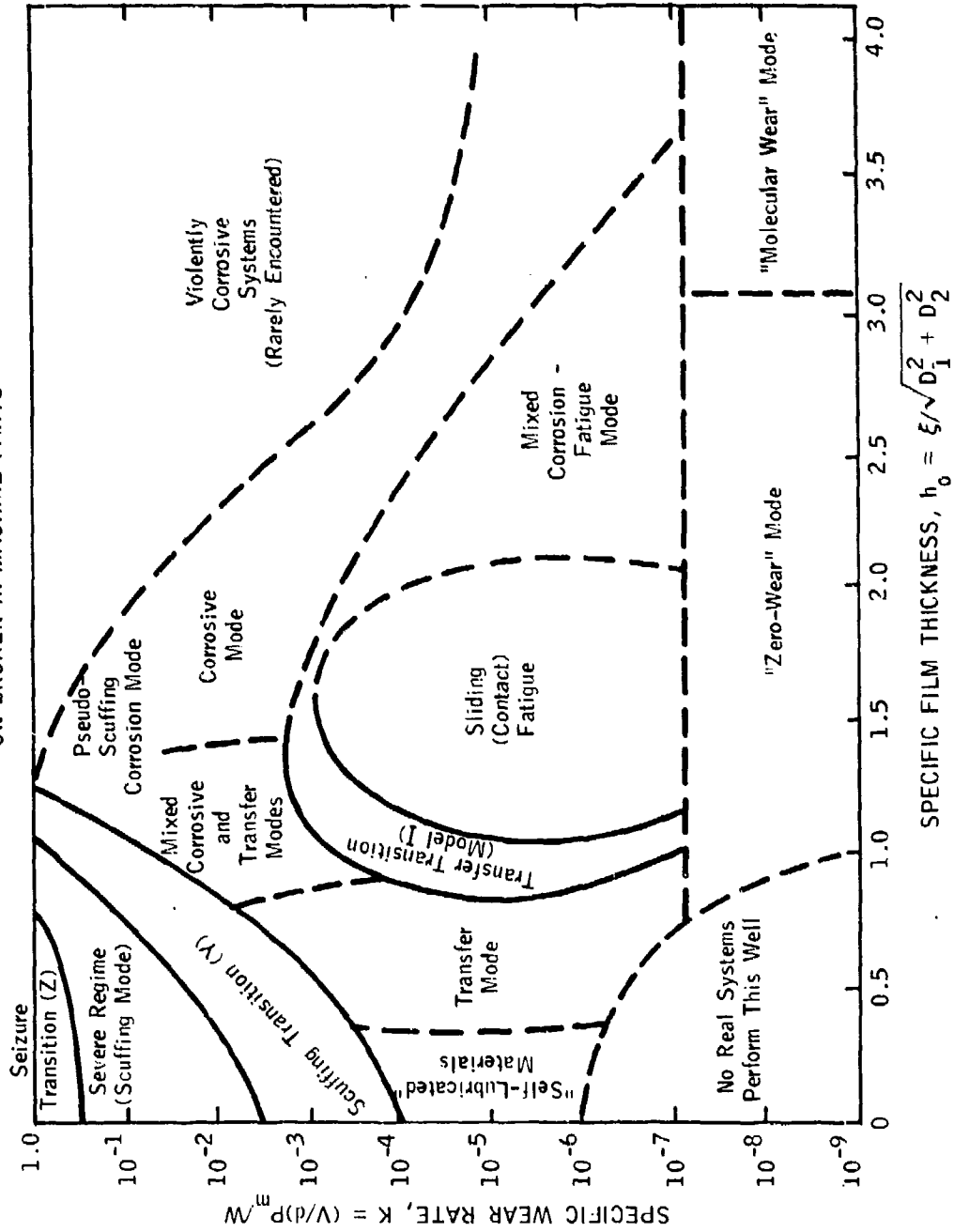
The plot represents the situation for a given system at any given time, but cannot include time as a third dimension. Perhaps some future worker can provide a series of plots at various times, as done in Figures 5.4-1 through 5.4-4, to show the important stages. At least, Models I, II, IIIA and IV are clearly shown, along with the three transition zones. It must be borne in mind that these are "forbidden zones" within which a machine cannot continue to operate; it must "jump" across, usually in the direction of higher specific wear rate. In comparison to the solid lines bounding the transition zones, the dashed lines are both arbitrary and ill-defined. In particular, the line between "zero-wear" and "molecular wear" should not be taken too seriously.

Figure 6.4-1 resembles in some ways the basic pattern used by K. L. Johnson (1970A) on which to build a grid of lines on which only one parameter is allowed to vary at a time. Such lines might, in the future, be added to Figure 6.4-1, to show what effect changing load, velocity and viscosity would have on the specific wear rate. Other lines might be drawn to represent changing "lubricity" and roughness, and one might even hope to indicate such time-dependent processes as break-in, fatigue and abrasion by such a grid. The following examples may help to clarify the many uses of Figure 6.4-1:

6.4.1 Increasing load will generate a curve leading to the left from a starting point in "ZERO or MOLECULAR WEAR" up to SEIZURE. If the metallurgy prevents seizure, the upper end will be in "SELF-LUBRICATED".

6.4.2 Decreasing viscosity produces another curve, with the same starting and end points but of a different shape.

Figure 6.4-1
REGIMES AND MODES OF WEAR
(EXCLUDING ABRASION)
ON BROKEN-IN MACHINE PARTS



6.4.3 Decreasing velocity will be more complex, starting nearly horizontal and curving up to SEIZURE or "SELF-LUBRICATED".

6.4.4 Decreasing work of adhesion would start off vertically, curving over to the usual end point.

6.4.5 Break-in might have started anywhere below the scuffing transition, shifting to the right and downward as if load were being decreased.

6.4.6 Abrasion would start in ADHESIVE, CORROSIVE, FATIGUE or MIXED, and tend to move upward and slightly to the right, perhaps leveling off at $K = 10^{-2}$ but never entering SEVERE (scuffing) or SEIZURE.

6.4.7 Fatigue would rise vertically from "ZERO-WEAR" to the higher part of SLIDING FATIGUE.

6.4.8 EP Lubrication would start in ADHESIVE moving upward and to the right into the MIXED and CORROSIVE modes. The shift to the right depends on counting the EP film as part of δ ; if it were not, the shift would be slightly to the left because the asperities would grow a little.

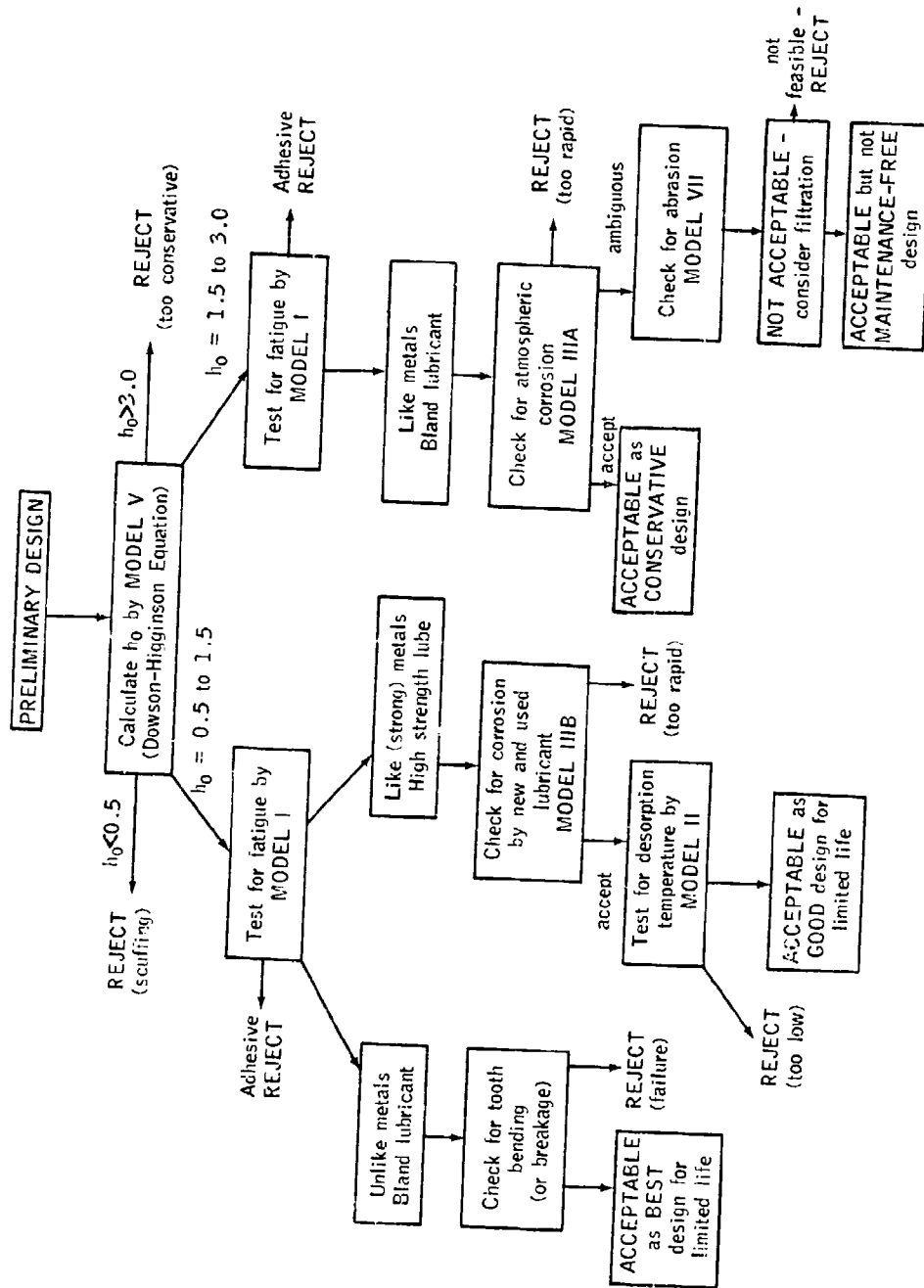
6.5 Combining the Models for Design Purposes

The tricks used in Section 6.2 to reduce the models to standard format for screening purposes may have their uses in design, but a great deal more will be required. An illustrative plan was worked out, under the guidance of Dr. L.S. Akin of General Electric, as shown in Figure 6.5-1. It begins with the assumption that the problem has been clearly stated; in this case, that a set of gears are required to work at a certain load and speed, within a few constraints on atmosphere and temperature. Akin (1971) has since released a much more complete version.

The first step required is to assume some design parameters. These will be based on the engineer's experience, personal or departmental, with similar problems. Some constraints may also be supplied by the customer, especially in military work. These may include use of one of a few specification lubricants, metals, etc., and frequently entail volume or weight limitations.

This first approximation gear set is then subjected to step-wise analysis. First, Model V is applied to determine the specific film thickness (h_0) at the most critical point where the tooth tip (addendum) contacts the root (dedendum). This may be done by means of the Dowson-Higginson equation (5.7-4), as shown in Table 6.5-1. The result sets the designer onto one of three pathways, indicated by the regimes on Figure 6.4-1. Of course, if $h_0 < 0.5$ there is no pathway as this leads to immediate seizure of like-metal gears. Thus, the three pathways would be $h_0 = 0.5$ to 1.5, $h_0 = 1.5$ to 3.0 and $h_0 \geq 3.0$. The last of these would be so conservative as to represent wasteful practice, especially in military work.

Figure 6.5-1
ILLUSTRATIVE DESIGN SCHEME FOR MILITARY
POWER GEARING



Pursuing the $h_0 = 0.5$ to 1.5 pathway, it is evident from Figure 6.4-1 that one may be in either the adhesive or fatigue mode. This is shown by Model I to depend on both metallurgy and lubricant. The designer will have to choose between unlike metals and high film strength lubricant (i.e., stearic acid additive in Table 5.3-1) at the second fork in Figure 6.5-1. If he chooses the metallurgical (Model IV) route, he will have to face the fact that metals sufficiently unlike to prevent adhesion tend to include one of lower strength than the other; thus, he will be limited by tooth bending or breakage and must reconsider whether his design is adequate for the shock loadings, etc., to be expected in military service, where extraordinary abuse must be anticipated. If acceptable, this design is nearly optimum for equipment of limited lifetime.

If he chooses the high film strength additive route in Figure 6.5-1, he must be prepared to accept the fact that such lubricants are more corrosive, and being less stable, also tend to increase their corrosivity more rapidly, than the bland lubricant of the left-hand branch. However, the greatest problem may be desorption temperature leading to scuffing in hot climates, etc. If this test is passed, then a good limited-life design is available.

When h_0 is 1.5 to 3.0, the designer is basically conservative. He must still test for adhesive wear by Model I, but will probably pass it. For such a set-up, only bland lubricant and like metals need to be considered. The conservative nature of the first choice indicates that a fairly long lifetime is contemplated, so the possibilities of corrosive and corrosion-fatigue wear (which were ignored on the first branch) must be taken into account. If the Model IIIA test is passed, a conservative design results.

It may prove that corrosion or corrosion-fatigue will be rapid enough to cause concern. A test is then made as to whether this will lead to an abrasive failure in which the primary wear particles start a cascade of secondary, tertiary, etc., particles. If this is not the case, then the design is still acceptable on a conservative basis.

If there is substantial danger of a cascade, then filtration may be considered. However, this violates the goal of this STAF in that such a system is NOT maintenance-free, and so would be acceptable only as a last resort. Use of anti-abrasive additives might provide a way out of this difficulty - but probably with some sacrifice of lubricant stability.

The scheme outlined above assumes that a number of gaps in the models will be filled; it is illustrative only, and definitely NOT ready for use by designers.

7. REVIEW AND EXPLANATION OF THE ANOMALIES

At last, with the models as well sorted out as is possible at this time, we can look again and see what, if anything, has been left unexplained by this new arrangement of old and new information. Perhaps some of the following discussion belabors the obvious, in light of what has already been said in discussion of the models, but it seems best to consolidate everything into focus.

7.1 The Base Case

It has long been believed that the vital link in lubrication with fatty oils was the free acid, which is either present or quite promptly produced by hydrolysis. This is quite in accordance with Model IIC, and perhaps that is all that is needed. The water film needed for hydrolysis is available, as shown in Figure 5.5-1, as long as the humidity is high enough according to Table 5.3-V. Even in the absence of such a film, the fat will usually carry enough dissolved water to give adequate acidity. This is vital, as esters do not adsorb strongly enough to provide much film strength.

No doubt the process described above accounts for the protective film that forms on a new part. Events may even progress beyond this, to the formation of a soap film, in accordance with Model IIIB, during break-in or even sooner. Thus, the anti-asperities are partly filled with soap. Finally, Model IIIC may add to this layer of soap an increment of surface resin. Though this is hardly needed to complete the break-in process, the double bonds of fatty oils make it very probable.

A mineral oil will not carry out this process with the same efficiency. For many years it was believed that "natural surfactants" were involved in Model IIC adsorption. Groszek (1967-8), Rudston (1971) and the writer (1971A) have all thrown this into disrepute. Only Model IIA, a relatively low energy process, is helpful, and the "natural surfactants" range from neutral to harmful. Model IIIB soap formation is possible only with very poorly refined (or partly oxidized) oils. Model IIIC resin tends to be soluble, and carbide formation may cause it to do as much harm as good. Thus, Model IIID is probably the main process that permits break-in and subsequent low-wear operation possible.

Steel and bronze are both capable of Model IIIC catalytic activity, but are easily poisoned by oxygen as shown in Figure 5.5-8. Their ability to perform in Model IIID may not be correlated with surface free energy, but steel is well known to emit exo-electrons.

This pair has very favorable anti-scoring characteristics. Iron and copper have a Model IVA (5%) miscibility temperature of only 17°K, as shown in Table 5.6-1, while iron and tin go to 304°K. The latter would be the more appropriate since the low γ of tin will cause it to predominate at the surface. However, this is just barely above room temperature (88°F), and Model IVA is much too naive to predict this system. Model IVB and Figure 5.6-1 do better, but the true situation involves both Fe_3C and Sn_6Cu_5 , for which parameters are not available. It can only be said that some further work on Model IV using both the blending equation (5.5-14) and more data on intermetallic compounds would be required to "predict" what everyone has known for 4,000 years--but if it predicted just one more pair as widely useful as steel on bronze, the work would be well spent.

7.2 Anomalies Involving Lead

The low V of lead places it so low on Figures 5.5-7 and 8 that it may be considered "non-catalytic", though Model IIIC implies that "negligible activity" would be more appropriate. The same factor should result in a very low E value in Model II. Thus, its exceptional performance is not predicted by the chemical models. Even when it forms a soap in Model IIIE, the low melting point and high solubility in oil preclude much aid to the load-sharing of Model V. Only Model IV sheds some light on this anomaly, since lead is the most immiscible of all metals. Figure 5.6-1 shows ten pairs with two phases; iron with 8 pairs is in second place. While Tables 5.6-I and II are not complete enough to tell the story, this is also predictable by Model IVA. Apparently the usefulness of lead in bearings depends largely on its ability to remain as a separate phase and exude when it is needed, to serve as a lubricant. The low γ value causes it to spread on most metals. This is an interesting case of the sort of phenomenon investigated by Bondi (1953).

Another peculiarity of lead is that it does not work - harden, being one of the few metals which anneal at or below room temperature. This is reflected in Model VIB, where abrasion is prevented by embedding the wear particles so deeply they become harmless.

The effect of lead-based additives is less clear-cut, as noted in 4.2. This question cannot be resolved by any of the models, as we do not have E values for these additives to put into Model IIC, nor enough data on the physical properties of lead sulfide, halides etc. to be sure that they would flow into the anti-asperities and provide EHD lift for Model V. However, this seems to be one of the best modes of action. Another closely related possibility is that the additives serve as homogeneous catalysts for the oxidation steps in Model IIIC and D. At any rate, investigation of the lead anomalies deserves high priority.

The effect of lead-based additives is less clear-cut, as noted in 4.2. This question cannot be resolved by any of the models, as we do not have E values for these additives to put into Model IIC, nor enough data on the physical properties of lead sulfide, halides etc. to be sure that they would flow into the anti-asperities and provide EHD lift for Model V. However, this seems to be one of the best modes of action. Another closely related possibility is that the additives serve as homogeneous catalysts for the oxidation steps in Model IIIC and D. At any rate, investigation of the lead anomalies deserves high priority.

7.3 Anomalies Involving Calcium

Calcium has been used so widely that it is surprising so little is known about its mode of action. One thing that is striking is that the lattice spacing of many calcium compounds is close to that of iron. This is not enough in itself to provide high E values for Model IIC, but the solid film people (Devine 1968) have shown it to be a strong factor in selection of appropriate heavy metal chalcogenides, such as MoS_2 , WTe_2 etc. to fit specific metal lattices. It is probable that the exceptionally large volume of the calcium atom fits it uniquely for some roles in additives. While this cannot be extended to other elements, there is a great deal that can be done to increase the number of applications of this very cheap, high film-strength additive.

The derivation of Equation (5.11-7) involves the Girifalco and Good correction for volume disparity of molecules which are in random orientation, so that the interacting area of each may be represented by $V_m^{2/3}$. This is certainly not true for asymmetric, oriented molecules such as calcium dialkylaryl sulfonate, calcium caprylate-acetate etc. Smith (1969A,B) has done valuable work on the orientation of molecules on mercury. This work should be repeated with gallium, since mercury is so irregular in its surface free energy and crystal form (See Appendix III). With such data available, Model IIC may prove to be adequate for this anomaly.

7.4 Other Elements

Of the elements listed in Section 3.4, only iodine warrants detailed discussion. As noted, this element appears to be unique. Most of the models to which so much time has been devoted are concerned with wear, and friction is a secondary consideration. If we can trust Equation (5.12-3) (which is an open question) iodine must also produce an extremely low wear rate. In fact, the F values in Figure 4-1 are out of the boundary range entirely; in no case did MacGregor (1964) report any value to compare with Furey's (1966).

Comparison with Figure 5.7-6 raises a suspicion that what we are seeing is an extreme case of shifting of Stribeck minimum to the left. Though the F values do not go as low as the 0.0005 shown by Christensen, it must be recognized that Furey's conditions would not necessarily produce the same F value at the Stribeck minimum. The question is, how can iodine produce such a situation? The only guide available is Model VI, and the only mechanism is reduction of the surface roughness. This cannot be attributed to selective corrosion of the asperities down to a "chemically polished" surface. Among the many pieces of evidence for this statement is the fact that iodine also works on glass/glass systems. It appears that some sort of polymer formation is going on, but it clearly obeys a different set of rules from those of Models IIC and D.

A recent paper by Brown (1968) of General Electric shows that an iodine-silicone complex is an effective low friction lubricant. This adds another piece to the puzzle. It appears that complex formation is a frequent part of the iodine anomaly. This calls to mind the fact that something very like hydrogen bonding takes place with halogens. There is also the fact, recently emphasized by Bagley (1971), that under pressure hydrogen bonded species such as alcohols appear to increase their degree of aggregation from the usual oligomers to quite high molecular weights under pressure. The iodine effect tends to increase with load, at least over a range, which reinforces this ad hoc theory.

It is therefore the writer's speculation that iodine works by the formation under pressure of a temporary polymer with substantial elasticity. According to Okrent's reasoning (1964), such a material would have quite substantial ability to support a load without increasing the friction over that of the unthickened oil. The effects would all disappear when the lubricant leaves the pressure zone.

This hypothesis can readily be tested by conducting a few tests at high pressure, with both low and high shear rates. Suitable equipment has been described by a number of laboratories.

7.5 Optima in Blended Lubricants

It should be obvious from the detailed discussion in Section 5.5.4 and 5.5.5 that the various blend anomalies are due to surface resin formation. Three detailed discussions are given, on specific phenomena.

7.5.1 The DuPont Patents

While this might have been discussed in Section 5.3.4, it seems more appropriate here as many of the liquids and all of the catalysts discussed in it are blends. The duPont bulletin (1971) is rather cautious about the mechanism, and concentrates on the many performance tests in which these alloys have shown up well. The name "LP alloys" is tied to lubricant producing on page 1, and to Laves Phase on page 8, so apparently the writer of the bulletin was less sure of the former concept than some of the inventors discussed below. Laves Phase refers to hard intermetallic compounds which separate from several types of alloys (Nevitt 1963). The prototypes are $MgZn_2$ (hexagonal), $MgCu_2$ (cubic) and $MgNi_2$ (hexagonal), but the current preferences are Co_2Mo_2Si and $CoMoSi$. These are quite hard ($P_m = 1000$ to 1500), indicating quite high surface free energy. Whether this is directly applicable in Equation (5.5-12) is open to question, but the DuPont data tends to support that idea.

Unlike solid solutions, two (or more) phase alloys are not subject to the Gibbs equilibrium, and any Laves phase present at the surface will remain there. The seven patents fall into three groups:

U.S. Patent 3257178 covers metal articles coated with Laves phase alloys, and offers only metallurgical theory. The phases are named for Dr. Fritz Laves, no reference given, and consist of compounds of one large and two small atoms, so arranged as to permit the most complete occupation of space. The ratio of radii may be 1.05 to 1.68.

U.S. Patent 3331700 is a division of the first, and adds some micrographs and details of coating procedure.

U.S. Patent 3361560 was filed later, but is very similar. These three do not mention lubrication, but cite the alloys as resistant to wear, abrasion, oxidation and corrosion.

U.S. Patent 3180012 covers shaped articles made from these alloys, including turbine blades, tools and dies.

U.S. Patent 3410732 is similar, and suggests use as seal faces and impact mills for breaking up chemical sludges.

U.S. Patent 3507775 is described as a "lubricant producing system", and is largely devoted to the subject of polymerizing light hydrocarbons to lubricant viscosity. Gasoline vapor and liquid are both cited as suitable starting materials, along with various "environmental media". This includes the chemical sludges mentioned above, and liquids such as are shown in Table 7-I.

U.S. Patent 3513084 goes on in the same vein, adding little of theoretical interest.

Table 7-I is of much interest, especially as most of the liquids are not in the classes considered polymerizable in Sections 5.5.4 and 5. The tests were run by rotating a ring of $\text{Co}_5\text{Mo}_2\text{Si}_2$ against one of 0.9 wt.% carbon steel at 180 ft/min. under the liquid. While the picture is muddled by the apparently pointless variation in load (PV), it is evident that some sort of optimum was approached, in coefficient of friction at least, by the blends. The relative wear coefficient, on the other hand, seems to negate Equation (5.12-3), and optimizes at octanol; only at the extremes are the two coefficients in agreement. No simple explanation will serve; perhaps interaction of maximum work of adhesion for one coefficient and ease of polymerization for the other would serve. The special properties of hexagonal metals may also be involved, since these would be shared by hexagonal intermetallic compounds. In any case, this anomaly has enough potential to deserve further study.

TABLE 7-1
FRICTION AND WEAR OF LAVES PHASE
ALLOY WITH VARIOUS LIQUID LUBES

<u>Example No.</u>	<u>Environmental Liquid</u>	<u>Coefficient of Friction</u>	<u>PV x1000</u>	<u>Total Wear (mils/100 hrs.)</u>	<u>Relative Wear Coefficient</u>
7,15	Gasoline	0.10	1200	<0.05*	<0.004*
24	Methanol	0.14	>100	0.3	<0.3
25	Ethanol	0.11	>400	1.1	<0.28
26	n-Butanol	0.12	>300	0.5	<0.17
27	n-Octanol	0.10	>500	<0.05*	<0.01*
28	Butyraldehyde	0.13	>100	1.0	<1.0
29	10 wt % Ethanol 90 Trichloroethylene	0.05	50	0.2	0.4
30	10 wt % n-Butanol 90 Trichloroethylene	0.02	50	1.4	2.8
Control	Trichloroethylene	0.3	27	44.	163.

* Reported as "0", re-interpreted on apparent precision of authors' means of measurement.

7.5.2 The Silicone Anomaly

In effect, Tabor (1965) has already taken care of this matter. Apparently silicone is so prone to polymerization that even copper can catalyze it. The resulting film tends to be brittle--too fragile to be much help in lubrication and probably even abrasive. In his second paper (1969), Tabor showed that stearic acid added to the silicone appeared to copolymerize with it, to form an excellent lubricant film. Assuming this is the mode of action for ester-silicone blends makes this a clear-cut case of Model IIIC.

7.5.3 Aromatic-Aliphatic Blends

The following is a condensation of a paper by Goldblatt and the writer (1971), which explains these blends primarily in terms of Model IIID:

"Recently a paper was published which demonstrated that the whole oil is a poorer lubricant than either its aromatic or paraffinic fraction. In this work Groszek (1967-8) showed that the portions eluted with pentane (the paraffins and naphthenes) and isopropanol (the aromatics and polars) from silica gel are superior lubricants to the original sample. On the other hand, Appeldoorn and Tao (1968B), working with pure polynuclear aromatics such as α -methylnaphthalene, demonstrated that paraffinic-aromatic mixtures behave synergistically. The purpose of this note is to suggest an explanation for the apparently contradictory results - i.e., that Groszek observed an antagonism and Appeldoorn and Tao observed a synergism.

"Based upon some other work (Goldblatt 1970), which demonstrates that the addition of certain additives (e.g., TCP) to mixed aromatic-paraffin stocks causes increased wear, it was decided to investigate this prowear effect observed by Groszek.

"A 1000 coastal distillate was separated into various fractions, one containing the saturates (paraffins and naphthenes), three containing different amounts of 1 ring, 2 and 3 ring, and 4 and 5 ring aromatics and one containing the non-hydrocarbon "polar" fraction. This latter cut probably includes much of the nitrogen, oxygen, and some of the sulfur compounds. This corresponds to Groszek's last fraction rather than his "surface active material". The aromatic cuts were analyzed mass spectrometrically and the details of this analysis appear in Table 7-II. As can be seen, all the cuts contain substantial amounts of aromatics ranging from one to five rings per molecule. The details of the alkyl and naphthenyl substitutions on these aromatic structures are omitted from Table 7-II for clarity.

"In Table 7-III are listed wear data for the 1000 coastal distillate oil and its fractions. As can be seen, the aromatic fractions tend to give lower wear. This improvement tends to become poorer as the percentage of polynuclears decrease. The poorest results are those obtained with the saturates cut. This trend of decreasing wear with increasing aromaticity is similar to the data presented by Groszek in Figures 19.3 and 19.4 appearing in his paper. However, he observes a maximum in wear which was not observed here, probably because we lumped all saturates together. His final fraction, in each case, shows a slight increase in wear similar to that found here for the nonhydrocarbon cut.

TABLE 7-II
MASS SPECTRAL ANALYSIS OF 1000 COASTAL DISTILLATE OIL

	<u>1st Aromatic Cut</u>	<u>2nd Aromatic Cut</u>	<u>3rd Aromatic Cut</u>
% Benzenes	50.7	49.9	39.5
% 2,3 ring	33.5	35.3	38.3
% 4,5 ring	7.2	8.3	13.0
% sulfur compounds (2,3,4,5 ring)	7.6	6.5	8.2
% sulfur	0.3	0.46	0.64

TABLE 7-III

WEAR DATA FOR COMPONENTS OF 1000 COASTAL DISTILLATE(a)

<u>Fraction</u>		<u>Wear Scar Diameter (mm)</u>
Saturates		0.43
1st Aromatic Cut		0.37
2nd Aromatic Cut		0.30
3rd Aromatic Cut		0.25
Nonhydrocarbon		0.33
63% Saturates	} Blend A	0.40
37% Mixed Aromatics(b)		
62% Saturates	} Blend B	0.47
36% Mixed Aromatics(b)		
2% Nonhydrocarbon		

(a) 4-Ball machine, 15 kg, 1200 rpm, 125°F, Dry Air, 15 min. These test conditions are not comparable to the 1 hr, 20°C test conditions in Ref. 1. The WSD are therefore expected to be different although the relative values are correct.

(b) Blended in their naturally occurring proportions. Contains about 50% single ring aromatics.

"The most important point is that our Blend A (Table 7-III) shows some improvement over the saturates alone due to replacing the aromatic cuts. On the other hand, reconstituting the original oil by adding the 2% of polar nonhydrocarbons (Blend B) gave a wear rate greater than that of any component, confirming Groszek's observations. Thus, addition of natural polar compounds to the mixed aromatic-saturates blend had the same effect as that observed for TCP. The differences observed between Appeldoorn and Tao on the one hand and Groszek on the other may very well be related to this prowear effect of compounds in mixed base stocks. Appeldoorn and Tao were working with pure aromatics. Addition of these to the paraffin produced only the beneficial behavior they reported. The oils with which Groszek was working contained large quantities of polar impurities, and, hence, he observed prowear on the total mixture.

"Two significant conclusions may be drawn from this work:

- (a) polar impurities within naturally occurring petroleum fractions very frequently have a detrimental effect upon the lubricating ability of the pure hydrocarbon fractions,
- (b) heavily alkylated polynuclear aromatics are less efficient anti-wear additives than a monoalkylated aromatic. This latter conclusion may be drawn from the fact that the additive effects reported by Appeldoorn and Tao are substantially greater than those observed in this work. While these conclusions appear to be completely validated for 52100 steel on the 4-Ball machine in air, it must be recognized that they have not been confirmed for any other concentrations, metals, machines and atmospheres than those shown in Table 7-III."

7.6 Competition of Additives For Surfaces

It is evident from the previous section that no simple model can begin to explain the intricacies of additive action. In highly idealized situations, such as those of Studt (1968), reversible chemistry (Model IIC) provides such easy answers as to constitute no anomaly at all, whereas most of the real field problems are related to Model IIIC and D. Admittedly, there are loose ends, but the writer feels confident that a modest investment of laboratory and mathematical work will fit these under the general heading of Model III.

7.7 Roles of Humidity And Oxygen

The reader is referred to Section 5.5.5 and 5.5.6 for a good deal of the explanation on the paradoxical effects of water vapor and oxygen. However, there is more to be said about water than about any other chemical species--a not uncommon situation, since ordinary water contains quite enough anomalies to satisfy most people! Table 7-IV shows the various forms of involvement that have been noted so far in this report. It is evident that not only is it impractical to eliminate water, but that the results would not all be beneficial. Instead, the goal should be to understand the ten or more interactions in Table 7-IV and to find means to counteract the harmful ones.

TABLE 7-1V

VARIOUS ROLES OF WATER IN LUBRICATION MODELS

<u>Model</u>	<u>Wear Mode</u>	<u>RH*</u>	<u>Role of Water, Vapor or Liquid</u>
I	Sliding Fatigue and High Transfer	<	Decreases zero-wear life and increases finite wear rate, probably by embrittlement.
		>	Increases zero-wear life and decreases finite wear, due to liquid film.
II	Adhesive or Locked Dislocation	Any	Displaces base stock, increases wear. Displaces or couples additives to oxide.
IIIA	Corrosion by O ₂	Any	"Catalytic" transfer aid, increases wear.
IIIB	Soap Formation	Any	"Catalytic" reaction aid, decreases wear.
IIIC	Dehydrogenation	Any	Poisons catalytic action of some metals.
IIID	Electron Transfer	Any	Destroys anionic radicals, increases wear.
IIIE	Soap Formation	Any	Reaction aid, decreases wear.
IV	Corrosion	Any	Increases scuff load (increases wear by IIIA).
VI	Rolling Fatigue	Any	Decreases life by embrittlement.
VII	Abrasion	>	Prevents adhesion to two-body situation, reduces wear.

* Relative Humidity < subcritical or > supercritical.
 "Any" humidity does not include 0 to 1 ppm H₂O by weight;
 effects above and below critical are not yet identified.

The situation on oxygen is similar, but not quite so complicated. As indicated in Figure 5.3-3, Rowe's data from a nitrogen atmosphere fits Model IB for dry air. On the other hand, some mechanism (perhaps Model IIID) is sensitive to a part per million or less of oxygen, as Bieber (1968) reported a drastic loss of lubricating ability at that level.

There is a great deal of work needed to make sure that all these conflicting mechanisms are clarified, but perhaps less than 100% understanding will serve as a basis for combatting the worst ones.

7.8 The Sharp Transition To Scuffing Wear

The transition at Y has received a great deal of attention, both because of its technical importance as a limiting condition in gear design (Section 4.1.2), but also its fascination as a scientific puzzle. Model IV, as already mentioned, shares the same fascination and represents a special aspect of the same problem. However, the principal concern in this Section is with identical metal parts.

Model I does not recognize loads approaching the scuffing level, but most of the others touch on this problem one way or another. Model II includes Equation (5.4-23), which purports to set up a critical condition for catastrophic desorption. Cameron and his students (Grew 1969) have taken this so literally as to list "desorption temperatures" for various additives; though there is some question as whether the term is applicable, the phenomenon is certainly clear-cut. It depends on the metallurgy, the base-stock and quite possibly on the running conditions. Most striking is the dependence on matching the molar volumes of additive and base oil (Askwith 1966). The writer (1971c) has demonstrated that a very similar case in emulsion technology can be explained on the basis of minimizing the entropy of mixing of additive and base oil, but this development still lacks rigor.

Models IIIA and B do not contain any equation specifically related to scuffing, but atmospheric corrosion is widely recognized as a factor. Roberts (1969) goes into considerable detail on this phenomenon as part of his paper on "Lubrication (Without Oils)". Additive corrosion used to be considered the whole basis of EP scuff prevention.

Models IIIC, D and E explicitly describe, in Equation (5.5-20), how the protective films of soap or resin can be expected to fail. Actually this equation is apt to give a slow "transition" when resin is tested under static conditions, it is the "snowball effect" in which a little loss of resin causes T_s to rise, which causes further loss of resin and so on. This is probably the most plausible of all explanations of the "seizure delay" noted by Pike (1970), if we assume that test parts come covered with a thin film of resin. Despite the "cleaning" given to such test parts, they are hopelessly contaminated by aerospace standards (Buckley 1966).

Model V carries, in Figures 5.7-7 and 8, a very convincing demonstration of the way an EHD film can go into instability. It seems quite unlikely that this model would work with additives present, but it might be related to the Blok (1937) postulate of a constant scoring value of T_s for any given viscosity of non-additive oils. The writer discussed Blok's paper (1970) at some length, considering all the various sources of instability known at that time, and concluded that the one factor that was constant was the viscosity of the oil at the asperity tip temperature, by Equation (5.4-6).

The derivation is much too long to quote here, but the outcome was that gears will not fail on non-additive oils of 100°F boiling range when the viscosity at T_g is over 1.87 ± 0.06 cps, and will probably fail below 1.18 ± 0.06 cps (Table 7-V). Between these values their failure is probabilistic. Similar results can be extracted from a paper by Fein (1967), with the pass-fail limits on the 4-ball machine at 2.7 times these values. This was attributed to differences in geometry. Blok protested, quite rightly, that it was the viscosity at T_b that controlled loss through the anti-asperities and held that it was bubble formation due to vaporization at T_g (Griebe 1970) that caused the breakdown. Tallian (1971) agrees that the viscosity at T_g is not the relevant factor.

Reconsideration of Table 7-V has led the writer to conclude that Blok is probably correct, especially since he unpublished data that show lubricants made by blending kerosene with heavy oil scuff at a lower temperature than straight-cut oils of the same viscosity. Since vapor pressure is often most appropriately handled as $\log(P_v)$, the total pressure column was converted to $\log(P_v + P_a)$. This function showed a definite relationship to scoring temperature: at T_L , it was 2.627 ± 0.057 , and at T_u it was 2.656 ± 0.049 . While the difference is significant only at a low confidence level, it does indicate that experiments in which $\log(P_v + P_a)$ was measured rather than estimated would be highly desirable. Further clarification of Model VC by Christensen will be awaited with the greatest interest.

Models VI and VII have nothing to offer on this matter, though it is well known that three-body abrasion (probably both kinds together) can prevent scuffing--at the price of high wear rates.

In short, we suffer from an embarrassment of too many explanations, and at present none of them can be definitely eliminated. Moreover, it seems that there will be several survivors, as Model IV cannot be eliminated and there appear to be at least two more mechanisms (additive and non additive) at work. However, hope is in sight to cut out the dead wood in the next year or two.

7.9 Effect of Anti-Wear Additives on Fatigue

Since Model VI was specifically brought in to deal with fatigue, and has been discussed in Section 5.8, there is little more to be said about Equation (5.8-1). However, that section was fairly specific to rolling fatigue, and the anomaly is not necessarily limited to that specific case. In addition, it seems probable (as indicated in Table 7-IV) that humidity plays more of a role than its own high surface free energy would predict by Equation 5.8-1.

The writer has not located any mathematical model for hydrogen embrittlement, nor for the specific symptoms of fatigue due to such embrittlement. There is a regular flood of articles under the headings "corrosion fatigue", "stress corrosion", "hydrogen embrittlement", etc. which rarely come to the attention of the lubrication engineer. The writer has been unable to even read all of these articles published during the contract period, let alone make a critical survey of them. A few that were found to be of special interest are listed in the bibliography (Hoar 1962, 1964, Scully 1963, Vitovec 1964, Burg 1967, France 1970, Naesar 1970). From the volume of publications it is clear that there are many unsolved problems, and many workers engaged in solving them. It would seem that all this activity might solve the problems of the lubrication engineers without effort on their part, but the writer believes better solutions will be reached sooner if the matter is not left entirely to the structural and corrosion engineers. In addition, some problems (especially in the U.S. Navy) seem to be so urgent that action is already

TABLE 7-V
Estimated Properties of Blok's Oils

At Standard Temperatures									
Oil No.	Viscosity (cstk)		Density at 60°F	Air Solubility at 77°F and 760 torr (% by volume)					
	50°C	100°F		210°F					
1	7.2	14.1	0.843	12					
2	14.5	33.3	0.857	11					
4	31.0	82.8	0.872	9					
5	82.0	249.7	0.884	8					
7	145.0	509.0	0.889	8					

At Minimum Scoring Temperature (T _L)										
Temperature °C	Viscosity (Centipoises)	Vapor Pressure (torr)	Air Solubility (Vol %)	Air Solubility at 760 torr Change from 77°F	Pressure of Air Plus Vapor (torr)		Surface Free Energy (ergs/cm ²)			
					485	470	409	374	393	24.2
122	250	1.77	19	7						
150	302	1.84	18	7						
165	365	1.82	17	8						
220	428	1.99	17	9						
290	482	1.92	17	9						

At Maximum Scoring Temperatures (T _H)										
Temperature °C	Viscosity (Centipoises)	Vapor Pressure (torr)	Air Solubility (Vol %)	Air Solubility at 760 torr Change from 77°F	Pressure of Air Plus Vapor (torr)		Surface Free Energy (ergs/cm ²)			
					485	470	409	374	393	24.2
150	302	1.24	20	8						
190	374	1.16	21	10						
230	446	1.15	19	10						
280	536	1.17	18	10						
305	588	1.17	18	10						

under way. A very recent paper by Schatzberg (1970B) provides some empirical answers for combatting fatigue induced by water; a new model which takes these into account is badly needed.

In trying to fit models to fatigue wear, we must not lose sight of the fact that two or more modes are possible. The situation depicted in Figure 5.3-2 is characterized by Tallian as "traction", in which the frictional force FW/N is applying tension at the crack. Rolling fatigue tends to pull cracks on both sides of the Hertz spot, and the model may be different--even in terms of what effect γ_{12} might have, unlikely though that seems.

A much more likely cause for "failure" of Equation (5.8-1) would be changes in γ_1 . Should this be replaced by σ_1 , the surface stress, which includes γ_1 plus dislocation and work-hardening energies? Equation (5.9-7) tends to show that for abrasion, things are not that simple, and that both γ_1 ($=300P_o^{1/3}$) and σ_1 (presumably $=300P_m^{1/3}$) would be needed.

In addition, there is the very important consideration that the chemical species at the surface after a long series of non-wear encounters, as shown in Figure 5.3-1, or wear encounters as shown in Figure 5.4-4, may no longer be metal at all - but carbide. This would be especially likely at low humidity due to the radical-quenching effect of H_2O . Kragelskii (1965) notes that many metals form "white layers" at the broken-in surface. In the case of iron, this can generally be identified as cementite (Fe_3C), more familiar as "white cast iron". Recently another iron carbide ($Fe_{20}C_9$) has been identified; for years it was known only by its characteristic X-ray lines. It is important to note that carbides are "ceramics", and hence fall on the lower line in Rabinowicz' (1965B) chart reproduced in Figure 7-1. Hence, they are far more prone to cracking; even though harder than metals, they are lower in γ_1 . Hence, carbide formation can result in greatly reduced fatigue life.

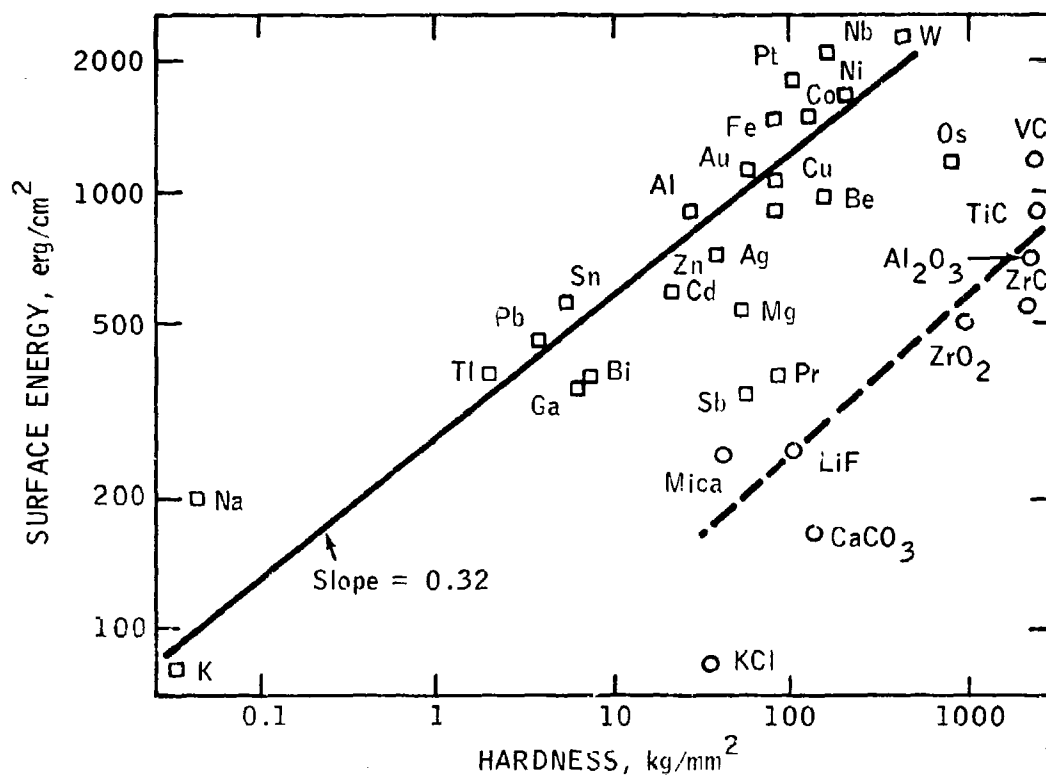
Finally, there is the by-product of carbide formation by Reaction (4.4-18), which is hydrogen. This would be a relatively small amount compared to that produced from water. However, it is well known that hydrogen embrittles only hard steels--that is, those with a high cementite content, from which we might deduce that the combination $Fe_3C + H_2$ gives a compound or complex which is exceptionally brittle. However, Vitovec (1964) has shown that result is subsurface bubbles of CH_4 , which cannot diffuse away and so builds up pressure.

In short, there is a great deal to be done to determine the parameters, but combining Models IIIC and VI appears to explain why there can be conflicting reports on the effect of additives on fatigue.

7.10 The Break-in Anomalies

Setting aside the asperity-cutting effects of break-in, important though they are, as being easily explained, we are left with quite a wide variety of phenomena that take place in the first few minutes or hours of operation. The results are so well known, and have been so well described by Crook (1958-9) that a very brief listing will serve. The gear, bearing or other device that has been properly broken in will carry at least twice the load that would have caused scuffing in its original condition. The wear rate will also be low as 1/25 of that originally found at the same load, and the friction is generally lower by as much as 50%, more or less in line with Equation (5.12-3).

Figure 7-1
CORRELATION OF SURFACE FREE ENERGY
WITH HARDNESS



Plot of surface energy at the melting point against hardness at room temperature, for some metals and non-metals.

Perhaps the greatest anomaly of break-in is that most test machines are run on new parts, suddenly brought to full load with no chance to build up whatever protective layers are responsible for the excellent performance of the machines they are supposed to stimulate. Some engineers justify this on the basis that the test without break-in provides a "safety factor". Actually, a factor which varies widely with the chemistry and physics of the system can hardly be justified; a true safety factor is a known allowance for uncertainties in the design equations, the materials of construction, and the overloads the average user imposes.

A second rationalization for this bad practice might be that extreme pressure lubrication was first widely applied in metal cutting. This is the one area in which virgin metal is encountered at every pass (except for the tool surface, which may or may not be subject to break-in). Hence, many of the test machines that are used to test gear and bearing lubricants were developed for the metal working oil formulators and purchasers, and have been thrust into other services with little or no thought. Fein (1967) has shown a good deal of what can be done simply by making adjustments to the test procedure on certain test machines. Most engineers, however, seem to blame the machine geometry, and are very loath to even consider the fact that they are trying to telescope years of service into a 10 or even 2 minute run, when they say that some machine does not correlate with field. Of all the test devices in common use, only the Ryder gear machine (ASTM Method D 1947) even approaches a realistic break-in period.

There is little choice in models for break-in among those listed. Models IIIC and D are the only ones which offer a reaction period that is comparable with the observed results. To these may be added the soap formation of Model IIIE in some circumstances. No doubt other effects, such as work-hardening, are important, but that is outside the scope of this report. Model IV might be considered in the special aspect of the diffusion of alloys by Equation (5.5-14), where the heat and dislocation speed up the diffusion of a low surface free energy component to where it can do the most good. It is also possible that the Feng version of Model II (Figure 54-5) will, when complete, be of some use in this connection.

7.11 Miscellaneous Anomalies

To preserve the pattern of Section 4, this group of anomalies are all relegated to subheadings, though some of them receive extended treatment while others are barely mentioned.

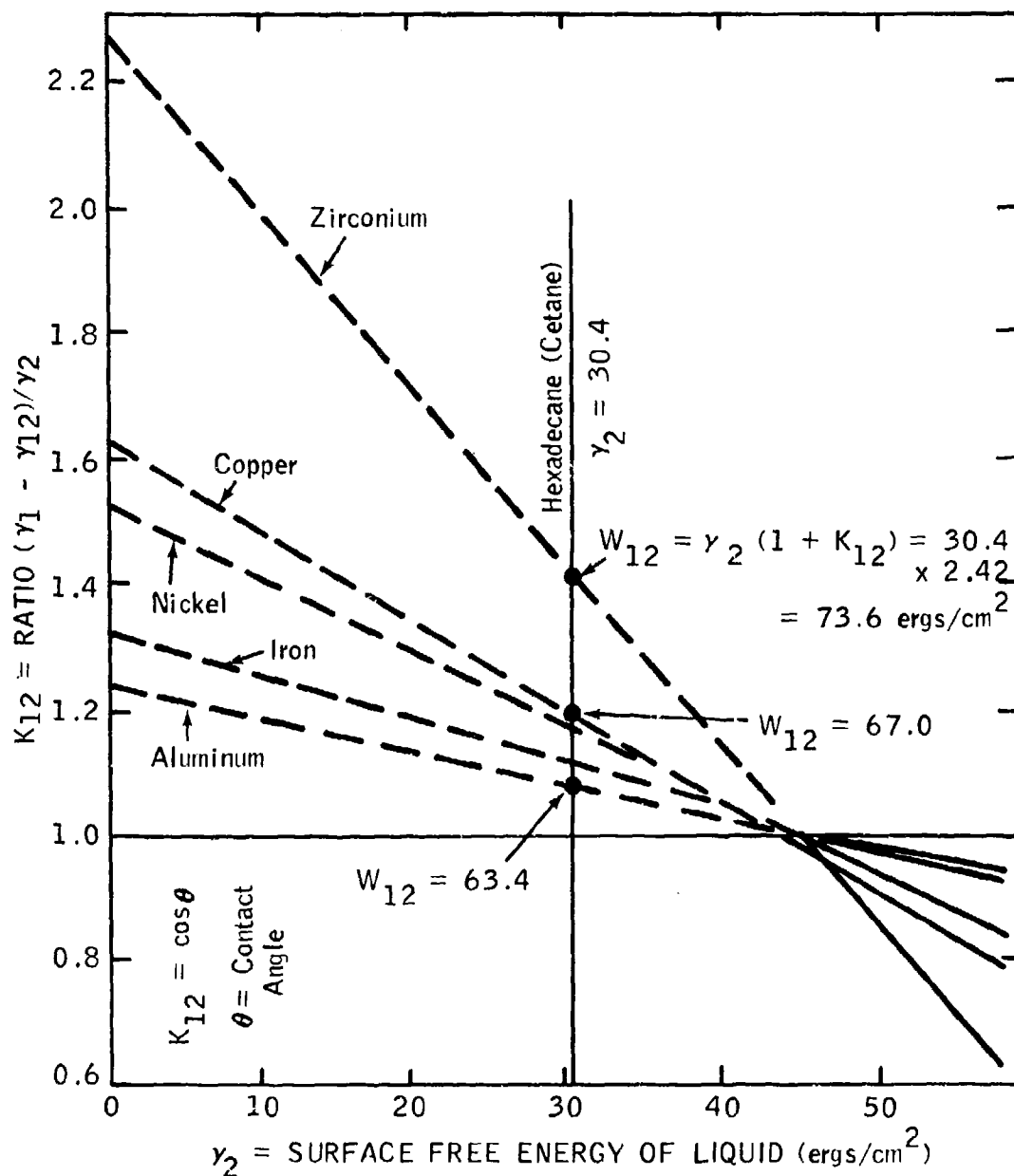
7.11.1 Anomalously Low Friction in Transmissions

Since this anomaly was put on the list, Li (1970) has investigated the matter further, with somewhat less startling results. F-values were found to decrease (without steps) in response to both time and temperature. Though isothermal conditions were not rigorously maintained in any test, and in some tests temperature was allowed to rise with time, the writer feels that Li's experiments show definite evidence of Model IIIC and V break-in, as outlined in 5.7.5. The "glaze" must have been rather high in oxygen content (and δ_H) since it resisted the solvent action of paraffinic oil, even at 500°F.

7.11.2 Anomalous Wetting Energy

This is illustrated in Figure 7-2, plotted from data by Bennett and Zisman (1968). Unfortunately, they did not use enough liquids to permit plotting a Hansen diagram, which might well have shown how the three partial parameters act on a metal which is buried under the variety of layers shown in Figure 5.5-1. (In this case, one or another of the iron oxides may be absent as the authors polished their specimens under water).

Figure 7-2
ZISMAN-GANS PLOT OF WETTING POWER
OF ORGANIC LIQUIDS ON METALS
(AT RELATIVE HUMIDITY - 0.6%)



The arithmetic on Figure 7-2 is based on the conclusion which was originally published in Germany by Philippoff (1960) and more recently by Gans (1970) independently in the U.S., that the work of adhesion A_{12} for liquids with γ_2 below the "critical surface tension" γ_c cannot equal the often quoted but incorrect " $2\gamma_2$ ". The A_{12} values shown are of dubious value, due to the hydrated oxide etc. layers, but agree well with Harkins (1950) and Clayfield (1957A). (See Appendix V.)

Another model to be tested here is the Zadumkin-Karashaev Equation (5.11-6). Since the energy involved comes from ordinary electrostatic forces, and the intervening layers are essentially all dielectric material, this should apply over substantial distances. Suitable contact potentials for the metals are listed by Bewig and Zisman (1964). As this seemed borderline to the present study, the necessary rather complicated calculations have not been carried out. However, the discussion below (7.11-4) on stearic acid multilayers gives some idea of the possibilities.

7.11.3 Group B Metals

Group B Metals have been analysed under Model IV, and found not to have any special properties not accounted for by their solubility parameters and molar volumes. (See 5.5). Conversion of these to surface free energies is discussed in Appendix IV.

7.11.4 Multilayers of Stearic Acid

A recent paper by Allen et al (1969A) tried to show that multilayers of stearic acid were of great value in boundary lubrication. The writer's comments are quoted below:

"The authors make an excellent case for the existence of ordered multilayers of stearic acid, and a plausible one for their importance in boundary lubrication. However, there is much evidence that such layers have no practical value when forces greater than a few dynes/cm are involved.

"On the positive side is a very recent paper by Takenaka (1971) in which multilayers built up by repeated application from a water surface showed a firm monoclinic crystallite system with a spacing of 23.8 Å and an inclination of 27 to 35°.

"On the negative side, Vold (1952) observed 20 years ago that even Blodgett layers on dilute HCl have about 22% of voids until compressed. Ries and Kimball (1958) showed that the void fraction varies across the film, from circular islands of 3000 to 50,000 Å that are 100% covered to large areas with nearly 100% voids. Spink (1967) showed that about 70% of the monolayer was readily removed by evaporation from mica or silver surfaces. Block and Simms (1967) showed 55% of the monolayer to be readily desorbed, and 61% readily exchanged, from steel surfaces. Timmons et al (1968) confirmed this, in more detail, as 60% by thermal desorption, 50% by solvent desorption and 60% by exchange from iron. Anderson et al (1969) applied this work to aluminum, platinum, copper and gold surfaces, with similar results.

"The point made by these six papers is that not even ONE layer of stearic acid is bound to metal tightly enough to resist 60% removal by even the mildest forces. The reason for this is evident from analysis of the cohesive energies of the various joints in the multilayer. Stearic acid rarely encounters bare metal; the ordinary contact is with a hydrous oxide surface such as $\text{FeO}(\text{OH})$. While initially the encounter must result in chemisorption, aging will harden this into covalent bonding such as $\text{FeO}(\text{OCOC}_{17}\text{H}_{35})$. Probably the 40% coverage is of this nature, and the other 60% is hydrogen bonded (H-bond), with Keesom (permanent dipole) and London "dispersion" energies also contributing. The second layer of acid can only contact the first through the hydrocarbon tails, and thus the bond has only the London energy. The third layer is again hydrogen bonded, and so forth. The resulting structure results

Joint	Cohesive Energy (kcal/mole)				
	Covalent	Hydrogen	Keesom	London	Total
1	0.40×100	0.60×5	0.60×1	0.60×1	44.2
2	0	0	0	1.00×1	1.0
3	0	1.00×5	1.00×1	1.00×1	7.0

In addition to the weak second joint, there is every reason to expect a further weakening due to liquid invasion of the structure. As pointed out by Levine and Zisman (1957) there is a recognizable difference between the Blodgett layers picked off a water surface and layers laid down by adsorption from nonvolatile solvents. Beerbower and Hill (1971C) show that this is predictable from the enthalpy and entropy relations. The exact amount of liquid depends on the H-bond, Keesom, and London cohesive energies of surfactant (i.e., stearic acid) and liquid, and the ratio of their molar volumes. While this work was primarily directed to interface layers in emulsions, it can equally well be used to explain the peaks noted by Askwith et al (1966). Thus, the multilayer will contain between 40 and 60% of liquid and be of a rather mushy consistency.

"The question is, if the authors feel a multilayer of this sort is so valuable, why do we not get all the benefits cited by using grease in the first place?

"As the writer showed (1971A), there is a strong antiwear effect from thick, semisolid films, but these are the result of catalytic oxypolymerization of the base oil-additive mixture at the rare encounters with bare metal. When such contact does occur, presumably at a fresh wear spot, this "friction polymer" forms. Since it is caused by wear rather than friction, and is an oligomer with O and CO links rather than a polymer, we prefer to call it "surface resin".

"While our laboratory has not had any opportunity to check out this matter, it might be of interest to note that Zadumkin et al have come out with a model for interfacial energies which helps to explain how these multilayers are formed (1965). In very condensed form, this states that the work of adhesion A_{12} of an organic liquid to a metal depends on the square of the contact potential of the metal against a non-polar liquid V_1 , two other metal constants, and the dielectric constant of the liquid

$$A_{12} = kV_i^2(\epsilon - 1)/(\epsilon + 1) \quad (7.11-1)$$

where k contains the other two metal constants. These are presumably not highly variable from metal to metal, as they relate to Thomas-Fermi transformations. This equation has been verified for liquid gallium and mercury against a number of pure organic liquids.

"As the Gibbs-Duhem principle requires that a system equilibrate with the minimum free energy, the work of adhesion ($-G$) will maximize, which leads a mixture to separate with the higher dielectric constant species accumulating near the interface. Taking the dielectric constants of hexadecane = 2.00 and of stearic acid = 2.34 at 20°C, and the contact potentials against hexane from Bewig and Zisman (1964), the relative works of adhesion may be calculated:

hexadecane on chromium	= 0.016k ergs/cm ²
stearic acid on chromium	= 0.019k
hexadecane on gold	= 0.0055k
stearic acid on gold	= 0.0068k

"Thus, chromium or alloys in which chromium forms the surface have discriminating power of 0.003k, while gold has only 0.0013k ergs/cm² and so will form a much more fragile layer".

Smith (1970) attributed multilayers of acid to soap formation.

7.11.5 Freshly Purified Cetane

The only anomaly here lies in the fact that the changes in the cetane which has been exposed to light are so subtle as not to have been readily detected. Without further investigation, the writer believes that the principal change is the presence of free radicals, which help in triggering off the Model IIIC reaction (5.5-17).

7.11.6 Complex Organic Phosphates

Time has not permitted any investigation of this matter, nor was the project funded for any laboratory work. It can only be speculated that these large molecules (castor oil-P₂O₅ reaction product and Ca₃(PO₄)₂ plus oleic acid, perhaps partly reacted) act through formation of soap-like films by Model IIIE.

7.11.7 Diesel Engine Scuffing

The anomaly involved at this point is not only that discussed under the competition of additives, where typical anti-wear additives increase wear. The real bomb-shell was the discovery by Rogers (1970) that a simulative test device gave ordinary wear on cast iron when dry, but rapidly shifted into "scuffing" wear on being lubricated.

Simultaneously, an exceptionally thick "white layer" developed. The author failed to make the obvious statement that this particular white layer was Fe₃C, either from caution or ignorance, but did offer the opinion that Fe₃C in the wear debris was caused by carbide formation using the carbon from the lubricant. At first, this seemed to be an unnecessary complication, as gray cast iron already contains enough carbon (in the form of graphite) that it can be converted to white cast iron (partially pure Fe₃C) by melting and quick chilling to prevent decomposition into ferrite and graphite.

Subsequent studies of the literature, especially Eischens' article (1969) showed that indeed hydrocarbon lubricants might undergo complete dehydrogenation by Model IIIC, to yield Fe_3C . The effect of this on fatigue has already been discussed in Section 7.9.

7.11.8 Suspension of Particles

This was fully covered under Section 5.9.3, in what might be designated as Model VIID. It should be emphasized once more, however, that a great deal remains to be done. At present, it is not possible to put together a consistent list of Hamaker constants, nor is any procedure available for computing them. It is highly probable that one can be developed from δ_D values (and γ values) for the material of the particle--but we do not always know what the particle is, nor do we always have δ_D values for it (Fe_2O_3 , for example, has never had its heat of vaporization determined due to low vapor pressure below its decomposition point). Fowkes has a new method of computation under development, but so far has not released details (1970). Hansen (1969) has shown that sedimentation of pigments can be correlated with his three parameters, plotting the same way as for solubility or wetting. Parfitt (1967) presented a review of the subject featuring the "DLVO" (Derjaguin-Landau-Verwey-Overbeek) model, which is considered to be more complete than the Hamaker-Vold version.

7.11.9 Delay of Transition

It was mentioned under Section 5.3.9 that transition delay might be caused by slow dissolution of surface resin formed from metal-working oils used in preparing test parts. Actually, this is not the most plausible explanation. It seems more likely that some fatigue phenomenon is taking place. Figure 7-3 shows Pike's (1970) 4-ball data on cetane without additive, replotted on log-log paper. It is evident that the data fits fairly well to the Lundgren (1949) formula, $W^{3d_0} = \text{constant}$ (see Section 5.3.2).

Unfortunately, the addition of stearic acid, shown by MacGregor (1964) to favor fatigue over adhesion, causes the negative slope to drop from 0.333 to about 0.065. This indicates that a mixed mode, probably "Quasi-Hydrodynamic" (see Table 2-I) has replaced the simple fatigue observed with cetane.

In addition, Appeldoorn (1966) shows data with a positive slope (Table 7-VI), for cetane on the 4-ball machine; no theory is likely to reconcile these data with Pike's.

7.11.10 Formation of Gold-Oxygen Layer

It has recently been confirmed (Runk 1971), and serves to emphasize the point made by Zisman (1969) that the wetting of metals is a fairly complex process unlike that of organics and ceramics. As discussed in Appendix V, metals appear to bond to organic liquids by an electron donor-acceptor energy closely related to hydrogen bonding, and the oxygen may well play a vital role. Pask (1970) felt that good bonding MUST involve non-London forces, and if at all possible, covalent energy. This anomaly has been assigned to Model II, since it clearly involves reversible surface chemistry.

Figure 7-3
TRANSITION DELAY TRAVEL AS A
POWER FUNCTION OF LOAD

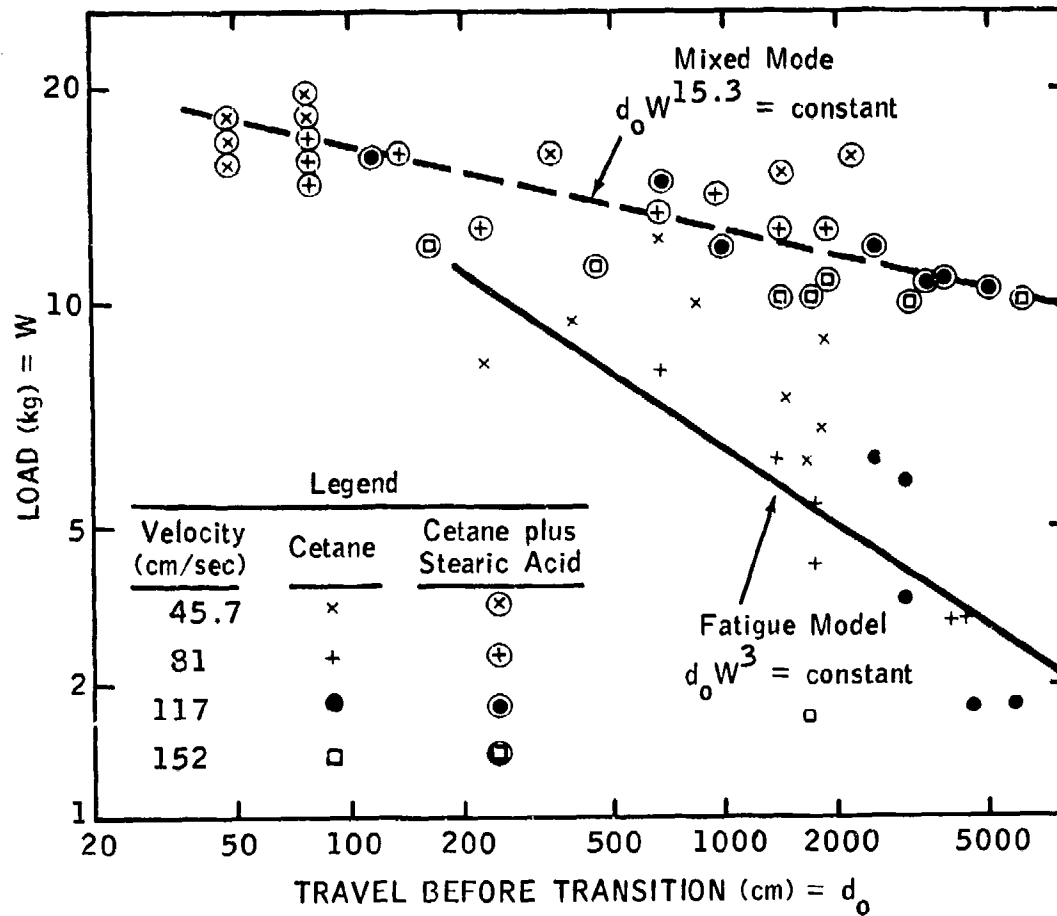


TABLE 7-VI

"ZERO-WEAR" PERIODS AT HIGH LOADS
ON THE 4-BALL MACHINE WITH CETANE
AS LUBRICANT

	<u>DELAY PERIOD IN MINUTES - 77°F STARTING TEMPERATURE</u>			
Load (kg.):	<u>5</u>	<u>10</u>	<u>30</u>	<u>50</u>
600 rpm	0.71	0.80	4.64	18.50
1200 rpm	--	0.74	5.00	6.85
1800 rpm	--	0.33	15.90	--

7.11.11 Water Solutions as Lubricants

There is a good deal going on in this area, all apparently more or less dependent on surface resin formation. However, it appears borderline to the scope of this report, and much of the information is proprietary, so this anomaly is merely cited as another success for Model IIIC.

7.11.12 "Bifurcated" Wear

Saibel (1970) has provided a very elegant solution for this matter, based on his equations for birth-and-death statistics of asperity contacts. Others (4.11.12) feel, with some justification, that the explanation is much simpler, and merely due to proximity to a transition point such as Y in Figure 2-1. In such a case, wear could continue on a "normal" basis indefinitely in the absence of a perturbation such as proposed by Blok (1970). However, once wear enters the scuffing mode, return to "normal" would be quite difficult, requiring a new break-in, as discussed in Section 4.8, at a much lower load.

One case came to light which scarcely can be explained by the "proximity to transition" theory. The Industrial Unit of Tribology at the University of Leeds in England reported that an oil soluble barium salt of an anti-smoke additive was put into diesel fuel and tested in a London taxi fleet. Wear on about half the vane pumps was doubled over that for the base fuel, while the others decreased to half the wear rate. All tests on metallurgy etc., revealed no differences. No explanation other than Saibel's statistical one has yet been offered.

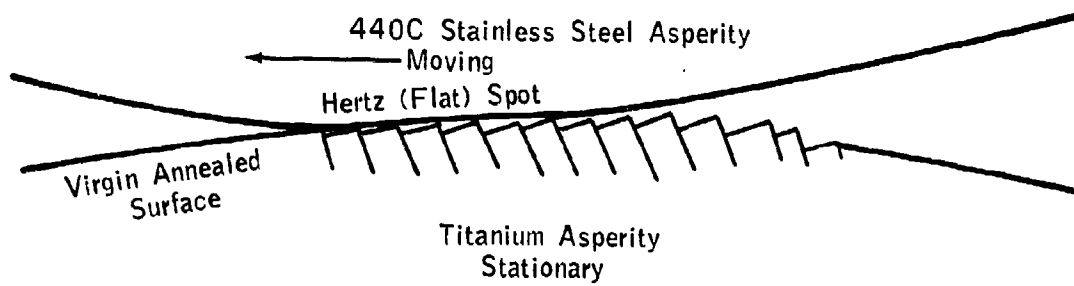
7.11.13 High Friction on Titanium

The trouble with titanium seems to be primarily associated with peculiar crystal structure (Buckley 1966). Most hexagonal metals are quite easy to lubricate; cobalt in particular gives good friction and wear even when lubricated only with its own oxide (Roberts 1969). The principal difference is in the ratio of prism lattice dimensions, c/a , where c is the spacing in the axial direction and a that measured across one of the six flats. Cobalt has a ratio of 1.624, while titanium is only 1.587. This difference is augmented by a tendency to slip parallel to the flat, rather than at right angles to the axis, so that rubbing a titanium surface tilts the prisms into a saw-tooth configuration. The resulting surface is shown in Figure 7-4. The effect may be compared to attempting to slide with bare feet on a bathroom floor paved with loose hexagonal tiles.

Rabinowicz (personal communication) doubts that the c/a ratio is the sole explanation, as other hexagonal metals with similar ratios lubricate normally. It is only the group IVA (Ti, Zr, Hf) which is peculiar. He also published a paper (1955) on lubricating titanium with a variety of synthetics, and feels iodine is not any better than chlorine and fluorine.

It is evident that the problem is fundamental to this metal (or group). Efforts are being made to alleviate it by alloying with tin (Johnson 1970B) or with high oxygen contents. However, the best approach would be to reduce the traction force (FW/N) on each asperity to such a point that it could not cause the tilting shown in Figure 7-4. Apparently iodine-based lubricants function in this way. They do not have any specific reaction with titanium, since they show the same low friction on other metals and even on glass. Even if the mechanism proposed in Section 5.3.3 proves to be unique, it may still be possible to make further improvements on the present iodine-silicone polymer (Brown 1968), and it appears that such a mechanism could at least be simulated with hydrogen bonding to replace halogen bonding. Such a system would at least be relatively non-corrosive.

Figure 7-4
PROBABLE MECHANISM FOR HIGH
FRICTION ON TITANIUM



7.11.14 Austenite Versus Martensite

The writer is not well qualified to investigate this matter, but has not turned up any further evidence to support Grew's theory. On the other hand, the various versions of Model IV do not seem to explain his results, so the matter remains open.

7.12 Recapitulation of Anomaly Explanations

In the preceding subsections an attempt has been made to deal with each anomaly in terms of which models are applicable. The results are summarized in Table 7-VII. It appears that most of the phenomena can be explained, at least qualitatively, in terms of the models. On the 28 cases considered, only one (Austenite vs. Martensite) was left completely unexplained, and that primarily due to lack of interest. In cases 7.3, 7.4 and 7.11.12 special purpose models had to be invoked that were not otherwise useful. The "hexagonal theory" arose twice; perhaps it should have had special billing as "Model IVC".

It is obviously not possible to base any reliable conclusions on a "body count", but the fact that Model III shows up 21 times in Table 7-VII is rather impressive. Much of this is due to the surface resin Models IIIC (10 times) and IIID (6 times).

Put in another way, the models have been tested as to their ability to explain extraordinary lubrication, in addition to the evaluation against ordinary lubrication in Sections 5 and 6. Each of them has earned some recognition, even though in some cases this is quite limited. Thus, all of them require inclusion in the over-all design manual which is the distant goal of this study. The weakest member is undoubtedly Model II as described. While it does represent a real situation, its usefulness will be trivial until the Feng dislocation transfer mechanism has been incorporated. In other words, simple adhesive wear is so rare as to be of very little interest, but transfer wear describes a mode which is worthy of further study. Such study would be motivated by a desire to prevent transfer in favor of fatigue, for reasons clear in Figures 6.4-1 and 6.5-1.

The encouragement gained from Table 7-VII is very substantial in terms of justification for proceeding towards this goal. The fact that eight of the explanations can be considered quantitative, and twelve qualitative (with the means at hand to upgrade them) is strong evidence that the phase of generalization discussed in Section 3.3 is indeed far advanced. Specifically, the established practices of using fatty oils, mineral oils, bronze-on-steel (7.1) leaded systems (7.2) and good break-in (7.10) have been given explanations which the writer feels are considerably sounder than any previous attempts. While less complete, the attempt at explaining the effect of calcium compounds (7.3) also represents a distinct advance in explaining an accepted practice.

TABLE 7-VII

SUMMARY OF EXPLANATIONS FOR THE ANOMALIES IN SECTION 7

Sub- Section	Anomaly	Applicable Models and Notes	Adequacy**
7.1	Base Case - Fatty oils	III B and C + V	B
	- Mineral oils	III D + V	B
	- Bronze on steel	IV	A
7.2	Lead	IV	A
7.3	Calcium	II C + Lattice matching	C
7.4	Iodine	"Temporary polymer"	D
7.5*	Blends	III C and D + V	B
7.6	Additive Competition	II C, III C and D	B
7.7	Humidity and Oxygen	I, II, III, IV, VI, and VII	C
7.8	Transition to Scuffing	II, III B-C-D, IV and V	A
7.9	Additives and Fatigue	III C and VI	C
7.10	Break-in	III B, C and D, plus physical smoothing	B
7.11.1	Low Friction in Transmissions	III C + V	B
7.11.2	Anomalous Wetting Energy	II	A
7.11.3	Group B Metals	IV and hexagonal theory	A
7.11.4	Stearic Acid Multilayers	II	A
7.11.5	Freshly Purified Cetane	III C	B
7.11.6	Complex Phosphates	III E	D
7.11.7	Diesel Scuffing	III C	A
7.11.8	Particle Suspension	VI D	B
7.11.9	Delay of Transition	I	B
7.11.10	Gold-Oxygen Layer	II B	C
7.11.11	Water Solution Lubes	III C	E
7.11.12	Bifurcated Data	Statistical theory	D
7.11.13	Titanium	Hexagonal theory	A
7.11.14	Austenite vs. Martensite	Not explained	-

* Counted as three cases (7.5.1 on LP alloys, 7.5.2 on silicone blends and 7.5.3 on aliphatic-aromatic blends.)

** Adequacy ratings: A = Quantitative
B = Qualitative
C = Plausible
D = Speculative

While the scuffing transition (7.8) was rated "A", it would have been more satisfying if one model had won out over all others. However, the results can be interpreted as providing several routes to preventing scuffing; there may not be a single "best answer." This anomaly clearly demands farther research, as does the closely related delay (7.11.9).

One other "A" rating deserves special mention. It appears to the writer that a perfectly valid explanation for diesel scuffing (7.11.7) has been synthesized in the course of this study, and that a few check tests may provide a solution to this vexing problem.

The limitation on the successes with the additive competition and atmospheric effects (7.5, 7.6 and 7.7) is largely due to the newness of Model IIID. As further research is made on this complex of chemical reactions, progress to "A" ratings should be rapid. (Actually, 7.5.2 on silicones would be so rated, but the forms of Table 7-VII did not permit such fine distinctions).

In the case of titanium friction and scuffing (7.11.13), an "A" explanation does not seem to lead to any easy solution. However, with the problem more clearly stated than in the past, we may hope for additional progress.

The success of Model IV on the "Group B" metals (7.11.3) is gratifying, and should lead rapidly to experimentation with other non-scuffing alloys (for use with steel shafts, etc.) that do not contain vigorous oxidation catalysts such as copper. All such work will certainly become part of the proposed manual.

The "B" rating on paricle suspension (7.11.8), when raised to an "A" level by further work, could have very dramatic effects on the concept of oil filtration and cleanliness. If simple additives (Tao 1970) can eliminate abrasive wear, we are at least a year closer to zero-maintenance design than would be possible by the use of filters.

Other "A" and "B" successes (7.11.1, 7.11.2, 7.11.4, 7.11.5 and 7.11.11) can only be counted as advances in general understanding since they are too specialized to provide much meat for manual writing. The same applies to some less successful explanations (7.11.6, 7.11.10, 7.11.12, 7.11.14).

Elevation of the friction-reduction by iodine to "A" status could be a major break-through, or not, depending on the nature of the solution. The ad hoc model proposed (7.4) would lead to a whole new class of additives, if verified, and yield some very easy routes to low friction and wear. If this theory of temporary electron-transfer bonds leads to lubricants as maintenance-free as the synovial fluid in animal joints, the proposed design manual could be quite brief.

Finally, the lack of complete success on fatigue (7.9) needs attention, even though rolling fatigue is still a minor problem because of other failures predominating. A clear-cut solution to this anomaly might well open up routes to sliding fatigue, thus solving some problems with Model I and delay of transition (7.11.9) and bringing the design manual closer.

7.13 Immediate Applications of Anomalies

It would seem desirable to take advantage of as many of the anomalies as possible without waiting for further research. In a few cases, this should be possible.

7.13.1 Lead

From all indications, the use of leaded alloys, platings and lubricants could be considerably expanded. In spite of the current popular hysteria on this metal, its use does not often create environmental problems, and there are many precedents to support this statement. (Actually, the incentive for lead-free gasoline is to prevent damage to the catalytic mufflers soon to be added to cars; toxicity appears to be a minor problem.) Use in many cases would not involve re-design, but merely calling for existing alloys and lubricants in unconventional places, in the full expectation of reduced maintenance.

7.13.2 Calcium

The promises are less definite for calcium, but the possibility of using high-calcium marine diesel type lubricants for other services should not be neglected. They have undoubtedly been tested, but perhaps not under realistic conditions of break-in.

7.13.3 Diesel Scuffing

While the discussion of this problem in 7.11.7 and 7.12 suggests the most probable cause of this problem, it does not provide a solution. The latter must come from observations, such as those by Montgomery (1969) that engines which develop proper "glaze" during break-in do not scuff. Hence, addition of anything tending to promote surface resin formation to the oil, or cylinder wall metal, may be expected to alleviate the problem.

7.13.4 Particle Suspension

While Model VII is far from complete, it is at least known that fatty acid will render Fe_2O_3 non-abrasive, while octadecyl amine does the same for SiO_2 . Any systems suffering from abrasive contamination with either of these, or similar compounds (Al_2O_3 , etc.) may be expected to show a dramatic response to these additives.

8. RECOMMENDED RESEARCH PLAN

It is evident that the Models discussed above go a long way toward explaining the various phenomena that occur in boundary lubrication, including those classed as "anomalous"; but there is still a considerable way to go before the models will be useful to the designer in assuring one-shot, lifetime lubrication for bearings operating in the boundary regime.

8.1 The Incentives for Further Work

The goal of the recommended effort is to extend the lubrication period of Army (and other) vehicles and equipment without incurring excessive wear - hopefully to the designed lifetime of the equipment.

The Army has a wide variety of lubrication needs, most of which are being attacked by supplying well-standardized lubricants for field servicing. However, the life of the lubricated equipment depends upon several factors:

1. The correct lubricant at the time and place that relubrication is due,
2. Personnel trained, equipped and motivated to do a proper job of maintenance,
3. Opportunity to carry out these duties before excessive wear takes place, and
4. Facilities for relubrication without abrasive or water contamination.

Even under non-combat conditions, the chances of getting all four factors at once are none too good. As a result, maintenance may come too late, or indeed even be harmful. For example, it has been noted (in civilian vehicles) that 90% of the wheel bearing failures occur within 1000 miles after relubrication. This sort of statistic is harder to obtain on military vehicles, but it seems unlikely to be more favorable.

On the other hand, the replacement of a sealed-for-life ball bearing requires a minimum of logistics. It carries with it a lubricant selected for that bearing and inserted under ideal conditions at the factory. The personnel need not be skilled beyond the elementary ability to recognize and take out a defective unit and replace it with another with the same model number. Application of this technique to engines, gearboxes, etc., will not be easy; but if a lifetime of about five years without excessive wear can be demonstrated - and this is not unreasonable - the result would be a dramatic decrease in POL logistics problems with only a modest increase in the logistics of prelubricated-and-sealed spare parts.

Beyond the improvement of logistics, there are clear benefits to be gained from improved lubrication itself. Jost (1966) has estimated potential savings (to British industry) of over \$ 1,000,000,000 per year from improved lubrication and reduction of friction, the least of which is the saving in the cost of lubricants; as follows:

ESTIMATED SAVINGS FROM BETTER
LUBRICATION

<u>Source of Savings</u>	<u>% of Total</u>
Reduction in energy consumption through lower friction	5.4
Reduction in manpower	1.9
Savings in lubricant costs	1.9
Savings in maintenance and replacement costs	44.7
Savings of losses consequential upon breakdown	22.3
Savings in investment due to higher utilization ratios and greater mechanical efficiency	4.3
Savings in investment through increased life of machinery	19.5
	100.0

Comparable savings should be demonstrable for any large user of lubricated machinery.

There are also incentives in the reduction of the amount of empirical testing that is now necessary to design a new machine element. Currently, a machine designer will typically select a bearing or a gear from a commercial catalog, thus automatically determining the metallurgy. The maintenance engineer selects a lubricant of the viscosity specified in the machine instruction booklet, and the lubricant formulator modifies one of his regular products to fit it if complaints start to build up. Occasionally, there are conferences, on a spot basis, if the machine designer faces an unusual problem, and there may be an attempt to review some possibilities before the design is frozen. However, this is all too rare.

Military designing differs from industrial problems mainly in that everyone involved knows that the lubricant must, barring exceptional circumstances, meet one or another of the existing MIL specifications. There may be some intervention by a technical expert from the procuring agency, if something out of the ordinary is being designed. However, the tendency is to let the contractor use his best judgement.

Handbook guidance is scanty, and it provides no factors for lubricant quality (other than MIL specs). The result is over-design, except in the aircraft and aerospace fields where weight is of prime importance. Where such optimization is required, an iterative - and expensive - shop program is usually employed in which a prototype is built, tested to failure, rebuilt and so on until an acceptable compromise is achieved.

In none of this is anybody to blame, but it is clear that great economies and greatly improved performance could be achieved if it were possible to DESIGN for zero maintenance in lubricated military equipment. The program recommended herein offers promise of such design.

8.2 Forecast of Possible Achievements

At present, we have seven mathematical models which partially predict the wear which will be experienced by a given bearing with a given load, a given metallurgy and a given lubricant. Seven different models are needed because each one essentially describes a single mode or mechanism of wear and all of them are important. The bearing, of course, sees all the modes - or whichever one happens to dominate - and a complete model would have to be a synthesis of all the fragmentary models, with suitable coefficients so as to yield the correct net wear rate in a real condition.

It now appears that such a synthesis could be made, given some additional theoretical work and some additional data; which would account for wear as it is normally encountered over the whole range of metallurgy, lubricants and conditions which are used. More significantly, such a combined model would also explain the anomalously low wear rates which are sometimes encountered and would open the way to obtain such low wear rates on a routine basis. And that would improve the normal wear expectancy to the point that heavy-duty military machinery could be designed to run until obsolete without the necessity for any field re-lubrication or wear-caused repairs.

The above is quite a realistic expectation. Many anti-friction bearings are already being supplied factory-lubricated for life, and some automobile engines have already been run as long as 60,000 miles without relubrication and without appreciable loss of performance.

The development of the model is a realistic expectation, too. Each of the seven component models accounts for a wear mode at least qualitatively, and some give good quantitative predictions. They also account, at least qualitatively, for nearly all the known instances of extraordinarily good lubricant performance. It certainly appears that foreseeable programs - detailed in the next sections - can probably lead to a complete and quantitative description of wear which will take into account all significant factors of metallurgy, lubricant and environment.

However, one more step is needed. A mathematical model, while an essential step in the development of the technology, is not a tool which is useful to shop people and machine designers. It needs to be translated, or converted, into a design manual useable by practical people, a manual which will provide charts of metallurgy vs. lubricant, load vs. wear, environment vs. additives --- all the working details necessary for a designer to engineer a bearing-lubricant system to meet his requirements.

The writing of such a manual would be a painstaking task, but it would be quite feasible with the aid of the completed boundary lubrication Model. It is estimated that the model could be completed in approximately two years, given the requisite resources, and that the Design Manual could be completed in approximately one more year.

8.3 The Plan of Attack

What is required is a design manual which will take into account all the variations in bearing metallurgy and geometry, in lubricant chemistry and physical properties, and in surrounding atmospheres. With such a manual, a machine designer could engineer a bearing-lubricant element as a system, with confidence that it will have an acceptable failure-free lifetime without the necessity for periodic maintenance. Such a manual could be written if the model discussed above were extended and quantified as now seems possible.

A program to arrive at a design manual would encompass three inter-related phases:

- Fill in the Remaining Gaps in the Models

The various models have been carried about as far as they can be with existing data resources, but there are still some important gaps in their coverage of the boundary phenomena. These gaps need to be filled in by further theoretical work and by further analysis of such data as are available. This task is estimated to require approximately 15 man-years to accomplish.

- Test the Models by Crucial Laboratory Experiments

In several instances, laboratory data are needed to furnish numerical coefficients for the symbolic equations already worked out, and these must be obtained in close consultation with the theoreticians. There are also cases where it is not yet possible to choose between two alternate formulations of models, and data are needed to select the right, or best, one. This task is estimated to require approximately 6 man-years to accomplish.

- Write the Design Manual

Translate the completed and quantified mathematical models into a form useful and intelligible to industrial factory designers and military planners. This task is estimated to require approximately 1.5 man years to accomplish.

In view of the great benefits to be derived by the field users, it is recommended that the completion of this work be considered at an early date. It is also suggested that sponsorship be shared by all the Armed Forces, NASA and DOT, under the general leadership of the Army, since all will benefit from the advent of zero-maintenance vehicle bearings.

- 224 -
APPENDIX I

NOMENCLATURE

Some symbols which appear only on one page of the text are defined there but not in this Appendix. Certain symbols which are used only for surface properties in Appendices III-VI are also omitted from Appendix I.

LATIN

- A = Arrhenius (pre-exponential) constant; length of cylindrical contact
 A_p = projected bearing area
 A_t = cross-sectional area of wear track (cm^2)
 A_{12} = work of adhesion (ergs/cm^2)
B = electric charging energy of metal (ergs-cm^2)
c = additive concentration in mole fraction
 C, C' = constants in finite wear equations
 C_1, C_2, C_2' = constants in metal compatibility equations
 C_a = concentration of abrasive powder (%)
 C_m = constant for metal in abrasive wear equation
 C_o = oxygen concentration in lubricant (gm/gm)
d = sliding distance (cm)
 d_o = zero-wear sliding distance (cm)
D = surface roughness (μin or μm)
 D_s = surface roughness after running in
E = energy (heat of adsorption (cal/mol or ergs/cm^2))
 ΔE = difference in heat of adsorption of additive (E_a) and base fluid (E_b) (cal/mol)
 E_r, E_s = energy of adsorption on rider and specimen (cal/mol)
 E_1, E_2 = Young's modulus of solids (psi)
 $1/E' = (1 - \nu_1^2)/E_1 + (1 - \nu_2^2)/E_2$
F = coefficient of friction
G = allowable fraction of τ_y for zero-wear
 G_R = G for 2000 passes
h = Planck's constant (6.5×10^{-27} erg sec)
 h_c = critical thickness of corrosion products film (cm)
 h_o = specific film thickness
H = Hertz contact dimension (in or cm)
 ΔH_s = heat of sublimation (cal/gm mol)
 ΔH_v = heat of vaporization (cal/gm mol)

- J = mechanical equivalent of heat (ft lb/BTU)
- k = Boltzman's constant (1.4×10^{-16} ergs/deg C)
- k_m = "wear coefficient" for metal-metal contact area
- k_1, k_2 = thermal conductivities (cal/sec-cm-°C); in 5.1.1, (BTU/ft-hr-°F)
- K = specific wear rate (archard constant)
- K_f = specific wear rate due to fatigue
- K_{12} = interfacial wetting factor
- L = number of revolutions or strokes
- L_o = L for zero-wear period
- M = molecular weight (gm/mol)
- n = number of molecules per unit area (cm^{-2}); exponent of load in simplified wear equations
- N = number of passes
- N_a = Avagadro's number
- N_o = N for zero-wear
- p = exponent of velocity in simplified wear equations
- "PV" = apparent pressure (W/A_p) times velocity (lb/ft-sec)
- q_o = maximum stress in Hertz contact area (psi or kg/mm^2)
- Q = activation energy for oxidation of metal (cal/mol)
- $r = 1/(1/r_1 + 1/r_2)$, the harmonic mean of surface radii (in or cm)
- r_1, r_2 = individual radii of surfaces (in or cm)
- R = molar gas constant (cal/mol-°K); R' is same (ergs/mol-°K)
- S = distance traveled per revolution or stroke (in or cm)
- ΔS = total entropy change associated with adsorption (eu)
- t = time (sec)
- t_o = vibrational time of adsorbed molecule (sec)
- T_b = bulk temperature of lubricant (°K)
- T_c = critical temperature (°K)
- T_m = melting point (°K)
- T_s = temperature of surface (°K)
- T_t = transition temperature at scuffing (°K)
- U = sliding velocity (cm/sec)
- V = wear volume (cm^3)
- V_m = molar volume (cm^3/mol)
- w = width of wear track (cm or in)
- w_o = w for end of zero-wear period (cm or in)
- W = load (gms or lbs)
- W_1 = load carried by asperities (lb)

- W_2 = load carried by EHD film (lb)
 x = ratio of molar diameters
 X = diameter of adsorbed molecule (cm)
 X_3 = mole fraction of alloying component

NOMENCLATURE - GREEK

- α = fractional film defect (for additive in Model II C)
 α_r, α_s = fractional film defects on rider and specimen
 β = fractional base fluid film defect
 γ = von Mises friction function for plastic flow $(1 + 3F^2)^{0.5}$
 γ_1 = surface free energy of lower phase (ergs/cm²)
 γ_2 = surface free energy of upper phase (ergs/cm²)
 γ_3 = surface free energy of second component in blend or alloy (ergs/cm²)
 γ_{12} = interfacial free energy (ergs/cm²)
 γ_m = surface free energy of blend or alloy (ergs/cm²)
 δ_D = London force solubility parameter (cal/cm³)^{0.5}
 δ_H = electron transfer (H-bond) contribution to solubility parameter (cal/cm³)^{0.5}
 δ_1, δ_2 = solubility parameters of metal pair (cal/cm³)^{0.5}
 ϵ = dielectric constant of lubricant; resistance to wear in 5.9
 η_o = viscosity at entrance (bulk) temperature (poise)
 η_s = viscosity at surface temperature
 θ = contact angle (deg)
 θ_1 = asperity slope (deg)
 ν_1, ν_2 = Poisson's ratio of solids
 ξ = thickness of lubricant film (in or m)
 ρ = density of oil (gm/cm³)
 ρ_o = at 60°F (15°C) (gm/cm³)
 σ = surface stress (ergs/cm²)
 τ_{max} = maximum shear stress in contact area (psi)
 τ_y = yield stress in shear of solid (psi)
 ϕ = fractional surface coverage by additive; ratio V_m (oxide)/ V_m (metal)
 ϕ_1 = volume fraction of higher solubility parameter metal

APPENDIX II

BIBLIOGRAPHY

- Akin, L. S., "An Interdisciplinary Lubrication Theory for Gears - with particular emphasis on the scuffing mode of failure", General Electric Co., Marine Turbine and Gear Dept., West Lynn, Mass. (1971).
- Akhmatov, A. S., "Molecular Physics of Boundary Lubrication", Moscow (1963) (Translation available from Israel Program for Scientific Translations, Kiryat Moshe, P. O. Box 7145, Jerusalem, Israel.)
- Allen, C. M., and Drauglis, E., "Boundary Layer Lubrication: Monolayer or Multilayer", Wear, 14, 363 (1969A).
- Allen, B. C., "The Surface Free Energy of Solid Molybdenum", J. Less Com. Met. 17, 403 (1969B).
- Allum, K. G., and Forbes, E. S., "The Load-Carrying Mechanism of Organic Sulfur Compounds - Application of Electron Probe Microanalysis," ASLE Trans. 11, 162-175 (1968).
- Anderson, J. L., Baker, R. A., and Forbes, J. F., "Application of Evaporative Rate Analysis to the Surface Properties of Metals", J. Coll. and Interface Sci. 31, 372-381 (1969).
- Anderson, J. L., "Evaporative Rate Analysis (ERA) Symposium", Org. Coat. Plast. Chem. ACS Preprint 30, No. 1, 442-457 (1970).
- Anonymous, "The Long, Hot Slide from Tokyo to Osaka", Ind. Res. 12, No. 2, 56 (Feb. 1970).
- Antler, M., "Organometallics in Lubrication", I&EC 51, 753-758 (1959).
- *Antler, M., "The Lubrication of Gold", Wear 6, 44-65 (1963).
- Antonoff, G., Chanin, M. and Hecht, M., "Equilibria in Partially Miscible Liquids", J. Phys. Chem. 46, 492-499 (1942).
- Appeldoorn, J. K. and Royle, R. C., "Lubricant Fatigue Testing", Lubrication Eng. 21, 45 (1965).
- Appeldoorn, J. K., Campion, R. J., Tao, F. F. et al., Tech. Rep. AFAPL - TR-66-89, Part I (August 1966).
- Appeldoorn, J. K. and Tao, F. F., Tech. Rep. AFAPL-66-89, Part II, (September 1967A).
- *Appeldoorn, J. K., "Physical and Chemical Aspects of Boundary Lubrication", Erdoel Kohle, 20, 559 (1967B).
- *Appeldoorn, J. K., Goldman, I. B. and Tao, F. F.; Tech. Rep. AFAPL - TR-66-89, Part III (July 1968A).
- Appeldoorn, J. K. and Tao, F. F., "The Lubricity Characteristics of Heavy Aromatics", Wear, 12, 117 (1968B).
- Appeldoorn, J. K., Goldman, I. B. and Tao, F. F., "Corrosive Wear by Atmospheric Oxygen and Moisture", ASLE Trans. 12, 140 (1969).

- Archard, J. F. and Hirst, W., "The Wear of Metals Under Unlubricated Conditions", Proc. Roy. Soc. A236, 397-410 (1956).
- *Archard, J. F., "Elastic Deformation and the Laws of Friction", Proc. Roy. Soc. A243, 190-205 (1957).
- *Archard, J. F., "The Temperature of Rubbing Surfaces", Wear, 2, 438 (1959).
- Askwith, T. C., Cameron, A., and Crouch, R. F., "Chain Length of Additive in Relation to Lubricants in Thin Film and Boundary Lubrication", Proc. Roy. Soc., 291A, 500-519 (1966).
- *ASTM, "Symposium on the Properties of Surfaces", STP 340, Amer. Soc. Test. Mat., Philadelphia, 1963.
- ASTM Annual Book of Standards, Parts 17 and 18, Amer. Soc. Test. Mat., Philadelphia, 1970.
- ASTM, "Hydraulic System Cleanliness", STP 491, Amer. Soc. Test. Mat., Philadelphia, 1971.
- Babb, S. E., Jr., "Parameters in the Simon Equation Relating Pressure and Melting Temperature", Rev. Mod. Phys. 35, 400-413 (1963).
- Babichev, M. A., "Investigation of the Abrasive Wear of Metals by the Brinell Method", Fric. and Wear in Mach., (transl. by ASME) 14, 1-29 (1962).
- Bagley, E. B., Nelson, T. P. and Scigliano, J. M., "Three-Dimensional Solubility Parameters and Their Relationship to Internal Pressure Measurements in Polar and Hydrogen-Bonding Solvents", J. Paint Tech., 43, No. 555, 35 (1971).
- Bayer, R. G., Clinton, W. C., Nelson, C. W. and Schumacher, R. A., "Engineering Model for Wear", Wear, 5, 378 (1962).
- Bayer, R. G., "Prediction of Wear in a Sliding System", Wear, 11, 319 (1968A).
- *Bayer, R. G. and Schumacher, R. A., "On the Significance of Surface Fatigue in Sliding Friction", Wear, 12, 173 (1968B).
- Bayer, R. G. and Ku, T. C., Personal Interview, April 22, 1970.
- Beatty, H. A., "Organolead Compounds as Lubricant Additives", First Int. Conf. on Organolead Chem. and Its Applns., U. S. Army, Natick Labs (1967).
- Beerbower, A. and Dickey, J. R., "Advanced Methods for Predicting Elastomer-Fluids Interactions", ASLE Trans. 12, 1-12 (1969).
- Beerbower, A., "A Critical Survey of Mathematical Models for Boundary Lubrication", ASLE Trans. 14, 90-104 (1971A).
- Beerbower, A., "Surface Free Energy: A New Relationship to Bulk Energies", J. Coll. Interf. Sci. 35, 126-132 (1971B).

- Beerbower, A. and Hill, M. W., "The Cohesive Energy Ratio of Emulsions - A Fundamental Basis for the HLB Concept", McCutcheon's Detergents and Emulsifiers Annual (1971C).
- Beerbower, A. and Goldblatt, I. L., "An Interpretation of Wear Observed with Natural Hydrocarbons", Wear 18, 421-425 (1971D).
- Beerbower, A. and Panzer, J., Comments on "Interaction Between Lubricants and Plastic Bearing Surfaces", Wear 18, 481-487 (1971E).
- Beerbower, A. and Garabrant, A. R., Comments on "Influence of Water Vapour on the Wear of Lightly Loaded Contacts", Wear 18, 492-496 (1971F).
- Beerbower, A., Comments on "Ordered Multilayered Films: Key to Effective Lubrication", by C. M. Allen, E. Drauglis, and N. F. Hartman, awaiting publication in ASLE Trans. (1972A).
- Beerbower, A. "The Environmental Capability of Liquid Lubricants", NASA Symposium on Liquid Lubricants, awaiting publication (1972B).
- Begelinger, A., "Questionnaire on the Relation Between Surface Condition and Friction, Wear and Lubrication - Summary Report", Metaalinstituut TNO, Delft, Netherlands (Sept. 1969).
- Bernett, M. K. and Zisman, W. A., "Effect of Adsorbed Water on the Critical Surface Tension of Wetting on Metal Surfaces", J. Coll. and Interf. Sci., 28, 243-249 (1968).
- Berry, W. E., "Stress-Corrosion Cracking and Its Relation to Petroleum Industry Materials", W. Va. Univ. - Tech. Bull. 86, p. 416, Oct. 1967.
- Bewig, K. W. and Zisman, W. A., "Surface Potentials and Induced Polarization in Nonpolar Liquids Adsorbed on Metals", J. Phys. Chem. 68, 1804-13 (1964).
- Fleber, H. E., Klaus, E. E. and Tewksbury, E. J., "A Study of Tricresyl Phosphate as an Additive for Boundary Lubrication", ASLE Trans. 11, 155-161 (1968).
- Bigelow, W. C., Glass, E. and Zisman, W. A., "Oleophobic Monolayers. II. Temperature Effects and Energy of Adsorption", J. Coll. Sci. 2, 563 (1947).
- Bikerman, J. J., "Thermodynamics, Adhesion and Sliding Friction", J. Lubr. Tech. (Trans. ASME Ser. F) 42, 243-247 (1970).
- *Bisson, E. E. and Anderson, W. J., "Advanced Bearing Technology", NASA SP-38, 1964.
- Blakely, J. M. and Maiya, P. S., "Surface Energies from Transport Measurements", in "Surfaces and Interfaces I - Chemical and Physical Characteristics", J. J. Burke, N. L. Reed and V. Weiss, eds., Proc. 13th Sagamore Army Mat. Res. Conf., Syracuse U. Press 1966.

- Blanks, R. F., and Prausnitz, J. M., "The Thermodynamics of Polymer Solubility in Polar and Nonpolar Systems", I&EC Fundamentals, 3, 1 (1964).
- Block, A. and Simms, B. B., "Desorption and Exchange of Adsorbed Octadecylamine and Stearic Acid on Steel and Glass", J. Coll. and Interface Sci. 25, 514-518 (1967).
- Blok, H., "Surface Temperature Under Extreme Pressure Conditions", Second World Petrol. Cong., Section 4, Paris (1937).
- Blok, H., "The Postulate About the Constancy of Scoring Temperature", 153-248, Proc. Interdisciplinary Approach to the Lubrication of Concentrated Contacts, NASA SP-237, Washington, D.C. (1970).
- Bodensieck, E. J., "Specific Film Thickness - An Index of Gear Tooth Surface Deterioration", Preprint, Aerospace Gear Comm., AGMA Meeting, Sept. 12-14 (1965).
- Bond, G. C., "Catalysis by Metals", Academic Press, London and New York, 1962.
- Bond, G. C., "Adsorption and Coordination of Unsaturated Hydrocarbons with Metal Surfaces and Metal Atoms", Disc. Farad. Soc. No. 41, 200 (1966).
- Bond, G. C., Personal Interview (March 25, 1970).
- Bondi, A., "The Spreading of Liquid Metals on Solid Surfaces", Chem. Rev. 52, 417-458 (1953).
- Bondi, A., "Physical Properties of Molecular Crystals, Liquids and Glasses", John Wiley & Sons, 1968.
- Boner, C. J., "Manufacture and Application of Lubricating Greases", Reinhold, N.Y. 1954.
- Bowden, F. P. and Tabor, D., "The Friction and Lubrication of Solids", Oxford University Press, London and New York, 1950.
- *Bowden, F. P. and Tabor, D., "Friction and Lubrication", John Wiley and Sons, N.Y., 1956.
- *Bowden, F. P. and Tabor, D., "The Friction and Lubrication of Solids", Clarendon Press, Oxford, 1964.
- Bowers, R. C., Cottingham, R. L., Thomas, T. N. and Zisman, W. A., "Boundary Lubrication Studies of Typical Fluoroesters", Lubr. Eng. 12, 245 (1956).
- Bradley, A., "Organic Polymer Coating Deposited from a Gas Discharge", Ind. Eng. Chem. Prod. Res. Develop., 9, #1, 101 (1970).
- *Brewer, L., "Prediction of High Temperature Metallic Phase Diagrams", in "High Strength Materials", V. F. Zackay, ed., Wiley, 1964.
- Brockley, C. A. and Fleming, G. K., "A Model Junction Study of Severe Metallic Wear", Wear 8, 374-380 (1965).

- *Brophy, J. E., Militz, R. O. and Zisman, W. A., "Dimethyl-Silicone-Polymer Fluids and Their Performance Characteristics in Unilaterally Loaded Journal Bearings", Trans. ASME 68, 355 (1946).
- Brown, E. D., "Methyl Alkyl Silicones. A New Class of Lubricants", ASLE Trans. 9, 31-35 (1966).
- Brown, E. D. and Owens, R. S., "The Development of a Non-Corrosive Non-Toxic Iodine Containing Lubricant and Cutting Fluid", Div. Petr. Chem. ACS Preprint 13, B5-B14 (1968).
- Brown, E. D., Jr., "Effect of Temperature on Lubricity of Lubricating Silicones," Wear 15, 131-135 (1970).
- Bryant, L. F., Speiser, R. and Hirth, J. P., "Some Interfacial Properties of Fcc Cobalt", Trans. of the Metallurgical Soc. AIME 242, 1145 (1968).
- Buckley, D. H. and Johnson, R. L., "Friction and Wear of Hexagonal Metals and Alloys as Related to Crystal Structure and Lattice Parameters in Vacuum," ASLE Trans. 9, 121 (1966).
- Buckley, D. H., "A LEED Study of the Adhesion of Gold to Copper and Copper-Aluminum Alloys", Tech. Note D-5351, NASA, Washington, D.C. (Aug. 1969).
- Buckley, D. H., "Interaction of Methane, Ethane, Ethylene and Acetylene with an Iron (001) Surface and Their Influence on Adhesion Studied with LEED and Auger", Tech. Note D-5822, NASA, Washington, D.C. (May 1970).
- *Buckley, D. H., "Friction, Wear and Lubrication in Vacuum", NASA SP-277, Sci. and Tech. Inf. Off., NASA, Washington, D. C. 1971
- *Cameron, A., "Principles of Lubrication", Longmans, London 1966.
- Campbell, W. E., Pilarczyk, K. and Papp, C. A., "Effect of Wettability of a Lubricant on Journal Bearing Performance", Proc. Conf. Lubr. & Wear, IME, London, 46-52 (1957).
- Campbell, W. E. and Lee, Jr., R. E., "Polymer Formation on Sliding Metals in Air Saturated with Organic Vapors", ASLE Trans. 5, 91 (1962).
- Carr, D. S., "Organolead Lubricant Additives", Ind. Lubr. 19, #12 463-4 (1967).
- Chaikin, S. W., "On Frictional Polymer", Wear 10, 49 (1967).
- Christensen, H., "Some Aspects of the Functional Influence of Surface Roughness in Lubrication", Wear 17, 149-162 (1971).
- Clayfield, E. J. et al, "The Spreading Pressures and Works of Adhesion of Liquid Hydrocarbons on Chrome-Steel and Chromium Surfaces", Second Int. Cong. of Surf. Act., Butterworths, London (1957A).
- Clayfield, E. J., Matthews, J. B. and Whittam, T. V., "The Importance of Oil-Metal Adhesion in Lubrication", Proc. Conf. Lubr. & Wear, IME, London, 326-332 (1957B).

- *Cocks, M. and Tallian, T. E., "Sliding Contacts in Rolling Bearings", ASLE Trans. 14, 32-40 (1971).
- Coffin, L. F., Jr., "A Study of the Sliding of Metals, with Particular Reference to Atmosphere", Lubr. Eng. 12, 50 (1956).
- *Coleman, W., "Gear Design Considerations", p. 551, Interdisc. Appr. to the Lubr. of Conc. Cont., NASA SP-237, Washington, D.C. (1970).
- Cornelius, D. F. and Roberts, W. H., "Friction and Wear of Metals in Gases up to 600 C", ASLE Trans. 4, 20-32 (1961).
- Crook, A. W., "Some Studies on Wear and Lubrication", Wear 2, 364-393, (1958-59).
- Currie, C. C. and Hommel, M. C., "Boundary Lubricating Characteristics of Organopolysiloxanes", Ind. Eng. Chem. 42, 2452-6 (1950).
- Dal, P. H. and Berden, W. J. H., "Bound Water on Clay", Science of Ceramics 2, 59-79 (1965).
- Davies, R. L. and Morris, A., Esso Pet. Ltd., personal interview (Sept. 22, 1969).
- *Davis, K. A., "A Study of the Effectiveness of Selected Antiwear Additives in Synthetic Esters", Air Force Materials Laboratory Technical Report AFML-TR-69-301 (July, 1970).
- de Boer, J. H., "Mobility of Molecules along Adsorbing Surfaces", from "Molecular Processes on Solid Surfaces", McGraw-Hill, New York, 1968.
- de Gee, A. W. J., Vaessen, G. H. G. and Begelinger, A., "The Influence of Composition and Structure on the Sliding Wear of Copper-Tin-Lead Alloys", ASLE Trans. 12, 44 (1969).
- de Gee, A. W. J., Vaessen, G. H. G. and Begelinger, A., "Influence of Phosphorus on the Load Carrying Capacity under Boundary Lubrication Conditions of Copper-6 Tin", ASLE Trans. 14, 116-123 (1971).
- Demorest, K. E., and Whitaker, A. E., "Effect of Various Lubricants and Base Materials on Friction at Ultrahigh Loads", ASLE Trans. 9, 160-170 (1966).
- Demorest, K., Personal interview (August 18, 1969).
- Devine, M. J. and Sander, L. F., "Interatomic Spacing Concept for Solid Lubricant-Metal Systems", presented at Symposium on Chemistry of Lubrication, Division of Petroleum Chemistry, Inc., Amer. Chem. Soc., San Francisco, Calif. (April 1968).
- Dickert, J. J. and Rowe, C. N., "Deposition of Gold on Rubbing Surfaces", Nature Phys. Sci. 231, 87-88 (May 24, 1971).

- Dietrich, V. I. and Honrath-Barkhausen, M.: "Zur Bildung widerstandserhöhender Beläge organischen Ursprungs auf elektrischen Kontakten, Zeit." für Angw. Phys., vol XI, Heft 10, 399 (1959).
- Donald, D. K., "Contribution of Charge to Powder Particle Adhesion", Org. Coat. & Plas. Chem. ACS Preprint 31, No. 2, 47-54 (1971).
- Dowson, D. and Higginson, G. R., "Elastohydrodynamic Lubrication", Pergamon Press, New York, 1966.
- Duckworth, W. E. and Forrester, P. G., "Wear of Lubricated Journal Bearings", Proc. Conf. on Lubr. and Wear, IME, London, 1957.
- Dudley, D. W., "Information Sheet - Gear Scoring Design Guide for Aerospace Spur and Helical Power Gears", AGMA 217.01, Am. Gear Manuf. Assoc., Washington, 1965.
- Duga, J. J., "Surface Energy of Ceramic Materials", DCIC Report 69-2, AD691019, Clearinghouse, Springfield, Va., 1969.
- du Pont, Petroleum Chemicals Division, "LP Alloys - Bulletin No. 1", May 1971.
- Eberhart, J. G., "The Surface Tension and Critical Properties of Liquid Metals" J. Coll. and Interf. Sci. 33, 191-2 (1970).
- Ehrlich, G., "Atomistics of Metal Surfaces", in "Surface Phenomena of Metals", S.C.I. Monograph No. 28, 13-38 (1968).
- Eischens, R. P., "Catalytic Studies Related to Boundary Lubrication", in "Boundary Lubrication: An Appraisal of World Literature", F. F. Ling, E. E. Klaus and R. S. Fein, eds., ASME, 61, 1969.
- Ernst, H. and Merchant, M. E., "Surface Friction of Clean Metals - A Basic Factor in the Metal Cutting Process", Proc. Spec. Summ. Conf. on Frict. and Surf. Fin., MIT Press, 76-101 (1940).
- Ernst, H. and Merchant M. E., "Chip Formation, Friction and High-Quality Machined Surfaces", Surface Treatment of Metals, Trans. ASM 29, 299 (1941).
- Eudier, M. and Youssef, H., "Considerations on the Theory of Friction: Friction Without Wear", Powd. Met. 12, No. 24, 462-470 (1969).
- *Evdokimov, V. D., "Exoelectron Emission in Sliding Friction," Dokl. Akad. Nauk, USSR, 175, 563 (1967).
- Everett, D. H., "Thermodynamics of Adsorption from Solution. Part 2 - Imperfect Solutions", Trans. Faraday Soc. 61, 2478 (1965).

- *Fein, R. S., "Transition Temperatures with Four Ball Machine", ASLE Trans. 3, 34 (1960).
- *Fein, R. S. and Kreuz, K. L., "Chemistry of Boundary Lubrication of Steel by Hydrocarbons", ASLE Trans. 8, 29 (1965A).
- Fein, R. S., "Effects of Lubricants on Transition Temperature", ASLE Trans. 8, 59-68 (1965B).
- Fein, R. S., "Operating Procedure Effects on Critical Temperature", ASLE Trans. 10, 373-385 (1967).
- *Fein, R. S. and Kreuz, K. L., "Cyclohexane Vapor Lubrication of Steel", ACS Div. of Pet. Chem. Preprints, 13, B27 (1968).
- *Fein, R. S., "Chemistry in Concentrated-Conjunction Lubrication", p. 489, Interdisc. Appr. to the Lubr. of Conc. Cont., NASA SP-237, Washington, D.C. (1970).
- Feng, I-M., "Metal Transfer and Wear", J. Appl. Phys. 23, 1011 (1952).
- Feng, I-M. and Rightmire, B. C., "The Mechanism of Fretting", Lubrication Engineering 9, 134 (June 1953).
- Feng, I-M., "A New Theory of Metal Transfer and Wear", Lubrication Engineering 10, 34-8 (1954A).
- Feng, I-M. and Uhlig, H. H., "Fretting Corrosion of Mild Steel in Air and in Nitrogen", J. Appl. Mech. 21, 395-400 (1954B).
- Feng, I-M., "An Analysis of the Effect of Various Factors on Metal Transfer and Wear Between Specimen Pairs of Same Metal and Same Shape, I. The Basic Scheme of Formulation of Metal Transfer and Wear", J. Appl. Phys. 26, 24 (1955). II. "Effect of the Surrounding Atmosphere", J. Appl. Phys. 26, 28 (1955).
- Feng, I-M. and Rightmire, B. G., "An Experimental Study of Fretting", Inst. Mech. Eng. 170, 1055-60 (1956A).
- *Feng, I-M. and Chang, C. M., "Critical Thickness of Surface Film in Boundary Lubrication", J. Appl. Mech. 23, 458-460 (1956B).
- *Feng, I-M., "The Influence of Surface Activity on Friction and Surface Damage", Proc. Second International Congress of Surface Activity, III, 539 Academic Press, New York, 1957A.
- Feng, I-M., "Plastic Roughening and Wear", International Conference on Lubrication and Wear, Inst. Mech. Eng. October 1-3, 1957B).

- Feng, I-M., "Mechanisms of Wear", Symposium on the Chemistry of Solid Surfaces, OOR, 1958.
- *Feng, I-M., "Pyrolysis of Zinc Dialkyl Phosphorodithionates", Wear 3, 309- (1960).
- *Feng, I-M. and Chalk, H., "Effects of Gases and Liquids in Lubricating Films on Lubrication and Surface Damage", Wear 4, 257-68 (1961).
- *Feng, I-M., "A New Approach in Interpreting the Four-Ball Wear Results", Wear 5, 275 (1962).
- Feng, I-M., Perilstein, W. L. and Adams, M. R., "Solid Film Deposition and Non-Sacrificial Boundary Lubrication", ASLE Trans. 6, 60-66 (1963).
- Finkin, E. F., "The Sliding of Copper-Based Sintered Material Against Steel in Paraffinic Mineral Oil", Wear 11, 341-353 (1968A).
- Finkin, E. F., "Abrasive Wear", in "Evaluation of Wear Testing", Spec. Tech. Pub. 446, Amer. Soc. Test. Mat., (1968B).
- Fitch, E. C., "Requirements for an Effective Program in Fluid Contamination Control", ASTM STP 491, pp. 39-49 (1971A).
- Fitch, E. C., "The Compatibility of Hydraulic Power Components with Contaminated Fluid Environments", Deutsche Messe- u. Ausstellungs-AG, Abt. Vb - copies available from author at School of Mechanical and Aerospace Engineering, Oklahoma State University, Stillwater, Oklahoma 74074 (1971B).
- *Fitzsimmons, V. G. et al., "Dimethyl-Silicone-Polymer Fluids and Their Performance Characteristics in Hydraulic Systems", Trans. ASME 68, 361 (1946).
- Forbes, E. S., Allum, K. G., Neustadter, E. L. and Reid, A. J. D., "The Load-Carrying Properties of Diester Disulfides", Wear 15, 341-352 (1970).
- Fowkes, F. M., "Surface Chemistry", in "Treatise on Adhesives and Adhesion", R. A. Patrick, ed., p. 362, Marcel Dekker, Inc. (1966).
- Fowkes, F. M., "Intermolecular and Interatomic Forces at Interfaces", in "Surfaces and Interfaces I - Chemical and Physical Characteristics", Burke, Reed & Weiss, eds., p. 197, Syracuse Univ. Press (1967).
- Fowle, T. I., "Interaction Between Bearing Metals and Lubricants", Paper 3, Joint Course on Tribology, The Institution of Metallurgists, London (1968).
- Fowles, P. E., personal communication, Nov. 30, 1970.
- Fox, P. J. and Soria-Ruiz, J., "Fracture-Induced Thermal Decomposition in Brittle Crystalline Solids", Proc. Roy. Soc. London, A317, 79-90, (1970).
- France, W. D., Jr., "Effects of Stress and Plastic Deformation on the Corrosion of Steel", Corrosion-NACE 26, No. 5, 189-199 (1970).

- Francis, H. A., "Interfacial Temperature Distribution Within a Sliding Hertzian Contact", ASLE Trans. 14, 41-54 (1971).
- Frank, R. G. and Swets, D. E., "Hydrogen Permeation Through Steel During Abrasion", J. Appl. Phys., 28, 380 (1957).
- Frewing, J. J., "The Influence of Temperature on Boundary Lubrication", Proc. Roy. Soc. A181, 23-42 (1942).
- Frewing, J. J., "The Heat of Adsorption of Long-Chain Compounds and Their Effect on Boundary Lubrication", Proc. Roy. Soc. A182, 270-285 (1943).
- *Fuks, G. I., "The Polymolecular Component of the Lubricating Boundary Layer", Ibid., 2, p. 159 (1964).
- Furey, M. J., "Titanium Coordination Compounds as Corrosion Inhibitors", U.S. Pat. 2,891,910 (June 22, 1959).
- *Furey, M. J. and Appeldoorn, J. K., "The Effect of Lubricant Viscosity on Metallic Contact and Friction in a Sliding System", ASLE Trans. 5, 149-159 (1962).
- Furey, M. J., "Oil Compositions Containing Anti-wear Additives", U.S. Pat. 3,180,910 (April 27, 1965).
- Furey, M. J., "The Action of Iodine in Producing Extremely Low Friction", Wear 9, 369 (1966).
- Gans, D. M., "Positive Final Spreading Coefficients", J. Paint. Tech., 42, No. 550, 653 (1970).
- *Gatos, H. C., "Structure of Surfaces and Their Interactions", in "Interdisciplinary Approach to Friction and Wear", NASA SP-181, p. 7-84, Washington, D.C. 1968.
- Gerdil, R. and Lucken, E. A. C., "Radical Anions Containing Sulfur Atoms in a Conjugated System", Proc. Chem. Soc. 1963, 144 (1963).
- Getzen, F. W., "Bulk-to-Surface Distribution Coefficients and Surface Activity Coefficients from Surface Tension Measurements", J. Coll. and Interf. Sci. 37, 668-677 (1971).
- Gilman, J. J., "Direct Measurement of the Surface Energies of Crystals", J. Appl. Physics. 31, 2208 (1960).
- Giltrow, J. P., "A Relationship Between Abrasive Wear and the Cohesive Energy of Materials", Wear 15, 71-78 (1970).
- Glicksman, M. E. and Vold, C. L., "Determination of Absolute Solid-Liquid Interfacial Free Energies in Metals", Acta Met. 17, #1, 1-11 (1969). (See also comments by R. J. Holylev and L. E. Murr, and response by authors, Scripta Met. 3, 783-792 (1969)).

- Feng, I-M., "Mechanisms of Wear", Symposium on the Chemistry of Solid Surfaces, OOR, 1958.
- *Feng, I-M., "Pyrolysis of Zinc Dialkyl Phosphorodithionates", Wear 3, 309- (1960).
- *Feng, I-M. and Chalk, H., "Effects of Gases and Liquids in Lubricating Films on Lubrication and Surface Damage", Wear 4, 257-68 (1961).
- *Feng, I-M., "A New Approach in Interpreting the Four-Ball Wear Results", Wear 5, 275 (1962).
- Feng, I-M., Perilstein, W. L. and Adams, M. R., "Solid Film Deposition and Non-Sacrificial Boundary Lubrication", ASLE Trans. 6, 60-66 (1963).
- Finkin, E. F., "The Sliding of Copper-Based Sintered Material Against Steel in Paraffinic Mineral Oil", Wear 11, 341-353 (1968A).
- Finkin, E. F., "Abrasive Wear", in "Evaluation of Wear Testing", Spec. Tech. Pub. 446, Amer. Soc. Test. Mat., (1968B).
- Fitch, E. C., "Requirements for an Effective Program in Fluid Contamination Control", ASTM STP 491, pp. 39-49 (1971A).
- Fitch, E. C., "The Compatibility of Hydraulic Power Components with Contaminated Fluid Environments", Deutsche Messe- u. Ausstellungs-AG, Abt. Vb - copies available from author at School of Mechanical and Aerospace Engineering, Oklahoma State University, Stillwater, Oklahoma 74074 (1971B).
- *Witzsimmons, V. G. et al., "Dimethyl-Silicone-Polymer Fluids and Their Performance Characteristics in Hydraulic Systems", Trans. ASME 68, 361 (1946).
- Forbes, E. S., Allum, K. G., Neustadter, E. L. and Reid, A. J. D., "The Load-Carrying Properties of Diester Disulfides", Wear 15, 341-352 (1970).
- Fowkes, F. M., "Surface Chemistry", in "Treatise on Adhesives and Adhesion", R. A. Patrick, ed., p. 362, Marcel Dekker, Inc. (1966).
- Fowkes, F. M., "Intermolecular and Interatomic Forces at Interfaces", in "Surfaces and Interfaces I - Chemical and Physical Characteristics", Burke, Reed & Weiss, eds., p. 197, Syracuse Univ. Press (1967).
- Fowle, T. I., "Interaction Between Bearing Metals and Lubricants", Paper 3, Joint Course on Tribology, The Institution of Metallurgists, London (1968).
- Fowles, P. E., personal communication, Nov. 30, 1970.
- Fox, P. J. and Soria-Ruiz, J., "Fracture-Induced Thermal Decomposition in Brittle Crystalline Solids", Proc. Roy. Soc. London, A317, 79-90, (1970).
- France, W. D., Jr., "Effects of Stress and Plastic Deformation on the Corrosion of Steel", Corrosion-NACE 26, No. 5, 189-199 (1970).

- Goddard, J. and Wilman, H., "A Theory of Friction and Wear During the Abrasion of Metals", *Wear* 5, 114-135 (1962).
- Goldblatt, I. L. and Appeldoorn, J. K., "The Antiwear Behavior of TCP in Different Atmospheres and Different Base Stocks", *ASLE Trans.* 13, 203-214 (1970).
- Goldblatt, I. L., "A Model for the Lubrication Behavior of Polynuclear Aromatics", *I&EC Prod. Res. and Dev.*, 10, 270-8 (1971).
- Goldman, I. B., "Corrosive Wear as a Failure Mode in Lubricated Gear Contacts", *Wear* 14, 431-444 (1969).
- Goldman, I. B., Appeldoorn, J. K. and Tao, F. F., "Scuffing as Influenced by Oxygen and Moisture", *ASLE Trans.* 13, 29-38 (1970).
- Good, R. J. and Elbing, E., "Generalization of Theory for Estimation of Interfacial Energies", *Ind. & Eng. Chem.*, 62, 54-78 (1970).
- Gordy, W. and Stanford, S. C., "Spectroscopic Evidence for Hydrogen Bonds: Comparison of Proton-Attracting Properties of Liquids. III." *J. Chem. Phys.* 7, 93-99 (1939).
- Grau, F. E. and Itoh, M. (1966) - quoted in Rabinowicz (1971B).
- *Greenwood, J. A. and Williamson, J. B. P., "Contact of Normally Flat Surfaces", *Proc. Roy. Soc. A295*, 300-319 (1966).
- Greenwood, J. A. and Tripp, J. H., "The Elastic Contact of Rough Spheres", *J. of Appl. Mech.*, 34, 153 (1967).
- Gregory, J., "The Calculation of Hamaker Constants", *Advan. Colloid. Interface Sci.* 2, 396-417 (1969).
- Grew, W. J. S., "Transition Temperatures of Lubricants", Ph.D. Thesis, Imperial Coll. of Sci. and Tech., Sept. 1969.
- Griebe, R. W., Winter, E. F. R. and Schoenhals, R. J., "Choking and Shock Phenomena in a Single Component Two-Phase Flow Including Vibrational Effects", *Warme- und Stoffubertragung*, Bd. 3, 7-18 (1970).
- Grosze, A. V., "The Relationship Between the Surface Tensions and Energies of Liquid Metals and Their Critical Temperatures", *J. Inorg. Nucl. Chem.* 24, 147-156 (1962).
- Grosze, A. V., "The Relationship Between Surface Tension and Energy of Liquid Metals and Their Heat of Vaporization at the Melting Point", *J. Inorg. Nucl. Chem.* 26, 1349 (1964).
- Groszek, A. J., "Preferential Adsorption of Compounds with Long Methylene Chains on Cast Iron, Graphite, Boron Nitride, and Molybdenum Disulfide", *ASLE Trans.* 9, 67-76 (1966).
- Groszek, A. J., "Wear-Reducing Properties of Mineral Oils and Their Fractions", *Proc. Instn. Mech. Eng.* 182, Pt 3N, 160-168 (1967-8).
- Groszek, A. J., "Heats of Preferential Adsorption of Boundary Additives at Iron and Iron Oxide/Liquid Hydrocarbon Interfaces", *ASLE Trans.* 13, 278-287 (1970).

Groszek, A. J., "BP Symposium on the Significance of the Heats of Adsorption at the Solid/Liquid Interface", BP Research Centre, Middlesex (5th March 1971).

* Groszek, A. J., "Role of Adsorption in Liquid Lubrication", NASA Symposium on Interdisciplinary Approach to Liquid Lubricant Technology (1972).

Grunberg, L. et al, "Hydrogen Diffusion in Water-Accelerated Rolling Surface Fatigue", Nature 188, No. 4757, 1182-3 (1960).

Guastalla, J., "Recent Work on Surface Activity, Wetting and Dewetting", J. Coll. and Interf. Sci. 11, 623-636 (1956).

Hamaker, H. C., "London-van der Waals Attraction Between Spherical Particles", Physica 4, 1058 (1937).

Hamaker, F. C., "London-van der Waals Forces in Colloidal Systems", Rec. Trav. Chim. 57, 61-72 (1938). (In English)

Hansen, C. M., "The Three-Dimensional Solubility Parameter - Key to Paint Component Affinities", J. Paint Tech., 39, No. 505, p. 105 and No. 511, pp. 505 and 511 (1967).

Hansen, C. M., "The Universality of the Solubility Parameter", I&EC Prod. Res. and Dev., 8, 2 (1969).

Hansen, C. M., "Characterization of Surfaces by Spreading Liquids", J. Paint Tech., 42, No. 550, 660 (1970A).

Hansen, C. M. and Beerbower, A., "Solubility Parameters", Encycl. Chem. Tech. 2nd ed. Supp. Vol., (1971).

Hansen, R. M. and Gardner, N. C., "A Field Emission Study of the Decomposition of Acetylene and Ethylene on Tungsten", J. Phys. Chem. 74, 3466-3453 (1970B).

Harkins, W. D. and Grafton, E. H., "Surface Tension and Molecular Attraction: On the Adhesional Work Between Mercury and Organic Liquids", J. Am. Chem. Soc., 42, 2534 (1920).

*Harkins, W. D. and Cheng, Y. C., "The Orientation of Molecules in Surfaces. VI. Cohesion, Adhesion, Tensile Strength, Tensile Energy, Negative Surface Energy, Interfacial Tension, and Molecular Attraction", J. Am. Chem. Soc., 43, 35 (1921).

Harkins, W. D. and Loesser, E. H., "Surfaces of Solids-Molecular Interaction Between Metals and Hydrocarbons", J. Chem. Phys., 18, 556 (1950).

Harris, T. A., "Rolling Bearing Analysis", Wiley, New York, 1966.

Hart, E. J., Gordon, S., and Thomas, J. K., "Rate Constants of Hydrated Electron Reactions with Organic Compounds", J. Chem. Phys. 68, 1271 (1964).

Helpinstill, J. G. and van Winkle, M., "Prediction of Infinite Dilution Activity Coefficients for Polar-Polar Binary Systems", I&EC Proc. Design and Dev. 7, 213-219 (1968).

- Hermance, H. W. and Egan, T. F., "Organic Deposits on Precious Metal Contacts", Bell Syst. Tech. Journ., 37, No. 3, 739 (1958).
- Hildebrand, J. H. and Scott, R. L., "The Solubility of Non-Electrolytes, 3rd Ed.", Dover, New York, 1950.
- Hoar, T. P. and West, J. M., "Mechano-Chemical Anodic Dissolution of Austenitic Stainless Steel in Hot Chloride Solution", Proc. Roy. Soc. A268, 304-315 (1962).
- Hoar, T. P. and Scully, J. C., "Mechanochemical Anodic Dissolution of Austenitic Stainless Steel in Hot Chloride Solution at Controlled Electrode Potential", J. Electrochem. Soc. 111, No. 3, 348-352 (1964).
- Hordon, M. J., "Adhesion of Metals in High Vacuum", in "Adhesion and Cold Welding of Materials in Space Environment", ASTM STP-431, 109-127 (1967).
- * Horth, A. C. et al., "Use of Laboratory Ball Joint Test to Predict Chassis Grease Performance", Paper 379B, presented at SAE Summer Meeting, St. Louis, Missouri (1961).
- * Hoy, K. L., "New Values of the Solubility Parameters from Vapor Pressure Data", J. Paint Tech., 42, No. 541, 76 (1970).
- Hudson, J. C., "Atmospheric Corrosion of Metals", Trans. Farad. Soc. 25, 177-252 (1929). (See especially p. 207-8).
- Hultgren, H. H., "Compatibility in Sliding Metals", B.S. Thesis, MIT (1956).
- Hurricks, P. L., "The Mechanism of Fretting - A Review", Wear 15, 389-409 (1970).
- Imanaka, O., "Surface Energy and Fracture of Materials", Kinzoku Hyomen Gijutsu 19, 424 (1968).
- * Jemmet, A. E., "Inter-Relation of Surface Chemistry of Silicones and Diesters at Elevated Temperatures", Wear 15, 137-141 (1970A).
- * Jemmet, A. E., "Review of Recent Silicone Work", Wear 15, 143-148 (1970B).
- Johnson, K. I. and Keller, D. V., "Effect of Contamination on the Adhesion of Metallic Couples in Ultra High Vacuum", J. Appl. Phys. 38, 1896-1904 (1967).
- Johnson, K. L., "Regimes of Elastohydrodynamic Lubrication", IME Jour. Mech. Eng. Sci. 12, 9-16 (1970A).
- Johnson, R. E. and Dettre, R. H., "Contact Angle Hysteresis: I. Study of an Idealized Rough Surface, pp. 112-135; II. Contact Angle Measurements on Rough Surfaces, pp. 136-144", in "Contact Angle, Wettability and Adhesion", Adv. in Chem. Ser. 43, ACS, Washington, D.C., 1964.

- Johnson, R. E. and Dettre, R. H., "Wettability and Contact Angles", in "Surface and Colloid Science", E. Matijevic, Ed., 2, 85: Wiley, 1968.
- Johnson, R. L., Godfrey, D. and Bisson E. E., "Friction of Surface Films Formed by Decomposition of Common Lubricants of Several Types", NACA TN 2076 (April 1950).
- Johnson, R. L., Informal talk at Int. Res. Group on Wear of Eng. Mat., Delft, Holland, April 2, 1970B).
- Jones, D. R. H. and Chadwick, G. A., "Experimental Measurement of the Solid-Liquid Interfacial Energies of Transparent Materials", Phil. Mag. 22 #176, 291-300 (1970).
- Jost, P., "Lubrication (Tribology)," Her Majesty's Stationery Office, London, 1966.
- Kagiya, T., Sumida, Y. and Inoue, T., "A Measure of the Electron-donating Power and Electron-accepting Power of Liquid Organic Compounds", Bull. Chem. Soc. Japa. 41, 767-773 (1968).
- Kanekar, C. R. and Khetrapal, C. L., "Estimation of Aromaticity from Dilution Shifts - An Extension of the Method for Compounds Without Protons", Curr. Sci. 36, 67 (1967).
- Kannel, J. W., "A Study of the Influence of Lubricants on High Speed Rollings-Contact Bearing Performance", Technical Report ASD-TDR-61-643, Part VIII (June 1968).
- Karashaev, A. A., Zadumkin, S. N. and Kuphno, A. I., "Temperature Dependence of the Surface Tension of Gallium and Its Interfacial Tension at the Interface with Some Nonpolar Organic Liquids", Poverkh. Yavleniya Rasplavakh 1968, 219-225 (1968).
- Keller, D. V., "Adhesion Between Solid Metals", Wear 6, 353-365 (1963).
- Khrushchov, M. M. and Babichev, M. A., "An Investigation of the Wear of Metals and Alloys by Rubbing on an Abrasive Surface", Friction and Wear in Machinery, Vol. 11, American Society of Mechanical Engineers, 1-12, 1956A.
- Khrushchov, M. M. and Babichev, M. A., "Investigation of the Effect of Abrasive Hardness on Wear of Metals", Friction and Wear in Machinery, Vol. 11, American Society of Mechanical Engineers, 13-19, 1956B.
- Khrushchov, M. M., "Resistance of Metals to Wear by Abrasion, as Related to Hardness", Proceedings of the Conference on Lubrication and Wear, London, Institution of Mechanical Engineers, 1957, pp. 655-659.
- Khrushchov, M. M. and Babichev, M. A., "Resistance to Abrasive Wear of Structurally Inhomogeneous Materials", Friction and Wear in Machinery, 12, ASME Transl. 5-24 (1958).

- Khrushchov, M. M. and Babichev, M. A., "Resistance to Abrasion and the Elastic Moduli of Metals and Alloys", in Russian, Dokl. Akad. Nauk. SSSR 131, No. 6, 1319-22; in English, Sov. Phys. Doklady 5, No. 2, 410-412 (1960).
- Khrushchov, M. M. and Babichev, M. A., "Correspondence Between the Relative Abrasive-Wear Resistance of Metals, Alloys and Some Minerals, and their Moduli of Elasticity", Fric. and Wear in Machinery 17, 1-8 (1962) ASME Transl. 1965A.
- Khrushchov, M. M. and Babichev, M. A., "Abrasive-Wear Resistance and the Modulus of Elasticity of Heat-Treated Steels", Fric. and Wear in Machinery 17, 9-18 (1962) ASME Transl. 1965B.
- Khrushchov, M. M. and Babichev, M. A., "The Effect of Heat Treatment and Work Hardening on the Resistance to Abrasive Wear of Some Alloy Steels", Fric. and Wear in Machinery 19, 1-15 (1965) ASME Transl. 1967.
- Kingsbury, E. P., "The Heat of Adsorption of a Boundary Lubricant", ASLE Trans. 3, 30 (1960).
- Kingsbury, E. P., "Experimental Observations on Instrument Ball Bearings", MIT Inst. Lab. Report E-2316, Sept. 1968.
- Kislyi, P. S. and Kuzenkova, M. A., "Estimation of the Surface Energy of Some Metals and Refractory Compounds", Porosh. Met. 9 (10), 39-43 (1969).
- *Klaus, E. E. and Bieber, H. E., "Effects of P³² Impurities on the Behavior of Tricresyl Phosphate on Steel", ASLE Transl. 8, 12 (1965).
- Klemgard, E. N., "The Manufacture of Lubricating Greases", Reinhold, N.Y. 1937.
- Kolfenbach, J. J. and Morway, A. J., "New Thickener System Extends Range of Multipurpose Greases", Fifth World Pet. Cong. VI, 239 (1959).
- Kostikov, V. I., Kharitonov, A. V. and Savenko, V. I., "Determination of Surface Energy for Titanium in the Solid Phase", Fiz. Met. Metalloid, 26, 568 (1968).
- Kotzé, I. A. and Kuhlmann-Wilsdorf, D., "A Theory of the Interfacial Energy Between a Crystal and its Melt", Appl. Phys. Letters 9, #2, 96 (1966).
- Kragelskii, I. V., "Friction and Wear", Transl. in Eng. by Butterworths, Ltd., 1965.
- Kramer, J., "Studies with the Geiger Point Counter on Worked Nonmetals", Z. Physik, 128, 538 (1950).
- Kreuz, K. L., Fein, R. S. and Rand, S. J., "Solubilization Effects in Boundary Lubrication", ACS Petr. Div. Preprint, A126 (Sept. 7-12, 1969).

- *Ku, T. C. and Pimbley, W. T., "Effect of Temperature on the Emission of Electrons from Abraded Surfaces of Beryllium, Calcium, Aluminum and Magnesium," J. Appl. Phys., 32, 124 (1961).
- Kubaschewski, O. and Hopkins, B. E., "Oxidation of Metals and Alloys", 2nd Ed. Academic Press, New York, 1962.
- Kubaschewski, O. et al., "Metallurgical Thermochemistry", 4th Ed., Pergamon, New York, 1967.
- *Kuznetsov, V. D., "Metal Transfer and Build-Up in Friction and Metal Cutting", 1st Ed., Pergamon Press, 1965-6.
- Lang, N. D. and Kohn, W., "Theory of Metal Surfaces: Charge Density and Surface Energy", Phys. Rev. B, 1, 4555-4568 (1970).
- Lee, L.-H., "Adhesion of High Polymers. II. Wettability of Elastomers", J. Poly. Sci. Part A-2 5, 1103-1118 (1967).
- Lee, L.-H., "Relationships Between Surface Wettability and Glass Temperatures of High Polymers", J. Appl. Poly Sci. 12, 719-730 (1968).
- Levine, O. and Zisman, W. A., "Physical Properties of Monolayers Adsorbed at the Solid Interface. II. Mechanical Durability of Aliphatic Polar Compounds and Effect of Halogenation", J. Phys. Chem. 61, 1188 (1957).
- Li, K. Y. and Ling, F. F., "The Sliding of Copper-Based Sintered Material Against Steel in Paraffinic Mineral Oil", Wear 15, 249-256 (1970).
- Likhtman, P. A., Rebinder, P. A., and Karpenko, G. V., "Effect of a Surface Active Medium on the Deformation of Metals", Her Majesty's Stationary Office, 1958.
- Ling, F. F. and Weiner, R. S., "A Bifurcation Phenomenon of Static Friction", Trans. ASME, Ser. E, 28, 213-7 (1962).
- Ling, F. F., et al., "Boundary Lubrication. An Appraisal of World Literature", American Society of Mechanical Engineers, New York, 1969.
- Lomakin, V. S., "Investigation of Wear of Sleeves and Piston Rings of Mud Pumps", Friction and Wear in Machinery (transl. by ASME) 11, 39 (1956).
- *Loomis, W. R. and Hady, W. F., "Lubrication with Some Polyphenyl Ethers and Super-refined Mineral Oils in 600 F (316 C) Inerted Pump Loop", NASA TN D-5096 (1969).
- Loomis, W. R. and Johnson, R. L., "Resin Additive Improves Performance of High Temperature Hydrocarbon Lubricants", NASA Tech. Brief 71-10394 (1971).
- Lundberg, G. and Palmgren, A., "Dynamic Capacity of Rolling Bearings", J. Appl. Mech. 16, No. 2, 165-172 (1949).
- MacGregor, C. W., "Handbook of Analytical Design for Wear", Plenum Press, New York 1964.
- Machlin, E. S. and Yankee, W. R., "Friction of Clean Metals and Oxides with Special Reference to Titanium", J. Appl. Phys. 25, 576-581 (1954).

- Maev, V. E., "Investigations on the Abrasive Properties of Small Solid Mineral Particles", *Fric. and Wear in Mach.* 19, ASME Transl. 51-64 (1965).
- Maffiolo, G., Vidal, J. and Renon, H., "Cohesive Energy of Liquid Hydrocarbons", *Ind. Eng. Chem. Fundam.* 11, 100-105 (1972).
- Mahncke, H., personal communication (1971).
- Maitland, A. H. and Chadwick, G. A., "The Cleavage Energy of Zinc", *Phil. Mag.* 16, 645-651 (1969).
- Matuszak, A. H. and Morway, A. J., "Synthetic Lubricating Composition", U.S. Pat. 2,889,281 (June 2, 1959).
- *Mayer, S. W., "Dependence of Surface Tension on Temperature", *J. Chem. Phys.* 38, 1803 (1963).
- *Mays, C. W., Vermaak, J. S. and Kuhlmann-Wilsdorf, D., "On Surface Stress and Surface Tension: II. Determination of the Surface Stress of Gold", *Surf. Sci.* 12, 134-140 (1968).
- *McClellan, A. L., "Tables of Experimental Dipole Moments", Freeman (San Francisco), 1963.
- *McCool, J. I., "Load Ratings and Fatigue Life Predictions for Ball and Roller Bearings", ASME Trans., Ser. F, *Jour. of Lubr. Tech.*, 92, 16-22 (1970).
- Merchant, M. E., "Friction and Adhesion", in "Interdisciplinary Approach to Friction and Wear", NASA SP-181, Washington, D.C., 1968.
- *Mints, R. I. and Kortov, V. S., "Exoelectronic Emission During the Deformation of the Surface of Austenitic Steels by the Action of Microshock", *Tr. Uralsk Politekhn Inst.*, 143, 15 (1965).
- Moeller, C. E. and Noland, M. C., "Cold Welding Tendencies and Frictional Studies of Clean Metals in Ultra-High Vacuum", ASLE Trans. 10, 146-157 (1967).
- Montgomery, R. S., "Run-In and Glaze Formation on Gray Cast Iron Surfaces", *Wear* 14, 99-105 (1969).
- *Montgomery, R. S., "Friction and Wear of Some Bronzes under Lubricated Reciprocating Sliding", *Wear* 15, 373-387 (1970).
- Moorthy, V. K. and Tooley, F. V., "Effect of Certain Organic Liquids on Strength of Glass", *J. Am. Cer. Soc.* 39, 215-7 (1956).
- Morecroft, D. W., "Reaction of n-Octadecane and Decolic Acid with Clean Iron Surfaces", *Wear* 18, 333-340 (1971).
- Morris, J. A., "Metallic Bearing Materials", in "Lubrication and Lubricants", E. R. Braithwaite, Ed., Elsevier Publ. Co., 1967.
- Mullins, W. W., in "Metal Surfaces: Structure, Energetics and Kinetics", 17 (American Society for Metals, Ohio, 1962).
- *Murlson, C. A., "Investigation of Thin Films of Organic Substances by Electron Diffraction", *Phil. Mag.*, 17, 201 (1934).

- *Murr, L. E., "Stacking-Fault Anomalies and the Measurement of Stacking-Fault Free Energy in F.C.C. Thin Films", Thin Sol. Films 4, 389-412 (1969).
- Myers, R. S., "Thermodynamics of Liquid Solutions, Parts A and B", Ph.D. Thesis, Emory U. (1969).
- Naeser, G., "Mechanical Activation of Solid Materials and Its Technological Significance", Int. Jour. Powder Met. 9, No. 2, 3-12 (1970).
- Nathan, G. K. and Jones, W. J., "Influence of the Hardness of Abrasives on the Abrasive Wear of Metals", Lubr. and Wear Fifth Conv., Inst. Mech. Eng., London, 215-221 (1967).
- Neale, M. J., et al., "Dry Rubbing Bearings - A Guide to Design and Material Selection", No. 68018, Engineering Sciences Data Unit, 251-259 Regent St., London, W. 1 (1968).
- Neumann, A. W. and Tanner, W., "The Temperature Dependence of Contact Angles - Polytetrafluoroethylene/n-Decane", J. Coll. and Interf. Sci. 34, 1-8 (1970).
- Neumann, A. W. and Good, R. J., "Thermodynamics of Contact Angles. I. Heterogeneous Solid Surface", J. Coll. and Interf. Sci. 38, 341-358 (1972).
- Nevitt, M. V., "Alloy Chemistry of Transition Elements", Table XIII, pp. 101-178, in "Electronic Structure and Alloy Chemistry of the Transition Elements", Ed. P. A. Beck, Interscience-Wiley, New York 1963.
- Nurse, R. W., "Surface Energy, Adhesion and Cohesion in Solids", Proc. 9th Conf. Silicate Ind., Budapest, 129-141 (1968).
- * O'Connell, J. P. and Prausnitz, J. M., "Application of Statistical Mechanics", Ind. Eng. Chem. 60, 36 (1968).
- O'Connor, J. J., Boyd, J. and Vallone, E. A., "Standard Handbook of Lubrication Engineering", McGraw-Hill, New York 1968.
- Okrent, E. H., "The Effect of Lubricant Viscosity and Composition on Engine Friction and Bearing Wear", ASLE Trans. 4, 97-108 (1961A).
- Okrent, E. H., "The Effect of Lubricant Viscosity and Composition on Engine Friction and Bearing Wear. II." ASLE Trans. 4, 257-262 (1961B).
- Okrent, E. H., "Engine Friction and Bearing Wear. III. The Role of Elasticity in Bearing Performance", ASLE Trans. 7, 147-152 (1964).
- Østvik, R. and Christensen, H., "Changes in Surface Topography with In", Proc. I. M. E. 183(3P), 57-65 (1968-9).
- * Padday, J. F. and Uffindell, W. D., "The Calculation of Cohesive and Adhesive Energies from Intermolecular Forces at a Surface", J. Phys. Chem. 72, 1407 (1968).
- Panzer, J., "Components of Solid Surface Free Energy from Wetting Measurements" J. Coll. and Interf. Sci., awaiting publication (1972).

- Parfitt, G. D., "Dispersion", J. Oil Col. Chem. Assoc. 50, 822-843 (1967).
- Pask, J. A., Personal Interview (Jan. 9, 1970).
- Peterson, M. B. and Johnson, R. L., "Factors Influencing Friction and Wear with Solid Lubricants", Lubrication Eng., 11, 325 (1955).
- Philippoff, W., "Grenzflächenerscheinungen an Kolloid", in "Kolloidchemisches Taschenbuch, 5. Aufl. Akademische Verlagsgesellschaft Geest and Portig K.-G., Leipzig, 1960.
- Pike, W. C. and Spillman, D. T., "Effects of Seizure-Delay on Transition Temperatures in the 4-Ball Machine", ASLE Trans. 13, 127-133 (1970).
- Prausnitz, J. M., "Molecular Thermodynamics of Fluid-Phase Equilibria", Prentice-Hall, Englewood Cliffs, New Jersey, 1969.
- Quayle, O. R., "The Parachors of Organic Compounds", Chem. Rev. 53, 439-589 (1953).
- Quinn, T. F. J., "The Effect of 'Hot-Spot' Temperatures on the Unlubricated Wear of Steel", ASLE Trans. 10, 158-168 (1967).
- Quinn, T. F. J., "An Experimental Study of the Thermal Aspects of Sliding Contacts and Their Relationship to the Unlubricated Sliding of Steel", Proc. Instn. Mech. Eng., 183, Pt3P, 129 (1968-9).
- Quinn, T. F. J., "Oxidative Wear Mechanisms, Chemical Effects at Bearing Surfaces", Conference at Swansea, Preprint pages 187-201 (January 1971A).
- Quinn, T. F. J., "Oxidative Wear Mechanisms", Wear 18, 413-420 (1971B).
- Rabinowicz, E. and Kingsbury, E. P., "Lubricants for Titanium", Metal Prog. (May 1955).
- Rabinowicz, E., "New Coefficients Predict Wear of Metal Parts", Prod. Eng. 39, 71-73 (June 23, 1958).
- Rabinowicz, E. and Mutis, A., "Effect of Abrasive Particle Size on Wear", Wear 8, 381-390 (1965A).
- Rabinowicz, E., "Friction and Wear of Materials", John Wiley and Sons, New York, 1965B.
- Rabinowicz, E., "Compatibility Criteria for Sliding Metals", in "Friction and Lubrication in Deformation Processing", New York, 90-101 (1966).
- Rabinowicz, E., "Lubrication of Metal Surfaces by Oxide Films", ASLE Trans. 10, 400-407 (1967).
- Rabinowicz, E., "The Determination of the Compatibility of Metals through Static Friction Tests", ASLE Trans. 14, 198-205 (1971A).
- Rabinowicz, E., "The Influence of Compatibility on Different Tribological Phenomena", ASLE Trans. 14, 206-212 (1971B).

- *Ramsey, J. A., "The Emission of Electrons from Aluminum Abraded in Atmospheres of Air, Oxygen, Nitrogen and Water Vapor", *Surf. Sci.* 8, 313 (1967).
- Reid, R. C. and Sherwood, T. K., "Properties of Gases and Liquids", 2nd Ed. McGraw-Hill, New York, 1966.
- Rhee, S. K., "Wetting of Ceramics by Liquid Aluminum", *J. Am. Cer. Soc.* 53, 386-389 (see also 409) (1970).
- Rhee, S. K., "Wetting of Ceramics by Liquid Metals", *J. Am. Cer. Soc.* 54, 332-4 (see also 376-381) (1971).
- Ries, H. E., Jr. and Kimball, W. A., "Electron Micrographs of Monolayers of Stearic Acid," *Nature* 4613, 901 (1958).
- Roach, A. E., Goodzeit, C. L. and Hunnicut, R. P., "Scoring Characteristics of Thirty-Eight Different Elemental Metals in High-Speed Sliding Contact with Steel", *Trans. ASME* 78, 1659 (1956).
- *Roberts, R. W. and Owens, R. S., "Titanium Lubrication", *Nature* 200, 357 (1963A).
- *Roberts, R. W., "Adsorption and Decomposition of Hydrocarbons on Clean Metal Films", *Brit. J. Appl. Phys.* 14, 485 (1963F).
- *Roberts, R. W., "Reactions of Saturated Hydrocarbons with Clean Rhodium Films", *Ann. N.Y. Acad. Sci.* 101, 766 (1968).
- Roberts, W. H., "Lubrication Without Oils", Paper No. 6 presented 30 Sept. - 1 Oct. 1969 at National Center of Tribology symposium UKAEA, Risley, Warrington, Lancs, England.
- Rogers, M. D., "The Mechanism of Scuffing in Diesel Engines," *Wear*, 15, 105 (1970).
- Rounds, F. G., "Effects of Base Oil Viscosity and Type on Bearing Ball Fatigue", *ASLE Trans.* 5, 172 (1962).
- Rounds, F. G., "Some Effects of Additives on Rolling Contact Fatigue", *ASLE Trans.* 10, 243 (1967).
- Rowe, C. N., "Some Aspects of the Heat of Adsorption in the Function of a Boundary Lubricant", *ASLE Trans.* 9, 100 (1966).
- Rowe, C. N., "A Relation Between Adhesive Wear and Heat of Adsorption for the Vapor Lubrication of Graphite", *ASLE Trans.* 10, 10 (1967).
- Rowe, C. N., Comments on "Wear" by J. F. Archard, *Interdisc. App. to Fric. and Wear*, NASA SP-181, p. 314 (1968).
- Rowe, C. N., "Role of Additive Adsorption in the Mitigation of Wear", *ASLE Trans.* 13, 179-188 (1970).
- Rowe, G. W. and de Gee, A. W. J., "Friction, Wear and Lubrication - Tribology - Glossary", *Org. for Econ. Co-op. and Dev. Paris*, (available from OECD Publications Center, Suite 1305, 1750 Pennsylvania Ave., N.W., Washington, D.C. 20006, phone (202)298-8755), 1969.

- Rudston, S. G. and Whitby, R. D., "The Effect of Model Lubricating Oil Constituents on the Wear of Steel", J. Inst. Petr., 57, 189-203 (1971).
- Runk, R. B., Shanefield, D. J., Brandner, J. L. and Radke, L. L., "Adhesion of Gold on Sapphire", Abst. in Cer. Bull. 50, 398 (Apr. 1971).
- Saibel, E., "A Statistical Approach to Run-In and the Dependence of Coefficient of Friction on Velocity", Paper IRG-70-4, Delft, Holland (April 2, 1970).
- Sakurai, T. and Baba, T. (title not translated), J. Jap. Petr. Inst. 1, 33-58 (1958).
- Sakurai, T. and Sato, K., "A Kinetic Study on the Reaction of Labeled Sulfur Compounds with Steel Surfaces during Boundary Lubrication," ASLE Trans. 8, 39-47 (1965).
- Sakurai, T. and Sato, K., "Study of Corrosivity and Correlation Between Chemical Reactivity and Load Carrying Capacity of Oils Containing Extreme Pressure Agents", ASLE Trans. 9, 77-87 (1966).
- Sakurai, T., Okabe, H. and Takahashi, Y., "A Kinetic Study of Labeled Sulfur Compounds in Binary Additive Systems During Boundary Lubrication," ASLE Trans. 10, 91-101 (1967).
- Sakurai, T. and Sato, K., "Chemical Reactivity and Load Carrying Capacity of Lubricating Oils Containing Phosphorus Compounds", ASLE Trans. 13, 252-261 (1970).
- Sakurai, T. and Okabe, H., "Wear Rate of Copper Under Boundary Lubrication", ASLE Trans. 14, 221-225 (1971).
- Schatzberg, P. and Felsen, I. M., "The Influence of Water and Oxygen on Rolling Contact Lubrication", ACS Petr. Div. Preprints 13, #2, B49-60 (1968).
- Schatzberg, P., "Influence of Water and Oxygen in Lubricating Oils on Sliding Wear", Lubr. Eng., 301 (Sept. 1970); comments 462 (Dec. 1970A).
- Schatzberg, P., "Inhibition of Water-Accelerated Rolling-Contact Fatigue", ASME Preprint 70LUB-9, 1970B.
- Schmidt, R. L., "I - Application of Theoretical Models to the Surface Tension of Binary Mixtures", Ph. D. Thesis, Emory U. (1967).
- Scully, J. C. and Hoar, T. P., "Mechanochemical Anodic Dissolution of Iron-Nickel Alloys in Hot Chloride Solution at Controlled Electrode Potential", Proc. 2nd Int. Cong. on Met. Corr., N.A.C.E., New York (1963).
- Senior, J. M. and West, G. H., "Interaction Between Lubricants and Plastic Bearing Surfaces", Wear 18, 311-324 (1971).

- Shain, S. A. and Prausnitz, J. M., "Thermodynamics and Interfacial Tension of Multicomponent Liquid-Liquid Interfaces", A.I.Ch.E. Jour. 10, 766 (1964).
- Shaw, P. E. and Leavey, E. W. L., "Friction of Dry Solids in Vacuo", Phil. Mag., Series 7, 10, 809-822 (1930).
- Shirley, D. A. and Goan, J. C., "Competitive Metalation of Some Nitrogen and Sulfur Containing Heterocycles", J. Organomet. Chem. 2, 304 (1964).
- Sikorski, M. E., Correlation of the Coefficient of Adhesion with Various Physical and Mechanical Properties of Metals", ASME Jour. of Basic Eng. 85, 279 (1963).
- Small, P.A., "Some Factors Affecting the Solubility of Polymers", J. Appl. Chem. 3, 71 (1953).
- Smith, A. J. and Cameron, A., "Preliminary Studies of Thick Surface Films", Special Discussions of the Faraday Society, No. 1 (1970).
- Smith, T., "Theoretical Equations of State and Molecular Configuration of Rod-Shaped Molecules on a Metal Surface: Alkanes, Alcohols, and Carboxylic Acids on Hg", J. Coll. Interf. Sci. 30, 183-199 (1969 A).
- Smith, T., "Spherical and Flat Shaped Molecules on a Mercury Surface", J. Coll. Interf. Sci. 31, 270-277 (1969B).
- Spielman, L. A. and Goren, S. L., "Capture of Small Particles by London Forces from Low Speed Liquid Flows", Envir. Sci. and Tech. 4, No. 2, 135-140 (1970).
- Spink, J. A., "Thermal Desorption of Stearic Acid Monolayers from Silver and Mica", J. Coll. and Interface Sci. 24, 61-70 (1967).
- Spurr, R. T. and Newcomb, T. P., "The Friction and Wear of Various Materials Sliding Against Unlubricated Surfaces of Different Types and Degrees of Roughness", Proceedings of the Conference on Lubrication and Wear, London, Institution of Mechanical Engineers, 1957, pp. 269-275.
- Spurr, R. T., "Frictional Behavior of Metals on a Crossed Cylinder Apparatus", Wear, 5, 55-59 (1962).
- Spurr, R. T., "The Coefficient of Friction of Metals", Wear 7, 330-333 (1964).
- Spurr, R. T., "The Coefficient of Friction of Metals at Slip", Wear, 10, 332 (1967).
- Spurr, R. T., "Boundary Lubrication of Metals", Wear 14, 207 (1969).
- Spurr, R. T., "The Wear Rate of Metals", Wear, 17, 279-283 (1971).
- Spurr, R. T., The Static and Dynamic Friction of Metals", Wear 19, 61-65 (1972).
- Stoloff, N. S., "Liquid Metal Embrittlement", in "Surfaces and Interfaces II", J. J. Burke, N. L. Reed and V. Weiss, eds., Sagamore Army Mat. Res. Conf. 14, 157-182, Syracuse U. Press (1968).
- Studt, P., "Correlation Between Adsorbability and Effectiveness of E.P. Additives in Lubricating Oils", Erdöl Kohle 21, #12:784 (1968).

- Tabor, D. and Winer, W. O., "Silicone Fluids: Their Action as Boundary Lubricants", ASLE Trans. 8, 69-77 (1965).
- Tabor, D. and Willis, R. F., "The Formation of Silicone Polymer Films on Metal Surfaces at High Temperatures and Their Boundary Lubricating Properties", Wear 13, 381 (1969).
- Takenaka, T., Nogami, K., Gotoh, H. and Gotoh, R., "Studies on Built-up Films by Means of the Polarized Infrared ATR Spectrum. I. Built-up Films of Stearic Acid", J. Coll. and Interface Sci. 35, 395-402 (1971).
- Tallian, T. E., Chiu, Y. P., et al, "Lubricant Films in Rolling Contact of Range Surfaces", A.S.L.E. Transactions 7, 2, p. 109 (1964).
- *Tallian, T. E. and McCool, J. L., "The Observation of Individual Asperity Interactions in Lubricated Point Contact", ASLE Trans. 11, 176-190 (1968).
- Tallian, T. E., Personal communication (1971).
- Tao, F. F., "The Role of Diffusion in Corrosive Wear", ASLE Trans. 11, 121 (1968A).
- Tao, F. F. and Appeldoorn, J. K., "The Ball-on-Cylinder Test for Evaluating Jet Fuel Lubricity", ASLE Trans., 11, 345 (1968B).
- Tao, F. F., "A Study of Oxidation Phenomena in Corrosive Wear", ASLE Trans. 12, 97 (1969).
- Tao, F. F. and Appeldoorn, J. K., "An Experimental Study of the Wear Caused by Loose Abrasive Particles in Oil", ASLE Trans. 13, 169 (1970).
- Tenwick, N. and Earles, S. W. E., "A Simplified Theory for the Oxidative Wear of Steels", Wear 18, 381-392 (1971).
- Thompson, R. A. and Bocchi, W., "A Model for Asperity Load Sharing in Lubricated Contacts", ASLE Trans. 15, 67-79 (1972).
- Thomsen, E. S., "Concerning Solubility Parameters", Farmaceuten, 30, 44-48 (1967).
- Timmons, C. O., Patterson, R. L. and Lockhart, L. B., Jr., "The Adsorption of C¹⁴-Labeled Stearic Acid on Iron", J. Coll. and Interface Sci. 26, 120-127 (1968).
- Tomlinson, G. A., "A Molecular Theory of Friction", Phil Mag., Series 7, 7, 905-939 (1929).
- Trapnell, B. M. W., "Paraffin Sorption on Clean Metals. Part 1: The Behaviour of Different Metals towards CH₄ and C₂H₂", Trans. Farad. Soc. 52, 1618 (1956).
- Turnbull, D., "Formation of Crystal Nuclei in Liquid Metals", J. Appl. Phys. 21, 1022 (1950).
- Udin, H., Sheler, A. J. and Wulff, W., "The Surface Tension of Solid Copper", AIMME Metal Trans. 185, 186-190 (1949).

- Uhlig, H. H., Feng, I-M., Tierney, W. D. and McClellan, A., "A Fundamental Investigation of Fretting Corrosion", NACA Tech. Note 3029, (1953).
- Vaessen, G. H. G. and de Gee, W. J., "Influence of Water Vapour on the Wear of Lightly Loaded Contacts", Preprint of Conf. on Chemical Effects at Bearing Surfaces", Wear 18, 325-332 (1971).
- Valori, R. R., Tallian, T. W. and Sibley, L. B., "Elastohydrodynamic Film Effects on Load-Life Behavior of Rolling Contacts", ASME Preprint 65-LUBS-11 (June 6-8, 1965).
- *Vaubel, G. and Baessler, H., "Determination of the Energy of Conduction States in Anthracene Crystals by Photoemission of Electrons from Sodium", Phys. Status Solo., 26, 599 (1968).
- Vere, R. A., "Lubricity of Aviation Turbine-Fuels", SAE Trans. 78, Sect. 4, 2237-45 (1969).
- Vermaak, J. S., Mays, C. W. and Kuhlmann-Wilsdorf, D., "On Surface Stress and Surface Tension: I. Theoretical Considerations", Surf. Sci. 12, 128 (1968).
- Vinogradov, C. V., Laing, K., and Pavlooskays, N. T., "Effects of Prooxidants and Antioxidants on the Lubricating Action of Petroleum Oils", Neftekjimiya, 1, 427 (1961).
- *Vinogradov, G. V., Nametkin, N. S. and Nossov, M. I., "Antiwear and Antifriction Properties of Polyorganosiloxanes and Their Mixtures with Hydrocarbons", J. Basic. Engr., Trans. ASME 747-753 (1965).
- Vitovec, F. H., "The Growth Rate of Fissures During Hydrogen Attack of Steels", Proc. A.P.I., 44 III, 179-188 (1964).
- Vold, M. J., "Molecular Cross Sections in Films of Fatty Acids on Water", J. Coll. Sci. 7, 196-8 (1952).
- Vold, M. J., "The Effect of Adsorption on the Van der Waals Interaction of Spherical Colloidal Particles", J. Coll. Sci. 16, 1-12 (1961).
- Warke, W. R. et al., "The Effect of Lead on Micro-Crack Initiation and Propagation in Alloy Steels - Final Report - Phase II", U.S. Army Tank Comm. Contract No. DA-20-113-AMC-10820(T), Technical Report No. P0752, AD 701 047 (November 1969).
- Weale, K. E., "Chemical Reactions at High Pressures", Chemical Engineering Series, Spon., London (1967).
- Weimer, R. F. and Prausnitz, J. M., "Screen Extraction Solvents This Way", Hydr. Proc. Petr. Ref., 44, #9, 237 (1965).
- Wenzel, R. N., "Surface Roughness and Contact Angle", J. Phys. Chem. 53, 1466-7 (1949).

- Westbrook, J. H., "Surface Effects on the Mechanical Properties of Non-Metals", in "Surfaces and Interfaces II", J. J. Burke, N. L. Reed and V. Weiss, eds, Sagamore Army Mat. Res. Conf. 14, 95-138, Syracuse U. Press (1968).
- Westwood, A. R. C. and Lye, R. G., "The Technological Significance of Surfaces and Interfaces", in "Surfaces and Interfaces II", J. J. Burke, N. L. Reed and V. Weiss, eds, Sagamore Army Mat. Res. Conf. 14, Syracuse U. Press (1968).
- Westwood, A. R. C., "A Conceptual Approach to Understanding Environment-Sensitive Mechanical Behavior", Proc. Mech. Fail. Prev. Group 11, 3-8 (1970A).
- Westwood, A. R. C. and Goldheim, D. L., "Mechanism for Environmental Control of Drilling in MgO and CaF₂ Monocrystals", J. Amer. Cer. Soc. 53, 142-147 (1970B).
- *Widom, B., "Intermolecular Forces and the Nature of the Liquid State", Science 157, 375 (1967).
- *Wigotsky, V. W., "Liquid and Solid Lubrication", Design News 23, 37- (Dec. 6, 1968).
- *Williams, R. A., "Investigation of Exoelectron Emission from Various Materials Using Abrasion and Ultrasonic Techniques", AD-64242-2 (1966).
- *Williamson, J.B.P., "Topography of Solid Surfaces", in "Interdisciplinary Approach to Friction and Wear", NASA SP-181, Washington, D.C., 1968.
- Wistreich, J. G., "Lubrication in Wire Drawing", Proc. Conf. Lube and Wear, Paper 4C, p. 505 (1957).
- Wittman, F., "On the Influence of Surface Energy on the Strength of a Porous Solid", Z. Angew Phys. 25, 160 (1968).
- *Wojciechowski, K. F., "Note on Metal Surface Energy", Acta Physica Polonica, XXVI, 185 (1964).
- Wu, S., "Estimation of the Critical Surface Tension for Polymers from Molecular Constitution by a Modified Hildebrand-Scott Equation", J. Phys. Chem. 72, 3332 (1968).
- Wu, S., "Surface and Interfacial Tension of Polymer Melts - 1 - Polyethylene, Polyisobutylene and Polyvinyl Acetate", J. Coll. and Interf. Sci. 31, 153 (1969).
- Zadumkin, S. N. and Karashayev, A. A., "Surface Energy at Metal/Dielectric Liquid Interfaces", Soviet Materials Science (Eng. Trans.) 1, No. 2, 86 (1965).

Zadumkin, S. N. and Temrokov, A. I., "Simple Methods for Calculation of Surface Energy and Surface Tension of Ionic Crystals", Izv. Vys. Uch. Zved. Fizika 11, No. 9, 40-51 (1968).

Zettlemoyer, A. C., "Chemistry and Metallurgy of Wetting Solid Surfaces", in "Ohmic Contacts Semicond. Symp.", ed: B. Schwartz, 48-66 (1968).

Zisman, W. A., "Relation of Equilibrium Contact Angle to Liquid and Solid Constitution", in "Contact Angle, Wettability and Adhesion", p.1, Advances in Chemistry Series, #43, American Chemical Society, Washington, D.C. (1964).

Zisman, W. A., "Surface Energetics of Wetting, Spreading and Adhesion", J. Paint Tech. 44, NO. 564, 42-57 (1972).

* References marked with an asterisk are not specifically keyed in the text, for various reasons. Some were dropped in favor of more recent work, others are of such general interest as to have influenced sections too numerous to mention, and still others are simply good background.

APPENDIX III

Reprinted from JOURNAL OF COLLOID AND INTERFACE SCIENCE, Volume 35, No. 1, January 1971
Copyright © 1971 by Academic Press, Inc. Printed in U.S.A.

Surface Free Energy: A New Relationship to Bulk Energies

A. BEERBOWER

Government Research Laboratories, Esso Research and Engineering Co., Linden, New Jersey 07036

Received May 27, 1970

By means of an equation containing two adjustable coefficients it is possible to relate the surface free energy to the energy of vaporization, using the Hansen parameters for London force energy, polar energy, and hydrogen-bonding energy. The technique is applicable to simple organic liquids, mixtures of simple liquids, and most liquid metals. Hydroxy compounds, acidic and basic organic liquids, certain hexagonal and irregular metals, and most fused halides require special versions of the basic equation.

1. ORGANIC LIQUIDS

Hildebrand and Scott (1) derived an equation relating surface free energy γ to energy of vaporization:

$$\gamma = K'(\Delta H_v - P\Delta V)^{2/3}N^{1/3}, \quad [1]$$

where ΔH_v is the molar heat of vaporization, $P\Delta V$ the work of vaporization (generally closely approximated by RT , the gas constant times the absolute temperature), V the molar volume, and N Avogadro's number. The relationship was stated to hold for "regular" substances such as hydrocarbons and some inorganic liquids. In addition, their numerical evaluation resulted in an arbitrary value of K' , and an exponent of γ equaling 0.86, which destroyed the dimensional balance. A more general relationship would be useful because of the improvement in understanding of surface phenomena, even though it is generally easier to measure a surface free energy than to calculate one.

Hansen (2) has shown that the energy of vaporization can be split into three components

$$\Delta H_v - RT = A + B + C, \quad [2]$$

where A is the contribution of the London forces, B that due to dipole forces, and C the energy of the hydrogen bonds, reduced

dipoles, and probably other interactions. It is possible to estimate A by London's equation (1) but the data for this are generally not available. A far better procedure uses the corresponding states principle and a "homomorph." The latter is a hydrocarbon of similar molecular shape to that of the compound in question. A is simply the energy of vaporization of the homomorph at the same reduced temperature (T/T_c) and molar volume. Charts for this purpose were published¹ by Weimer and Prausnitz (3), but they tend to give slightly higher values than were used by Hansen (2). The writer (4) extended these charts but actually used Hansen's. Values in the present article are taken from reference 4 and Hansen's later article (5).

Hansen originally obtained B by trial and error fitting in a set of three-dimensional models depicting the solubility of polymers in the liquids to be evaluated. He subse-

¹ This very valuable article contains a number of misprints, which can be quite confusing at first reading. Figures 1-3 actually plot cal/cc rather than cal/gm mole as stated. The writer believes that Fig. 1 really refers to normal and iso paraffins, though it is labeled "normal." Equation 39 appears to lack the factor " RT " in the last two terms. The solubility parameter of a hexane-iso-octane blend appears to be high.

SURFACE FREE ENERGY

quently showed (5) that quite precise values could be obtained by:

$$B = \frac{12108}{V} \cdot \frac{\epsilon - 1}{2\epsilon + n^2} (n^2 + 2) \mu^2, \quad [3]$$

where ϵ is the dielectric constant, n the index of refraction, and μ the dipole moment. The writer later showed that good approximations could be obtained by

$$B = 336 \mu^2 \quad [4]$$

or

$$B = [RT(\epsilon - 1)(\epsilon - n^2)]/[\epsilon(n^2 + 2)], \quad [4A]$$

which require fewer data. Hansen's and the writer's values were expressed in terms of partial polar solubility parameter δ_p , from which

$$B = V\delta_p^2. \quad [5]$$

The "hydrogen-bonding" energy C is the most difficult to obtain directly. Hansen (5) demonstrated that acceptable values of C or the partial parameter δ_H could be calculated simply for hydroxy compounds. His equation, slightly modified by the writer (4), is

$$C = 4650 m, \quad [6]$$

where m is the number of OH groups. He apparently did not recognize an extension of this rule to the monocarboxylic acids, but his C values are well fitted by using $m = 0.5$.

In the study reported below, B and C values from references 4 and 5 were used where available. To fill in gaps, μ values from McClellan (6) were converted to B values with the use of Eq. [4], and C was determined by difference with the use of Eq. [2]. In a few cases, B and C values for functional groups were estimated on the basis of family relationships along the lines of Eq. [6].

In expanding Eq. [1] to cover complex liquids, it was assumed that the energy of surface formation would not include the full values of B and C , since these forces are specific in direction. The A forces, being omnidirectional, are carried at full strength. When we let aB and bC represent the values corrected for the number of molecular pairs

which resist separation during surface formation, and $K = K'/N^{1/3}$, Eq. [1] becomes:²

$$\gamma = K(A + aB + bC)/V^{2/3}. \quad [7]$$

Computer evaluation of this equation gives $K = 0.07147$, $a = 0.643$, $b = 0.620$ with a correlation coefficient of 0.984 for 100 liquids at 25°C. Regular liquids, electron donors, and electron acceptors were included, but donor-acceptors containing OH and COOH groups were not. The γ values were interpolated from Quayle (7) to 25°C.

This value of K came to the attention of a colleague, Dr. E. G. Baker. He commented (8) that some of his work had led to a similar factor since "the molecules of most liquids tend to occupy positions, on the average, at the corners of regular octahedra. Once that postulate is made the number of nearest-neighbors may immediately be calculated as 11.247 from knowledge of the total dihedral angle expressed as a multiple of 2π . If such structures persist throughout liquids, up to and including the surface layers, the number of nearest-neighbors would drop to 8 at the interface. The latter result can easily be deduced by constructing a surface layer out of half-octahedra. In the nest of half-octahedra, the edges of the square bases are shared. Accordingly, the fraction of "bonds" between nearest-neighbors that are broken at the interface relative to those existing in the interior, would be $(11.247 - 8.000)/11.247 = 0.2887$." Performing the necessary calculation of multiplying by 4.185×10^7 cal/erg and dividing by $2N^{1/3}$ (since cutting 1 cm² of liquid produced 2 cm²) we obtain $K = 0.07152$. Both of us feel that such agreement by two different approaches and with no adjustment whatever, implies that Dr. Baker's value of a 28.87% decrease in number of neighbor

² It would be very easy to divide this equation into a dispersion term γ^d and a "polar" term γ^p , in keeping with the practice of several recent authors, or to go farther than they have and separate the latter into a purely polar γ^p and an H-bonding γ^h . However, the writer feels that to do so at present might further disturb an already controversial situation, as he has not yet demonstrated what relationship such values would have to those already in use.

BEERBOWER

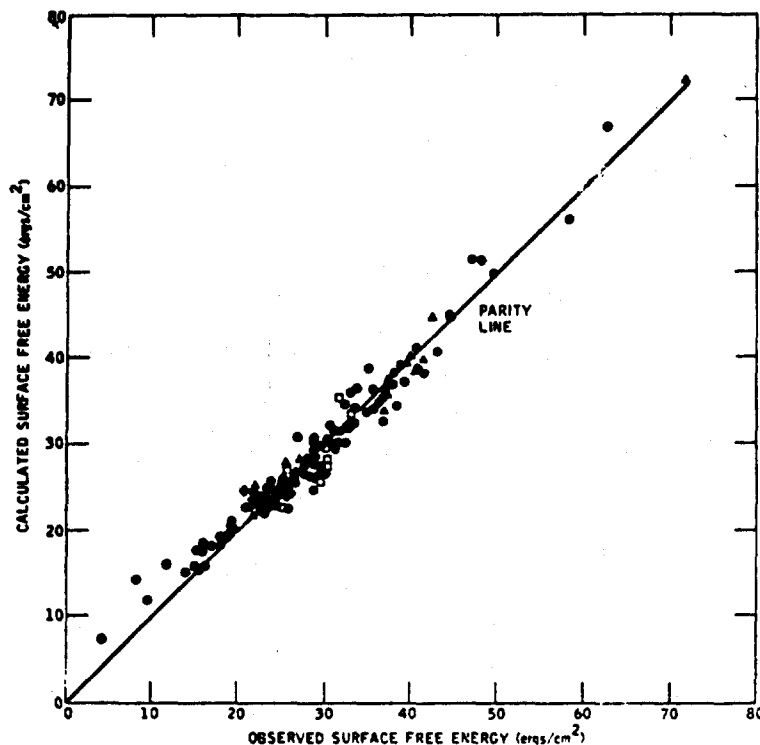


FIG. 1. Comparison of calculated and observed surface free energies for general class of liquids (●), paraffinic monohydric alcohols (◆), acids, phenols, and amines (▲), and some commercial mixtures of general class liquids (□).

bonds at the surface has fundamental significance.

The values of a and b are less fundamental. They can even be considered equal without any great loss of accuracy of correlation. Such equality would be consistent with the thinking of Weimer and Prausnitz (3), who lumped B and C together with a coefficient between 0.100 and 0.208 for liquid-liquid extractions. Even when they were kept separate, Hansen (5) found both a and $b = 0.25$ to fit his data on 10,000 polymer solutions, and the writer (4) found $a = b = 0.19$ for rubber swelling. The resulting correlation is shown in Fig. 1, based on

$$\gamma = 0.0715 [A + 0.632(B + C)]/V^{2/3} \quad [8]$$

It is generally believed that proton donors such as chloroform and acceptors such as acetone cannot hydrogen-bond to themselves. However, the evidence here is so clear that a bond of the same general properties exists in each of these pure liquids

that some explanation is required. Possibly, the equality of a and b implies that the bond is due to an induced dipole (3), though it seems more likely that these factors both represent a correction for the entropy of formation of molecular doublets.

Electron donor-acceptor liquids fall into two groups. The first of these is the paraffinic monohydroxy alcohols, which are so strongly hydrogen bonded as to resist pair-breaking and so give an exceptionally low value of b . As the value of K obtained independently for this group was essentially the same as for the other liquids, Baker's value of 0.0715 is used. A computed run on 15 alcohols resulted in $a = 1.044$ and $b = 0.060$. In view of the small number of data points, there would be essentially no loss in accuracy in rounding these off to

$$\gamma = K(A + B + 0.06C)/V^{2/3} \quad [9]$$

The points, plotted in Fig. 1, fall as close to the line as could be desired. Apparently, the

SURFACE FREE ENERGY

strong hydrogen bonding causes the lower energy dipole bonds to behave as if they were London forces.

Although it may seem paradoxical, the glycols and glycerol had to be excluded from this class. The same applies to ring alcohols such as benzyl, furfuryl, and cyclohexyl. Both groups fit into the general class. If all these cases are due to steric hindrance, it would appear likely that heavily hindered tertiary alcohols would behave in a similar manner. However, triethyl carbinol (7) shows only 25.2 ergs/cm²; this would class it with the other paraffinic monohydroxy alcohols.

The last group is more heterogeneous but seems to be logically consistent. The compounds included are the acids, phenols, and amines, but not the amides. Computer analysis of 16 data points yielded $a = 2.018$ and $b = 0.45$. After rounding off a and adjusting b , we obtained

$$\gamma = K(A + 2.0B + 0.481C)/V^{2/3} \quad [10]$$

The extraordinary behavior of the polar energy, which apparently works twice, can be attributed to the imperfection of the vapor of these compounds. It is known that the vapor of acetic acid is essentially all dimerized; this, of course, leads to a low value of ΔH_v . This effect results in a lower ΔH_v than is needed to account for the high surface free energy. It appears that the dimer is held together by dipole forces rather than hydrogen bonds. The dimerized vapor also accounts for the special value $m = 0.5$ for acids, noted under Eq. [6].

These points (3 acids, 3 phenols, 9 amines, and water) are shown in Fig. 1. Water fits best with this group, though its A , B , and C parameters had to be adjusted from Hansen's tentative values (5) to fit both Eqs. [2] and [9]. The values arrived at were $A = 1040$, $B = 1095$, and $C = 7720$ cal per mole.

The scatter may be attributed to literature errors on γ , to a lack of precision of A and B , to variations in a and b in violation of the assumption that all compounds must fit Eq. [8], [9], or [10] with no gradations in between, or to a mixture of causes. Literature values below 15 ergs/cm² are especially suspect. One group found difficult to handle

was the n -paraffin hydrocarbons, for which the calculated results are too high by an amount that increases as some power of V . This is believed to represent increasing deviation from Baker's octahedral geometry due to their elongated shape.

A number of commercial liquids for which A , B , C , and γ were known are also plotted in Fig. 1. These are mostly hydrocarbon solvents, lubricants, and rubber process oils. The fit is sufficiently good that Eq. [8] has been adopted for estimating the solubility parameters of such liquids from surface free energy measurements.

II. LIQUID METALS

The liquid metals present a somewhat simpler picture than the organic liquids so far considered, and their properties at the melting point have already been correlated on a common basis with some organics by Bondi (9). Grosse (10) developed an equation for most of the metals closely related to [1]:

$$\gamma = 0.0665 \Delta H_v/V^{2/3} \quad [11]$$

(obtained by combining his equation [3] with his final one on page 1361). This was put into better form by Schonhorn (11), who based his analysis on the statistical mechanics "scaled particle theory" of Mayer (12):

$$\gamma = 0.0737 \Delta E_v/V^{2/3} \quad [12]$$

This differs from the conclusion reached for the organic liquids only by a factor of 1.03 and by the absence of the polar and H bond terms. Schonhorn limited this equation to the cubic and tetragonal metals; this might well be considered consistent with Baker's octahedral model. Both Grosse and Schonhorn found it necessary to set up a separate equation for the hexagonal and rhombohedral metals. Schonhorn's version is again the more logical, and consists simply of Eq. [12] multiplied by $(12/2)^{1/3}$. The results of substituting Baker's value of $K = 0.0715$ into these two equations are shown in Fig. 2. One special case is that of bismuth, which Grosse found behaves as a cubic metal despite its hexagonal structure. He attributed this anomaly to its other peculiarity

BEERBOWER

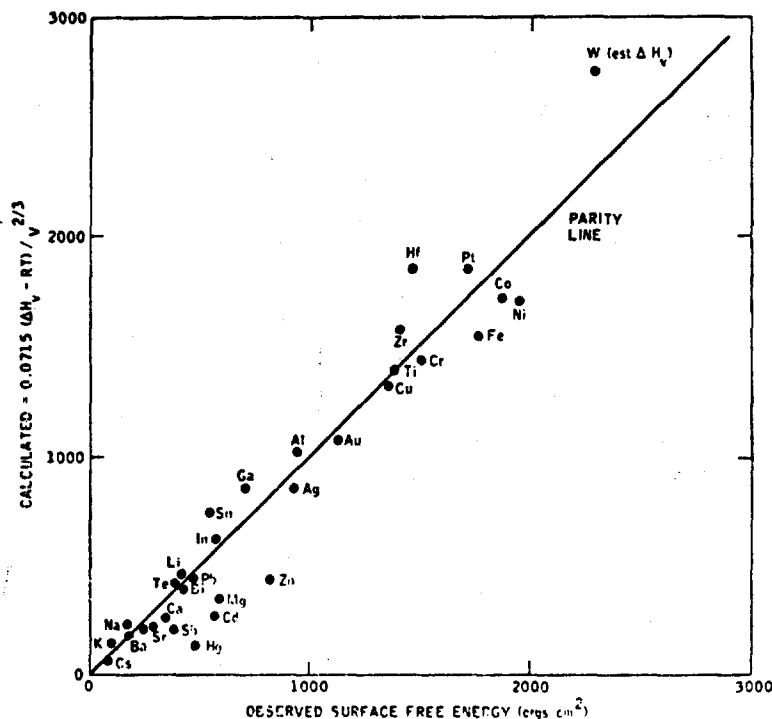


FIG. 2. Surface free energies of the liquid metals at their melting points

of expansion on freezing. The data for calcium are uncertain enough to fit either system, and those for germanium appear to be useless owing to impurities. However, most of the other metals are correlated by the simplest of the equations:

$$\gamma = 0.0715 \Delta E_v / V^{2/3} \quad [13]$$

Additional difficulties arise in applying this "hexagonal rule." The worst problem lies in the existence of other classifications than that used by Grosse. Hildebrand and Scott (1) classify antimony and bismuth as "sheet structure" and mercury as "complex", along with gallium, uranium, and manganese. An additional complication they show is that many metals undergo transition from cubic to hexagonal (or vice versa) before melting. Hence, we can say only that liquid mercury, zinc, cadmium, antimony, and magnesium require the equation:

$$\gamma = 0.130 \Delta E_v / V^{2/3} \quad [14]$$

III. FUSED SALTS

The surface free energies of fused alkali halides have received a great deal of attention, and there is a scattering of data on other inorganic salts. However, the picture is weak in terms of oxides, phosphates, and carbides, and totally blank on sulfides. Analysis of the surface free energy of halides may well start with those of the trivalent metals, arsenic, antimony, and bismuth. (No surface data were readily available on any tetrahalide except CCl_4 , which is already correlated in Eq. [8].) The available data fit quite well into Eq. [13], despite the fact that some of these halides are rhombohedral or hexagonal in crystal form. This casts some doubt on Schonhorn's reasoning on the basis for his $(12/2)^{1/3}$ rule, though not on its numerical usefulness. As that reasoning was based on Grosse's assumption that "some important elements of the crystal structure . . . persist in the liquid state," and, as this assumption has been disproved by Hildebrand for gallium (1), it was already of

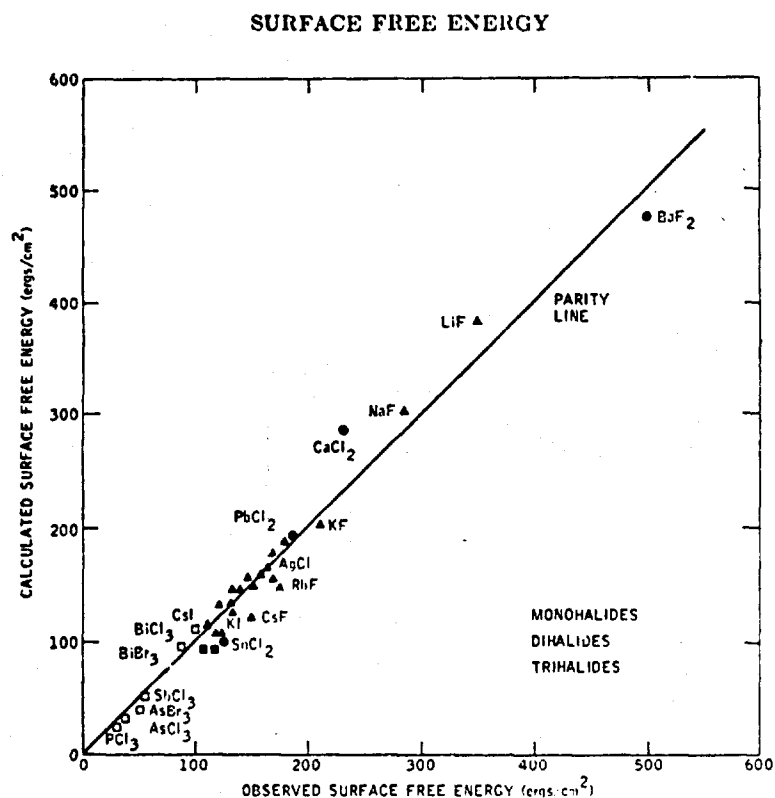


FIG. 3. Surface free energy of the fused metal halides (extrapolated to 298°K)

dubious value. Others have since failed to find any such order in other liquids. The fit of the six available points is shown in Fig. 3. The energies of vaporization were calculated from Kubaschewski's (13) values for latent heat of evaporation at 25°C, and the surface free energies extrapolated to the same temperature, with the use of equations of the form discussed in detail by Duga (14).

The monohalides were next examined. Fitting an equation of the type of [14] proved impossible, as a positive intercept was required:

$$\gamma = 0.0238 \Delta E_v / V^{2/3} + 50. \quad [15]$$

To account for this intercept, it appeared logical to turn to the organic acids and amines, where a similar situation arose (Eq. [10]). Both classes are distinctly ionic. By adding in additional polar energy (ΔE_p , presumably already includes $B = 336 \mu^2$, per Eq. [4]), and then reducing the London

energy by an empirical divisor, it was possible to obtain a good fit with:

$$\gamma = 0.0244 (\Delta E_v + 228 \mu^2) / V^{2/3} = K(0.342 A + 2B) / V^{2/3}. \quad [16]$$

The dipole moments were obtained from McClellan (6). The results are plotted in Fig. 3.

No satisfactory explanation can be offered for the 0.342. Even substituting a regular tetrahedron model for the half-octahedron results only in a factor of 0.511, and further reduction would require assumptions which hardly seem justified. It is interesting that Mayer (12) had no trouble obtaining good γ values from the compressibility of these liquids, so that the anomaly is apparently associated with ΔE_p . Perhaps the more complicated cell models cited by Patterson (15) will help to clarify this matter.

The data on dihalides are very scarce and

BEERBOWER

no dipole moments are available. The farthest we can go is a simple equation:

$$\gamma = 0.0559 \Delta E_p / V^{2/3}, \quad [17]$$

which implies a position intermediate between the mono- and trihalides. The six data points available are shown in Fig. 3.

CONCLUSIONS

The octahedral model served well for the general class of liquids with weak through moderate interactions between molecules, even when complicated by the free electron forces in liquid metals. However, very long molecules or those exerting specific interactions such as hydrogen acceptor-donor, acid-base, or ionic forces require special values of one or both of the adjustable parameters, and monohalides violate the geometric model completely. Thus, one general equation and five specific ones cover all the liquids so far investigated.

ACKNOWLEDGMENT

This work was supported in part by U. S. Army Contract No. DAH19-69-C-0033, administered by the Research Technology Division, Army Research Office, Arlington, Virginia.

REFERENCES

1. HILDEBRAND, J. H. AND SCOTT, R. L., "The Solubility of Nonelectrolytes," 3rd ed. Reinhold, New York, 1950.
2. HANSEN, C. M., *Jour. of Paint Tech.*, **39**, #505, 105 (1967).
3. WEIMER, R. F., AND PRACSNITZ, J. M., *Hydrocarbon Proc. Petr. Ref.*, **44**, 237 (1965).
4. BEERBOWER, A., AND DICKEY, J. R., *ASLE Trans.*, **12**, 1 (1969).
5. HANSEN, C. M., AND SKAARUP, K., *Jour. of Paint Tech.*, **39**, #511, 505 (1967).
6. McCLELLAN, A. L., "Tables of Experimental Dipole Moments," W. H. Freeman, San Francisco, 1963.
7. QUAYLE, O. R., *Chem. Rev.* **53**, 439 (1953).
8. BAKER, E. G., Private communication, March 24, 1969.
9. BONDI, A., *Chem. Rev.* **52**, 417 (1953).
10. GROSSE, A. V., *J. Inorg. Nucl. Chem.*, **26**, 1349 (1964).
11. SCHONHORN, H., *J. Phys. Chem.* **71**, 4578 (1967).
12. MAYER, S. W., *J. Phys. Chem.* **67**, 2160 (1963).
13. KUBASCHOWSKI, O., *et al.*, "Metallurgical Thermochemistry," 4th ed. Pergamon Press, New York, 1967.
14. DEGA, J. J., DCIC Report 69-2 (AD691019) Clearinghouse, Springfield, Virginia, June, 1969.
15. PATTERSON, D., AND RASTOGI, A. K., *J. Phys. Chem.* **74**, 1067 (1970).

APPENDIX IV

THE SURFACE FREE ENERGY OF SOLIDS

IV.1 Introduction

The importance of the surface free energy of solids in lubrication was vaguely recognized many years ago, but it was not until Prof. Rabinowicz' (1965) book appeared that the central role of this energy was brought into focus. Despite the crude methods and data he was forced to use at that time, he made a good case; in a very real sense, it was out of his work that the possibility of this STAF arose. This Appendix is largely devoted to updating his work, applying modern chemical engineering techniques to the correlation of the spotty data available and to the prediction of missing values. Fortunately, there has been a convergence of interests among metallurgists, ceramic experts and paint technologists which has resulted in much new insight on solids. (This Appendix first appeared in Progress Report No. 1, Sept. 9, 1969, but has been largely re-written since that time.)

IV.2 Definitions

It is not possible to discuss the surfaces of solids until certain terms have been defined. This is particularly true because of the widespread abuse of the phrase "surface tension." This term was apparently first coined by von Segner in 1751 for liquids, in which true tension is rarely exhibited; its spread to solids amounts to a semantic disaster.

It might well be mentioned that the term "surface" is itself misleading, since every surface must, in reality, be an interface. However, as a matter of convention, we will continue to use surface to represent the interface of a solid or liquid against a gas or its own vapor. The word interface thus represents the area of contact of two liquids, or solids, or one of each. Tension, if used at all, will apply only to the bulk tensile stress in solids.

The reader must be warned that some authors reverse these symbols, and that others reverse the meanings; the results approach chaos (Mullins 1962, Johnson 1968, Vernaak 1968, Zadumkin 1968). In this STAF, the symbols and definitions above and below will be strictly followed.

IV.2.1 Surface Free Energy (properly specific surface free energy) is the central property of interest to those working with the interfacial properties of matter. It is defined as the reversible work required to create a unit area of the surface at constant volume, temperature and chemical potential. Thus, it is a Gibbs free energy and not that defined by Helmholtz. It is almost universally designated by " γ ", and is valid for all pure liquids and solids. Although this strict definition would make it inapplicable to multicomponent systems, where the surface free energy of the mixture

$$\gamma_m = \gamma + \sum_i \gamma_i (v_i/v) \quad (IV-1)$$

where μ_i and Γ_i are the chemical potential and excess surface per unit area of component i , this fine distinction will be neglected for the present.

The origin of the term "tension" in this connection was in Von Segner's concept of a "contractile skin" of special surface material whose tension resisted the "internal pressure" of the liquid. The correlation of bulk and surface properties, with no need for special densities or energies at the surface, should help to dispel the idea of this "skin" which is, unfortunately, still being taught. Actually, the second law of thermodynamics requires that each system seek the lowest free energy configuration, which accounts for the spherical shape of drops, capillary rise and other phenomena that so puzzled the scientists of the 17th and 18th centuries. It is interesting that if von Segner had thought in terms of energies rather than forces, his model would conform almost exactly to Appendix III where the surface free energy is shown to balance the cohesive energy density ($\Delta E_v/V$). The latter term is believed to correspond almost exactly to the old idea of internal pressure (Hildebrand 1950) though not all agree (Bagley 1971).

IV.2.2 Total Surface Energy has not been involved in such semantic controversy, perhaps because it is not used so often. It consists of the free energy plus an entropy term:

$$E = \gamma + T \frac{d\gamma}{dT} \quad (IV-2)$$

Many authors refer to this property simply as "surface energy", which is quite legitimate. Unfortunately, this term is also sometimes used carelessly for the surface free energy, so it is best avoided.

IV.2.3 Surface Stress. For a solid, it is also necessary to consider the reversible work done in extending the surface by one unit area. This is best referred to as the surface stress, σ . While γ is a scalar (non-directional) energy, σ is a tensor quantity and is equal to

$$\sigma = \gamma + \frac{d\gamma}{dS} \quad (IV-3)$$

where dS is the specific reversible surface strain. For liquids, $\sigma = \gamma$.

IV.2.4 Surface Distortion cannot be defined thermodynamically, but is very real. It represents the total of the various stored mechanical energies such as dislocations, and elastic tensions or compressions, over and above the Surface Stress. The effect is clearly visible during corrosion, when the distorted spots invariably corrode first. It also has more subtle symptoms, such as the discharge of "Kramer" (1950) electrons which blacken photographic film, generate H_2O_2 , and perhaps contribute to forming surface resin.

IV.3 Measurement Techniques and Calculation Methods

In contrast to liquids, whose surface properties are easily measured, solids require difficult and often indirect techniques. Nothing approaching the ring or capillary method is available; the nearest approach to that was Rabinowicz' correlation of surface free energy with pyramid hardness (Figure 7-1), which has so far yielded only rough approximations. The methods discussed below have been reviewed in greater detail by Duga (1969) but some of the analysis is new.

IV.3.1 Direct Measurements

The outstanding procedure is the "zero creep method", first brought to reliability by Udin (1949) and since used by many others. It is carried out by hanging a series of thin wires or foils in an inert atmosphere at a controlled temperature near the melting point. Monocrystal specimens are preferred but multicrystal ones have been shown to introduce less than 10% error, for which an approximate correction can be made. Unfortunately, this method can only be applied to materials with a fair amount of ductility, and even with those it must be run at near the melting point to avoid intolerably long waiting for the decision as to which load will neither rise due to surface force nor stretch due to gravity. The surface free energy is numerically equal to this critical load (in dynes) divided by the circumference of the specimen (in cm.), as ergs/cm². Methods for adjusting the data from the undesirably high temperatures at which they are determined are discussed in Appendix VII.

The other direct method has been discussed briefly in Section 6.8.1. It depends on the Griffith principle, that the work required to extend a crack is expended in generating new surface. There has been much controversy about this method since its application by Gilman (1960), on both theoretical and practical grounds. Unfortunately, again, this method can rarely be checked on the same materials for which zero creep data is available, since the criteria are essentially opposite. The Gilman method requires non-ductile specimens, so is generally run at liquid nitrogen temperature.

The practical problem is to overcome the effects of residual ductility in the specimens; this is handled fairly well by breaking at a series of strain rates, and extrapolating the results to zero strain rate. Theoretical points include the argument that really this method measures σ rather than γ , which raises a question of the sign of $d\gamma/dS$ in Equation (IV-3). Some feel it is positive so that σ is always greater than γ ; others, who are more oriented to the calculations from lattice parameters (see IV.3.4 below), tend to regard it as negative, even to the point of driving γ to negative values (Mullins 1962, Zadumkin 1963, Johnson 1968, Vermaak 1968). This question is probably only of academic interest compared to that raised by Fox (1970), who estimated large temperature rises in the tip of the crack (Figure 5.8-1, point A-A'). These were based both on very approximate calculations, and on observations of crack-initiated detonations in crystalline explosives. This temperature rise was more than enough to explain the deviations noted below in IV.3 below. As Fox's calculations were too crude to serve as a correction factor, this method is definitely NOT recommended.

IV.3.2 Measurements of Liquid Interactions

Most of the discussion on solid-liquid interactions is properly relegated to Appendix V. However, there is one case which need not be postponed, as it is relatively simple - the interaction of a solid with its own melt. This does require use of the controversial rule proposed in 1907 by Antonoff (1942), that the interfacial free energy is the difference between the surface free energies of the two phases measured against their common vapor:

$$\gamma_{12} = \gamma_2 - \gamma_1 \quad (IV-4)$$

(The convention 1 = lower phase and 2 = upper phase will be used in subscripts.) This has to be applied to phases that are mutually saturated, as surely a solid and its melt will be.

The first technique, by Turnbull (1950), measured γ_{12} by means of the maximum degree of supercooling required to make isolated droplets of the liquid nucleate homogeneously. By reasoning too complicated to cite here, he was able to show that combining this ΔT with ΔH_f , T and two estimated constants led to a solution for γ_{12} . Since γ_2 , the liquid surface free energy, is readily measured, the addition of this to γ_{12} yields the desired γ_1 for the solid.

The second technique (Glicksman 1969) involved measuring the dihedral angle between adjoining crystals, Ψ , and the lattice tilt misorientation angle θ . While these angles are not independent, it appears better to measure both. Then,

$$\gamma_{12} = E_0 \ln \theta/2 (A' - \frac{1}{\theta} \cos (\Psi/2)) \quad (IV-5)$$

where A' is a constant (eliminated in a regression procedure), and E_0 is a function of the Burgers vector (lattice spacing) and the elastic constants of the solid, to be measured in separate tests at the melting point. This technique has not been as thoroughly tested as Turnbull's but appears to give good results (IV.4 below).

Both of these methods have the same limitation as Udin's of giving γ_1 near the melting point and so requiring adjustment to the desired temperature. The use of other liquids solves this problem but introduces many others. Perhaps the greatest sacrifice is loss of the quite reasonable assurance of a clean interface in the Turnbull and Glicksman methods. Where a solid surface must be fabricated and brought into interaction with a liquid, contamination is almost inevitable, and drastic cleaning procedures are in order (Buckley 1966), but forming the solid from the liquid prevents most of the possibilities.

Zisman (1964) and his group have done a great deal of work on contact angles, from which arose the concept of a "critical surface tension", γ_c . This is the surface free energy of the liquid, from a "homologous" series of hydro- and halo-carbons, which will just spread on the solid. Though Zisman has issued many warnings against using γ_c as the surface free energy of the solid, some experimenters persist in doing so - to their own discredit. One of the most dramatic warnings was by Bennett and Zisman (1968); as shown in Figure 7-2, they found γ_c to be the same for all metals. The true meaning of γ_c will be discussed in Appendix V.

IV.3.3 Calculation Methods

It is highly desirable to have a system for calculating surface free energies of solids, because of the limited supply (and accuracy) of literature values, and also for increased understanding. As will be seen in Appendices V and VII, there are unanswered questions on interfacial matters and also on the entropy of surface formation which a good mathematical model of surface free energies would help to answer. Two approaches have been tried; one is based on bulk energies and parallels Appendix III, while the other is more fundamental.

IV.3.3.1 Calculation from Bulk Energies

If the reasoning in Appendix III is as sound as the results indicate, it should be possible to calculate not only γ values for solids but even partial values as suggested in Footnote 2, page 254. Several possible modes offer themselves; the simplest being to substitute the heat of sublimation (ΔH_s) for that of vaporization and change the molar volume to that of the solid. A less heroic approach is to use the measured value of γ_2 at the melting point, and adjust it via the heat (ΔH_f) and volume (ΔV_f) change of fusion to the solid just below melting. Suitable heat values are listed by Kubaschewski (1967) for many substances. These concepts are by no means new, having been forecast by Bondi (1953) and further developed by others (Duga 1969). What is new is the additional degree of flexibility afforded by the Hansen parameters, as demonstrated in Appendix III. Discussion of the latter will be given in Appendix V.

IV.3.3.2 Calculation from Lattice Parameters

An amazing number of papers have been published on generation of surface properties from the basic lattice spacings, inter-atomic forces and electron distributions. Many of the results have been ridiculous, including the negative values for γ mentioned above, but the results are getting closer to reality. In a recent paper, many of the metals were predicted (Lang 1970) to within experimental error. The sole exception was lead, which might possibly tie in with its anomalous behavior (4.2, 7.2).

The most significant finding of these workers is that each pair of faces on anisotropic crystals has a surface free energy unlike the other pairs. This is really not surprising when one examines a crystal lattice model; all three pairs have clearly different atomic arrangements, even for elements; for compounds, the difference is even more striking. Some of the computations are detailed enough to show the concentration of free energy at corners (Bruce 1965); this is in rough agreement with the experimental dislocation energies in Section 5.6.5.

One method deserves special mention because of its very close ties to the Glicksman method (IV.3.2). It was developed by Kotzé (1966), and started from the same E_o function for simple tilt boundaries:

$$E_o = Gb/4\pi (1 - \nu) \quad (\text{IV-6})$$

where G is the modulus of rigidity, b the Burgers vector and ν Poisson's ratio, all measured by the melting point. From this and a few other considerations, including averaging in E_o for twist boundaries ($Gb/2\pi$),

$$\gamma_{12} = \frac{0.85}{16\pi} \left[\frac{1}{1 - \nu} + 2 \right] Gb\theta_m \quad (\text{IV-7})$$

where θ_m is the maximum angle of misorientation. Taking this as 25° and ν as $1/3$,

$$\gamma_{12} = 0.0258 Gb \quad (\text{IV-8})$$

IV.4 Comparison of Experimental and Calculated Results

In order to implement Rabinowicz' theories, as well as those of the interfacial workers in Appendix V, it is necessary to examine the tools which are available in a critical manner. The following sections attempt this, but time has not permitted inclusion of all the latest data. The reader should go back of mid-1970 or earlier to collect the flood of experimental results coming from all parts of the world, and regard the following only as a beginning to an ever-sharpening focus on the γ values of solids.

IV.4.1 Organic Solids

In contrast to the profusion of data on organic liquids, very little has been done on organic crystals. Up to the cut-off date (February 1971 on Chemical Abstracts and Engineering Index) only one study (Jones 1970) had been reported. He used the Glicksman method on camphene and succinonitrile. The results appear plausible, but there is only the heat of fusion theory against

which to compare them. His results on water and phosphorus are subject to checks; the water data disagrees with nucleation and some theories, but checks very well with Kotzé. The phosphorus data checks both nucleation and heat of fusion quite well. Fortunately, this neglect is no great loss to lubrication theory.

More relevant is the work on polymers and plastics, which have increasing importance for oil-less and lubricated bearings (see 5.1). Some very good data have been obtained from polymer melts (Lee 1967, 1968; Wu 1969) though there are two questions on extrapolation to room or working temperature. The first concerns the degree of crystallinity. Polymers which simply become glassy are no problem, but many undergo partial crystallization at a fairly sharp temperature, leaving the rest of the polymer as an "atactic" glassy viscoelastic liquid. Should γ be corrected for the heat of fusion of the "isotactic" portion? Fortunately, this would be a small correction and can be ignored for a first approximation. The second is one which haunts all workers on solids - is the surface of the same composition as that of the liquid? As mentioned in 5.5.4, the Gibbs principle states that at equilibrium the system will achieve the configuration with the least free energy. In simple hydrocarbon polymers, this will lead to the atactic phase dominating the surface so that the γ estimated from the liquid tests will be correct. However, many polymers are complex in the sense that each link contains groups of two different cohesive energy densities. As in the case of the monohydric alcohols (Appendix III), this may lead to some sort of surface orientation if the geometry of the molecule permits. Thus, while the dimethyl silicones can exhibit only one kind of surface consisting of methyl groups somewhat modified by the -O-Si-O-Si- backbone, the methyl tetradecyl silicones (Brown (1970)) can exhibit remarkably wax-like characteristics under some circumstances, while other conditions bring out responses typical of the backbone. Even more impressive are liquid mixtures; as discussed in Appendix VI, these will show surfaces typical of the total mixture on a short-time scale (such as foaming in a distillation tower) but reflect the properties of the lower γ component on a long-time basis. As liquids approach the glass transition point, the meaning of "short time" must be expanded to approach infinity, due to the increased viscous resistance to segregation of chemical types or groups. This parallels the phenomenon of "plastic memory", in which physical distortions held in a polymer are frozen, only to have the piece revert to its original shape on warming.

Thus, a piece of plastic may have one surface, when cooled from its melt, which corresponds quite closely to that of the melt, and quite another surface when sliced below its glass transition temperature. The latter would be a true sampling of all the chemical groups on a numerical basis, as opposed to the essentially Gibbs situation on the cooled melt, and hence would show a higher γ value. Other possibilities arise when a surface cooled by some other medium than air is considered; presumably water quenching would call forth quite a different Gibbs situation, with any hydrogen bonds as exposed as possible, while metal etc. molds would doubtless cause special surfaces more related to Appendix V. Some of these would have higher γ values than the cold-cut surface. However, annealing in air would restore the γ value extrapolated from the melt.

In view of these peculiar variations in surface composition, it is not surprising that variations in γ_c are found, nor that they increase with increasing complexity of the polymers. Low values of γ_c appear to match fairly well with γ values extrapolated from melts, but at higher values γ_c tends to be lower. This is due to the fact that the probe liquids used cannot interact with all the forces at the polymer surface (Appendix V).

Wu (1968) provided an excellent fit of the γ_c data on most of the common plastics, with an equation developed from Hildebrand (1950). However, it contains several features that make it unacceptable on any other than a crude empirical basis. It is dimensionally unbalanced, and is keyed to the number of atoms in the monomer. Wu builds up his energies from the Small (1953) system, and so his results include the London, Keesom and some of the electron acceptor "H-bond" forces. As shown by Panzer (1972), this gives a very inadequate picture of wetting energy, but Wu's is the only system that permits building up γ_c from the structural formula and so must be mentioned. The experimental measurement of the partial surface free energies is taken up in Section 5.11 and Appendix V; this is the recommended approach for all polymers and plastics.

IV.4.2 Metallic Solids

Until recently, surface free energy values for solid metals simply were not available, and many surface chemists working mainly with liquids still believe that to be the case. As recently as 1965, Rabinowicz was able to find only the values for liquid metals discussed in Appendix III, and for a few solid non-metals. Since then, the materials scientists have made a good deal of progress. Direct measurements on nine metals are shown in Figure IV-1; these were obtained by Udin (1949), Blakely (1966) and Allen (1969B). The comparison is with data on the liquid near the melting point as compiled by Grosse (1964). The very low value for nickel was verified by repeated experiments by Blakely; the low position of the whole iron group is probably due to negative volume changes on fusion. The cobalt value is by Bryant (1968), and is believed correct. A low value for molybdenum in Progress Report No. 1 has been replaced by a later one (Ehrlich 1968).

Also plotted in Figure IV-1 are a number of results obtained by combining Grosse's value for the liquid with γ_{12} . Most of the latter are from Turnbull (1950), but Bi is from Glicksman (1969) and Pb (same method) was reported by Jones (1970) from unpublished data by R. L. Morris. Agreement with the Udin method is extremely gratifying, as are the high correlation coefficients of the Udin method alone (0.982) or the three combined (0.981). Thus, we may say that the problem of predicting surface free energies of solid metals just below the melting point is solved by multiplying the liquid value by 1.14, with a few exceptions due to negative change of volume on fusion.

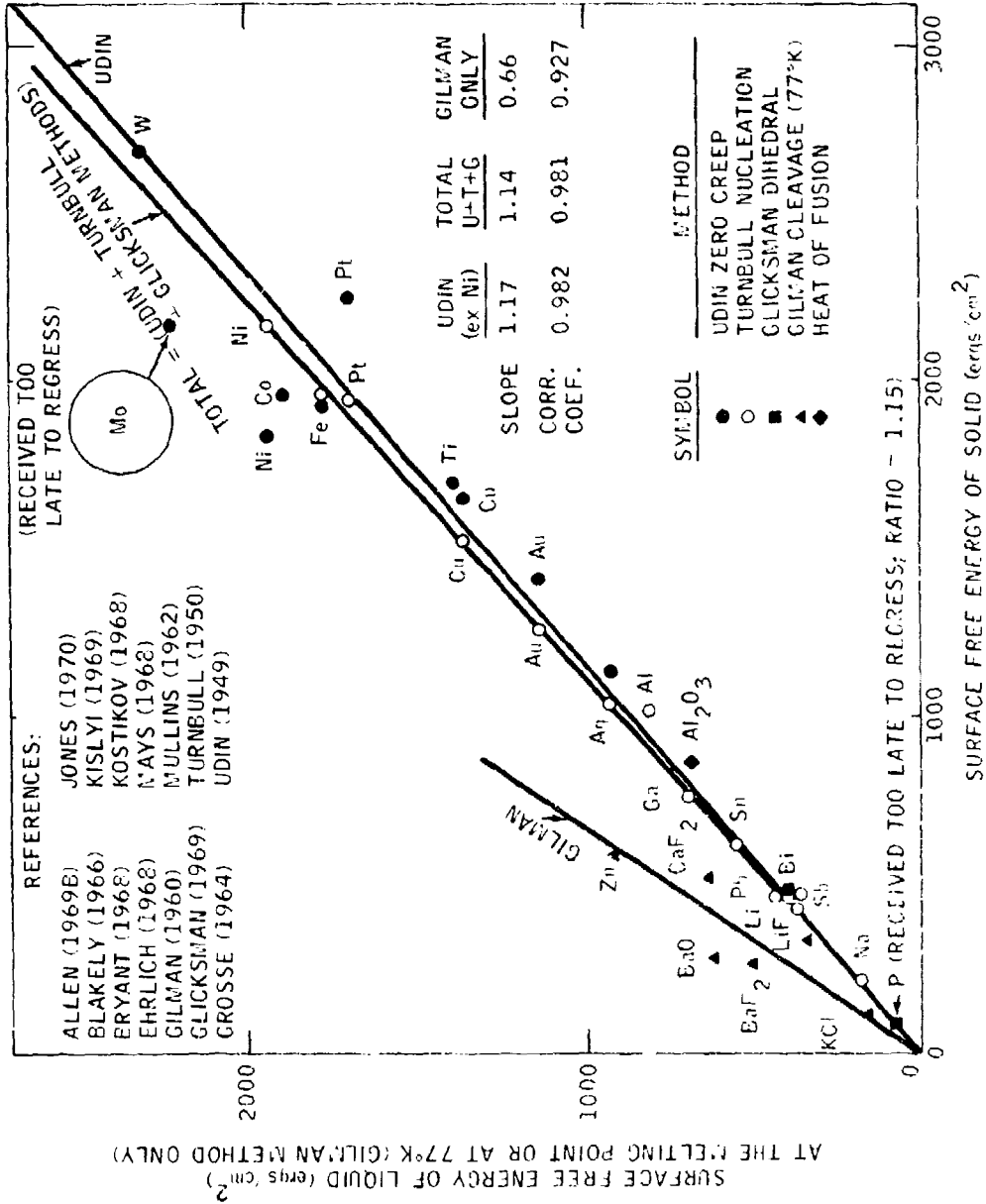
The single Gilman cleavage value shown is for an exceptionally brittle metal, zinc (Maitland 1969). It falls far below the line. This cannot be attributed to its hexagonal structure, as other hexagonals (Ti, Co) fit the line quite well. The fault must lie in the cleavage method, probably due to the Fox (1970) temperature rise as the negative $d\gamma/dS$ idea seems increasingly untenable.

IV.4.3 Ceramic (Inorganic Non-Metal) Solids

Work on ceramics has largely been limited to the Gilman method. As shown in Figure IV-1, the results line up quite well with that for zinc, and show a fairly respectable correlation coefficient of 0.927. Obviously, the conclusion must be that the Gilman method does not yield results which are comparable with the zero creep or other methods, and which are far lower than the liquid values. One might set up an empirical correction factor of $1.14/0.66$ and multiply all Gilman results by 1.73, but it would seem wiser to wait until some substances have been run by all the methods. It would not be easy to find a material brittle enough for the Gilman and ductile enough for the Udin method, but some of Gilman's samples could be tested for nucleation or dihedral angle. (He reported several for which no γ_2 was available, that are not shown in Figure IV-1.) Perhaps in the uncorrelated 1970-71 data there is enough evidence to make this decision. Meanwhile, casual scanning of it (including Jones' P and H_2O) indicates that the three methods that agree are good enough. A single point on Figure IV-1 was derived by $\gamma_2 + 0.0715 \Delta H_f/V^{2/3}$; it was for Al_2O_3 , and appears to fit the line quite well, so this route is also open.

Nurse (1968) gives a number of other methods for use on ceramics. Some are not relevant, but others are quite provocative if regarded as possible sources for surface distortion energies.

Figure IV-1



APPENDIX V

INTERFACIAL ENERGIES OF PURE LIQUIDS ON SOLIDS

V. 1 Introduction

It was anticipated, when Appendices III and IV were first prepared, that they would provide more or less direct solutions to the various interfacial energies involved in lubrication. These may be classified as follows: (1) metal/metal, (2) ceramic/metal, (3) ceramic/ceramic, (4) organic/ceramic and (5) organic/metal. It now appears that only classes (1), (2) and (3) can be solved in such wholesale fashion and these all concern unlubricated systems, borderline to the scope of this STAF. Class (4) proves to be of only transitory interest, since it only covers oil wetting a film of corrosion products that will soon be swept away. The main objective was class (5), and it is evident from Sections 5.5.4 and 5.5.5 that metals with higher γ_1 (or harder; see Figure 7.1) than copper or silver are only wetted by lubricants for the brief time it takes to decompose the lubricant (and perhaps to convert the metal to carbide). Thus, class (5) proves to be limited to the softer metals (babbitt, bronze, lead) which are usually paired with steel, and it is necessary to establish a class (6) covering the interfacial energy of oil against the surface resin formed by its decomposition.

V. 2 Definitions

As before, it is necessary to deal with energies that have been misnamed and re-named to the point of chaos. The convention 1 = lower phase and 2 = upper phase (Philippoff 1960) will be continued. Interfacial free energy has already been defined in Appendix IV and discussed in Sections 5.8, 5.11 and 7.11.2. Equation (IV-4) and (IV-5) are both special cases of the general equation

$$\gamma_{12} = \gamma_{1v} - \gamma_{2v}K_{12} \quad (V-1)$$

where K_{12} is the ratio discussed in 7.4 and Figure 7-1. For the Antonoff (1942) situation $K_{12} = 1.000$. If there is a contact angle (θ), $K_{12} = \cos \theta$, and for strongly wetting systems $K_{12} > 1$, even up to 6. (Philippoff 1960, Gans 1970).

V. 2.1 Spreading Pressure

An important aspect of Equation (V-1) is the "v" subscripts, indicating that γ_{1v} and γ_{2v} are measured against the vapor common to both phases, rather than air. This difference is usually trivial for γ_{2v} which tends to differ from γ_2 by less than 1% because the lower phase is frequently the less volatile, since it is a solid (or a dense liquid). The difference between γ_1 and γ_{1v} can have much more dramatic effects; it is defined by

$$\pi = \gamma_1 - \gamma_{1v} \quad (V-2)$$

This is the spreading "pressure", which is not a pressure at all but an energy. The writer would like to see it more appropriately renamed, but will use the archaic "pressure" in this Appendix even though some (Clayfield 1957A) use this term for "spreading coefficient" (see V. 2.3). Where possible without creating

technical problems, the "v" subscripts will be omitted. Thus, Equations (V-1) and (V-2) combine to

$$\gamma_{12} = \gamma_1 - \pi - \gamma_2 K_{12} \quad (V-2A)$$

Spreading pressure at equilibrium can be estimated from the vapor adsorption isotherm and the Gibbs adsorption equation (Zettlemoyer 1968), but with lubricants the low vapor pressure means that equilibrium may not be attained for a long time. Even without this complication, the problem is a formidable one, since the vapor adsorption isotherm is not easy to measure and even more difficult to predict.

When $K_{12} > 1.0$, the spreading pressure as such disappears, but an equivalent problem arises. The use of Equation (IV-4) is so set about with rules (Antonoff 1942) that it is a major task to perform a prediction. First, the solubility of each phase in the other must be computed. This can be done (Prausnitz 1969, Good 1970), but with increasing difficulty as the compounds increase in polarity.

Surface free energies must then be computed as discussed in Appendix VI. However, the experimental approach is not easy either, since Antonoff required 10 days of equilibration for phenol-water, and 30 days for isobutyric acid or isoamyl alcohol-water interfaces.

It should never be thought that such precautions are unnecessary because the phases are "immiscible." Literally all substances are mutually soluble to some extent; even the solubility of mercury in i-octane can be both computed and measured at about 5 μ mole/liter (Thomsen 1968). Thus, Equations (IV-4) and (V-1) are deceptively simple, though such low solubilities as that of mercury in i-octane can be neglected.

V. 2.2 Work of Adhesion

This term, at least, appears to be universally accepted. It is the mechanical work (a special sort of free energy) exerted in pulling a unit area of phase 2 away from phase 1, and is calculated by

$$A_{12} = \gamma_1 + \gamma_2 - \gamma_{12} = \gamma_{12} (1 + K_{12}) \quad (V-3)$$

It is important to realize that A_{12} and γ_{12} behave in opposite ways; poor adhesion is characterized by high γ_{12} and low A_{12} , while good wetting typically shows high A_{12} and low γ_{12} . In fact, even negative values of γ_{12} have been seriously discussed, but the writer considers these to be merely mathematical abstractions expressing demands for free energy which are soon filled. Even the poorest wetting cannot produce a zero value of A_{12} ; the universality of London forces assures that K_{12} will always be greater than -1.0; very rarely is it even as low as -0.866 ($\theta = 150^\circ$).

V. 2.3 Spreading "Coefficient" (Free Energy)

Another combination of γ_1 , γ_2 and γ_{12} which has some usefulness is the spreading free energy

$$F_{21} = \gamma_1 - \gamma_2 - \gamma_{12} - 2\gamma_2 = \gamma_2(K_{12} - 1) \quad (V-4)$$

This describes the spreading of phase 2 or phase 1; for the inverted case, if phase 1 can be floated on 2,

$$F_{12} = \gamma_2 - \gamma_1 - \gamma_{12} = A_{12} - 2\gamma_1 = \gamma_1 (K_{12} - 1) \quad (V-5)$$

As can be seen from these equations, F is in no sense a coefficient, and use of this term should be discouraged. Apparently "spreading pressure" means F_{21} in England (Clayfield 1957A).

V. 2.4 Adhesion "Tension" (Free Energy)

Among the other left-overs from past ages is the concept of an "adhesion tension." This should properly be called adhesion free energy, and is defined by

$$B_{12} = K_{12} \gamma_2 = A_{12} - \gamma_2 = \gamma_1 - \gamma_{12} \quad (V-6)$$

B_{12} is not very useful within the scope of this STAF.

V. 2.5 Heat of Immersion

The value needed for this STAF is the heat of immersion (Section 5.4), sometimes called "heat of wetting." It is related to the total surface energy (IV. 2.2), and is defined by

$$E_{12} \equiv A_{12} - T \Delta S_{12} = A_{12} - T (dA_{12}/dT) = (1 + K_{12}) E_2 - \gamma_2 T (dK_{12}/dT) \quad (V-7)$$

Use of this equation requires measuring A_{12} or K_{12} at more than one temperature, which the surface chemist rarely does. The importance of the entropy term ($T\Delta S_{12}$) varies with the system. Philippoff (1960) cited work showing $T\Delta S_{12}$ to represent 38 to 40% of E_{12} for organic/inorganic interfaces. This will be further discussed in Appendix VII, but it is of interest to note here that E_{12} shows only slight variation with temperature.

V. 2.6 Heat of Adsorption

Generally means "from the vapor phase", and so should differ from the heat of immersion by a heat of vaporization. Both must be expressed in consistent units, which requires knowledge of the surface coverage in moles/cm². As an approximation, the "molecular diameter" used in Equation (5.4-8) may be used, so the heat of adsorption

$$H_{12} = E_{12} + \frac{1}{2} H_V J / (4/3) \pi^{2/3} N_a^{1/3} V_m^{2/3} \quad (V-8)$$

where J is the mechanical equivalent of heat (ergs/cal). Of course, if the "vapor" is a fixed gas (above T_c), $\Delta H_V \approx 0$ and $H_{12} = E_{12}$.

The same term is often used for the differential heat of adsorption from solution, ΔE in Equation (5.4-21), with quite confusing results. Methods for ΔE are discussed in Appendix VI, under "Heat of Displacement."

V. 3 Calculation and Measurement of Interfacial Energies

While Good (1970) has developed excellent methods for calculating liquid/liquid interfacial energies, he expresses strong reservations about the use of these or other proposed computations on liquid/solid systems. However, for those willing to study through some 125 equations, his paper does offer some hope for going beyond his stated limitations. In Section V.4 some attempts will be shown for computing solid/solid interfacial free energies from the γ_1 values in Appendix IV. However, the rest of this section is limited to the many methods for measurements at the liquid/solid interface.

V. 3.1 Contact Angle Method

The basic technique for contact angle measurement is simple, but the interpretation can present formidable problems. One of these is evaluation of the spreading "pressure" (π), as mentioned in V.2.1. All too frequently it is either ignored or assumed to be zero, with chaotic results. Gans (1970) gives an excellent summary of the methods that may be used without getting into the difficulties of vapor adsorption. Using the extrapolation procedure in Fig. 7-2, he obtained F_{12} values for liquids spreading on liquids. By analogy, this should also apply to smooth, uniform solids wetted by liquids.

On less idealized solids, complications arise (Zettlemoyer 1968, Zisman 1972). Surface roughness has an effect on contact angle which can be estimated by well-known methods (Wenzel 1949), but heterogeneity creates a different type of problem. In this case, there is a difference between advancing and receding contact angles known as hysteresis (Johnson 1964, Neumann 1972). The advancing angle relates to the low energy portions of the surface, and the receding angle to the higher energy portions. The worst problem is the ubiquity of subtle surface contamination. The current horrible example was that a considerable literature was built up on the "contact angle of water on gold," until Zisman (1972) showed that, in hydrocarbon-free atmospheres, water wets gold readily and completely.

Despite all these hazards, the contact angle method has given much help to those concerned with adhesion to plastics (Zisman 1964, 1972). Perhaps it would have been more useful in lubrication if it were not for the high γ_1 of metals which leads to $K_{12} > 1.0$, and the irreversible chemistry noted in 5.4.4.

Contact angle data are not meaningful until analysed into some sort of pattern. A number of attempts have been made to do this; only three will be discussed below.

V. 3.1.1 The Straight Line Assumption

Zisman (1964) set up a "homologous" series of liquids designed to provide non-polar interactions with solids. We now know that the higher γ_2 liquids actually are both polar and H-bonded (Panzer 1972), but this series proved to yield straight lines when $\cos \theta$ was plotted against γ_2 as shown in Figure 7-2. Other series, including those known to H-bond, tended also to give straight lines with a different γ_c . The "non-polar" series has received the most attention because of its apparent dependence on London forces alone.

This line can be described by γ_c and the slope $m (= \Delta K_{12} / \Delta \gamma_2)$:

$$K_{12} = m (\gamma_c - \gamma_2) + 1 \quad (V-8)$$

which provides an analytical solution to the problem solved graphically in Figure 7-2. By combining Equation (V-8) and (V-3),

$$A_{12} = (2 + m\gamma_c) \gamma_2 - m \gamma_2^2 \quad (V-9)$$

This can be differentiated with respect to γ_2 and set equal to zero to locate the maximum work of adhesion:

$$dA_{12}/d\gamma_2 = 2 + m\gamma_c - 2m\gamma_2 = 0 \quad (V-10)$$

from which

$$\gamma_2 = 0.5\gamma_c + 1/m \quad (V-11)$$

For aluminum, $\gamma_c = 45$ and $m = 0.0052$, so the maximum work of adhesion comes at $\gamma_2 = 200$; for zirconium ($m = 0.028$), it comes at $\gamma_2 = 60$ ergs/cm². Thus, it appears that for all the metals in Figure 7-2 (and all others up to $m = 0.044$, which would be a very energetic metal) the principle stated by Campbell (1957) that a partially wetting liquid provides optimum lubrication may be valid. However, it must be remembered that the surfaces in Figure 7-2 (Bennett 1968) were prepared in such a way as to leave a hydrated oxide surface, and also that the linearity of Equation (V-8) is limited to Zisman's hydrocarbon-halocarbon series (Panzer 1972). The latter certainly does not include anything approaching $\gamma_2 = 200$; such a liquid would have to be either ionic or metallic (Appendix III).

Even with these reservations, it is still interesting to check what the A_{12} maxima would be. Combining Equations (V-9) and (V-11),

$$(A_{12})_{\max} = 1/m + \gamma_c + 0.25 m \gamma_c^2 \quad (V-12)$$

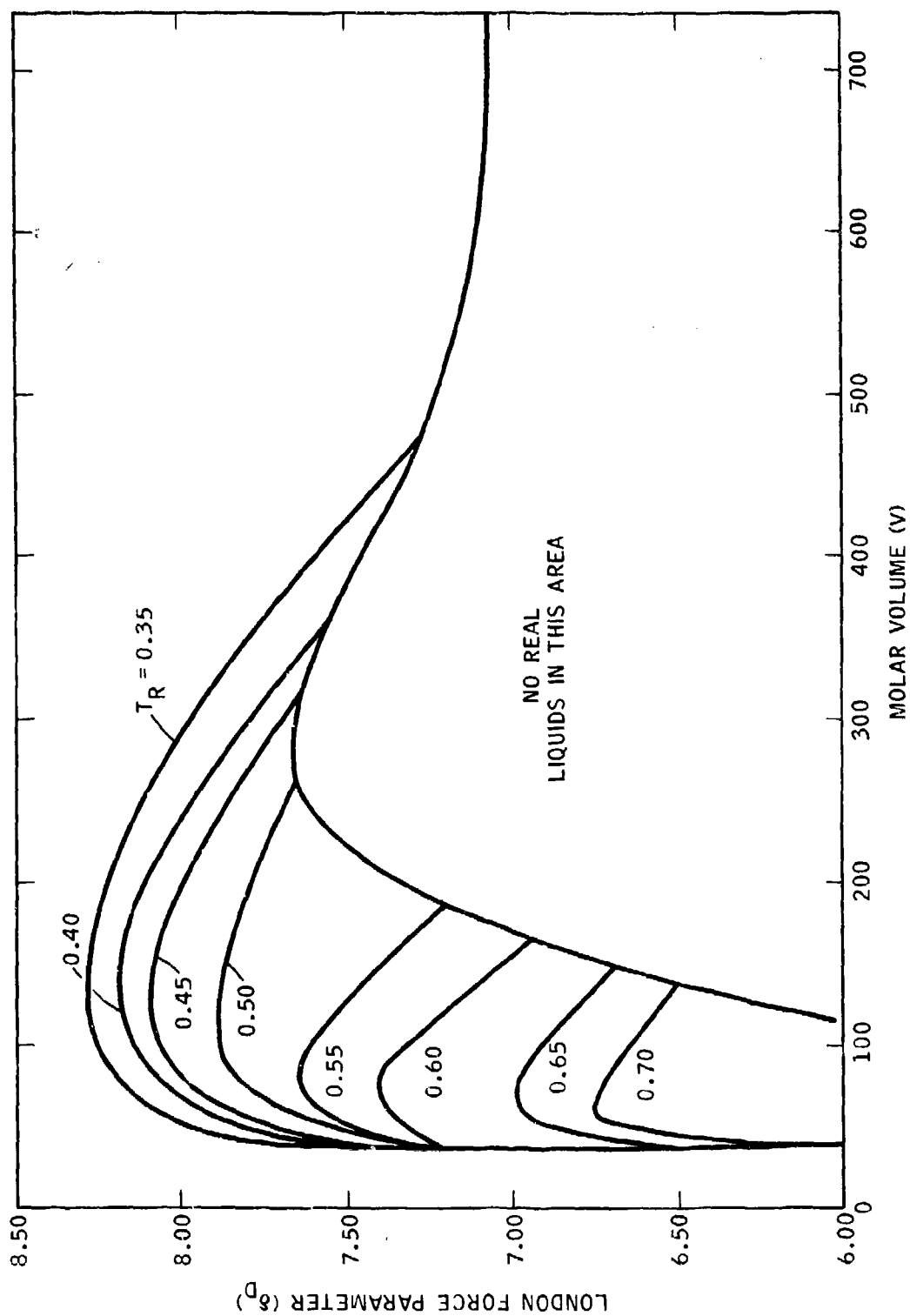
The result for aluminum is 236, and that for zirconium 96 ergs/cm². Both are appreciably higher than the $2\gamma_c$ frequently quoted. To complete the picture, the contact angles of these hypothetical optimum lubricants would be 51.5° on zirconium and 80.8° on aluminum.

V. 3.1.2 The Hansen Plot Approach

The Hansen partial solubility parameters were discussed briefly in Section 5 and Appendix III, and are covered quite thoroughly in Appendix VIII. However, a few improvements in the system have been made which should be covered before proceeding further.

V. 3.1.3.1 A new homomorph chart for δ_D was recently devised, and is awaiting publication (Beerbower 1972B), for normal and isoparaffin hydrocarbons of essentially unlimited molar volume (Figure V-1). It presumably combines the best features of those by Blanks (1964) and Beerbower (1969), and may be used for determining the London force partial solubility parameter (δ_D) of any non-cyclic compound for which V and T_R can be estimated. Maffiolo (1972) has just published an elegant method for computing cohesive energies, but its relation to Figure V-1 has not been tested.

Figure V-1
HOMOMORPH CHART FOR NON-CYCLIC COMPOUNDS



V. 3.1.2.2 A valuable new correlation which offers a simple route to the dispersion parameter, and can also be applied to liquids of indefinite composition, has recently been made by W. M. Salathiel (personal communication, 1971). He showed that 88 compounds in Appendix VIII for which sodium D-line refractive indices (n_D) were available at 25°C were fitted by the equation

$$\delta_D = 4.22 (n_D^2 - 1) + 3.75 \quad (V-13)$$

to within ± 0.5 units. Inclusion of 64 more compounds for which values were available only at other temperatures did not change the slope but did increase the scatter. The writer added unpublished values for 21 petroleum solvents, which resulted in only minor readjustment of Equation (V-13), as shown in Figure V-2.

V. 3.1.2.3 A partial table of group contributions to the polar and electron transfer parameters was published by Hansen (1971) (see Appendix VIII). A more complete version is awaiting publication (Beerbower 1972B). These are of use in estimating the properties of synthetic lubricants, including even those which have not yet been made. By this means it should be possible to "design" a lubricant to match a given surface for which the three partial parameters are known, or to minimize A_{12} if that is desired for combatting fatigue.

V. 3.1.2.4 Broadening the scope of δ_H from the original concept of hydrogen bonding has been accomplished gradually, until now it appears best to describe it as the "electron transfer parameter." Kagiya (1968) repeated the measurements of Gordy (1939) and found that many of the older data were inaccurate. He classed these measurements as electron donor energy, and correlated them with ionization potential, Lewis base number (pK_b), iodine charge-transfer and coordination power with diethyl zinc. Electron acceptor energy, measured by shift of the C=O band, was less impressive but did correlate with Lewis acid number (pK_a).

For use as an engineering tool, the writer feels that the "donor" energy already shown to correlate with $V\delta_H^2$ (Beerbower 1969) is all that is needed. This encompasses all the interactions, by using the scaling factor b in Appendix III, Equation [7] at 1,000 for vaporization, 0.643 for surface formation and 0.25 for solution. This loss of scientific exactitude relieves us of the necessity for strict accountability for "donor" and "acceptor", and permits viewing $V\delta_H^2$ as the energy of an electron transaction.

V. 3.1.2.5 As many authors have pointed out, δ_H can not be expected to obey the geometric mean rule which is central to the solubility parameter concept

$$\Delta E_{12} = (\Delta E_1 \cdot \Delta E_2)^{0.5} \quad (V-14)$$

This fact had to be recognized in preparing Appendix VIII. The geometric mean, as shown by Small (1953), leads to the form

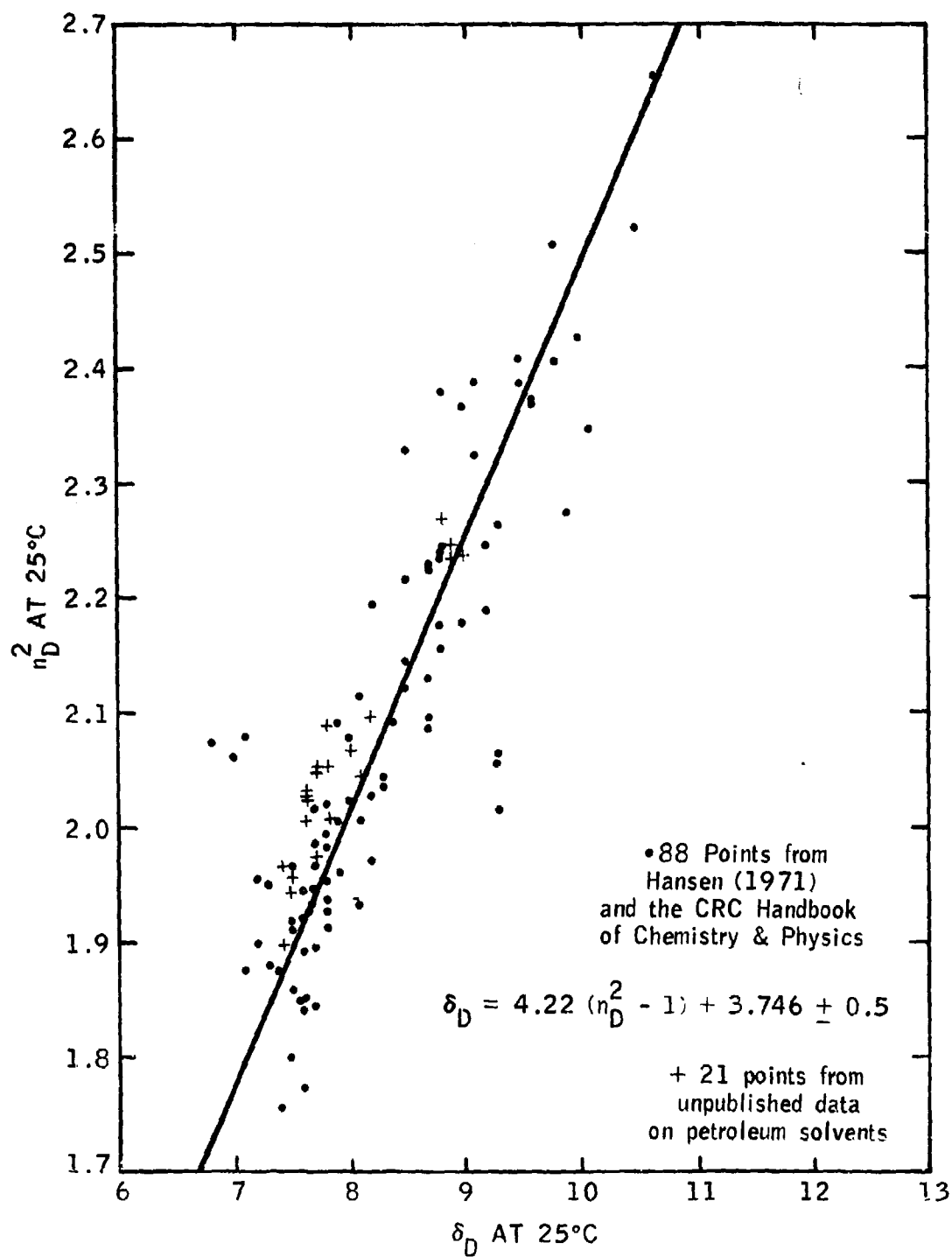
$$\delta = \sum (\gamma_i \delta_i) / \sum \gamma_i \quad (V-15)$$

This worked out well for δ and δ_p , but not for δ_H where the energy $V\delta_H^2$ proved to be the better group contribution.

Zettlemoyer (1968) observed that, in cases where the geometric mean

Figure V-2

PREDICTION OF LONDON PARAMETER
FROM REFRACTIVE INDEX



was inappropriate, the arithmetic mean could be used, and this approach will be followed for δ_H as an engineering approximation.

V. 3.1.2.6

The original Hansen plots were used for polymer solubility, and the contour circles (representing the three projections of a spheroid on the δ_D/δ_H , δ_H/δ_P and $\delta_P/2\delta_D$ planes) were drawn at the "almost completely soluble" (see Figures 5.4-10, 11 and 12). This concept was expanded by Beerhower (1969) to cover elastomers, and the contours were drawn at 25% swelling of elastomers. The third version (Hansen 1970) used $\cos \theta$ as the plotted variable, and the contour was drawn at $\cos \theta = 1.0$ to enclose all spreading cases. His paper gave data on two plastics, and also a mixture of them which proved to be quite different from what would be expected. He also showed that two chromated "tinplate" surfaces showed appreciable response to δ_H . This is discussed in V. 3.9.2.

It is evident that these plots provide a very powerful tool for data analysis. However, aside from the untested Equation (5.11-7), no method is available to convert them to work of adhesion. A recent advance in processing contact angle data is discussed in the next section.

V. 3.1.3 The Panzer Plot Approach

Panzer (1972) followed up the idea expressed in Appendix III, Footnote 2, and converted the partial parameters listed in Appendix VIII to partial surface free energies. Having reviewed all the various methods for analysing contact angle data and found Hansen's (1970) to be the best, he wanted to go a step further. One fault in the plots discussed in the above Section is that they take no account of the molar volume (V). To the paint technologists, this is of no great moment as most of their solvents fall into the class $V = 100 \pm 20 \text{ cm}^3$, and for most of their solutes $V \rightarrow \infty$. This is not true for lubricants. Panzer saw that the type of equation suggested by Fowkes would simplify this and other problems:

$$\gamma_2 = \gamma_2^d + \gamma_2^p + \gamma_2^h \quad (\text{V-16})$$

where γ^d represents the London force contribution, γ^p the Keesom force contribution and γ^h the electron transfer contribution, with room for expansion if ionic (γ^i) or metallic (γ^m) forces are involved.

As was to be expected from the scatter in Appendix III Figure 1, some problems were encountered with poor fitting. Panzer solved this by adjusting all three parameters proportionately to add up to the observed γ_2 . These adjusted partial surface free energies were then plotted, just as the partial δ values are, in a Hansen type plot.

The results, based on the number of probe liquids shown in Table V-I, proved to be somewhat simpler than those from the Hansen plots. Though ellipsoids were required in several cases with the γ plots, a bimodal response obtained with the δ plots was eliminated. The centers found are shown in Table V-I. However, it is necessary to give serious thought to the conversion of these energies into work of adhesion, since Panzer did not deal with that step. Fowkes (1964) worked from the premise that

$$\gamma_{12} = \gamma_1 + \gamma_2 - 2\sqrt{\gamma_1^d \gamma_2^d} \quad (\text{V-17})$$

where only London forces crossed the interface.

TABLE V-I
RESULTS OF PANZER PLOTS

<u>Solid</u>	<u>Number Of Probe Liquids</u>	<u>γ^d</u>	<u>γ^p</u>	<u>γ^h</u>	<u>γ_{12}</u>
n-Octacosane	40	21.8	0.6	1.1	23.5
Polymethyl methacrylate	78	25.9	5.3	1.7	32.9
Versamide 930	79	26.8	3.3	1.5	31.6
Lithium Stearate	70	22.8	2.0	1.0	25.8

However, this has gradually had to be extended to include terms for other forces. Combining (V-17) and (V-3), and adding p and h terms,

$$A_{12} = 2\sqrt{\gamma_1^d \gamma_2^d} + 2\sqrt{\gamma_1^p \gamma_2^p} + \gamma_{12}^h \quad (V-18)$$

Since γ^h probably does not obey the geometric mean rule, as discussed in the previous section, γ_{12}^h remains unresolved. Acting on Zettlemoyer's (1968) suggestion that the arithmetic mean could be successfully substituted, it very tentatively proposed that

$$\gamma_{12}^h = \gamma_1^h + \gamma_2^h \quad (V-19)$$

would provide an easily testable completion to Equation (V-18). Any group charged with continuing this program should be instructed to replot all the Hansen charts mentioned in the various sections, to determine whether the Panzer-Hansen method leads to plausible values of A_{12} , via Equation (V-19) or some alternative route (i.e., the harmonic mean).

V. 3.2 The Panzer Powder Wetting Method

Panzer (1972) reported work closely related to the contact angle studies in the same paper, based on powder wetting. This idea can be traced back to various studies on sedimentation volume etc., but took the unique form of titrating a powder with the probe liquid until the next drop wetted the container wall. This point can be related to the adhesion "tension" (free energy) B_{12} . Results can be obtained with both wetting and non-wetting liquids, and plots of titration volume against B_{12} show a maximum. Panzer prepared both δ and γ plots (see V.3.1.2 and 3) for versamide and lithium hydroxy stearate and found them similar to his contact angle plots. More recently, he has used this technique on aluminum powder (personal communication) and Goldblatt has tried it on iron powder (personal communication) as prepared by Groszek (1970). Both metals were found to show appreciable δ_p and δ_H energies. Problems in preparing relevant metal powders are discussed in V.3.6 below, and the results are discussed in V.3.9.2

V. 3.3 Liquid Metal Interfacial Methods

Although liquid-liquid interfaces are outside the scope of this STAF, it seems relevant to include a Hansen plot of Harkins' (1920) data for work of adhesion on mercury (Figure V-3). It is evident that this metal, like chromated tin, participates in electron transfer bonding. Mention has been made of the work by Zadumkin (1965) on mercury and Karashayev (1968) on gallium. The former is included in Figure V-3, but the gallium data is too scanty for a Hansen plot.

Bridging the gap is Smith's (1969 A and B) use of a film balance for measurements on mercury. The most startling result was that fatty acids with less than 15 carbons stand with the COOH away from the metal while the longer acids take the conventional position of COOH down.

Presumably liquid metal data can eventually be used in predicting A_{12} on solid metals by using ΔH_f as shown in Appendix IV. However, mercury is too irregular for such studies, and there is not enough data yet on liquid regular metals to test this idea.

V. 3.4 The Film Balance Method

Use of the Langmuir-type film balance for measuring work of adhesion is relatively rare, but offers some advantages over the contact angle method. The version developed by Washburn and Anderson seems well adapted to the liquid/solid interface problem.

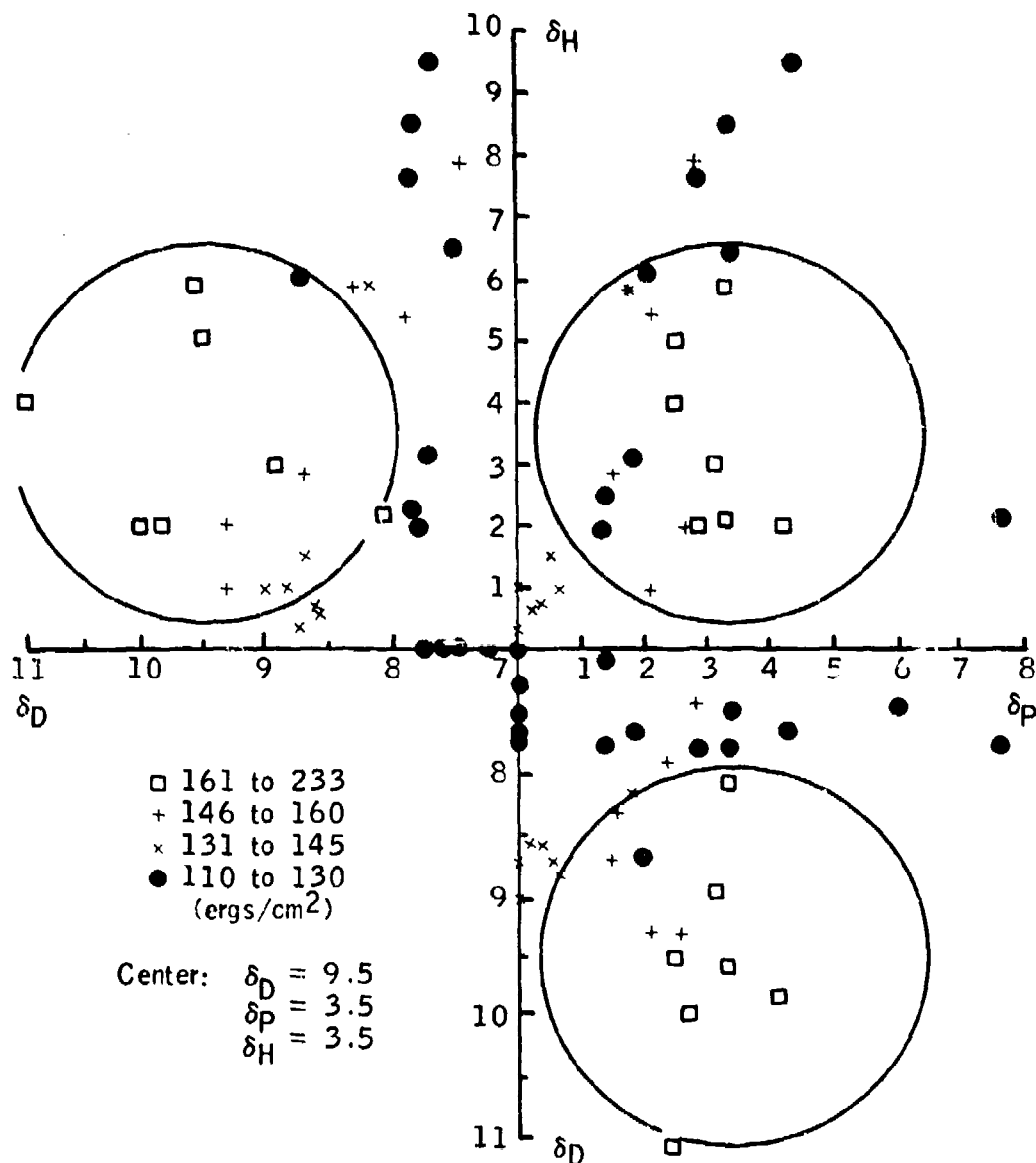
Clayfield (1957A) measured the adhesion of a variety of pure hydrocarbons to chrome-steel and chromium surfaces, and later (1957B) extended the study to new and used lubricating oils. The procedure is quite simple: The cleaned metal plate is placed in the trough and the water level raised to just cover it. A monolayer of a suitable compound such as n-octadecanol is floated on the water and 0.02 ml of hydrocarbon dropped in so it breaks through the film and the water to wet the metal. The octadecanol layer is then pressed up with the film balance, and the force/cm to just prevent spreading of the oil on the metal is recorded as the critical film pressure (F_c). The situation is then as shown in B of Figure V-4. Calibration of the apparatus by varying the depth of water permits evaluation of the contact angles, from which the work of adhesion on 16.5% chrome steel is

$$A_{12} = 0.525F_c + 13.3 + 2\gamma_2 \quad (V-20)$$

The results for some typical hydrocarbons on chromium surfaces are shown in Table V-II. These are the extreme values found for isoparaffins, naphthenes and aromatics, and led Clayfield to conclude that the composition of the oil did not cause drastic changes in A_{12} . He also found that there was a great difference in solids. Organics gave F_c values (not converted to A_{12} , for unstated reasons) of 13 to 28, chromium gave 7 to 20, and various chrome steels gave 0 to 14. Eight other steels containing less than 1.6% chromium, and aluminum, showed hydrophilic surfaces ($F_c < 0$), and could not be tested by this method. Even the chrome steels, when ion bombarded and first wet with water, became hydrophilic. The lipophilic surfaces reported in Table V-II were first wet with any of several organics. Hexane, cyclohexane, benzene and ether apparently all gave similar results. Evidently Model IIIC surface resin is involved in this phenomenon.

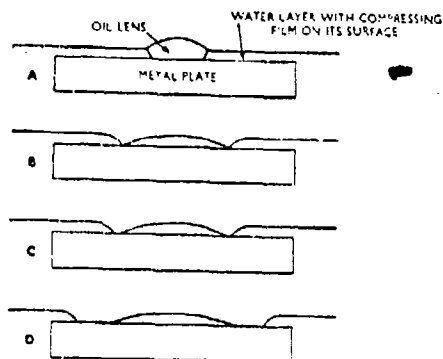
Figure V-3

WORK OF ADHESION OF
LIQUIDS ON MERCURY



Data from: Girifalco and Good, J. Phys. Chem. 61, 904-9 (1957), except the value for nitroethane was altered to conform to Harkins' value in "Physical Chemistry of Surface Films", Reinhold, 1952, page 29. Four acids were not plotted as they show evidence of chemical reaction with the metal surface.

FIGURE V-4



Changes in the oil lens/metal plate/water layer system in measuring spreading pressure of oil on a metal surface. A, Initial stage with high compressing film pressure. B, Just prior to the balance-point with compressing film pressure just higher than the critical film pressure. C, Break-away of water from oil lens with compressing film pressure just lower than the critical film pressure. D, Water layer almost completely retracted with compressing film pressure much lower than the critical film pressure.

TABLE V - II

Typical Works of Adhesion On
Chromium by Washburn - Anderson Balance

Hydrocarbon	F_c (dynes/cm)	A_{12}^2 (ergs/cm ²)
7-butyl tridecane	22.0	78.8
7,12-dimethyl 9,10-di-n-hexyl octadecane	7.0	63.0
1,1-dihexahydrobenzyl undecane	11.7	80.2
1,4-dicyclohexyl butane	12.6	81.1
1,6-diphenyl hexane	17.0	93.4
1,4-di-n-heptyl benzene	9.3	76.2

This method gave plausible results, but the question of the nature of the surface renders it of dubious value.

V. 3.5 The Guastalla Wetting Balance

Guastalla (1956) devised a modification of the Wilhelmy method in which a plate of the metal is withdrawn from the liquid while recording the force-distance diagram. Return of the metal to the liquid in the same way gives a hysteresis loss unless the plate is smooth, uniform, rigid and free from oriented film on the withdrawal. Limited data on iron (M. W. Hill, personal communication) showed A_{12} values of 79 to 92 for three esters.

This method, like that of Clayfield, is subject to all sorts of variations in the surface preparation. Hill polished his steel in air and then solvent washed, so the results may be comparable to Clayfield's but not to Bennett's (1968).

V. 3.6 Heat of Immersion (Liquid Phase)

The study of heats of immersion by direct calorimetry actually preceded Young's initial statement of Equation (V-1) in 1805, since Leslie reported a value in 1802. A very recent report by Groszek (1971) contains the minutes of a meeting on calorimetry, consisting of two general papers, one on the direct and four on the flow method of calorimetry. Both are discussed below, but have so much in common that a number of points may be discussed as if they were one method.

In all such experiments, the solid is reduced to powdered form, since the energy output is only from 10 to 100 ergs/cm² and a powder of at least 5 m²/gm is required to get a precise reading. An auxiliary experiment is required to determine the surface area of another sample of the same powder, usually by the "BET" cyogenic nitrogen isotherm method. The whole problem lies in the preparation of the powder, and may be divided into the usual two parts: (1) Is the surface contaminated? (2) How much strain energy was stored from the powdering process? To these we must add two special questions (3) Is this surface relevant to the lubrication process? (4) Is a chemical reaction taking place?

In answer to (1), it is very nearly impossible to prepare a powder on this humid, contaminated Earth which can be described as "pure" without serious reservations. Furthermore, the calorimetric procedures do not provide the necessary information for a clear-cut decision on this matter. One can only try successively refined cleaning techniques until no further change in E_{12} takes place, and this does not prove cleanliness.

In (2) as in (1), it is very nearly impossible to make a powder which does not contain strain energy. Presumably the worst of the strain can be removed by annealing, but the preponderance of edges and corners (Figure 5.5-9) cannot be eliminated without sintering the powder. The question of detection of these excess energies (see Figure 5.4-6) is discussed below.

Question (3) is a very unpleasant one, and the answer must be, at best, a qualified negative. Unless the study involves metal cutting, where the lubricant sees raw metal every pass, powder surfaces will not resemble the service condition very closely. Where a break-in process is involved, they are definitely misleading.

Question (4) can probably be answered by close study of the contents of the calorimeter after the test, or by some sort of desorption experiments.

V. 3.6.1 Direct Calorimetry

The procedure is simply to break a capsule of the powder under the liquid in the calorimeter and measure the temperature rise. Zettlemoyer (1968) and Tideswell (Groszek 1971) have reviewed this matter. It is possible to map the energetics of heterogeneities by taking heat of immersion on powder precoated with varying amounts of the vapor of the same liquid (Zettlemoyer). Tideswell concentrated on the relatively neglected problem of wetting by mixtures (see Appendix VI), and his curves could be interpreted as showing that "Graphon" (a graphitized carbon black) has active sites. He expressed considerable surprise at these shapes; they did not fit any of the usual patterns. Of course, it must be recognized that the graphite crystal is extremely anisotropic, having a low (120 to 220 ergs/cm²) surface free energy on the flats, and a very high γ on the sides. The latter would relate to the high boiling point of about 6000°C.

V. 3.6.2 Flow Calorimetry

This important new technique has been applied primarily to solutions and so is relegated to Appendix VI.

V. 3.7 Heat of Adsorption (Vapor Phase)

As mentioned in V. 2.5, heat of adsorption usually implies adsorption from the vapor phase, including fixed gases. The catalyst workers have done a great deal of good work on metal-organic interaction; most of it is difficult reading for the outsider. Eischens (1969) has done much to translate this data into lubrication terms, and Bond (1962) to relate it to the physical chemistry of metals. However, the data tend to be taken on the lighter hydrocarbons and fixed gases, so the applicability of the methods to lubricants has not been clearly established. There is a serious problem of delivering sufficient vapor to the metal surface to permit good calorimetry, when even the lightest lubricants require 200°C or more to generate 10 torrs of vapor pressure. This is above the range desired by most lubrication engineers. Another problem is the fact that such molecules tend to "chemisorb", with irreversible chemical changes, even at room temperature, as shown by Morecroft (1971). Such chemical reactions are readily detected by catalyst methods, and in fact were predictable from the data on C₄ and lighter hydrocarbons (Eischens 1969).

The method most favored for calorimetry (Bond 1962) uses a wire or film of the metal, under adiabatic conditions. The metal specimen is calibrated to be its own resistance thermometer, providing that any chemical changes do not affect its integrity. Powdered metals can also be used but the problems mentioned above are all present. Wires can be drawn and annealed with considerable assurance that subsequent cleaning, by ion sputtering in vacuum for instance, will remove the contamination and some of the work hardening. The resulting surface is not usually homogeneous (Figure 5.4-6) energetically. Films are most often vapor deposited, by the hot filament, ion sputtering or similar methods. There is reason to believe they are more reactive than the same metal would be in bulk (R. L. Johnson 1970).

V. 3.8 Heat of Desorption (Evaporation)

A very new method is described by Anderson (1970) who terms it "Evaporative Rate Analysis." In brief, it requires preparation of a "clean" surface, to which is added essentially one monolayer of the liquid by deposition from a volatile solvent such as cyclopentane. The liquid must be radioactive enough that the radiation from less than a monolayer can be monitored readily. The specimen is placed on a heating stage under a Geiger counter, and a small, steady flow of gas passed over it until the counter shows complete desorption. The experiment is run at several temperatures, and the evaporation rate at each is used in the Clausius-Clapeyron equation, as if it were a vapor pressure, to calculate an apparent heat of desorption. This, of course, is the sum of the heat of adsorption plus that of vaporization (V.2.6).

Results from this method are too few to judge its value, but the usual problems of surface preparation are all present. One new bit of information from Anderson's work is that water vapor displaced most additives from oxidized aluminum.

V. 3.9 Dynamic Methods

Although a relation between heat of adsorption and friction/wear reduction was implicit in the thinking of many earlier workers, no one seems to have attempted to calculate E from dynamic tests until Frewing (1943) did so. His model was limited to adsorption from solutions (Appendix VI) but with the methods now available it is possible to re-examine a great deal of data, taken for less specific purposes on a variety of pure liquids lubricating solids.

V. 3.9.1 The Stick-Slip Transition

In an earlier paper, Frewing (1942) reported the temperatures (T_t) at which an abrupt transition from smooth sliding in a Bowden-Leben (sphere on platen, see Section 5.3) took place with various compounds, when the temperature of the platen was raised by external heat. A number of these temperatures are listed in Table V-III, along with the melting points (T_m) of the compounds. Frewing found a definite relation between T_t and T_m . In all tests with hydrocarbons (hexadecane, diphenylmethane, paraffin wax, biphenyl and bis-*p*-biphenyl methane), alcohols (lauryl and ceryl), ketones (methyl heptadecyl, myristone and benzophenone) and amides (acetamide, pelargonamide and myristamide) $T_t = T_m$.

The acids showed a fairly constant difference of $T_t - T_m = 70 \pm 5^\circ\text{C}$. Those below pelargonic are not reported since rapid evaporation and corrosion led to problems in getting the data. The methyl esters showed $T_t - T_m = 50 \pm 5^\circ\text{C}$., but the stearates of various alcohols showed a response expressible by $T_t - T_m = 60 (28 - n) \pm 5^\circ\text{C}$., where n is the number of carbons in the alcohol. (The values in Table V-III are correct; Frewing's Figure 7 has the ordinate scale misnumbered). The glycol and glycerol ester data, and that on dimethyl esters, are too scanty to draw any conclusions except that they are unlike the simple esters of either class.

TABLE V - III

Temperatures of Melting (T_m) and
Transition (T_t) for Various Compounds ($^{\circ}\text{C}$)

Compound	T_m	T_t	ΔT
Pelargonic Acid	12	90	68
Capric Acid	30	95	65
Lauric Acid	47	120	73
Myristic Acid	57	125	68
Palmitic Acid	63	130	67
Stearic Acid	70	145	75
Oleic Acid	14	85	71
Elaidic Acid	45	120	75
Methyl Laurate	0	45	45
Methyl Myristate	18	65	47
Methyl Stearate	38	95	47
Methyl Arachidate	53	110	57
Methyl Cerotate	82	135	53
Ethyl Stearate	33	90	57
Butyl Stearate	28	80	52
Hexyl Stearate	28	75	47
Lauryl Stearate	44	85	41
Stearyl Stearate	60	85	25
Cerotyl Stearate	72	77	5
Ferric Stearate	111	113	2
Glycol Dimyristate	61	85	24
Glycol Distearate	76	115	39
Glycerol Trimyristate	56	80	24
Glycerol Tristearate	71	105	34
Dimethyl Succinate	19.5	55	35
Dimethyl Sebacate	28	35	7

Frewing was unable to analyse his data mathematically, 30 years ago. It would certainly be worthwhile to subject the excellent block of data to modern analytical methods. The Kingsbury-Rowe method will be discussed in 3.8.3.

Another possible method of analysis, which was not tried, is the Hansen plot. However, it is evident that normal esters with the same total C, H and O count, which would have the same partial parameters, will not give the same T_c when chosen from the methyl esters and the stearates. For example, methyl stearate (C_{19} , 95°C .), ethyl stearate (C_{20} , 90°C .), methyl arachidate (C_{21} , 110°C .) and butyl stearate (C_{22} , 80°C .) which would plot quite close together, can obviously not be fitted with a circle.

This contrasts strongly with the good fit obtained in Figures 5.11-1, 2 and 3, where Bowden-Leben machine friction values were plotted. Frewing did not report enough friction data for this purpose, nor did Senior and West (1971) heat their apparatus. It appears, despite this lack of confirming evidence, that there is reason to regard T_c as basically unsuited to Hansen plotting. One reason would be that the parameters all decrease with increasing temperature, and not at the same rate (Hansen 1971).

The Panzer plot (V. 3.1.3) has not been tested, but it obviously will encounter the same problem on esters.

V. 3.8.2 Metal Cutting Friction

As far as the writer knows, the work of Ernst (1941) shown in Figures 5.11.4 and 5 is unique. However, it obviously has a good deal to recommend it, this being one of the few cases where a truly uncontaminated solid surface can be contacted with a liquid. While some doubt was expressed in Section 5.11 as to whether the δ_H value reported for aluminum was real, recent data on powder wetting (Panzer, personal communication) has given similar data on "clean" aluminum powder using liquids quite unlikely to undergo Reaction (5.11-8). Thus, we have a number of cases of metal wetting in which both δ_p and δ_H are important, as shown in Table V-IV. Hence it appears that Fowkes' (1966) assumption that electron transfer across an interface to metal does not take place is disproved.

A moderate extension of the cutting method is to plot breaking strength for the Hansen contours. A plot of data from Imanaka (1968) is shown in Figure V-5, which illustrates the Rehbinder effect of decreasing the crushing strength of Al_2O_3 . The contour is 2.15 kg force, and all data except that on water are satisfactorily resolved. Figure V-6 shows data by Moorthy (1956), which shows the Joffe effect of increasing the fracture strength of soda-lime glass. The contour surface is at 20% increase over that under water, or 29% over that in air.

TABLE V - IV

Partial Solubility Parameters of Metal Surfaces

<u>Metal</u>	<u>Author (year)</u>	<u>δ_D</u>	<u>δ_{p*}</u>	<u>δ_H</u>
Chromated "Tin Plate A"	Hansen (1970)	5.0	-0.3	5.2
Chromated "Tin Plate B"	Hansen (1970)	6.9	-0.2	6.3
Iron Powder (new)	Goldblatt (unpublished)	8.1	5.7	3.0
Iron Powder**	Goldblatt (unpublished)	8.6	1.9	3.0
Aluminum, Fresh Cut	Ernst (1941)	8.4	2.6	6.5
Aluminum Powder	Panzer (unpublished)	7.9	3.0	7.1
Mercury (liquid)	Harkins (1920)	9.5	3.5	3.5

* Negative values represent mathematical artifacts rather than any real "negative energy"

** Ground under hexane per Groszek (1969)

Figure V-5
THE REHBINDER EFFECT

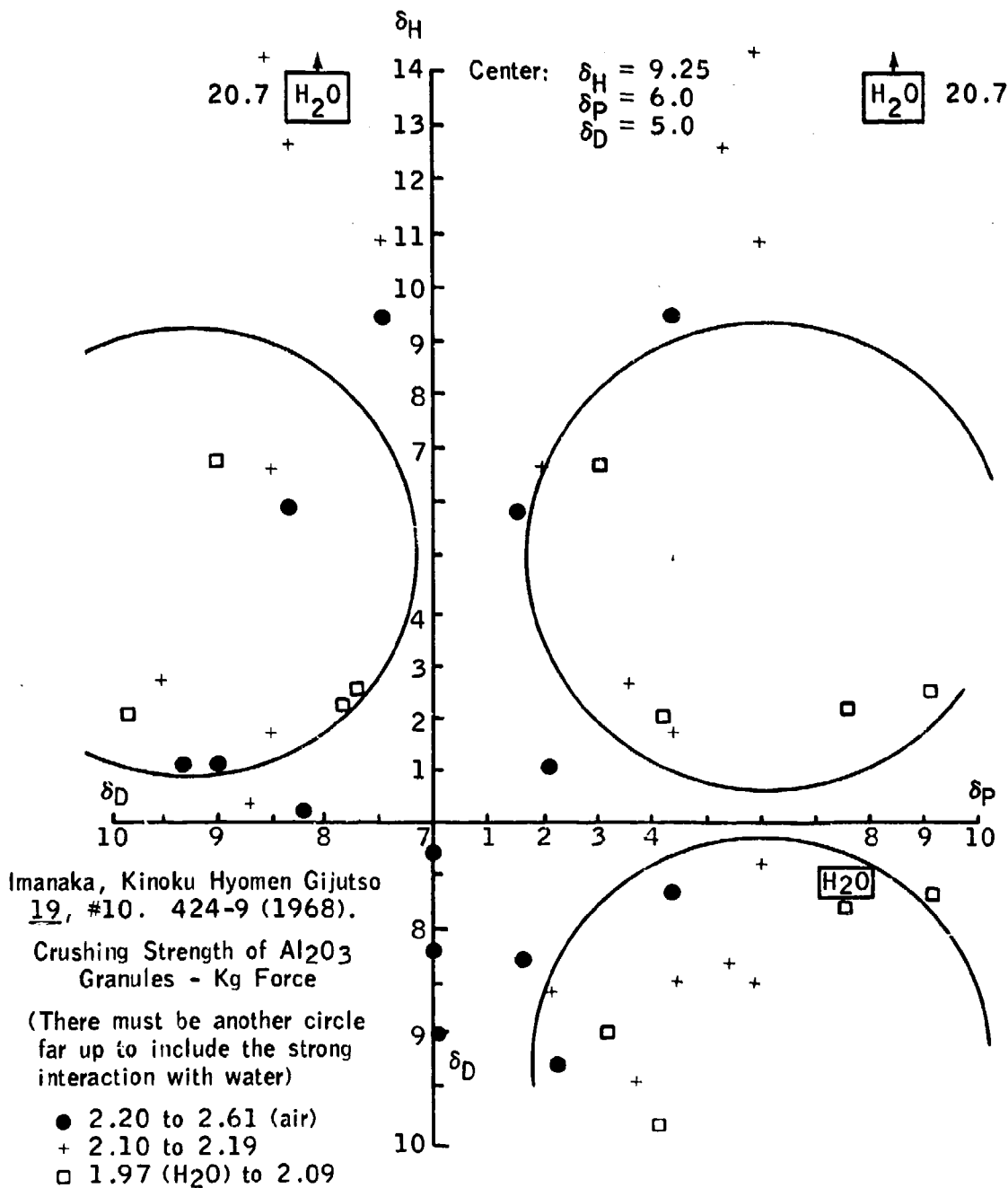
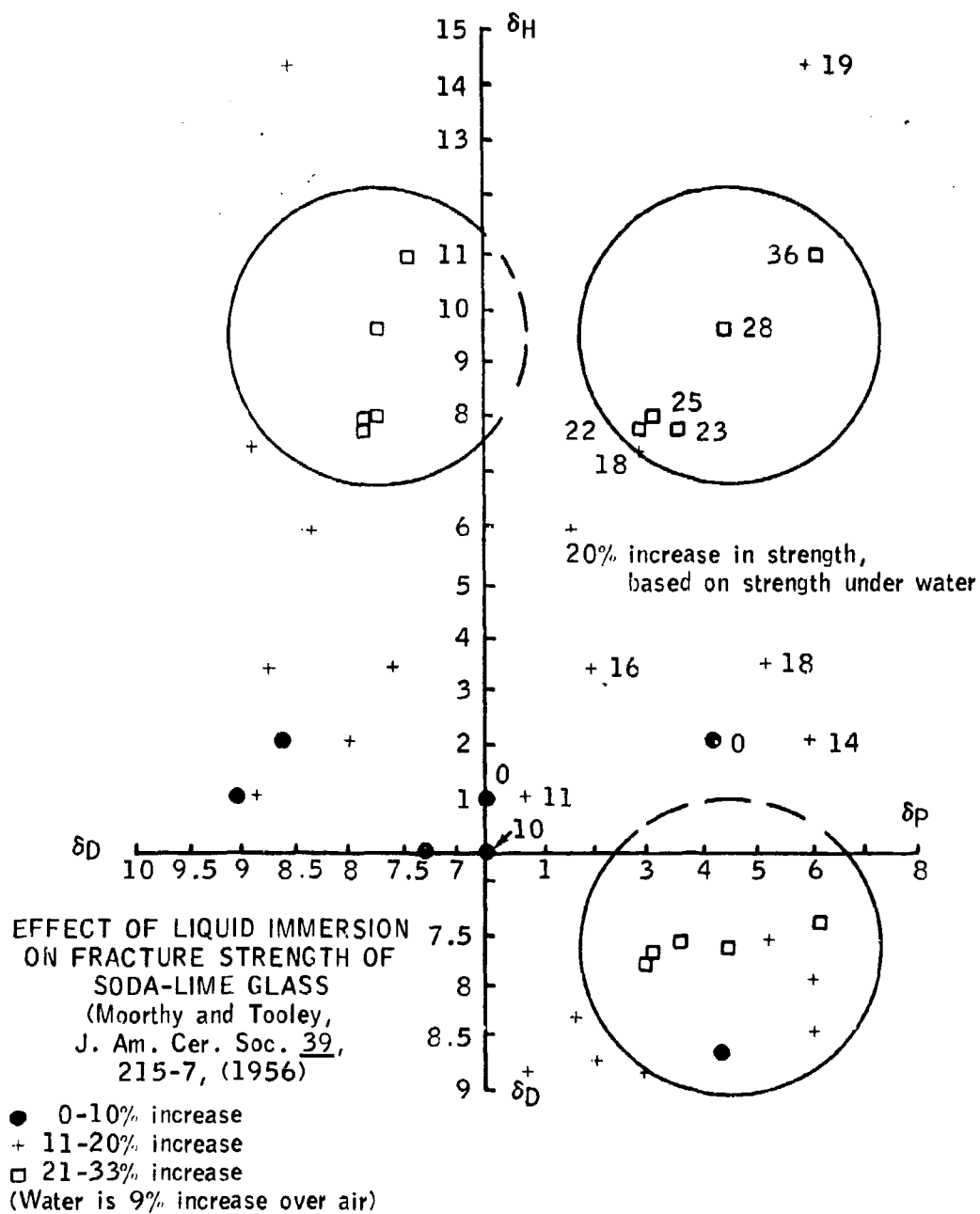


Figure V-6
THE JOFFÉ EFFECT



V. 3.8.3 The Kingsbury-Rowe Method

Two examples of the use of Model IA to obtain energies of "adsorption", or more likely chemisorption, were shown in Tables 5.4-III and IV. Garabrant (personal communication) noted that the function (E/T_s) was far more constant than E . At the time it was not realized that Frewing (1943) had predicted, for stick-slip conditions presumably corresponding to adhesive wear, the film defect (α) and hence (E/RT_t) would be constant for any given compound. While Frewing had intended this to apply to the adsorption of an active additive from an inert solvent (Appendix VI), its applicability to a pure liquid appears at least plausible.

The use of Model IA requires two pieces of data to arrive at an α value, while Frewing's (1942) data provides only T_t . Such data could be analyzed by Equation (5.4-24), modified as indicated in 5.4.1 to give

$$T_t = \frac{E}{2R} \left(1 - \frac{\exp(-E/RT_t)}{3.23 \times 10^{-5} U (M/T_m)^{0.5}} \right) \quad (V-21)$$

This work has not been carried out because the Kingsbury equation requires an iterative solution for E , and more pressing matters prevented setting up such a program. Had Frewing varied the velocity (U), the applicability of Equation (V-21) could have been tested very easily since either E or T_t , and their ratio, would have to vary with U , but he always used 0.005 cm/sec. Other experimenters have varied velocity, but apparently have not covered such a wide range of pure liquids and have tended to use solutions (Grew 1969) as discussed in Appendix VI.

In view of de Boer's (1968) objections on the t concept used in developing it, perhaps work with Equation (V-21) should be deferred in favor of developing some new model. The modification from 5.4.2 cannot be used, since it requires two readings on each lubricant to evaluate k_m^1 , and Frewing's data consists only of T_t .

V. 3.9 Conclusions

It is evident that the outcome of this review of test methods is largely negative, in that most of them are applicable only to irrelevant surfaces. The results are summarized in Table V-V. Clearly, the one method which can be clearly related to the low wear rates with which this STAF is concerned is the Kingsbury-Rowe method. While this has been applied only to ball-on-cylinder data, there is no reason to doubt its applicability to other geometries. It must be recognized that the constant value of E/RT_s noted above was computed from the model which de Boer (1968) considers inappropriate, so that more work is necessary along the lines of Equation (5.4-19) to be sure this outcome is not a coincidence. However, at the present time there is every reason to place the main emphasis on collecting data suitable for this model.

TABLE V - V

Methods for Heat of Immersion in Pure Liquids

Experimental	Solid Surface	Preparation	Remarks
Contact Angle*	Flat	Polished in air	Could be run on broken-in bearings
Powder Wetting	Powder	Ground in air or liquid	Probably irrelevant to bearings
Liquid Metal*	Calculated	Idealized	Definitely irrelevant to bearings
Film Balance*	Flat	Displacement of water	Relevant only to anti-asperities
Guastalla Plate*	Flat	Polished in air	Possibly adaptable to realistic surfaces
Heat of Immersion**	Powder	Ground in air or liquid	Probably irrelevant to bearings
Heat of Adsorption**	Film or wire	Vacuum deposited or ion-sputtered	Definitely irrelevant to bearings
Frewing Dynamic	Ball on flat	Polished in air	Difficult to calculate E value
Metal Cutting*	Lathe cut	Freshly cut	Relevant for high wear rates
Kingsbury-Rowe	Any configuration	Broken-in	Relevant for low wear rates

* Reports only on A_{12} , so dA_{12}/dT must also be obtained for E_{12}

** Measures complete E versus α curve; others measure average or one point.

V. 4. Solid/Solid Interfacial Free Energy

Rabinowicz (1965) undertook to establish the relations between A_{12} for the two metals and their friction-wear properties, mainly in unlubricated sliding. His basic equations are

$$\left. \begin{aligned} A_{12} &\approx 2 \gamma_1 \text{ for identical surfaces} \\ A_{12} &\approx 3/4 (\gamma_1 + \gamma_2) \text{ for compatible surfaces} \\ A_{12} &\approx 1/2 (\gamma_1 + \gamma_2) \text{ for incompatible surfaces} \end{aligned} \right\} \quad (V-22)$$

where "compatible" and "incompatible" are as defined in 5.6.2.

In addition, he derives a number of model equations which deserve further testing. The diameter of a hemispherical particle produced by adhesive wear

$$D_p \approx 6 E_1 A_{12} / (v_1 \tau_y)^2 \quad (V-22)$$

where E_1 , v_1 , and τ_y refer to the wearing surface. This can be simplified by assuming $v_1 = 1/3$ and $\tau_y E_1 = 0.003$ to

$$D_p = 60,000 A_{12} / P_m \quad (V-23)$$

Another model, considering only the properties of the wearing surface, gives

$$D_p = 12,000 \gamma_1 / P_m \quad (V-24)$$

From this relation, he derives a flash temperature

$$T_s - T_b = 9400 F \gamma_1 U / J (k_1 + k_2) \quad (V-25)$$

where 9400 is the units conversion factor for T in $^{\circ}F$, γ_1 , in ergs/cm^2 for the softer material, and U in $\text{ft.}/\text{min.}$

His model for abrasive wear requires two equations. The critical abrasive size is that below which there is a strong dependence of wear rate on size, while above it the rate is independent of size. For 3-body abrasion

$$D_c = 120,000 \gamma_1 / P_m \quad (V-26)$$

and for 2-body abrasion

$$D_c = 24,000 \gamma_1 / P_m$$

His Figure 7.15 indicate that D_c often exceeded these values, probably because average particle sizes rather than maximum sizes were plotted.

Finally, he proposes that under boundary lubrication conditions the effective work of adhesion is

$$A_e = \alpha A_{12} + (1 - \alpha) A_1 \quad (V-27)$$

where α is the fractional film defect and A_1 the work of adhesion of the lubricated surfaces. In the writer's opinion, the latter is negligible, and hence the diameter of the lubricated wear particle

$$D_L = \alpha D_p \quad (V-28)$$

Rabinowicz was concerned because another model, based on friction effects, gave

$$D_L = \alpha^{0.5} D_p \quad (V-29)$$

To the writer, this is merely another case of the ambiguous definition of α . If the more rigorous definition in Equation (5.4-12) is accepted, then

$$D_L = (\alpha_r \alpha_s)^{0.5} D_p$$

and Equation (V-29) simply becomes the special case where α_r or $\alpha_s = 1.00$.

APPENDIX VI

SURFACE AND INTERFACIAL FREE ENERGIES OF MIXTURES

VI. 1. Introduction

While the surfaces of blended liquids are immensely more complicated than those of pure ones, a great deal less can be said about them. The structure of this Appendix will generally follow that of Appendix V, except that only one problem exists on nomenclature. It is the common use of "heat of adsorption" for what will be called here "heat of displacement." This is the ΔE required in Equation (5.4-22) for Model IIC, and may now be defined more specifically by

$$\Delta E = E_{13} - E_{12} \quad (\text{VI} - 1)$$

where E_{13} is the heat of immersion in pure additive.

The point which needs emphasis, first, last and always, is that every substance is "surface active" under the proper circumstances. Put in another way, in every blend containing two substances which differ in more than very minor details, the composition at the surface will be different from that in the bulk. This is the result of the famous Gibbs principle, which states that every system will equilibrate into the configuration having minimum free energy.

The above statements are generally recognized to be true, though not usually expressed so emphatically. What is not so widely recognized is that the "surface" is but one of an infinite number of possible interfaces, and that the composition which gives the minimum free energy at the air interface is quite unlikely to appear where the blend interacts with another liquid or solid. For example, a solution of 1% stearic acid in cetane will show very nearly 0% acid at the air interface, about 40% at a metal interface (see 7.11.4) and close to 100% at an interface with water.

VI. 2. Computation of Interfacial Free Energies of Blends

There have been several approaches taken to establish the free energy at the air-liquid interface. Hildebrand (1950) set up a system based on total solubility parameters, and Clever's students Schmidt (1967) and Myers (1969) improved on it. They took care of deviations from actuality by making adjustments to the molar area, which Hildebrand had defined in terms of molar volume (V) to the $2/3$ power. Getzen (1971) recently summed up all such work and reduced it to easily usable form, but his method need not be discussed here since it does not lead to interfacial energies.

Shain (1964) took a more general approach by calculating the activity coefficients of a solute in two immiscible solvents, and relating them to concentrations at the interface. The method is too complex to quote here, and appears to be limited to liquids forming more or less regular solutions. However, it is undoubtedly capable of being expanded by use of the Hansen partial parameters. Whether such expansion can be extended to metal/liquid interfaces remains to be seen.

Everett (1965) attempted to set up a system for the amount of adsorption at solid interfaces. However, it is better adapted to correlating data than to predicting it.

VI. 3. Measurement of Interfacial Energies of Blends on Solids

In general, the test methods used for pure liquids (Appendix V) can be run on blends. However, interpretation of the results can present serious problems in some cases, while the additional freedom to vary concentration makes others easier to interpret. The following methods involve problems which justify ruling them out without discussion:

1. Contact angle.
2. Powder wetting.
3. Liquid metal tests.
4. Heat of immersion by direct calorimetry.
5. Heat of adsorption - vapor phase.
6. Work of adhesion by metal cutting.

The remaining methods, plus an electrical effect not covered in Appendix V, are discussed below.

VI. 3.1 Heat of Displacement by Flow Micro-Calorimeter

One of the most popular tools at present is the flow calorimeter developed by Groszek (1966, 1967-8, 1970, 1971). In this device, a small bed of the powder to be studied is packed between layers of inert powder with appropriate temperature sensors imbedded. A steady flow of a pure hydrocarbon is passed through the bed until thermal equilibrium is established. The system is calibrated with small "injections" of electrical heating.

VI. 3.1.1 Steady Flow Technique

In this procedure, the pure hydrocarbon is suddenly replaced with a dilute solution of the additive, and recording begun. The rise in temperature is proportional to the heat of displacement (ΔE), and its plot against time

corresponds to a plot of ΔE versus $(1 - \alpha)$, the fraction of surface covered by additive. When the experiment has gone as far as desired (often to $\alpha = 0$) the flow of pure solvent is resumed and the differential heat of desorption is recorded. Some combinations desorb completely; others show apparently permanent chemisorption.

As an added experiment, a second additive may be used to displace the first. There have been fewer of these experiments than of the single-additive type, but one investigation by Jaycock (Groszek 1971) covered the very important situation in which water is the first "additive."

VI. 3.1.2 Pulse Injection Technique

Alternatively, small pulses of more concentrated additive solution are injected into the solvent stream. There seem to be some cases where it is desirable to use both techniques, but the steady flow is usually favored.

VI. 3.1.3 Concentration-Step Technique

The best procedure is to pursue the first concentration until heat evolution ceases, after which a stronger solution is used, and so forth. This permits application of the Langmuir equation, in modified form, as a check on the fraction of surface coverage $(1 - \alpha)$.

Far too many data have been reported on metals and oxides (Groszek 1971) for review here. The method is very promising, despite the inevitable problems with powders.

VI. 3.2 Wettability Transition Temperature

A method resembling that of Guastalla (V.3.6) but not fundamentally related was used by Bigelow (1947). A square of carefully cleared platinum was dipped repeatedly into a solution of fatty acid in dicyclohexyl or cetane, until the surface became repellant to the solution. This system was then heated and tested until a temperature was reached at which the dipper remained wetted. This was considered to be the temperature at which a constant (unknown) value of $(1 - \alpha)/\alpha$ existed. The experiment was repeated at several concentrations.

Plotting the log of concentration against the reciprocal of absolute temperature gave a slope which, handled by the Van't Hoff equation, provided a heat of displacement. Typical results (from bicyclohexyl) were stearic acid = 10.0 kcal/mole and octadecanol = 10.0 kcal/mole. These identical values seem rather unlikely in light of present knowledge, and the method has not been used extensively.

VI. 3.3 Rectification Effect Transition

Sakurai (1953) found that a small DC current flowed between a flat plate and a spherical surface separated by a lubricant film. This effect vanished abruptly with an increase in load or in temperature. Assuming, as usual, that this represents a definite value of $(1 - \alpha)/\alpha$, the log concentration - reciprocal temperature calculation gave the following ΔE values on platinum:

Myristic acid in cetane	= 10.4 kcal/mole
Stearic acid in cetane	= 10.6 kcal/mole
Palmitic acid in decalin	= 10.6 kcal/mole
Iron palmitate in cetane	= 12.1 kcal/mole
Iron stearate in cetane	= 12.7 kcal/mole

Because this paper is available only in Japanese, it seems to have been neglected and no further use of the method made (Grew 1969).

VI. 3.4 The Frewing Dynamic Method

Frewing (1943) extended his work on pure compounds to solutions in white mineral oil. This gave him the additional degree of freedom needed to perform calculations of heat of displacement. The reasoning was as described above (VI.3.1.2), as was the calculation method. The transition point was taken again as the stick-slip. Grew (1969) takes exception to this practice, since stick-slip is highly apparatus-dependent, but concedes that stick-slip usually begins simultaneously with the sharp increase in friction which he regards as the best indication of transition.

The data were handled in the way outlined above. Typical values are shown in Table VI-I. The relevance of these values is uncertain in view of Frewing's practice of running each test on a fresh track, presumably coated with hydrous oxide. His data indicate that adsorption was reversible.

VI. 3.5 The Cameron Dynamic Method

Askwith (1966) used the same mathematics to process data from the more relevant surfaces produced by a 4-ball machine operated at 200 rpm, and Grew (1969) carried the work further. The results were most illuminating, especially the "chain-matching" effect shown in Figure VI-1. Briefly, it appears that the optimum fatty acid to use in a given n-paraffin is that with the same chain length. The writer has explained this (Beerbower 1971C) on the basis that the optimum comes when molar volumes are matched because this minimizes the "ideal" entropy of mixing (Hildebrand 1950; see also 7.11.4).

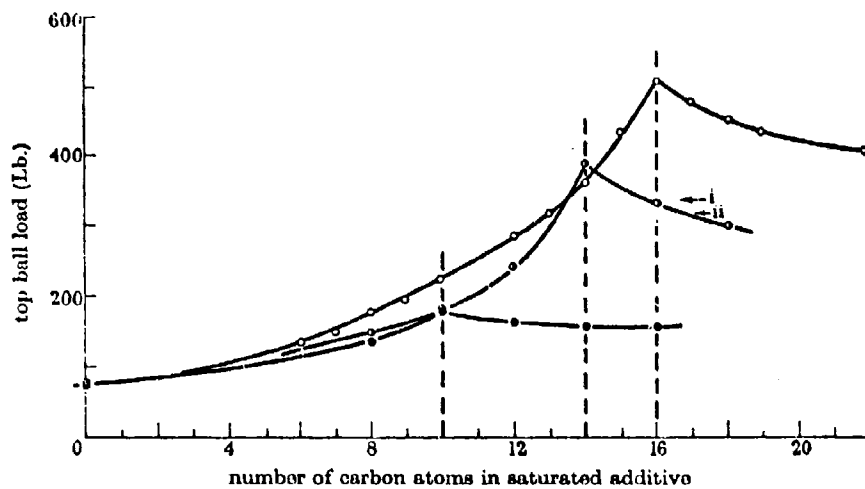
This method is presently the most fully developed dynamic test for ΔE , and can presumably be applied to essentially any test machine in which bulk temperature is controlled independently of frictional heating. However, it depends

TABLE VI-I

HEATS OF DISPLACEMENT FROM WHITE OIL BY
FREWING (1943) DYNAMIC METHOD

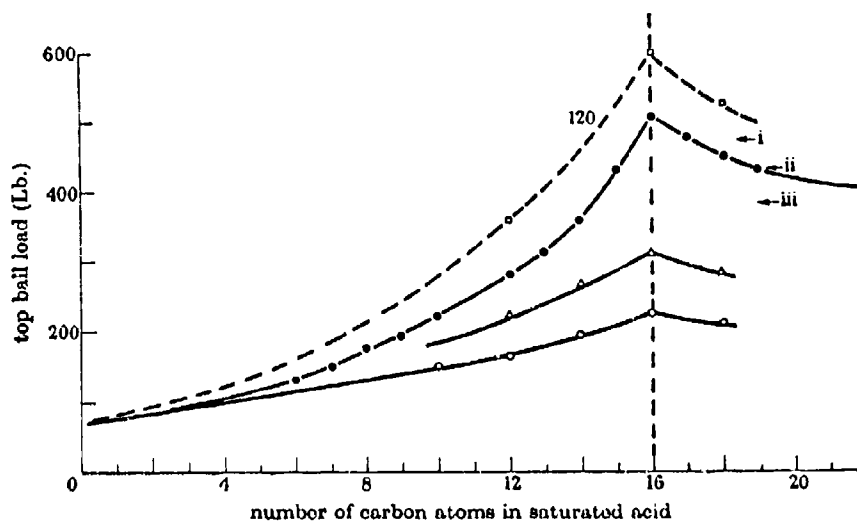
<u>Additive</u>	<u>ΔE (cal/mole)</u>
Capric Acid	12,500
Myristic Acid	13,000
Stearic Acid	13,000
Oleic Acid	13,500
α -Bromo Stearic Acid	10,000
α -Iodo Stearic Acid	10,000
α -Hydroxy Stearic Acid	13,500
Methyl Stearate	8,600
Ethyl Stearate	3,900
n-Butyl Stearate	3,200
n-Hexyl Stearate	6,900
n-Octadecyl Stearate	4,900
Glycol Distearate	10,500
Glycerol Tristearate	7,800
Octadecyl Acetate	7,500
Octadecyl Chloride	14,509
Octadecyl Iodide	7,500
1-Nitro Octadecane	13,000
Octadecyl Cyanide	4,300
Octadecyl Thiocyanate	4,700

FIGURE VI-1



A - Scuffing tests with hexadecane (○), tetradecane (◐) and decane (●) with a range of acids. (i) oleic acid, and (ii) elaidic acid in tetradecane.

All concentrations = 0.003 Molar



B - Scuffing tests with 0.03M additives in hexadecane: acids (□, 120 rev/min. ●, 200); amines (Δ) and alcohols (○). (i) Elaidic and erucic acids; (ii) brassidic acid. (iii) oleic acid.

on detection of a friction transition, so that a sensitive measure of friction is essential. The results must be supplemented with E_{12} values (Appendix V) to obtain the full picture for Model IIC. One problem not yet solved is that desorption from martensitic steels has proved impractical so austenitic steels must be used.

VI. 3.6 The Rowe Dynamic Method

This has been discussed briefly under Model IIC (see 5.5.4). It cannot be recommended as a means for gathering E_{12} and ΔE data until further experimental and theoretical work is completed. However, it does have the advantage of using both wear and friction data and so may be considered more sophisticated than the Cameron dynamic method.

VI. 3.7 Conclusions

Though more complicated than for pure liquids, wetting by mixtures is in fairly good shape as a source of design manual data. The methods are summarized in Table VI-II, with the Cameron dynamic method currently in the best position.

TABLE VI - II

METHODS FOR HEAT OF DISPLACEMENT

<u>Experimental</u>	<u>Solid Surface</u>	<u>Preparation</u>	<u>Remarks</u>
Flow Calorimeter	Powder	Ground Under Liquid	Probably Irrelevant to Bearings
Wettability Transition	Flat	Polished in Air	Doubtful Relevance
Rectification Transition	Ball on Flat	Polished in Air	Doubtful Relevance
Friction Transition	Ball on Flat	Polished in Air	Relevance Uncertain
Cameron Dynamic	Four Ball	Worn Track	Relevant for Low Wear Rates
Rowe Dynamic	Ball on Disk	Worn Track	Relevant for Medium Wear Rates

APPENDIX VII

SURFACE AND INTERFACIAL ENTROPIES

VII. 1. Introduction

The need for entropy values in boundary lubrication is two-fold. As indicated in Appendix IV, most of the surface free energy data on solids (γ_s) can be obtained only near or at the melting point, and requires adjustment to T_s or T_b . A lesser problem of the same sort is adjustment of liquid (γ_l) values from the usual 20 or 25°C. The other sort of problem is the conversion of free energy or work of adhesion to total energy (E) or heat of immersion (E_{12}). As shown in Appendices V and VI, some of the most relevant test methods yield E_{12} and ΔE values direct, so this Appendix will make only a minimum effort on those points. Indeed, there is relatively little work to report on ΔS_{12} .

In this Appendix, the emphasis is on predictive methods. Correlation methods are cited only where predictions cannot be made. Experimental methods are omitted, as these are all well known.

VII. 2. Surface Entropy of Organic Liquids

The literature on $d\gamma/dT$ is extremely prolific. This interest can be traced to the pioneer work of Eötvös, who correctly identified the two key parameters in 1886. His equation

$$\gamma = k_E (T_c - T - 6)/V^{2/3} \quad (\text{VII-1})$$

where k_E is the "Eötvös constant", T_c the critical temperature and V the molar volume, is still rated as useful by Reid (1966). The temperature correction of 6°K was added in 1893 by Ramsay, and is trivial except near T_c . Unfortunately, Equation (VII-1) is accurate only for non-polar liquids of low molecular weight, for which $k_E = 2.12$. It decreases with polarity and increases with molecular weight, so a higher ketone or ester may also have $k_E = 2.12$ by coincidence.

A more accurate correlation was suggested by van der Waals in 1894:

$$\gamma = k_v T_c^{1/3} P_c^{2/3} (1 - T_R)^{1.2} \quad (\text{VII-2})$$

where P_c is the critical pressure and T_R the reduced temperature (T/T_c). The factor k_v and exponent 1.2 were supposed to be universal constants for all materials, but this has not proved to be very accurate (Reid 1966). Better results are obtained with

$$k_v = 0.133 \alpha_c - 0.281 \quad (\text{VII-3})$$

where α_c is the Riedel factor, but large errors result with polar compounds, due in part to variation of the exponent from 0.99 to 1.23. However, elimination of $k_v T_c^{1/3} P_c^{2/3}$ gives a simplified form

$$\gamma = \gamma_o (1 - T_R)^{1.2} \quad (\text{VII-4})$$

where γ_o is the (extrapolated) value at 0°K. Reid (1966) recommends this for adjusting γ to any temperature.

The most elaborate system is that of Macleod, further developed by Sugden and put into final form by Quayle (1953),

$$\gamma = (P (\rho - d)/M)^4 \quad (\text{VII-5})$$

where P is the "Parachor", a constant for each liquid which is claimed to be independent of temperature, M the molecular weight, ρ the density of the liquid and d that of the vapor. In most cases, d is negligible and the equation becomes simply

$$\gamma = (P/V)^4 \quad (\text{VII-6})$$

The Parachor can be calculated with fairly good accuracy from tabulated values for various functional groups. Lee (1967) has made a comparison of this system of "building blocks" against Small's (1953), on the basis of predicting values of γ_c for polymers, and came to the conclusion that Small's were better. However, the latter are only useful at 25°C. It must be recognized that part of the apparent constancy of P is due simply to the high exponent 4, which has a strong tendency to hide significant deviations in γ .

A third set of building blocks are those due to Lydersen, but most readily available in Reid (1966). Values of T_c may be built up by using them in the equation

$$T_c = T_b / (0.567 + \Sigma \Delta_T - (\Sigma \Delta_T)^2) \quad (\text{VII-7})$$

where T_b is the boiling point at one atmosphere. If needed, P_c and V_c can be built up by similar procedures. The T_c values may then be used in the Watson equation as expressed by Bondi (1968).

$$\Delta H_v = H_o^o (1 - T_R)^{0.38} \quad (\text{VII-8})$$

where H_o^o is the extrapolated heat of vaporization at 0°K. Bondi provides building blocks for H_o^o . This can be shown to be essentially consistent with Equation (VII-1).

It would be desirable to have the separate contributions of the A, B and C energies of Appendix III to dy/dT . As worked out by Panzer (1972), see V.3.1.3,

$$\gamma = \gamma^d + \gamma^p + \gamma^h = KA/V^{2/3} + KaB/V^{2/3} + Kbc/V^{2/3} \quad (\text{VII-9})$$

Differentiating the first term,

$$d\gamma^d/dT = KdA/V^{2/3}dT - 2\alpha\gamma^d \quad (\text{VII-10})$$

Substituting ΔH_v from Equation (VII-8) for A leads to the complicated

$$d\gamma^d/dT = K (0.38 H_D^0 / (1 - T_R)^{0.62} - R) / V^{2/3} - 2\gamma\alpha/3 \quad (\text{VII-11})$$

where H_D^0 is the heat of vaporization of the homomorph at 0°K.

A simpler approach uses one of Hildebrand's (1950) approximations

$$d(\ln\delta_D)/dT \approx -1.25d \quad (\text{VII-12})$$

where α is the thermal expansivity, dV/VdT .

From this and $A = V\delta_D^2$, algebraic manipulation of the first term in Equation (VII-9) gives

$$d(\ln\gamma^d)/dT \approx -2.17\alpha \quad (\text{VII-13})$$

This is not only far from rigorous, but also is not as simple as it appears to be, since α itself is a complicated function of T_R . Bondi shows that $\rho\alpha$, which is identical to $d\rho/dT$, is essentially constant over the range $0.4 < T_R < 0.8$, but conversion of Equation (VII-13) to this form does not eliminate the problem as ρ remains in the equation.

Similar treatment of Equation (VII-1) yields

$$d(\ln\gamma^d)/dT = -1.38\alpha - 2.12/\gamma^d V^{2/3} \approx -3.7\alpha \quad (\text{VII-14})$$

and of Equation (VII-6) yields

$$d(\ln\gamma)/dT = -4.0\alpha \quad (\text{VII-15})$$

Obviously, these cannot all be right, even allowing for the fact that Equation (VII-15) includes polar as well as non-polar liquids.

A better solution is offered by differentiating Equation (VII-4)

$$d(\ln \gamma^d)/dT = -11/9 (T_c - T) \quad (\text{VII-16})$$

which eliminates both α and ρ . This should certainly be valid for regular liquids and the homomorphs, using T_c values from Equation (VII-7).

Duga (1969) took another approach by combining Equation (VII-5) with a vapor pressure relationship and the Clausius-Clapeyron equation

$$T \ln P_v = -a\gamma (M/(\rho - d))^{2/3} + b \quad (\text{VII-17})$$

(a and b are not the same as in VII-9) which he feels gives justification for a factor of 6/5 rather than 11/9 in Equation (VII-16). The difference is trivial; it is the fact that these two approaches resulted in essentially the same relationship that is important.

The polar contribution to $d\gamma/dT$ has never been worked out, but Equations [3], [4] and [4A] in Appendix III should contain the necessary information. Even though $d\mu/dT$ is essentially zero, Equation [3] presents a formidable problem of differentiation as the result will contain α , $d\epsilon/dT$ and dn/dT in a complex pattern. The molar refraction has been used as a correction to Equation (VII-6), but only over the range 20-30°C. It has the effect of calculating a sort of apparent density from n values and yet another set of building-blocks. The problem is the lack of dn/dT values over a wide range, which also limits the usefulness of Equation [4A]. Thus, we are left with the admittedly crude Equation [4] as a working tool. Its weakness can easily be demonstrated, using dipole moments from Bondi's (1968) Table 14.28 for the alkyl-methyl ketones, where the C=O group contributes 2.81 ± 0.03 esu. Conversion to δ_p values by Equations [4] and [5] gives values which are at variance with those of Equation [3] and Hansen's nearly identical experimental values in Appendix VIII, Table I.

However, as an approximation we can use

$$d(\ln \gamma^p)/dT = -2a \alpha/3 \quad (\text{VII-18})$$

since $d\mu/dT = 0$.

The contribution of hydrogen and other electron transfer bonding included in C was relatively well worked out by Bondi (1968), from whose earlier work Equation [6] in Appendix III was derived. The details are given in Appendix VIII, page 907. Since Equation [6] is so well documented, we may use it without many reservations, the only obvious one being that Bondi may well have included some B energy in the C energy values.

$$d(\ln \gamma^h)/dT = mb(dC/CdT) - 2mb\alpha/3 \quad (\text{VII-19})$$

where dC/dT is taken from Bondi's tabulation.

Assembling these three parts, we can now write with considerable confidence for all organic liquids:

$$-dy/dT = 1.22/\gamma^d(T_c - T) + 2a \alpha/3\gamma^p + 2mb \alpha/3\gamma^h - mbdCk\gamma^h dT$$

(VII-20)

The temperature coefficients of the partial solubility parameters are shown in Appendix VIII, p. 328. Blanks (1964), Weimer (1965) and Helpinstill (1968) published lists giving values of δ_p (usually symbolized as " λ ") and τ , which is equal to $(\delta_p^2 + \delta_h^2)^{0.5}$. While their values are reasonably consistent, some serious problems arise at this point. In the first place, the two later articles give higher values of δ_p at 298°K than Blanks, whose chart was followed by Hansen (1967) and Beerbower (1969). Hopefully, Figure V-1 resolves this discrepancy, but these authors also present values for λ and τ at other temperatures which are not consistent with the equations in Appendix VIII. By analogy, the equations in Appendix VII should be used with some caution, until they have been compared with compilations of γ data such as Quayle (1953) which cover considerable ranges of T.

VII. 3. Surface Entropy of Liquid Ceramics

Some work has been done to correlate dy/dT data on fused salts and oxides by Duga (1969). However, there are some serious problems in predicting dy/dT for materials on which no experimental data exists. This is frequently the case for T_c , which requires much higher temperatures than ΔH_v . Values of T_c for organic compounds may be calculated by Equation (VII-7), but there are no building-blocks for the inorganic compounds in Lydersen's tables (Reid 1966).

However, consistent values of T_c are obtainable from Equation (VII-16) when γ values are available at three temperatures. These may then be used to construct the entire curve from T_c to 0°K. The results tend to justify the common practice of treating dy/dT as constant over the narrow ranges in which experimental γ values are usually available, since most of the curvature takes place in the upper 20% of the range. Generally, γ values extrapolated to 298°K on the linear assumption have proved to be correct to within about 2%.

VII. 4. Surface Entropies of Liquid Metals

The only metal for which T_c had then been determined experimentally was mercury, but Grosse (1962) estimated T_c values for many metals from the densities of liquid and vapor at high temperatures. These were then used in Equation (VII-1) to correlate the available γ data on the liquid phase of those metals. The results were quite plausible in some cases, but in others the results appear quite discrepant. Mercury is, as usual, quite anomalous. The well-known high dy/dT exceeds even that predicted by $T_c = 1733^\circ\text{K}$. His values of the slope in Equation (VII-16) vary from 0.249 for Cd to 1.282 for Na, compared with the accepted value of 1.222 or 1.200.

Eberhart (1970) had T_c values for the five alkali metals, as well as a newer value for Hg of $1758 \pm 5^\circ\text{K}$. Grosse's values for Na and K proved to be about 10% too high. He tested the "corresponding states" version of Equation (VII-1)

$$\gamma_o V_c^{2/3} = K_E T_c \quad (\text{VII-21})$$

where γ_o is the value of γ extrapolated to 0°K , V_c is V at T_c and the accepted value of K_E is 4.3.

The K_E results varied from 3.7 for Hg through 2.2 for Na to 1.8 for Rb and Cs, showing that metals do not follow the corresponding states principle. The data were well fitted by the empirical

$$\gamma_o (V_c - 27 \pm 4) = (1.66 \pm 0.02) T_c \quad (\text{VII-22})$$

In order to check this against Grosse's T_c values, it would be necessary to estimate V_c for the 15 metals, and reliable methods are not available. Meanwhile, Equation (VII-1) can be used to estimate γ from Grosse's T_c and γ_o values.

VII. 5. Surface Entropy of Solids

Conversion of the above equations to use on solids does not present any serious problem. Both Kubaschewski (1967) and Duga (1969) proceed to use ΔH_s as a replacement for ΔH_v , with considerable justification. The fact that the coefficient of thermal expansion (α) is a great deal lower for solids than for liquids does not create much difficulty, if we accept the validity of Equation (VII-15). Presumably, the solid will follow the same rule, with $\gamma_s = 1.14 \gamma$, as in V.4.2, and $\alpha_s \approx 0.01 \alpha$. Thus, the slope from T_m to 0°K will be considerably flatter than s from T_m to $T_c - 6$, and the slope will be predictable from α_s/α data when such is available.

Equations have not yet been developed for dividing the surface entropy of organic solids into d, p and h component. However, the fact that the surface properties are all strongly dependent on V leads the writer to believe that simply substituting α_s for α in the appropriate equations will serve the purpose.

VII. 6. Entropy of Liquid/Liquid Interfaces

In contrast to the extensive literature on air/liquid interfacial entropies, there has not been much done with liquid/liquid interfaces. The methods of Good (1970) are applicable, but are not emphasized in his article. Since such interfaces are outside the scope of this STAF, no attempt will be made here to carry this work forward.

VII. 7. Entropy of Liquid/Solid Interfaces

As there are no accepted prediction methods for the air/solid or liquid/liquid interfaces, it is to be expected that the liquid/solid interfacial entropy is not yet predictable. In fact, there is not even much experimental data on this matter. Neumann(1970) has contributed a study of the variation with temperature of contact angle of organic liquids on plastics, and Rhee (1970, 1971) has done the same for liquid metals on ceramics. The latter study resulted in the conclusion that the Zisman (1964) linear relation of $\cos \theta$ to γ_s is obeyed, so that dA_{12}/dT can be calculated. This is, of course, merely one of the latest and best of various articles on high temperature wetting since Bondi's (1953) classic review, but it is quite difficult to generalize anything from them.

The most important category for the present purpose is the entropy of organic liquid/solid metal interfaces, and no articles on that subject have been located.

If the "heat of immersion" (E) in V.2.5 is regarded as a true heat rather than an energy, the function E/T_s becomes the entropy of immersion. As shown in 5.4.2, this is essentially constant at 40.8 for hydrocarbons in air on 52100 steel, with a standard deviation of about 1.3. Though this is based on questionable assumptions, it is a very practical engineering tool for a dynamic measure of interfacial entropy.

VII. 8. Entropy of Mixed Liquid/Solid Interfaces

Since this is the most complicated of all such systems, it can be classed as "unpredictable by present methods." Very few experimental results have been reported, and there is not even enough theory to analyze such data as exists.

VII. 9. Conclusions

There is more than adequate theory for the prediction of the surface entropies of organic liquids. However, as the complexity is increased towards the goal of mixed liquids on solid metals, theory and even experiment become completely inadequate. Thus, even if works of adhesion were known for these systems, no means for converting them to heats of immersion is available.

As concluded in Appendices V and VI for entirely different reasons, the best way to obtain heats of immersion and heats of displacement is by the dynamic methods for friction and/cr wear.

Reprinted from *ENCYCLOPEDIA OF CHEMICAL TECHNOLOGY*, Supplement Volume, 2nd ed.
Copyright © 1971 by John Wiley & Sons, Inc.

SOLUBILITY PARAMETERS

Solubility parameter concepts have found wide and increasing use in many areas of industrial and academic endeavor because of the simplicity with which significant predictions can be obtained. These concepts are generally applied to solvent selection in the industrial community, while the calculation of solubilities and thermodynamic properties have concerned the more theoretical workers. Hildebrand's initial work was based on the solution of nonelectrolyte solids in nonpolar solvents, although such topics as gas-in-liquid solubility, liquid-liquid miscibility, metallic solutions, polymer solutions, and correlations with surface phenomena and critical properties were discussed (1, 2). Burrell (3-6) applied the solubility parameter to polar solvents and polar polymers, and Hansen (7-12) has described relationships with organic and inorganic pigments, proteins, and biological materials, and even inorganic salts. Based on these results, it appears that a solubility parameter study can provide systematic information on physical interactions for any material which interacts suitably (dissolves, swells, or absorbs) when contacted with a sufficient number of solvents (energy probes). It is assumed that there is a close similarity between the cohesive energy densities of the interacting, well-defined solvents and that of the substrate material, and thus a solubility parameter may be assigned to the material.

Historical Background

Hildebrand and Scott designated the energy of vaporization per cubic centimeter as the *cohesive energy density* (*ced*) and its square root as the *solubility parameter*, δ . Thus,

$$\delta = \left(\frac{\Delta H_v - RT}{V} \right)^{1/2} = \left(\frac{\Delta E_v}{V} \right)^{1/2} = (ced)^{1/2} \quad (1)^*$$

where ΔH_v and ΔE_v are the heat and energy of vaporization, respectively, and V is the molar volume. As suggested by Crowley (13) the unit $(\text{cal}/\text{cm}^3)^{1/2}$ is designated as a "hildebrand." This parameter is important in the estimate of the heat of mixing for two nonpolar liquids, given by Hildebrand as:

$$\Delta H^M \approx \Delta E^M = \phi_1 \phi_2 (x_1 V_1 + x_2 V_2) (\delta_1 - \delta_2)^2 \quad (2)$$

* Correction made for this STAF, to $\Delta H_v - RT$.

SOLUBILITY PARAMETERS

The heat of mixing ΔH^M and the energy of mixing ΔE^M are equal when there is no volume change on mixing. The ϕ 's are the volume fractions of the liquids, and the x 's are their mole fractions.

Consideration of the free energy equation

$$\Delta G^M = \Delta H^M - T\Delta S^M \quad (3)$$

quickly shows that the negative ΔG^M values necessary for solution to occur can be achieved by reducing ΔH^M , which in turn means that δ_1 and δ_2 should be similar in value. The entropy of mixing ΔS^M can be assumed to be positive, and generally does not receive much attention, at least from the practical approaches to using solubility parameter theory.

Burrell (3-6) was the first to apply the solubility parameter to practical (polar) systems. He grouped a large number of solvents into three classes according to their "low," "medium," and "high" hydrogen bonding capacities, and used these groupings together with the solubility parameter itself to aid in solvent selection in the paint industry. Following this lead, various refinements were proposed to quantify a hydrogen bonding parameter (14, 15), and ultimately a three-parameter system using the solubility parameter, the dipole moment, and a hydrogen bonding parameter (based on shifts in the 4-micron band for methyl deuterioxide) was proposed (13, 16).

Other approaches to account for polar bonding have been developed along the lines proposed by Van Arkel (17) and Hildebrand (17a), and particularly by Prausnitz and co-workers (18-20). The basis of this approach is that the cohesive energy arises from both the permanent dipole molecular interactions and the London "dispersion" type atomic interactions. The latter have been estimated as being equal to the energy of vaporization of a homomorph at the same reduced temperature, T/T_c , where T_c is the critical temperature. The homomorph of a polar molecule is a nonpolar molecule having very nearly the same size and shape as those of the polar molecule. Each solvent is assigned a polar solubility parameter and a nonpolar solubility parameter. This division has been used to estimate solubilities (18, 20), to aid in solvent selection for extractions (19), and to calculate activity coefficients (21). A somewhat similar approach to division of the cohesive energy was described by Gardon (22) in which a fractional polarity was estimated.

In any of these systems, as well as the one proposed by Hansen, described in more detail below, a proper estimate of the nonpolar contribution is important. The homomorph concept appears to be the current best choice, since use of ionization potentials in various potential equations does not account for the effects of inner shell electrons. On the other hand, this approach tacitly assumes that the hydrocarbon homomorph's entire cohesive energy is due to London forces, which is not exactly true. This is an area for future research.

If it is assumed (7-12) that the cohesive energy, ΔE , arises from contributions from hydrogen bonding ΔE_H , as well as permanent-dipole-permanent-dipole interactions, ΔE_P , and nonpolar interactions, ΔE_D , the following equation can be written:

$$\Delta E = \Delta E_D + \Delta E_P + \Delta E_H \quad (4)$$

Dividing this equation by the molar volume of a solvent, V , gives:

$$\frac{\Delta E}{V} = \frac{\Delta E_D}{V} + \frac{\Delta E_P}{V} + \frac{\Delta E_H}{V} \quad (5)$$

SOLUBILITY PARAMETERS

or

$$\delta^2 = \delta_D^2 + \delta_P^2 + \delta_H^2 \quad (6)$$

where

$$\delta = (\Delta E/V)^{1/2} \quad (7)$$

is the usual equation for the solubility parameter,

$$\delta_D = (\Delta E_D/V)^{1/2} \quad (8)$$

is the dispersion component of the solubility parameter,

$$\delta_P = (\Delta E_P/V)^{1/2} \quad (9)$$

is the polar component of the solubility parameter, and

$$\delta_H = (\Delta E_H/V)^{1/2} \quad (10)$$

is the hydrogen bonding component of the solubility parameter. Permanent dipole-induced dipole interactions are generally small compared to the other forces (24), with all errors being largely grouped into the δ_H component. These parameters are given in Table 1 for a number of solvents. The parameters listed in Table 1 were developed through independent calculations for the individual values where data were available and have been checked by numerous solubility evaluations (7, 8, 10-12) and compared to other systems for their accuracy (25). The nonpolar contribution was estimated from homomorph considerations; the hydrogen bond values agree well with ΔH_v measurements of about 4,650 cal for each OH group, and the polar contribution was calculated from a slight modification of Böttcher's equation (26):

$$\delta_P^2 = \frac{12,108}{V^2} \cdot \frac{\epsilon - 1}{2\epsilon + n_D^2} (n_D^2 + 2) \mu^2 \quad (11)$$

where V is the molar volume, ϵ is the dielectric constant (static value), n_D is the index of refraction for D light (sodium), and μ is the dipole moment expressed in Debye units (10^{-18} (esu)(cm)).

It must be emphasized at this point that "hydrogen bonding" is being used rather loosely in this article, and that some more ambiguous term such "weak chemical bonds," or perhaps "association bonds" might be better. However, historical considerations favor continuation of this loose usage, at least for the present article, with the understanding that some π -bonds, quadrupole and octapole interactions, and probably other yet unnamed forces are included in δ_H and ΔE_H .

The energies calculated as described fit equation 4 or 6 very well where all four terms can be estimated independently. These quantities can also be estimated from the parameters in the other systems described above by use of the simplified equations of Beerbower (25), such as

$$\delta_P = 18.3 \mu / \sqrt{V} \quad (11a)$$

but parameters so calculated may be in error by ± 1.7 hildebrand. A better solution is to extend the "group contributions" mentioned above for $-\text{OH}$ to most of the common functional groups.

The group concept was first applied to total parameters by Small, but his work was updated and extended by Hoy (23). They felt that $V\delta$ contributions from por-

Table 1. Solubility Parameters of Various Liquids at 25°C

Class	Code	Name	Molar volume V	Parameters hildebrands,		
				δ_D	δ_P	δ_H
paraffin hydrocarbons	1	<i>n</i> -butane	101.4	6.9	0	0
	2	<i>n</i> -pentane	116.2	7.1	0	0
	3	<i>i</i> -pentane	117.4	6.7	0	0
	4	<i>n</i> -hexane	131.6	7.3	0	0
	5	<i>n</i> -heptane	147.4	7.5	0	0
	6	<i>n</i> -octane	163.5	7.6	0	0
	7	2,2,4-trimethylpentane	166.1	7.0	0	0
	8	<i>n</i> -nonane	179.7	7.7	0	0
	9	<i>n</i> -decane	195.9	7.7	0	0
	10	<i>n</i> -dodecane	228.6	7.8	0	0
	11	<i>n</i> -hexadecane	294.1	8.0	0	0
	12	<i>n</i> -eicosane	359.8	8.1	0	0
	13	cyclohexane	108.7	8.2	0	0.1*
	14	methylcyclohexane	128.3	7.8	0	0.5
aromatic hydrocarbons	14.1	<i>cis</i> -decahydronaphthalene	156.9	9.2	0	0
	14.2	<i>trans</i> -decahydronaphthalene	159.9	8.8	0	0
	15	benzene	89.4	9.0	0*	1.0
	16	toluene	106.8	8.8	0.7	1.0
	16.1	naphthalene*	111.5	9.4	1.0	2.9
	17	styrene	115.6	9.1	0.5	2.0
	18	<i>o</i> -xylene	121.2	8.7	0.5	1.5
	19	ethylbenzene	123.1	8.7	0.3	0.7
	19.1	1-methylnaphthalene	138.8	10.1	0.4	2.3
	20	mesitylene	139.8	8.8	0	0.3
	21	tetrahydronaphthalene	136.0*	9.6*	1.0	1.4
	21.1	biphenyl	154.1	10.5	0.5	1.0
	22	<i>p</i> -diethylbenzene	156.9	8.8	0	0.3
halohydrocarbons	23	methyl chloride	55.4	7.5*	3.0	1.9
	24	methylene dichloride	63.9	8.9	3.1	3.0
	24.1	bromochloromethane	65.0	8.5	2.8	1.7
	25	chlorodifluoromethane	72.9	6.0	3.1	2.8
	26	dichlorofluoromethane	75.4	7.7	1.5	2.8
	27	ethyl bromide	76.9	8.1	3.9	2.5
	27.1	1,1-dichloroethylene	79.0	8.3	3.3	2.2
	28	ethylene dichloride	79.4	9.3*	3.6	2.0
	28.1	methylene di-iodide*	80.5	8.7	1.9	2.7
	29	chloroform	80.7	8.7	1.5	2.8
	29.1	1,1-dichloroethane	84.8	8.1	4.0	0.2
	29.2	ethylene dibromide	87.0	9.6	3.3	5.9
	30	bromoform	87.5	10.5*	2.0	3.0*
	31	<i>n</i> -propyl chloride	88.1	7.8	3.8	1.0
	32	trichloroethylene	90.2	8.8	1.5	2.6
	33	dichlorodifluoromethane	92.3	6.0	1.0	0
	34	trichlorofluoromethane	92.8	7.5	1.0	0
	35	bromotrifluoromethane	97.0	4.7	1.2	0
	36	carbon tetrachloride	97.1	8.7	0	0.3
	37	1,1,1-trichloroethane	100.4	8.3	2.1	1.0
	38	tetrachloroethylene	101.1	9.3	3.2*	1.4
	39	chlorobenzene	102.1	9.3	2.1	1.0
	39.1	<i>n</i> -butylchloride	104.9	8.0	2.7	1.0
	39.2	1,1,2,2-tetrachloroethane	105.2*	9.2	2.5	4.6
	40	bromobenzene	105.3	10.0	2.7	2.0
	41	<i>o</i> -dichlorobenzene	112.8	9.4	3.1	1.6
	42	benzyl chloride	115.0	9.2*	3.5	1.3

Table 1 (continued)

Class	Code	Name	Molar volume, V	Parameters hildebrands,		
				δ_D	δ_P	δ_H
ethers	42.1	1,1,2 2-tetrabromoethane ^a	116.8	11.1	2.5	4.0
	43	1,2-dichlorotetrafluoroethane ^a	117.0	6.2	0.9	0
	44	1,1,2-trichlorotrifluoroethane	119.2	7.2	0.8	0
	45	cyclohexyl chloride	121.3	8.5	2.7	1.0
	46	1-bromonaphthalene	140.0	9.9	1.5	2.0
	47	trichlorobiphenyl ^d	187.0	9.4	2.6	2.0
	48	perfluoromethylcyclohexane	196.0	6.1	0	0
	49	perfluorodimethylcyclohexane ^d	217.4	6.1	0	0
	50	perfluoro- <i>n</i> -heptane	227.3	5.9	0	0
	51	furan	72.5	8.7	0.9	2.6
	51.1	epichlorhydrin	79.9	9.3	5.0	1.8
	51.2	tetrahydrofuran	81.7	8.2	2.8	3.9
	51.3	1,4-dioxane	85.7	9.3	0.9	3.6
	51.4	methylal ^c CH ₂ (OCH) ₂	88.8	7.4	0.9	4.2
	52	diethyl ether	104.8	7.1	1.4	2.5
	53	bis(2-chloroethyl) ether	117.6	9.2	4.4	2.8 ^a
	53.1	anisole ^c	119.1	8.7	2.0	3.3
	53.2	di-(2-methoxyethyl) ether	142.0	7.7	3.0	4.5
	53.3	dibenzyl ether ^c	192.7	8.5	1.8	3.6
	53.4	di-(2-chloro- <i>i</i> -propyl) ether ^c	146.0	9.3	4.0	2.5
ketones	54	bis-(<i>m</i> -phenoxyphenyl) ether	373.0	9.6	1.5	2.5
	55	acetone	74.0	7.6	5.1	3.4
	56	methyl ethyl ketone	90.1	7.8	4.4	2.5
	57	cyclohexanone	104.0	8.7	3.1	2.5
	58	diethyl ketone	106.4	7.7	3.7	2.3
	58.1	mesityl oxide	115.6	8.0	3.5	3.0
	59	acetophenone	117.4	9.6 ^a	4.2	1.8
	60	methyl <i>i</i> -butyl ketone	125.8	7.5	3.0	2.0
	61	methyl <i>i</i> -amyl ketone	142.8	7.8	2.8	2.0
	61.1	isophorone	150.5	8.1	4.0	3.6
aldehydes	62	di-(<i>i</i> -butyl) ketone	177.1	7.8	1.8	2.0
	63	acetaldehyde ^c	57.1	7.2	3.9	5.5
	63.1	furfuraldehyde	83.2	9.1 ^a	7.3	2.5
	64	butyraldehyde	88.5	7.2	2.6 ^a	3.4 ^a
	65	benzaldehyde	101.5	9.5	3.6	2.6
esters	66	ethylene carbonate	66.0	9.5	10.6	2.5
	66.1	γ -butyrolactone	76.8	9.3	8.1	3.6
	66.2	methyl acetate	79.7	7.6	3.5	3.7
	67	ethyl formate	80.2	7.6	4.1	4.1
	67.1	propylene carbonate	85.0	9.8	8.8	2.0
	68	ethyl chloroformate	95.6	7.6	4.9	3.3
	69	ethyl acetate	98.5	7.7 ^a	2.6	3.5 ^a
	69.1	trimethyl phosphate	99.9	8.2	7.8	5.0
	70	diethyl carbonate	121.	8.1	1.5	3.0
	71	diethyl sulfate	131.5	7.7	7.2	3.5
	72	<i>n</i> -butyl acetate	132.5	7.7	1.8	3.1
	72.1	<i>i</i> -butyl acetate	133.5	7.4	1.8	3.1
	72.2	2-ethoxyethyl acetate	136.2	7.8	2.3	5.2
	73	<i>i</i> -amyl acetate	148.8	7.5	1.5	3.4
	73.1	<i>i</i> -butyl <i>i</i> -butyrate	163.	7.4	1.4	2.9
	74	dimethyl phthalate	163.	9.1 ^a	5.3 ^a	2.4
	75	ethyl cinnamate	166.8	9.0	1.0	2.9
	75.1	triethyl phosphate	171.0	8.2	5.6	4.5
	76	diethyl phthalate	198.	8.6	4.7	2.2
	76.1	di- <i>n</i> -butyl phthalate	266.	8.7 ^a	4.2	2.0
	76.2	<i>n</i> -butyl benzyl phthalate	306.	9.3	5.5	1.5

(continued)

Table 1 (continued)

Class	Code	Name	Molar volume, V	Parameters hildebrands,		
				δ_D	δ_P	δ_H
nitrogen compounds	77	tricesyl phosphate	316.	9.3	6.0	2.2
	78	tri- <i>n</i> -butyl phosphate	345.	8.0	3.1	2.1
	79	<i>t</i> -propyl palmitate ^c	330.	7.0	1.9	1.8
	79.1	di- <i>n</i> -butyl sebacate	339.	6.8	2.2	2.0
	79.2	methyl oleate ^d	340.	7.1	1.9	1.8
	79.3	dioctyl phthalate	377.	8.1	3.4	1.5
	80	di- <i>n</i> -butyl stearate ^c	382.	7.1	1.8	1.7
	81	acetonitrile	52.6	7.5	8.8	3.0
	81.1	acrylonitrile	67.1	8.0	8.5	3.3
	82	propionitrile	70.9	7.5	7.0	2.7
	83	butyronitrile	87.0	7.5	6.1	2.5
	84	benzonitrile	102.6	8.5	4.4	1.6
	85	nitromethane	54.3	7.7	9.2	2.5
	86	nitroethane	71.5	7.8	7.6	2.2
	87	2-nitropropane	86.9	7.9	5.9	2.0
	88	nitrobenzene	102.7	9.8	4.2	2.0
	89	ethanolamine	60.2	8.4	7.6	10.4
	89.1	ethylene diamine	67.3	8.1	4.3	8.3
	89.2	1,1-dimethylhydrazine ^c	76.0	7.5	2.9	5.4
	89.3	2-pyrrolidone	76.4	9.5	8.5	5.5
	90	pyridine	80.9	9.3	4.3	2.9
	91	<i>n</i> -propylamine	83.0	8.3	2.4	4.2
	92	morpholine	87.1	9.2	2.4	4.5
	93	aniline	91.5	9.5	2.5	5.0
	93.1	<i>N</i> -methyl-2-pyrrolidone	96.5	8.8	6.0	3.5
	94	<i>n</i> -butylamine	99.0	7.9 ^a	2.2 ^a	3.9 ^a
	95	diethylamine	103.2	7.3	1.1	3.0
	95.1	diethylenetriamine	108.0	8.2	6.5	7.0
	96	cyclohexylamine	115.2	8.5	1.5	3.2
	96.1	quinoline	118.0	9.5	3.4	3.7
	97	di- <i>n</i> -propylamine	136.9	7.5	0.7	2.0
	98	formamide	39.8	8.4	12.8	9.3
	99	dimethylformamide	77.0	8.5	6.7	5.5
	99.1	<i>N,N</i> -dimethylacetamide	92.5	8.2	5.6	5.0
	99.2	tetramethylurea	120.4	8.2	4.0	5.4
	99.3	hexamethyl phosphoramide ^c	175.7	9.0	4.2	5.5
sulfur compounds	100	carbon disulfide	60.0	10.0	0	0.3
	101	dimethyl sulfoxide	71.3	9.0	8.0	5.0
	101.1	ethanethiol ^c	74.3	7.7	3.2	3.5
	102	dimethyl sulfone ^b	75.	9.3	9.5	6.0
acid halides and anhydrides	103	diethyl sulfide	108.2	8.3	1.5	1.0
	104	acetyl chloride	71.0	7.7	5.2	1.9
	104.1	succinic anhydride ^b	66.8	9.1	9.4	8.1
monohydric	105	acetic anhydride	94.5	7.8 ^a	5.7 ^a	5.0 ^a
	120	methanol	40.7	7.4	6.0	10.9
	121	ethanol	58.5	7.7	4.3	9.5
	121.1	ethylene cyanohydrin (hydraacrylonitrile)	68.3	8.4	9.2	8.6
alcohols	121.2	allyl alcohol ^c	68.4	7.9	5.3	8.2
	122	1-propanol	75.2	7.8	3.3	8.5
	123	2-propanol	76.8	7.7	3.0	8.0
	123.1	3-chloro- <i>n</i> -propanol	84.2	8.6	2.8	7.2
	124	furfuryl alcohol	86.5	8.5	3.7	7.4
	125	1-butanol	91.5	7.8	2.8	7.7
	126	2-butanol	92.0	7.7	2.8	7.1

Table 1 (continued)

Class	Code	Name	Molar volume, V	Parameters hildebrands,		
				δ_D	δ_P	δ_H
	126.1	2-methyl-1-propanol	92.8	7.4	2.8	7.8
	126.2	benzyl alcohol	103.6	9.0	3.1	6.7
	127	cyclohexanol	106.0	8.5	2.0	6.6
	128	1-pentanol	109.0	7.8	2.2	6.8
	129	2-ethyl-1-butanol	123.2	7.7	2.1	6.6
	129.1	diacetone alcohol	124.2	7.7	4.0	5.3
	129.2	1,3-dimethyl-1-butanol	127.2	7.5	1.6	6.0
	130	ethyl lactate	115.	7.8	3.7	6.1
	130.1	n-butyl lactate	149.	7.7	3.2	5.0
	131	ethylene glycol monomethyl ether	79.1	7.9	4.5	8.0
	132	ethylene glycol monoethyl ether	97.8	7.9	4.5	7.0
	132.1	diethylene glycol monomethyl ether	118.0	7.9	3.8	6.2
	132.2	diethylene glycol monoethyl ether	130.9	7.9	4.5	6.0
	133	ethylene glycol mono-n-butyl ether	131.6	7.8	2.5	6.0
	133.1	2-ethyl-1-hexanol	157.0	7.8	1.6	5.8
	134	1-octanol	157.7	8.3	1.6	5.8
	134.1	2-octanol	159.1	7.9	2.4	5.4
	134.2	diethylene glycol mono-n-butyl ether	170.6	7.8	3.4	5.2
	135	1-decanol	191.8	8.6	1.3	4.9
	136	"tridecyl alcohol" ^d	242.	7.0	1.5	4.4
	136.1	"nonyl" phenoxy ethanol ^d	275.	8.2	5.0	4.1
	137	oleyl alcohol ^d	316.	7.0	1.3	3.9
	137.1	triethylene glycol mono-oleyl ether	418.5	6.5	1.5	4.1
acids	140	formic acid	37.8	7.0	5.8	8.1
	141	acetic acid	57.1	7.1	3.9	6.6
	141.1	benzoic acid ^b	100.	8.9	3.4	4.8
	142	n-butyric acid ^c	110.	7.3	2.0	5.2
	142.1	n-octioic acid ^c	159.	7.4	1.6	4.0
	143	oleic acid ^d	320.	7.0	1.5	2.7
	143.1	stearic acid ^b	326.	8.0	1.6	2.7
phenols	144	phenol	87.5	8.8	2.9	7.3
	144.1	1,3-benzenediol ^b	87.5	8.8	4.1	10.3
	145	m-cresol	104.7	8.8	2.5	6.3
	145.1	o-methoxyphenol ^c	109.5	8.8	4.0	6.5
	146	methyl salicylate	129.	7.8	3.9	6.0
	147	"nonyl" phenol ^d	231.	8.1	2.0	4.5
water	148	water ^c	18.0	7.6 ^a	7.8 ^a	20.7 ^a
polyhydric alcohols	149	ethylene glycol	55.8	8.3	5.4	12.7
	150	glycerol	73.3	8.5	5.9	14.3
	150.1	propylene glycol	73.6	8.2	4.6	11.4
	150.2	1,3-butanediol	89.9	8.1	4.9	10.5
	151	diethylene glycol	95.3	7.9	7.2	10.0
	152	triethylene glycol	114.0	7.8	6.1	9.1
	153	hexylene glycol	123.0	7.7	4.1	8.7
	154	dipropylene glycol ^d (mixed isomers, see Vol. 10, p. 651)	131.3	7.8	9.9	9.0

^a Altered from previously published value.

^b Solid, treated as supercooled liquid.

^c Values uncertain.

^d Impure commercial product of this nominal formula.

SOLUBILITY PARAMETERS

tions of a molecule would be additive, and obtained good precision. However, hydrogen bonding is usually additive on an energy ($V\delta^2$) basis (28). The near-constancy of μ for each group in McClellan's (27) Appendix B, along with equation 11a led to correlating both $V\delta_P$ and $V\delta_H^2$. The former showed greater precision and freedom from hydrocarbon portion effects, and so was used in Table 2 while the hydrogen bonding columns use $V\delta_H^2$. The precision shown is the full range for the data (about ± 2 standard deviations).

Table 2. Group Contributions to Partial Solubility Parameters

Function and group	Polar parameter, $V\delta_P$, (cal·cc) ^{1/2} /mol	H-bond parameter, $V\delta_H^2$, cal/mol	
		Aliphatic	Aromatic
—F	225 \pm 25 ^a	~0	~0
—Cl	300 \pm 100	100 \pm 20 ^a	100 \pm 20 ^a
>Cl ₂	175 \pm 25	165 \pm 10 ^a	180 \pm 10 ^a
—Br	300 \pm 25	500 \pm 100	500 \pm 100
—I	325 \pm 25 ^a	1000 \pm 200 ^a	
—O—	200 \pm 50	1150 \pm 300 ^b	1250 \pm 300 ^{ab}
>CO	390 \pm 15	800 \pm 250 ^b	400 \pm 125 ^a
—COO—	250 \pm 25	1250 \pm 150	800 \pm 150 ^a
—CN	525 \pm 50	500 \pm 200 ^b	550 \pm 200 ^a
—NO ₂	500 \pm 50	400 \pm 50 ^b	400 \pm 50 ^a
—NH ₂	300 \pm 100 ^a	1350 \pm 200 ^c	2250 \pm 200 ^{ab}
>NH	100 \pm 15	750 \pm 200	
—OH	250 \pm 30	4650 \pm 400 ^c	4650 \pm 500
(—OH) _n	$n(170 \pm 25)$	$n(4650 \pm 400)$	$n(4650 \pm 400)$ ^a
—COOH	220 \pm 10	2750 \pm 250	2250 \pm 250 ^a

^a Two or less compounds tested, confidence limits by analogy.

^b Unpublished infrared data included in correlation.

^c Data from (28), corrected to 25°C and $V\delta_P^2$ subtracted. For important steric shielding effects, see his Tables 7.6 and 7.7 (page 205).

Most of the data were taken from Table 1, using compounds having only one functional group. In addition, excess heats of vaporization from Bondi (28) and Weimer (19), and from gas-liquid chromatography by Martire (29), were corrected for dipole interaction and used for hydrogen bonding. An unpublished infrared method similar to that cited by Crowley (13) was also used. Some δ_P values from equation 11a were used where Table 1 data were sparse (ie, on —F).

The reader is cautioned against indiscriminate addition of functional groups as is permitted in Small's system. For —OH, δ_H is additive and δ_P nearly so; but the effect of adding a second chlorine reduces δ_P and may or may not double δ_H . Most spectacular is the effect of ortho —COO— groups in phthalate; they combine to quadruple δ_P . Addition of an ether group causes such complex effects that Hoy (23) calls the products "chameleon"; some of the benefits are discussed below under emulsions, but mathematical prediction requires further study.

Practical Use of the Solubility Parameter

Solvent Selection for Coatings. The most widespread practical use of the solubility parameter has been within the paint and related industries since these are intimately associated with solvent selection. Indeed, most of the practical develop-

SOLUBILITY PARAMETERS

ments outlined in the previous section were by workers in the paint field. The usual procedure is to perform a solubility-parameter study by contacting the solute (polymer) in question with a limited number of solvents chosen specifically to examine behavior at all levels of the parameters concerned. These data are then plotted in a suitable manner and a region of solubility is defined by those solvents found to dissolve the particular polymer. Plotting the data is a straightforward procedure when only two solvent parameters are used, but requires more effort when the three-dimensional systems are employed (Fig. 1). Various means to plot three parameters have been suggested including projections along each of the three axes (12, 25), use of triangular coordinates (30), and contour plotting (16). It has also been suggested that the δ_p vs δ_H plot in the Hansen system is sufficiently accurate for most practical purposes (Fig. 2). It should be remembered, however, that cyclic, halogenated, and a few other special solvents have relatively high δ_D components, as do most polymers, and are, therefore, somewhat more potent than indicated by this plot. Fig. 1 also has the advantage that the solubility region is a circle rather than an irregular shaped body as is found in the other systems. A computer can be very useful in calculations and in plotting.

Having defined a region of solubility, one can proceed to use it in solving practical problems. Solvent selection can be systematically worked out according to the requirements of the solvent for evaporation rate, flash point, toxicity, etc, and finally the requirement that the solvent or solvent blend chosen lie within the region of solubility. Many practical solutions to this problem involve boundary solvent mixtures, since hydrocarbon diluents are used as much as possible for economic reasons. A rule for the average solubility parameter of a mixed solvent based on the volume fractions of the solvents is sufficiently accurate in practice. The effect of diluents (nonsolvents) is seen since the average solubility parameter approaches a boundary as their concentration increases. One can also systematically choose a mixed, good solvent composed exclusively of nonsolvents, by choosing nonsolvents located, respectively, on opposite sides of the region of solubility. It is possible to make use of combinations of alcohols and hydrocarbons in such situations, perhaps including a third, slow, good solvent as insurance that the last solvent leaving the film is a good one. Plasticizers can contribute to the average solubility parameter of a system and should not be neglected in calculations or graphic solutions to problems.

In general, one can quickly determine all possible combinations of solvents which will solve a particular solubility problem. It may be useful to remember that the solution viscosity at high polymer concentration can be decreased by selectively using solvent blends where the solvent viscosity itself is low, and where the solubility parameter of the solvent approaches that of the polymer. Returning to the example of an alcohol-hydrocarbon mixed solvent, it is well known that additions of 1-butanol (viscosity = 2.96 cP) to xylene (viscosity = 0.87 cP) will produce this viscosity reduction effect in spite of the greater neat viscosity of the 1-butanol. Had ethanol been chosen instead of 1-butanol, the effect would have been more pronounced because of its lower viscosity and higher δ_H . Similar examples can be found by considering solubility parameter plots, such as Fig. 1 or 2.

Selection of Other Coating Ingredients. In addition to solvent selection one can use solubility-parameter (energy) concepts to help understand and solve other types of practical problems. Burrell's articles are filled with examples. Liquid miscibility plots can be constructed, if desired, and problems concerning polymer compatibility

SOLUBILITY PARAMETERS

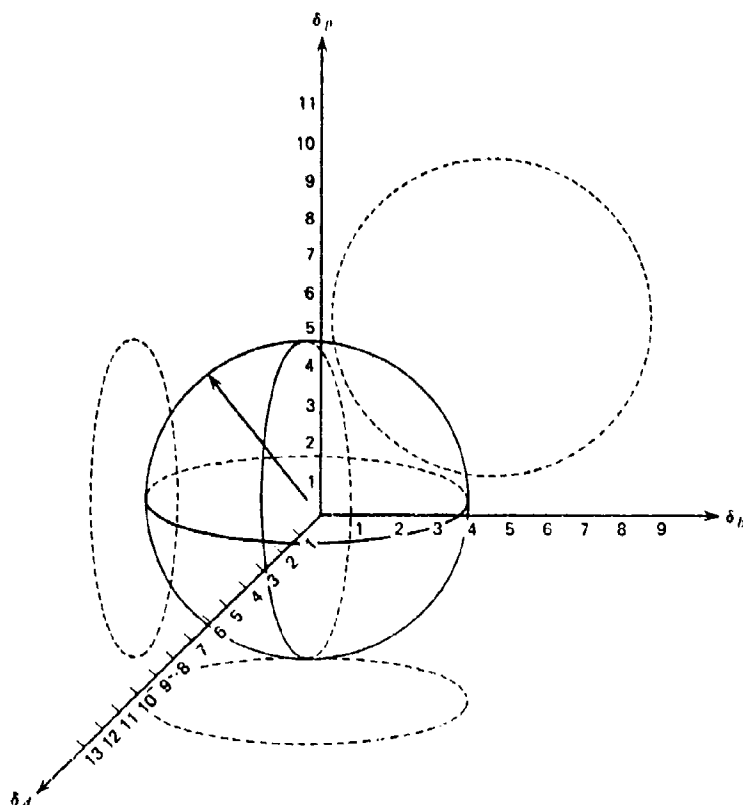


Fig. 1. Solubility plot for poly(methyl methacrylate) based on solution in solvents of different delta values. The circles represent areas within which the solubility is 10% or more.

can be systematically approached since polymers having essentially the same solubility parameters (dissolve in the same solvents) are more likely to be compatible because of their physical similarity. Crystallinity and high molecular weight may far outweigh these factors, however. Other examples include the formulation of thixotropic systems where (in alkyd systems) one customarily reacts a small amount of hydrocarbon insoluble material into the system late in the synthesis of the vehicle. These hydrocarbon insoluble portions form loosely bound domains in hydrocarbon solvent; these domains provide body to the system while at rest and are easily broken by shear (brushing) to allow even flow during application. Small additions of alcohol will also destroy the domains and the thixotropic behavior, illustrating that one does not always want good solvents.

Some work on the relation of solubility parameters to pigment dispersion has been reported, but this has not been explored as much as the importance of the process warrants (31-33). In general, if a pigment suspends for prolonged periods in the liquids used in a solubility-parameter study of its surface properties, that pigment will be easily wet by a suitable binder. The most suitable binder from this point of view

SOLUBILITY PARAMETERS

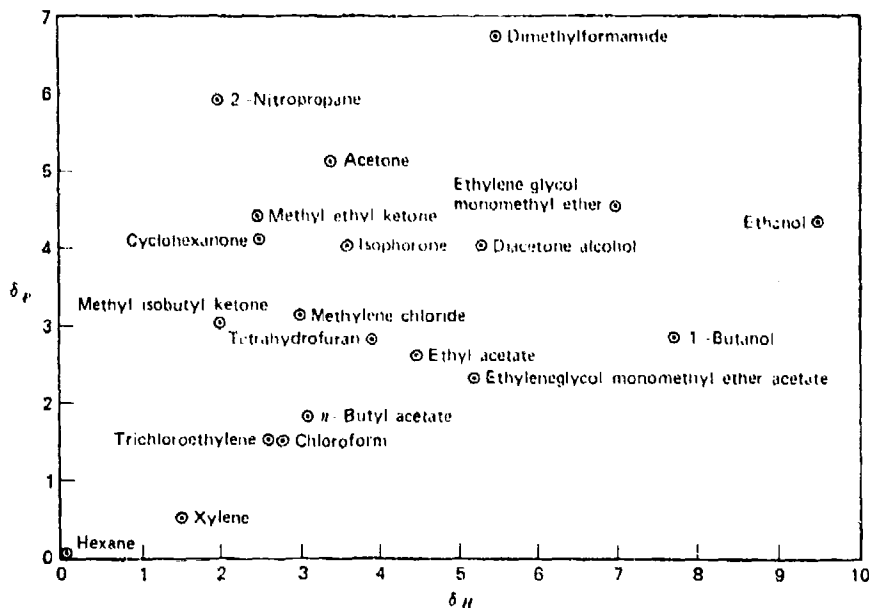


Fig. 2. Solubility parameter plot for common solvents.

would be one dissolving in the same solvents that suspend the pigment. Adsorption seems to be greater in a poor solvent than in a good one, but stability may be greater in a better solvent since the polymer molecules apparently extend more in the better solvent maintaining greater interparticle distances (31-34). Adsorption of polymers as well as surface-active agents is better considered in terms of nonsolubility rather than solubility, since the Gibbs principle requires that the total system free energy become stabilized at the lowest possible value. According to the particular situation this may be arranged to occur with high energy portions being adsorbed on a high energy solid surface, or perhaps in a water phase. Low energy portions may remain in an organic vehicle, or if they are not compatible therein (eg hydrocarbon, silicone), they will appear at the lowest energy surface available, the air-liquid interface.

Dispersion-type coatings can also be analyzed from a solubility parameter point of view. The general principle is to distribute the film former in a stabilized manner, in a relatively fast evaporating medium, be it water or hydrocarbon solvent. Film formation from the dispersed state requires the flowing together of the dispersed particles. This intimate intermingling of the particles is effected by a liquid known as a *coalescing solvent*, which is added to impart the required mobility to the polymer molecules. To be effective, the slowly evaporating, coalescing solvent must be such that the solubility parameter of the last solvent to volatilize is located within the region of solubility for the film-forming material. Organosols are formulated on similar principles, with a boundary solvent mixture in the initial stable system. The solvent improves with the loss of the poorer solvent and a film is formed, aided by the application of heat in most cases.

In general, visual observations of 10% "solutions" are suitable for a solubility parameter study. Higher or lower concentrations may be used in particular problems.

SOLUBILITY PARAMETERS

Low degrees of swelling (solution) in noncrosslinked polymer systems essentially define concentric regions surrounding those usually described as "soluble" on a solubility parameter plot.

Other Studies on Polymers. Beerbower (25) has systematized selection of cross-linked elastomers for use in contact with various types of liquids. This is illustrated in Figure 3, where the swelling of polysulfide rubber has been plotted on the plane obtained by opening out the three-dimensional corner of Figure 1 along the δ_D axis and flattening it. Each liquid appears in each quadrant, so that this presentation is 50% redundant. The 25% swelling contours are presented here as rectangles as a simplification to permit expressing them as "pass or fail" limits, but could have been shown as the projections of two ellipsoids. This figure is of special interest since it unexpectedly revealed that the rubber consisted of a block copolymer—a finding which was later verified by independent investigation.

A third method of presentation is shown in Figure 4. This is a computer procedure, as it requires simultaneous evaluation of δ_D , δ_P and δ_H for the elastomer, two weighting factors for the differences in δ_P and δ_H , the maximum possible swelling, Q_{max} , and a constant related to the relative molar volumes of the liquid and elastomer (between crosslinks). As there is some question as to the true constancy of the last factor, it is suggested that investigators develop their own program for such problems, and especially for copolymers. Only vulcanized natural rubber was evaluated by the computer procedure, but results on twelve other elastomers were correlated by the flattened three-dimensional approach. The results were successful in terms of predicting "pass" or "fail" on the 25% swell criterion in 97% of over 1000 data points.

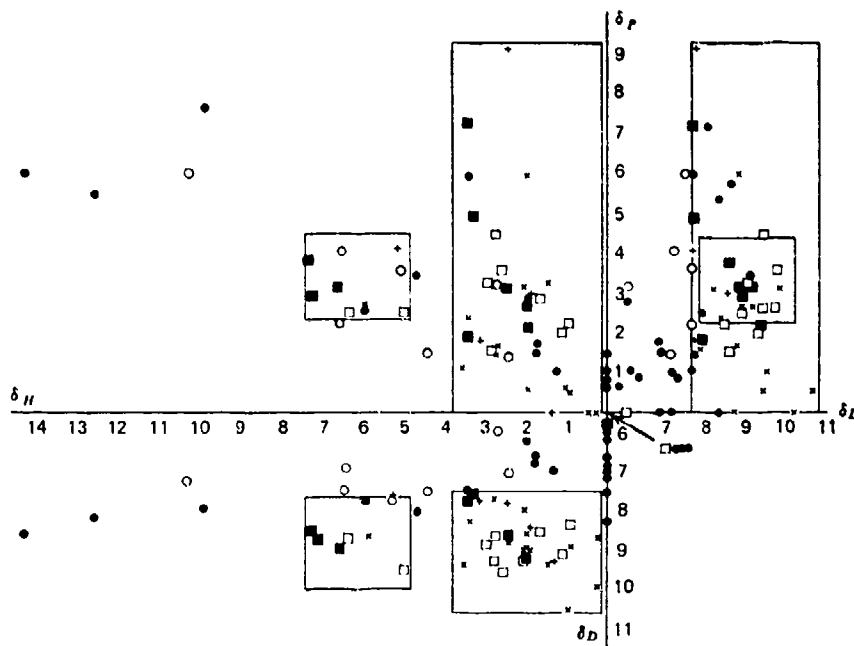


Fig. 3. Bimodal 25% swell contour of polysulfide rubber (CST). LEGEND: ■, greater than 350% swell; □, = 101 to 350% swell; ×, 51 to 100%; +, 26 to 50%; ○, 11 to 25%; and ● 0 to 10%.

SOLUBILITY PARAMETERS

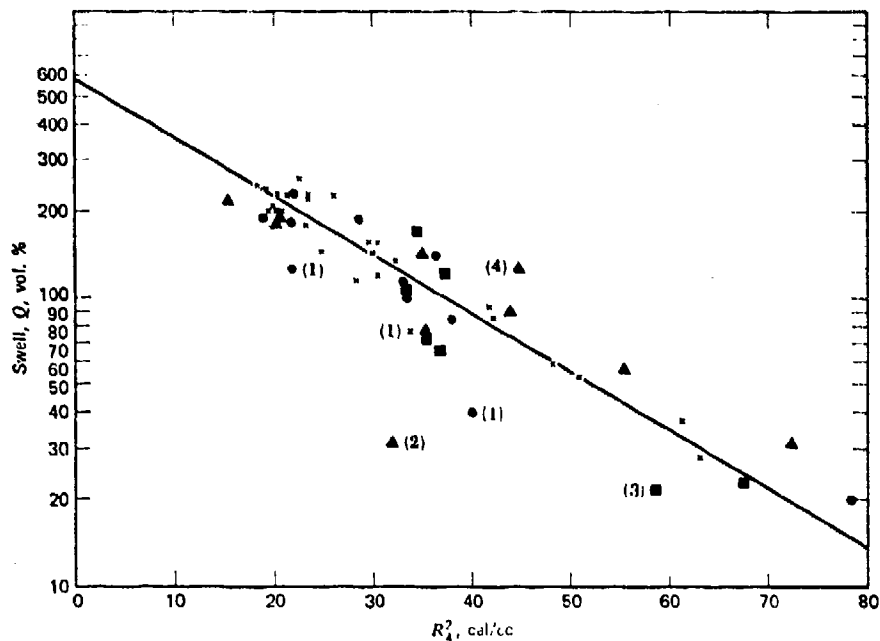


Fig. 4. Correlation of swell of natural rubber with radius of spheroid; all values of swell were normalized for vulcanization level of 2.75 pph sulfur. The equation of the line is $\log_{10} Q = \log_{10} Q_{\max} - 0.08 R_A^2$; $R_A^2 = (\delta_D - 8.8)^2 + 0.19 (\delta_P + 3.9)^2 + 0.19 (\delta_H - 3.4)^2$. Legend: \times , binary mixtures from ref. 35; \bullet , pure compounds from ref. 35; \blacktriangle , pure compounds from ref. 36; and \blacksquare , pure compounds from ref. 37. (1) indicates hexane-ethyl acetate system; (2), aniline; (3), CCl_4/F_2 ; and (4), benzaldehyde.

Another important property of a polymer is its wettability. This has been characterized by Zisman (38) in a *critical surface tension*, γ_c , defined as the surface free energy of the most energetic nonhydrogen-bonded liquid to wet the polymer completely (ie, contact angle = 0°). Wu (39) has been able to correlate these γ_c values with the solubility parameters of the polymers as calculated by Small's (40) method. His preferred equation is dimensionally unbalanced, but he also offers a second, balanced equation which gives about the same results. As an example, Wu calculates γ_c for polyisoprene in the following way:

The monomer is considered in simple groups, with the double bond which enters into polymerization disregarded. "Force constants" according to Small are tabulated, multiplied by the number of groups of this class, and summed up:

$-\text{CH}_2$	$1 \times 214 = 214$
CH_2	$1 \times 133 = 133$
$\text{CH}-$	$1 \times 28 = 28$
$-\text{CH}=\text{CH}-$	$1 \times 222 = 222$
H	$1 \times 90 = 90$
ΣF	$= 687$

This is substituted into the equation

$$\gamma_c = 0.229(\Sigma F)^2 d^{1.47} / x^{0.33} M^{1.47} \quad (11b)$$

SOLUBILITY PARAMETERS

where d is the polymer density, x the number of atoms in the monomer and M the monomer molecular weight. The result of this calculation is $\gamma_c = 30.7$, compared with 31 by actual measurement. Presumably, the constants more recently computed by Hoy (23) would give approximately the same value.

An alternative approach was published by Hansen (40a), in which the cosine of the contact angle is used in place of the solubility on a plot similar to Figure 1. The circles are then drawn to enclose all liquids which spread on the surface. The result is a set of three partial parameters to characterize the surface, rather than a γ_c value. The technique, like Zisman's, may be applied to metallic and other surfaces as well as plastics.

Surface Free Energies. Hildebrand (2) established the relationship between solubility parameter and surface free energy as a simple quadratic equation, but unfortunately was unable to provide a theoretical value for the constant in it. Even more unfortunately, he then set up a dimensionally unbalanced equation which has been widely used, with confusing results (see preceding section). Beerbower (41) has carried the analysis through on a three-dimensional parameter basis, and was able to correlate the surface free energies of most organic liquids, fused salts, and liquid metals with one equation:

$$\gamma = 0.0715V^{1/2}[\delta_D^2 + 0.632(\delta_P^2 + \delta_H^2)] \quad (12)$$

Special equations were required for aliphatic alcohols, for alkali halides, for five metals roughly grouped as "irregular," and for γ_c . The constant was derived from the number of nearest neighbors lost in surface formation, assuming that the molecules tend to occupy, on the average, the corners of regular octahedra. This postulate has other justifications, but the greatest is that it yields a value of 0.07152, while empirical fit of the data on organic solvents had previously given 0.07147.

Hildebrand (2) suggests that the solubility parameters of blends may be estimated by summing the parameters of the components multiplied by their volume fractions. This works well enough for polymer interactions (7, 25) but cannot be applied to surface free energies of blends due to enrichment at the surface in accordance with the Gibbs-Duhem principle of minimizing the free energy of the system. This approach presumably gives the instant free energy of a freshly formed surface, which is useful in such fast-moving processes as fractional distillation. Hildebrand's solution to this problem is not entirely satisfactory, though Clever (41a) has done a great deal of work on evaluating it and has developed a computer program for the purpose. The predictions are quite accurate but are made so at the cost of using the molar surface areas of the components as adjustable parameters. The deviation from the "real" areas as expressed by a $V^{1/2}$ function is minor in regular liquids but becomes sizable with increasing irregularity. An alternative approach was worked out by Shain (42) and applied by Sprow (43) with good success, again for simple mixtures. Beerbower (25) reported use of the volume blending rule along with chromatographic separation for the solubility parameters of petroleum fractions, and more recently has used equation 12 to estimate these from the surface free energies. This again falls into the regular solution category, and there is still need for much work in prediction of surface free energies from three-dimensional parameters for blends of irregular liquids. In addition, the rate of attaining the Gibbs-Duhem equilibrium has not been adequately predicted.

Liquid-Liquid Interactions. One of the factors often overlooked in the use of solubility parameters is the vital importance of the molar volumes when predicting

SOLUBILITY PARAMETERS

solubilities, and such rules-of-thumb as "liquids differing by 2 hildebrands are incompletely miscible" can be quite misleading. The reason is that disparity of molar volume plays a dual role here, as it builds up not only $\Delta\delta$, but also the entropy. Hildebrand's equation (ref. 1 (43a) (eq. 10.3) shows this very clearly, and has been used by Beerbower (25) to correlate the aniline point (ASTM Method D-611) with the solubility parameters and molar volumes at 25°C of hydrocarbon solvents. Assuming that the "consolute temperature" (CST) comes at the 50%-by-volume point, which Francis (44) shows is usually true, and using 10.6 as the empirical solubility parameter of aniline (approximately $\delta_p^2 + 0.25[\delta_p^2 + \delta_H^2]$) he arrived at the relation

$$\delta = 10.6 - \left[\frac{4R(A + 460)}{1.8(V + 91.1)} \right]^{1/2} \quad (13)$$

where $R = 1.9864$, the gas constant in cal/(°C)(mole). This expression fits the aniline point (A , in °F) and molar volumes of 41 hydrocarbon solvents within ± 0.8 hildebrand. However, the relationship fails for olefins and esters, where the CST does not fall near 50%-by-volume point. Hildebrand's equation contains means for adjusting to other consolute volumes, but these were not tested.

It will be noted that the above example uses the single parameter, with a somewhat arbitrary adjustment for δ_p and δ_H . For liquid-liquid extractions, this is not adequate, and Weimer (19) has developed methods for handling polar-nonpolar interactions. Helpinstill (21) extended this to polar-polar systems. Unfortunately, both articles contain misprints, and (19) in particular needs correction. Figures 1-3 in this article actually plot cal/cm³ rather than cal/g-mol as stated, and equation 9 lacks the factor "RT" in the last two terms. Worst of all, the homomorph charts in these articles yield δ_p values that are higher than those from Blanks (18) which were the basis for successful correlations (8, 10, 11, 25, 38, 45). Even more unfortunately, Beerbower (25) propagated the problem by extending the same charts to higher molar volumes, but he did not make use of them. In order to take advantage of the values in Table 1, it is necessary to continue use of the Blanks chart.

Despite these difficulties, the two articles on liquid-liquid extraction make a very important point. Both use a two-part parameter, the polar and hydrogen-bonding forces being lumped together in the following expression:

$$\tau^2 = \delta_p^2 + \delta_H^2 \quad (14)$$

This parameter, τ , is used with a correlation factor, or as defined by Weimer, a correction term which in effect becomes a factor. The need for this has been attributed to failure of real systems to meet one of Hildebrand's assumptions (19), and to the directional nature of the polar and hydrogen-bond forces (38). In any case, the need for this correction is very real. The values found for various situations are as follows:

Correction Factor, b	Liquid Interacting With	Reference
0.250	polymers, surfactants, pigments	11
0.191	vulcanized polyisoprene	25
0.632	its own vapor	38
0.208, 0.202	paraffins	19, 21
0.170, 0.224	olefins	19, 21
0.100, 0.106	aromatics	19, 21

SOLUBILITY PARAMETERS

Since the last three categories were evaluated on the basis of the homomorph charts questioned above, they are not quite comparable with the others. It is to be hoped that resolving this problem will tend to reduce the scatter of the liquid-liquid factors.

The selectivity of an extraction solvent "1" for a mixture of A and B is defined as the ratio of their activity coefficients at infinite dilution in 1. This is equal to the mole ratio of A to B in the extract obtained by treating an equimolar mixture of A and B with an infinite amount of solvent. Each of these infinite dilution activity coefficients " a_2^∞ " may be obtained by the following equation:

$$\ln a_2^\infty = V_2[\delta_{D1} - \delta_{D2}]^2 + b(\tau_1 - \tau_2)^2/RT + 1 - (V_2/V_1) + \ln(V_2/V_1) \quad (14A)$$

where b is the correction factor (see above). While greater accuracy might be obtained by use of the three individual parameters, this has not been demonstrated and the example cited (21) indicates little need for improvement.

The last three terms of equation (14A) represent the Flory-Huggins entropy correction. Since V_2 appears in almost every term of this equation, selectivity depends both on the differences in the partial parameters and on the molar volumes of the two components to be separated. Because of this, it is possible to separate chemically similar liquids of unequal molar volumes, as well as dissimilar liquids of equal molar volumes. If both these factors vary, it is possible for the two effects to enhance or cancel each other; this is in agreement with the experimental evidence.

Emulsions. Winsor (46) predicted that the properties of emulsions could be related to the "ratio of the dispersing tendencies on the oil and water faces of the surfactant region." He was unable to quantify these forces, but Beerbower (45) did so by equating them to the cohesive energies of the mixtures of oil with the lipophile tail of the surfactant and of water with the hydrophile head. Both mixtures were calculated on the basis of three-dimensional solubility parameters, though this was only a formality where the oil was a paraffin hydrocarbon ($\delta = \delta_D$). Making the logical assumption that the volume swelling of the surfactant film was equal on both sides, he was able to produce an expression of these forces meeting all of Winsor's requirements.

However, this equation still contains ϕ , the volume fraction of each liquid which swells the surfactant layer, and this cannot be precisely evaluated at present. One method used to bypass this problem is to consider only those emulsions in which a perfect "chemical match" has been made (ie, δ_D , δ_P , δ_H are identical for oil versus lipophile, and for water versus hydrophile). The equation then reduces to a form independent of ϕ , for this special case of Winsor's ratio R :

$$R_0 = \frac{V_L \delta_{*L}^2}{V_H \delta_{*H}^2} \quad (15)$$

where V_L and V_H are the partial molar volumes of the lipophile tail and hydrophile head; δ_{*L}^2 and δ_{*H}^2 are defined by

$$\delta_{*}^2 = \delta_D^2 + 0.25(\delta_P^2 + \delta_H^2) \quad (16)$$

the 0.25 correction factor being based on Hansen's work (11).

This permits relation of R_0 to the well-known hydrophile-lipophile balance (HLB, see Vol. 8, p. 131) which Becher (47) showed correlates much of the data on

SOLUBILITY PARAMETERS

nonionic emulsions. Since HLB is defined as $20M_H/(M_L + M_H)$ where M is molecular weight,

$$R_o = \frac{\delta_{*L}^2}{\delta_{*H}^2} \left(\frac{20}{HLB} - 1 \right) \frac{d_H}{d_L} \quad (17)$$

where d_H and d_L are the densities of head and tail.

This valuable relationship helps to validate both the Winsor theory, which lacked numerical data, and the HLB theory, which was entirely empirical. Another approach to the swelling fraction problem was to assume that $\phi = 0.5$. This resulted in an equation which correlated the data on emulsions made in water, formamide, and mixtures of these, but not those made in glycols.

Use of these equations for the design of O/W (oil-in-water) emulsions made with ethoxylated surfactants requires only the assumption that the supply of emulsifier is adequate to cover at least 50% of the droplet surface. The steps are as follows:

1. Determine V_o and δ_{*o} for the oil to be emulsified. Unless the oil is exceptionally polar or hydrogen-bonded, the value of δ or δ_D may be used for δ_* . If a surface free energy is available, equation 12 may be used as an approximation.

$$\delta_{*o} \cong \sqrt{\gamma/0.0715 V_o^{1/3}} \quad (17a)$$

2. Correlation of literature data for the optimum value of R_o for oil in water emulsions leads to the working version of equation 17:

$$HLB_o = 20 \delta_{*o}^2 / (\delta_{*o}^2 + 38.4) \quad (17b)$$

where HLB_o is the required HLB value for the emulsifier.

3. An emulsifier is selected which meets the above criteria of HLB_o and $\delta_{*L} = \delta_{*o}$. The term δ_{*L} is determined by Small's method (37), calculating the ΣF values down to but not including the first ether or ester ($-O-$) linkage. A third criterion, based on experience, is that $V_L = V_o$. Rarely is a single emulsifier available which meets all three criteria, and it is customary to blend two or more. This practice is especially beneficial when different types of lipophile are blended (47), probably because of increased entropy.

4. All that remains is to set the percentage of emulsifier. Becher (47) provides some calculation methods, but it is probably best to make a test series to determine the balance of economy versus stability.

Solubility of Gases. Hildebrand (1) gave a chart which is reasonably accurate for predicting the solubility at 25°C of simple gases in regular liquids with solubility parameters from 6 to 10. This work has been greatly extended by Prausnitz (48), who removed not only the temperature limitation but also other limitations. Their approach is basically that of "condensing" the gas to a hypothetical state having a liquid-like volume. This hypothetical fluid is then blended with the solvent on essentially a liquid miscibility basis. The key information is the molar volume and solubility parameter of the gas as "condensed" at 25°C. Appropriate values for common gases are listed in Table 3. These are used in the following equation:

$$\frac{1}{X_2} = \frac{f_2^L}{f_2^G} \exp \frac{V(\delta_1 - \delta_2)^2 \phi_1^2}{RT} \quad (17c)$$

where X_2 is the mol fraction of the gas in solution, f_2^G is the fugacity of the pure gas at

SOLUBILITY PARAMETERS

initial conditions (taken as one atmosphere partial pressure) and f_2^L is the fugacity of the hypothetical liquefied gas. The latter is obtained from Fig. 5, adapted from Prausnitz (48). The critical temperature (T_c) and pressure (P_c) of the solute gas are also required. For gases of ordinary low solubility, ϕ_1 (the volume fraction of solvent) may be taken as unity.

Table 3. "Liquid" Volumes and Solubility Parameters for Gaseous Solutes at 25°C*

Gas	V , cc/g-mol	δ , (cal/cc) ^{1/2}
N ₂	32.4	2.58
CO	32.1	3.13
O ₂	33.0	4.0
Ar	57.1	5.33
CH ₄	52	5.68
CO ₂	55	6.0
Kr	65	6.4
C ₂ H ₄	65	6.6
C ₃ H ₈	70	6.6
Rn	70	8.83
Cl ₂	74	8.7

* J. M. Prausnitz and F. H. Shair, *A.I.Ch.E.J.* 7, 682 (1961); also reference 48.

Special methods are required for the light gases H₂, He, and Ne, which require corrections based on quantum mechanics, and for reactive gases such as HCl, SO₂ and NH₃. Hydrogen-bonding gases are given special treatment (48).

Effects of Temperature on Solubility Parameters. The success cited above in handling miscibility and gas solubility problems at various temperatures from the parameters at 25°C is due to a feature of the regular solution model, cited by Prausnitz (48). This is that the value of the complex functions

$$V_2\phi_1^2(\delta_1 - \delta_2)^2 \text{ and } V_1\phi_2^2(\delta_1 - \delta_2)^2 \quad (18)$$

are independent of temperature (as long as the composition remains constant). Since ϕ_1 and ϕ_2 vary only slightly with temperature, $(\delta_1 - \delta_2)$ is often nearly temperature in-

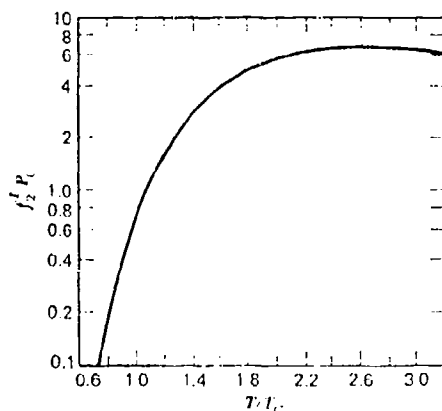


Fig. 5. Fugacity of hypothetical liquid at 1 atmosphere.

SOLUBILITY PARAMETERS

dependent. Hildebrand (2) gave an estimate of the variation of individual solubility parameters of nonpolar liquids

$$\frac{d\delta_D}{dT} = -1.25\alpha\delta_D \quad (19)$$

where α is the temperature coefficient of expansion, $d(\ln V)/dT$. This is not very exact, as he warns the reader, and he suggests a more sophisticated method. However, it is possible to derive an even more exact relationship from the well-known Watson equation for variation of ΔH_v with temperature:

$$d\delta_D/dT = -\delta_D[\alpha/6 + 0.6 T_c^{1.2}/\delta_D^2(T_c - T)^{2.2}] \quad (20)$$

It is now evident that the "constancy" of $(\delta_1 - \delta_2)$ is true only when the critical temperatures of the two materials are comparable, or a happy combination of α , T_c , and δ_D exists.

The polar parameter may be handled more simply, since μ is independent of temperature. Differentiation of equation 11a gives

$$d\delta_P/dT = -\delta_P\alpha/2 \quad (21)$$

There is no rigorous way of arriving at values of the temperature coefficient of the hydrogen bonding parameter, but Bondi (28) has provided empirical values at 100°C along with some of the ΔE_H values cited in Table 2. Assuming as above that $d(\Delta E_P)/dT = 0$, his numbers should reflect only $d(\Delta E_H)/dT$. Dividing them by the excess heats of vaporization and averaging the four results leads to

$$d\delta_H/dT = -\delta_H(1.22 \times 10^{-3} + \alpha/2) \quad (22)$$

Processing some of Weimer's data (19) the same way gives several more results of about the same magnitude, though averaging slightly lower.

By way of example, the rates of change for two liquids are shown in Table 4.

Table 4. Rates of Change for Two Liquids

Liquid	Equation		
	19, $d\delta_D/dT$	21, $d\delta_P/dT$	22, $d\delta_H/dT$
acetone*	-11.1×10^{-3}	-3.0×10^{-3}	-6.1×10^{-3}
1-propanol	-9.3×10^{-3}	-1.6×10^{-3}	-14.5×10^{-3}

* The value for $d\delta_D/dT$, as calculated by equation 20, would be -10.7×10^{-3} , an insignificant improvement.

This points up the importance of the level of hydrogen bonding, since it is generally believed that these bonds weaken rapidly with temperature. Actually, this is true only for alcohols and is due to equation 22 being the sum of the two.

Effects of Pressure on Parameters. Large increases in pressure tend to increase all the solubility parameters because of the decrease in V , and may be considered in a general way to be equivalent to reductions in temperature. Compressibility measurements afford a means to study cohesive energy, as pointed out by Hildebrand (2), and currently by Bagley (49).

A very interesting extension of the solubility parameter concept has been made by

SOLUBILITY PARAMETERS

Giddings (50) who applied it to supercritical gases compressed to liquid-like densities. The results have been useful in predicting the correct gas to use in high-pressure gas chromatography, and also in other problems relating to solubility in these peculiar fluids.

The above examples should be sufficient to demonstrate how various types of physical-chemical problems can be analyzed systematically and simply in terms of the energy concepts made possible by suitable interpretation of the solubility parameter. Understanding physical phenomena in terms of energies allows analysis of how materials can be expected to interact, a prime requisite for solving everyday industrial problems.

Theoretical Implications of the Solubility Parameter

The theoretical implications of an understanding of energy interactions among materials are too numerous to relate here. Prausnitz (48) has gone into this in some detail, and has demonstrated the interchangeability of solubility parameters, Flory-Huggins interaction parameters, and activity coefficients. In doing so, he emphasizes a point often overlooked, that the definition of δ in equation 1 describes the energy of vaporization required to expand the vapor isothermally to infinite volume. He also relates this type of correlation to the more general Prigogine and corresponding states theories (51). However, there is still work needed to tie in Hansen's work with Maron's (52), and Patterson's (53). The notable absence here of numbers related to acceptor-donor interactions has disturbed numerous people, but this arose only in the surface-free-energy work (41) and could be easily handled by correction factors. The success of solubility parameter concepts in explaining the data as completely as they do has been said to rest upon compensating errors; if so, the compensation is excellent. It has also been suggested (54) that the Hansen solubility-parameter system should be inverted, the solvents being represented as spheres having radii proportional to $(RT/V)^{1/2}$, thus leading to reducing radii with increasing molecular weight (ie, polymers as points helping to explain incompatibility more readily). This last consideration has generally been resolved in an arbitrary manner by treating the material concerned as the volume on solubility parameter plots, since this is generally what is of greatest concern in a given situation. The success of the solubility parameter in the (partial) characterization of inorganic salts and other materials in terms of the properties of organic liquids, suggests that terms can be included in equations 4 and 6 to include the energies arising from ionic and metallic type interactions. Work on surface-active agents and also bearing materials is being continued. Questions concerning entropy are yet to be resolved, but we do know that the free energy must be close to zero in a boundary region on a solubility plot. The Flory-Huggins parameter should also be close to 1/2 in the same region.

In spite of these many questions, some significant progress has been made in the area of relating surface phenomena to bulk liquid properties. The correlation of Hildebrand and Scott has been rewritten in terms of the Hansen solubility parameters with excellent correlation for most liquids (41).

Conclusion. It is hoped that this brief exposition of the past performance and the expected future of a very useful practical tool will stimulate more interest and action on the part of practical and theoretical workers alike. There is much to be done and, hopefully, the three-parameter nature of the solubility parameter will not impede progress. If there are three (or more) independent effects, quite simply, three

SOLUBILITY PARAMETERS

(or more) parameters are required to describe them. Certainly there are other effects in the solubility question, but the δ_D , δ_P , and δ_H parameters have demonstrated significance, with molar volume as a necessary fourth parameter in most cases.

The challenge to understand the physical interactions among all types of materials in terms of their energy properties should be recognized and met, not only in bulk systems, but also at interfaces.

ACKNOWLEDGMENT: The work reported in this article was supported in part by Army Contract No. DAH19-69-C-0033, administered by the Research Technology Division, Army Research Office, Arlington, Va.

Bibliography

1. J. Hildebrand and R. Scott, *Regular Solutions*, Prentice-Hall, Englewood Cliffs, N.J., 1962.
2. J. Hildebrand and R. Scott, *Solubility of Non-Electrolytes*, 3rd ed., Reinhold Publishing Corp., New York, 1949.
3. H. Burrell, *Am. Chem. Soc., Division of Organic Coatings Plastics Chemistry, Preprints* **28** (1), 682-708 (1968).
4. H. Burrell, *Offic. Dig.* **27** (369), 726 (1955).
5. H. Burrell, *Offic. Dig.* **29** (394), 1159 (1957).
6. H. Burrell, *VI Federation d'Associations de Techniciens des Industries des Peintures, Vernis, Emaux et Encres d'Imprimerie de l'Europe Continentale*, Congress Book, 1962, p. 21.
7. C. M. Hansen, *Ind. Eng. Chem. Prod. Res. Dev.* **8**, 2 (1969).
8. C. M. Hansen, doctoral dissertation, Technical University of Denmark, Danish Technical Press, Copenhagen, 1967.
9. C. M. Hansen, *Farg Lack* **14** (1), 10-22; (2), 23-25 (1968).
10. C. M. Hansen, *J. Paint Technol.* **39** (505), 104 (1967).
11. C. M. Hansen, *J. Paint Technol.* **39** (511), 505 (1967).
12. C. M. Hansen and K. Skaarup, *J. Paint Technol.* **39** (511), 511 (1967).
13. J. D. Crowley, G. S. Teague, and J. W. Lowe, *J. Paint Technol.* **38** (496), 296 (1966).
14. E. P. Lieberman, *Offic. Dig.* **34** (444), 30 (1962).
15. M. Dyck and P. Hoyer, *Farbe Lack* **70**, 522 (1964).
16. J. D. Crowley, G. S. Teague, and J. W. Lowe, *J. Paint Technol.* **39** (504), 19 (1967).
17. A. E. Van Arkel and S. E. Ules, *Rec. Trav. Chim.* **55**, 407 (1936); A. E. Van Arkel, *Trans. Faraday Soc.* **42B**, 81 (1946).
- 17a. Reference 1, p. 167.
18. R. F. Blanks and J. M. Prausnitz, *Ind. Eng. Chem. Fund.* **3**, 1 (1964).
19. R. F. Weimer and J. M. Prausnitz, *Hydrocarbon Proc. Petr. Ref.* **44**, 237 (1965).
20. H. G. Harris and J. M. Prausnitz, *Ind. Eng. Chem. Fund.* **8**, 180 (1969).
21. J. G. Helpinstill and M. Van Winkle, *Ind. Eng. Chem. Proc. Res. Dev.* **7**, 213 (1968).
22. J. L. Gardon, *J. Paint Technol.* **38** (492), 43 (1966).
23. K. L. Hoy, *J. Paint Technol.* **42** (541), 76 (1970).
24. R. J. Good, in *Treatise on Adhesion and Adhesives*, R. L. Patrick, ed., Marcel Dekker, Inc., New York, 1967.
25. A. Beerbower and J. R. Dickey, *A.S.L.E. Trans.* **12**, 1 (1969).
26. C. J. F. Böttcher, *Theory of Electric Polarization*, Elsevier, New York, 1952, Chap. 5.
27. A. L. McClellan, *Tables of Experimental Dipole Moments*, Freeman, Inc., San Francisco, 1963.
28. A. Bondi, *Physical Properties of Molecular Crystals, Liquids, and Glasses*, John Wiley & Sons, Inc., New York, 1968.
29. D. E. Martire and P. Riedl, *J. Phys. Chem.* **72**, 3478 (1968).
30. J. P. Teas, *J. Paint Technol.* **40**, 19-25 (1968).
31. P. Sorensen, *J. Oil Colour Chemists' Assoc.* **50**, (3), 226 (1967).
32. K. Skaarup, *Farg Lack* **14**, (2), 28-42; **14**, (3), 45-56 (1968).
33. A. Vinther and A. Peterson, *Verfkronek* **40**, 286-9 (1967).
34. W. D. Schaeffer, *Am. Ink Maker* **43** (5), 54 (1965).
35. G. Gee, *Trans. Inst. Rubber Ind.* **18**, 266-281 (1943).

SOLUBILITY PARAMETERS

36. B. J. Eiseman, Jr., *Refrigeration Eng.* **57**, 1171 (1949).
37. Anonymous, *Enjay Butyl Rubber Chemical Resistance Handbook*, Enjay Chemical Co., New York, 1964.
38. W. A. Zisman, in *Contact Angle, Wettability and Adhesion, Advances in Chemistry Series No. 43*, American Chemical Society, Washington, D.C., 1964, pp. 1-54.
39. S. Wu, *J. Phys. Chem.* **72**, 3332 (1968).
40. P. Small, *J. Appl. Chem.* **3**, 71 (1953).
- 40a. C. M. Hansen, *J. Paint Tech.* **42** (550), 660 (1970).
41. A. Beerbower, *J. Coll. Interf. Sci.*, **35**, 126 (1971).
- 41a. H. L. Clover, *J. Coll. Interf. Sci.*, awaiting publication.
42. S. A. Shain and J. M. Prausnitz, *A.I.Ch.E.J.* **10**, 766 (1964).
43. F. B. Sprow and J. M. Prausnitz, *Trans. Faraday Soc.* **62**, 1105 (1965).
- 43a. Reference 1, p. 143.
44. A. W. Francis, *Critical Solution Temperatures, Advances in Chemistry Series No. 31*, American Chemical Society, Washington, D.C., 1961.
45. A. Beerbower and J. Nixon, *Am. Chem. Soc. Petrol. Div. Preprints* **14** (1), 62 (1969).
46. P. Winsor, *Solvent Properties of Amphiphilic Compounds*, Butterworth Scientific Publications, Ltd., London, 1954.
47. P. Becher, *Emulsions, Theory and Practice*, 2nd ed., *Am. Chem. Soc. Monograph Series No. 162*, Reinhold Publishing Corp., Inc., New York, 1965.
48. J. M. Prausnitz, *Molecular Thermodynamics of Fluid-Phase Equilibria*, Prentice-Hall, Englewood Cliffs, N.J., 1969.
49. E. B. Bagley, T. P. Nelson, J. W. Barlow, and S.-A. Chen, *Ind. Eng. Chem. Fundamentals* **9**, 93 (1970).
50. J. C. Giddings, N. M. Myers, L. McLaren, and R. A. Keller, *Science* **162**, 67 (1968).
51. J. M. Prausnitz, *Chem. Eng. Sci.* **20**, 703 (1965).
52. S. H. Maron and C. A. Daniels, *J. Macromol. Sci.-Phys.* **B2** (3) 449-461 (1968); **B2** (3), 463-477 (1968); **B2** (4), 591-602 (1968); **B2** (4), 743-767 (1968); **B2** (4), 591-602 (1968).
53. D. Patterson, *J. Polymer Sci. Part C Polymer Symp.* No. 16, 3379 (1968).
54. T. Kahler and S. L. Knudsen, Student Report, Technical Univ. of Denmark, 1967.

CHARLES HANSEN

PPG Industries, Inc.

ALAN BEERBOWER

Esso Research and Engineering Co

APPENDIX IX

LIST OF EXPERTS INTERVIEWED*

Adam, N. K. - Prof. (retired) Surf. Chem., Southampton, England

Akin, L. S. - General Electric Co., Marine and Turbine Gear Dept., West Lynn, Mass.

Anderson, J. L. - U. of Tennessee, Chattanooga, Tenn.

Antler, M. - Bell Telephone Labs., Columbus, Ohio

Appeldoorn, J. K. - Senior Research Associate, Esso Italiana, Rome, Italy

Archard, J. F. - U. of Leicester, England

Askwith, T. C. - Tribology Centre, U. of Leeds, England

Bayer, R. G. - I.B.M., Endicott, N.Y.

Begelinger, A. - T.N.O., Delft, Holland

Blok, A. - Prof. Mech. Eng., Technische Hogeschool, Delft, Holland

Bond, G. C. - Brunel Univ., Uxbridge, England

Bondi, A. - Shell Development Co., Emeryville, Calif.

Brown, E. D. - General Electric Co., Silicones Div., Waterville, N.Y.

Buckley, D. H. - NASA, Lewis Research Center, Cleveland, Ohio

Cameron, A. - Prof. Mech. Eng., Imperial College, London, England

Christensen, H. - SINTEF, Tech. U. of Norway, Trondheim, Norway

Ciruna, J. - Imperial Oil Enterprises, Sarnia, Ontario

Clever, H. L. - Prof. Chem., Emory U., Atlanta, Ga.

Davies, J. T. - Prof. Chem. Eng., U. of Birmingham, England

Davies, R. L. - Esso Research Centre, Abingdon, Berks, England

de Gee, A. W. J. - T.N.O., Delft, Holland

Demorest, K. - Chief of Lubrication Branch, NASA Marshall Space Flight Center, Huntsville, Pa.

Duga, J. J. - Battelle Memorial Institute, Columbus, Ohio

*Each person mentioned in this list is receiving a copy of this STAF.

IX - 2

Egan, T. F. - Bell Labs, Holmdel, N.Y.

Fein, R. S. - Texaco Research Center, Beacon, N.Y.

Feng, I-M. - Esso Research and Engineering Co., Linden, N.J.

Feurstenau, D. W. - Prof. Mat. Sci. and Eng., U. of Cal., Berkeley, Cal.

Finkin, E. F. - Mechanical Tech. Inc., Latham, N.Y.

Fowkes, F. M. - Prof. Coll. Chem., Lehigh U., Bethlehem, Pa.

Fowles, P. E. - Mobil Research Center, Princeton, N.J.

Goldblatt, I. R. - Esso Research and Engineering Co., Linden, N.J.

Goldman, I. B. - Western Electric Co., Princeton, N.J.

Good, R. J. - Prof. Chem. Eng., State U. of N.Y., Buffalo, N.Y.

Grew, W. J. S. - Imperial College, London, England

Groszek, A. J. - BP Research Centre, Sunbury-on-Thames, England

Hansen, C. M. - P.P.G. Industries, Springdale, Pa.

Hermance, H. W. - (Retired), Bell Labs., Holmdel, N.J.

Johnson, R. L. - Chief of Lubr. Branch, NASA Lewis Research Center, Cleveland, Ohio

Kingsbury, E. P. - MIT Instrumentation Lab, Cambridge, Mass.

Klaus, E. E. - Prof. Chem. Eng., Penn. State U., University Park, Pa.

Ku, T. C. - I.B.M., Endicott, N.Y.

Leslie, R. L. - Vickers Inc., Troy, Mich.

Neumann, A. W. - Prof. Mech. Eng., U. of Toronto, Ontario, Canada

Oliver, D. R. - U. of Birmingham, England

Panzer, J. - Esso Research and Engineering Co., Linden, N.J.

Pask, J. A. - Prof. Ceram. Eng., U. of Cal., Berkeley, Cal.

Philippoff, W. - Esso Research and Engineering Co., Linden, N.J.

Prausnitz, J. M. - Prof. Chem. Eng., U. of Cal. Berkeley, Cal.

Rabinowicz, E. - Prof. Mech. Eng., MIT, Cambridge, Mass.

IX - 3

Robbins, E. J. - Risley Tribology Centre, Warrington, England

Rowe, C. N. - Mobil Research Center, Princeton, N.J.

Saibel, E. - Carnegie Inst., Pittsburgh, Pa.

Salomon, G. - T.N.O., Delft, Holland

Smith, A. J. - Imperial College, London

Tabor, D. - Prof. Surface Chem., Cambridge, England

Tao, F. F. - Esso Research and Engineering Co., Linden, N.J.

Vaessen, G. H. G. - T.N.O., Delft, Holland

Weale, K. E. - Prof. Chem. Eng., Imperial College, London

Wilkinson, C. S. - McDonnell Douglas Co., Santa Monica, Cal.

Zisman, W. A. - Naval Res. Lab., Washington, D.C.

APPENDIX X

PUBLICATIONS RESULTING FROM THIS CONTRACT

- "A Critical Survey of Mathematical Models for Boundary Lubrication"
ASLE Trans. 14, 90-104 (1971).*
- "Surface Free Energy: A New Relationship to Bulk Energies", J. Coll. and
Interf. Sci. 35, 126-132 (1971).**
- "Solubility Parameters", (with C. M. Hansen), Encyl. Chem. Tech. 2nd ed.
Supp. Vol. 889-910 (1971).
- "The Environmental Capability of Liquid Lubricants", NASA Symposium,
on Interdisciplinary Approach to Liquid Lubricant Technology,
awaiting publication (1972).

* Received Alfred E. Hunt Award from ASLE as best paper of 1971.

** More than 70 requests for reprints from all over the world have been
received.